# Monitoring, Explaining and Predicting the Stabilization Process of Coastal Dunes in Israel Using Remote Sensing and Geographic Information Systems (GIS) Means: The Case of Ashdod and Nizzanim

**Thesis submitted for the degree**
**Doctor of philosophy**

**By**

Noam Levin

**Submitted to the Senate of Tel-Aviv University**

**February 2006**

**This work was carried out under the supervision of**

**Prof. Eyal Ben-Dor**

**and**

**Dr. Giora J. Kidron**

# Acknowledgments

| | |
|---|---|
| *There are children of the valley,* | *יש ילדים של העמק,* |
| *there are children of the mountain,* | *ילדים של ההר,* |
| *and there are children of the sands.* | *ויש ילדים של החולות.* |
| *I am a child of the sands,* | *אני ילד של חולות,* |
| *and when these disappear,* | *וכאשר הם נעלמים,* |
| *gone is the place, in which I was born,* | *נעלם לי הדבר שבו נולדתי,* |
| *and whoever chooses to,* | *ומי שרוצה,* |
| *may call it a homeland.* | *יכול לקרוא לזה מולדת* |
| | |
| *(Amos Keinan)* | *(עמוס קינן)* |

Many people have inspired me and helped me throughout my research. Some of them are mentioned in the respective chapters, and many more deserve my warm thank you.

I would like to first give my thanks to my friends at the Society for the Protection of Nature in Israel (SPNI), where I have worked for almost seven years as head of the GIS unit during and between my B.A. and M.A. studies. These include my companions in the GIS unit, Lisa Oz, Ronnie Sade, Rachel Rodnitsky and Guy Nizry, the people from Deshe, Yoav Sagi and Edna Barnea, and many others – Uri Ramon, Hava Lahav, Raya Rudich, Mimi Ron, Binat Schwartz, Iris Han, Lihi Ben-Horin, Yossi Shak, Nir Papai, Yaakov Shaked, Yohanan Darom, Moshe Pearlmutter, Yael Peretz, Eran Binyamini, Yael Cohen, Noa Peled, Yonat Magal, Yisrael Tauber and Tali Finish. Working in the SPNI gave me a lot of professional experience in GIS, where I am indebted to Yaari Ginot who accepted me to work with him (at first in a big digitizing project) and later on as he moved to the Ministry of Environment, I have replaced him. But more than this, the SPNI was for many years my second home, not just in spending a lot of hours there, but more as serving as a place where I liked to be with many friends having a purposeful aim – of preserving Israel's open landscapes.

One of the most influential people there for me was and is Yair Farjun – a poet, a visionary, biblical prophet and guru, that is now almost identified with the Dunes of Ashdod, whom I am honored to have as a friend. Working closely with him at the office and in the field, I got to love this piece of land – yellow and ever changing – the coastal sand dunes of Ashdod/Nizzanim. I would also like to thank his wife Neta, and their kids for their warm hospitality. As we were working on the coastal dunes project within the SPNI, I was wondering what will be the theme of my M.A. thesis. I was ready to abandon any academic aspirations, when Tamar Achiron-Frumkin asked if I could estimate vegetation cover over the dunes from aerial photographs. This was the beginning of both my M.A. and Ph.D. theses, and I thank her for this initial push.

I was drawn to study Geography principally because of my love to maps since I was a kid and collected stamps. In the first year of my B.A. the courses I was most excited about were those related to Cartography, then given by Avi Degani and Zion Shitrug, GIS, by Yitzhak Benenson and Remote Sensing – given by Eyal Ben-Dor, who became my supervisor for both the M.A. and Ph.D. degrees, and to whom I owe my emergence as a specialist in Remote Sensing, as well as financial support. Giora Kidron joined Eyal in supervising me in my Ph.D thesis, and is warmly thanked not just for the great coffee he makes and the joint field trips, but also for developing my writing and critical reading skills. Other sources of inspiration for me within Tel Aviv University included Hadas Saaroni, Michael Roman, and Rosalie Sitman, as well as many of my friends during those years: Alexandra Chudnovski, Rachel Lugassi, Daniela Heller, Keren Patkin, Karine Hamm, Edna Barco, Tal Feingersh, Alexander (Sasha) Koltunov, Michael Winograd, Semantha Gluckman, Smadar Barkan, Sara Levin, Noa Feller, Ravit Aizic and Eitan Maze. I would also like to thank all my friends that ventured with me into the dunes to help with field measurements, or just for the fun of it: Yaron Yaakov, Oded Potchter, Rami Almog, Matt Freedman, Michael Gilmont, Efrat Klipstein, Ayelet Leibowitch, Assa Kedar, Shuli Zeik and Sandra Bähnk. The work with Avi Shmida from the Hebrew University of Jerusalem has stimulated my interest in ecology and I feel privileged for being able to work together. Many people from Israel's Nature and Parks Authority and the Green Patrol have also given me valuable help: Zeev Kuler, Ofri Cohen, Ravid Pik, Yoav Eshel, Shay Cohen, Zvi Horesh, Alon Galili, Naomi Altshuler, Gile’ad Altman, Yoel Dov and Noam Eldan.

I would like to thank my loving parents, David and Dvora Levin for all their support and love, as well as for sacrificing their digital camera – the hero of the second chapter of this thesis. To Adi, my brother, Sharon, his wife, and to Yael my sister, I thank for their friendship. I would also like to express my love to my grand parents, Maty and Avraham Sternhartz, and Zehava and Shmuel Levin. I would like to thank Ruth and Jeremy Kark for accepting me into their family.

Finally, it is my greatest pleasure to express here my love and thank you to Salit, my wife, and to our two lovely sons – Peleg and Yuval – that I hope will come to know these lovely dune areas – here in Israel, and those in Brasil.

# Contents

# Abstract

Coastal sand dunes present a complex system in which a-biotic, biological and human factors interact. Due to the proximity of large human populations to these areas, and their unique physical and biotic properties, the processes shaping coastal sand dunes demand better scientific understanding. This is especially relevant in the face of the ongoing global changes. In this thesis my objectives were to analyze the physical and human factors that affect the spatial and temporal variability in the process of coastal dune stabilization. To achieve these goals an interdisciplinary and multi-scale approach was adapted, combining tools from remote sensing, Geographic Information Systems (GIS) and geomorphologic field work. The main study area was the Ashdod-Nizzanim dunes, the largest remaining area of coastal dunes in Israel. The scientific papers comprising this thesis (in which each chapter is built as a paper) are organized along three axes, which include a methodological axis, a temporal axis and a spatial axis. The first axis aims at developing new methods to study sand dunes applying remote sensing and GIS tools; the second axis aims at studying the temporal changes in the dune dynamics and the physical and human factors responsible for these changes; and the third axis aims at quantifying the factors affecting or indicating the spatial variability in sand movement. Following are the major contributions and findings of this study, along these three axes:

**Methodological axis**. New methods were developed in this study for (a) Extracting of topographic information of dunes (slope, aspect and height) from shading effects appearing in satellite (e.g. Landsat) images, in areas where the mineralogy of the surface is homogeneous and there is no vegetation cover (Chapter 1); (b) Determining the color of sand, the content of free iron oxides and fine particles of sand samples using a digital camera, with an accuracy similar to that achieved with a field spectrometer (Chapter 2); (c) Calculating dune movement rates of sand dunes using a new method developed in this work that can be applied in

complex cases where different parts of a dune are moving at different rates. This method was applied to historical maps (Chapter 3) as well as to aerial photographs (Chapter 4); and (d) assessing the chlorophyll content of biological soil crusts over sand dunes at various depths in the field using a field spectrometer (Chapter 8), thus enabling to find the factors governing its presence over the coastal dunes.

**Temporal axis**. This part of the work focused on a study of the movement rates of coastal dunes in Israel since the 19th century, using both historical maps and aerial photographs. Analyzing the best map of the region generated in the 19th century (The Survey of Western Palestine by the Palestine Exploration Fund, 1871-1877) and comparing more recent maps by applying modern GIS methods, I found that the dunes were mobile during the first half of the 20th century, moving at an average rate of 5.1 m/year (Chapter 3). Based on an analysis of historical aerial photographs between 1944-1999, climatic records and historical archives, I demonstrated that the direct impact of human activities, and especially the presence of nomadic societies (the Bedouins) and their herds was responsible for changes in the dune mobility and stabilization processes along the Mediterranean coast of Israel (chapter 4). Time series of sand erosion/deposition rates, as measured in the field using erosion pins were studied with respect to meteorological time series of wind and rainfall. These were used to explain the low effect of rainfall on sand and dune movement along Israel's coastal dunes (Chapter 6).

**Spatial axis**. In this axis, the relationships between topography, vegetation, wind and sand mobility were explored. At first it was demonstrated that it is possible to map the aerodynamic surface roughness (Z0) over a dunes field with accuracy higher than 64% using a digital elevation model from which the relative height was calculated and using vegetation indices derived from a medium resolution satellite image (Chapter 5). These factors also

explained nearly 70% of the spatial variation of erosion/deposition rates as measured in the field by 315 erosion pins that were examined monthly along four transects from the coastline towards the dune edge over two years (Chapter 6). In both Chapters 5 and 6 I also examine the effect of upwind variables on sand drift variables and quantify this effect using directional filters. Vegetation cover is commonly used as an indicator of dune activity. However, different processes may occur at similar levels of vegetation cover: stability or mobility, erosion or deposition. To identify whether certain perennial plant species may serve as indicators for these different aeolian processes, a graphic exploratory data analysis method was developed and applied (Chapter 7). Using statistical tools, this approach enabled me to identify several plant species that can serve as useful indicators for different environments and the aeolian processes shaping them, including stable (Retama raetam, Stipagrostis lanata), erosive (Silene succulenta) or undergoing sand accumulation (Ammophila arenaria). Performing a detailed spectral survey of surface and subsurface properties (the content of chlorophyll, fine particles and free iron oxides) of three dunes in the heart of the Nizzanim-Ashdod study area, it was shown that chlorophyll content is higher in the most stable areas, as well as at the north facing slopes. Surface stability was able to explain 64% of the variability in the chlorophyll content, but only 26% of the variability in the content of fine particles and only 17% of the variability of free iron oxides. It was therefore shown that sand rubification is a weak indicator of dune stabilization processes, and is more related to the dune age or to its source material (Chapter 8).

The tools developed in this thesis, the identification of biotic and a-biotic indicators of dune stabilization, and the uncovering of the human role in this process in Israel, will enable efficient monitoring of coastal dune processes worldwide, as well as to predict future trends. This is especially valuable given the current global changes in climate and land use, which affect sand dunes around the world.

# Preface

As a child growing up in Tel-Aviv and not far from the sea, the landscape of sand dunes was part of my childhood. Whether they were coastal dunes between my neighborhood and the beach where we would see wild hares running in the sand, or ancient sand dunes that have transformed into aeolionite ("Kurkar") hills with their magnificent cross beddings and ancient carved graves, they were both a wonderful area waiting to be explored at a walking distance from home. These landscapes are slowly disappearing however, the sand dunes being covered with high-rise buildings and new roads, and exposures of "Kurkar" stones are now hard to find in the city.

During the course of my university studies I worked for seven years in the Society for the Protection of Nature in Israel, on various mapping projects related to the preservation of open landscape areas in Israel. The subject of one of those projects was the conservation of the coastal dunes of Israel. As part of that project I rediscovered the landscape of dunes, especially those south of Ashdod, and started to map the current and historical extent of coastal dunes and their vegetation using historical maps, aerial photographs and satellite images. This thesis is therefore a consequence of that work.

Coastal dunes are not only an attractive landscape that together with the adjacent beach is drawing tourists. Nor is it only an area where we may witness the working of evolution, with endemic species that have adapted to these special conditions. As sand dunes are highly porous, they form a perfect medium that captures and stores rainfall in underground aquifers. In addition, the preservation of coastal dunes, as well as of other coastal landscapes (such as mangroves) is an effective way to protect the hinterland from surges of the sea. The fact that a large part of the world's population is living near the coast, adds another challenge in understanding and protecting this unique ecosystem, a desert-like ecosystem that penetrates into every possible climate zone, and maybe the most dynamic of all geologic landscapes. In the face of future climate changes and increasing human pressures, which may lead to the re-activation or to the stabilization of coastal dunes, this is all the more important.

In this study I have tried to study coastal dunes in a multi-disciplinary approach, combining human, biotic and a-biotic aspects, at several spatial and temporal scales, using both field and remote sensing methods. I hope that the readers of this work will gain a new insight of coastal dune areas, and upon visiting such an area, will be able to understand that the landscape that they witness is ever changing, and will not be the same when they return to see it again.

d

# Introduction

## 1. Coastal dunes

### 1.1 Geomorphology of coastal dunes

Desert and coastal dunes cover about 10% of the land area between latitudes 30˚N and 30˚S (Sarnthein, 1978). Sand dune areas are dynamic in nature, with the dunes changing their location, length, or height, depending on the dune type (Tsoar, 2001). Dunes span a height range from about 30cm to over 300m, but they are generally poorly mapped around the world, due to their dynamic nature and their remoteness (Cooke et al., 1993). The physical properties of sand and its movement as sand grains and as sand dunes were first studied and described by Bagnold (1941). This work, considered a classic in aeolian geomorphology, focused mainly on desert dunes. Since then, many books and publications have been written on this subject (e.g. McKee, 1979; Pye and Tsoar, 1991; Wiggs, 2001). Wasson and Hyde (1983) found that the two factors determining the type of dune that will form are wind regime and availability of sand, whereas the presence of vegetation has only a secondary influence, and the wind power has no influence on the type of dune that will form. In experiments that studied the influence of the flow regime upon dunes, it was found that the surface is created with an orientation that aspires to maximize the transport of sand, aiming at an orientation perpendicular to the winds' direction (Rubin and Hunter, 1987; Rubin and Ikeda, 1990).

Coastal dunes are different from desert dunes, being of a younger age (up to 10,000 years, related to the last glacial period and low sea level, 18,000 years ago; Hesp, 2000; Tsoar, 2001), experiencing higher rates of sand deposition (Illenberger and Rust, 1988), having additional stress factors exerted on their plants due to salt spray and availability of underground water near the beach (Danin, 1991), and being closer to population centers, are more influenced by human activities. One of the classical books about coastal dunes is that of Ranwell (1972), that covers also their development and ecology.

Several dune forms may be identified at a coastal dune field (Pethick, 1984; Hesp, 2000; Tsoar, 2001):

- **Foredunes**, originating at the landward edge of the beach, parallel to the shoreline. They are formed by the wind blown sand deposition within vegetation, and are usually preceded by incipient embryo dunes.

- **Blowouts**, being an erosional dune landform. They are typically saucer-, cup or trough-shaped depressions or hollows formed by wind erosion of a pre-existing sandy substrate or dune.
- **Transgressive** dunefields of **transverse** or **barchan** dunes that migrate inland form as a response to rising sea level and/or climatic change, in regions with high sediment supply, strong winds, and on coasts experiencing erosion, where foredunes are only temporary or missing. It is common that in a transgressive dune field several dune ridges may be identified, that are separated by **dune slack** areas.
- **Parabolic** dunes are characterized by short to elongate trailing ridges that terminate downwind in U-, or V-shaped depositional lobes. Parabolic dunes typically evolve from blowouts or from transgressive dune fields that are in the process of stabilization.
- **Nebkha (coppice)** dunes are sand hammocks that are formed by isolated clumps of vegetation that act as sand traps. These can reach up to 30m high and 100m across; variations in shape depend upon the shape of the canopy.

## 1.2 The coastal dunes of Israel

The origin of the sand forming the coastal dunes of Israel is from the mountains of Ethiopia, from which it is carried first by the Nile River and then by the Mediterranean long shore current towards the shore of Israel (Nir, 1989). The coastal dunes of Israel are mostly comprised of quartz as is common in most dune areas (Muhs, 2004). Calcium carbonate is present in only minor amounts, mostly less than 7 per cent (Emery and Neev, 1960). The reddish color of the sand is due to a thin coating of iron oxides following oxidation and weathering processes, whereas the color of beach sand was lost during long shore transportation as iron was reduced (Emery and Neev, 1960). Archaeological remains covered by these coastal dunes indicate that aeolian sand forming the current stage of coastal dunes started to encroach on the coastal plain of Palestine/Israel between the $7^{th}$ and $9^{th}$ centuries A.D. (Tsoar, 1990). This encroachment of sand is attributed by some to climatic changes (Issar, 1995; Issar and Yakir, 1997), or as claimed by Reifenberg (1947, 1950) and Rubin (1989), to processes of soil erosion in Palestine, caused by changes in human land uses, following the occupation of the area by the Arabs from the hands of the Byzantine Empire.

Shaped by the SW and W winter storm winds, the coastal dunes of Israel were formed as transverse dunes, advancing towards the NE direction (Goldsmith et al., 1990). Aeolian sand was able to penetrate and develop coastal dunes only where the coastal sea cliff does not exist, or where streams breach it (Tsoar, 1990). Estimations of the coastal dunes movement rates in the 1940's and early 1950's range was found to be between 2-6 m/year (Reifenberg, 1947; Reifenberg, 1951; Tsoar and Blumberg, 2002a). However, during the early 1950's the dunes began to stabilize, their movement rate decelerating, and their shape changing from transverse to parabolic dunes. In addition to the stabilization process, the area covered by coastal dunes in Israel has diminished from 462 $km^2$ (Tsoar, 1990), to only 185 $km^2$ at the end of the 1990's (Frumkin-Ahiron et al., 2003), due to the quarrying of sand, and the construction of cities, military bases and water reservoirs over dune areas.

**Table 1**: Major studies that have been conducted about coastal dunes in Israel, according to their theme, study area and year.

| **Dunes area** | **Theme** | **Reference** |
|---|---|---|
| Acre | Vegetation of the dunes | Orshan, 1955 |
| General | *Ammophila arenaria* as a pioneer plant | Tsuriel, 1959 |
| General | Mediterranean beaches of Israel | Emery and Neev, 1960 |
| El-Arish | Sand and dune movement | Tsoar, 1970 |
| Caesarea Dunes | Photogrammetry of dune movement | Shtoch and Finkel, 1973 |
| Caesarea Dunes | Photogrammetry of dune movement | Gat, 1974 |
| Caesarea Dunes | Plant communities and succession | Kutiel et al., 1979/80 |
| Sharon Park | Silt and clay sedimentation during plant succession | Danin and Yaalon, 1982 |
| Netiv ha Asara | Vegetation and its habitats | Nukrian, 1988 |
| Southern dunes | The role of cyanobacteria in dune stabilization | Danin et al., 1989 |
| Neve Yam | The influence of vegetation on sand transport | Gertner, 1989 |
| Atlit | Sand transport | Harel, 1990 |
| General | Aeolian transport measurements and wind | Goldsmith et al., 1990 |
| Nizzanim Dunes | The influence of coastal cliffs on sand movement inland from the beach | Blumberg, 1989 |
| General | Dune development | Tsoar, 1990 |
| Nizzanim Dunes | The influence of coastal cliffs on sand movement inland from the beach | Tsoar and Blumberg, 1990 |

| | | |
|---|---|---|
| Nizzanim Dunes | The influence of coastal cliffs on sand movement inland from the beach | Tsoar and Blumberg, 1991 |
| Netiv ha Asara | Dynamics of dune vegetation since 1945 | Danin and Nukrian, 1991 |
| Holon | Effects of urbanization | Peery and Dmiel, 1995 |
| Sharon Park | Changes in vegetation 1918-1991 | Kosovsky et al., 1996 |
| Sharon Park | Landscape changes in the past 50 years | Kutiel P. and Sharon H., 1996 |
| Sharon Park | The role of biogenic soil crusts in the succession of dune vegetation | Kutiel et al., 1996 |
| Caesarea Dunes | Annual plants | Kutiel, 1997 |
| General | Stabilized efforts of dunes during the British mandate period | Liphschitz and Biger, 1997 |
| Rishon Lezion | Soil microbial biomass | Sarig et al., 1999 |
| Sharon Park | Recreational impacts on soil and vegetation | Kutiel et al., 1999 |
| Sharon Park | The effects of removing shrub cover | Kutiel et al., 2000 |
| Ashdod Dunes | Dune movement rates | Barzilay, 2001 |
| Ashdod Dunes | Dune activity and the formation of parabolic dunes | Tsoar and Blumberg, 2002a |
| Ashdod Dunes | The effect of vegetation removal on sand transport | Tsoar and Blumberg, 2002b |
| Ashdod Dunes | Vegetation establishment and invasion by *Acacia Saligna* 1965-1999 | Cohen, 2002 |
| Ashdod Dunes | Mapping of the rubification process | Levin, 2002 |
| Ashdod Dunes | Photogrammetry and volume changes | Arnold, 2003 |
| General | Conservation – a policy report | Frumkin-Ahiron et al., 2003 |
| Ashdod Dunes | Vegetation establishment and invasion by *Acacia Saligna* 1965-1999 | Kutiel et al., 2004 |
| Ashdod Dunes | Mapping of the rubification process | Ben-Dor et al., 2006 |

Most of the studies of coastal dunes in Israel have been focused in the past in areas north of Tel Aviv (see Table 1). As the largest area of remaining coastal dunes in Israel is now between the cities of Ashdod and Ashkelon, this area has recently been declared as a Long Term Ecological Research (LTER) station, and many studies are being conducted there in the past five years. However, most of the studies so far have focused on only a single aspect, and a holistic research integrating the human, biotic and a-biotic

components of this system was still lacking. Such in-depth holistic studies are few also in coastal dunes around the world (e.g. Liddle and Greig-Smith, 1975a, b; Rutin, 1983). We have thus aimed in this study to understand and quantify the relative weight of the physical and human factors influencing the stabilization process of coastal dunes, and the spatial and temporal variability of this process. The present study therefore presents a new and important approach to bridge the above gap. The main study area was the Ashdod-Nizzanim dunes, the largest remaining area of coastal dunes in Israel.

## 1.3 Stabilization processes of coastal dunes

The stabilization of coastal dunes is a complex process, involving interactions and feedback mechanisms between a-biotic factors (mainly the wind regime, characteristics of the sand grains, aeolian input of dust, evolution of a soil profile, and the level of underground water) and biotic factors (mainly the development of vascular and of microphytic vegetation, the activity of animals, and human land uses).

The stabilization or re-activation of sand dunes may thus be a result of either climate changes (e.g. Anthonsen et al., 1996; Lancaster, 1997) or of human activities (e.g. Al-Dabi et al., 1997; Tsoar and Møller, 1986).

Dune stabilization processes are commonly described by many studies as follows (Danin and Yaalon, 1982; Tsoar and Møller, 1986; Danin et al., 1989; Danin, 1991; Hesp, 1991): (1) With sufficient rainfall (above 50 mm/year) pioneer plants of perennial grasses germinate; (2) The presence of vegetation leads to a decrease in the wind speed, causing a local deposition of sand forming biogenic hillocks (nebkhas) and at a lower rate also the trapping of fine-grained particles transported via aerosols that are washed by the rainfall; (3) This amelioration in the water regime enables the development of filamentous cyanobacteria and the formation of a biogenic crust; (4) This in turn increases surface roughness, leading to less sand movement, enabling plant succession, an increase in nutrient levels and a decrease in stress levels for the plants. Due to the low field capacity of sand, the frequency and distribution of rainfall events may be more important than overall rainfall amounts, especially in desert environments.

Another important phenomenon in the soil formation process over sand dune environments is the rubification process. The rubification is defined as a pedogenesis stage in which iron is released from primary minerals to form free iron oxides that coat quartz particles in soils with a thin reddish film (Buol et al. 1973). The free iron oxides coat the quartz particles and provide a reddish chroma to the matrix as well as stability

(Ben-Dor and Singer 1987). In fact, differences in iron oxide mineralogy (red hematite vs. yellow goethite) may be used to understand differences in the pedoclimate (see Singer et al., 1998; Balsam et al., 2004).

In addition to the increase in vegetation cover, and the decrease in the movement of sand grains, stabilizing dunes also experience morphological and topographic changes. Thus, "*the establishment of vegetation on the crest changes the dynamics of barchan and transverse dunes, so that not all the sand eroded from the windward side is carried to the lee slip-face; some is trapped by plants. Consequently, there is a change in the shape of the windward slope from convex to concave, and the dune gradually becomes parabolic*" (Tsoar and Blumberg, 2002a). This process was observed on coastal dunes in Israel, Denmark, and elsewhere (see Anthonsen et al., 1996). Later on in the stabilization process, the whole topography of the sand dunes changes gradually, with the formation of sand hills lower than the initial dunes and with moderate slopes; these may then undergo processes of re-sedimentation, that will then fill the former interdune areas (see Zonneveld, 1999; Ringrose, 1996; Tsoar and Møller, 1986).

The coastal dunes of Israel are undergoing processes of stabilization by vegetation since the establishment of the state of Israel, in 1948. This is attributed to the low energy wind regime and changes in human land uses along the coast (Danin and Nukrian, 1991; Tsoar and Blumberg, 2002a), however the role of the human factor was not yet studied.

## 1.4 Physical factors affecting the stabilization or reactivation of sand dunes

Amongst the various physical factors that influence dunes some may encourage stabilization while others may encourage mobility. The magnitude of these factors changes both spatially (between and within a field dune) and temporally (along the year and between subsequent years and decades). These various factors are related to sand mobility in what can be described as positive and/or negative feedback loops (Tsoar and Møller, 1986).

Indices of sand mobility are traditionally based on precipitation, evaporation and wind magnitude. Lancaster (1988) has suggested the following mobility index that was then applied in many studies, based on his findings in the Namib and Kalahari deserts:

$$M = W/(P/PE) \qquad (1)$$

Where W = the percentage of the time the wind is blowing above the threshold velocity for sand transport
P = annual rainfall
PE = potential annual evapotranspiration

According to Lancaster (1988), dunes will be fully active when the values of M are higher than 200 and inactive when M is lower than 50. However, this index is only capable of predicting the general level of aeolian activity on a timescale of decades or longer (Lancaster and Helm, 2000). As demonstrated by Tsoar and Werner (1998) and Tsoar (2002, 2004) wind regime is the most important physical factor in determining the mobility of dunes. They recommend using another index for calculating the winds' drift potential, following Fryberger (1979):

$$DP = \sum q \, , \, q \approx U^2 (U - U_t) / 100 * t \qquad (2)$$

Where DP = the scalar sum of potential sand fluxes
q = the drift potential for a certain wind sector
U = wind velocity
$U_t$ = the threshold wind velocity for sand movement
t = the time the wind blew above the threshold

Using the DP values for each sector, the Resultant Drift Potential (RDP) can be calculated as the vector sum of the sector sand fluxes q. They have thus suggested the following equation to differentiate between vegetated and un-vegetated dunes. Following Equation 3 sand dunes in areas where the annual rainfall is higher than 50mm are un-vegetated and mobile under wind conditions in which M is above 1.

$$M = DP / (1000 - 750*RDP/DP) \qquad (3)$$

Where DP = the parameter presented in Equation 2 of the potential maximum at of sand that could be eroded by the wind during a year.
RDP/DP = an index of the directional variability of the wind that is the ratio of the resultant drift potential to the drift potential of the

wind (where unidirectional winds result in RDP/DP close to unity, while multidirectional equally spread winds result in RDP/DP values close to zero).

However, under the influence of human activities (as detailed in the following section) dunes may be either active or stabilized in contrast to the favoring climatic factors. As the quantity of sand flux is a function of third power of the wind speed (Bagnold, 1941), it will also be affected by the factors influencing wind speed (that is, the factors determining the aerodynamic surface roughness, or $Z_0$). It should also be remembered that with increased sand movement, erosion leads to the exposure of the roots of plants, deposition may bury plants, and saltating sand grains impact and injure plant tissues (Hesp, 1991; Danin, 1996). Thus, to explain the spatial variability in wind speed and in sand mobility within a dune field or within a single dune, the following factors are known to be of importance:

- Topography: Wind speed and sand movement are expected to increase with the relative height and available wind fetch (see Yeaton, 1988; McKenna Neuman et al., 1997; Bauer and Davidson-Arnott, 2002; Sauermann et al., 2003; Hesp et al., 2004). Maximum sand erosion is commonly found on the steepest part of the windward slope (Wiggs, 2001), however with increasing slope angle sand transport decreases (Iversen and Rasmussen, 1999) and heavier sand grains are left behind at lower elevations (White and Tsoar, 1998);
- Vegetation: The higher is the vegetation cover and height, and depending on its spatial arrangement, wind speed and sand movement will be lower (Lettau, 1969; Wasson and Nanninga, 1986; Yeaton, 1988; Wolfe and Nickling, 1993; Lancaster and Baas, 1998; Dong et al., 2001);
- Biogenic crust. Depending on their cover and type biogenic soil crusts stabilize the soil and inhibit sand erosion by the wind (Belnap and Gillette, 1998; McKenna Neuman et al., 2005);
- Surface moisture content. During and following rainfall surface moisture content rises, decreasing the effective amount of sand transported by the wind (Sherman et al., 1998; Arens et al., 2004; Cornelis et al., 2004; Wiggs et al., 2004);
- Underground water table. In places where the water table is less than two meters below the surface plant growth on sand dunes may be related to the water table height (Ranwell, 1972; Munoz-Reinoso and de Castro, 2005);

- Aeolian deposition of fine particles. Dust deposited during dust storms may penetrate into the soil by rainfall events that commonly follow events of Sharav (Alpert and Ziv, 1989; Zaady et al., 2001;Chen et al., 2002). A higher content of fine particles may lead to a higher cover of vascular plants and biogenic soil crusts, due to the higher retainment of water, thus enhancing stabilization (Tsoar and Møller, 1986), as well as enhance the cementing of quartz grains by clay minerals.

## 1.5 Human factors affecting the stabilization or reactivation of sand dunes

Human activities may change and impact coastal systems faster than physical factors related to climate changes (Gabriel and Kreutzwiser,2000). In addition, human disturbances are usually not cyclic, and therefore do not allow the natural system enough time to recover.

As with the physical factors, human activities over sand dunes may either lead to their stabilization or reactivation, depending on the type of activity and its intensity:

- Livestock grazing, surface trampling and cutting of dead and live vegetation by nomadic populations. Changes in the intensity of these activities may either reactivate stabilized dunes, or stabilize active dunes (Meir and Tsoar,1996; Barth,1998). Thus, the trampling of biogenic soil crusts by the movement of people and their livestock, and the human uses of dune plants (Bailey and Danin, 1981) may lead to a decrease in the surface aerodynamic roughness, and increase the erosion of sand by the wind.
- Planting of vegetation to stabilize dunes, as these were often regarded in the past as a menace to agricultural areas, transportation lines, settlements and the navigability of rivers (for a description of dune stabilization efforts in Israel, see Liphschitz and Biger, 1997).
- Planned stabilization of dunes is often done using plants that are not native to the area, and thus may lead to their invasion by exotic plants, especially in areas disturbed by human activities, changing the ecological system of the dunes (van der Meulen and Salman, 1996; Wiedermann and Pickart, 1996; Hilton and Harvey, 2002; Kim, 2004). This problem is now also studied in the coastal dunes of Israel with respect to the invasive tree *Acacia saligna* (Kutiel et al., 2004).
- Disturbances related to military activities, that by removing vegetation cover and biogenic soil crusts may lead to reactivation of dunes, as happened after the first

Gulf War in Kuwait (Al-Dabi et al.,1997), or following war-time military training in England (Hewett, 1970).

- Disturbances to the vegetation and biogenic soil crusts as a consequence of recreational activities, such as off-road vehicles (ORVs) and hikers (Curr et al., 2000; Lemauviel and Roze, 2003). To a certain degree, the compaction of soil along tracks and paths increases the water content of dry sand dune soils, and thus enhances the growth of vegetation (Liddle and Greig-Smith, 1975a). Along heavily used trails however no vegetation will be found. Studying an area of stabilized dunes in the Sharon Park of Israel, Kutiel et al. (1999) have found that the impact of high visitor use is localized and limited to the trail boundaries and their immediate surroundings (6 m axis perpendicular to the trails), while the effect on low-use trails is dispersed over a larger area, apparently because the trail borders are less visually defined to the visitor.
- Changes in sand supply due to the building of coastal facilities, as well as dams, and other structures. The building of dams along the Nile River (and especially the Aswan dam), as well as the dense network of irrigation canals in the Delta of the Nile, resulted with the slow destruction of the delta (Frihy, 1988; Stanley, 1996; Stanley and Warne, 1998). However, the present rate of sand transport of sand supply to Israel's coast, derived from the Nile Delta, its submarine cone, and the beaches of north Sinai, is expected to persist unchanged for the foreseeable future (Almagor et al., 2000). Nonetheless, the construction of ports and marinas along the Israeli coast has been shown to cause beach accretion in the upstream area of the marine structure, and erosion on the downstream, to a distance of even 2 km or more (Shoshany et al., 1996; Almagor et al., 2000; Klein and Zviely, 2001). The trapping of sands by new marine structures reduces the volume of sand that is transported and causes an overall deficit of sand along the coast. This may be offset by nourishment projects (Matias et al., 2004).
- Mining of minerals from sand dunes as well as from beached and development of built areas. These activities destroy sand dunes, as has been the case over many coastal dune areas and beaches in Israel (Almagor et al., 2000; Frumkin-Ahiron et al., 2003). However, areas where dune mining was practiced in the past may some times be rehabilitated (Lubke and Avis, 1998).

The sensitivity of coastal dunes to human impacts is a function of their morphodynamic type, as defined by Rust and Illenberger (1996): Retentive dune systems, being vegetated,

are sensitive and fragile. Mobile dunes that form the major component of transgressive dune systems are robust and resilient. This morphodynamic classification is particularly useful because the two types of dune systems have diametrically opposed sensitivities and hence different management requirements.

In areas where dunes are being stabilized as a result of human actions (whether in purpose or indirectly), the ecological consequences are now being questioned. In such areas, not only does the landscape change, populations of sand-living organisms decrease as a result of the loss their habitat – shifting sand, and are replaced by other organisms, more adapted to stabilized dunes (Kutiel et al., 2000). In Israel, this may result with the loss of species that are endemic to the Israeli coastal dunes. As a result experiments are being conducted that aim at reactivating stabilized dunes to restore their ecological values (Kutiel et al., 2000; Arens et al., 2004). Similar efforts are now starting also in the Ashdod and Nizzanim Dunes (Tsoar and Blumberg, 2002b).

## 1.6 Remote sensing of coastal dunes

### 1.6.1 Introduction

Remote sensing is the science and art of obtaining information about an object, area or phenomenon through the analysis of data acquired by a device that is not in contact with the object, area or phenomenon under investigation (Lillesand and Kiefer, 1994). The sensors used may be mounted on a spaceborne platform (e.g. satellite) or taken to the field (e.g. digital camera). Another distinction between different sensors is whether that are passive, measuring the solar reflected energy, or active, measuring the energy reflected from the controlled pulse of energy that they have emitted themselves.

Sand dunes differ from each other in their size and shape (depending on the wind regime, the amount of sand available to build them, vegetation cover; Wasson and Hyde, 1983), in their mineralogy, color and grain size (reflecting their sources and evolution through time), and in their state: active or stabilized. All these characteristics can be determined using remote sensing means that give a new regional insight into processes shaping the dunes, and into past climate regimes.

Sand dunes present an ideal target for monitoring by remote sensing methods, enabling a worldwide coverage with repetitive and quantitative measurements of biophysical and geophysical variables. As coastal dunes cover smaller areas than desert dunes, low spatial resolution sensors (~ 1km) are not appropriate, and typically coastal dunes studies will utilize sensors whose spatial resolution is between 30m (e.g. Landsat) to 1m or less (e.g.

Ikonos and aerial photographs). In this section (for the full version see Levin and Ben-Dor, in press) an overview of the great variety of applications remote sensing has to offer for studying dune areas is given. The focus will be put on coastal dunes and wherever available give examples from case studies along the coastal dunes of Israel, and especially from the dunes of Ashdod and Nizzanim.

### 1.6.2 Remote sensing studies concerning the mineralogy of dunes

During the past few years it was shown that soil spectra across the Visible-Near InfraRed- Short Wave InfraRed (VIS-NIR-SWIR) region are characterized by significant chromophores (e.g. OH, Fe3+, CO3 and COOH) enabling qualitative and quantitative analysis of soil properties (Ben-Dor 2002). This is mostly done today with advanced hyperspectral sensors that can provide a full spectrum out of every acquired pixel. Accordingly, remote sensing of sand dunes in general and using hyperspectral sensors in particular enables to rapidly and quantitatively map the mineralogy of sand dunes.
As the spectral reflectance of quartz is relatively flat and high exhibiting few absorption features (White et al., 1997; Ben-Dor et al., 1998), the spectral reflectance properties of sand dunes will be influenced by even small quantities of clay minerals, iron oxides, organic material, biogenic crust or vegetation.
While many soil properties can be detected across the NIR-SWIR regions of the spectrum, soil color in the human visible range (0.4-0.7 μm) is related to the presence of pigments or chromophores that absorb radiation in different wavelengths and intensities. Organic matter, water molecules, iron oxides, carbonates and chemical composition of transition metals in clay minerals are the major components affecting soil color (Ben-Dor et al., 1998). Traditionally, Munsell soil color charts are used to describe soil color visually, by assigning hue, value and chroma indices. This method is slowly being replaced by more accurate spectral measurements in the field (e.g. Torrent et al., 1983, Mathieu et al., 1998). In addition, various studies have applied remote sensing techniques in the field or using air- and space-borne sensors to map the mineralogic content (e.g iron oxides and carbonates) of sand dunes, to map relative-age zones, and to study the source-areas contributing to a dune field (see El-Baz, 1978; Blount et al., 1990; White et al., 1997; Pease et al., 1999; White et al., 2001; Bullard and White, 2002). Levin (2002) and Ben-Dor et al. (2006) have demonstrated the ability of a CASI airborne hyperspectral sensor to map low concentrations of iron-oxides over the Ashdod Dunes.

### 1.6.3 Remote sensing studies concerning the vegetation over dunes

The spectral reflectance of electromagnetic radiation from vegetation is dependent upon several factors, among them are the chlorophyll absorption, the geometry of the leaves, the morphological and physiological characteristics of the plant, the type of soil, the solar incidence angle and the climatic conditions (Barret and Curtis, 1992). Characteristic spectral reflectance curves of several desert habitats and of dominant desert vegetation (including key species common also to Israel's coastal dunes, e.g. *Ammophila arenaria*, *Artemisia monosperma* and *Retama raetam)* were collected using a field spectrometer by Pinker and Karnieli (1995).

Biological soil crusts, which can be formed by communities of several types of microphytes including mosses, lichens, fungi, green and blue-green algae as well as bacteria, are a common and widespread phenomenon in arid and semi-arid landscapes (Lange et al., 1992). Much attention has also been given for the spectral study of cyanobacteria soil crust over sand dunes (for desert dunes in Israel - Karnieli and Sarafis, 1996; Karnieli, 1997; Karnieli et al., 1999; for semi-arid regions in Australia – O'Neill, 1994).

Based on the spectral characteristics of vegetation many vegetation indices that serve as estimators for green vegetal biomass have been developed. These are usually based on the reflectance in the near-infrared band (that is related to the leaves of the plant) and in the red band (that is related to the chlorophyll absorption). A review and a comparison of some of the most popular vegetation indices is given by Broge and Leblanc (2000). Karnieli (1997) has suggested an index for mapping cyanobacterial crust covering sand dunes, using the red and blue bands, and tested it over the Nizzana dunes, Israel.

Remote sensing estimations of vegetation cover using the VIS-NIR spectral range are considered difficult in arid and semi-arid regions where vegetation cover is sparse (lower than 25%-35%), due to the soil background reflectance (Tueller, 1987). Nevertheless, maps showing classes of vegetation cover for almost the entire coastal dunes of Israel are presented by Frumkin-Ahiron et al. (2003) based on Normalized Difference Vegetation Index (NDVI) values calculated from a Landsat image of August 1999, whereas maps showing classes of historical vegetation cover (between 1965-1999) for the Ashdod dunes based on aerial photographs were created by Kutiel et al. (2004).

Classifying coastal dune fields into separate vegetation units or habitats was considered impossible until lately (Lucas et al., 2002), however new studies using hyperspectral sensors are showing promising results (Lucieer et al., 2003; Til et al., 2004; de Lange et al., 2004; Kempeneers et al., 2004).
Further improvement in this respect may be achieved by combining several images based on the phenological characteristics of the dunes' vegetation (see Schmidt and Karnieli, 2000; Karnieli, 2003).

### 1.6.4 Remote sensing studies of the activity of sand dunes

Active sand dunes areas may be identified based on their mineralogy (as in Jacobberger, 1989 and Paisley et al., 1991), or by mapping the extent of bare sand (as in Janke, 2002), using Landsat satellite images. However, most studied analyzing the mobility of sand dunes are usually done using time series of aerial photographs, from which the dunes movement rate is then analyzed by locating the position of the front of the dune (slip face) at successive times (e.g. Hunter et al., 1983; Illenberger and Rust, 1988; Gay, 1999; Jimenez et al., 1999). This method was also utilized by Tsoar and Blumberg (2002a) to analyze the dunes movement rate for 15 dunes south of Ashdod, identifying their decreasing movement rate, from 3.36 m/year between 1944-1956, to 1.90 m/year between 1980-1990. A new method for calculating the migration rate of parabolic dunes was recently introduced by Bailey and Bristow (2004).

### 1.6.5 Remote sensing studies of the topography of sand dunes

However important are studies concerning the movement of sand dunes, to fully understand their dynamic nature, they should be treated as 3D objects, and their topographic characteristics should be analyzed (Andrews et al., 2002). Knowledge of dune topography is extremely important for remote sensing as it influences the radiation reaching the sensor through shading and shadowing effects. As dunes' topography change with time, dune movement (analyzed above) and topography are two factors that should be assessed for a better remote sensing interpretation. Once a Digital Elevation Model (DEM) is created several attributes can be measured (such as the surface height and angles of exposure and slope) and compared between measurements done in different times. The following methods for extracting DEMs and surface roughness characteristics are commonly applied for sand dunes and desert areas: photogrammetry (e.g. Brown and Arbogast, 1999; Arnold, 2003, over the Ashdod Dunes), RAdio

Detection And Ranging (RADAR; see Blumberg and Greeley, 1993; Blumberg, 1998; Qong, 2000 and also Rabus et al., 2003) and LIght Detection And Ranging (LIDAR; see Lefsky et al., 2002). LIDAR measurements of dunes are becoming widely used for studying volumetric changes in relation with physical and human impacts (e.g. Rango et al., 2000; de Stoppelaire et al. 2001; Woolard and Colby, 2002), as well as providing a new method to derive the effective aerodynamic roughness length ($Z_0$) and displacement height ($d_0$), as in de Vries et al. (2003).

## 2. Research aims

In spite of the importance of coastal dune areas as a unique desert-like landscape in different climates, as a habitat for specifically adapted plants and animals, and their various roles for human society (serving as an underground water aquifer, as a line of protection from the sea, and as an area for tourism), coastal dune research is less developed than that of desert dunes. Especially lacking are studies that incorporate human, biotic and a-biotic aspects, at several spatial and temporal scales, using both field and remote sensing methods (see Sherman, 1995). Only using such an approach can we gain a synoptic view of the various components of this ecosystem.

The research aim was therefore to understand and quantify the relative weight of the physical and human factors influencing the stabilization process of coastal dunes, and the spatial and temporal variability of this process.

More specifically to:

- Develop new remote sensing and geographic information system (GIS) methods for monitoring sand dune areas.
- Monitor the changes in the stabilization process of the Israeli coastal dunes in the past century, analyzing the spatial and temporal variability.
- Identify the physical and human factors affecting dune stabilization at different temporal and spatial scales..

## 3. Outline of the articles comprising the Ph.D. thesis

Based on the above outline several peer-reviewed scientific articles in English and in Hebrew were published and others will be soon submitted. Table 2 provides a short summary to the papers that are included in this study. The Ph.D. thesis is comprised of the following eight articles that may be classified into three themes: the development of novel remote sensing and GIS techniques for monitoring sand dunes, a temporal-historical analysis of the mobility of the Israeli coastal dunes and the factors influencing it, and a spatial study of various physical factors and indicators of dunes' stability.

**Table 2**: The chapters and scientific papers comprising the thesis.

| Theme | Chapter | Name | Authors | Status |
|---|---|---|---|---|
| Articles devoted to the development of new remote sensing and GIS techniques for monitoring sand dunes | 1 | Topographic Information of Sand Dunes as Extracted from Shading Effects Using Landsat Images | Levin N., Ben-Dor E. and Karnieli A. | Published in 2004 in *Remote Sensing of Environment*, 90: 190-209 |
| | 2 | A digital camera as a tool to measure colour indices and related properties of sandy soils in semi-arid environments | Levin N., Ben-Dor E. and Singer A. | Published in 2005 in *International Journal of Remote Sensing*, 26 (24): 5475 - 5492 |
| Articles devoted to a temporal analysis of the Israeli coastal dunes mobility | 3 | The Palestine Exploration Fund map (1871-1877) of the Holy Land as a tool for analyzing landscape changes: the coastal dunes of Israel as a case study | Levin N. | Published in 2006 in *The Cartographic Journal*, 43 (1): 1-24 |
| | 4* | Monitoring sand dune stabilization along the coastal dunes of Ashdod-Nizanim, Israel, 1945-1999 | Levin N., and Ben-Dor E. | Published in 2004 in *Journal of Arid Environments*, 58: 335-355 |
| Articles devoted to the factors influencing the spatial variability in sand movement and to indicators of dune activity | 5 | Prediction of surface roughness ($Z_0$) over a stabilizing coastal dune field based on vegetation and topography | Levin N., Ben-Dor E., Kidron G.J, and Yaakov Y. | In review in *Geomorphology* |
| | 6 | The spatial and temporal variability of sand erosion across a stabilizing coastal dune field | Levin N., Kidron G.J. and Ben-Dor E. | In review in *Sedimentology* |
| | 7 | A field quantification of coastal dune perennial plants as indicators of surface stability, erosion or deposition | Levin N., Kidron G.J. and Ben-Dor E. | To be submitted to *Plant and Soil Science* |
| | 8 | The relationship between coastal dunes' stabilization and the content of biogenic soil crusts, free iron-oxides and fine particles – a field spectral analysis | Levin N., Kidron G.J. and Ben-Dor E. | To be submitted to *Remote Sensing of Environment* |

* A Hebrew version of this paper was published as follows: Levin N., Ben-Dor E. and Kidron G.J, 2003, The influence of human factors on the temporal changes in the stabilization rate of the Ashdod-Nizzanim dunes, *Horizons in Geography*, 57-58: 224-241 (in Hebrew; abstract in English in p. viii). See in the appendix.

Following is a description of the order of the scientific papers and their relations to each other as well as to the general line of research.

## 3.1 The development of new remote sensing and GIS techniques for monitoring sand dunes

Throughout the articles included in this thesis an intensive use of remote sensing and geographic information systems (GIS) has been made to analyze the spatial and temporal properties of dune stabilization processes. Part of the research was therefore devoted to develop new remote sensing and GIS methods to enable better and more accurate quantification of the variables studied. Some of these techniques deserved their own articles, whereas some are included in the methods of other articles.

*In the first article* the topographic properties of active sand dunes are treated, and a new method for extracting the height, slope and aspect of dunes is presented based on the principle of "shape from shading". In this paper it was shown that shading effects assessed by Landsat can be treated as a signal that stores important topographic information, especially when the spectral characteristics of a surface are homogenous, as they are in mobile dunes.

When dealing with sand dunes, whether stabilized or active, the properties of the sand however cannot be considered homogeneous when large areas are involved. Due to chemical and physical weathering processes that occur as sand is transported by the wind, exposed to the elements, and in interaction with vegetation, the properties of the sand itself change. Among those changing properties are the colour of the sand, its mineralogy and granulometry.

*In the second article*, a method to characterize the colour of soil samples is presented, and related chemical and physical properties of the soil (content of iron oxides and of fine particles), using a digital camera, instead of subjective munsell charts or expensive field spectrometers. These variables, may serve as indicators of the stabilization process, as will be discussed in the subsequent articles.

Other indicators for the stabilization process of coastal dunes include the movement rate of sand dunes, and the presence of biogenic soil crusts. As part of this thesis new techniques for these issues have been developed and are incorporated in the more geomorphologic-oriented articles.

*In the fourth article* a new GIS method is presented for calculating the movement rate of dunes, that is adapted for the case of dunes are stabilizing. In such cases, it is shown that the traditional method for estimating the dunes' movement rate results with overestimates, due to the fact that not all the parts of a dune are advancing at all, or at the same rate. The method proposed is based on integrating the whole area over which the dune advanced for the calculation, instead of using only a few selected lines to measure the advance rate.

As for the presence of biogenic crust, *in the eighth article* a new method is presented to measure its reflectance in the field along a vertical micro-profile. This was achieved by using a specially constructed Subsurface Biogenic Crust Sampler, that enabled to remove 2mm layers of sand one after the other, and thus to measure the reflectance at several layers. Furthermore, a study on the effect of moisture on spectral indices related to the chlorophyll content has been conducted, and a relationship was established between the content of fine particles in a sand sample and its spectral properties in the short wave infra-red region of the electromagnetic spectrum. Using these techniques it was possible to quantify the content of biogenic soil crust and of fine particles in the field, and relate them to the variables of surface aspect and surface stability (mobile or stabilized, erosion or deposition) that occur in different places on the dune.

The combination of all these new methods with established remote sensing technique for analyzing vegetation cover (using vegetation indices such as NDVI and SAVI), together with directional filtering methods, enabled to obtain quantitative relationships between various indicators of dunes' activity, and the spatial factors of vegetation and topography, as will be detailed in articles 5-8.

## 3.2 Analyzing temporal changes in the mobility of the Israeli coastal dunes

The activity of sand dunes changes with time both on a micro-scale (minutes-hours-days) and on the meso-scale (months-years-decades). On the meso-scale these changes may be due to either physical changes in the climate and in the sediment supply, or due to changes in human activities over the dunes. A historical analysis of such changes is commonly done using historical maps, aerial photographs and satellite images, and is usually limited therefore to the past decades only.

*In the third article* the possibility of using historical maps for studying the mobility rate of coastal dunes is presented. As is discussed there, the accuracy of a historical maps should be assessed before using it for landscape changes. To this end two sets of historical maps were used: the Survey of Western Palestine executed in the 1870's by the Palestine Exploration Fund, at a scale of 1:63,360, and topocadastric maps of Palestine executed in the 1930's-40's by the British Mandate Department of Survey at a scale of 1:20,000. From these two sets of geo-referenced and digitized maps a study of the dunes movement rate in six regions along the coast of Israel was then executed, going farther back than has been previously done.
*In the fourth article* an analysis of the temporal changes in the stabilization process of the Israeli coastal dunes in the past 60 years is presented, focusing on the case study of the Ashdod and Nizzanim dunes. In this part of the research the trends of dune stabilization and re-activation were studied using historical aerial photographs since 1944/5. To explain the trends that were discovered an extensive array of both physical and human factors are discussed, to reveal the causes of dune stabilization in the study area.

## 3.3 Analyzing factors influencing the spatial variability in sand movement

The first variable to understand with respect to the spatial variability of sand movement is the wind field, as after all sand grains are moved by the wind.
*In the fifth article* the aim was to quantify the spatial variability in the wind speed, or to be more specific, in the aerodynamic surface roughness ($Z_0$) across a coastal dune field, focusing on two areas: the Ashdod dunes and those of Bet Yanay.

Understanding the spatial variability of the wind field and how it is influenced by vegetation and topography are a key for better models of dune stabilization. In this chapter the importance of analyzing the influence of the area upwind of a selected location to understand its wind speed characteristics was demonstrated. The same principle was expected to be true also for the movement of sand, as measured in the field.

*In the sixth article* the rates of erosion and deposition of sand that were measured using erosion pins across the dunes of Ashdod and Nizzanim at 315 locations for 25 periods along two years (2002-2004) are presented. Using this dataset the effect of wind and of rainfall on sand movement along Israel's coastal dunes is explored. In addition, the spatial variability in sand movement was quantified, as governed by vegetation cover and topography upwind of the erosion pins.

*In the seventh article* it was shown that even when no measurements of sand erosion and deposition are conducted, the composition and cover of the perennial plants at a certain location may indicate whether it is stable or active, and whether it is undergoing erosion or deposition. To this end nine perennial plant species that are abundant across these coastal dunes, were analyzed using a specially devised visual exploratory data analysis method (the gradient visualization) in combination with established statistical methods.

*In the eighth article* a detailed analysis of changes in the soil properties in a small basin surrounded by three dunes was conducted. The soil properties that were mapped based on spectral features as measured in the field were the content of fine particles, free iron oxides and biogenic soil crusts. Studying in detail the spatial variability in these variables, in a basin that has begun stabilizing only 30 years ago, was intended to reveal the differences in the temporal responses of these indicators to dune stabilization.

## References for Introduction

Al-Dabi H., Koch M., Al-Sarawi M. and El-Baz (1997), Evolution of sand dune patterns in space and time in north-western Kuwait using Landsat images, *Journal of Arid Environments*, 36: 15-24

Almagor, G., Gill, D., and Perath, I., 2000, Marine sand resources offshore Israel, Marine Georesources and Geotechnology, 18: 1-42

Alpert, P., and Ziv, B., 1989, The Sharav cyclone: observations and some theoretical considerations, *Journal of Geophysical Research*, 94 (D15): 18,495-18,514

Andrews B.D., P.A. Gares and J.D. Colby, 2002, Techniques for GIS modeling of coastal dunes, Geomorphology, 48: 289-308

Anthonsen K.L., L.B. Clemmensen and J.H. Jensen, 1996, Evolution of a dune from crescentic to parabolic form in response to short-term climatic changes: Rabjerg Mile, Skagen Olde, Denmark, Geomorphology, 17: 63-77

Arens S.M., Q. Slings and C.N. de Vries. 2004. Mobility of a remobilized parabolic dune in Kennemerland, The Netherlands, Geomorphology, 59: 175-188

Arnold D., 2003, Photogrammetry and geospatial analysis of coastal sand dunes dynamics at the southern coastal plane of Israel, unpublished M.A. thesis, the Department of Geography, Bar-Ilan University

Bagnold, R.A., 1941, The Physics of Blown Sand and Desert Dunes, Methuen, London, 265 p.

Bailey, C., and Danin, A., 1981, Bedouin plant utilization in Sinai and the Negev, Economic Botany 35 (2): 145 –162.

Bailey S.D. and C.S. Bristow, 2004, Migration of parabolic dunes at Abberffraw, Anglesey, north Wales, Geomorphology, 59: 165-174

Balsam, W., Ji, J., and Chen, J., 2004, Climatic interpretation of the Luochuan and Lingtai loess sections, China, based on changing iron oxide mineralogy and magnetic susceptibility, Earth and Planetary Science Letters, 223, pp. 335-348

Barret E.C. and L.F. Curtis, 1992, Introduction to environmental remote sensing, Chapman and Hall, London, 426p

Barzilay E., 2001, The Geomorphologic Changes in the Coastal Dunes of Ashdod between the Mid-1940's till the Mid-1990's, unpublished M.A. thesis, Ben Gurion University of the Negev, Israel (in Hebrew)

Bauer B.O. and Davidson-Arnott R.G.D., 2002, A general framework for modeling sediment supply to coastal dunes including wind angle, beach geometry, and fetch effects, Geomorphology, 49: 89-108

Belnap J. and D.A. Gillette, 1998, Vulnerability of desert biological soil crusts to wind erosion: the influences of crust development, soil texture, and disturbance, Journal of Arid Environments, 39: 133-142

Ben-Dor E., 2002, Quantitative Remote Sensing of Soil Properties, Advances in Agronomy 75: 173-243

Ben-Dor, E., J.R. Irons, and G. Epema, 1998, Soil reflectance, In Remote Sensing for the Earth Sciences, edited by Rencz, A.N., in Manual of Remote Sensing Volume 3, edited by Ryerson R.A. (New York: John Wiley & Sons, Inc.), pp. 111-188

Ben-Dor E., and A. Singer, 1987, Optical density of vertisol clays suspensions in relation to sediment volume and dithionite-citrate-bicarbonate extractable iron. Clays and Clay Minerals, 35: 311-317

Ben-Dor E., N. Levin, A. Singer, A. Karnieli, O. Braun and G.J. Kidron, 2006, Quantitative Mapping of the Soil Rubification Process on Sand Dunes Using an Airborne CASI Hyperspectral Sensor, Geoderma, 131: 1-21.

Blount G., M.O. Smith, J.B. Adams, R. Greeley and P.R. Christensen, 1990, Regional aeolian dynamics and sand mixing in the Gran Desierto: evidence from Landsat Thematic Mapper images, Journal of Geophysical Research, 95 (B10): 15,463-15,482

Blumberg, D., 1989, The effect of the Sea Cliff on Inland Encroachment of Aeolian Sand as Shown on the Ashklon-Ashdod Beach, unpublished M.A. thesis, Department of Geography, Ben Gurion University of the Negev, Israel, 121p.

Blumberg D.G., 1998, Remote sensing of desert dune forms by polarimetric synthetic aperture radar (SAR), Remote Sensing of Environment, 65: 204-216

Blumberg D.G. and R. Greeley, 1993, Field studies of aerodynamic roughness length, Journal of Arid Environments, 25: 39-48

Broge N.H. and E. Leblanc, 2000, Comparing prediction power and stability of broadband and hyperspectral indices for estimation of green leaf area index and canopy chlorophyll density, Remote Sensing of Environment, 76: 156-172

Brown D.G. and A.F. Arbogast, 1999, Digital photogrammetry change analysis as applied to active coastal dunes in Michigan, Photogrammetric Engineering and Remote Sensing, 65 (4): 467-474

Bullard J.E. and K. White, 2002, Quantifying iron oxide coatings on dune sands using spectrometric measurements: an example from the Simpson-Strzelecki Desert, Australia, Journal of Geophysical Research, 107 (B6): 2125-2135

Buol S.W., F.D. Hole, and R.J. McCracken, 1973, Soil Genesis and Classification, The Iowa State University Press, Ames pp. 360

Chen X.Y., Spooner N.A., Olley J.M. and Questiaux D.G., 2002, Addition of aeolian dusts to soils in southeastern Australia: red silty clay trapped in dunes bordering Murrumbidgee River in the Wagga Wagga region, Catena, 47: 1-27

Cooke R.U., A. Warren and A.S. Goudie, 1993, Desert Geomorphology, London: UCL Press

Cornelis, W.M., Gabriels D. and Hartmann R., 2004, A parameterization for the threshold shear velocity to initiate deflation of dry and wet sediment, Geomorphology, 59: 43-51

Curr R.H.F., Koh A., Edwards E., Williams A.T. and Davies P., 2000, Assessing anthropogenic impact on Mediterranean sand dunes from aerial digital photography, Journal of Coastal Conservation, 6: 15-22

Danin A., 1991, Plant adaptations in desert dunes, Journal of Arid Environments, 21: 193-212

Danin A., 1996, Plants of Desert Dunes, Springer-Verlag, Berlin, 177 p.

Danin A., Bar-Or Y., Dor I. and Yisraeli T., 1989, The role of cyanobacteria in stabilization of sand dunes in southern Israel, Ecologia Mediterranea, 15: 55-64

Danin A. and R. Nukrian, 1991, Dynamics of dune vegetation in the Southern Coastal area of Israel since 1945, Documents Phytosociologiques, XIII: 281-296

Danin A. and Yaalon D.H., 1982, Silt plus clay sedimentation and decalcification during plant succession in sands on the Mediterranean coastal plain of Israel, Israel Journal of Earth Sciences, 31: 101-109

Dong Z., Gao S. and Fryrear D.W. (2001), Drag coefficients, roughness length and zero-plane displacement height as disturbed by artificial standing vegetation, Journal of Arid Environments, 49: 485-505

El-Baz F., 1978, The meaning of desert color in Earth orbital photographs, Photogrammetric Engineering and Remote Sensing, 44 (1): 69-75

Emery K.O. and D. Neev, 1960, Mediterranean beaches of Israel, Ministry of Development, Geological Survey, Bulletin No. 26, Jerusalem, Israel, pp:1-22

Frihy O.E., 1988, Nile delta shoreline changes: aerial photographs study of a 28-year period, Journal of Coastal Research, 4 (4): 597-606

Frumkin-Ahiron T., R. Frumkin, R. Roudich, A. Melloul, N. Levin and N. Papay, 2003, Conservation of the Coastal Sand Dunes – a Policy Report, The Surveys Unit – Open Landscape Institute – The Society for the Protection of Nature in Israel, The Ministry of Environment, The Nature and Parks Authority, The Jewish National Fund, The Water Commission and the Jerusalem Institute for Israel Studies, 126 p. (in Hebrew)

Fryberger S. G., (1979), Dune forms and wind regime, In: McKee Edwin D. (ed.), *A Study of Global Sand Seas*, Geological survey professional paper 1052, Washington, D.C. : United States Geological Survey, 137-169

Gabriel, A.D., Kreutzwiser, R.D., 2000, Conceptualizing environmental stress: a stress-response model of coastal sandy barriers, Environmental Management, 25 (1): 53 –69

Gat G., 1974, A Graphic-Quantitative Description of Sand Dune Areas Using Aerial Photographs, unpublished M.A. thesis, Department of Geography, Tel Aviv University

Gay S.P., 1999, Observations regarding the movement of barchan sand dunes in the Nazca to Tanaca area of southern Peru, Geomorphology, 27: 279-293

Gertner Y., 1989, The Influence of Vegetation on the Rates of Erosion and Deposition of Wind Blown Sand in the Coastal Dunes of Neve Yam, unpublished M.A. thesis under the supervision of M. Inbar, P. Kutiel and V. Goldsmith, Department of Geography, University of Haifa (in Hebrew)

Goldsmith V., Rosen P. and Gertner Y., 1990, Eolian transport measurements, winds, and comparison with theoretical transport in Israeli coastal dunes, in Coastal dunes: form and process, Nordstrom K.F., Psuty N.P. and Carter R.W.G. (eds.), John Wiley & Sons LTD., pp. 79-101

Guyot G., F. Baret, and S. Jacquemoud, 1992, Imaging spectroscopy for vegetation studies, in Imaging spectroscopy: fundamentals and prospective applications, Toselli F. and Bodechtel J. (eds.), pp. 145-165

Harel R., 1990, The Change in Space and Time in the Balance of Wind Blown Sand in the Dunes of Atlit Bay, unpublished M.A. thesis under the supervision of H. Kutiel and V. Goldsmith, Department of Geography, University of Haifa (in Hebrew).

Hesp P.A., 1991, Ecological processes and plant adaptations on coastal dunes, Journal of Arid Environments, 21: 165-191

Hesp P.A., 2000, Coastal Sand Dunes, Form and Function, Massey University, CDVN Technical Bulletin No. 4

Hesp P.A., Davidson-Arnott R., Walker I.J. and Ollerhead J., 2004, Flow dynamics over a foredune at Prince Edward Island, Canada, Geomorphology, in press (14 p.)

Hewett D.G., 1970, The colonization of sand dunes after stabilization with Marram Grass (*Ammophila arenaria*), Journal of Ecology, 58: 653-668

Hilton M. and Harvey N., 2002, Management implications of exotic dune grasses on the Sir Richard Peninsula, South Australia, Coast to Coast, pp. 186-189

Huete A.R., 1988, A soil-adjusted vegetation index (SAVI), Remote Sensing of Environment, 25: 295-309

Hunter R.E., Richmond B.M. and Alpha T.R., 1983, Storm-controlled oblique dunes of the Oregon coast, Geological Society of America Bulletin, 94: 1450-1465

Illenberger W.K. and I.C. Rust, 1988, A sand budget for the Alexandria coastal dunefield, South Africa, Sedimentology, 35: 513-521

Issar, A. (1995). 'Climatic changes and the history of the Middle East', American Scientist, 83, 350-355.

Issar, A. and Yakir, D. (1997). 'The Roman period's colder climate', Biblical Archaeologist, 60 (2), 101-106.

Iversen J.D. and Rasmussen K.R., 1999, The effect of wind speed and bed slope on sand transport, Sedimentology, 46: 723-731

Jacobberger P.A., 1989, Reflectance characteristics and surface processes in stabilized dune environments, Remote Sensing of Environment, 28: 287-295

Janke J.R., 2002, An analysis of the current stability of the Dune Field at Great Sand Dunes National Monument using temporal TM imagery (1984–1998), Remote Sensing of Environment, 83: 488-497

Jimenez J.A., L.P. Maia, J. Serra and J. Morias, 1999, Aeolian dune migration along the Ceara coast, north-eastern Brazil, Sedimentology, 46: 689-701

Karnieli A., 1997, Development and implementation of spectral crust index over dune sand, International Journal of Remote Sensing, 18 (6): 1207-1220

Karnieli, A., 2003, Natural vegetation phenology assessment by ground spectral measurements in two semi-arid environments, International Journal of Biometeorology, 47: 179-187

Karnieli A., G.J. Kidron, C. Glaesser and E. Ben-Dor, 1999, Spectral characteristics of cyanobacteria soil crust in semiarid environments, Remote Sensing of Environment, 69: 67-75

Karnieli A. and V. Sarafis, 1996, Reflectance spectroscopy of cyanobacteria within soil crusts – a diagnostic tool, International Journal of Remote Sensing, 17 (8): 1609-1615

Kempeneers P., S. de Backer, S. Delalieux, B. Nechad, W. Debruyn, P. Coppin, K. Ruddick, and P. Scheunders, 2004, HYPERWAVE Generic classification technique for Hyperspectral Data, a Powerpoint presentation presented at: Stereo & Vegetation, May 6 2004

Kim K.D., 2004, Invasive plants on disturbed Korean sand dunes, Estuarine, Coastal and Shelf Science, in press, 12p.

Klein, M., and Zviely, D., 2001, The environmental impact of marina development on adjacent beaches: a case study of the Herzliya marina, Israel, Applied Geography, 21: 145-156

Kosovsky A., Perevolotsky A. and Gavish D., 1996, Changes and Stability in the Perennial Vegetation in the area of the Sharon Park between the Years 1918-1991, unpublished scientific report presented to the Jewish National Fund (in Hebrew)

Kutiel P., 1997, The annual vegetation of the Northern Sharon dunes, Ecology and Environment, 4 (1): 25-34 (in Hebrew)

Kutiel P., Danin A., and Orshan G., 1979/80, Vegetation of the sandy soils near Caesarea, Iarael. I. Plant communities, environment and succession, Israel Journal of Botany, 28: 20-35

Kutiel P., O. Cohen, M. Shoshany and M. Shub, 2004, Vegetation establishment on the southern Israeli coastal sand dunes between the years 1965 and 1999, Landscape and Urban Planning, 67: 141-156

Kutiel P., Dangur H., Moses H. and Levi S., 1996, The role of biogenic soil crusts in the succession process of the Sharon dunes, Ecology and Environment, 3: 177-184 (in Hebrew)

Kutiel P., Peled Y. and Geffen E., 2000, The effect of removing shrub cover on annual plants and small mammals in a coastal sand dune ecosystem, Biological Conservation, 94: 235-242

Kutiel P. and Sharon H., 1996, Landscape changes in the Sharon Park area in the past 50 years, Ecology and Environment, 3: 167-177 (in Hebrew)

Kutiel P., Zhevelev H. and Harrison R., 1999, The effect of recreational impacts on soil and vegetation of stabilized coastal dunes in the Sharon Park, Israel, Ocean and Coastal Management, 42: 1041-1060

Lancaster N., 1988, Development of linear dunes in the southwestern Kalahari, Southern Africa, Journal of Arid Environments, 14: 233-244

Lancaster N., 1997, Response of eolian geomorphic systems to minor climate change: examples from the southern Californian deserts, *Geomorphology*, 19: 333-347

Lancaster N. and A. Baas, 1998, Influence of vegetation cover on sand transport by wind: field studies at Owens Lake, California, Earth Surface Processes and Landforms, 23: 69-82

Lancaster N. and P. Helm, 2000, A test of a climatic index of dune mobility using measurements from the southwestern United States, Earth Surface Processes and Landforms, 25: 197-207

de Lange R., M. van Til and S. Dury, 2004, The use of hyperspectral date in coastal zone vegetation monitoring, EARSeL eProceedings 3,2/2004, pp. 143-153

Lange O.L., G.J. Kidron, B. Budel, A. Meyer, E. Kilian and A. Abeliovich, 1992, Taxonomic composition and photosynthetic characteristics of the 'biological soil crusts' covering sand dunes in the western Negev Desert, Functional Ecology, 6: 519-527

Lefsky M.A., W.B. Cohen, G.G. Parker and D.J. Harding, 2002, LIDAR remote sensing for ecosystem studies, BioScience, 52 (1): 19-30

Lemauviel S. and Roze F., 2003, Response of three plant communities to trampling in a sand dune system in Britanny (France), Environmental Management, 31 (2): 227-235

Lettau H. (1969), Note on aerodynamic roughness-parameter estimation on the basis of roughness-element description, Journal of Applied Meteorology, 8: 828-832

Levin N., 2002, Quantitative Mapping of the Soil Rubification Process on the Coastal Sand Dunes of Israel Using an Airborne CASI Hyperspectral Sensor: The Sand Dunes of Ashdod as a Case Study, unpublished M.A. thesis, Department of Geography and Human Environment, Tel-Aviv University, Israel (in Hebrew)

Levin N. and E. Ben-Dor, in review, Remote sensing as a tool for monitoring coastal sand dunes – a review, an invited chapter to a book edited by Prof. Pua Bar (Kutiel) titled: Conservation and Management of Mediterranean Coastal Sand Dunes in Israel: Dilemmas and Challenges at Nitzanim Sand Park; Submitted in September 2004

Liddle M.J. and Greig-Smith P., 1975a, A survey of tracks and paths in a sand dune ecosystem, I. Soils, Journal of Applied Ecology, 12: 893-908

Liddle M.J. and Greig-Smith P., 1975b, A survey of tracks and paths in a sand dune ecosystem, II. Vegetation, Journal of Applied Ecology, 12: 909-919

Lillesand T.M. and R.W. Kiefer, 1994, Remote Sensing and Image Interpretation, John Wiley & Sons, Inc., 3rd edition, New York

Liphschitz, N., and Biger, G., 1997, Sand dunes reclamation by vegetation in Palestine during the British mandate period, Horizons in Geography, 46 –47: 21 –38 (in Hebrew)

Lubke, R.A., and Avis, A.M., 1998, A review of the concepts and application of rehabilitation following heavy mineral dune mining, Marine Pollution Bulletin, 37 (8-12): 546-557

Lucas N.S., Shanmugam S. and Barnsley M., 2002, Sub-pixel habitat mapping of a coastal dune ecosystem, Applied Geography, 22: 253-270

Lucieer A., P. Fisher and A. Stein, 2003, Texture-based segmentation of high-resolution remotely sensed imagery for identification of fuzzy objects, Proceedings of the 7th International Conference on GeoComputation, University of Southampton, United Kingdom, 8 - 10 September 2003

Mathieu, R., M. Pouget, B. Cervelle, and R. Escadafal, 1998, Relationships between satellite-based radiometric indices simulated using laboratory reflectance data and typic soil color of an arid environment, Remote Sensing of Environment, 66: 17-28

Matias, A., Ferreira, O., Dias, J.A., and Vila-Concejo, A., 2004, Development of indices for the evaluation of dune recovery techniques, Coastal Engineering, 51: 261-276

McKee E.D., 1979, A Study of Global Sand Seas, Geological Survey Professional Paper 1052, Washington

McKenna Neuman C., N. Lancaster and W.G. Nickling, 1997, Relations between dune morphology, air flow, and sediment flux on reversing dunes, Silver Peak, Nevada, Sedimentology, 44: 1103-1113

McKenna Neuman C., C. Maxwell and C. Rutledge, 2005, Spatial and temporal analysis of crust deterioration under particle impact, Journal of Arid Environments, 60: 321-342

van der Meulen F. and Salman A.H.P.M., 1996, Management of Mediterranean coastal dunes, Ocean and Coastal Management, 30 (2-3): 177-195

Muhs D.R., 2004, Mineralogical maturity in dune fields of North America, Africa and Australia, Geomorphology, 59: 247-269

Munoz-Reinoso J.C. and de Castro F.J., 2005, Application of a statistical water-table model reveals connections between dunes and vegetation at Donana, Journal of Arid Environments, in press, 17p.

Nir Y., 1989, Sedimentological Aspects of the Mediterranean Coast of Israel and Northern Sinai, The Geological Survey of Israel, Report no. GSI\39\88, Jerusalem

Nukrian R., 1988, Vegetation and its Habitats in the Dunes South of the Shikma River, unpublished M.A. thesis, Department of Botany, Hebrew University of Jerusalem (in Hebrew)

O'Neill A.L., 1994, Reflectance spectra of microphytic soil crusts in semi-arid Australia, International Journal of Remote Sensing, 15 (3): 675-681

Orshan, G., 1955, A vegetation map of the sand dunes in the Southern Acre Plain, Israel Exploration Journal, 5: 109-113

Paisley E.C.I., N. Lancaster. L.R. Gaddis and R. Greeley, 1991, Discrimination of active and inactive sand from remote sensing: Kelso Dunes, Mojave Desert, California, Remote Sensing of Environment, 37: 153-166

Pease P.P., G.D. Bierly, V.P. Tchakerian and N.W. Tindale, 1999, Mineralogical characterization and transport pathways of dune sand using Landsat TM data, Wahiba Sand Sea, Sultanate of Oman, Geomorphology 29: 235-249

Peery G. and Dmiel R., 1995, Urbanization and sand dunes in Israel: direct and indirect effects, Israel Journal of Zoology, 41: 33-41

Pethick J., 1984, An Introduction to Coastal Geomorphology, Edward Arnold, London

Pinker R.T. and A. Karnieli, 1995, Characteristic spectral reflectance characteristics of a semi-arid environment, International Journal of Remote Sensing, 16 (7): 1341-1363

Pye K. and Tsoar H. (1991), Aeolian sand and sand dunes, London, Unwin Hyman

Qong M., 2000, Sand dune attributes estimated from SAR images, Remote Sensing of Environment, 74: 217–228

Rabus B., M. Eineder, A. Roth and R. Bamler, 2003, The shuttle radar topography mission – a new class of digital elevation models acquired by spaceborne radar, ISPRS Journal of Photogrammetry and Remote Sensing, 57: 241-262

Rango A., M. Chopping, J. Ritchie, K. Havstad, W. Kustas and T. Schmugge, 2000, Morphological characteristics of shrub coppice dunes in desert grasslands of Southern New Mexico derived from scanning LIDAR, Remote Sensing of the Environment, 74: 26–44

Ranwell D.S., 1972, *Ecology of Salt Marshes and Sand Dunes*, London: Chapman and Hall, 258pp.

Rast M., 1991, Imaging spectroscopy and its applications in spaceborne systems, European Space Agency, SP-1144, 143p.

Reifenberg, A. (1947). The Soils of Palestine, Studies in Soil Formation and Land Utilization in the Mediterranean, London, Thomas Murby & Co.

Reifenberg, A. (1950). The War between the Sown Land and the Wilderness, Jerusalem, The Bialik Institute, 132 p. (in Hebrew).

Reifenberg, A. (1951). 'Caesarea, a study in the decline of a town', Israel Exploration Journal, 1, 20-32

Ringrose S., 1996, The geomorphological context of calcrete deposition in the Dalmore Downs area, Northern Territory, Australia, Journal of Arid Environments, 33: 291-307

Rubin, R. (1989). 'The debate over climatic changes in the Negev, fourth-seventh centuries C.E.', Palestine Exploration Quarterly, 121, 71-78

Rubin D.M. and Hunter R.E. (1987), "Bedform alignment in directionally varying flows", Science, 237, pp. 276-278

Rubin D.M. and Ikeda H. (1990), "Flume experiments on the alignment of transverse, oblique and longitudinal dunes in directionally varying flows", Sedimentology, 37, pp. 673-684

Rust I.C. and Illenberger W.K., 1996, Coastal dunes: sensitive or not?, Landscape and Urban Planning, 34: 165-169

Rutin J., 1983, Erosional Processes on a Coastal Sand Dune, De Blink, Noordwijkerhout, The Netherlands, Ph.D. Thesis, Kaal B.V. Amsterdam

Sabins F.F., 1996, Remote Sensing, Principles and Interpretation, W.H. Freeman and Company, 3rd edition, New York

Sarig S., Fliessbach A. amd Steinberger Y., Soil microbial biomass under the canopy of coastal sand dune shrubs, Arid Soil Research and Rehabilitation, 13: 75-80

Sarnthein M., 1978, Sand deserts during glacial maximum and climatic optimum, Nature, 272: 43–46

Sauermann G., Andrade Jr. J.S., Maia L.P., Costa U.M.S., Araujo A.D. and Herrmann H.J., 2003, Wind velocity and sand transport on a barchan dune, Geomorphology, 54: 245-255

Schmidt H. and A. Karnieli, 2000, Remote sensing of the seasonal variability of vegetation in a semi-arid environment, Journal of Arid Environments, 45: 43-59

Sherman D.J., 1995, Problems of scale in the modeling and interpretation of coastal dunes, Marine Geology, 124: 339-349

Sherman D.J., Jackson D.W.T., Namikas S.L. and Wang J., 1998, Wind-blown sand on beaches: an evaluation of models, Geomorphology, 22: 113-133

Shoshany, M., Golik, A., Degani, A., Lavee, H., and Gvirtzman, G., 1996, New evidence for sand transport direction along the coastline of Israel, Journal of Coastal Research, 12 (1): 311-325

Shtoch L. and Finkel H., 1973, Dune Movement near the Menashe Rivers Project, unpublished scientific report no. 199, available (in Hebrew) at the library of the University of Haifa

Singer, A., Schwertmann, U. and Friedl, J., 1998, Iron oxide mineralogy of Terre Rosse and Rendzinas in relation to their moisture and temperature regimes, *European Journal of Soil Science*, 49, pp. 385-395

Stanley, D.J., 1996, Nile delta: extreme case of sediment entrapment on a delta plain and consequent coastal land loss, Marine Geology, 129: 189-195

Stanley, D.J., and Warne, A.G., 1998, Nile delta in its destruction phase, Journal of Coastal Research, 14 (3): 794-825

de Stoppelaire G.H., J. Brock, C. Lea, M. Duffy and W. Krabill, 2001, USGS, NPA, and NASA investigate horse-grazing impacts on Assateague Island dunes using airborne LIDAR surveys, USGS Open File Report 01-382, July 2001, 4p.

Til M. van, A. Bijlmer and R. de Lange, 2004, Seasonal variability in spectral reflectance of coastal dune vegetation, EASReL eProceedings 3 (2/2004): 154-165

Torrent, J., U. Schwertmann, H. Fechter, and F. Alferez, F., 1983, Quantitative relationships between soil color and hematite content, Soil Science, 136 (6): 354-358

Tsoar H., 1970, The Dunes of El-Arish, unpublished M.A. thesis, The Hebrew University of Jerusalem

Tsoar, H., 1990, Trends in the development of sand dunes along the southeastern Mediterranean coast, in Dunes of the European Coasts, Catena Supplement, 18, ed. by Bakker, Th.W., Jungerius, P.D., and Klijn, J.A., 51-60.

Tsoar H., 2001, Types of Aeolian Sand Dunes and Their Formation, in: Balmforth N.J., & A. Provenzale (Eds.): Lecture Notes in Physics 582, pp. 403-429, Berlin Heidelberg: Springer-Verlag

Tsoar H., 2002, Climatic factors affecting mobility and stability of sand dunes, in *Proceedings of ICAR5/GCTE-SEN Joint Conference*, International Center for Arid and Semiarid Land Studies, Texas, Publication 02-2: 423-426

Tsoar H., 2004, The effect of climate change on mobility and stability of coastal sand dunes, in Physics Survey of Irregular Systems, 15-18 August 2004, Fortaleza, Brazil, Abstract book, pp. 26-27

Tsoar H. and D. Blumberg, 1990, The effect of coastal cliffs on inland encroachment of aeolian sand to the southern coastal plain of Israel, Horizons in Geography, 31: 155-168 (in Hebrew)

Tsoar H. and D.G. Blumberg, 1991, The effect of sea cliffs on inland encroachment of aeolian sand, Acta Mechanica (supplementum), 2: 131-146

Tsoar, H. and D.G. Blumberg, 2002a, Formation of parabolic dunes from barchan and transverse dunes along Israel's Mediterranean coast, Earth Surface Processes and Landforms, 27: 1147-1161

Tsoar H. and D.G. Blumberg, 2002b, The Effect of Vegetation Removal on the Rate of Aeolian Sand Transportation and the Morphologic and Dynamic Changes in the Dunes of Ashdod, Annual report presented to the Jewish National Fund, Research no. 90-2-537-01 (in Hebrew), available at: http://www.geocities.com/parkholot1/tsohar2002.pdf

Tsoar H. and Møller J.T., 1986, The role of vegetation in the formation of linear sand dunes, *Eolian Geomorphology Proceedings from the 17th annual Binghamton Geomorph. Symp.*, 75-95

Tsoar H. and Werner I., (1998), Reevaluation of sand dunes' mobility indices, *Journal of Arid Land Studies*, 7S: 265-268

Tsoar, H. and Y. Zohar, 1985, Desert dune sand and its potential for modern agricultural development. In Desert Development, ed. by Gradus Y., pp. 184-200, D. Reidel Pub. Co.

Tsuriell E.D., 1959, Physiological – Ecological Studies on Ammophila arenaria as a Pioneer Plant for Israel's Sand Dunes, unpublished PhD thesis, The Hebrew University of Jerusalem, Israel

Tueller P.T., 1987, Remote sensing science applications in arid environments, Remote Sensing of Environment, 23: 143-154

de Vries A.C., W.P. Kustas, J.C. Ritchie, W. Klassen, M. Menenti and J.H. Prueger, 2003, Effective aerodynamic roughness estimated from airborne laser altimeter measurements of surface features, International Journal of Remote Sensing, 24 (7): 1545-1558

Wasson R.J., and R. Hyde, 1983, Factors determining desert dune type, Nature, 304: 337-339

Wasson R.J. and Nanninga P.M., 1986, Estimating wind transport pf sand on vegetated surfaces, Earth Surface Processes and Landforms, 11: 505-514

Welch R., 1989, Desktop mapping with personal computers, Photogrammetric Engineering and Remote Sensing, 55 (11): 1651-1662

White K., J. Walden, N. Drake, F. Eckardt, and J. Settle, 1997, Mapping the iron oxide content of dune sands, Namib Sand Sea, Namibia, using Landsat Thematic Mapper data. Remote Sensing of Environment, 62:30-39

White K., A. Goudie, A. Parker and A. Al-Farraj, 2001, Mapping the geochemistry of the Northern Rub' Al Khali using multispectral remote sensing techniques, Earth Surface Processes and Landforms, 26: 735-748

White B.R. and Tsoar H., 1998, Slope effect on saltation over a climbing sand dune, Geomorphology, 22: 159-180

Wiedermann A.M. and Pickart A., 1996, The *Ammophila* problem on the Northwest Coast of North America, Landscape and Urban Planning, 34: 287-299

Wiggs G.F.S., 2001, Desert dune processes and dynamics, Progress of Physical Geography, 25 (1): 53-79

Wiggs G.F.S., Baird A.J. and Atherton R.J., 2004, The dynamic effects of moisture on the entrainment and transport of sand by wind, Geomorphology, 59: 13-30

Wolfe, S. A. and W. G. Nickling (1993). The protective role of sparse vegetation in wind erosion. Progress in Physical Geography 17(1): 50-68

Woolard J.W. and J.D. Colby, 2002, Spatial characterization, resolution, and volumetric change of coastal dunes using airborne LIDAR: Cape Hatteras, North Carolina, Geomorphology, 48: 269-287

Yeaton, R.I. (1988), Structure and function of the Namib dune grasslands: characteristics of the environmental gradients and species distributions, Journal of Ecology, 76: 744-758

Zaady E., Offer Z.Y. and Shachak M. (2001), The content and contributions of deposited aeolian organic matter in a dry land ecosystem of the Negev Desert, Israel, *Atmospheric Environment*, 35: 769-776

Zonneveld I.S., 1999, A geomorphological based banded ('tiger') vegetation patterm related to former dune fields in Sokoto (Northern Nigeria), Catena, 37: 45-56

van Zyl J.J., 2001, The shuttle radar topography mission (SRTM): a breakthrough in remote sensing of topography, Acta Astronautica, 48 (5-12): 559-565

*In the first article* the topographic properties of active sand dunes are treated, and a new method for extracting the height, slope and aspect of dunes is presented based on the principle of "shape from shading". In this paper it was shown that shading effects assessed by Landsat can be treated as a signal that stores important topographic information, especially when the spectral characteristics of a surface are homogenous, as they are in mobile dunes.

Available online at www.sciencedirect.com
SCIENCE DIRECT®
Remote Sensing of Environment 90 (2004) 190–209
Remote Sensing of Environment
www.elsevier.com/locate/rse

# Topographic information of sand dunes as extracted from shading effects using Landsat images

N. Levin[a,*], E. Ben-Dor[a], A. Karnieli[b]

[a] The Department of Geography and Human Environment, Tel-Aviv University, P.O. Box 3904, Ramat Aviv, Tel Aviv 69978, Israel
[b] J. Blaustein Institute for Desert Research, Ben Gurion University of the Negev, Sede Boker, Israel

Received 9 September 2003; received in revised form 8 December 2003; accepted 13 December 2003

**Abstract**

Topographic variations affect the reflectance properties of the Earth's surface and are often removed in remote sensing studies, especially when significant terrain variations exist. In this study, however, we show that shading effects assessed by Landsat can be treated as a signal that stores important topographic information, especially when the spectral characteristics of a surface are homogenous. The coastal transverse dunes of the Ashdod area, and the desert linear dunes of Nizzana (both located in Israel), were selected to investigate the abovementioned idea. The dune heights in these areas are 10 m on average (relative to their surroundings) and have maximum slopes of 33°. An innovative method for extracting slope, aspect, and height data for sand dunes using Landsat Thematic Mapper (TM) and Enhanced Thematic Mapper Plus (ETM+) images was developed, based on the regularity and periodicity of dunes' landscapes. Using two Landsat images representing different sun zenith and azimuth angles, reflectance values of each image were converted to cos($i$) values ($i$ = incident angle between the surface normal and the solar beam radiation), applying histogram matching methods. The slope and aspect of each pixel were determined as those that give the best prediction of the observed value of cos($i$). Height profiles were then extracted, using simple trigonometric relationships. The accuracies of heights and slopes along selected profile lines were to the order of 1 m and 3°, respectively (at a spatial resolution of 15 m). Best results were obtained when the images included one from the summer and the other from the winter, corresponding to maximum difference in solar zenith and azimuth angles. Errors in heights were attributed to surface heterogeneity (e.g., presence of biogenic soil crusts in the rainy season), geometric correction errors, cast shadows, and Bidirectional Reflectance Distribution Function (BRDF) effects. Comparison to Advanced Thermal Emission and Reflection Radiometer (ASTER) 3D information showed that the proposed method is better in representing the topographic variation of the area than the digital elevation model (DEM) produced by ASTER.


*Keywords:* Landsat; Shape from shading; Sand dunes; Digital elevation models

## 1. Introduction

### 1.1. Shading effects in remote sensing

Environmental phenomena measured by electromagnetic radiation can be treated either as noise or as a signal, depending on the theme under study. For example, the absorption of gases in the atmosphere can be seen either as noise masking reflectance or as a signal that can be processed to show the spatial distribution of these gases (e.g., Gao et al., 1993). Topographic shading and cast shadows can introduce errors into accurate analysis of satellite images since they mask significant spectral features and hamper signal based mapping. Consequently they are usually treated as noise that needs to be removed (Ekstrand, 1996; Shepherd & Dymond, 2002; Smith et al., 1980). Nevertheless, shading also stores information about topographic characteristics (in our case, of sand dunes), and in this sense, the noise becomes an important signal that should be extracted and analyzed.

Digital elevation models (DEMs) are a digital representation of topographic surfaces, containing only elevation data (Carter, 1988). The traditional methods to measure heights and create DEMs are (Toutin, 2001): (1) photo-clinometric methods (the use of information

* Corresponding author. Tel.: +972-2-6798365; fax: +972-3-6406243.
*E-mail address:* levinnoa@post.tau.ac.il (E. Ben-Dor).

0034-4257/$ - see front matter © 2004 Elsevier Inc. All rights reserved.
doi:10.1016/j.rse.2003.12.008

from either shadowing or shading; also termed photometric stereo or shape from shading); (2) photogrammetric methods (using stereo pairs of aerial photographs, or satellite images, e.g., SPOT or ASTER, Welch et al., 1998); (3) radar (e.g., the shuttle radar topography mission; Rabus et al., 2003); (4) and laser altimeters (Rango et al., 2000). As aerial photogrammetry and laser altimeters are expensive and not applicable over wide range areas, remote sensing from satellite images may provide a favorable solution.

Variation in the reflectance of the visible range has been used to extract information on the mean slope of the waves in the sea, using aerial photographs (Cox & Munk, 1954), laser (Shaw & Churnside, 1997), or satellite images (Melsheimer & Kwoh, 2001). In the urban environment, cast shadows were used in several studies to determine building heights (Cheng & Thiel, 1995; Hartl & Cheng, 1995). Ichoku et al. (1996) took advantage of the spatial behavior of shading on Landsat-TM images with respect to channels and other topo-morphologic features in order to detect drainage channel networks. Planetary remote sensing used photoclinometry to determine the topography of the moon, Mars (mostly in the polar regions) and other planets since the 1960s (Bridges & Herkenhoff, 2002; Fenton & Herkenhoff, 2000; Howard et al., 1982; Wildey, 1975). The only attempt, however, to the best of our knowledge, to extract topographic information of the Earth's surface from optical satellite images based on their shading effects, was that of Lodwik and Paine (1985). They have empirically calibrated reflectance values (from two images, with different sun elevations) to maximum slope data assuming a linear relationship between the two, over the Barnes icecap on Baffin Island (in an area ranging between 2300 and 3300 ft above sea level). Using this method they were able to extract a generalized DEM, that corresponded more to a trend surface, than to detailed contours. In addition, no quantitative assessment of the accuracy of their method was given. A previous attempt to quantify dunes' topographic parameters from satellite images was done by Qong (2000), that suggested a method for estimating Root Mean Square (RMS) of a dune's slope and height from Synthetic Aperture Radar (SAR) images.

Zhang et al. (1999) compare several algorithms that were developed for the extraction of shape-from-shading (SFS) on a single image (as generally applied by the photoclinometric studies of Mars) and conclude that existing SFS techniques produce generally poor results with either synthetic data or real images. One of their recommendations for future research was to use multiple images where the light source is moved—an approach that we will develop in the following sections.

Determination of topography by passive remote sensing was done mostly by multi-look angle platforms, whereas the shade option was neglected. This is mostly because shading over heterogeneous areas may be difficult to assess due to the varying albedo characteristics of the landscape targets. Sand dunes are high albedo targets that may be considered homogeneous. In this study, we used sand dunes and treated their shading effects on imagery as a signal, in order to develop a new method of extracting topographic information from nadir viewing platforms. Developing a method for extracting dune attributes from optical satellite images can be of great value for studying the movement of shifting dunes on both regional and continental scales, and related environmental hazards. In addition, dunes' surface presents a challenge different from that of icecaps, due to the periodicity of the surface, and the smaller height range of dunes' surfaces.

### 1.2. Sand dunes—geomorphologic properties

Desert and coastal dunes cover about 10% of the land area between latitudes 30°N and 30°S (Sarnthein, 1978). Sand dunes areas are dynamic in nature, with the dunes changing their location, length, or height, depending on the dune type (Tsoar, 2001). An example of the speed with which dunes' topography changes can be given from the coastal dunes of Ceara, Brazil, where barchan dunes that reach heights of 50 m move at an average rate of 17.5 m/year (Jimenez et al., 1999).

Dunes span a height range from about 30 cm to over 300 m, but they are generally poorly mapped around the world, due to their dynamic nature and their remoteness, and their extent of area is usually known more accurately than their height (Cooke et al., 1993). The main factors that influence the shape of a dune are the wind regime, sand supply, vegetation cover, and grain size. Linear dunes are formed under bidirectional wind regimes, while transverse dunes are formed under a unidirectional wind regime and an ample supply of sand (Wasson & Hyde, 1983).

Vegetation cover on sand dunes depends on several factors: wind speed and wind regime, rainfall, evaporation, water table height, dust accumulation, and anthropogenic disturbances (Pye & Tsoar, 1990; Tsoar & Illenberger, 1998). In areas with more than 100 mm/year of rainfall, only strong wind energies, or significant anthropogenic influences (such as grazing) can keep the dunes bare of vegetation. An increase in vegetation cover can influence the morphology of the dunes (Tsoar & Blumberg, 2002), inhibits the movement of sand, and eventually stabilizes the dunes.

Dune dynamics is an important indicator of desertification processes that are influenced by both man and climate change. Studies of dune surface stability, dune movement rate or sand transport rate are usually based on field measurements using iron rods (as in Kadmon & Leschner, 1995), topographic field surveys (as in Andrews et al., 2002), or through the visual or digital identification of the dunes' location in successive years from aerial photo-

graphs (e.g., Gay, 1999; Jimenez et al., 1999; Levin & Ben-Dor, in press), and are therefore limited in their scope. Once a DEM is constructed, various types of geomorphological analyses can be made, e.g., elevation change maps, elevation profiles, volumetric change calculations, identification of areas of erosion or deposition, etc. (Andrews et al., 2002). Incorporation of the third dimension from archived satellite images can therefore enhance our understanding of dune processes, and enable us to analyze larger areas.

### 1.3. Sand dunes—spectral properties

Sand dunes present an ideal target for monitoring by remote sensing methods, due to their remoteness and lack of data. The reflectance spectra of sand dunes as received on the sensor is dependent upon: (1) the characteristics of the dunes and their surface; (2) the geometry between the sun, the surface, and the sensor; and (3) atmospheric attenuation. The reflectance spectrum of sand dunes is influenced, in addition to vegetation cover, by their mineralogy (Ben-Dor et al., 1999; White et al., 1997), texture (Gerbermann & Neher, 1979), and presence of biogenic soil crusts (Karnieli et al., 1999).

The reflectance of sand is also dependent upon Bidirectional Reflectance Distribution Function (BRDF) effects (Romanova, 1964). BRDF effects become important for sand and crust surfaces especially at solar zenith angles greater than 30° (Cierniewski & Karnieli, 2002). BRDF effects are governed by the sun-object-sensor geometry, and are characterized by two specific areas of minimum and maximum reflectance (Pellikka et al., 2000). Where the scattering angle (the angle between the target source (the sun) and the target observer (the sensor) vectors) is zero, the area generally appears brighter than the rest of the image, and is therefore termed a "hotspot". At the largest scattering angles, a dark area is found. BRDF effects are different than shading effects. Although they also occur on horizontal surfaces, they are more wavelength dependent and specific. BRDF effects are stronger when the viewing angle of the sensor is wider, and their importance is of second order (in relation to shading effects) on nadir viewing sensors, such as Landsat, or when the area analyzed is relatively small (i.e., the scattering angle between the sun and the sensor in the area is constant).

Based on the previous review that summarized the importance of dune morphology and shading effects, the objectives of this study were:

- Study whether the relatively coarse spatial resolution of Landsat images (between 15 and 120 m) enables the characterization of desert and coastal dunes, according to shading effects on the images;
- Study the shading effects on transverse and linear dunes, as influenced by their orientation and the sun's zenith and azimuth angles;
- Develop and apply a method for extracting slope/aspect/height information of sand dunes from shading effects as seen on Landsat images;
- Determine the accuracy of the method when applied on Landsat TM and ETM+ images, compared to height profiles extracted from photogrammetrically derived DEMs over sand dunes.

## 2. Materials and methods

### 2.1. Research area

Two research areas were selected at the center and the south of Israel (Fig. 1), each representing a different kind of sand dune:

1. Coastal sand dunes south of the city of Ashdod, Israel (area A in Fig. 1). These are barchan and transverse dunes, shaped by the strong southwesterly winter winds. These dunes are in general going through a process of stabilization (since 1948) and morphological change from transverse to parabolic dunes (Levin & Ben-Dor, in press; Tsoar & Blumberg, 2002).
2. Desert linear dunes of the Negev (near Nizzana), on both sides of the Israel–Egypt border (area B in Fig. 1). The dunes in this area are shaped by a bidirectional wind regime, alternating between southwesterly winds and northwesterly winds. The utilization of the desert's resources in this area, and the resulting changes in the dunes' landscape were shown in the literature of the past two decades to be dependent upon the geopolitical situation, and the accessibility of the area to the Bedouin population (e.g., Tsoar & Møller, 1986). The influence of human settlement, and particularly sheep herding, upon the dunes in this area, through trampling, collection of dry vegetation and grazing, have transformed those dunes from semi-stabilized and vegetated linear shape to a much more dynamic braided and seif shape. When the pressure of nomadic population decreases, the dunes start to stabilize.

The spatial and morphometric characteristics of these dunes are summarized in Table 1. From this table, it is postulated that significant differences between the two dune types emerge. While the height characteristics of the dune areas are quite similar (average height of 10.5 m, standard deviation of about 4 m), the average and variance of the slope values are greater in the linear dunes of Nizzana. In addition, the linear dunes of Nizzana present two slip faces (alternating between N and S) and these comprise 41.6% of the dunes' area, while those of Ashdod have only one slip face (generally facing NE) comprising only 13.1% of their respective area.

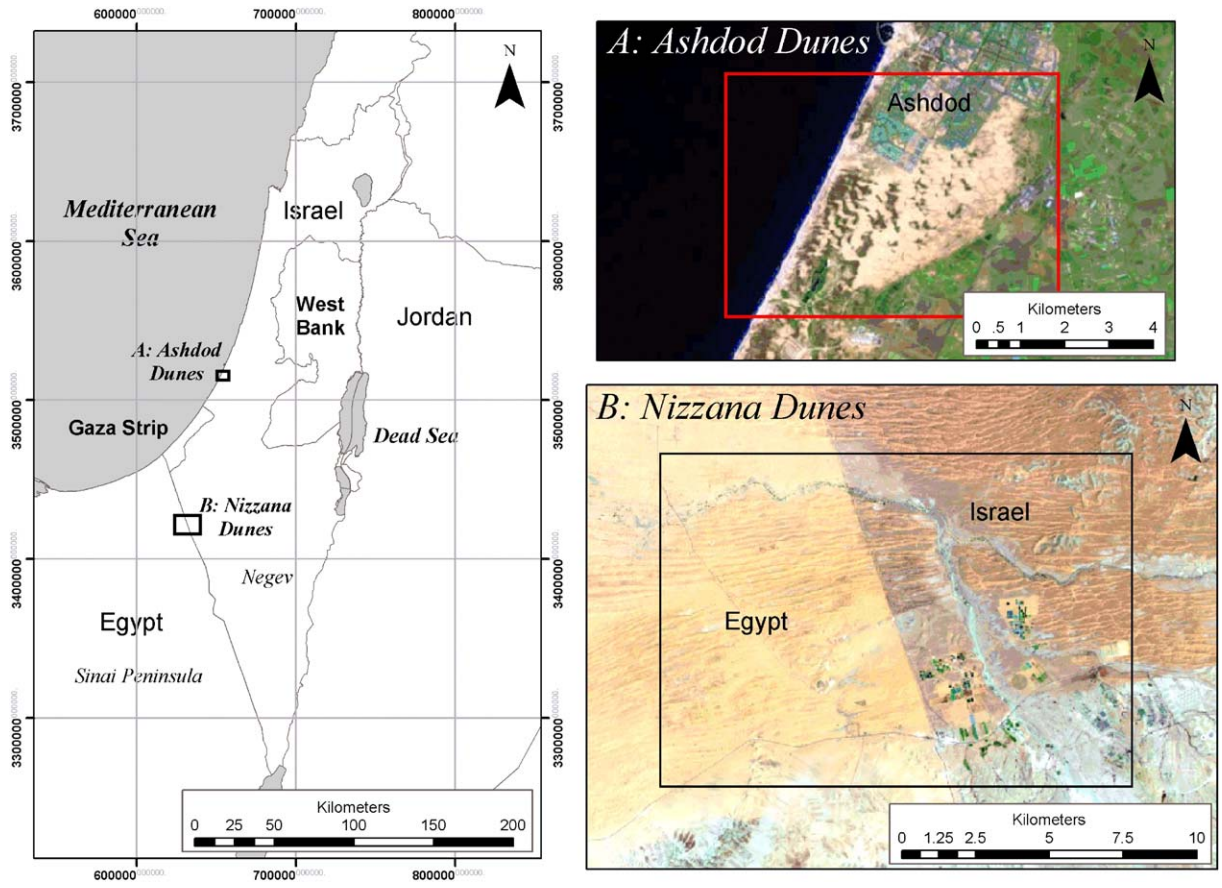


Fig. 1. Location map of the research area (projection UTM 36N), presented over a false color composite image of Landsat 7 ETM+ image (bands 7, 4, 2), from August 7, 1999.

### 2.2. Landsat imagery

Six Landsat images were selected for this study in order to represent two generations of Landsat sensors, and to study the influence of the time of year on the shading effects. Table 2 provides the details of the images used.

The spectral, spatial, and temporal characteristics of the Thematic Mapper (TM) sensor onboard Landsat 5, and the Enhanced Thematic Mapper Plus (ETM+) sensor placed onboard Landsat 7, are quite similar (Masek et al., 2001; Teillet et al., 2001). The main improvements of the ETM+ over the TM are in the improved resolution of the thermal band, the supplement of a panchromatic band, and the availability of two calibration modes from radiances into DN; the low and high gain modes are selected according to the time of year (the sun's position) and the average albedo of the Landsat scene. All Landsat images were converted from DN to radiance values, and then corrected atmospherically using the MODTRAN 3 radiative transfer model (Abreu & Anderson, 1996). Satellite images over the Ashdod dunes were geo-rectified to Israel Transverse Mercator (ITM) coordinate system (Mugnier, 2000) using 10–20 ground control points (GCP's) located on an orthophoto, using the triangulation method available in Envi 3.4 package (Research Systems, 2001). Satellite images over the Nizzana dunes were left in UTM coordinate system (as they were received), and the DEM was converted from ITM to UTM using standard projection tools.

### 2.3. High resolution DEMs of the dunes areas

As the average height of the dunes is about 10 m, the Survey of Israel DEMs constructed from 1:50,000 maps is unsatisfactory, as it is based on 10-m contours (Hall et al., 1999). For our work, we used detailed DEMs created by photogrammetric methods from aerial photographs. The DEMs were created from detailed contours (vertical spacing of 0.5 m) that were measured photogrammetrically. The data from the contours were converted into a DEM using the triangulation method described by Zhu et al. (2001), as implemented in the Idrisi software (Eastman, 2001).

### 2.4. ASTER DEM data

The Advanced Thermal Emission and Reflection Radiometer (ASTER) sensor, onboard the EOS-AM1 platform, acquires along-track stereo data for topographic mapping, at 15 m resolution, with a base-to-height (B/H) ratio of 0.6 (Welch et al., 1998). With the above B/H

Table 1
Main characteristics of the dunes investigated

| | Ashdod, Israel's coastal plain | Nizzana, Negev desert |
|---|---|---|
| Landsat path/row | path 174, row 038 | path 174, row 039 |
| Location | 34°65′ E, 31°77′ N | 34°37′ E, 30°94′ N |
| Elevation above sea level (m) | 0–50 | 150–250 |
| Average yearly rainfall (mm) | 485 | 90 |
| Perennial vegetation cover, late 1990s (%) | 25 | 14 |
| Dune type | transverse/parabolic | longitudinal/seif |
| Mean and standard deviation of height (m) | $\mu=10.7$, $\sigma=4.3$ | $\mu=10.2$, $\sigma=4.0$ |
| $\lambda$ (m) | 300 | 150–200 |
| Mean and standard deviation of slope (deg) | $\mu=4.7$, $\sigma=2.9$ | $\mu=6.1$, $\sigma=5.0$ |
| Orientation of the crest line of the dunes | NW–SE | West–East |
| % area of flat places | 0.0 | 13.9 |
| % area of N facing slopes | 11.2 | 22.6 |
| % area of NE facing slopes | 13.1 | 6.5 |
| % area of E facing slopes | 11.0 | 4.1 |
| % area of SE facing slopes | 8.6 | 7.6 |
| % area of S facing slopes | 10.0 | 19.0 |
| % area of SW facing slopes | 14.4 | 8.1 |
| % area of W facing slopes | 20.5 | 7.3 |
| % area of NW facing slopes | 11.2 | 10.9 |

ratio and correlations to within $\pm 0.5$ to $\pm 1.0$ pixel, the error of a single (relative) height measurement for ASTER was originally (prelaunch) expected to be between $\pm 12$ and $\pm 25$ m (Welch et al., 1998). Evaluations of vertical accuracy resulting from stereocorrelation indicated that RMSEz values of approximately $\pm 7$ to $\pm 15$ can be expected with images of good quality and adequate ground control (Hirano et al., 2003). Although the ASTER DEM was not expected to be detailed enough in the case of the Israeli dunes, it is able to give a base height (meters above sea level), while in other dune fields of the world, where the dunes are higher, it may be more relevant.

ASTER DEM data available on the web (http://edcdaac.usgs.gov/gov/) that corresponded to the study areas, was found only for the Ashdod dunes. The Local Granule ID of the image used was: ASTER_DEM20020610100628.hdf.

## 3. Theory and methods: shading effects on sand dunes

### 3.1. Solar radiation models

According to Dubayah and Rich (1995, p. 406) "There are three sources of illumination on a slope:

- Direct irradiance, which is strongly influenced by illumination angle, and includes self-shadowing by the slope itself and shadows cast by nearby terrain;
- Diffuse sky irradiance, where a portion of the overlying hemisphere may be obstructed by nearby terrain;
- Direct and diffuse irradiance reflected by nearby terrain towards the point of interest."

Shading can be modeled to a first degree as a function of how directly the sun's rays are incident upon the slope, that is, a function of cos($i$) (Ekstrand, 1996, p. 152):

$$\cos(i) = \cos(e)\cos(z) + \sin(e)\sin(z)\cos(\phi_s - \phi_n) \quad (1)$$

where $i$ = incident angle between the surface normal and the solar beam, $e$ = surface normal zenith angle or terrain slope, $z$ = solar zenith angle, $\phi_s$ = solar azimuth angle, and $\phi_n$ = surface aspect of the slope angle.

To determine whether a point is in shadow, the zenith angle to the horizon should be calculated and compared with the solar zenith and azimuth angles. In sand dunes, the maximum angle of slope (the angle of repose) is 33° (Bagnold, 1954). This angle is reached in the slip face of active sand dunes, and beyond it dry sand is unstable. In three of the Landsat images used, the solar zenith angle was less than 57° (i.e., sun elevation greater than 33°) and thus no shadowing was expected. In the other Landsat images that were used (January 1987, December 1994 and January 2001), we estimated that there were only small shadowing effects, based on solar zenith angles between 58° and 62°. For our analysis, we presumed that under clear sky conditions, spatial variability in radiation is dominated by the illumination

Table 2
Time of year, and sun zenith and azimuth angles for the six Landsat images selected for the research

| Sensor | TM | TM | TM | ETM+ | ETM+ | ETM+ |
|---|---|---|---|---|---|---|
| Date | 8-8-1985 | 18-1-1987 | 7-12-1994 | 7-8-1999 | 14-1-2000 | 21-5-2000 |
| Solar zenith | 34.2 | 62.4 | 61.8 | 28.6 | 58.6 | 24.6 |
| Sun azimuth | 108.6 | 142.6 | 148.1 | 116.6 | 151.6 | 112.5 |

angle, so the diffuse sky irradiance can be neglected (Dubayah & Rich, 1995).

### 3.2. Factors affecting shading on dunes

On bare sand dune areas (active dunes with dry sand and almost no vegetation cover) several factors determine the shading effects observed by a sensor:

- The zenith and azimuth angles of the sun. The greater the sun's zenith angle, and the more its azimuth angle is perpendicular to the crest of the dune, the greater are the shading effects. As Landsat is a sun-synchronous satellite, the time of year (and not the time of day) is the main factor determining the position of the sun with respect to the ground, and hence the shading. Thus, in the northern hemisphere, we expected shading to be more evident in winter (November–February) than in summer (May–August).
- The orientation of the dunes with respect to the sun direction. We expected those parts of a dune where the slope is steep (at the slip face) to exhibit the greatest shading effects. Thus, when the incident angle (i) between the slip face and the radiation source is either 0° or 180° we expected to have the most pronounced shading effects. This supposition was confirmed by

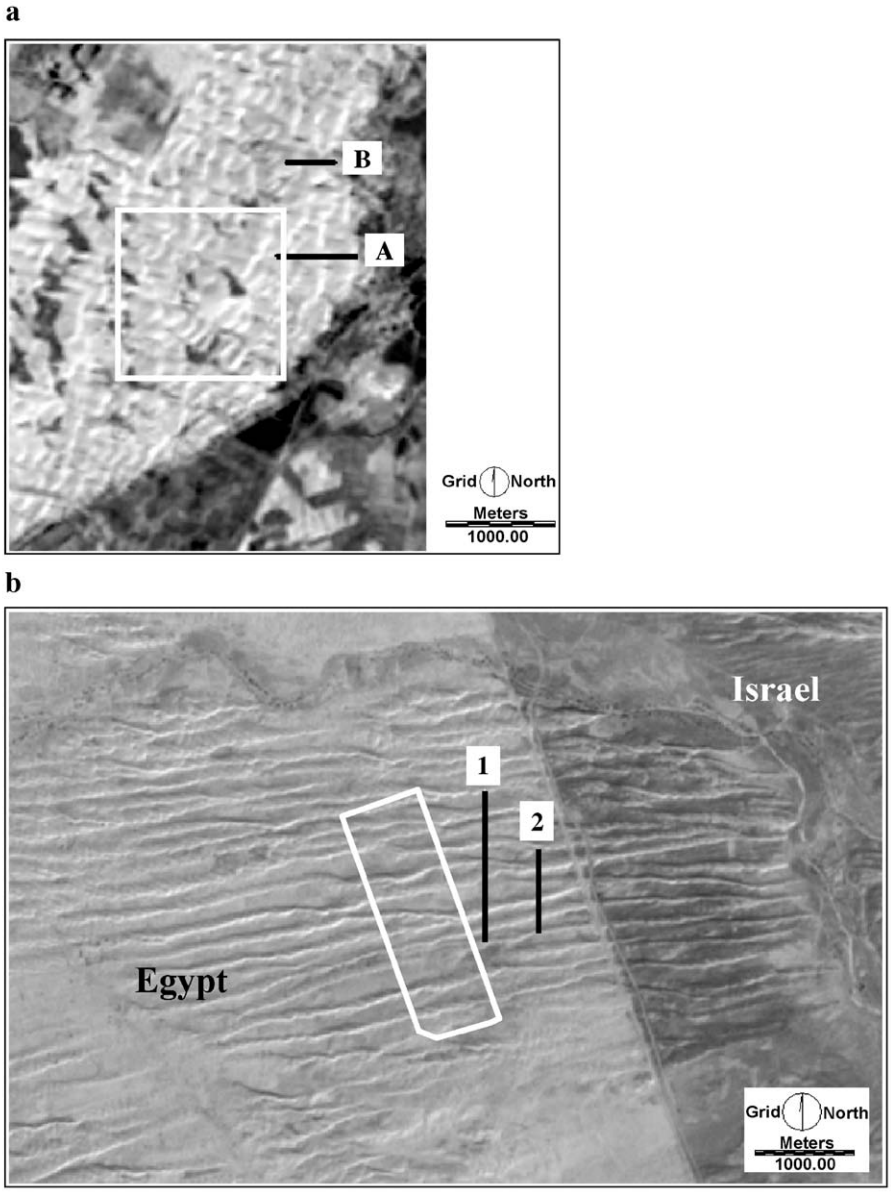


Fig. 2. (a) Transverse dunes of Ashdod (band 4 of Landsat 5 TM image, 8-8-1985). The white rectangle marks the area used for the calibration of reflectances to cos(i) values. Relative elevations were calculated along profile lines A and B. (b) Linear dunes of Nizzana (Panchromatic band of Landsat 7 ETM+, January 14, 2000). The white rectangle marks the area used for the calibration of reflectances to cos(i) values. Relative elevations were calculated along profile lines 1 and 2.

Blumberg (1998, p. 10) using SAR images, where for linear dunes "a look direction that is parallel to the crest line decreases the visibility of the dunes". He reported however that for transverse dunes, a look direction parallel to the mean crest line is optimal for showing the dunes and inter-dune regions.

- The topographic structure of the dune. Active sand dunes will have slip faces with angles of 33°. When dunes are stabilizing, as is the case along the coast of Israel (Tsoar & Blumberg, 2002) slip faces will be less pronounced and be covered with more vegetation, and thus, with time fewer shading effects will be evident, due to an increase in mixed vegetation-shading signal.

The magnitude of observed shading effects can be calculated from the variance of reflectances observed in an area. Expected shading effects for a given time of day and year can be calculated using a DEM (see Section 4.1), using Eq. (1), where the variance in cos(*i*) gives the shading effect. In addition, calculated cos(*i*) values can be compared with the reflectance values observed in the Landsat images, for each of its spectral bands, in order to evaluate which bands are best for extracting topographic information (see Section 4.2). Correlation coefficient values between cos(*i*) and reflectances depend upon the homogeneity of the dunes' surface (therefore those parts of the dunes with no vegetation cover were analyzed), accuracy of the geometric correction and of the DEM, and the dynamic range of reflectances and cos(*i*) values.

### 3.3. Extracting dune slope and aspect from topographic effects

Eq. (1) presents the shading effect as dependent on the sun's position (zenith and azimuth angles) with respect to the surface and the topography of the surface itself (slope and aspect). Given two images taken at different times (sun's position known), close enough in time so that no significant changes in the topography or the land cover emerge, they can be used as a database, from which the slope and the aspect of the surface can be extracted from the reflectance values of the images. This is based on the idea that variation in the reflectance of the dunes' surface is only governed by the shading effects.

Accordingly, the proposed method, which was developed to account for the slope and aspect information, is applicable only within areas of uniform land cover, and thus, is feasible only for dry sand dunes that are bare of vegetation, and have no biogenic soil crusts. This is because all these factors can change the reflectance of the dune significantly and create a bias.

#### 3.3.1. The proposed method

The problem presented here is actually solving for the values of two variables from two equations. As it is not possible to isolate either the slope or the aspect variables from Eq. (1), the following method is proposed:

- For each pixel, a lookup table consisting of 192 possible combinations of slope and aspect were calculated (12 values of slope between 0° and 33° with intervals of 3°, 16 values of aspect between 0° and 337.5° with intervals of 22.5°). Cos(i) values were calculated for all these combinations.
- Cos(i) values were estimated from the reflectance values in the images (see Section 3.3.2).
- For each of the 192 combinations, the difference between the actual value of cos(i) in the image, and the lookup table cos(i) was checked:

$$\text{Difference}_j = \text{abs}[\cos(i)_{j,\text{date}-a} - \cos(i)_{\text{date}-a}] + \text{abs}[\cos(i)_{j,\text{date}-b} - \cos(i)_{\text{date}-b}] \quad (2)$$

  where j = 1 − 192 combinations, date-a = image from time a, date-b = image from time b, abs = absolute difference.
- Each pixel is assigned to those slope and aspect values that give the smallest difference between the calculated and actual cos(i) values.

The method proposed assumes lambertian reflectance and no cast shadows.

#### 3.3.2. Calibration of observed reflectance values to cos(i) values

In order to apply the proposed method, reflectance values of the images need to be calibrated to cos(*i*) values. While photoclinometric studies of Mars are based on visually

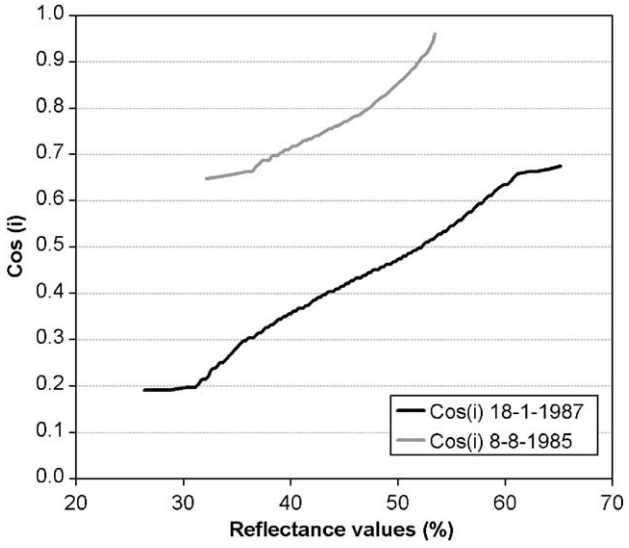


Fig. 3. Empirical calibration functions derived for the Ashdod 1985 and 1987 scenes, from reflectance values to cos(*i*) values, as derived by histogram matching techniques.

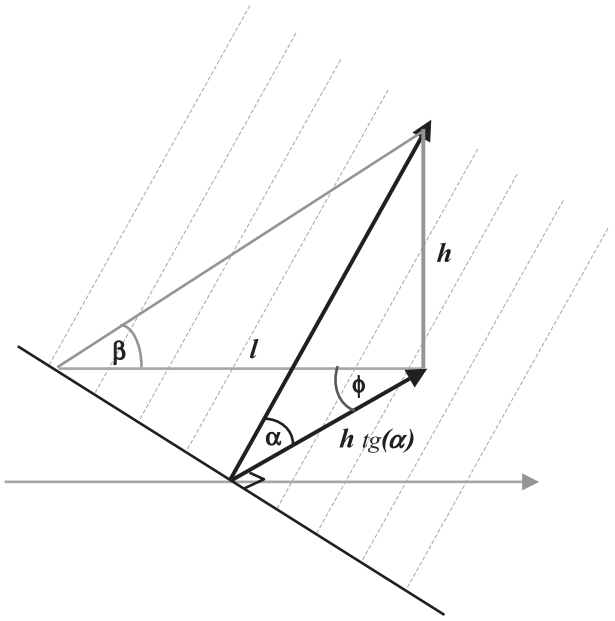


Fig. 4. Extraction of relative elevations ($h$) along a profile line from images of maximum slope ($\alpha$) and aspect. The angle $\phi$ is the difference between the profile line azimuth and the azimuth of the surface. The gray arrow represents the direction of the profile line, the side $l$ of the triangle represents the size of a pixel along the profile line, and the angle $\beta$ stands for the slope along the profile line.

identifying flat areas in the image (e.g., in Fenton & Herkenhoff, 2000), we propose a method that is based on the regularity of dunes' landscapes. The proposed empirical calibration method is based on the availability of a DEM of the same dune type, rotated and stretched so it will have the same characteristics of the area under study (that is: dunes' orientation, height, spacing etc.). The calibration steps are as follows:

- Atmospheric correction is performed for all images.
- The area with less than 5% vegetation cover is extracted using Normalized Difference Vegetation Index (NDVI) (Eastman, 2001) values, as a reference.
- The distribution of reflectance values over the bare area is calculated for each of the images, over selected areas (shown as white rectangles in Fig. 2a and b).
- A DEM with similar dune characteristics is used to calculate cos(i) values for the time of the two images. For this purpose, it is enough to have a detailed DEM for a small test area (established by photogrammetry or laser altimetry) of sand dunes with similar characteristics.
- The distribution of cos(i) values is calculated for the two dates.
- A histogram matching is performed between reflectance values and cos(i) values.

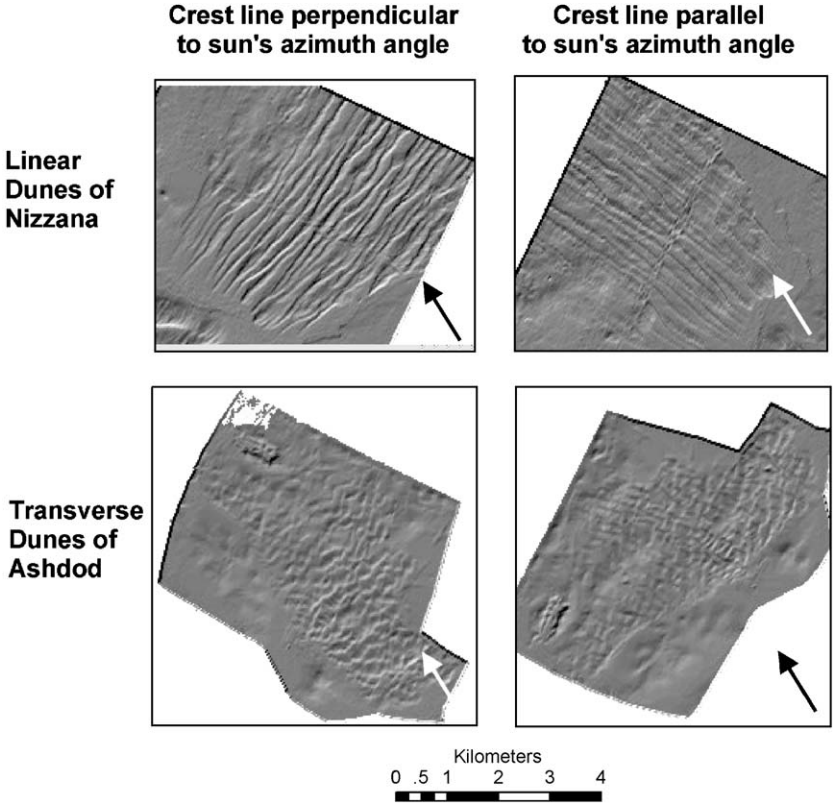


Fig. 5. Influence of the sun's azimuth angle and the dune's orientation on the simulated shading effects (for the month of December), on the linear dunes of Nizzana and the transverse dunes of Ashdod. Cos($i$) values of all four images were linearly stretched between the values of 0.25–0.75. The arrow presents the sun azimuth angle in December 22nd.

The area selected for calibrating the reflectance values to cos($i$) values in the dunes of Ashdod covers 2.25 km$^2$ ( ~ 25% of the area of the dunes analyzed), presented in white in Fig. 2a. This area may be used for the calibration of reflectance to cos($i$) on transverse coastal dunes, typical along many coastal areas worldwide. The area used for the same calibration over the dunes of Nizzana covers an area 1.05 km$^2$ ( ~ 10% of the Egyptian side of the area, or ~ 5% of the total area of the dunes analyzed), and is presented in Fig. 2b. This area may be used for the calibration of reflectance to cos($i$) on linear dunes, typical to many desert areas in the world.

From Fig. 3 (calibration functions of the two Landsat TM images, over the Ashdod dunes) it can be seen that the calibration functions are nonlinear, hence using linear correlation functions to calibrate from reflectance values to cos($i$) is not appropriate (as presumed by Lodwick & Paine, 1985), and empirical calibration functions should be used.

### *3.4. Extraction of elevations from slope and aspect maps along profile lines*

The slope and aspect maps derived by the proposed method present the maximum slope ($\alpha$) and its orientation relative to north. In order to calculate the relative heights along a profile line from those values of slope and aspect, one needs to extract from the maximum slope $\alpha$ in a pixel, the slope $\beta$ in the direction of the profile line. Fig. 4 describes the problem geometrically, and the following equations describe the relations between angles $\alpha$, $\beta$, and $\phi$, mathematically.

$$l = h * \tan\alpha / \cos\phi \tag{3}$$

$$\tan\beta = \tan\alpha / \cos\phi \tag{4}$$

where $l$ = length of pixel along the profile line, $h$ = height difference between adjacent pixels along the profile line,

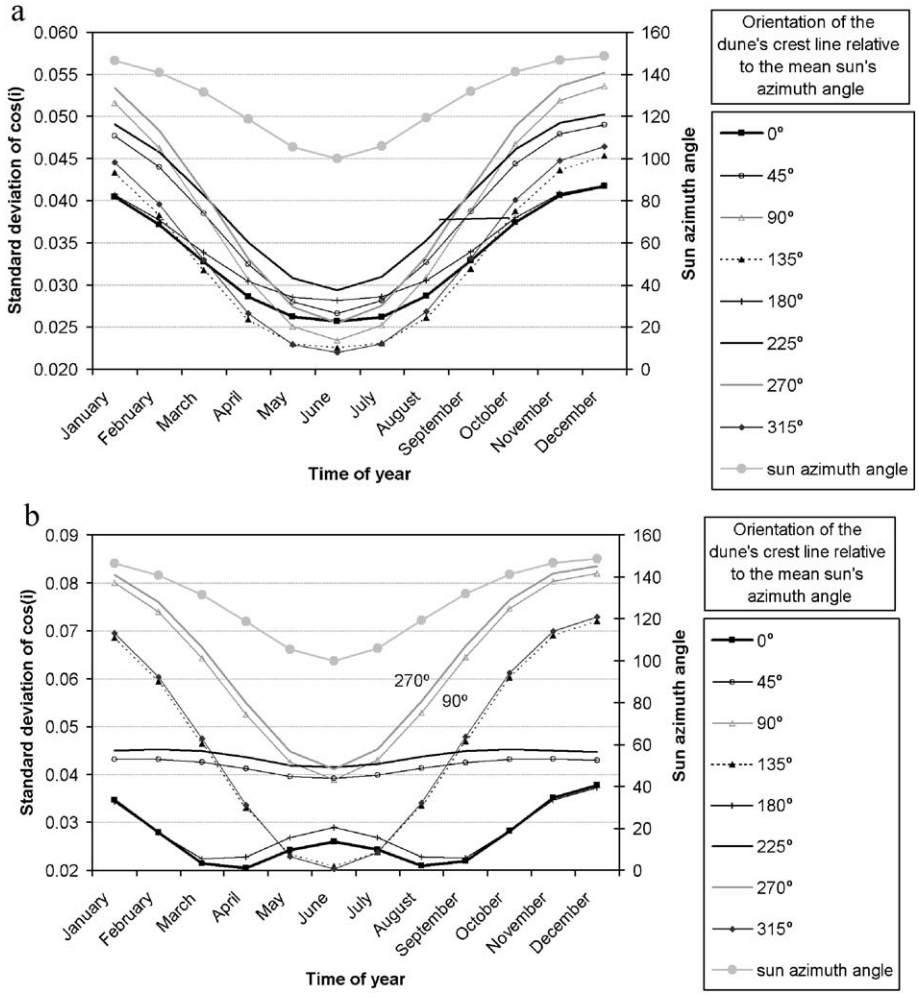


Fig. 6. Standard deviation of cos($i$) values, as a factor of the time of year, and the orientation of the dune's crest line relative to the look direction (sun's azimuth angle). (a) Transverse dunes of Ashdod (dune's crest line azimuth: 135°). (b) Linear dunes of Nizzana (dune's crest line azimuth: 0°).

$\alpha$ = maximum slope angle, $\beta$ = slope in the direction of the profile line, $\phi$ = difference between the aspect angle of the maximum slope and the azimuth of the profile line.

## 4. Results

### *4.1. Simulating topographic effects on dunes in Landsat images*

Shading effects were simulated using detailed DEMs of Ashdod and Nizzana dunes (described previously in Section 2.3) in order to study the influence of two of the factors mentioned above: the time of the year and the dune's orientation. The DEMs were resampled to a spatial resolution of 30 m to match the TM spatial resolution, and rotated by 45° increments, so that eight DEMs were created representing transverse dunes (Ashdod) and linear dunes (Nizzana), with orientations of 0°, 45°, 90°, 135°, 180°, 225°, 270°, and 315°. Shading was simulated on these DEMs by calculating cos(*i*) values for the 22nd of each month (thus representing the winter and summer solstice, and the fall and spring equinox) at the time of day corresponding to the overpass of Landsat TM (10:00 am). All in all, 96 simulated cos(*i*) images (8 orientations × 12 months) were created for each of the dune fields (Fig. 5).

The amount of the simulated shading (estimated by calculating the standard deviation of cos(*i*) values, over the DEM of those sand dunes) is presented in Fig. 6a (for the transverse dunes of Ashdod) and in Fig. 6b (for the linear dunes of Nizzana). As the overall distribution of the aspect (orientation of the surface relative to the north) is more uniform on the transverse dunes of Ashdod (Table 1), the general trend is similar in the different months of the year, with shading effects greater in winter than in

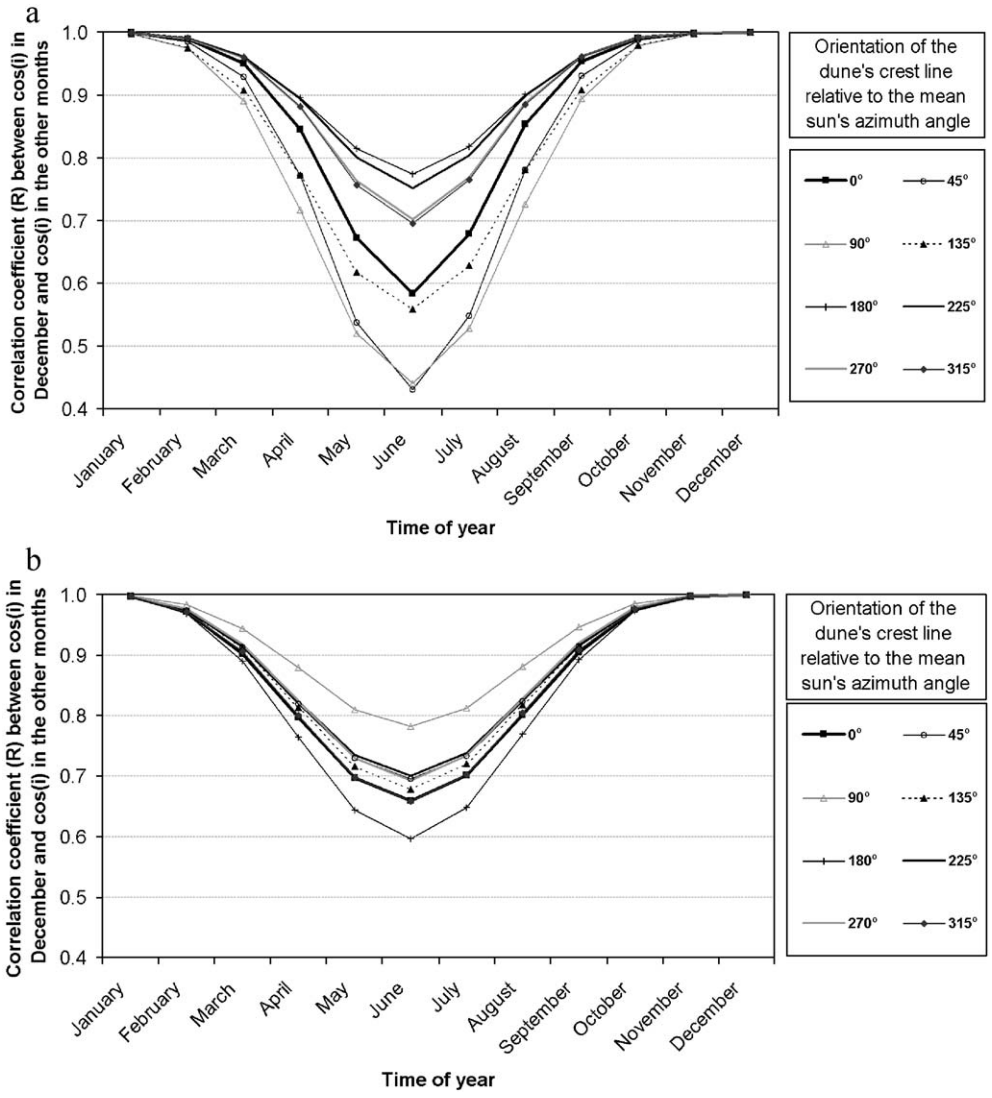


Fig. 7. Correlation coefficient values between cos(*i*) in December, and cos(*i*) in the other months of the year. (a) Transverse dunes of Ashdod (dune's crest line azimuth: 135°). (b) Linear dunes of Nizzana (dune's crest line azimuth: 0°).

summer (Fig. 6a). The favorable orientation of the dune's crest line for achieving maximum shading effects in wintertime is at angles orthogonal (90° and 270°) to the dune's crest line (in contrast to the findings of Blumberg, 1998 that were based on visual interpretation of SAR images).

The spatial pattern of the linear dunes of Nizzana is much more regular, with aspect values distributed less evenly (as seen in Table 1 and in the greater range of values in Fig. 6b relative to Fig. 6a). The general trend of standard deviation of cos(*i*) values for linear dunes (Fig. 6b) exhibits greater differences between the different orientations. The greatest shading effects are expected when the sun's azimuth angle is perpendicular to the dune's crest line orientation (at 90° and 270°), the maximum values achieved at wintertime. However, for some orientations (45° and 225°) there are no differences between the months of the year.

When comparing the shading effects on linear (Nizzana) and transverse (Ashdod) dunes, it appears from Fig. 6a and b that they will be more pronounced on linear dunes (as the standard deviation of cos(*i*) is higher in Fig. 6b). This may be explained by the higher average and standard deviation of the slope (Table 1) in the linear dunes of Nizzana. This is due to the fact that the active slip face of linear dunes shifts (in the case of the Nizzana dunes, between the northern and the southern sides) in the different seasons in response to the alternation between the two main wind directions (Tsoar & Møller, 1986), while in the transverse dunes of Ashdod the aspect of the slip face is stable throughout the year.

Fig. 7a and b present the correlation coefficients between cos(*i*) values in December and cos(*i*) values in the other months of the year. The general pattern emerging is as expected, with minimum correlation occurring between the summer and winter months in both locations. We hypothesize that for the extraction of topographic information from reflectances, the best results will be achieved when using those bands with high correlation to cos(*i*) values, and when combining pairs of images with the least correlation between them. Accordingly, the most recommended months to derive topography will be a combination of a wintertime image (highest correlation with cos(*i*) values) and a summertime image (least correlated with the wintertime image).

### *4.2. Correlation between Landsat bands and simulated shading effects*

#### *4.2.1. Ashdod transverse dunes*

Fig. 8 presents the images of cos(*i*) and band 4 (band 4 was chosen as it is less affected by atmospheric scattering, and because the dynamic range of the sand reflectance is higher in the NIR than in the VIS) of the Landsat 5 TM from August 1985, January 1987, December 1994 and of Landsat 7 ETM+ from August 1999. As observed on the Landsat 5 TM images of 1985, 1987 and 1994, and on the Landsat 7 ETM+ image of January 2000 (not shown) the shading effects clearly reveal the morphology of the dunes. However, on the Landsat 7 ETM+ images of

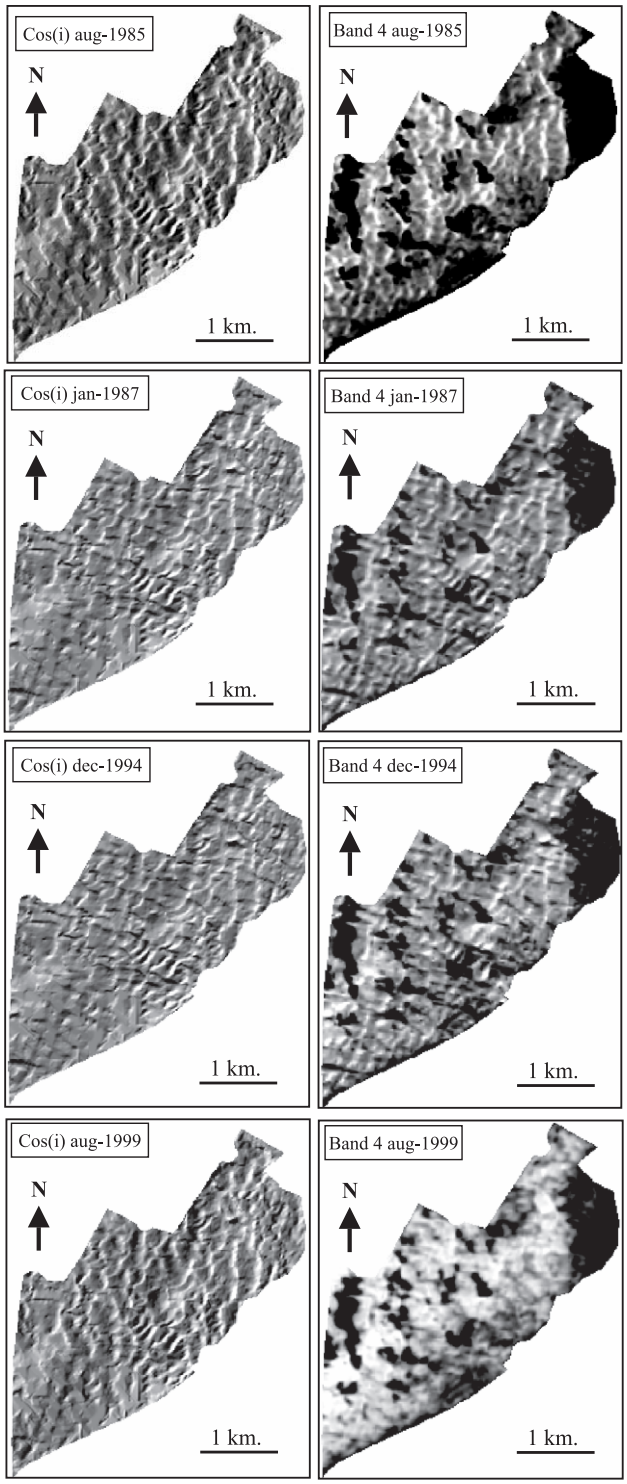


Fig. 8. Comparison of simulated shading (cos(*i*)) and reflectances as measured by Landsat TM/ETM+ band 4, on the transverse dunes of Ashdod. Note the correlation between the pairs of images.

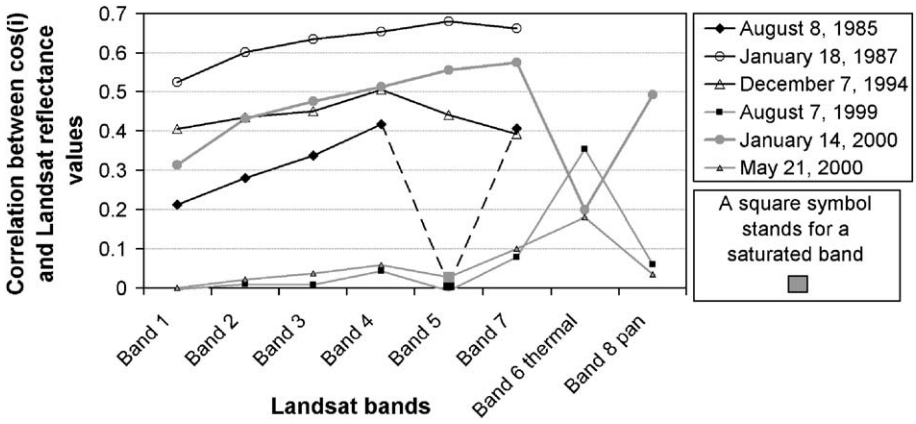


Fig. 9. Correlation coefficients between cos(*i*) values and reflectances on Landsat 5 TM and Landsat 7 ETM+ bands, over the eastern part of the Ashdod dunes. The thermal band of Landsat 5 was not analyzed due to its poor resolution (120 m).

summer 1999 and spring 2000 (not shown) no shading effects were evident.

To examine this observation quantitatively, Fig. 9 presents the correlation coefficients between the calculated cos(*i*) values and the Landsat reflectance values (in the areas with less than 5% vegetation cover—an area containing more than 15,000 pixels) for all the bands over the entire span of years, for the Ashdod dunes.

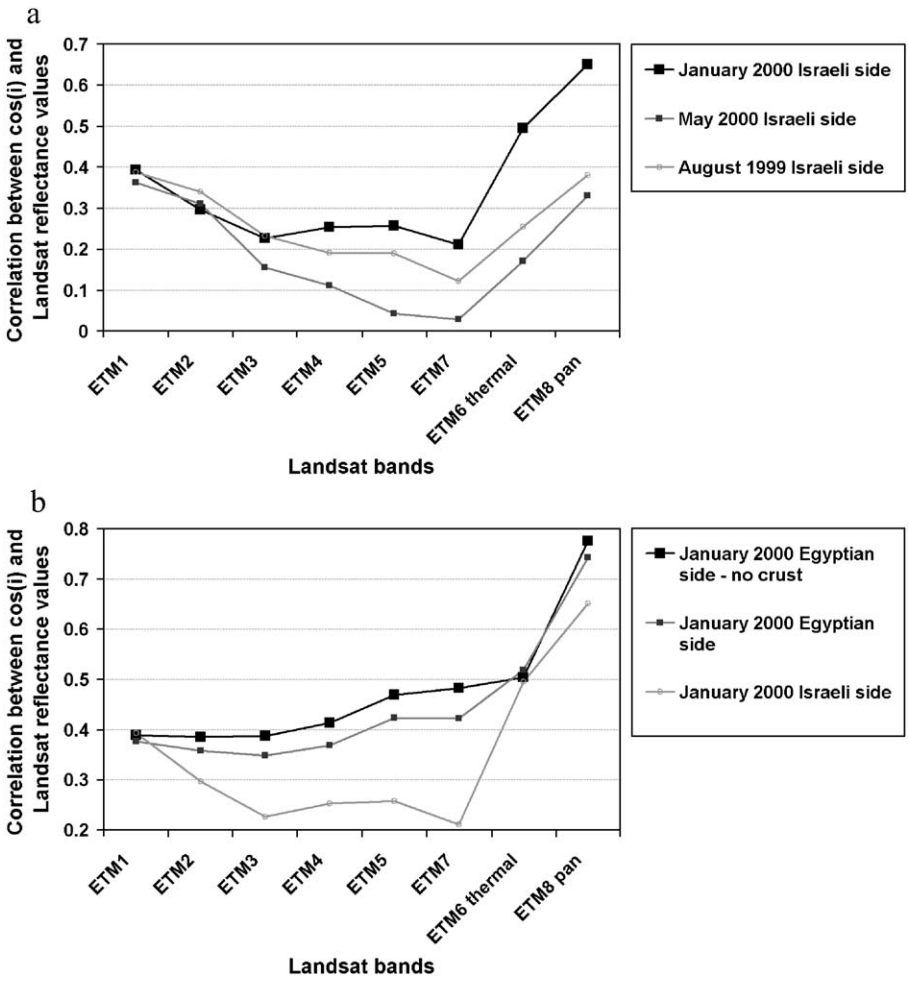


Fig. 10. Correlation coefficients between cos(*i*) values and reflectances on Landsat 7 ETM+ bands, over the Nizzana dunes. (a) Israeli side of the Nizzana dunes, for the months of January, May and August. (b) For the month of January 2000, with the following regions of interest: (1) Israeli side of the border, (2) Egyptian side of the border, (3) Egyptian side of the border with the crusted areas filtered out.

From Fig. 9 several observations can be made:

- Correlation between the shading and the topographic effects is higher in the winter than in the summer, as expected.
- The low correlation between cos(i) and ETM+ band 6 (of January 2000) is probably due to cirrus clouds, barely apparent in the visible bands, but masking the dunes in the thermal band (band 6).
- No correlation was found between cos(i) and reflectance values in the images of August 1999 and May 2000, over the entire range of bands. However, correlation was found on the other Landsat 7 ETM+ image, of January 2000. As the radiometric performance of the ETM+ is supposed to be similar to the TM (Masek et al., 2001), our explanation for the lack of correlation in the images of summer 1999 and spring 2000 is related to the stabilization process of the Israeli coastal dunes that accelerated during the 1990s (Tsoar & Blumberg, 2002). As dunes stabilize, vegetation cover increases and the dune's topography changes, therefore of those Landsat 7 ETM+ images used, only the 2000 winter image (when the sun is lower) was still able to discern the dune's shape.

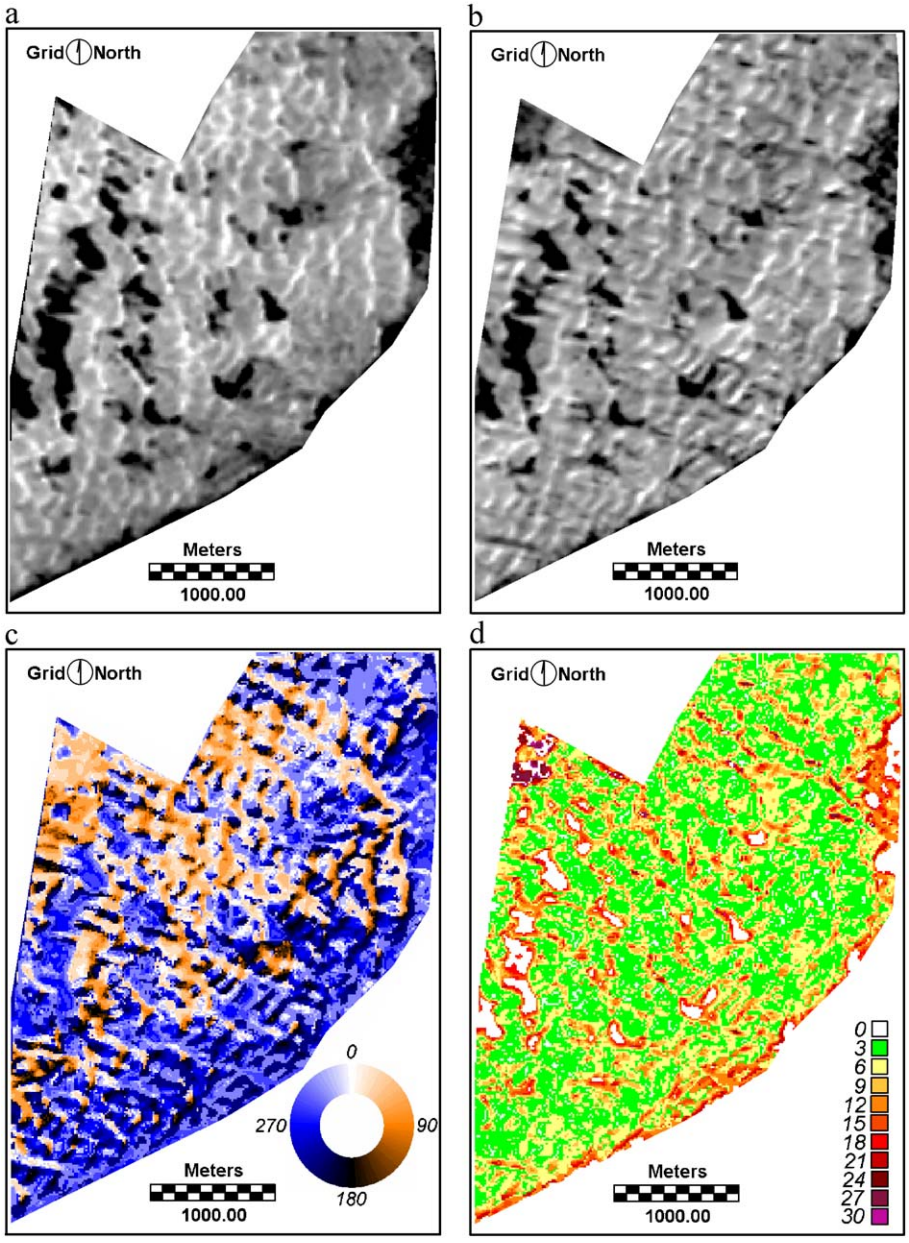


Fig. 11. (a) Landsat 5 TM image band 4, August 1985, Ashdod dunes. (b) Landsat 5 TM image band 4, January 1987, Ashdod dunes. (c) Aspect map derived from the above Landsat images. (d) Slope map derived from the above Landsat images.

*4.2.2. Nizzana linear dunes*

Fig. 10a presents the correlation coefficients between cos(*i*) values and Landsat reflectance values found over the Nizzana dunes. A distinction was made between the Israeli side of the border (where the dunes are stabilized, vegetation cover is higher, and the inter-dune areas and the slopes are covered by biogenic soil crusts, Fig. 1) and the Egyptian side of the border (where the dunes are active). Furthermore, in Fig. 10b we compare the correlation coefficients obtained when the region of interest (on the Egyptian side of the border) included or excluded areas with biogenic soil crust (which is quite sparse in the Egyptian side; these areas were marked out from the analysis using the Crust Index (CI) developed by Karnieli, 1997).

The main observations from Fig. 10a and b are as follows:

- In general, correlation coefficients between cos(i) values and reflectances are higher in wintertime.
- The correlation of the thermal band of the ETM+ is usually higher than that of the optical bands, although its spatial resolution is coarser (60 m vs. 30 m).
- The correlation of the panchromatic band is the highest, probably due to its finer spatial resolution (15 m).

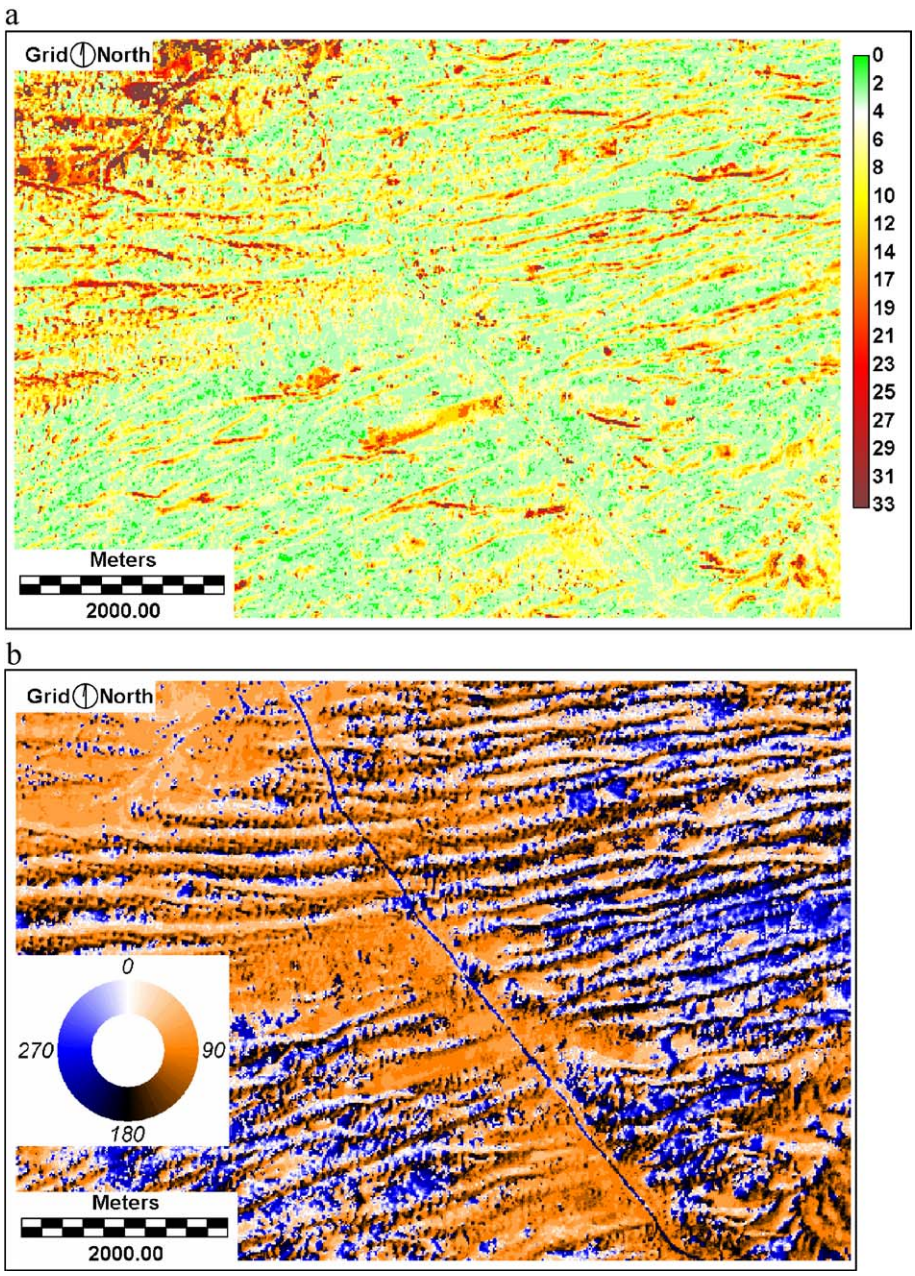


Fig. 12. Slope (a) and aspect (b) maps of the Egyptian side of the Nizzana dunes, derived from Landsat 7 ETM+ panchromatic images of August 1999 and January 2000.

- Correlation coefficients are influenced by the homogeneity of the sand dune's surface. On the Israeli side of the border, where vegetation cover and crust development are greater than on the Egyptian side, correlation coefficient values are lower. On the Egyptian side of the border, correlation coefficients improve when focusing on areas of bare sand and where there is no biogenic soil crust cover.

### *4.3. Topographic information extracted from Landsat images*

The method developed in Section 3 was applied to the Landsat TM images of August 1985 and January 1987, for the eastern part of the Ashdod sand dunes that are relatively bare of vegetation. The two images were rectified to the Israel Transverse Mercator coordinate system using the triangulation method, to a spatial resolution of 15 m. Band 4 of the TM was used for that purpose, for the same reasons given in Section 4.2.1. Landsat 7 ETM+ panchromatic images from 1999–2000 were not used, as explained in Section 4.2.1.

Over the linear dunes of Nizzana, the panchromatic band of Landsat 7 ETM+ was used to derive the slope and aspect images. This band was used as it presented the highest correlation coefficients and has the finest spatial resolution. In addition, three temporal combinations were examined (August 1999–January 2000, August 1999–May 2000, and January 2000–May 2000), in order to examine the stability of the method and the best temporal combination for the extraction of topographic information. Our hypothesis was that the best results would be achieved if a winter and a summer image would be used as a pair based on the two extremes they represent.

The Landsat 5 TM images that were used for the above calculation (for the Ashdod dunes) and their resulting slope and aspect maps are given in Fig. 11. In the northeastern part of the area shown, where vegetation cover is minimal, the structure of transverse dunes is extracted and clearly seen. The extracted DEM includes dunes that are beyond the extent of the available DEM (as during the time when the Landsat images were acquired, these dunes were not built over yet by the development of the city of Ashdod) and beyond the area used for calibrating from reflectance to

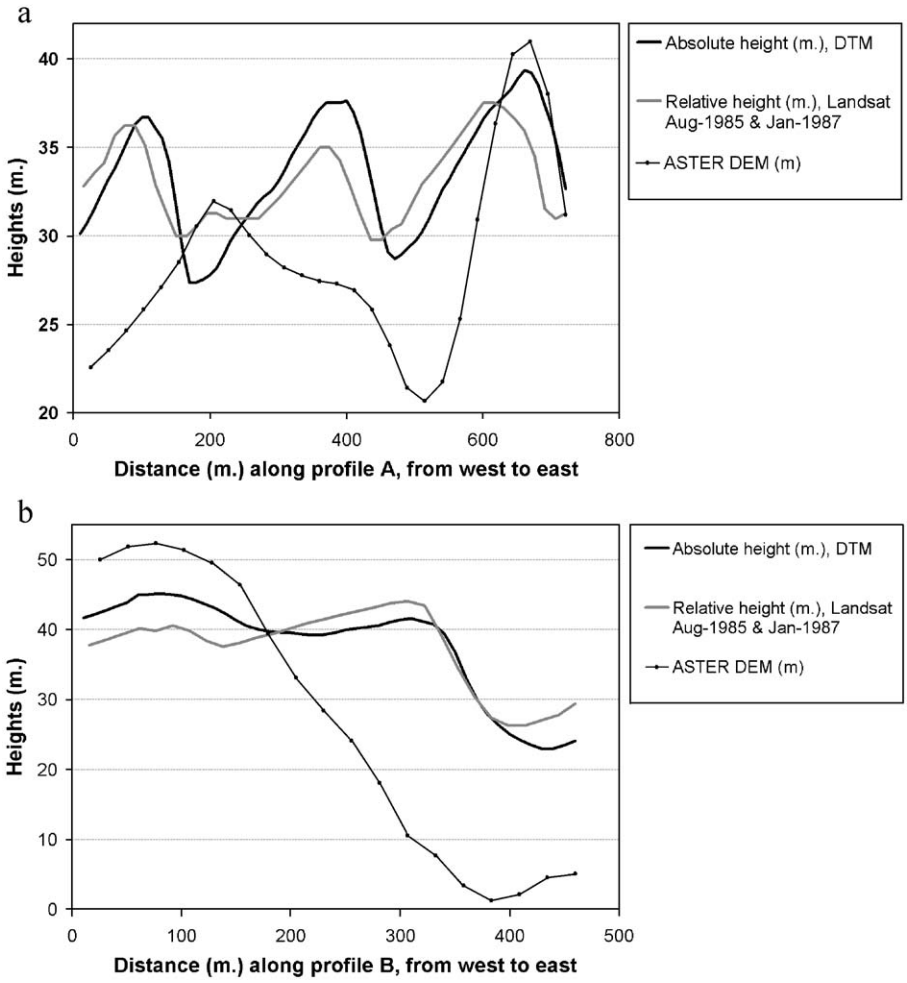


Fig. 13. Transverse dunes of Ashdod. (a) Heights calculated along profile line A. (b) Heights calculated along profile line B.

cos($i$). Slope and aspect maps were calculated also for the linear dunes of Nizzana (Fig. 12).

To examine the reliability of these results, the slope, aspect and height values were measured along two profile lines from west to east along the Ashdod dunes, and from south to north along the Nizzana dunes. The profile lines were aligned normally to the orientation of the dunes' slip faces, in order to achieve the best estimates of the slopes, as was done in similar studies (e.g., Bridges & Herkenhoff, 2002; Fenton & Herkenhoff, 2000). These profile lines and their positions are shown in Fig. 2a and b.

Over each profile, the slope, aspect and height were measured from available detailed DEM information (mentioned in Section 2.3) which was used as a reference, and for the Ashdod dunes also from the ASTER DEM data. Slope and aspect were also extracted along the profile lines from the Landsat images, and relative elevations were calculated from these in the method described in Section 3.4.

Fig 13a and b present the extracted heights along the profile lines of Ashdod (A and B). From these figures, it can be clearly seen that the DEM produced by ASTER is inadequate in mapping dune areas (where the dunes heights are about 10 m). However, the height profiles extracted from the Landsat TM images follow closely those extracted from the detailed DEMs. A quantitative analysis (Table 3) reveals high correspondence between DEM elevations and those extracted from Landsat images: $R = 0.63$ for profile A, $R = 0.88$ for profile B, and that the average absolute differences between height changes along profile lines of both DEMs are only 0.9 m.

In Fig. 14a and b, the extracted heights along the profile lines of Nizzana are presented, calculated from three combinations of Landsat 7 ETM+ images: (1) August 1999–January 2000, (2) August 1999–May 2000, and (3) January 2000–May 2000. Table 3 presents a quantitative analysis of the profiles along the Nizzana dunes; as the elevation errors accumulate along the profile lines, the average absolute difference is much smaller for changes in heights along a profile line, than for the elevations themselves. From Table 3 and from a careful observation of Fig. 14a and b, it is clear that the worst results were obtained using the August 1999–May 2000 combination (lowest $R$ values), and the best results using the August 1999–January 2000 combination (highest $R$ values and lowest differences of elevation). Based on these results, our previous hypothesis that using a combination of a winter image with a summer image was confirmed. The average absolute errors of the slope (Table 3) were about 3° (for the combinations of winter and summer images), which is similar to the slope intervals defined in our lookup table for calculating slope values from reflectances (Section 3.3.1). These errors can be reduced by applying smaller intervals than those used by us for identifying the slope and aspect.

One of the causes for errors in our method, evident in the Nizzana dunes, was due to the heterogeneity of the surface. Shortly after the first effective rainfall, a peak in the photosynthetic activity of the biogenic soil crust takes place, more or less around January (Schmidt & Karnieli, 2002). During the winter of 2000, only 4.8 mm of rain accumulated until January 14th (the date of one of the images used). However, apparently even this meager amount of rainfall was sufficient for the influence of the crust on topographic information extraction from Landsat images of August 1999 and January 2000 to be seen in Fig. 15. On the right hand side of the figure, it can be seen that the heights extracted from the Landsat images deviate from those of the detailed DEM. In this same place (around the distance of 800 m), the values of the crust index increase, and as the homogeneity of the surface is damaged, the elevations extracted become less reliable.

Table 3
Accuracy of elevations and slopes extracted from Landsat 7 ETM+ images over the dunes of Nizzana along profile lines 1 and 2, and from Landsat 5 TM images over the dunes of Ashdod along profile lines A and B, compared with the data extracted from detailed DEM

| Study area | | Nizzana | | | | | | Ashdod | |
|---|---|---|---|---|---|---|---|---|---|
| Sensor used | | Landsat 7 ETM+ panchromatic band (15 m resolution) | | | | | | Landsat 5 TM band 4 (30 m resolution) | |
| Length of profile lines | | Line 1: 1560 m, Line 2: 830 m | | | | | | Line A: 720 m, line B: 460 m | |
| Landsat images used | | Aug 1999 and Jan 2000 | | Jan 2000 and May 2000 | | Aug 1999 and May 2000 | | August 1985 and January 1987 | |
| Profile line | | 1 | 2 | 1 | 2 | 1 | 2 | A | B |
| Comparison with DEM elevations | $R$ | 0.86 | 0.74 | 0.81 | 0.77 | 0.14 | 0.35 | 0.63 | 0.88 |
| | Average absolute difference | 4.7 | 4.6 | 8.2 | 4.6 | 8.8 | 13.3 | 2.2 | 3.1 |
| Comparison with changes in DEM elevations along profile lines | $R$ | 0.67 | 0.76 | 0.63 | 0.75 | 0.00 | 0.00 | 0.44 | 0.74 |
| | Average absolute difference | 1.1 | 1.0 | 1.2 | 1.1 | 2.5 | 2.8 | 0.9 | 0.9 |
| Comparison with DEM slopes (along profile line) | $R$ | 0.59 | 0.48 | 0.46 | 0.46 | 0.00 | 0.14 | 0.45 | 0.73 |
| | Average absolute difference | 2.9 | 3.3 | 3.6 | 1.3 | 5.9 | 7.6 | 3.6 | 3.4 |

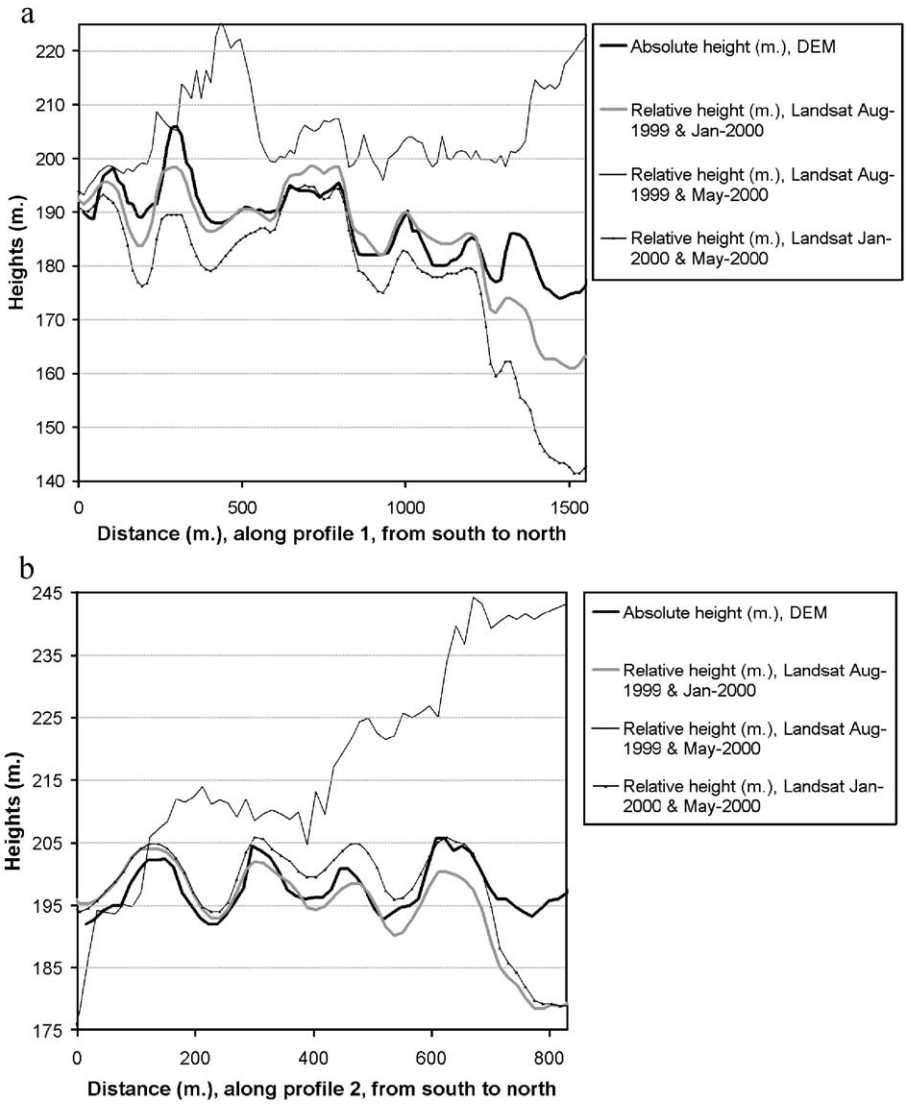


Fig. 14. Linear dunes of Nizzana. (a) Heights calculated along profile line 1. (b) Heights calculated along profile line 2.

### 4.4. Discussion

The study of sand dune areas is challenging, as not only does the land cover (vegetation, biogenic soil crusts, human uses) vary in space and time, the topographic features of the landscape may change over short time spans of several years or even months! Measuring these dynamics is essential to the understanding of these areas.

The method proposed in this study treats what is usually considered as unwanted additional variability in satellite images (the topographic effects) as a signal, and estimates the slope and aspect of the dune terrain, using two Landsat images taken at different times of the year. The photometric stereo method developed here requires, in addition to a pair of satellite images taken at different sun angles, knowledge of the dune type studied and a sample DEM of such a dune. In general, it is possible to create such information as a library for further utilization. Calibration of reflectances to $\cos(i)$ values is then possible to extract slope and aspect parameters of each pixel, by searching the best fit between $\cos(i)$ observed values and those resulting from all possible combinations of slope and aspect angles. With a spatial resolution 10 times higher (15 m in ETM+ band 8, and 30 m in the other optic bands) than that of the dune's spacing (150–300 m), subtle topographic features of sand dunes could be extracted, reaching an average accuracy of 3° in the estimation of slopes. Calculated relative elevations along selected profile lines, yielded highly accurate results, to the order of 1 m (for pixels the size of 15 m) that is 1/10 of the average dune height. These accuracies were obtained in two areas of sand dunes, each having different characteristics: one of transverse coastal dunes, and the other of linear desert dunes. This method can thus be substituted for ASTER DEM in areas of sand dunes, where the ASTER accuracy (between $\pm 7$ and

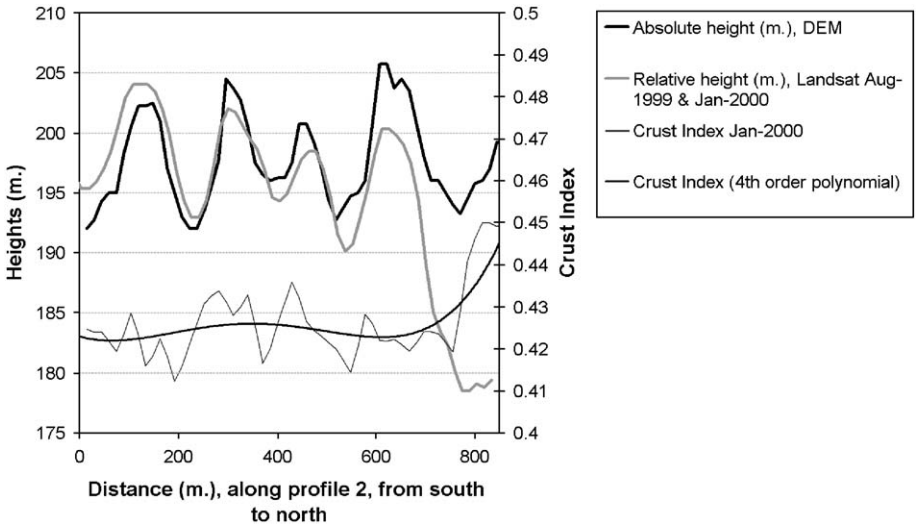


Fig. 15. Linear dunes of Nizzana: heights and crust index values calculated along profile line 2.

± 15 m) is not satisfactory. Best results were obtained for a combination of a winter and a summer image, offering maximum difference of sun position with respect to the surface. In addition, orientation of the dunes at an angle normal to the sun azimuth enhances shading effects, and is thus favorable for the success of shape from shading algorithms.

In spite of the good results that were obtained by the proposed method and its ease of use, we can identify several limitations, as follows:

(a) The method can be applied only to homogenous surfaces (i.e., dunes, snow, glaciers), where differences in the reflectance are the result of shading effects (i.e., no vegetation, crust or rocks are present).
(b) In order to calculate slope and aspect images from satellite images, over large areas, BRDF effects should be dealt with prior to the processing of the images.
(c) Dune sand is a high albedo target, and in spite of the dynamic range improvements of Landsat-7 ETM+ over Landsat-5 TM, images may still suffer from saturation problems. As Karnieli et al. (2002) noted, Landsat 7 images taken over light targets in Israel suffered occasionally from saturation (especially band 3), prior to the correction of the gain modes in July 2001.
(d) One of the major limitations of applying the proposed method is in the need to have some DEM information for the proper sand dune type in question, to calibrate reflectances into cos(i) values. In this regard, Breed and Grow (1979) used satellite images of uniform 1:1,000,000 scale and worldwide coverage as a base for quantitative and qualitative studies of large-scale eolian landforms. They were able to discriminate (visually) between the following dune types: linear, crescentic, star, parabolic and dome-shaped. They have also measured the dunes' length, width (or diameter) and wavelength (spacing). Among their findings is that "patterns made by dunes of the same type are similar, despite their occurrence in widely distant sand seas, because the relationships of mean length, width (or diameter), and wavelength are similar among dunes of each type, regardless of differences in size, form, or geographic location".

Based on the findings of Breed and Grow (1979), we suggest creating a DEM library (lookup table) for dunes. In this library, there will be a collection of high-resolution DEMs for the different dune types-barchan, parabolic, transverse, linear, star, and so on. For each dune type, several parameters will be recorded, such as the dune's mean length, width, spacing, orientation, and height. To apply these sample DEMs in order to predict the expected shading on a given sand dune's area, the DEM will be chosen according to the dune type and then rotated and stretched to fit the actual orientation and spacing (that can be visually estimated). These steps will enable the calibration of reflectance values to cos($i$) and the calculation of sand dune characteristics for sand dunes all over the world with minor efforts, based on a few high-resolution measurements, using the proposed method.

Photometric stereo methods for the extraction of topographic information have several important advantages, for example: (1) DEM with a high spatial resolution (the spatial resolution of the sensor); (2) the extraction of topographic information from satellite images acquired by early Landsat MSS and TM missions. So far, optical satellite images were used to gain information regarding the spatial extent of sand dunes, their vegetation cover and mineralogical composition. The method developed offers new opportunities for studies of eolian geomorphology, adding the ability to analyze dynamic aspects of sand dunes topography in time and space.

## Acknowledgements

We wish to thank the following people and institutions for their help: the GIS units of the Society for the Protection of Nature in Israel and the Jewish National Fund, for the use of spatial databases available for the area. We also thank the Hebrew University of Jerusalem Minerva Arid Ecosystem Research Center for providing us with the Nizzana rainfall data, and Dr. Dan G. Blumberg from the Department of Geography and Environmental Development, Ben Gurion University of the Negev, for providing us the Landsat TM image of January 1987. In addition, we thank the anonymous reviewers for their helpful comments and contribution to the manuscript. This work was done as part of a PhD thesis, in the Department of Geography and Human Environment, at Tel Aviv University.

## References

Abreu, L. W., & Anderson, G. P. (1996). *The MODTRAN 2/3 Report and LOWTRAN 7 MODEL*. North Andover, MA, USA: Ontar Corporation.

Andrews, B. D., Gares, P. A., & Colby, J. D. (2002). Techniques for GIS modeling of coastal dunes. *Geomorphology*, *48*, 289–308.

Bagnold, R. A. (1954). *The physics of blown sand and desert dunes*. London: Chapman & Hall, first published in 1941, 265 pp.

Ben-Dor, E., Irons, J. R., & Epema, G. (1999). Soil reflectance. In A. N. Rencz (Ed.), *Remote Sensing for the Earth Sciences—Manual of Remote Sensing, vol. 3* (pp. 111–188). New York: John Wiley & Sons.

Blumberg, D. G. (1998). Remote sensing of desert dune forms by polarimetric synthetic aperture radar (SAR). *Remote Sensing of Environment*, *65*(2), 204–216.

Breed, C. S., & Grow, T. (1979). Morphology and distribution of dunes in sand seas observed by remote sensing. In E. D. Mckee (Ed.), *A study of global sand seas. Geological Survey Professional Paper, vol. 1052* (pp. 253–302). Washington: United States Geological Survey.

Bridges, N. T., & Herkenhoff, K. E. (2002). Topography and geologic characteristics of aeolian grooves in the south polar layered deposits of Mars. *Icarus*, *156*, 387–398.

Carter, J. R. (1988). Digital representations of topographic surfaces. *Photogrammetric Engineering and Remote Sensing*, *54*(11), 1577–1580.

Cheng, F., & Thiel, K. -H. (1995). Delimiting the building heights in a city from the shadow in a panchromatic SPOT-image: Part 1. Test of forty-two buildings. *International Journal of Remote Sensing*, *16*(3), 409–415.

Cierniewski, J., & Karnieli, A. (2002). Virtual surfaces simulating the bidirectional reflectance of semi-arid soils. *International Journal of Remote Sensing*, *23*(19), 4019–4038.

Cooke, R. U., Warren, A., & Goudie, A. S. (1993). *Desert geomorphology*. London: UCL Press.

Cox, C., & Munk, W. (1954). Measurement of the roughness of the sea surface from photographs of the sun's glitter. *Journal of the Optical Society of America*, *44*(11), 838–850.

Dubayah, R., & Rich, P. M. (1995). Topographic solar radiation models for GIS. *International Journal of Geographical Information Systems*, *9*(4), 405–419.

Eastman, J. R. (2001). Idrisi 32 release 2. *Guide to GIS and Image Processing*, *vol. 2*. USA: Clark University, 144 pp.

Ekstrand, S. (1996). Landsat TM-based forest damage assessment: Correction for topographic effects. *Photogrammetric Engineering and Remote Sensing*, *62*(2), 151–161.

Fenton, L. K., & Herkenhoff, K. E. (2000). Topography and stratigraphy of the northern Martian polar layered deposits using photoclinometry, stereogrammetry, and MOLA altimetry. *Icarus*, *147*, 433–443.

Gao, B. C., Heidebrecht, K. B., & Goetz, A. F. H. (1993). Derivation of scaled surface reflectances from AVIRIS data. *Remote Sensing of Environment*, *44*, 145–163.

Gay Jr., S. P. (1999). Observations regarding the movement of barchan sand dunes in the Nazca to Tanaca area of southern Peru. *Geomorphology*, *27*, 279–293.

Gerbermann, A. H., & Neher, D. D. (1979). Reflectance of varying mixtures of a clay soil and sand. *Photogrammetric Engineering and Remote Sensing*, *45*(8), 1145–1151.

Hall, J. K., Weinberger, R., Marco, S., & Steinitz, G. (1999). Test of the accuracy of the DEM of Israel, Report TR-GSI/1/99, Ministry of National Infrastructures, Jerusalem. *Geological Survey of Israel.*

Hartl, Ph., & Cheng, F. (1995). Delimiting the building heights in a city from the shadow on a panchromatic SPOT-image: Part 2. Test of a complete city. *International Journal of Remote Sensing*, *16*(15), 2829–2842.

Hirano, A., Welch, R., & Lang, H. (2003). Mapping from ASTER stereo image data: DEM validation and accuracy assessment. *ISPRS Journal of Photogrammetry and Remote Sensing*, *57*, 356–370.

Howard, A. D., Blasius, K. R., & Cutts, J. A. (1982). Photoclinometric determination of the topography of the Martian north polar cap. *Icarus*, *50*, 245–258.

Ichoku, C., Karnieli, A., Meiseles, A., & Chorowicz, J. (1996). Detection of channel networks on conventional digital satellite images. *International Journal of Remote Sensing*, *8*, 1659–1678.

Jimenez, J. A., Maia, L. P., Serra, J., & Morais, J. (1999). Aeolian dune migration along the Ceara coast, north-eastern Brazil. *Sedimentology*, *46*, 689–701.

Kadmon, R., & Leschner, H. (1995). Ecology of linear dunes: Effect of surface stability on the distribution and abundance of annual plants. *Advances in GeoEcology*, *28*, 125–143.

Karnieli, A. (1997). Development and implementation of spectral crust index over dune sands. *International Journal of Remote Sensing*, *18*(6), 1207–1220.

Karnieli, A., Ben-Dor, E., Yunden, B., & Lugassi, R. (2002). *Radiometric saturation of Landsat-7 ETM+ data over the Negev desert, Israel: Problems and solutions*. 1st International Symposium on Recent Advances in Quantitative Remote Sensing, 16–20 Sept., 2002, Valencia, Spain.

Karnieli, A., Kidron, G. J., Glaesser, C., & Ben-Dor, E. (1999). Spectral characteristics of Cyanobacteria soil crust in semiarid environments. *Remote Sensing of Environment*, *69*, 67–75.

Levin, N., & Ben-Dor, E. (2003). Monitoring sand dune stabilization along the coastal dunes of Ashdod-Nizanim, Israel, 1945–1999. *Journal of Arid Environments* (In Press, Corrected Proof, Available online 14 October 2003).

Lodwik, G. D., & Paine, S. H. (1985). A digital elevation model of the Barnes ice-cap derived from Landsat MSS data. *Photogrammetric Engineering and Remote Sensing*, *51*(12), 1937–1944.

Masek, J. G., Honzak, M., Goward, S. N., Liu, P., & Pak, E. (2001). Landsat-7 ETM+ as an observatory for land cover: Initial radiometric and geometric comparisons with Landsat-5 Thematic Mapper. *Remote Sensing of Environment*, *78*, 118–130.

Melsheimer, C., & Kwoh, L. K. (2001). *Sun glitter in Spot images and the visibility of oceanic phenomena*. 22nd Asian Conference on Remote Sensing, 5–9 November 2001, Singapore.

Mugnier, C. J. (2000). Grids and Datums: The State of Israel. *Photogrammetric Engineering and Remote Sensing*, *66*(8), 915–917.

Pellikka, P., King, D. J., & Leblanc, S. G. (2000). Quantification and reduction of bi-directional effects in aerial CIR imagery of deciduous forest using two reference land surfaces types. *Remote Sensing Reviews*, *19*, 259–291.

Pye, K., & Tsoar, H. (1990). *Aeolian sand and sand dunes*. London: Unwin Hyman.

Qong, M. (2000). Sand dune attributes estimated from SAR images. *Remote Sensing of Environment*, *74*, 217–228.

Rabus, B., Eineder, M., Roth, A., & Bamker, R. (2003). The shuttle radar topography mission—a new class of digital models acquired by spaceborne radar. *ISPRS Journal of Photogrammetry and Remote Sensing*, *57*, 241–262.

Rango, A., Chopping, M., Ritchie, J., Havstad, K., Kustas, W., & Schmugge, T. (2000). Morphological characteristics of shrub coppice dunes in desert grasslands of Southern New Mexico derived from scanning LIDAR. *Remote Sensing of Environment*, *74*, 26–44.

Research Systems (2001). *ENVI version 3.4, 4990 Pearl East Circle, Boulder, CO 80301*. USA: The Environment for Visualizing Images.

Romanova, M. A. (1964). *Air survey of sand deposits by spectral luminance, authorized translation from the Russian, Consultants Bureau, New York*. New York, NY: Consultants Bureau (158 pp.).

Sarnthein, M. (1978). Sand deserts during glacial maximum and climatic optimum. *Nature*, *272*, 43–46.

Schmidt, H., & Karnieli, A. (2002). Analysis of the temporal and spatial vegetation patterns in a semi-arid environment observed by NOAA AVHRR imagery and spectral ground measurements. *International Journal of Remote Sensing*, *23*(19), 3971–3990.

Shaw, J. A., & Churnside, J. H. (1997). Scanning-laser glint measurements of sea-surface slope statistics. *Applied Optics*, *36*(18), 4202–4213.

Shepherd, J. D., & Dymond, J. R. (2002). Correcting satellite imagery for the variance of reflectance and illumination with topography. *International Journal of Remote Sensing*, 1–12 (preview article).

Smith, J. A., Lin, T. L., & Ranson, K. J. (1980). The Lambertian assumption and Landsat data. *Photogrammetric Engineering and Remote Sensing*, *46*(9), 1183–1189.

Teillet, P. M., Barker, J. L., Markham, B. L., Irish, R. R., Fedosejevs, G., & Storey, J. C. (2001). Radiometric cross-calibration of the Landsat-7 ETM+ and Landsat-5 TM sensors based on tandem data sets. *Remote Sensing of Environment*, *78*, 39–54.

Toutin, Th. (2001). Elevation modeling from satellite visible and infrared (VIR) data. *International Journal of Remote Sensing*, *22*(6), 1097–1125.

Tsoar, H. (2001). Types of Aeolian sand dunes and their formation. In N. J. Balmforth, & A. Provenzale (Eds.), *Lecture Notes in Physics*, *vol. 582* (pp. 403–429). Berlin: Springer.

Tsoar, H., & Blumberg, D. G. (2002). Formation of parabolic dunes from barchan and transverse dunes along Israel's Mediterranean coast. *Earth Surface Processes and Landforms*, *27*, 1147–1161.

Tsoar, H., & Møller, T. (1986). The role of vegetation in the formation of linear sand dunes. In W. G. Nickling (Ed.), *Aeolian geomorphology.* Boston: Allen & Unwinn (pp. 75–95).

Tsoar, H. T., & Illenberger, W. K. (1998). Reevaluation of sand dunes' mobility indices. *Journal of Arid Land Studies*, *7S*, 265–268.

Wasson, R. J., & Hyde, R. (1983). Factors determining desert dune type. *Nature*, *304*, 337–339.

Welch, R., Jordan, T., Lang, H., & Murakami, H. (1998). ASTER as a source for topographic data in the late 1990's. *IEEE Transactions on Geoscience and Remote Sensing*, *36*(4), 1282–1289.

White, K., Walden, J., Drake, N., Eckardt, F., & Settle, J. (1997). Mapping the iron oxide content of dune sands, Namib sand sea, Namibia, using Landsat Thematic Mapper data. *Remote Sensing of Environment*, *62*, 30–39.

Wildey, R. L. (1975). Generalized photoclinometry for Mariner 9. *Icarus*, *25*, 613–626.

Zhang, R., Tsai, P. S., Cryer, J. E., & Shah, M. (1999). Shape from shading: A survey. *IEEE Transactions on Pattern Analysis and Machine Intelligence*, *21*(8), 690–706.

Zhu, H., Eastman, J. R., & Toledano, J. (2001). Triangulated irregular network optimization from contour data using bridge and tunnel edge removal. *International Journal of Geographical Information Science*, *15*(3), 271–286.

*In the second article*, a method to characterize the colour of soil samples is presented, and related chemical and physical properties of the soil (content of iron oxides and of fine particles), using a digital camera, instead of subjective munsell charts or expensive field spectrometers. These variables, may serve as indicators of the stabilization process, as will be discussed in chapter 8 of this thesis.

*International Journal of Remote Sensing*
Vol. 26, No. 24, 20 December 2005, 5475–5492

Taylor & Francis
Taylor & Francis Group

# A digital camera as a tool to measure colour indices and related properties of sandy soils in semi-arid environments

N. LEVIN*†, E. BEN-DOR† and A. SINGER‡
†Department of Geography and Human Environment, Tel Aviv University, Israel
‡Seagram Center for Soil and Water Sciences, Hebrew University of Jerusalem, Rehovot, Israel

(*Received 6 January 2004; in final form 17 January 2005*)

Soil colour carries important information regarding the soil's chemical and physical properties. However, common practices for measuring soil colour, either by Munsell charts or by field/laboratory spectrometers, are insufficient, due to the subjective and nonquantitative character of the Munsell charts, and to the high cost and inconvenience of field spectrometers. We present herein, a method to characterize the colour of soil samples, and related chemical and physical properties of the soil, using a digital camera, and an array of coloured plastic chips, that are used for calibration purposes. Using 370 samples of sandy soils, we have demonstrated that both RGB values from digital images and their derived soil indices, correlate highly with similar measurements performed by a field spectrometer. When checked against free iron oxide content and against the percentage of fine particles in a sub-sample set of 42 soils, the redness index as measured by the digital camera gave similar or better correlations than those obtained from a field spectrometer, against both free iron oxides and fine particle contents ($R^2$ of 89% for the iron oxides, and of 81% for the fine particles). We propose the use of a digital camera as a field analytical tool to determine precisely: soil colour, iron oxide and fine particle content. Further study in this direction, with other soil population and more soil properties, is strongly advised in order to launch this as a vastly applicable and generic method.

## 1. Introduction

The spectral characteristics of the soil are determined by the chemical and physical soil-related properties (Ben-Dor 2002). Thus various scanning and sensing technologies were developed as proximal sensors for a range of soil properties which have important agronomic implications for precision agriculture (Viscarra Rossel and McBratney 1998, Adamchuk *et al.* 2004). While many of these properties can be detected only in the near-infrared–short-wave infrared (NIR–SWIR) regions of the spectrum, soil colour in the human visible range (0.4–0.7 μm) is related to the presence of pigments or chromophores that absorb or scatter radiation in different wavelengths and intensities. Organic matter, water molecules, iron oxides, carbonates and chemical composition of transition metals in clay minerals are the major chemical components affecting soil colour; while grain size, as a physical chromophore, also plays an important role in affecting this colour (Ben-Dor *et al.* 1998). Traditionally, Munsell soil colour charts are used to describe

*Corresponding author. Email: levinnoa@post.tau.ac.il

*International Journal of Remote Sensing*
ISSN 0143-1161 print/ISSN 1366-5901 online 
http://www.tandf.co.uk/journals
DOI: 10.1080/01431160500099444

soil colour visually, by assigning hue, value and chroma. This method, however, suffers from several drawbacks: (1) it oversimplifies colour identification due to its use of a limited number of colour chips; (2) unlike reflectance it is not a continuous quantitative physical variable; and (3) it may be influenced by variables independent of soil sample properties, such as operator's fatigue, illumination conditions, etc. (Mathieu *et al*. 1998).

Spectrometers and chroma meters permit more physically based characterization of soil colour, and are becoming an alternative tool to Munsell charts (Torrent *et al*. 1983, Mathieu *et al*. 1998, Konen *et al*. 2003). However, these are quite expensive and are inconvenient for field operation, and thus, are not available for many people in general, and for colour measurement in particular. A low-cost alternative is to use digital cameras for imaging and measuring colours. The development of solid-state charge coupled device (CCD) sensors had already begun in the late 1970s and early 1980s (King 1995). Digital cameras have several advantages over 35 mm photography, as they avoid inconsistencies in film development and errors introduced during scanning (Dean *et al*. 2000), and provide greater sensitivity than standard film (King 1995). Low cost digital cameras may also have advantages over narrow band imaging for most remote sensing applications, as they decrease the needs for precise calibration and accurate modelling of the physical characteristics of the scene (atmosphere, Bidirectional Reflectance Distribution Function (BRDF), etc; King 1995). Digital cameras have been used scientifically in many applications to date, e.g. to measure the colour of food surfaces (Yam and Papadakis 2004); to identify damage in maize plants (Sena *et al*. 2003); to locate characters in scene images (Wang and Kangas 2003); to automatically monitor snow cover in Antarctica (Hinkler *et al*. 2002); and various others as reviewed by King (1995). Several studies have demonstrated the benefits of using close range imaging systems to study soil sample attributes: 35 mm photography was used to map the soil surface in three dimensions (Warner 1995), or to analyse soil pore structure (Robertson and Campbell 1997); while Adderley *et al*. (2002) used an Olympus polarizing microscope and a three chip video camera to measure the colour of soil thin-sections. Using a digital camera in the laboratory and under 'ideal' lighting conditions, Viscarra Rossel and Walter (2002) were able to predict the content of soil organic carbon (SOC) for soil samples collected in Brittany, France; they found better correlations when the samples were moistened, and concluded that colour measurements using either RGB image-intensity values or Commission Internationale de l'Eclairage (CIE) L*a*b*/CIE Luv colour coordinates show good responses to SOC (with a higher content of SOC darkening the soil). In a follow-up study they found that predictions of SOC using simple colour models from a digital camera were comparable, or even better, than those obtained from a partial least-squares regression, implemented on spectral reflectance data measured by a FieldSpec Pro visible and NIR spectrometer (Viscarra-Rossel *et al*. 2003).

It should be noted, however, that using spectrometers, unique absorption features of minerals can be quantified; using a digital camera, however, only three bands are available—red, green and blue (these can be transformed into other colour coordinates, such as the CIE L*a*b*)—from which spectral indices can be derived.

Digital cameras therefore offer a new and simple opportunity to characterize soil samples. As with standard remote sensing applications, care should be taken when analysing images photographed with digital cameras. To avoid inconsistencies due to the light source, a controlled source of artificial illumination is commonly used to

light the target of interest (Sena *et al*. 2003, Yam and Papadakis 2004). For accurate calibration, the quantum efficiency curves of the CCD and the lens transmission spectra should also be known (Dean *et al*. 2000). However, these are often not supplied by the digital cameras' manufacturers, as they are regarded as an industrial secret. In many studies standard colour chips (Yam and Papadakis 2004), painted wooden panels (King 1995, Dean *et al*. 2000), or just a standard white reference (Webster and Mollon 1997), were imaged within the scene ('in-flight calibration') to enable calibration of the RGB values. Calibration is needed due to differences in the illumination conditions, and to contrasts within the image scenes themselves. Other artefacts that are encountered when using CCD arrays on digital cameras include: a brightness fall-off towards the corners of the image, partly due to obliquity in the view away from the nadir axis, and partly due to vignette effects from the lenses (Dean *et al*. 2000); adjacency effects that smooth the boundaries between objects; and BRDF effects (King 1995). To the best of our knowledge, other than the works on soil organic carbon by Viscarra Rossel and Walter (2002) and Viscarra Rossel *et al*. (2003), there has been no work to date that showed the ability of a simple digital camera, to serve as a practical tool for characterizing soil properties such as free iron oxides and measuring amounts of fine particles.

The percentage of free iron oxides in sand dunes and in sandy soils may represent their stage in the rubification process (Norris 1969, Walker 1979). The rubification is defined as a pedogenesis stage in which iron is released from primary minerals to form free iron oxides that coat quartz particles in soils with a thin reddish film (Buol *et al*. 1973). The free iron oxides coat the quartz particles and provide a reddish chroma to the matrix as well as stability (Ben-Dor and Singer 1987). There is abundant evidence that many dune sands become reddened with time and that this process is promoted by warm temperatures, oxidizing conditions, and the periodic presence of moisture (Norris 1969). Williams and Yaalon (1977) have demonstrated reddening in sand dune under laboratory weathering conditions. Their research showed that organic matter is not necessary to initiate the process. Thus the percentage of iron oxides in sand dunes may indicate their age, source materials, and transport paths, as demonstrated by White *et al*. (1997) and White *et al*. (2001) using Landsat satellite images; whereas in Terre Rosse and Rendzina soils (Rhodoxeralfs and Xerochreys, respectively, according to the US Department of Agriculture) differences in iron oxide mineralogy (red hematite vs yellow goethite) were interpreted by Singer *et al*. (1998) to be due to differences in the pedoclimate (see also Balsam *et al*. 2004).

The amount of fine particles increases during sand succession and dune stabilization processes (Danin and Yaalon 1982) and in sandy soils is important for estimating the water-holding capacity of these soils as it determines the availability of water to plants (Tsoar and Zohar 1985). Differences in the particle size of soils influence their reflectance; wherein if multiple scattering dominates, as is usually the case in the visible and NIR, the reflectance is expected to decrease as the grain size increases (Clark 1999). This was indeed observed by Okin and Painter (2004) who studied sand plumes from abandoned agricultural fields, in which effective particle size decreased towards the toe of the plume. Analysing a hyperspectral Airborne Visible/Infrared Imaging Spectrometer (AVIRIS) image, they demonstrated the expected negative correlation between effective grain size of sand in the plume, and its reflectance, with the most significant correlations in the SWIR.

This paper presents a simple method for using a digital camera to measure soil colour, and assesses the accuracy of soil colour indices derived from the digital camera, with respect to those obtained from a field spectrometer, and with chemical measurements of the iron oxides and of the percentage of fine particles in the samples. The methodology was designed to meet the following operational criteria:

1. images should be taken with a standard digital camera in natural daylight;
2. reference chips used for calibration should be simple and available to all;
3. no knowledge about the camera's characteristics is required; and
4. data capture and analysis using commercially available software.

## 2. Methods

### 2.1 *The soil samples*

The soil samples that we collected included sand samples from the coastal dunes of Israel covering a range of colours (from light yellow to light red) attributed to the soil rubification stage. Altogether, 370 soil samples were analysed, most of them (368) were collected from the coastal dunes between the cities of Ashdod and Ashkelon (south to Tel-Aviv, Israel), along several NW–SE transects going from the beach inland. While most of the coastal dune sand samples represent the surface of the dunes, 21 samples were taken from a depth of 2 cm below the surface, and eight were collected from places with exposed 'Hamra' (Haploxeralfs in the USDA soil classification terminology) soils. Two additional samples were collected from the surface of sand dunes in the Arava valley in southern Israel, 225 km south of the coastal dune study area. All samples were gently crushed (as the samples were taken from very sandy soils) by hand, or by lightly tapping with a hammer (in the case of hard aggregates found in samples taken from Hamra soil) and then air-dried for three days. No further treatments (removal of organic matter or calcium carbonate, sieving, etc.) were applied, so as to not alter the samples. This was done to keep the samples as close as possible to their natural composition, in order to represent the dune status under a remote sensing means.

### 2.2 *Camera settings*

After air-drying the soil samples for three days in an indoor environment, they were placed in the laboratory on a simple sheet of white A4 paper, situated on a small chair (at a height of 44 cm above the floor). The samples were carefully flattened by gently tapping on a hard-cover book that was set on top of the sand sample, in order to avoid shading effects due to possible microtopography. The thickness of the levelled sand sample was about 5 mm. The sand was rimmed by a piece of cardboard with 12 coloured plastic chips (key holders). The coloured plastic chips included duplicates of six colours (red, green, blue, white, grey and black; see figure 1).

A 1.3 megapixel digital camera (Olympus CAMEDIA C-920) was held on a tripod, with the lens facing downward, towards the sand sample. The distance from the camera lens to the sand sample was 50 cm. Images were taken in Tel-Aviv, Israel (April–June, 2003) under the following camera settings: no flash, no artificial lighting system, daylight diffuse conditions (the Sun did not light the sand samples directly) in a room with wide open windows (facing north), resolution $1280 \times 960$ pixels (of which the sand sample itself occupied ca. $270 \times 190$ pixels), and high

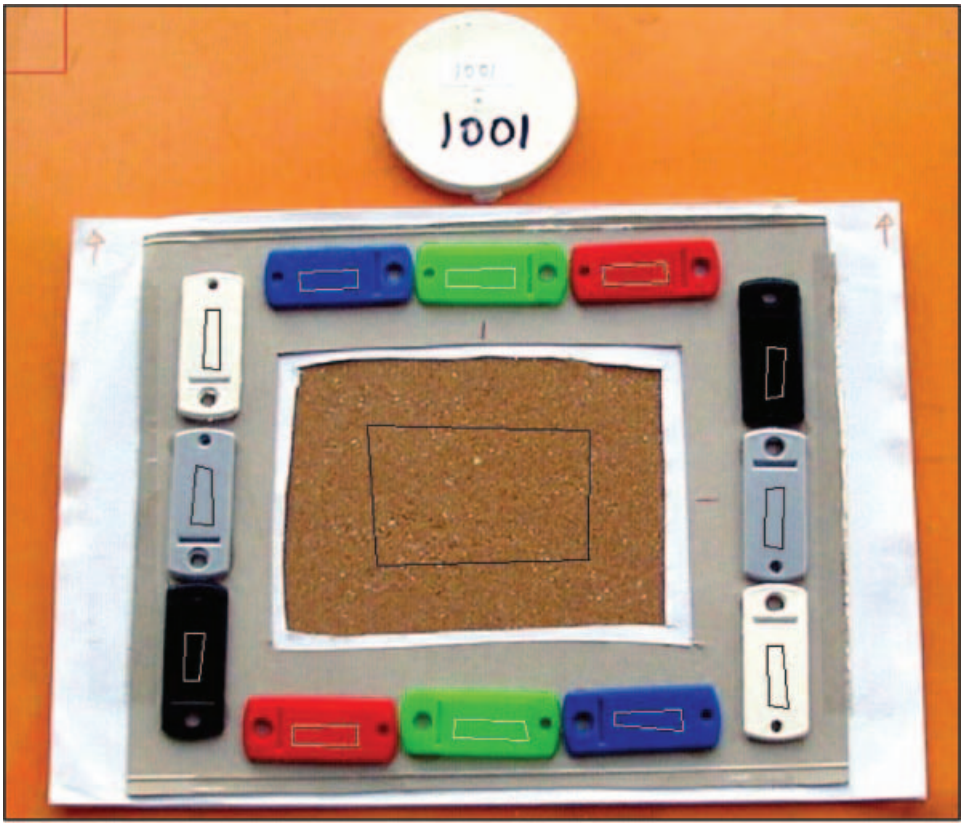


Figure 1. Arrangement of plastic colour chips around a soil sample (serial number 1001). Regions of interest (ROIs) drawn in ENVI over the plastic colour chips and the soil sample are presented in a thin white or black line.

quality (HQ) mode—JPG (Short for Joint Photographic Experts Group (JPEG) 2004) standard compression. Although JPG files are not recommended for research purposes (Yam and Papadakis 2004), our results show that the compressed (JPG) file did not hamper the accurate identification of the samples' colour. An important reason for preferring JPG images is the high compression ratio they offer for 24-bit images, thus allowing a greater number of photographs to be taken in a single session, especially on field trips.

### 2.3 *ASD measurements*

All soil samples were measured by a high performance single-beam field spectroradiometer—the Analytical Spectral Devices FieldSpec Pro (ASD 2001)—measuring throughout the visible to SWIR wavelength range (350–2500 nm). Soil samples were measured in the laboratory by attaching the contact probe ('potato') to the soil sample, and extracting for each sample the average of 20 readings, using the bare fiber mode and using the ASD's illumination. A white reference panel (made of halon) was used to calibrate the measurement to reflectance values in the same geometry. In addition, the reflectance of the plastic colour chips was also measured with the ASD, to enable an empirical line calibration (Smith and Milton

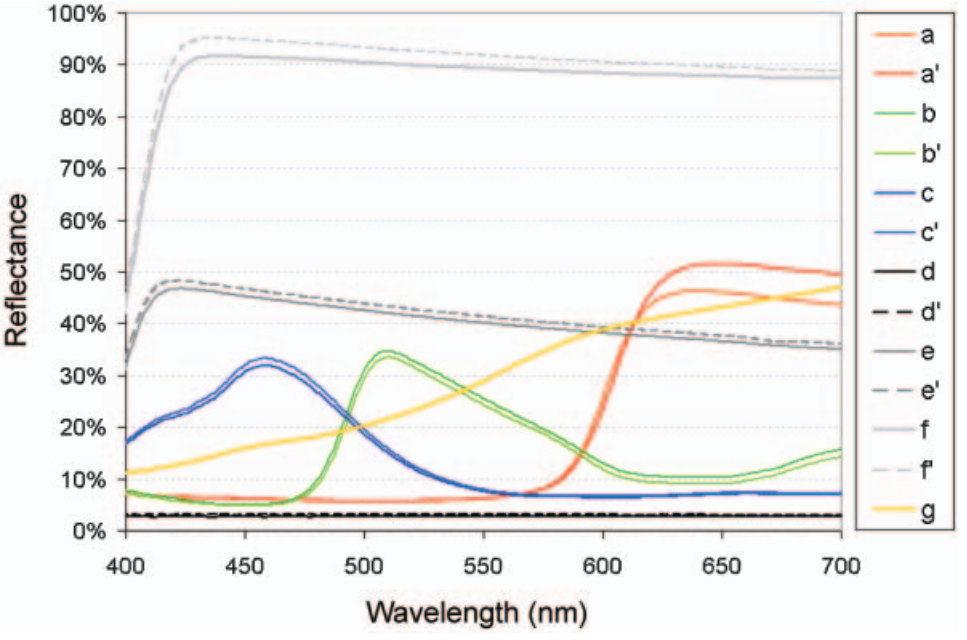


Figure 2. The reflectance spectra of the 12 plastic colour chips (two colour chips for each colour) and sand sample 1001, as measured by the field spectrometer (ASD). The captions of the spectral curves stand for the following reference objects: red chip (a, a′); green chip (b, b′); blue chip (c, c′); black chip (d, d′); grey chip (e, e′); white chip (f, f′); and a selected sand sample (g; sand sample number 1001).

1999). Figure 2 presents the reflectance spectra of a soil sample (serial number 1001) and of the 12 plastic colour chips used.

### 2.4 *Calibration of the camera digital number values to reflectance values*

Data encoded by the digital camera are scaled into 0–255 (8 bits) digital numbers (DN) in three bands (RGB) and saved in JPG format. We processed the digital images using ENVI 3.4 software (Research Systems 2000). Over each image, we defined 13 regions of interest (ROIs; 12 for the 12 colour chips, and one for the sand sample), covering the central part of these objects, so as to avoid adjacency effects (as recommended by Dean *et al.* 2000), as seen in figure 1. For each plastic colour chip, we averaged the values of RGB from the ROIs. These RGB values are referred to here as DC-RAW (digital camera raw data). Two calibration methods were applied to the measured RGB values: relative and absolute.

With the relative calibration, a linear regression line was found between the RGB values of the plastic chips of each soil sample (for each of the RGB values) and those of the image in an arbitrarily selected soil sample (the sample shown in figures 1 and 2). The average $R^2$ for all samples ($N$=370) and bands was 99.6%. Using the regression line coefficients, the RGB values of the soil sample (in each image) were corrected to match the illumination conditions of the first image. These RGB values are referred to here as DC-RGB (digital camera RGB).

Absolute calibration to reflectance values was based on measuring the spectral reflectance of the plastic chips with the ASD (figure 2). An exponential regression line was found between the digital camera's RGB values of the plastic chips (in each

image) and the ASD's reflectance values (at 640, 510 and 460 nm, representing red green and blue colour, respectively)—the average $R^2$ for all samples and bands was 93.7% ($N$=370). These regression lines were applied to the RGB values of the soil samples, in order to transform them into reflectance values, referred to here as DC-R (digital camera reflectance).

### 2.5 *Calculation of soil colour indices*

The following soil colour indices were calculated (Madeira *et al*. 1997, Mathieu *et al*. 1998):

$$\text{Brightness Index} \quad \text{BI} = \text{sqrt}\left\{\left(\text{B}^2 + \text{G}^2 + \text{R}^2\right)/3\right\} \tag{1}$$

$$\text{Saturation Index} \quad \text{SI} = (\text{R} - \text{B})/(\text{R} + \text{B}) \tag{2}$$

$$\text{Hue Index} \quad \text{HI} = (2 * \text{R} - \text{G} - \text{B})/(\text{G} - \text{B}) \tag{3}$$

$$\text{Colouration Index} \quad \text{CI} = (\text{R} - \text{G})/(\text{R} + \text{G}) \tag{4}$$

$$\text{Redness Index} \quad \text{RI} = \text{R}^2/\left(\text{B} * \text{G}^3\right) \tag{5}$$

where R=red band (640 nm when using the ASD); G=green band (510 nm when using the ASD) and B=blue band (460 nm when using the ASD).

We have used soil colour indices, as they were shown by Mathieu *et al*. (1998), to be good predictors of each of the soil colour components (expressed in Helmholtz coordinates). These indices were calculated for each of the sand samples four times: (i) from the raw DN values of the digital camera prior to their calibration (DC-RAW); (ii) from the self-calibrated DN values of the digital camera (DC-RGB); (iii) from the reflectance calibrated values of the digital camera (DC-R); and (iv) from the reflectance values of the ASD spectrometer (ASD-R).

As these indices are mostly ratio indices, we expected them to reduce shading and BRDF effects that may be present in the images, due to viewing angle with respect to the direction from which the light is coming (Lillesand and Kiefer 1994, King 1995). This is because a ratioed image of a scene effectively compensates for the brightness variation caused by the differences in the topography, and emphasizes the colour content of the data. In this study, we assumed that using a contact probe device to measure the reflectance with the ASD will significantly reduce major BRDF effects.

In addition, we have examined the performance of two other colour models, in predicting the content of free iron oxides and fine particles. The two colour models that we studied in comparison with the RGB model, were the CIE L*a*b* and the CIE L*C*H°. The CIE (1978) colour spaces form the foundation of device-independent colour for colour management, and are meant to be true representations of colours as perceived by the human eye (Amazys Holding 2004). In the CIE L*a*b*, L* is a measure of lightness of an object, and ranges from 0 (black) to 100 (white), a* is a measure of redness (positive a) or greenness (negative a), and b* is a measure of yellowness (positive b) or blueness (negative b). The coordinates a* and b* approach zero for neutral colours (white, greys and black). The higher the values for a* and b*, the more saturated the colour is. The CIE L*C*H° system is the same

as the CIE L*a*b* colour space, except that it describes the location of a colour in space by use of polar coordinates, rather than rectangular coordinates. L* is the same as above, C* is a measure of chroma (saturation), and represents the distance from the neutral axis, and H° is a measure of hue and is represented as an angle ranging from 0° to 360°.

We have calculated the colour coordinates in these two additional models, applying the formulas used in the software EasyRGB-PC$^{TM}$ (Logical 2004).

### 2.6 *Measurement of iron oxides and fine particles in the soil samples*

From the entire soil sample population, a set of 42 soil samples was selected for chemical measurements. The samples were selected according to their spectral soil colour indices, so as to cover the whole range of colour in the population. For each of those soil samples, two replications were used for the extraction of iron oxides, using the method described by Mehra and Jackson (1960). In this extraction, dithionite—citrate–bicarbonate (DCB) was used to extract the free iron into the solution for analytical determination. These values of free iron oxide content are referred to here as DCB-Fe. From the same set of 42 soil samples, an amount of 40 g was taken to analyse the content of fine particles (silt and clay) in the soil, as described in Kidron (2001). Table 1 presents the basic statistics of the content of free iron oxide and fine particles, as well as those of the Munsell value, hue, and chroma, as found using Munsell colour chart (Munsell 1923).

The samples' content of organic matter was not measured, as it was considered to be non-significant with in dune areas in Israel, as reported by Kutiel *et al.* (1996) (less than 1% of the coastal dunes and Hamra soils in Israel).

## 3. Results

Table 2 presents the linear correlation coefficients obtained for the RGB values, and their derived soil indices (between the digital camera and the ASD), as calculated from the above four sets: DC-RAW, DC-RGB, DC-R and ASD-R. Figure 3 presents some of the scatter plots for these variables. Both table 2 and figure 3 demonstrate the high correlation that exists between measurements performed by the digital camera and the ASD ($r$ values along the diagonal of the table are mostly greater than 0.9). As for the stability (that is, how well do the values of a certain variable correlate when measured either by the ASD or by the digital camera), the

Table 1. Descriptive statistics of the amount of free iron oxides and fine particles, as found in the 42 samples that were subject to chemical analysis in the laboratory.

| | Average | Standard deviation | Coefficient of variation | Minimum | 1st quartile | Median | 3rd quartile | Maximum |
|---|---|---|---|---|---|---|---|---|
| % Fe | 0.078 | 0.100 | 0.779 | 0.022 | 0.030 | 0.037 | 0.060 | 0.393 |
| % Fine particles | 6.01 | 11.13 | 0.54 | 0.18 | 0.39 | 0.86 | 5.38 | 44.78 |
| Munsell value | 9.8 | 0.7 | 14.8 | 7.5 | 10.0 | 10.0 | 10.0 | 10.0 |
| Munsell hue | 6.1 | 1.3 | 4.5 | 4.0 | 5.0 | 6.0 | 7.0 | 8.0 |
| Munsell chroma | 4.0 | 1.0 | 4.0 | 2.0 | 3.5 | 4.0 | 4.0 | 6.0 |

Table 2. Linear correlation coefficients ($r$) between RGB values and their derived soil indices, as measured by the digital camera (DC-RAW: raw RGB values; DC-RGB: relative RGB values calibrated by the RGB values of the colour chips; DC-R: RGB values converted into reflectance values) and the ASD field spectrometer.

| | | DC-RAW | | | | | | | | DC-RGB | | | | | | | | DC-R | | | | | | | |
|---|---|---|---|---|---|---|---|---|---|---|---|---|---|---|---|---|---|---|---|---|---|---|---|---|---|
| | | R | G | B | BI | SI | HI | CI | RI | R | G | B | BI | SI | HI | CI | RI | R | G | B | BI | SI | HI | CI | RI |
| ASD-R | R | 0.92 | 0.94 | 0.82 | 0.94 | −0.38 | −0.39 | −0.45 | −0.64 | 0.96 | 0.93 | 0.87 | 0.96 | −0.49 | −0.26 | −0.44 | −0.69 | 0.97 | 0.91 | 0.82 | 0.96 | 0.15 | 0.05 | 0.08 | −0.74 |
| | G | 0.89 | 0.96 | 0.87 | 0.95 | −0.48 | −0.47 | −0.53 | −0.65 | 0.92 | 0.94 | 0.92 | 0.96 | −0.60 | −0.32 | −0.53 | −0.70 | 0.94 | 0.93 | 0.88 | 0.96 | 0.00 | −0.02 | −0.03 | −0.77 |
| | B | 0.80 | 0.91 | 0.89 | 0.91 | −0.57 | −0.50 | −0.57 | −0.59 | 0.81 | 0.88 | 0.94 | 0.90 | −0.72 | −0.37 | −0.59 | −0.63 | 0.85 | 0.91 | 0.94 | 0.90 | −0.23 | −0.10 | −0.19 | −0.73 |
| | BI | 0.90 | 0.95 | 0.84 | 0.94 | −0.43 | −0.43 | −0.48 | −0.64 | 0.93 | 0.94 | 0.91 | 0.96 | −0.57 | −0.30 | −0.50 | −0.69 | 0.95 | 0.93 | 0.87 | 0.96 | 0.04 | 0.01 | 0.00 | −0.76 |
| | SI | −0.25 | −0.49 | −0.67 | −0.48 | 0.74 | 0.58 | 0.68 | 0.42 | −0.18 | −0.41 | −0.63 | −0.40 | 0.84 | 0.46 | 0.66 | 0.34 | −0.25 | −0.49 | −0.70 | −0.36 | 0.81 | 0.37 | 0.62 | 0.48 |
| | HI | −0.19 | −0.44 | −0.54 | −0.39 | 0.71 | 0.71 | 0.79 | 0.69 | −0.24 | −0.44 | −0.56 | −0.41 | 0.79 | 0.53 | 0.73 | 0.65 | −0.23 | −0.42 | −0.52 | −0.32 | 0.57 | 0.42 | 0.55 | 0.69 |
| | CI | −0.25 | −0.50 | −0.67 | −0.48 | 0.77 | 0.64 | 0.73 | 0.49 | −0.23 | −0.46 | −0.65 | −0.44 | 0.89 | 0.53 | 0.76 | 0.54 | −0.26 | −0.49 | −0.66 | −0.37 | 0.75 | 0.43 | 0.64 | 0.64 |
| | RI | −0.65 | −0.80 | −0.73 | −0.75 | 0.62 | 0.63 | 0.76 | 0.96 | −0.79 | −0.83 | −0.79 | −0.83 | 0.66 | 0.41 | 0.64 | 0.96 | −0.74 | −0.74 | −0.67 | −0.76 | 0.00 | 0.12 | 0.10 | 0.94 |

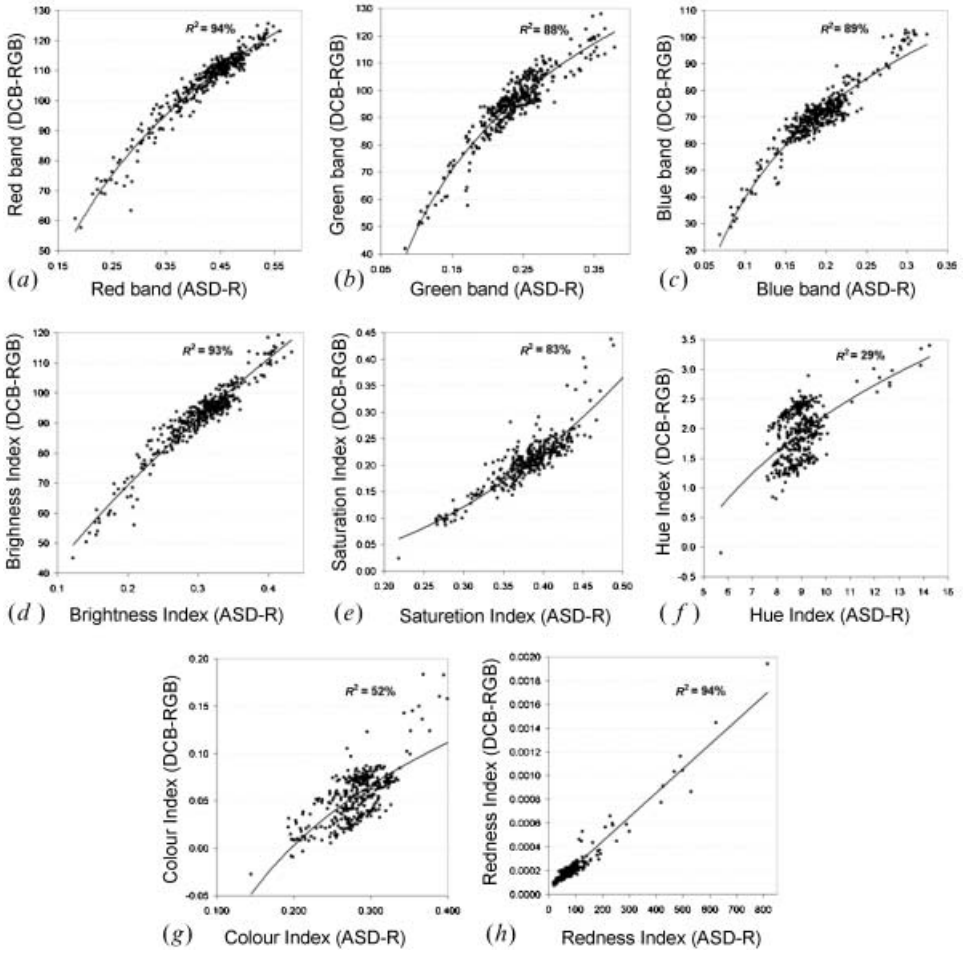


Figure 3. Scatter plots between various variables ((*a*) red band; (*b*) green band; (*c*) blue band; (*d*) Brightness Index; (*e*) Saturation Index; (*f*) Hue Index; (*g*) Colour Index; (*h*) Redness Index) measured by the digital camera and the field spectrometer (ASD).

soil indices can be ranked in the following decreasing order: Redness Index, Brightness Index, Saturation Index, Colour Index and Hue Index. Note that the correlations achieved between the ASD measurements and the uncalibrated digital camera measurements (DC-RAW) were almost as high as the calibrated digital camera measurements.

A comparison between DCB-Fe values of 42 selected soil samples, with the various soil indices (presented in table 3 and figure 4), reveals that similar results are obtained with either the digital camera or the ASD; the best spectral soil index (calculated from RGB values) being the Redness Index (with linear $r$ values greater than 0.85 for both the digital camera and the ASD spectrometer). In fact, correlation coefficients with the digital camera were similar, if not higher, than those achieved with the ASD. One should note that the relationship between the redness index and the free iron oxide content is of a logarithmic trend line (in figure 4). A similar relationship (using a parabolic fit, however) was interpreted by

Table 3. Linear correlation coefficients ($r$) between the content of iron oxides (DCB-Fe) values of 42 selected soil samples, and soil indices as calculated from RGB values, measured by the digital camera and the ASD field spectrometer (*95% significance, **99% significance).

| Correlation with DCB-Fe | | DC-RAW | DC-RGB | DC-R | ASD-R |
|---|---|---|---|---|---|
| Spectral soil index | BI | −0.73** | −0.75** | −0.69** | −0.72** |
| | SI | 0.73** | 0.76** | 0.16 | 0.53** |
| | HI | 0.78** | 0.66** | 0.35* | 0.86** |
| | CI | 0.80** | 0.76** | 0.27 | 0.63** |
| | RI | 0.92** | 0.92** | 0.86** | 0.89** |

Torrent *et al*. (1983) in Brazil, to represent a saturation in their redness rating index (that was based on Munsell colour charts), with respect to the hematite content of the soil.

Similar results were obtained for the relationship between spectral indices and the content of fine particles in the soil samples, as presented in figure 5 and table 4. This relationship follows a linear trend line; however, we used a logarithmic scale for the $x$-axis in this figure. Again, the best index for the fine particles was found to be the Redness Index (with linear $r$ values greater than 0.82 for both the digital camera and the spectrometer). In addition, the digital camera performed better than the ASD, in predicting the content of the fine particles based on spectral indices.

Evaluating four different colour models (RGB, CIE L*a*b*, CIE L*C*H° and Munsell) with respect to the ability of their colour coordinates to predict the content of fine particles and free iron oxides, we found that the poorest performance was that obtained by the Munsell charts ($r$ values not surpassing −0.70; see table 5). As for the other colour models, whose coordinates were calculated from the digital images, the RGB model and the two CIE models performed equally well (the best $r$ values reaching about −0.75). The best results were obtained with those colour variables that are directly related to the brightness of the soil sample (R, G, B and L*); whereas, the variables related to the redness of the soil sample obtained lower correlation values ($r \sim \pm 0.65$, for a* and H°). However, the spectral colour indices discussed above, and most notably the redness index, were found to be the best predictor of both DCB-Fe and of fine particle content.

## 4. Discussion

We have demonstrated the ability of a simple digital camera combined with simple plastic colour chips to capture RGB values of soil samples. From these, various soil colour indices were calculated. We found that soil colour indices in general, and those relating to the brightness or the redness of a soil sample in particular, may be calculated from digital camera images, with accuracies similar to or better than those achieved by an ASD. From these, accurate predictions of the free iron oxide and of fine particle contents can then be done, using either the digital camera or the ASD field spectrometer. Regarding the performance of a digital camera with respect to a field spectrometer, similar results were obtained by Viscarra Rossel *et al*. (2003) for the prediction of soil organic carbon. The fact that the accuracy achieved by the digital camera and the ASD spectrometer were quite similar, with different types of light sources (direct artificial light in the ASD, diffuse daylight with the digital camera), may be evidence that the sand samples behaved as lambertian reflecting surfaces. It may also be explained by the fact that a much larger, and hence

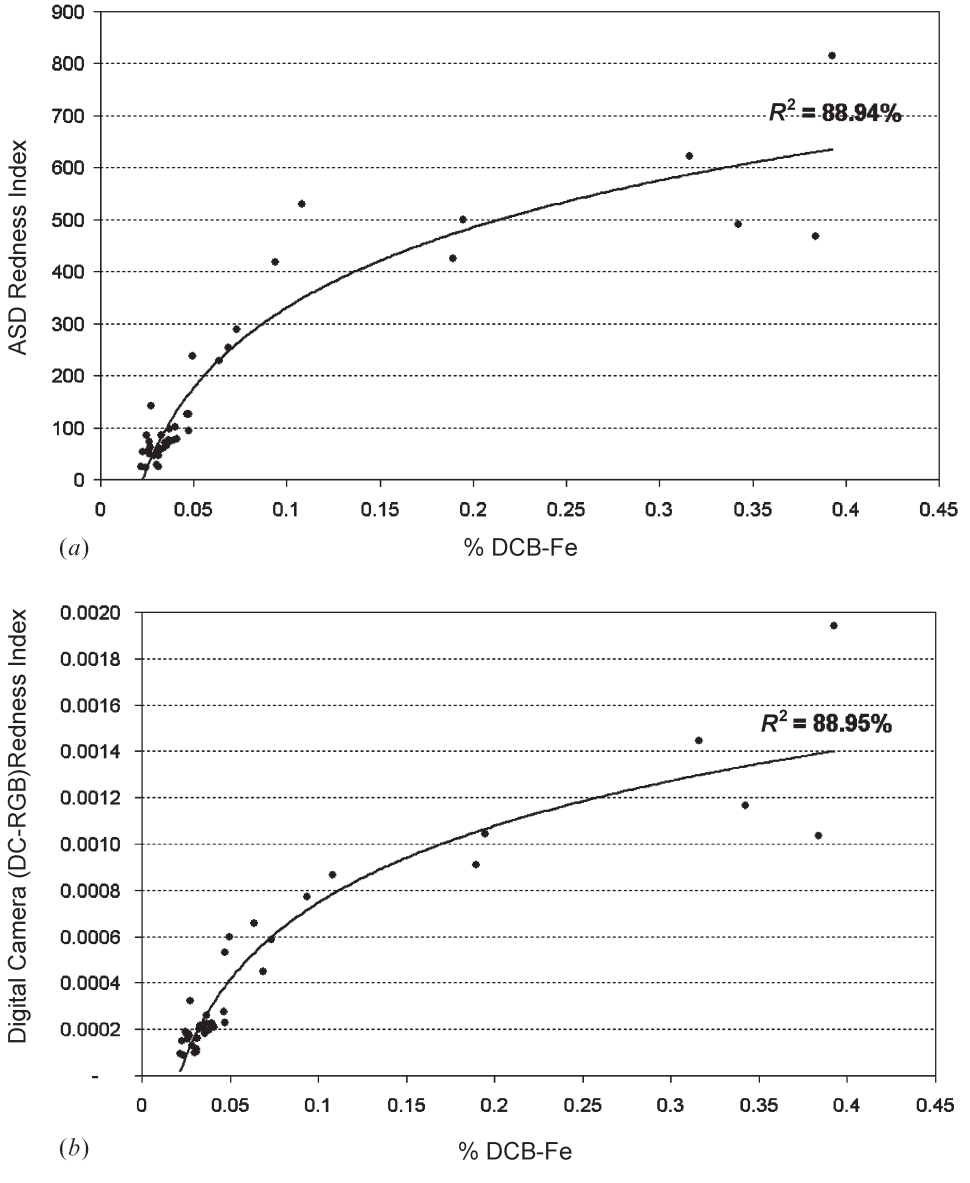


Figure 4. A scatter plot between the content of iron oxides (DCB-Fe) measured in the laboratory and the spectral redness index as measured (*a*) by the field spectrometer (ASD), and (*b*) by the digital camera.

representative, area of the soil sample was imaged by the digital camera (140 sq cm), as compared to the less than 2 sq cm imaged by the ASD, thus compensating for the higher accuracy expected from a sophisticated ASD field spectrometer.

With the Redness Index, high correlations were found between both the soil samples' free iron oxide content (DCB-Fe) and the fine particle percentages. In our study, we found that sandy soils with higher amounts of fine particles were darker than soils with a lower percentage of fine particles. This may seem to be contrary to the expected (see Clark 1999); however, in our case there was a high correlation between the content of free iron oxides and fine particles ($R^2$=93.5%). As noted by

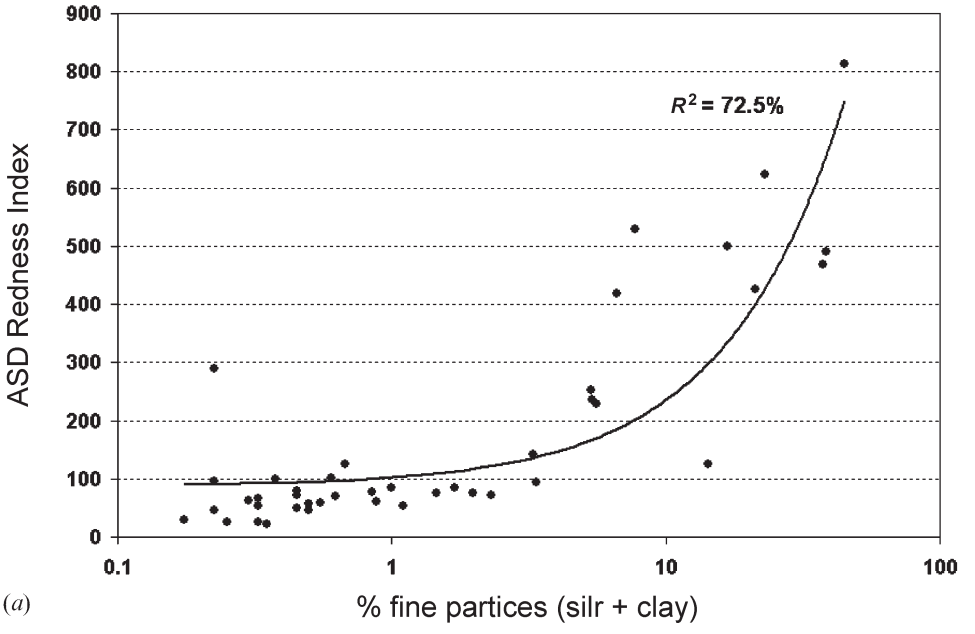


(*a*)

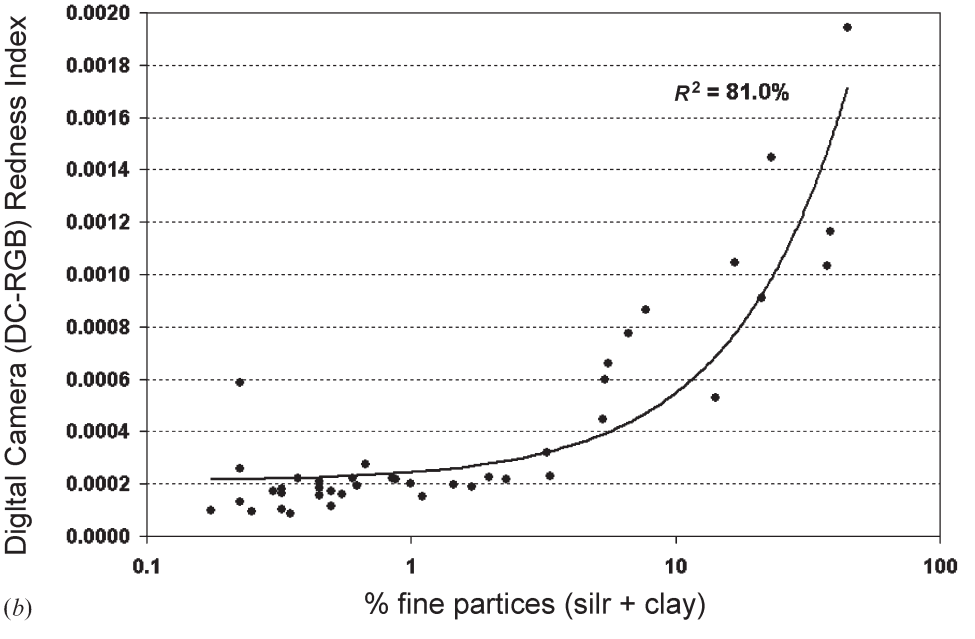


(*b*)

Figure 5. A scatter plot between the content of fine particles as measured in the laboratory and the spectral redness index as measured (*a*) by the field spectrometer (ASD), and (*b*) by the digital camera.

Dematte *et al.* (2004), as well as by Sanchez-Maranon *et al.* (2004), high iron content contributes to low reflectance; and hence, the fine particle inverse correlation with the reflectance values is explained by the occurrence of iron oxides.

We found the Redness Index to be the best spectral index for predicting both DCB-Fe ($R^2$=88.9%) and the content of fine particles ($R^2$=81%) in our soil sample

Table 4. Linear correlation coefficients ($r$) between content of fine particles of 42 selected soil samples, and soil indices as calculated from RGB values measured by the digital camera and the ASD field spectrometer (*95% significance, **99% significance).

| Correlation with % fine particles | | DC-RAW | DC-RGB | DC-R | ASD-R |
|---|---|---|---|---|---|
| Spectral soil index | BI | −0.74** | −0.75** | −0.69** | −0.71** |
| | SI | 0.64** | 0.70** | 0.09 | 0.46** |
| | HI | 0.73** | 0.66** | 0.31* | 0.80** |
| | CI | 0.72** | 0.73** | 0.22 | 0.56** |
| | RI | 0.89** | 0.90** | 0.83** | 0.85** |

population. We found that applying a spectral index was preferable to using simple colour coordinates, whether they belong to the RGB model or to the CIE models. Higher content of free iron oxides had two effects: lowering the brightness of the soil samples (as expressed in the negative correlation with R, G, B, L* and the Munsell value), and reddening them (as expressed in the positive correlation with a*, and the negative correlation with H° and the Munsell hue).

Although we were successful in quantifying soil colour indices and related soil properties using a digital camera, we may note the following limitations for this method: (1) changing illumination conditions may have more influence on the accuracy achieved when images are taken in the field; (2) images taken by different cameras can only be compared after they are calibrated to the same reference; and (3) soil samples should be levelled before images are taken to reduce shading artefacts, due to possible microtopography and BRDF. These artefacts are, however, partially compensated for when using ratio indices.

Organic matter may change the spectral slope of the VIS–NIR region (Ben-Dor *et al.* 1997), and accordingly the RI. Indeed, organic matter was demonstrated by Viscarra Rossel and Walter (2002) and Viscarra Rossel *et al.* (2003) to lower the reflectance of soils as measured by a digital camera. However, this can happen only when the organic matter content reaches a significant threshold (above 2%; Baumgardner *et al.* 1985). If the organic matter is fresh, then signatures of

Table 5. Linear correlation coefficients ($r$) between the content of fine particles and iron oxides (DCB-Fe) as measured in 42 soil samples, and several colour coordinates used in the following colour models: RGB, CIE L*a*b*, CIE L*C*H° and Munsell. All the calculations referring to the digital colour models were based on the DC-RGB values (the calibrated RGB values).

| Colour model | Colour coordinate | % fine particles | DCB-Fe |
|---|---|---|---|
| RGB | **R** | −0.75 | −0.74 |
| RGB | **G** | −0.76 | −0.76 |
| RGB | **B** | −0.71 | −0.73 |
| CIE L*a*b*: | **L*** | −0.76 | −0.77 |
| CIE L*a*b*: | **a*** | 0.62 | 0.65 |
| CIE L*a*b*: | **b*** | 0.09 | 0.17 |
| CIE L*C* H° | **C*** | 0.19 | 0.28 |
| CIE L*C* H° | **H°** | −0.62 | −0.63 |
| Munsell | **Value** | −0.68 | −0.69 |
| Munsell | **Chroma** | 0.31 | 0.39 |
| Munsell | **Hue** | −0.59 | −0.62 |

chlorophyll can be also present at around 680 nm (Ben-Dor *et al*. 1997). The organic matter content (fresh and mature) within a sand dune area (far from vegetation spots), as well as in typical 'Hamra' soil, is fairly low in the selected area (less than 1%; see Kutiel *et al*. 1996), and thus, not spectrally significant. As demonstrated by Danin *et al*. (1989), even when the silt + clay content in cyanobacterial crusts over desert dunes in Israel is 30%, the organic matter is less than 2%. However, in proximity to vegetation pockets, caution must be taken when using the proposed method. Along these areas, both organic matter and chlorophyll content may be masking the spectral response of the iron oxides.

## 5. Conclusions

In conclusion, the method presented here offers the possibility of using a digital camera as an alternative tool for a three-band field spectrometer in the VIS range; and it may also be applied in the field, thus allowing an easy, objective, and fast way to quantitatively measure soil colour variables. These may then be related to the amount of free iron oxides, content of fine particles, and probably also to organic carbon—all of which are important soil properties, which may also serve as indicators of the stage in the stabilization process of sand dunes. Further research may be applied to more soil populations, and to additional soil properties such as water and lime content, and to biogenic crusts, as they all affect the soil colour properties.

**Acknowledgments**

We thank Ms Ziva Hohman from the Soil and Water Department of the Faculty of Agriculture from the Hebrew University of Jerusalem for conducting the DCB iron extractions. We also express our thanks to Dr Giora J. Kidron and Sabra Rahel from the Geography and Human Environment Department of Tel Aviv University, for helpful comments on the manuscript. This work was done as part of a PhD thesis, in the Department of Geography and Human Environment, at Tel Aviv University. We appreciate the remarks made by the two anonymous referees, and thank them for their contribution to the improvement of this manuscript.

## References

ADAMCHUK, V.I., HUMMEL, J.W., MORGAN, M.T. and UPADHYAYA, S.K., 2004, On-the-go soil sensors for precision agriculture. *Computers and Electronics in Agriculture*, **44**, pp. 71–91.

ADDERLEY, W.P., SIMPSON, I.A. and DAVIDSON, D.A., 2002, Colour description and quantification in mosaic images of soil thin sections. *Geoderma*, **108**, pp. 181–195.

AMAZYS HOLDING, 2004, Color spaces. Available online at: http://www.i1color.com/knowledge/ (accessed 8 November 2004).

ASD, 2001, Analytical Spectral Devices. Available online at: http://www.asdi.com/ (accessed 13 November 2003).

BALSAM, W., JI, J. and CHEN, J., 2004, Climatic interpretation of the Luochuan and Lingtai loess sections, China, based on changing iron oxide mineralogy and magnetic susceptibility. *Earth and Planetary Science Letters*, **223**, pp. 335–348.

BAUMGARDNER, M.F., SILVA, L.F., BIEHL, L.L. and STONER, E.R., 1985, Reflectance properties of soils. *Advances in Agronomy*, **38**, pp. 1–44.

BEN-DOR, E., 2002, Quantitative remote sensing of soil properties. *Advances in Agronomy*, **75**, pp. 173–243.

Ben-Dor, E. and Singer, A., 1987, Optical density of vertisol clays suspensions in relation to sediment volume and dithionite—citrate–bicarbonate extractable iron. *Clays and Clay Minerals*, **35**, pp. 311–317.

Ben-Dor, E., Inbar, Y. and Chen, Y., 1997, The reflectance spectra of organic matter in the visible near infrared and short wave infrared region (400–2,500 nm) during a control decomposition process. *Remote Sensing of Environment*, **61**, pp. 1–15.

Ben-Dor, E., Irons, J.R. and Epema, G., 1998, Soil reflectance. In *Remote Sensing for the Earth Sciences*, A.N. Rencz (Ed.), pp. 111–188, in *Manual of Remote Sensing*, vol. 3, R.A. Ryerson (Ed.) (New York: John Wiley & Sons).

Buol, S.W., Hole, F.D. and McCracken, R.J., 1973, *Soil Genesis and Classification* (Ames: Iowa State University Press).

CIE, 1978, Commission Internationale de l'Eclairage, Recommendations on uniform colour spaces, colour difference equations and psychometric colour terms, Supplement No.2 to publication CIE No. 15 (E-1.3.1) 1971/(TC-1.3) 1978, Bureau Central de la CIE, Paris.

Clark, R.N., 1999, Spectroscopy of rocks and minerals, and principles of spectroscopy. In *Manual of Remote Sensing, Volume 3, Remote Sensing for the Earth Sciences*, A.N. Rencz (Ed.) (New York: John Wiley & Sons), pp. 3–58.

Danin, A. and Yaalon, D.H., 1982, Silt plus clay sedimentation and decalcification during plant succession in sands on the Mediterranean coastal plain of Israel. *Israel Journal of Earth Sciences*, **31**, pp. 101–109.

Danin, A., Bar-Or, Y., Dor, I. and Yisraeli, T., 1989, The role of cyanobacteria in stabilization of sand dunes in southern Israel. *Ecologia Mediterranea*, **15**, pp. 55–64.

Dean, C., Warner, T.A. and McGraw, J.B., 2000, Suitability of the DCS460c colour digital camera for quantitative remote sensing analysis of vegetation. *ISPRS Journal of Photogrammetry and Remote Sensing*, **55**, pp. 105–118.

Dematte, J.A.M., Campos, R.C., Alves, M.C., Fiorio, P.R. and Nanni, M.R., 2004, Visible-NIR reflectance: a new approach on soil evaluation. *Geoderma*, **121**, pp. 95–112.

Hinkler, J., Pedersen, S.B., Rasch, M. and Hansen, B.U., 2002, Automatic snow cover monitoring at high temporal and spatial resolution, using images taken by a standard digital camera. *International Journal of Remote Sensing*, **23**, pp. 4669–4682.

JPEG, 2004, JPEG home page. Available online at: http://www.jpeg.org/ (accessed 20 November 2003).

Kidron, G.J., 2001, Runoff-induced sediment yield over dune slopes in the Negev Desert. 2: Texture, carbonate and organic matter. *Earth Surface Processes and Landforms*, **26**, pp. 583–599.

King, D.J., 1995, Airborne multispectral digital camera and video sensors: a critical review of system designs and applications. *Canadian Journal of Remote Sensing*, **21**, pp. 245–273. Available online at: http://www.carleton.ca/~dking/paper1.html (accessed 10 November 2003).

Konen, M.E., Burras, C.L. and Sandor, J.A., 2003, Organic carbon, texture, and quantitative colour measurement relationships for cultivated soils in North Central Iowa. *Soil Science Society of America Journal*, **67**, pp. 1823–1830.

Kutiel, P., Dangur, H., Moses, H. and Levy, S., 1996, The place and role of biogenic crusts in the succession process of the Sharon dunes. *Ecology and Environment*, **4**(3), pp. 177–183 (in Hebrew).

Lillesand, T.M. and Kiefer, R.W., 1994, *Remote Sensing and Image Interpretation*, 3rd edn (New York: John Wiley & Sons).

Logicol S.R.l., 2004, EasyRGB-PC$^{TM}$, Software home page. Available online at: http://www.easyrgb.com/index.html (accessed 8 November 2004).

Madeira, J., Bedidi, A., Cervelle, B., Pouget, M. and Flay, N., 1997, Visible spectrometric indices of hematite (Hm) and goethite (Gt) content in lateritic soils:

the application of a Thematic Mapper (TM) image for soil-mapping in Brasilia, Brazil. *International Journal of Remote Sensing*, **18**, pp. 2835–2852.

MATHIEU, R., POUGET, M., CERVELLE, B. and ESCADAFAL, R., 1998, Relationships between satellite-based radiometric indices simulated using laboratory reflectance data and typic soil colour of an arid environment. *Remote Sensing of Environment*, **66**, pp. 17–28.

MEHRA, O.P. and JACKSON, M.L., 1960, Iron oxide removal from soils and clays by dithionite–citrate system buffered with sodium bicarbonate. *Clays and Clay Minerals*, **7**, pp. 317–327.

MUNSELL, A.H., 1923, *A Color Notation* (Baltimore: Munsell Color Company).

NORRIS, R.M., 1969, Dune reddening and time. *Journal of Sedimentary Petrology*, **39**(1), pp. 7–11.

OKIN, G.S. and PAINTER, T.H., 2004, Effect of grain size on remotely sensed spectral reflectance of sandy desert surfaces. *Remote Sensing of Environment*, **89**, pp. 272–280.

RESEARCH SYSTEMS, 2000, *ENVI User's Guide*, ENVI version 3.4 (Boulder: Research Systems).

ROBERTSON, E.A.G. and CAMPBELL, D.J., 1997, Simple, low-cost image analysis of soil pore structure. *Journal of Agricultural Engineering Research*, **68**, pp. 291–296.

SANCHEZ-MARANON, M., SORIANO, M., MELGOSA, M., DELGADO, G. and DELGADO, R., 2004, Quantifying the effects of aggregation, particle size and components on the colour of Mediterranean soils. *European Journal of Soil Science*, **55**, pp. 551–565.

SENA, D.G., PINTO, F.A.C., QUEIROZ, D.M. and VIANA, P.A., 2003, Fall Armyworm damaged maize plant identification using digital images. *Biosystems Engineering*, **85**, pp. 449–454.

SINGER, A., SCHWERTMANN, U. and FRIEDL, J., 1998, Iron oxide mineralogy of Terre Rosse and Rendzinas in relation to their moisture and temperature regimes. *European Journal of Soil Science*, **49**, pp. 385–395.

SMITH, G.M. and MILTON, E.J., 1999, The use of the empirical line method to calibrate remotely sensed data to reflectance. *International Journal of Remote Sensing*, **20**, pp. 2653–2662.

TORRENT, J., SCHWERTMANN, U., FECHTER, H. and ALFEREZ, F., 1983, Quantitative relationships between soil colour and hematite content. *Soil Science*, **136**, pp. 354–358.

TSOAR, H. and ZOHAR, Y., 1985, Desert dune sand and its potential for modern agricultural development. In *Desert Development: Man and Technology in Sparselands*, Y. Gradus (Ed.) (Dordrecht: D. Reidel), pp. 184–200.

VISCARRA ROSSEL, R.A. and MCBRATNEY, A.B., 1998, Laboratory evaluation of a proximal sensing technique for simultaneous measurement of soil clay and water content. *Geoderma*, **85**, pp. 19–39.

VISCARRA ROSSEL, R.A. and WALTER, C., 2002, Towards a quantitative assessment of field soil organic carbon using proximally sensed digital imagery. In *17th World Congress of Soil Science*, Bangkok, Thailand, 14–21 August 2002, symposium no. 48, paper no. 1523.

VISCARRA ROSSEL, R.A., WALTER, C. and FOUAD, Y., 2003, Assessment of two reflectance techniques for the quantification of field soil organic carbon. In *Fourth European Conference on Precision Agriculture*, J. Stafford and A. Werner (Eds) (Berlin: Wageningen Academic Publishers), pp. 697–703.

WALKER, T.R., 1979, Red color in dune sands. In *A Study of Global Sand Seas*, Geological Survey Professional Paper 1052, E.D. McKee (Ed.) (Washington: United States Geological Survey), pp. 61–81.

WANG, K. and KANGAS, J.A., 2003, Character location in scene images from digital camera. *Pattern Recognition*, **36**, pp. 2287–2299.

WARNER, W.S., 1995, Mapping a three-dimensional soil surface with hand-held 35 mm photography. *Soil and Tillage Research*, **34**, pp. 187–197.

WEBSTER, M.A. and MOLLON, J.D., 1997, Adaptation and the colour statistics of natural images. *Vision Research*, **37**, pp. 3283–3298.

WHITE, K., WALDEN, J., DRAKE, N., ECKARDT, F. and SETTLE, J., 1997, Mapping the iron oxide content of dune sands, Namib Sand Sea, Namibia, using Landsat Thematic Mapper data. *Remote Sensing of Environment*, **62**, pp. 30–39.

WHITE, K., GOUDIE, A., PARKER, A. and AL-FARRAJ, A., 2001, Mapping the geochemistry of the Northern Rub, Al Khali using multispectral remote sensing techniques. *Earth Surface Processes and Landforms*, **26**, pp. 735–748.

WILLIAMS, C. and YAALON, D.H., 1977, An experimental investigation of reddening in dune sand. *Geoderma*, **17**, pp. 181–191.

YAM, K.L. and PAPADAKIS, S.E., 2004, A simple digital imaging method for measuring and analyzing colour of food samples. *Journal of Food Engineering*, **61**, pp. 137–142.

*In the third article* the possibility of using historical maps for studying the mobility rate of coastal dunes is presented. As is discussed there, the accuracy of a historical maps should be assessed before using it for landscape changes. To this end two sets of historical maps were used: the Survey of Western Palestine executed in the 1870's by the Palestine Exploration Fund, at a scale of 1:63,360, and topocadastric maps of Palestine executed in the 1930's-40's by the British Mandate Department of Survey at a scale of 1:20,000. From these two sets of geo-referenced and digitized maps a study of the dunes movement rate in six regions along the coast of Israel was then executed, going farther back than has been previously done.

# The Palestine Exploration Fund map (1871-7) of the Holy Land as a tool for analyzing landscape changes: the coastal dunes of Israel as a case study

Levin Noam
Department of Geography and Human Environment, Tel Aviv University
10 Zelig St., Tel Aviv, Israel

## Abstract

The Palestine Exploration Fund (PEF) maps (1871-1877) are highly praised for their accuracy and completeness; however no systematic analysis of their accuracy has been done to date. To study the potential of these 1:63,360 maps for a quantitative analysis of land cover changes over time, I have compared them to 20th century topographic maps. The map registration error of the PEF maps was 74.4m using 123 control points of triangulation stations and a 1st order polynomial. The median RMSE of all control and test points (n = 1104) was 153.6m. As a case study of land cover changes, the area of coastal dunes as shown on the PEF maps was compared with that shown on British Mandate 1:20,000 topo-cadastral maps from ca. 1930. In five of the six areas analyzed the yearly dunes movement rate was above the estimated annual error due to data resolution (2.96 m/year). The rate of dune movement south of Acre was found to be between 3.9-6.3 m/year (depending on the method used for map registration) between 1874-1930, meaning that the current stage of coastal dunes in Israel has begun encroaching about 1,200 years ago, presuming no major change in the climatic conditions. Care should be taken when analyzing historical maps as it cannot be assumed that their accuracy is consistent at different parts or for different features depicted on them.

# 1. Introduction

## 1.1 Historical maps as a tool for studying landscape changes

In numerous studies modern historical maps have been used to analyze urban and landscape changes, to mention only a few examples from the USA (Rumsey and Williams, 2002), Austria (Hall et al., 2003), Argentina (Kitzberger and Veblen, 1999), Australia (Harvey, 2003), Great Britain (Coppock, 1968; Roper, 2003), Egypt (Stanley and Warne, 1993) and Israel (Schick, 1955; Kark, 1997a; Zvieli et al., 2003). Although historical maps are accessible to students, researchers and the general public in specialized libraries, their transformation into a digital format has been shown to increase their use dramatically (compare Hunt and Smith, 1985, with: Pearson et al., 1994; Rumsey and Williams, 2002; Roper, 2003).

As noted by Karmon (1960), the value of a map as a historical source obviously depends on the reliability and correctness of the measurements and notes on which it is based. However, as written by Coppock (1968, p. 41): "It is a truism to say that before a map or map series is used as a source of data on land use, it must be properly evaluated, *but this has not always been done*" (my emphasis). As for the reconstruction of past land uses, one should bare in mind that differences in interpretation or in the accuracy with which the location and type of land uses are recorded on historical maps, may lead to the identification of changes which are only apparent on the maps, but have no base in reality.

## 1.2 Historic maps registration methodology

The majority of registration methods consist of the following four steps (Zitova and Flusser, 2003): feature detection, feature matching, transform model estimation and image resampling and transformation. If possible, prior to registration maps should be evaluated for systematic errors (e.g. incorrectly placed geographic reference system). Ideally, to analyze the accuracy of a historical map (as is done for example when analyzing the classification results of satellite images), one would like to have a “ground-truth” base-map describing the land-cover as it was. As this is usually not the case, analyzing the accuracy of a historic map is commonly based on comparing it to a later map that was surveyed and drawn using more accurate methods. This can be done in two ways: (1) by comparing the distances between selected points on the maps analyzed (as in Bonisch, 1967), or (2) by identifying the location (in x,y coordinates) of the same place in the two maps – i.e. by compiling a table and a map showing the name and coordinates of a place in both maps (for examples see Warren, 1880; Karmon, 1960; Margary, 1977; Vuorela et al., 2002; Hall et al., 2003). To this end, point features (termed Control Points (CPs); e.g. river meetings, crossroads, settlements, buildings, mountain tops, etc., according to

the scale of the map) are preferred over line or polygon features, as the former can be pinpointed more accurately than the latter.

Whether this comparison is done using the raw data of longitudes and latitudes, from the visual or photographical overlay of maps (e.g. using the photographic method suggested by Margary, 1977) or by scanning them and rectifying them using Geographic Information Systems (GIS), three points should be kept in mind: (1) the points should be well defined; (2) the control points on which the comparison is based should be chosen from entities that did not change their location over the time period separating the two maps, with respect to the scale of the maps (e.g. triangulation stations and mountain tops are preferable over sand dunes); (3) errors in identifying places might result from misidentification of place names in of the maps. In addition, one may also analyze the features that were omitted from the map under consideration (that is, to analyze the completeness of the map).

## 1.3 Transformation model estimation

Once the control points are detected and matched for both maps/images, the parameters for a mathematical transformation are derived. This may be done using a global model that uses a set of well defined CPs for estimating one set of mapping function parameters valid for the entire image. Alternatively, local mapping functions treat the image as a set of patches and the function parameters depend on the location of their support in the image; this leads to the tessellation of the image, usually a triangulation, and to the defining of parameters of the mapping function for each patch separately (Zitova and Flusser, 2003).

One of the most frequently used global models uses bivariate polynomials of low degrees fitted using a least-squares trend model. A trend model, derived from *n* control points expressed as follows (Buiten and Putten, 1997, p. 59):

$$x = f(X, Y) + u \quad (1)$$

$$y = f(X, Y) + v \quad (2)$$

may consist of a lower-order polynomial, e.g. of the 1st order:

$$x = a_1 + a_2X + a_3Y + u \quad (3)$$

$$y = b_1 + b_2X + b_3Y + v \quad (4)$$

where: (X, Y) = master coordinate system with points ($X_i$, $Y_i$); i = 1,2,…,n; ($x$, $y$) = slave coordinate system with points ($x_i$, $y_i$); i = 1,2,…,n; and ($u_i$, $v_i$) being the residual pair corresponding to the i-th control point after the least square adjustment, assuming a redundant number of control points available for the transformation model. Such mapping functions do not map the CPs onto their counterparts exactly, as the least square technique averages out the local geometric distortion equally over the entire image.

If a map or an image are distorted locally then local methods such as piecewise linear mapping, piecewise cubic mapping together with Akima's quintic approach apply the combination of the CP-based image triangulation and of the collection of local mapping functions each valid within one triangle (Zitova and Flusser, 2003). As reported by Doytsher (2000) this method is considered today a popular approach. Local models were as well recommended in several studies that dealt with historical maps where geometric irregularities are not evenly distributed (Shimizu and Fuse, 2004; Vuorela et al., 2002; Cousins, 2001; Weir, 1997). However, triangulation is very sensitive to the number and quality (coverage, spatial accuracy) of CPs (Vuorela et al., 2002).

Other methods include radial basis functions and elastic registration however these are not commonly available in commercial image processing packages and were therefore not applied here (Zitova and Flusser, 2003; Fogel and Tinney, 1996).

## 1.4 Evaluation of the map registration accuracy

The residuals ($u_i$, $v_i$) give an estimate of the error of each control point in the x and y axes, whereas the total error for each point is given by:

$$\text{Total error} = \text{SQRT}\ (u^2 + v^2) \tag{5}$$

and the overall model error, called the *Root Mean Squared Error* is computed as (Verbyla, 2002, p. 155):

$$\text{RMS error} = \text{Square Root}\ [\ (\text{sum of total errors squared}) / n\ ] \tag{6}$$

Ideally, the residual vectors (u, v) should be independent of their 'place' or the type of the control point (e.g. building or rivers confluence) and isotropic. In addition to the RMS error, when dealing with satellite images an uncertainty term the size of diagonal ($\sqrt{2}$) of the spatial resolution of the images should be included to derive the accuracy (Hall et al., 2003).

Errors in data collection may be classified into gross errors (due to carelessness of the observer), systematic errors (that introduce a bias into the observations) and random errors (Thapa and Bossler, 1992). Historical maps belong to secondary methods of data collection, whereas primary methods of data collection include ground surveying, aerial and terrestrial photographs and remote sensing (Thapa and Bossler, 1992). As such, secondary methods of data collection are prone to all the errors contained in the primary methods (personal, instrumental and environmental), as well as errors related to dealing with paper maps. These include the following errors, listed in Table 1.

| Error number | Error type | Error size: best and worst case estimates (mm) |
|---|---|---|
| 1 | Error in plotting control points | 0.17 – 0.32 |
| 2 | Compilation error | 0.3 – 0.32 |
| 3 | Error introduced in drawing | 0.06 – 0.18 |
| 4 | Error due to map generalization | Depending on map scale |
| 5 | Error in map reproduction | 0.1 - 0.2 |
| 6 | Error in colour registration | 0.17 – 0.3 |
| 7 | Deformation of the material | 0.25 – 0.48 |
| 8 | Error introduced due to the use of the wrong scale | |
| 9 | Uncertainty in the definition of a feature | Depending on type of feature |
| 10 | Error due to feature exaggeration | Depending on map scale and type of feature |
| 11 | Error in digitization or scanning | 0.25 |

**Table 1**: Errors in secondary methods of data collection (after Thapa and Bossler, 1992)

Assuming that a linear relationship exists between the total error and the individual errors, the total error may be computed using the law of propagation of errors:

$$\text{Total error} = (e_1^2 + e_2^2 + e_3^2 + e_5^2 + e_6^2 + e_7^2 + e_{11}^2)^{0.5} \quad (7)$$

Where $e_x$ refers to the errors listed in Table 1. In the worst case scenario, the total RMS error will be equivalent to 0.81 mm at map scale (plus additional errors related to the type of feature and the map scale, as described in Table 1).

In addition to RMSE, two other methods for estimating the alignment error of the map registration are recommended (Zitova and Flusser, 2003; Vuorela et al., 2002): (1) Test Point Error (TPE): Test points (also termed as check points) are CPs that were deliberately excluded from the calculation of the mapping parameters; (2) Consistency check using multiple cues: here, the image registered by the method under investigation is compared with the same image registered by another comparative method.

## 2. Research goals

The Survey of Western Palestine was conducted by the British society of the Palestine Exploration Fund (PEF) during the years 1871-1877 (described in detail below). This survey is to this day highly praised for its accuracy and completeness, however, no systematic analysis of the accuracy of the PEF maps has yet been done. To demonstrate the potential of historical maps to analyze geomorphologic processes, and to assess the value of the PEF maps for the reconstruction of past land-cover, the following goals were set:

- Create a digital version of the PEF maps;
- Assess the horizontal and vertical accuracy of the PEF maps and their adequacy for evaluating changes in the coastal dunes of Israel;
- Evaluate whether different features (e.g. springs, mosques, etc.) may have been mapped at different accuracies;
- Assess spatial variations in the accuracy of the map;
- Evaluate changes in the area covered by the coastal dunes between the 1870s (as depicted on the 1:63,360 PEF maps) to ca. 1930 (based on British Mandate 1:20,000 topo-cadastral maps).

# 3. The accuracy of the PEF maps

## 3.1 Background

### 3.1.1 Early mapping of Palestine during the 19th century

The area known as Palestine was under Ottoman control from 1517 until World War I. During that period several land registration surveys were conducted, in which the size, type and ownership status was registered. Modern land registration was first introduced in 1865 following the Ottoman Land Code of 1858 and replaced a situation of complete anarchy (Kark and Gerber, 1984; Kark, 1997b). However, a basic component of land registry was still missing – the compulsory measuring and mapping of the land. Nonetheless, a detailed literal definition of the geographical boundaries of each parcel appeared in many of these surveys, and is some cases large scale maps of villages and their lands were also drawn (at the scale of 1:10,000), although very few of the maps survived (Kark and Gerber, 1984).

Systematic surveys of Palestine were performed in the 19th century almost only by European organizations and individuals, mainly the French and the British, but also the German, Russians, Dutch, Americans and other nationalities (Ben-Arieh, 1972; Gavish, 1991; Rosen, 1992; Goren, 2001; Goren, 2002; Frumin, 2005; Gavish, 2005). The first trigonometrically based topographic map of Palestine was the 1:100,000 map surveyed by Pierre Jacotin during the military campaign of Napoleon from Egypt to Acre in 1799. These measurements were conducted only along the coast and in the lower Galilee, and completed however, in a very short time – two months. Six sheets of the *Carte topographique de l'Egypte* were dedicated for Palestine, but they were heavily criticized, because of the haste with which the survey was performed and the addition of imaginary information (Gavish, 1991, 2005). A detailed analysis of the geometric, thematic and toponymic errors in Jacotin's map is given by Karmon (1960).

Goren (2002, p. 92) reports on the many calls for an organized survey of Palestine that were made during the 19th century, "recognizing the ineffectiveness of the haphazard collection of data by a lone traveller working for a short time wherever he happened to be". Interest in the mapping of Palestine increased due to its biblical significance, and for scientific reasons (e.g. the determination of the altitudes along the Jordan valley). However, the mapping of the country was delayed because it was not especially important, either strategically or geo-politically, for the European nations until the last quarter of the 19th century (Moscrop, 2000; Moscrop, 2002; Goren, 2002). Interest in the region grew at that time following the Crimean War (that ended in 1856), and especially with the building of the Suez Canal by France, and its opening in 1869. The British and the French were then colonial rivals, and as the French began mapping the Galilee in 1870, and with a pending war between Russia and the Ottoman Empire (which indeed

erupted in 1876), the British came to understand that it is in their interest to have good maps of Palestine (Goren, 2002).

### 3.1.2 The Palestine Exploration Fund (PEF) mapping

The establishment of the British Research Society of the Palestine Exploration Fund (PEF) in 1865 and its success later on have been attributed to a combination of factors (Goren, 2001): the renewal of Britain's strategic interest in Palestine and the intensification of English religious, missionary and scientific interest in the Holy Land/Palestine. The study objectives of the PEF focused on the archaeology, topography, geology and natural sciences of the Holy Land/Palestine, as well as the manners and costumes of the inhabitants of the land. These were accompanied by a renewed British national military interest (as was the case between the years 1865-1885 and 1909-1917) in Palestine. This interest triggered the involvement of the Royal Engineers Corps in the work of the PEF, both in funding its work and supplying the professional surveyors, with the aims of mapping the Holy Land/Palestine and gathering information (Moscrop, 2002). The highlight of the PEF's work in Palestine (which included archaeological work and the publication of a scientific journal: the Palestine Exploration Quarterly) is with no doubt the Survey of Western Palestine. The survey was conducted by a small group of professional surveyors from the Royal Engineering Corps, and was first led by captain R.W. Stewart and Mr. Charles F. Tyrwhitt Drake (1871-1872), then by lieutenant Claude Reignier Conder (1872-1875) and finally by lieutenant Horatio Herbert Kitchener (1877).
A detailed description of the surveying process is given in various sources (Conder and Kitchener, 1881-1883; Shatner, 1951; Elster, 1956; Gavish, 1991; Hodson, 1999; Gavish, 2005) and provides the following information regarding the maps:

- The scale of the final maps was an inch to the mile (1:63,360), and they included 26 sheets (Conder and Kitchener, 1880). The size of the sheets is 55*x*44 cm., covering 15' from north to south and 22' from east to west, with each sheet covering an area of ~970 sq.km.
- All the maps were based on a projection devised by Sir Henry James (Director General of the Ordnance Survey, from 1854 to 1875; the exact type of this projection is not known, see Hodson, 1999) using a central meridian of 35º15' east of Greenwich, a perpendicular of 32ºN, and the Clarke 1866 reference ellipsoid (Hodson, 1999; Mugnier, 2000).
- Although based on triangulation, the detail had been surveyed using compass and cavalry sketching board (Close 1932, as cited by Colleir, 2002).

The features depicted on the maps reflect their dual purpose, describing both the contemporary topography as well as the conditions in the Biblical and Classical eras (Hopkins, 1968). Topography was depicted using light-brown shading (replaced by an unattractive light-black shading in a later edition), based on the principle of "the steeper the darker", a method common to the so called "British National Style" of the first half of the 19th century (Jones, 1974; Hodson, 1999; Collier et al., 2003). Built-up areas were depicted in red with little detail. Hydrographic elements were shown in cyan, and vegetation types and geographic names in black (see Figure 1 – for extracts from the PEF maps and symbology used on the map). Special emphasis was given to local geographic names and these were placed on the maps and listed alphabetically in a special index (with a total number of about 9,000 names).

Forty years later, a new era in the mapping of Palestine began during World War I with the extensive use (by both the German and the Australian and British forces) of aerial photographs for producing town maps and updating the PEF maps (Amiran, 1953; Gavish and Biger, 1985; Collier, 1994; Kedar, 1999; Mugnier, 2000). The establishment of the Department of Surveys in Tel-Aviv under the British Mandate in 1920, where the main offices of the Survey of Israel are located to the present day, led to a new triangulation and survey of Palestine, which replaced the PEF map. A detailed history of the development of the British mapping during the Mandate is given by Gavish (1991, 2005).

### 3.1.3 Previous Accuracy assessments of the PEF maps

Today the PEF maps are highly regarded for their accuracy of measurements, their completeness in describing the hydrographic and archaeological landscape, and for their construction of local toponymies. These maps were considered the best maps of the Holy Land/ Palestine for at least 50 years, serving as a basis for updated and new maps, e.g. in the time of World War I and for archaeological surveys (Elster, 1956; Hopkins, 1968; Gavish, 1991; Frankel, 1998; Hodson, 1999; Gavish, 2005). The difference in the calculated and measured lengths of the check base of the triangulation on the Plain of Esdraelon was a mere 0.03%, and this was regarded at the time as a proof for the accuracy of the survey (Hodson, 1999).

There appears to be little work to date however, that has attempted to determine the horizontal and vertical accuracy of the PEF maps as a whole, with the exception of several localized studies (e.g. Frankel, 1998; Ben-Porat, 2003). The PEF maps were used by Warren (1880) as base maps to check the errors in latitudes and longitudes of places taken during his 1867 reconnaissance. Based on this work Warren estimated that 60 out of 134 stations and other well-defined points of his survey were within an expected error limit of 20 seconds latitude and

longitude (equivalent to ca. 26m).

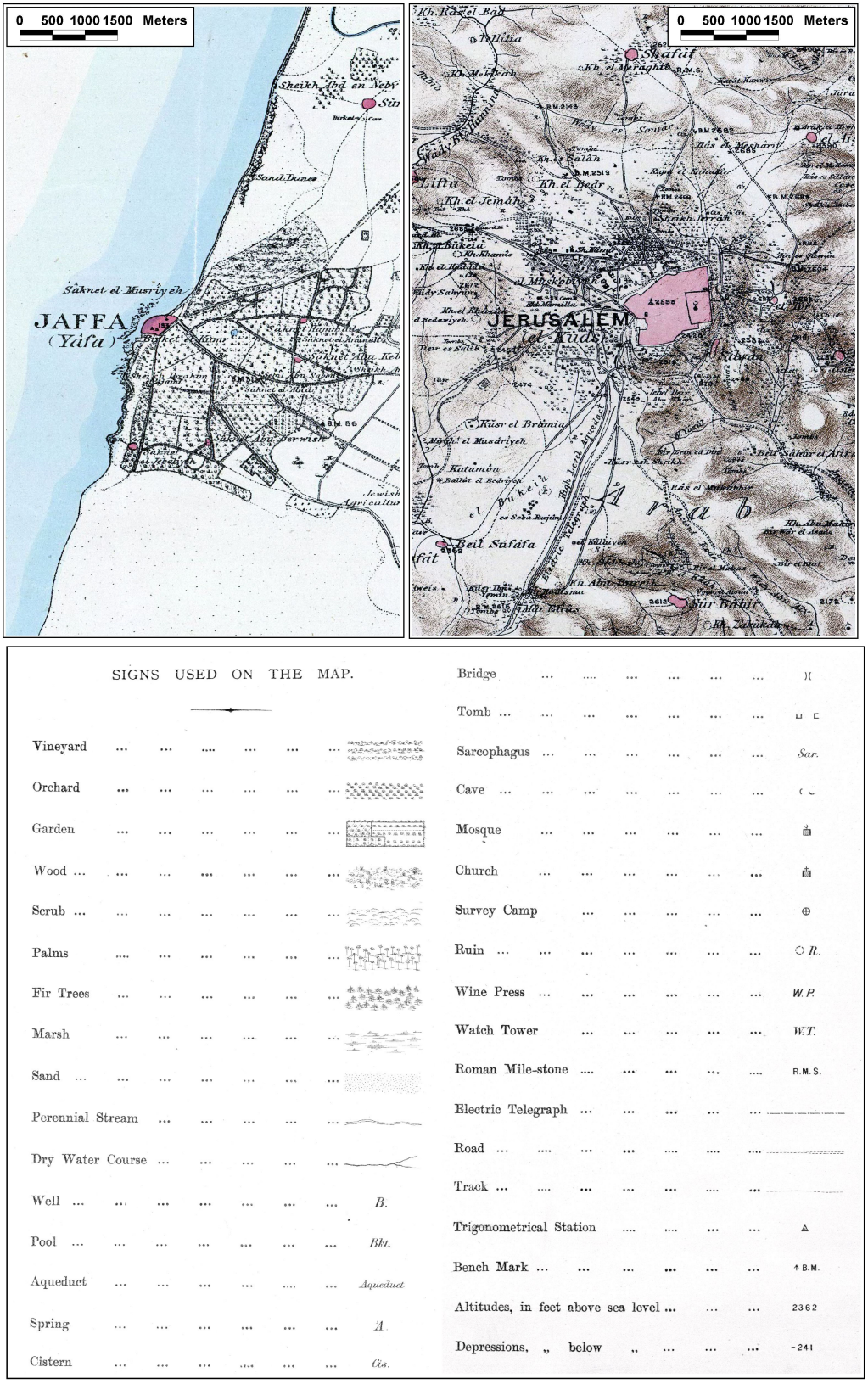


**Figure 1**: Examples of the symbology used on the PEF map: extracts of the map from the areas of Jerusalem and Jaffa, and the table of signs used on the map.

Errors were attributed largely to those places which could not be observed directly from the surrounding hills, and therefore could only be fixed by a series of compass observations. Hopkins (1968, p. 33) contains a brief quantitative evaluation of PEF map horizontal accuracy stating: "A cartotest on the PEF map revealed a block shift of 19 seconds to the west and an average discrepancy of 1.1 seconds to the north in latitude, when compared with the 1:100,000 maps of the Survey of Palestine". Relating to vertical accuracy he reported that: "A check on the heights shown on the Samaria sheet revealed an average difference of 35 feet compared with the corresponding Survey of Palestine map". No further details are given by Hopkins (1968) regarding the methods used to calculate these figures.

## 3.2 Materials and methods

### 3.2.1 Scanning the maps

The 26 sheets of the PEF maps were obtained digitally as JPG files at a resolution of 300 dpi from the Jewish and National University Library at Jerusalem. The coastal sheets of the British 1:20,000 mandate topo-cadastral maps were obtained by Frumkin-Ahiron et al. (2003) from the library of maps at the Department of Geography and Human Environment, at Tel-Aviv University, and scanned at a resolution of 150 dpi creating JPG files. These maps were then rectified to Israel's new grid (Israel Transverse Mercator; see Mugnier, 2000), and digitized to create a GIS layer of the coastal land cover ca. 1930 by the GIS unit of the Society for the Protection of Nature in Israel, as part of a report describing the changes taking place over Israel's coastal dunes in the past 60 years (Frumkin-Ahiron et al., 2003). The survey of these maps began in 1928 using plane tables and their publication followed the surveys immediately. Thus, most of the 1:20,000 mandate topo-cadastral coastal sheets used were published between 1928-1932. As the year of survey is not always mentioned on them, it was assumed that their land cover relates to the year 1930 (±2 years).

Finally, for the collection of control points (CPs) from modern maps, I have used a digital version of the 1:50,000 topographic maps of the Survey of Israel from the 1990s, scanned at a resolution of 150 dpi and registered to Israel's new grid, distributed within Turbo CD 4.0 software (2002; accessed: http://www.pazlogistics.com).

### 3.2.2 Piecing together the 26 sheets

Prior to the collection of CPs from the PEF maps, all were put into one file. As the exact type of the projection used is not known (Hodson, 1999), I have rectified each one of the 26 sheets to geographic (longitude/latitude) coordinates, as these are given along the edges of the maps, at

intervals of 10 seconds. To that end, in most cases 24 CPs were collected from each sheet, ~16 of them along the edges and from the corners of the sheet, and ~8 from the sheet's interior, at the crossings of longitudes and latitudes (according to the tics of longitude and latitude drawn along the maps edges). Figure 2 identifies the distribution of the CPs over sheet number six.

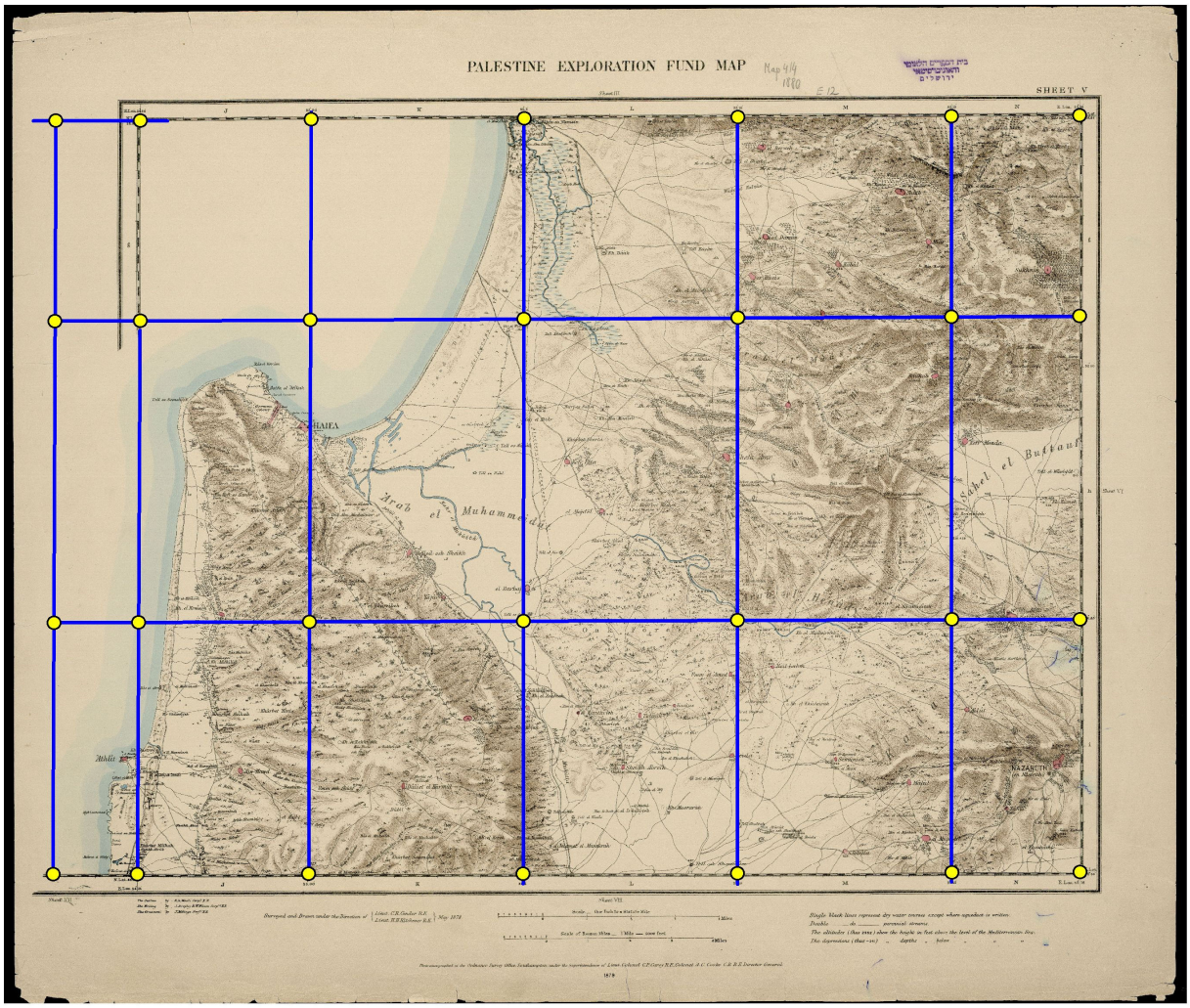


**Figure 2:** The distribution of CPs over PEF map sheet number six, as an example for the CPs used for the rectification of the scanned sheets to the geographic grid (longitude and latitude coordinates).

To account for non-systematic bending, stretching, shrinking or local deformations that might have occurred to the paper on which the PEF maps were printed, I applied a local affine transformation (a facet model), using the triangulation method (which is actually a piecewise 1$^{st}$ degree transformation) available in ENVI 3.4 remote sensing software package (Research Systems, Inc., 2001), as recommended also by Shimizu and Fuse (2004).

To preserve the original resolution of the scanned maps, the spatial resolution of the individual sheets following the rectification was set to 0.00004 decimal degrees (~ 4 metres). All the rectified sheets were then pieced together to form one file, its dimensions being 38,334 columns

over 56,250 rows, weighing 6.3 GB before compressions, and 240 MB after being compressed to the ECW (ERMapper Compress Wavelets technology; accessed: http://www.ermapper.com) format.

### 3.2.3 Collection of Control Points

Control Points (CPs) were collected from the PEF maps in comparison to 1:50,000 topographic maps of the Survey of Israel, while along the coast 1:20,000 topographic British Mandate maps were also used. Altogether 1,150 CPs were collected, 1,093 CPs from the 1:50,000 maps, 57 CPs from the 1:20,000 maps. The CPs collected included all 166 triangulation stations (and some bench marks) depicted on the PEF maps (even if they were not identified in contemporary maps), and other features (e.g. mosques, buildings, springs, etc.). The rectification of the maps was done once with all matched CPs (n = 1,104 after the omission of CPs whose identification was either vague or lacking). Following Crowell et al. (1991) the maps were also rectified using only the well defined set of the triangulation stations CPs (n = 123 after the omission of CPs whose identification was either vague or lacking, or that their error was greater than 200m). In Table 2 a summary description is given for all those 1,104 CPs that were used for rectifying the maps and for analyzing their accuracy. The distribution of these CPs is given in Figure 3.

### 3.2.4 Rectification of the PEF maps in three ways

The pieced together PEF maps (and the GIS layers digitized from them), were rectified from geographic coordinates (latitude and longitude) into Israel's new grid (Israel Transverse Mercator, or ITM, projection) using ENVI 3.4 (Reseacrh Systems, 2001) for the scanned maps, and Idrisi 32.2 (Clark Labs, 2002) for the digitized vector layers, in three ways:

- Standard map projection tools (using a bilinear interpolation) from geographic coordinates to Israel New Grid coordinate system (Israel Transverse Mercator, ITM projection; Mugnier, 2000). This method was used to assess the amount of a systematic shift existing in the PEF maps.
- Polynomial transformation of the 1$^{st}$, 2$^{nd}$ and 3$^{rd}$ orders (using a bilinear interpolation). This method was used both to analyze the accuracy of the PEF maps (using equations 1-6). However, as in this method a global transformation is applied to all the CPs, they do not coincide with their appropriate positions.
- A local affine transformation, as applied in the triangulation (with bilinear interpolation) method, in ENVI 3.4. This method ensures that each one of the CPs used is located exactly in its appropriate position, and has the advantage of giving a much better fit

between, for example, between the coastline on the PEF maps and the modern coastline. However, in this method rubber sheeting might change local orientations of features (see Figure 4 for an example). This transformation was applied twice, once using all 1,104 CPs and then when using only the well defined set of 123 triangulation stations. In both cases, 162 CPs were added at regular intervals of 1km (taking into consideration the block shift of the maps, as described below) along sandy and straight parts of the coastline assuming no changes in the orientation and location of the coastline since the PEF map, in order to force the coastlines to fit well.

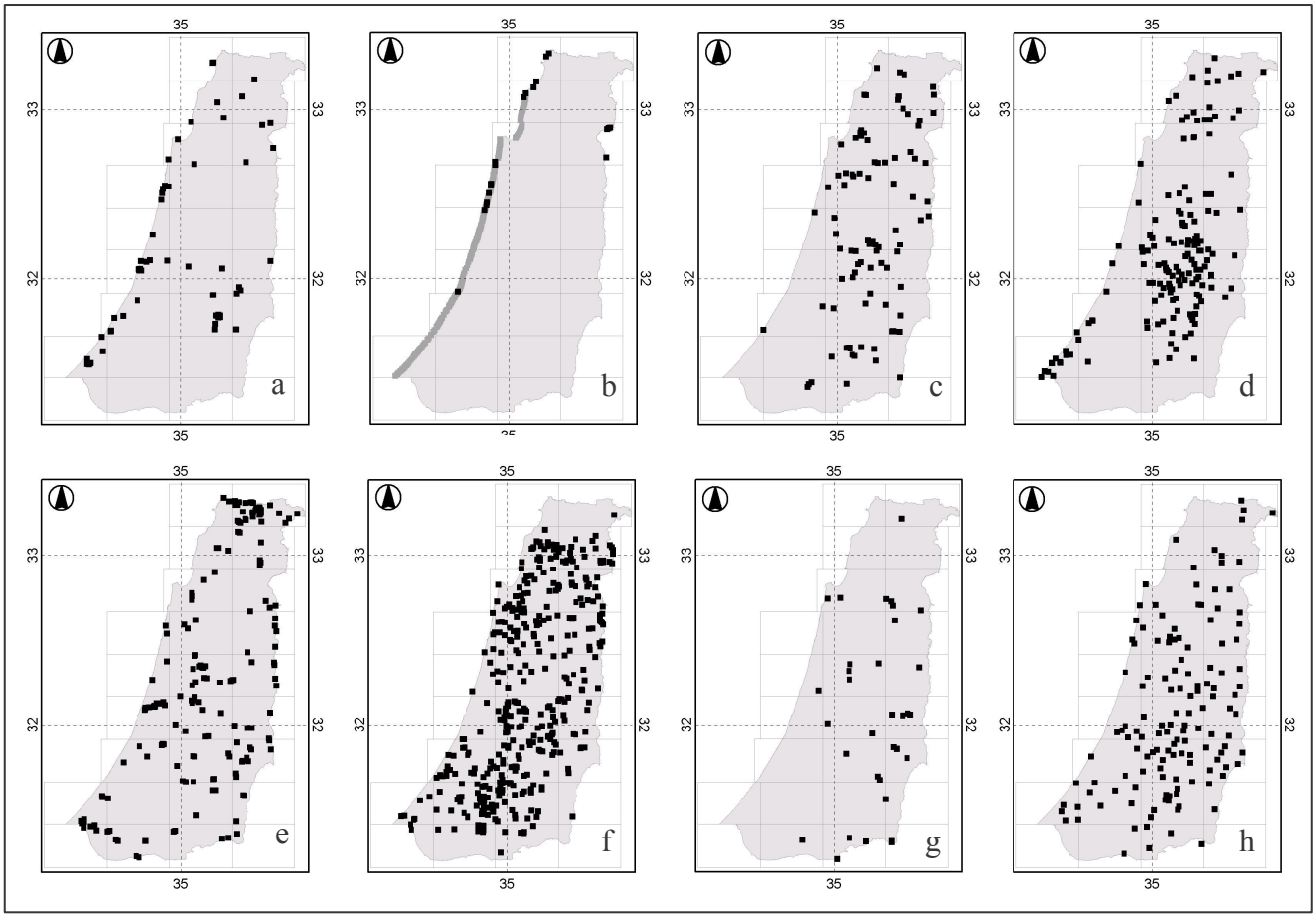


**Figure 3:** Distribution of the CPs used for the accuracy analyses. In the background are shown the extent of the PEF map and the layout of the 26 sheets. The CPs are shown separately for each type of feature, as follows: (a) Buildings; (b) Coastal features (the grey dots along the coast were only used for the local affine transformation, as explained in the text); (c) Hydrographic point features; (d) Mosques; (e) Hydrographic features along rivers; (f) Center points of polygonal features of ruins or settlements; (g) Topographic point features; (h) Trigonometric stations.

**Table 2**: Summary list of control and test points used in the map registration process and in the analyses of accurac

| Type | N collected from: | | | Vertical accuracy | | | Horizontal accuracy | | | Remarks |
|---|---|---|---|---|---|---|---|---|---|---|
| | 1:50,000 maps | 1:20,000 maps | Every 1km along sandy (non-built) coastline stretches | N with heights depicted both on PEF and 20th century maps | RMSE Heights (m) | Median vertical error (m) | RMSE Location (m), based on 1st order polynomial | | Median error in Location, based on 1st order polynomial | |
| | | | | | | | N=123 | N=1104 | N=123 | |
| Buildings | 49 | 21 | | 3 | 56.1 | 17.2 | 222.6 | 220.9 | 107.6 | Buildings, walls, road junctions in built areas, bridges, etc. |
| Coastal features | 23 | 2 | 162 | | | | 363.0 | 355.3 | 219.7 | Bending points of the coast, islands |
| Hydrographic point features | 92 | | | | | | 270.5 | 266.5 | 184.2 | Springs, wells |
| Mosques | 144 | 16 | | 7 | 21.6 | 12 | 202.1 | 201.0 | 121.7 | |
| Hydrographic features along rivers | 180 | 8 | | | | | 340.6 | 341.1 | 225.5 | Confluence of two rivers, bending points of rivers |
| Center points of polygonal features of ruins or settlements | 390 | 9 | | 59 | 49.2 | 12.8 | 284.5 | 283.8 | 181.6 | |
| Topographic point features | 34 | | | 16 | 19.7 | 18.7 | 352.5 | 338.3 | 166.3 | Mountain tops, cliffs, caves |
| Trigonometric stations | 135 | 1 | | 102 | 14.4 | 10.9 | 164.3 | 165.9 | 56.3 | |
| Trig stations subset used for registration | 122 | 1 | | | 14.8 | 11.0 | 74.4 | 80.3 | 51.7 | |
| Total | 1047 | 57 | 162 | 187 | 31.3 | 11.6 | 272.6 | 271.2 | 153.6 | |

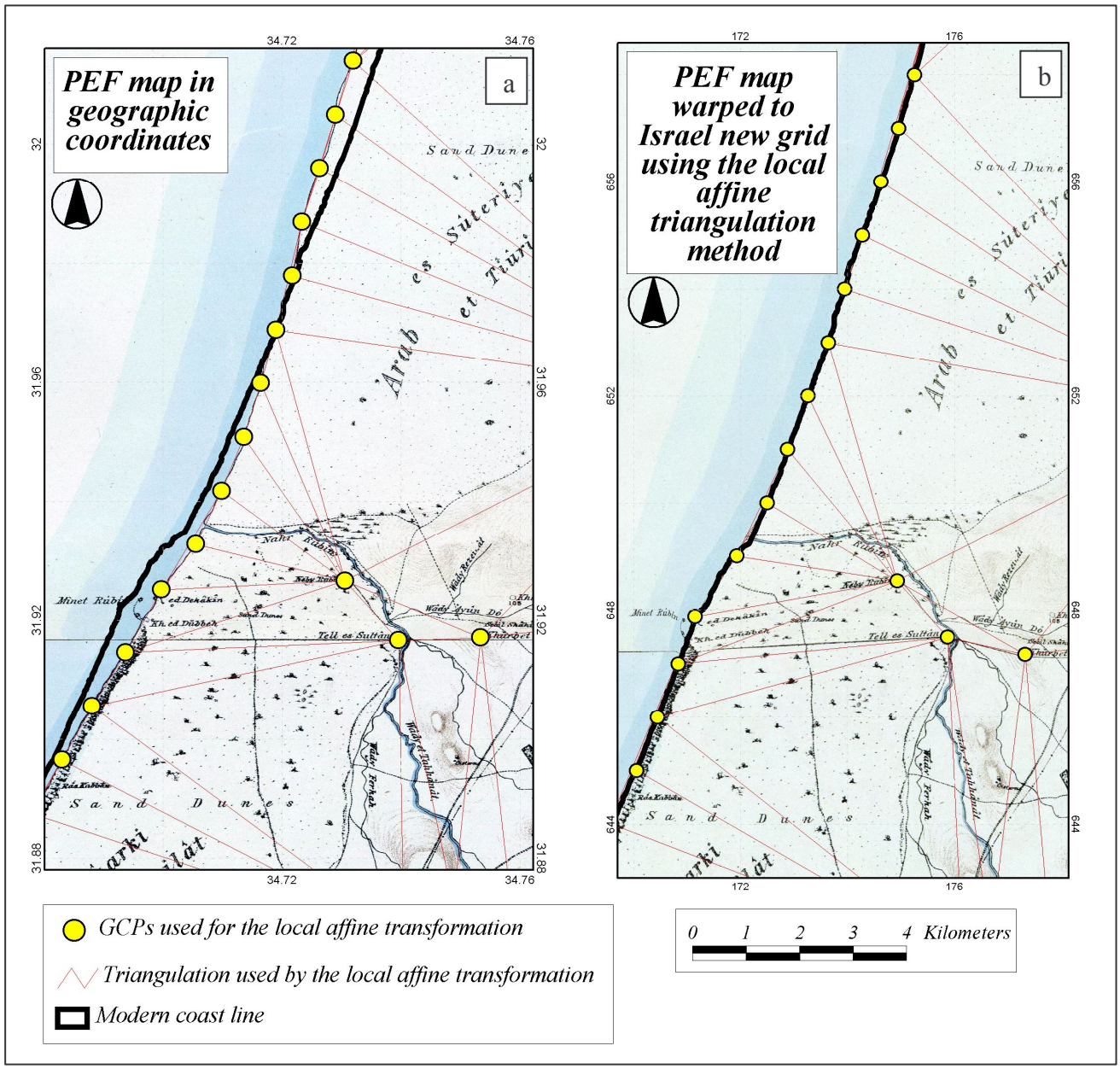


**Figure 4:** Warping of the PEF map using the local affine transformation, as applied in the triangulation method in Envi 3.4 software: (a) The mosaicked PEF map in geographic coordinates, overlaid by the modern coastline. Notice the inconsistent discrepancies between the modern and the PEF coastlines, in this part of the map (North west of the village of Yebnah); (b) The local affine warped version of the PEF map. Notice the perfect fit achieved between the two coastlines.

### 3.2.5 Accuracy Assessments

I have performed three types of accuracy assessments, as recommended by Zitova and Flusser (2003): (1) Calculation of RMSE for each of the types of CPs collected; (2) When only a subset of the 123 triangulation points were used as CPs, and the remaining subset of triangulation points as well as other groups of CPs serving as test points (TPs) and their RMSE was assessed; (3) In addition, different transformations were compared

with respect to their RMSE and land cover changes: 1st. 2nd and 3rd order polynomials, as well as a piecewise linear transformation (triangulation).

| Sheet no. | Number of CPs | 1st degree RMSE (metres) | 1st degree RMSE (mm) |
|---|---|---|---|
| 1 | 24 | 24.5 | 0.39 |
| 2 | 24 | 22.0 | 0.35 |
| 3 | 37 | 22.9 | 0.36 |
| 4 | 22 | 26.8 | 0.42 |
| 5 | 24 | 26.8 | 0.42 |
| 6 | 28 | 36.5 | 0.58 |
| 7 | 24 | 13.6 | 0.21 |
| 8 | 28 | 31.7 | 0.50 |
| 9 | 24 | 20.1 | 0.32 |
| 10 | 24 | 20.9 | 0.33 |
| 11 | 28 | 19.7 | 0.31 |
| 12 | 24 | 18.8 | 0.30 |
| 13 | 24 | 13.4 | 0.21 |
| 14 | 24 | 30.5 | 0.48 |
| 15 | 24 | 17.2 | 0.27 |
| 16 | 32 | 29.4 | 0.46 |
| 17 | 24 | 19.9 | 0.31 |
| 18 | 24 | 27.9 | 0.44 |
| 19 | 21 | 19.2 | 0.30 |
| 20 | 28 | 35.8 | 0.57 |
| 21 | 24 | 18.8 | 0.30 |
| 22 | 21 | 30.5 | 0.48 |
| 23 | 22 | 19.6 | 0.31 |
| 24 | 28 | 18.3 | 0.29 |
| 25 | 24 | 21.5 | 0.34 |
| 26 | 21 | 34.6 | 0.55 |
| **Total** | **652** | **24.7** | **0.39** |

**Table 3**: RMSE of CPs collected for the rectification of the 26 sheets prior to their piecing together in geographic coordinates.

## 3.3 Results: the horizontal and the vertical accuracies of the PEF maps

Figure 5 presents the mosaicked map in geographic coordinates. Table 3 lists the RMS value of the CPs collected for each one of the 26 sheets. The average potential error introduced therefore is 24.7 metres; this error seemed reasonable, as this figure is equal to only 0.39 mm for a map with a scale of one inch to the mile. As a piecewise linear transformation was used to warp each on of the sheets into geographic coordinates, it had forced adjacent sheets to meet well as shown in several examples in Figure 6 (showing selected meeting places of adjacent sheets). Notice however the existence of discontinuities between some of the sheets, resulting from variation in the symbology applied to the same features, or due to different interpretations of the landscape, as is the case with the depiction of the oak forest between sheets 10 and 13, or with the depiction of the coastal dunes and the open forest between sheets 7 and 10. However, between most of the sheets and for most of the features, there is an excellent continuity between adjacent sheets. Figure 7 presents a scatter plot showing the differences between the positions of the 123 triangulation stations CPs as depicted on the PEF maps (when projected from the original geographic coordinates to Israel Transverse Mercator grid without using any CPs), with respect to their true location on the ITM grid. From Figure 7 as well as from Table 2 several patterns emerge:

a) A systematic shift does exist in the PEF maps, being on average 481 metres (18.3 seconds) to the west, and 85 metres (3.1 seconds) to the north (as calculated from the 123 triangulation stations using a conformal projection, assuming no rotation and no scaling). These figures are similar to those reported by Hopkins (1968): a block shift of 19 seconds to the west and 1.1 seconds to the north.

b) The average registration error, based on the RMSE calculated from 123 CPs of triangulation stations is 74.4 metres, when a $1^{st}$ order polynomial is applied (for $2^{nd}$ and $3^{rd}$ order polynomials the registration error decreases to 70.4m and 67.0m, respectively). These figure are reasonable, given:
(1) the error introduced during the registration stage of the individual sheets into geographic coordinates (24.7m);
(2) the total error introduced in secondary methods of data collection, equal to 0.81mm in the worst case scenario (Thapa and Bossler, 1992). For the 1:63,360 PEF map this equals 51.3m, and for the current 1:50,000 topographic maps this equals 40.5m.
(3) altogether this error accumulates to: $( 24.7^{2} + 51.3^{2} + 40.5^{2} )^{0.5} = 69.9$m.

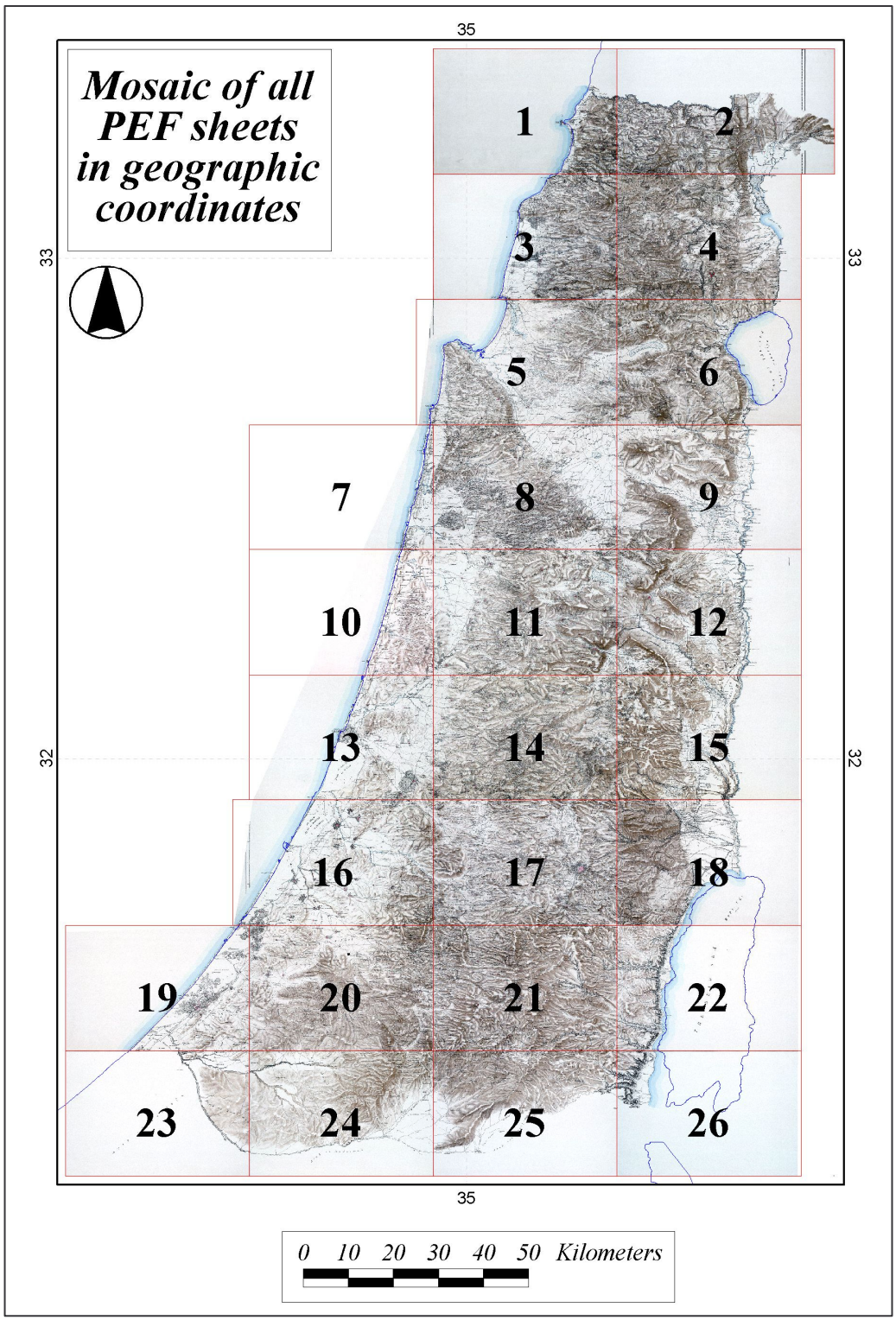


**Figure 5:** The full mosaic of all the 26 sheets of the PEF, in geographic coordinates, overlaid by modern coastlines (notice the changes in the coastline of the Dead Sea).

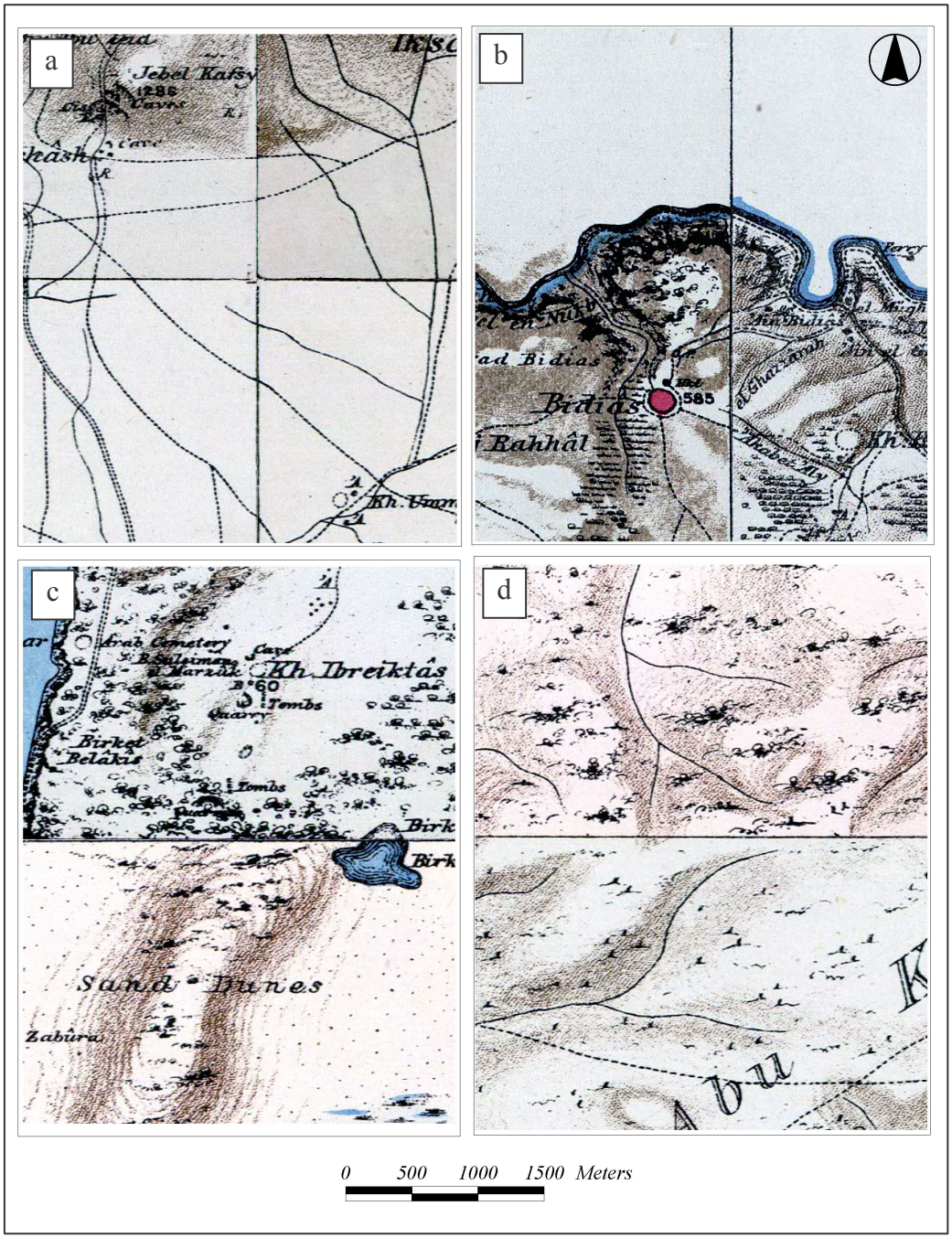


**Figure 6:** Examples of places where adjacent sheets meet (a) Sheets 5, 6, 8 and 9. Notice the fine continuity of the linear features between the sheets; (b) Sheets 1 and 2. Notice the change in the symbology of the perennial river. While on sheet 1 the blue coloring is below the river, on the right sheet it is above the river; (c) Sheets 7 and 10; Notice the change in the interpretation of the landscape; on the southern sheet a symbol of sand dunes is used, while on the northern sheet, an area of stabilized dunes with trees is drawn; (d) Sheets 10 and 13. Notice that in the northern an open oak forest is depicted, while on the southern sheet the trees are cut down, and only stumps are left.

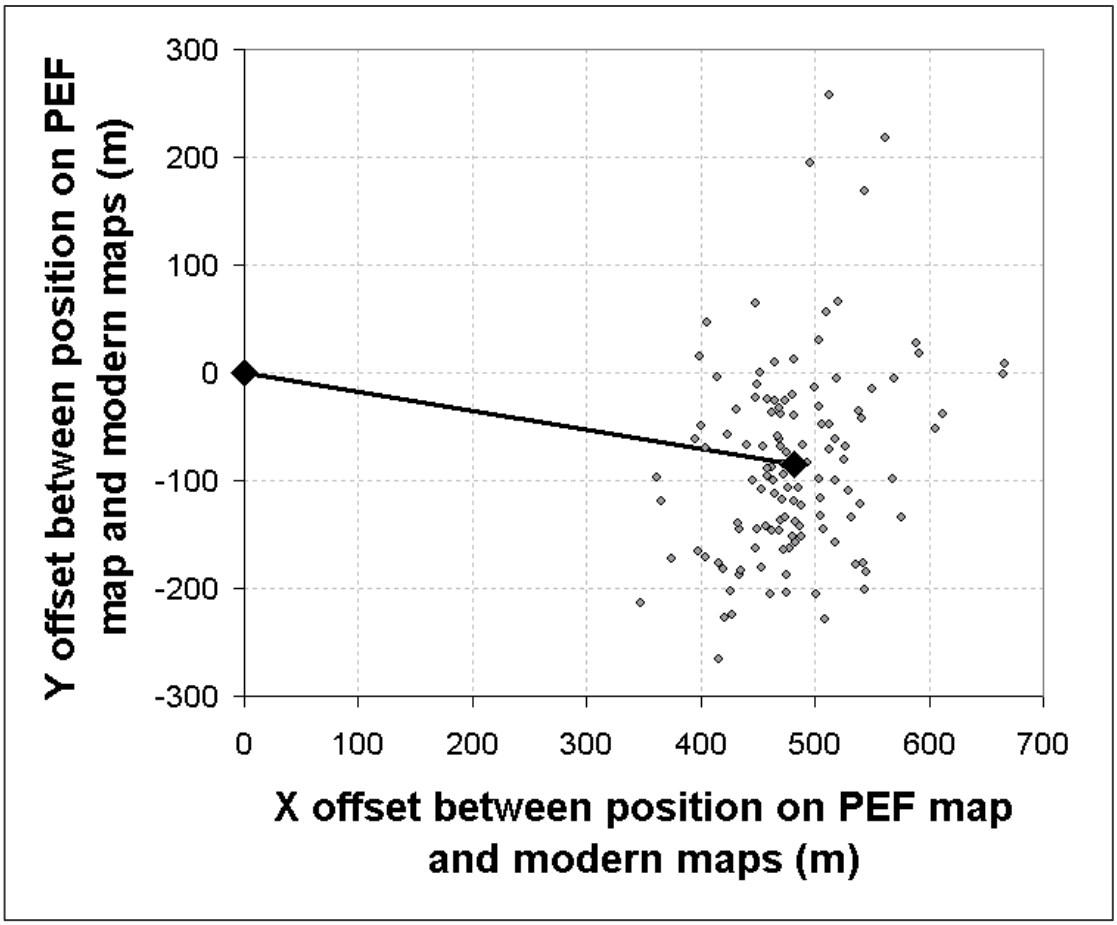


**Figure 7:** A scatter plot showing the differences between the positions of the 123 triangulation station CPs as depicted on the PEF maps, with respect to their true location on the ITM grid. Notice the systematic shift in the positions of features in the PEF map.

c) When the 123 triangulation stations were randomly partitioned into two subsets, one serving for calculating a 1st order polynomial transformation (n = 63), and the other serving as test points (n = 60), the average RMSE of the test points was 78.0m (standard deviation of 5.1m, given 30 runs).

d) When all other collected CPs were used as test points, it can be seen that different features were mapped with different accuracies, in the following decreasing order (of median RMSE in location; see Table 2): (1) Trigonometric stations, buildings, mosques, topographic point features, central points of ruins, hydrographic point features, coastal features and hydrographic features along rivers. The RMSE of all test and control points combined together was 272.6m (the median being 153.6m). The results of 2nd and 3rd order polynomials were almost identical to those obtained with the 1st order polynomial, and are therefore not shown.

e) The coastal features that were used as test points exhibited a rather large horizontal error (median RMSE of 219.7m). This may have an impact on estimates of dune movement analysis. However, as will be seen below, the dunes have advanced across a longer distance.

f) The errors in the positions of the CPs form a cloud of points, with no correlation between the errors in the X and Y axes. From this it can be concluded that a first order polynomial transformation is sufficient and there is no need to apply a higher order polynomial to the PEF maps (see Buiten and Putten, 1997). The four CPs that are outside the main cloud of points shown on Figure 7 were not excluded, as they are the only CPs located in the area of Lebanon and Mt. Hermon, to the north of all other CPs.

As for the average vertical accuracy of the PEF maps, the median error in heights, based on 187 CPs collected (for which the elevation was written on both the PEF maps and modern topographic maps), was found to be 11.6 metres (RMSE of 31.3 metres). This figure of vertical error closely resembles that mentioned by Hopkins (1968): 35 feet. The vertical error of the triangulation stations was found to be the lowest: only 10.9 metres (RMSE of 14.4 metres). Ben-Porat (2003) documents a vertical error of 68 m in the determination of the height of the Hula Lake as measured by the PEF surveyors, attributing it to an incident in which a barometer was broken and no calibration was performed. As before, different features were mapped with different vertical accuracies (see Table 2), in the following decreasing order (for median RMSE): Trigonometric stations, mosques, central points of ruins, topographic point features, buildings and central points of ruins.

As for spatial patterns, no correlation was found between either the horizontal or vertical errors of the CPs, with the variables of longitude, latitude or distance from the nearest trigonometric station.

The reasonable registration error of the map (RMSE=74.4m) with respect to the theoretical expected error (69.9m) suggested that it is possible to use the PEF maps to assess land cover changes. As historical maps have been widely used to study shoreline changes (Crowell et al., 1991; Morton et al., 2004), in this study I attempted to assess their potential use for studying dune dynamics. To this end, a detailed error (uncertainty) budget analysis was conducted, as will be described in the following part of this paper.

# 4. Analysis of landscape changes in Israel using the PEF maps: the coastal dunes as a case study

## 4.1 Background

Since the time when the PEF maps were constructed Palestine/Israel has and still is undergoing many changes in its land cover and land uses. One of the major changes results from the increasing development of open landscape areas (which intensified after the establishment of the state of Israel, in 1948): e.g., the extent of coastal dunes in Israel has diminished from 462 $km^2$ (Tsoar, 1990), to only 185 $km^2$ at the end of the 1990s (Frumkin-Ahiron et al., 2003), due in part to the quarrying of sand, and the construction of cities, military bases and water reservoirs. In addition, the remaining dunes are undergoing processes of stabilization by vegetation, due to changes in land use along the coast, mainly the ending of the practice of the "mawasi" agricultural system (in which the high level of coastal underground water was used for growing grapes, palm trees and other crops; see Tsoar and Zohar, 1985) and grazing by Arab and Bedouin local populations since the establishment of the state of Israel (Tsoar and Blumberg, 2002; Chapter 4 of this thesis).

This state of affairs however, was not always so. Sand dunes areas are dynamic in nature, changing in location, length, or height, depending on the dune type (Tsoar, 2001). Archaeological remains covered by coastal dunes indicate that aeolian sand started to encroach on the coastal plain of Palestine/Israel between the $7^{th}$ and $9^{th}$ centuries A.D. (Tsoar, 1990). This encroachment of sand is attributed by some to climatic changes (Issar, 1995; Issar and Yakir, 1997), or as claimed by Reifenberg (1947, 1950) and Rubin (1989), to soil erosion in Palestine, caused by changes in human land use, following the occupation of the area by the Arabs from the hands of the Byzantine Empire. The harbour of Caesarea, built by Herod 2,000 years ago, is an example where restricting sand movement resulted in the formation of sand dunes in Caesarea to the south and east (Reifenberg, 1951).

Shaped by the SW and W winter storm winds, the coastal dunes of Israel were formed as transverse dunes, advancing towards the northeast. Coastal dunes developed where aeolian sand was able to penetrate such as these areas where coastal sea cliffs did not exist or where breached by streams. Estimates of the rate of coastal dune movement in the 1940s and early 1950s range between 2-6 m/year (Reifenberg, 1947; Reifenberg, 1951; Tsoar and Blumberg, 2002; Chapter 4 of this thesis). However, during the early 1950s the dunes began to stabilize, their movement rate decelerating, and their shape changing from transverse to parabolic dunes (Tsoar and Blumberg, 2002). Estimates of the rate of movement of coastal dunes over longer periods of time, prior to their stabilization, may identify some of the factors that influenced their mobility

for more than millennia. Historical maps, such as those of the PEF and British Mandate maps, offer such a possibility.

## 4.2 Materials and Methods

### 4.2.1 Digitization of coastal land cover

Coastal land cover was digitized from both the PEF and the British Mandate maps, creating GIS layers of historical land uses and land cover along the coast.

### 4.2.2 Analysis of the average movement rate of the coastal dunes of Israel

Once all the maps were rectified into ITM projection and digitized, an analysis of the average movement rate of the dunes was performed, along six areas of coastal dunes in Israel (listed in Table 4). The areas were selected based on the criteria of an unambiguous depiction of coastal dune areas on both PEF and British Mandate maps. Two types of sand dune areas were therefore excluded from the analysis: (1) dune areas where various stages of vegetation succession exist, and therefore exhibited both areas of active dunes and stabilized ones (e.g. east and south-east of Caesarea), (2) dune areas where extensive areas of "mawasi" agriculture are depicted on the maps (PEF or British Mandate maps) – most of the southern coastal dunes of Israel).

The analysis of dune movement was done in the method developed in Chapter 4 of this thesis, summarized briefly below. For each dune area, the area of the dunes is calculated for both the PEF maps and the British Mandate maps. As the dunes in Israel advance towards the north-east (Tsoar, 1990), a polyline depicting the average dune front was interpolated. Across this line, the dunes were expected to advance. This line was automatically extracted as the skeleton line, using a vectorizing technique (Peuquet, 1981). This was applied to all polygons to the north and to the east (the direction in which the dunes are moving) of the area depicted in the PEF map as dunes, that resulted from a union operation performed between the dune areas digitized from both maps. Vectorizing was done using the Linevec command in Idrisi 32.2 (Clark Labs, 2002), and the resulting polylines were then generalized using the Linegen command (tolerance 25m) in Idrisi 32.2 (Clark Labs, 2002), following Douglas and Peucker (1973).

The yearly average movement rate of the dunes was calculated as follows (see Table 4):

(8) Average yearly movement rate =

(Area of dunes on British Mandate maps - Area of dunes on PEF maps)

/ Length of the dunes front

/ Number of years between the maps, 1874 (±3 years) to 1930 (±2 years) = 56 years

**Table 4**: Yearly average dune movement rates along six coastal dunes areas in Israel, from the north to the south.

| | Modern name of dune area | Akhziv | Bay of Haifa | Poleg | Rishon le Zion | Yavne | Ashdod | Total | Nilotic dunes | |
|---|---|---|---|---|---|---|---|---|---|---|
| | Northern limit (name depicted on PEF or British Mandate maps) | North of Wadi Hazirta | Nahr Namein | South to Bass el Hindi | Jaffa | Nahr Rubin | Nahr Sukereir | | Dunes belonging to the Nile littoral cell, excluding Akhziv | |
| | Southern limit (name depicted on PEF or British Mandate maps) | North of Nahr Mefshukh | Nahr el Mukutta | Nahr el Falik | Nahr Rubin | Nahr Sukereir | Ibtah River | | | |
| | PEF sheet number | 3 | 5 | 10 | 13 | 13 , 16 | 16 | | | |
| | | | | | | | | | | |
| **Map registration method and number of CPs** | 1st order polynomial, 123 CPs | 2.20 | **4.38** | **3.82** | **4.58** | **11.72** | **3.99** | **5.85** | **6.32** | **Dune movement rate (m/year), given in bold if above annual error** |
| | 2nd order polynomial, 123 CPs | 2.19 | **4.35** | **3.75** | **4.50** | **11.68** | **4.00** | **5.82** | **6.29** | |
| | 3rd order polynomial, 123 CPs | 2.20 | **4.34** | **3.78** | **4.40** | **11.60** | **3.89** | **5.76** | **6.22** | |
| | 1st order polynomial, 1104 CPs | 2.27 | **4.37** | **3.83** | **4.51** | **11.68** | **3.94** | **5.83** | **6.28** | |
| | Triangulation, 123 CPs +162 CPs every 1km along the coastline | 2.35 | **4.55** | **4.11** | -0.32 | **9.84** | **5.35** | **5.07** | **5.43** | |
| | Triangulation, 1104 CPs +162 CPs every 1km along the coastline | 2.23 | **3.79** | **5.43** | 0.98 | **4.39** | **5.40** | **3.78** | **3.98** | |
| | | | | | | | | | | |
| | Number of CPs in dune areas | 12 | 17 | 8 | 21 | 22 | 18 | 90 | 78 | |
| | Median RMSE of CPs in dune areas (m) | 140.9 | 166.0 | 59.8 | 231.1 | 403.2 | 172.6 | 185.2 | 193.4 | |

This analysis was performed for each of the transformations used, so that a comparison between the 1st, 2nd and 3rd order polynomial transformations as well as the local affine transformation can be done.

### 4.2.3 Uncertainty budget assessment for analyzing dune movement

Any accuracy (or more appropriately uncertainty) assessment of historic maps must consider the full range of uncertainty budget associated with the map. This includes not only the registration RMS, but also that associated with digitizing, surveying, interpolation, etc. Following similar studies that have estimated the error budget when mapping shoreline changes and cliff retreat rates based on historical maps and aerial photographs (Morton et al., 2004; Zviely and Klein, 2004; Shoshany et al., 1996; Crowell et al., 1991), or when estimating the accuracy of spatial data used in GIS (Thapa and Bossler, 1992) the following approach was adapted, such that the total error in feature position on any map is derived from:

$$Fp = \text{sqrt}\ (R^2 + S^2 + D^2 + FB^2) \qquad (9)$$

Where R = registration error (RMSE).
S = survey error (errors in mapping the dunes' boundary)
D = digitization error (errors in digitizing the dunes in GIS)
FB = feature boundary error (errors related to uncertainty in the dunes boundary)

The possible resolution of identifying annual changes in dune movement can then be derived using the following equation:

$$\text{Resolution} = \text{sqrt}\ (Fp_{map\ x}^2 + Fp_{map\ y}^2) / n \qquad (10)$$

Where Fp = Feature position error, defined above.
n = number of years between surveys/maps.

## 4.3 Results

### 4.3.1 Calculation of the possible resolution for dune movement analysis

Before reporting the results of dune movement rates, I first considered the possible resolution based on the maps used (i.e., the annual error in dune movement rate) as

estimated using equations 9 and 10 above). The assumptions for the **worst case** were the following (see Table 5):

1. For the PEF map, the **registration error** was 74.4m, which is equal to 1.17mm on the map. As the 1:20,000 British Mandate maps were rectified by Frumkin-Ahiron et al. (2003), it was assumed that they possess a similar registration error, equal to 23.5m in that scale.
2. Crowell et al. (1991) present an estimation of the **survey error** in shoreline mapping when this was done using plane tables prior to the use of aerial photography. This equals to 0.65mm on the map. When analyzing dune movement, survey errors may occur both at the shoreline and at the dunes edge. Summing these two possible error sources, arriving at 0.92mm on the map ($0.92 = (0.65^2 + 0.65^2)^{0.5}$). For the British Mandate maps this equals 18.4m. As the PEF surveyors did not use plane tables but cavalry boards, that are considered less accurate, the possible error was further doubled to 1.84mm on the map, that is equal to 116.5m.
3. The **digitization error** as estimated by Crowell et al. (1991) is equal to 0.5mm on the map. Summing this value for each of the three possible errors in the digitization of both the shoreline, the dunes' edge and the average dunes front, an estimated digitizing error of 0.87mm was reached ($0.87 = (0.5^2 + 0.5^2 + 0.5^2)^{0.5}$), equivalent to 54.9m for the PEF map, and 17.3m for the British Mandate maps.
4. Finally, the **error in the boundary of the dunes**, is related to two types of errors:

   (a) Uncertainty regarding the time of the survey. The PEF survey began in 1871 and ended in 1877, whereas the topo-cadastral 1:20,000 maps along the coast were surveyed and published between the years 1928-1932. Taking the mid-year of each survey (1874 and 1930, respectively) there is an uncertainty of ±3 years for the PEF map and of ±2 years for the topo-cadastral maps. As dunes move, the location of the boundary may change depending on the year in which it was surveyed. Assuming that the dunes movement rate was then 4 m/year (based on estimates for ca. 1950, before the stabilization process of the Israeli coastal dunes began; Tsoar and Blumberg, 2002, and Chapter 4 of this thesis), the estimated error for the PEF map was 12m (0.19mm), and 8m (0.4mm)for the topo-cadastral maps.

**Table 5**: Maximum worst-case estimated measurement errors for coastal dune movement. Error values are given in metres, as well as in millimetres relating to the original maps used. See the text for detailed explanations.

| | Time period | | | | | |
|---|---|---|---|---|---|---|
| | PEF map (1:63,360) | | | British Mandate topo-cadastral maps (1:20,000) | | |
| Measurement errors | m. | mm | remarks | m. | mm | remarks |
| Registration error | 74.4 | 1.17 | 1st order polynomial based on 123 CPs of triangulation stations | 23.5 | 1.17 | Assuming same error in registration as with the PEF maps |
| Survey error | 116.5 | 1.84 | Assuming twice the error of British Mandate maps, due to the use of cavalry board and not plane tables | 18.4 | 0.92 | Based on estimated of Crowell et al. (1991) related to the original raw data error associated with shoreline mapping using plane tables (1880-1930) |
| Digitization error | 54.9 | 0.87 | Crowell et al. (1991) | 17.3 | 0.87 | Crowell et al. (1991) |
| Dune boundary error due to uncertainty in the time of the survey and the symbology | 64.5 | 1.02 | ±3 years, assuming movement rate of 4 m/year, and an additional average error of 1 mm in defining the dunes landward edge | 8 | 0.4 | ±2 years, assuming movement rate of 4 m/year |
| Total dune position error | 162.1 | 2.6 | | 35.4 | 1.8 | |
| Combined dune position error (m) | $165.9 = ( 162.1^{2} + 35.4^{2} )^{0.5}$ | | | | | |
| Resolution (annualized error), m/year | 2.96 = 165.9 / 56 | | | | | |

(b) The symbols used to delineate dune areas. The coastline on both maps is marked in unmistakable way. So is also the dunes edge on the topo-cadastral maps. On the PEF map however, although the dunes are clearly shown using a dotted area, their landward edge is sometimes clearly depicted using a dotted line (see Figures 1 and 4), but in some cases their exact landward boundary is not given. Out of all the length of landward dunes' edge analyzed from the PEF maps, 50% was well defined. In the other 50%, determination of the landward edge of the dunes was based on visual interpolation, connecting the landward points marking the dunes' area. Assuming an error of 2 mm in determining the landward extension of the dunes in such cases, and multiplying this by 50%, an additional error of 1mm is added to the PEF maps, reaching 1.02mm ($1.02 = (0.19^2 + 1.0^2)^{0.5}$), equivalent to 64.5m.

The root of the sum of the squares of these errors adds to 162.1m for the PEF map, and 35.4m for the topo-cadastral maps. The root of the sum of the squares of these errors is 165.9m. Dividing this figure by the number of years between the two surveys, 56 years, results with a possible detecting resolution (annual error) of 2.96m/year.

### 4.3.2 Coastal dune movement analysis

All of the six areas of coastal dunes analyzed, exhibited a net increase in the size of the coastal dune area, regardless of the method used for registering the maps, thus indicating dune movement. This can be clearly seen both in the maps of each of these regions, given in Figure 8, and in the numeric figures given in Table 4. However, this should be checked with respect to data resolution, as calculated above. Indeed, the movement rate of the Akhziv dunes (2.19-2.35 m/year) is much lower than the worst case estimate of the annual error (2.96 m/year). These dunes are outside the area of the Nile littoral cell (Almagor et al., 2000), and are mainly composed of calcium and not of quartz (Emery and Neev, 1960), in contrast with all the other coastal dunes areas included in this study. The Akhziv dunes have not been studied much (however, see Bowman, 1972). These dunes may be less mobile than the other dunes due to (1) their higher content of carbonates (90%) leading to a coarser grain size both on the beach and on the dunes themselves with respect to those south of Acre (Nir, 1989; Emery and Neev, 1960); (2) The supply of sand along the coast of Israel diminishes with distance from the Delta of the Nile, and sand supply north of Acre is even lower than that reaching the bay of Haifa,

as it is mostly based on local sources of sand (Nir, 1989). As the sand supply is small, the dunes themselves and their thickness will be lesser (Bowman, 1972).

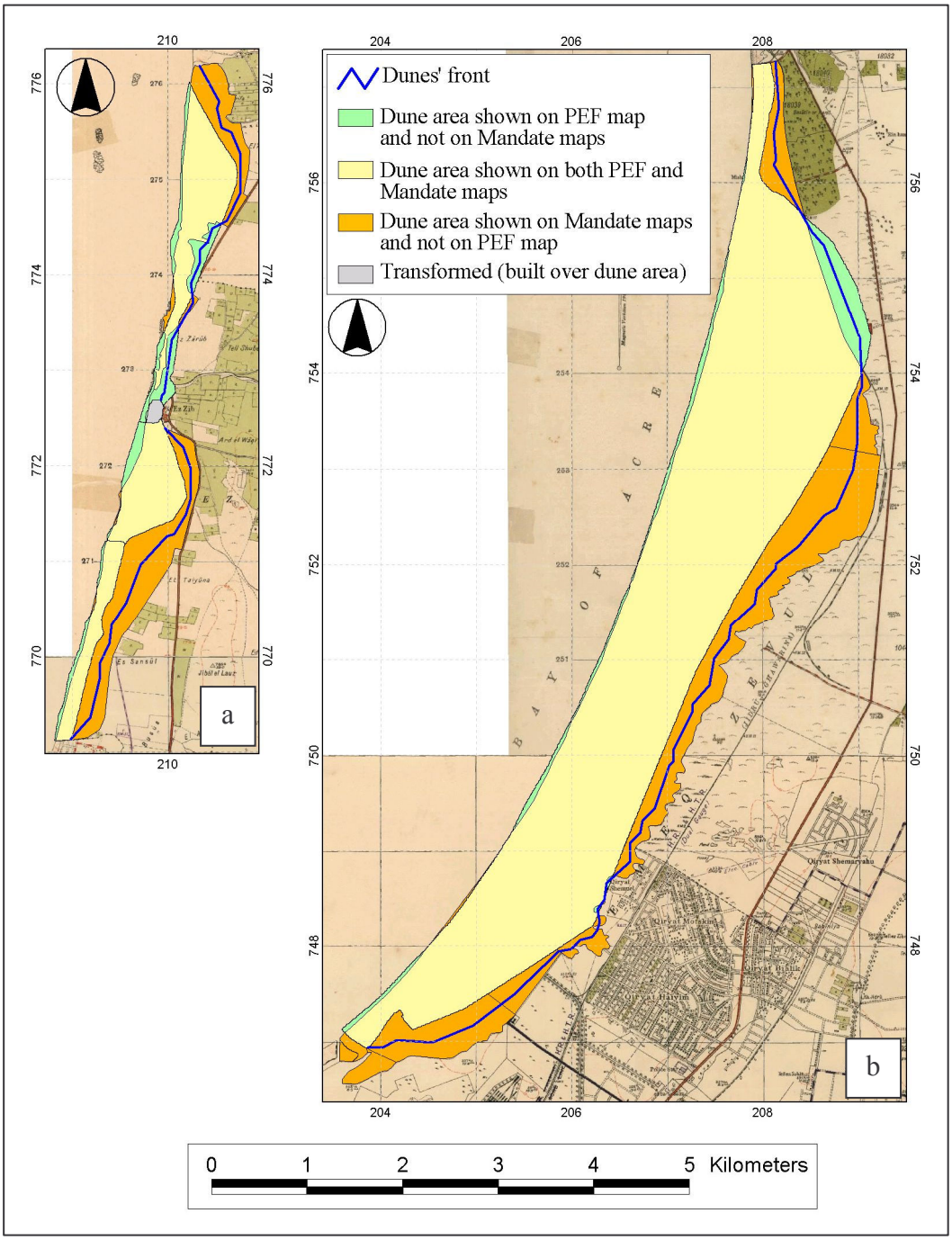


**Figure 8:** Analysis of dune movement between the 1870's to the 1930's, based on the PEF map (here shown is the digitized layer after a local affine triangulation based on all available CPs) and the British Mandate maps. Overlaying the 1:20,000 British Mandate maps, are GIS layers digitized from both maps, expressing the differences in dune areas shown on the maps, as listed in Table 2. (a) Dunes of Akhziv; (b) Dunes of the Bay of Haifa; (c) Dunes of Poleg; (d) Dunes of Rishon le Zion; (e) Dunes of Yavne; (f) Dunes of Ashdod. The line of the dunes' front refers to the interpolated average location of the dunes' landward edge, based on both maps (see text for details).

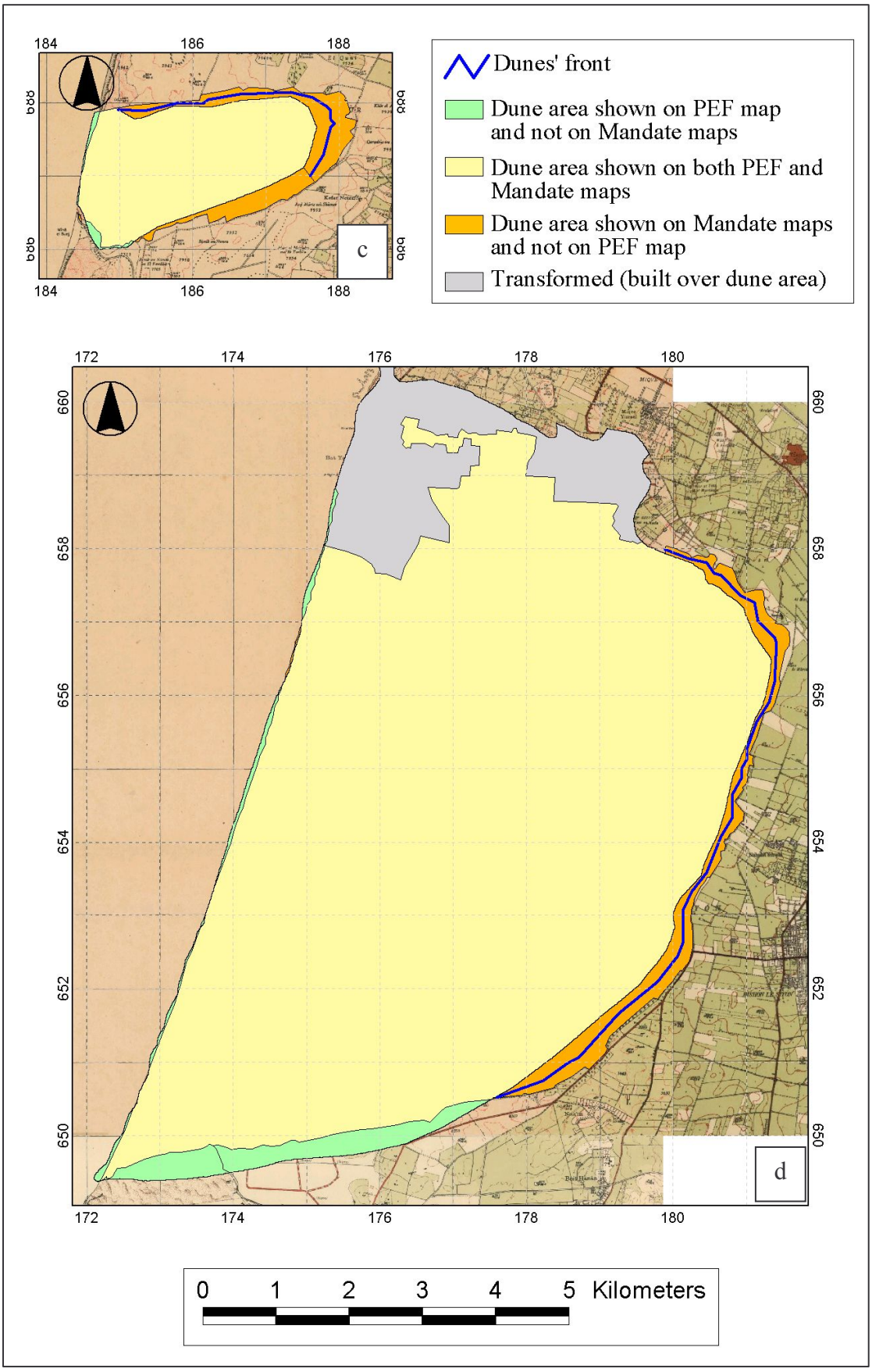
184
186
188
664
662
660
c
Dunes' front
Dune area shown on PEF map and not on Mandate maps
Dune area shown on both PEF and Mandate maps
Dune area shown on Mandate maps and not on PEF map
Transformed (built over dune area)
172
174
176
178
180
660
658
656
654
652
650
d
0 1 2 3 4 5 Kilometers

**Figure 8 c,d**

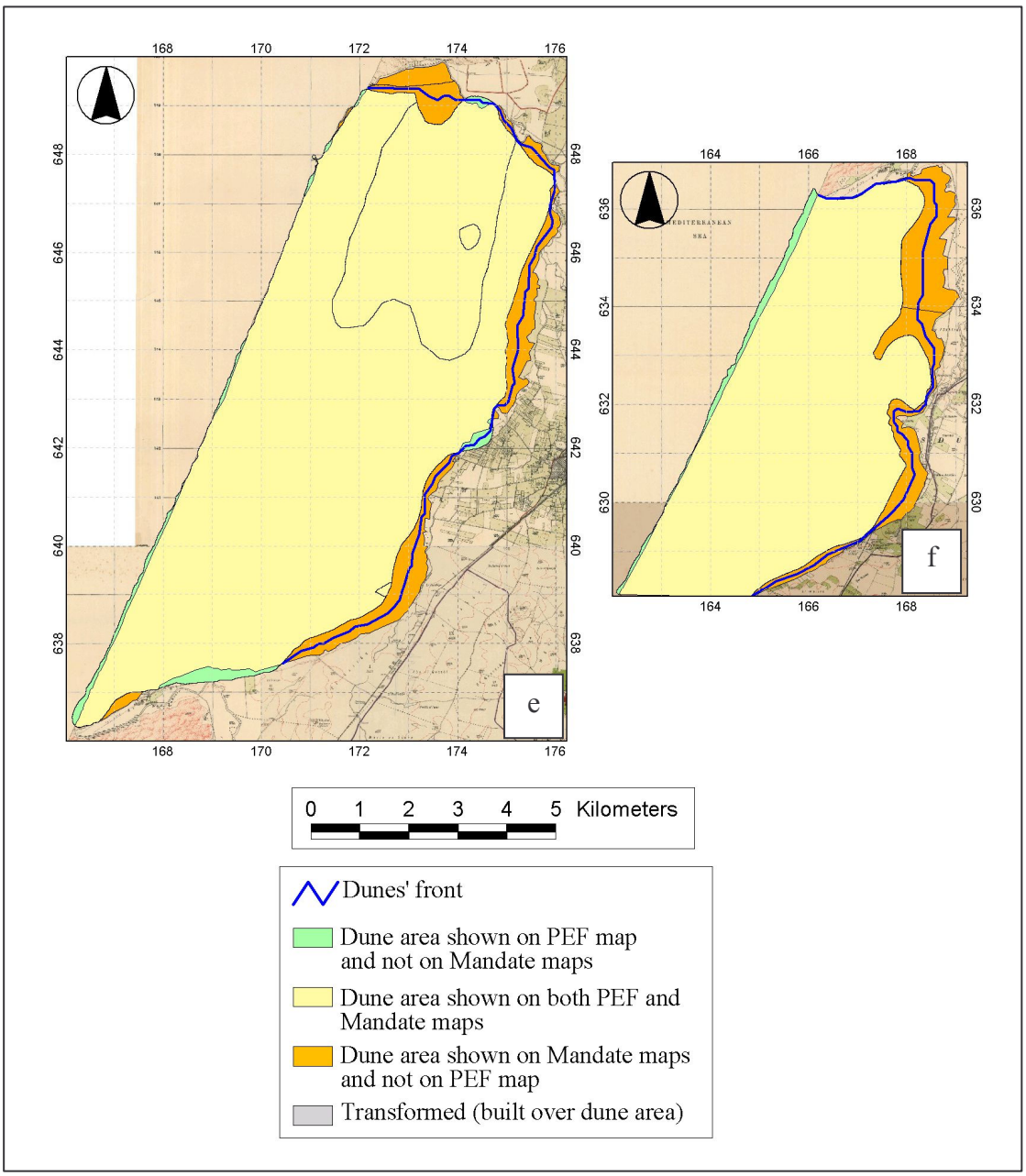


**Figure 8 e,f**

This, combined with their coarser grain size, may lead a lower drift potential and higher stabilization rates. The Akhziv dunes will be therefore excluded from the following analysis.

Overall, the average distance over which the dunes belonging to the Nile littoral cell advanced between 1874-1930 was found to be between 223-354 metres (depending on the registration method used).The corresponding yearly rate of advance of 3.98-6.32 m/year (depending on the registration method used) is thus well above the worst case estimate of annual data resolution error (2.96 m/year).resulting from the different map registration methods are given in Table 5, as are the accuracies of the CPs corresponding

to the areas of the dunes analyzed (the points that formed the local affine triangulation transformation around each of the dune areas). Notice that when using polynomial transformations, the dune movement rate figures were quite stable regardless of the polynomial order used, and regardless of the number of the CPs. However, when a local piecewise affine (triangulation) method was used, with additional CPs placed along sandy stretches of the coastline (forcing it to fit to the present date coastline), estimates of dune movement rates changed. In fact, the two areas that exhibited largest differences in dune movement rates (Rishon le Zion and Yavne) were also the two areas in which largest errors in CPs were found (median RMSE of 231.1m and 403.2m, respectively). The overall movement rate obtained (3.98-6.32 m/year) are close to estimates of dune movement reported in the literature (see Chapter 4 of this thesis; Tsoar and Blumberg, 2002; Reifenberg, 1951; Reifenberg, 1947) for the 1940s and 1950s, that were up to 6 m/year.

## 5. Discussion

Any accuracy (or more appropriately uncertainty) assessment of historic maps must consider the full range of uncertainty associated with the map. This includes not only the registration RMS, but also that associated with digitizing, surveying, interpolation, etc. Estimates of map uncertainty can then be calculated and reported in accordance with the principles of error propagation.

When comparing the positional accuracy of the PEF map (or any other historical map) with a modern map, and when analyzing land cover changes between the two maps, errors may result for various reasons:

1). **The source accuracy** of the historical maps which is comprised of the following:

- **Distortions** of the material (paper) from which they are made that occurred due to the printing process as well as with the passage of time. Deformation of the paper due to the printing process may amount to up to 1.25% in length and 2.5% in width (Thapa and Bossler, 1992).
- **Survey control** (rectification error of the map) – as in the case presented here, this is comprised of two stages: first rectifying each of the individual map sheets, and then of rectifying the mosaicked map.
- **Cartographic** – the scale of the map, the degree of generalization of features, the quality of the plotting/drawing process, and the type and size of the symbols used. The smaller

is the scale and the larger and less defined will be the symbols used on it, the greater will be the errors introduced.

Altogether the source accuracy of the PEF maps was found to be 74.4m (equivalent to 1.17mm), using a 1st order polynomial based on 123 triangulation stations CPs. Using 2nd and 3rd order polynomials further decreased the error to 70.4m and 67.0m (respectively), however it was preferred to use a 1st order polynomial, as no correlation was found between the x- and y-residuals (Buiten and Putten, 1997). This amount of error seemed reasonable, given the expected error of 69.9m when combining the registration RMSE of the individual sheets (24.7m), and the worst case scenario of errors in secondary methods of data collection (i.e. the maps from which the triangulation stations were collected and identified): 0.81mm (51.3m for the PEF map, and 40.5m for the topographic maps from the 1990s; see Thapa and Bossler, 1992).

2). **Interpretation uncertainty** that is comprised of the following:

- **Field survey** – the accuracy of the field survey, both with respect to the scale and details included in it, the time devoted to complete the survey, the surveying equipment, and the surveyors skills. Here we estimated for exaggeration that the PEF survey contains double the errors than with the topo-cadastral survey, as in the former cavalry boards and compasses were used, whereas in the latter plane tables were used for the field mapping. Following the estimation of Crowell et al. (1991) with respect to mapping the shoreline and with respect to the scale of the maps used in this study, the error in dune location on the British topo-cadastral maps was estimated as 18.4m (equivalent to 0.92mm), and 116.5m on the PEF map (equivalent to 1.84mm).
- **Digitizing** – this relates to both the resolution in which the map was scanned, and to the care and methods used to digitize the features of interest. In this study it relates to the digitization of the coastline, of the dunes landward boundary, and the interpolation of the average dunes' front in between the two. Following the estimation of Crowell et al. (1991) of a digitizing error of 0.5mm, and summing it three times (according to the law of propagation of errors) to account for digitizing errors of each of the above mentioned features, amounted to an error of 54.9m for the PEF map, and 17.3m for the British Mandate maps.

3). **Feature boundary visibility** – this relates to how well defined are the features both in the field, and then on the map. In this respect it may be stated that the line of advance of active dunes over non-dune areas is quite sharp, and is less ambiguous and less time-variant than the

location of the shoreline at a given moment in time. Nonetheless, to be on the safe side it was assumed here that the uncertainty in the position of both features is the same. As for the features visibility on the maps themselves, the coastline is a well defined feature, and so is also the dunes landward boundary in 50% of the cases, where it is lined by a dotted line (see Figures 1 and 4). Where this line was not so well defined on the PEF map, we estimated an additional error of 2mm (or 63.36m, after multiplying it by the maps' scale and by the percentage of the uncertain length). In addition, the feature boundary as seen by the surveyors depends on the time in which the survey, sue to the dynamics of shifting dunes. Assuming an uncertainty of three years for the PEF maps (1871-1877) and of two years for the topo-cadastral maps (1928-1932), and a movement rate of 4 m/year at that time, there was an additional error of 12m and 8m (respectively) for these maps.

Summing all these errors together led to an estimated error of 165.9m. This value was higher than the median RMSE of some of the features (trigonometric stations, buildings, mosques), similar to that of topographic point features, and lower than median RMSE found for springs, rivers and coastal features. When dividing the total estimated by the time period between the two surveys (1874-1930, 56 years), the resulting estimated annual resolution was 2.96 m/year. Thus, this is the minimum movement rate that can be reliably detected using this set of historical maps. Calculated movement rates for all but one of the dune areas analyzed were higher than this value (3.9-6.3 m/year, depending on the registration method used), thus indicating that the dunes were indeed active then. The only area whose estimated movement rate was within data noise was that of Akhziv – an area with different characteristics, as the source for its sand is not from the Nile river, rather local (Almagor et al., 2000).

Not only did the areas of coastal dunes analyzed present a net increase in their area, therefore indicating the expected inland penetration of the dunes towards the north-east, the overall value of dune movement rate calculated (3.9-6.3 m/year, depending on the registration method used) matched well with those reported in the literature for the British Mandate period and the years between 1944-1956: 2-6 m/year (Reifenberg, 1947; Reifenberg, 1951; Tsoar and Blumberg, 2002; Chapter 4 of this thesis). Nevertheless, over- and under-estimations of the dunes' movement rate values were found for two of the southern dune areas analyzed (Rishon le Zion and Yavne). It was only in these two areas that the median RMSE of the CPs in the dunes area was greater than 200 metres (due to inaccuracies in the measurement of the coastline there, when compared to the orientation of the modern coastline, assuming no changes between the

two). Thus, in areas where the local accuracy is lower, quantitative estimates of dune mobility (or of other spatial patterns in landscape changes) are less reliable. This may be estimated when comparing the results of different registration methods, as done in Table 5.

## 6. Conclusions

The following conclusions may therefore be drawn:

- When conducting a least-squares coordinate transformation, it is recommended that the number of control points to be four times the number of coefficients in the least-squares polynomial function (Mather, 1995). However, since the error distribution associated with well-defined points differs from that associated with non-descript points – more CPs are not necessarily better. As can be seen in Table 2, the RMSE of the different features remained the same, when using the well defined set of 123 triangulation stations as CPs, and when using all available 1,104 CPs.
- The average accuracy of a historical map may conceal local areas in which the accuracy is lower, resulting for example from problems encountered during field mapping. Local assessments of accuracies should be performed when only a part of the map is analyzed, in order to know how reliable that part of the map is with respect to the whole map.
- Local warping or rubber sheeting may insert large errors into the transformed map, when forcing it to fit points that were either misidentified by the user, or that were poorly mapped originally. Local warping may be therefore recommended in the following cases: (1) When rectifying a scanned map on which a coordinate grid is plotted, so that all intersections as well as the map border will be forced to their respective locations, in order to assure that adjoining sheets will meet well. (2) When rectifying an image that has local distortions, that are independent on the type of feature shown, as in images acquired by airborne platforms, due to its tilt as well as topography. (3) When wishing to allow a visual comparison of selected features between different maps (e.g. the coastline in this study), disregarding local distortions that may affect areas in between the features used for the transformation.
- The coastal dunes of Israel were indeed active during the 19$^{th}$ and early 20$^{th}$ century, experiencing a similar wind regime to that of the mid 20$^{th}$ century.
- Using an average figure of 5.1 m/year (between 3.9-6.3 m/year estimates of dune movement of the dunes belonging to the Nile littoral cell) and extrapolating backwards, presuming no major change in the climatic conditions, the current stage of coastal dunes in Israel has begun encroaching about 1,200 years ago, based on the maximum extent of

the coastal dunes, reaching about six kilometres south of Jaffa. This geomorphologic evidence resulting from an analysis of historical maps, confirms published estimations of the age of the coastal dunes of Israel (Tsoar, 1990), that are based on archaeological findings.

- The high level of mapping achieved by the Royal Engineering Corps surveyors, allows a reconstruction of the Holy Land/Palestine/Israel's geography as it was in the 1870s, just a few years before the great transformations it underwent, from a forgotten and neglected corner of the Ottoman Empire, into a modern country. However, it should be borne in mind that the accuracy of the map varies spatially, and for the different features depicted on it.

## Acknowledgments

I wish to thank Richard Cleave of Rohr Productions and the Jewish and National University Library at the Hebrew University of Jerusalem, for the scanned maps of the PEF, and Michael Winograd and Guy Nizry from the Department of Geography and Human Environment of Tel Aviv University for their technical assistance. I also thank Zvika Mednik of the Department of Geography and Human Environment, Tel Aviv University for the 1:20,000 British Mandate maps, and the GIS unit of the Society for the Protection of Nature in Israel, for the use of GIS layers relating to the coastal dunes of Israel. I also wish to thank Ruth Kark and Salit Kark from the Hebrew University of Jerusalem, and Michael Gilmont, for reviewing the manuscript. I thank Eyal Ben-Dor and Yuval Portugali from Tel Aviv University for using their lab facilities during this study. In addition I thank the anonymous reviewers for their helpful comments and contribution to the manuscript. This work was done as part of a Ph.D. thesis, in the Department of Geography and the Human Environment, at Tel Aviv University.

## References

Almagor, G., Gill, D., and Perath, I. (2000). ‘Marine sand resources offshore Israel’, Marine Georesources and Geotechnology, 18, 1-42.

Amiran, D. (1953). ‘Topographic maps of Israel from the days of World War I’, Eretz-Yisrael, 2, 33-40.

Ben-Arieh, Y. (1972). ‘The geographical exploration of the Holy Land’, Palestine Exploration Quarterly, 104, 81-92

Ben-Porat, A. (2003). 'The height of the Hula Lake: a survey error as a tool for determining the genealogy of maps', Abstracts of the Israeli Geographic Union Conference, Bar-Ilan University, Israel, 21-23.12.2003, 18-19.

Bonsich, F. (1967). 'The geometrical accuracy of 16th and 17th century topographical surveys', Imago Mundi, 21, 62-69.

Bowman, D. (1972). 'Akhziv – Rosh ha Nikra, Morphology and Sediments of the Coastal Plain'. The Department of Geography, The Hebrew University of Jerusalem.

Buiten, H.G. and van Putten, B. (1997). 'Quality assessment of remote sensing image registration – analysis and testing of control point residuals', ISPRS Journal of Photogrammetry and Remote Sensing, 52, 57-73.

Clark Labs. (2002) Idrisi Version 32.2, Clark Labs, The Idrisi Project, Clark University, 950 Main Street, Worcester MA 01610-1477 USA

Close, C.F. (1932). 'A fifty-year retrospective', Empire Survey Review, 1, 146-150

Collier, P. (1994). 'Innovative military mapping using aerial photography in the First World War: Sinai, Palestine and Mesopotamia 1914-1919', The Cartographical Journal, 31, 100-104.

Collier, P. (2002). 'The impact on topographic mapping of developments in land and air survey: 1900-1939', Cartography and Geographic Information Science, 29 (3), 155-174

Collier, P., Forrest, D. and Pearson, A. (2003). 'The representation of topographic information on maps: the depiction of relief', The Cartographical Journal, 40 (1), 17-26.

Conder, R.R. and Kitchener, H.H. (1880). Map of Western Palestine*, in 26 Sheets*, from surveys conducted for the Committee of the Palestine Exploration Fund, London.

Conder, R.R. and Kitchener, H.H. (1881-1883). The Survey of Western Palestine*,* Memoirs of the Topography, Orography, Hydrography and Archaeology, 3 Vols., Palestine Exploration Fund, London.

Coppock, J.T. (1968). 'Maps as sources for the study of land use in the past', Imago Mundi, 22, 37-49.

Cosuins, S.A.O. (2001). 'Analysis of land-cover transitions based on 17th and 18th century cadastral maps and aerial photographs', Landscape Ecology, 16, 41-54.

Crowell, M., Leatherman, S.P., and Buckley, M.K. (1991). 'Historical shoreline change: error analysis and mapping accuracy', Journal of Coastal Research, 7 (3), 839-852.

Douglas, D.H., and Peucker, T.K. (1973). 'Algorithms for the reduction of the number of points required to represent a digitized line or its caricature', The Canadian Cartographer, 10 (2), 112-122.

Doytsher, Y. (2000). 'A rubber sheeting algorithm for non-rectangular maps', Computers & Geosciences, 26, 1001-1010.

Elster, Y. (1956). 'The British Palestine Exploration Fund map', in Atlas of Israel, ed. by Elster, Y., Gliead, M., Amiran, D., Rosenan, N., Girdon, M., Zidon, M. and Kadmon, N., p. I/6, The Department of Surveys, Ministry of Labour, and the Bialik Institute, the Jewish Agency, Jerusalem, Israel, (in Hebrew)

Emery, K.O. and Neev, D. (1960). Mediterranean beaches of Israel, Ministry of Development, Geological Survey, Bulletin No. 26, Jerusalem, Israel, pp1-22

Fogel, D.N. and Tinney, L.R. (1996). Image Registration using Multiquadric Functions, the Finite Element Method, Bivariate Mapping Polynomials and Thin Plate Spline, Technical Report 96-1, National Center for Geographic Information and Analysis, U.S.A.

Frankel, R. (1998). 'Some notes on the work of the survey of Western Palestine in Western Galilee', Palestine Exploration Quarterly, 130, 99-105.

Frumin, M. (2005). 'The arrangement of the major roads in Syria, Lebanon and Palestine in the descriptions of a Russian officer 1834-1835', presented in Cartography and GIS 2005 Meeting, Tel Aviv University, March 17th, 2005 (in Hebrew)

Frumkin-Ahiron, T., Frumkin, R., Roudich, R., Melloul, A., Levin, N. and Papay, N. (2003), Conservation of the Coastal Sand Dunes – a Policy Report, The Surveys Unit – Open Landscape Institute – The Society for the Protection of Nature in Israel, The Ministry of Environment, The Nature and Parks Authority, The Jewish National Fund, The Water Commission and the Jerusalem Institute for Israel Studies, 126 p. (in Hebrew)

Gavish, D. (1991). Land and Map (Karka ve Mapa), Yad Yitzhak Ben Zvi, Jerusalem, (in Hebrew).

Gavish, D. (2005). A Survey of Palestine During the Period of the British Mandate, 1918-1948, Routledge Curzon, London

Gavish, D. and Biger, G. (1985). 'Innovative cartography in Palestine 1917-1918', The Cartographical Journal, 22, 38-44.

Goren, H. (2001). 'Scientific organizations as agents of change: the Palestine Exploration Fund, the Deutsche Verein zur Erforschung Palastinas and nineteenth-century Palestine', Journal of Historical Geography, 27 (2), 153-165.

Goren, H. (2002). 'Sacred, but not surveyed: nineteenth-century surveys of Palestine', Imago Mundi, 54, 87-110.

Hall, D.K., Bayr K.J., Schoner, W., Bindschadler, R.A. and Chien, J.Y.L. (2003). 'Considerastion of the errors inherent in mapping historical glacier positions in Austria from the ground and space (1893-2001)', Remote Sensing of Environment, 86, 566-577.

Harvey, J.T. (2003). 'Locating the Eureka Stockade: use of a Geographical Information System (GIS) in a historiographical research context', Computers and the Humanities, 37, 223-234.

Hodson, Y. (1999). 'An introduction to the publication of the map and memoirs', in Survey of Western Palestine, including a Survey of Eastern Palestine: Introductory Essays, ed. by Jacobson, D.M. and Hodson, Y., pp. 33-71, Archive Editions in association with The Palestine Exploration Fund, The United Kingdom.

Hopkins, I.W.J. (1968). 'Nineteenth-century maps of Palestine: dual-purpose historical evidence', Imago Mundi, 22, 30-36.

Hunt, J. and Smith, R. (1985). 'Nineteenth century maps: some cartographical problems and solutions', The Cartographic Journal, 22, 50–53.

Issar, A. (1995). 'Climatic changes and the history of the Middle East', American Scientist, 83, 350-355.

Issar, A. and Yakir, D. (1997). 'The Roman period's colder climate', Biblical Archaeologist, 60 (2), 101-106.

Jones, Y. (1974). 'Aspects of relief portrayal on 19th century British military maps', The Cartographical Journal, 11, 19-33.

Kark, R. (1997a). 'Land purchase and mapping in a mid-nineteenth-century Palestinian village', Palestine Exploration Quarterly, 129, 150-161.

Kark, R. (1997b). 'Mamluk and Ottoman cadastral surveys and early mapping of landed properties in Palestine', Agricultural History, 71 (1), 46-70.

Kark, R. and Gerber, H. (1984). 'Land registry maps in Palestine during the Ottoman period', The Cartographic Journal, 21, 30-32.

Karmon, Y. (1960). 'An analysis of Jacotin's map of Palestine', Israel Exploration Journal, 10 (3), 155-173.

Kedar, B.Z. (1999). The Changing Land: Between the Jordan and the Sea: Aerial Photographs from 1917 to the Present, Yad Yitzhak Ben Zvi, Jerusalem.

Kitzberger, T. and Veblen, T.T. (1999). 'Fire-induced changes in northern Patagonian landscapes', Landscape Ecology, 14, 1-15.

Margary, H. (1977). 'A proposed photographic method of assessing the accuracy of old maps', Imago Mundi, 29, 78-79.

Mather, P.M. (1995). 'Map-image registration accuracy using least-squares polynomials', International Journal of Geographical Information Systems, 9 (5), 543-554

Morton, R.A., Miller, T.L. and Moore, L.J. (2004). National Assessment of Shoreline Change: Part 1. Historical Shoreline Changes and Associated Coastal Land Loss along the U.S. Gulf of Mexico, U.S. Geological Survey open-file report 2004-1043, U.S. Department of the Interior, U.S. Geological Survey, Centre for Coastal and Watershed Studies, St. Petersburg, FL 33701

Moscrop, J.J. (2000). Measuring Jerusalem, The Palestine Exploration Fund and British Interests in the Holy Land, Leicester University Press, London and New York.

Moscrop, J.J. (2002). 'Strangers within the gates: the Royal Engineers and the Palestine Exploration Fund 1865-1870', Cathedra, 103, 53-68 (in Hebrew).

Mugnier, C.J. (2000). 'Grids and datums: the State of Israel', Photogrammetric Engineering and Remote Sensing, 66 (8), 915-917.

Nir Y., 1989, Sedimentological Aspects of the Mediterranean Coast of Israel and Northern Sinai, The Geological Survey of Israel, Report no. GSI\39\88, Jerusalem

Pearson, A., Carter, P., and Gallmeier, R. (1994). 'The application of digital mapping techniques to the tithe map of the Parish of Newport, Pembrokeshire', The Cartographic Journal, 31, 105-112.

Peuquet, D. J. (1981). 'An examination of techniques for reformatting cartographic data part 1: The raster-to-vector process', Cartographica, 18 (1), 34-48.

Reifenberg, A. (1947). The Soils of Palestine, Studies in Soil Formation and Land Utilization in the Mediterranean, London, Thomas Murby & Co.

Reifenberg, A. (1950). The War between the Sown Land and the Wilderness, Jerusalem, The Bialik Institute, 132 p. (in Hebrew).

Reifenberg, A. (1951). 'Caesarea, a study in the decline of a town', Israel Exploration Journal, 1, 20-32.

Research Systems, Inc., (2001). ENVI Version 3.4, 4990 Pearl East Circle, Boulder, CO 80301, USA: The Environment for Visualizing Images.

Roper, C. (2003). 'Historical mapping is still under-valued and under-used', The Cartographic Journal, 40 (2), 131-134.

Rosen, B. (1992). 'Mapping the coastline of Israel by the British navy', Cathedra, 64, 59-78 (in Hebrew)

Rubin, R. (1989). 'The debate over climatic changes in the Negev, fourth-seventh centuries C.E.', Palestine Exploration Quarterly, 121, 71-78.

Rumsey, D. and Williams, M. (2002). 'Historical maps in GIS', in Past Time, Past Place: GIS for History, ed. by Knowles, A.K., ESRI, USA.

Schick, A. (1955), 'The landscape of Palestine in the 1870s', in Atlas of Israel, ed. by Elster, Y., Gliead, M., Amiran, D., Rosenan, N., Girdon, M., Zidon, M. and Kadmon, N., p. VIII/1, The Department of Surveys, Ministry of Labour, and the Bialik Institute, the Jewish Agency, Jerusalem, Israel, (in Hebrew).

Shatner, Y. (1951). The Map of the Land of Israel (Eretz-Yisrael) and its History, The Bialik Institute, Israel (in Hebrew).

Shimizu, E. and Fuse T. (2004). 'Rubber-sheeting of historical maps in GIS and its application to landscape visualization of old-time cities: focusing on Tokyo of the past', International Workshop on Asian Approach toward Sustainable Urban Regeneration, September 4-7, 2004, The University of Tokyo, Japan.

Shoshany, M., Golik, A., Degani, A., Lavee, H., and Gvirtzman, G. (1996). 'New evidence for sand transport direction along the coastline of Israel', Journal of Coastal Research, 12 (1), 311-325

Stanley, D.J. and Warne, A.G. (1993). 'Nile delta: recent geological evolution and human impact', Science, 260, 628-634.

Thapa, K. and Bossler, J. (1992). 'Accuracy of spatial data used in geographic information systems', Photogrammetric Engineering and Remote Sensing, 58 (6), 835-841.

Tsoar, H. (1990). 'Trends in the development of sand dunes along the southeastern Mediterranean coast', in Dunes of the European Coasts, Catena Supplement, 18, ed. by Bakker, Th.W., Jungerius, P.D., and Klijn, J.A., 51-60.

Tsoar, H. (2001). 'Types of Aeolian Sand Dunes and Their Formation', in Lecture Notes in Physics 582, ed. by Balmforth N.J., & Provenzale A., pp. 403-429, Berlin Heidelberg: Springer-Verlag.

Tsoar, H. and Blumberg, D.G. (2002). 'Formation of parabolic dunes from barchan and transverse dunes along Israel's Mediterranean coast', Earth Surface Processes and Landforms, 27, 1147-1161.

Tsoar, H. and Zohar, Y., (1985). 'Desert dune sand and its potential for modern agricultural development'. In Desert Development, ed. by Gradus Y., pp. 184-200, D. Reidel Pub. Co.

Verbyla, D.L. (2002). Practical GIS Analysis, Taylor & Francis, London and New York.

Vourela, N., Alho, P. and Kalliola, R. (2002). 'Systematic assessment of maps as source information in landscape-change research', Landscape Research, 27 (2), 141-166.

Warren, R.E. (1880). 'Limits of error in latitudes and longitudes of places obtained during the reconnaissances made in Palestine', Palestine Exploration Fund Quarterly Statement, 243-246.

Weir, A.J.C. (1997). 'A century of forest management mapping', The Cartographic Journal, 34, 5–12.

Zitova, B. and Flusser, J. (2003). 'Image registration methods: a survey', Image and Vision Computing, 21, 977-1000.

Zviely, D., Galili, E. and Rosen, B. (2003). 'The port of Acre and its approaches in modern nautical charts', Horizons in Geography (Ofakim be Geografia), 56, 62-78 (in Hebrew, abstract in English).

Zviely, D., and Klein, M. (2004). 'Coastal cliff retreat rates at Beit-Yannay, Israel, in the 20th century', Earth Surface Processes and Landforms, 29, 175-184

*In the fourth article* a new GIS method is presented for calculating the movement rate of dunes, that is adapted for the case of dunes are stabilizing. In such cases, it is shown that the traditional method for estimating the dunes' movement rate results with overestimates, due to the fact that not all the parts of a dune are advancing at all, or at the same rate. The method proposed is based on integrating the whole area over which the dune advanced for the calculation, instead of using only a few selected lines to measure the advance rate. This method is then applied for an analysis of the temporal changes in the stabilization process of the Israeli coastal dunes in the past 60 years is presented, focusing on the case study of the Ashdod and Nizzanim dunes. In this part of the research the trends of dune stabilization and re-activation were studied using historical aerial photographs since 1944/5. To explain the trends that were discovered an extensive array of both physical and human factors are discussed, to reveal the causes of dune stabilization in the study area.

ELSEVIER

Journal of Arid Environments 58 (2004) 335–355

Journal of Arid Environments

www.elsevier.com/locate/jnlabr/yjare

# Monitoring sand dune stabilization along the coastal dunes of Ashdod-Nizanim, Israel, 1945–1999

N. Levin*, E. Ben-Dor

*Department of Geography and Human Environment, Tel-Aviv University, P.O.B. 39040, Ramat Aviv 69978, Israel*

Received 10 May 2002; accepted 20 August 2003

**Abstract**

Temporal changes in the stabilization process along the coastal dunes of Israel were assessed using a series of 23 aerial photographs taken over the period 1944–1999. The stabilization rate was then quantified using a specially developed method for the calculation of sand dune movement and by the calibration of the gray-scale images into vegetation cover maps. An episodic reactivation of the dunes during the 1970s was identified and examined with respect to various physical and human factors. The Mediterranean climate along the coast of Israel and the low wind energy are favorable for the stabilization of sand dunes in the absence of human activity. It was shown that military maneuvers and recreational traffic (pedestrians and off-road vehicles) increased fragmentation but did not lead to the reactivation of the dunes. Based on archival records and interviews with officials who have worked in the area over the past 25 years, it was concluded that the apparent changes in the stabilization process should be attributed to changes in the grazing and vegetation cutting practices of Bedouin farmers along the coast of Israel between the late 1960s and the late 1970s, concomitant with the changing policies of successive Israeli governments.


*Keywords:* Coastal dunes; Bedouin; Israel; Stabilization; Aerial photographs; Land uses

*Corresponding author.
*E-mail addresses:* levinnoa@post.tau.ac.il (N. Levin), bendor@post.tau.ac.il (E. Ben-Dor).

0140-1963/$ - see front matter © 2003 Elsevier Ltd. All rights reserved.
doi:10.1016/j.jaridenv.2003.08.007

## 1. Introduction

Among the important phenomena in sand dune areas are the process and degree of stabilization, which are controlled and governed by diverse environmental factors. The dune stabilization process is a positive feedback mechanism (Tsoar and Moller, 1986) in which the following sequence can be found: where the accumulation of sand is low (as in the dunes' crest), increase in soil moisture content allows an increase of vegetation density; as a result, there is a decrease in the area of exposed sand, an increase in the accumulation of eolian fine particles, and the formation of a biogenic crust that, in turn, leads to a decrease in the sand saltation.

This process endangers endemic species of flora and fauna that specifically adapted to the habitat of shifting sands, and in the long run may lead to the loss of one of the most unique landscapes in Israel—the coastal sand dunes along the Mediterranean Sea (Kutiel, 2000). As a consequence of land use changes, these coastal dunes are undergoing a process of stabilization since the late 1940s (Tsoar and Blumberg, 2002). Prior to 1948, the dunes were utilized by man in two ways: (1) the vegetation was used by the local Arab and Bedouin inhabitants for firewood and building materials, and by their livestock for grazing, and (2) employment of the traditional "mawasi" system of agriculture (mawasi in Arabic means "suction", referring to water that has been sucked out to the surface). In the "mawasi" system, plots in the inter-dune area were cultivated, and the sand was cleared out down to the water table, in order to make water more available for plants (Tsoar and Zohar, 1985). Following the establishment of the state of Israel in 1948, vegetation on the sand dunes was no longer disturbed by man and was therefore able to spread more efficiently on the dunes, thus stabilizing them as the zootic climax was replaced by a climatic climax.

Using aerial photographs of the Ashdod region between 1944 and 1995, Tsoar and Blumberg (2002) monitored changes in the dunes' movement rate, while Kutiel et al. (2003) monitored changes in the vegetation cover between 1965 and 1999. In another study, Danin and Nukrian (1991) used aerial photographs taken between 1945 and 1986 to examine changes in the area covered by vegetation units along the coastal dunes south of Ashkelon (see Fig. 1 for the exact location). In general, all the researchers noted that an overall trend of stabilization has occurred between the 1940s and the present. However, closer examination of their data reveals a period of time when the dunes were reactivated (apparently not considered by them): between 1965 and 1980 the stabilization process (expressed in a decrease of the dunes' movement rate and an increase in the vegetation coverage) came to a temporary halt and even reversed. To explore the possible reason for this shift, and to determine the factors predominantly responsible for it, the data on movement of dunes were extracted using a precise analytical method and a wider area of dunes was studied in this paper. Another parameter that was particularly important for the above exploration was to increase the temporal resolution over the time period in question.

The purpose of this study was, thus, to suggest an environmental mechanism and factor to explain the temporal changes in the dunes' stabilization process along the southern coastal dunes of Israel over the past 50 years. This goal was achieved by,

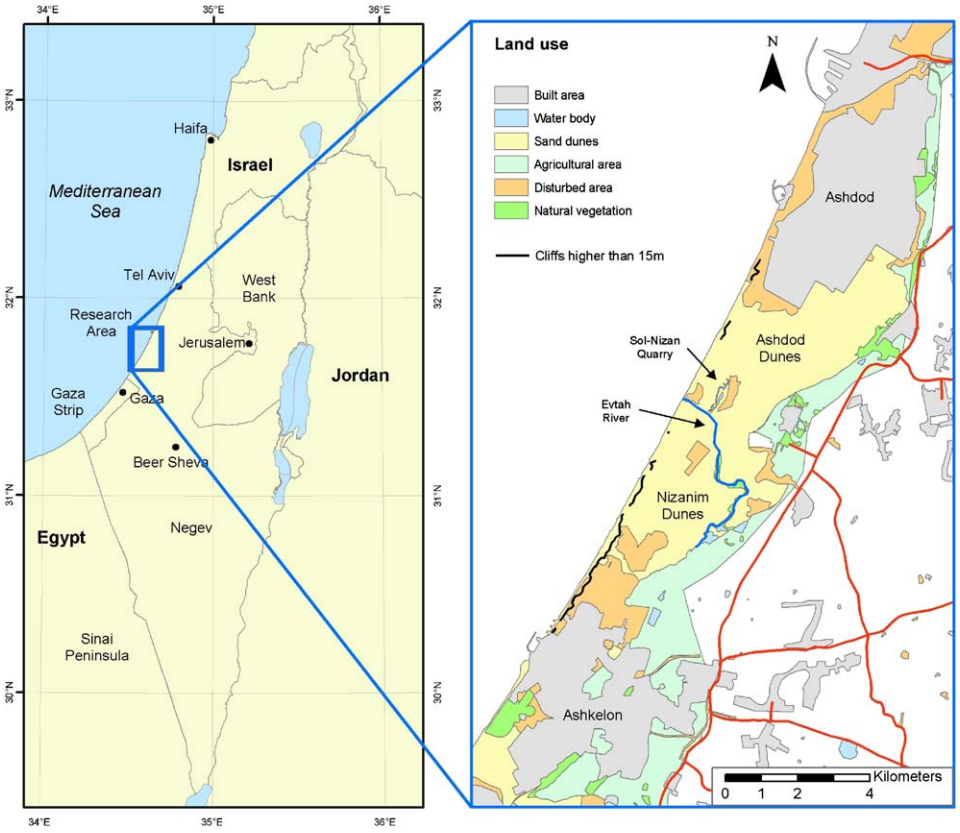


Fig. 1. Research area location in Israel, and the land use map of the research area (the map is partially based on GIS layers created by the GIS unit of the Society for the Protection of Nature in Israel).

first, precisely locating the phenomena in question both in time and space and, then, exploring all relevant and possible physical and human factors documented in this area. To that end, a new methodology and approach were developed and applied to a series of aerial photographs taken over the elapsed time.

## 2. Methodology

### 2.1. Research area

The area selected for this study consists of coastal sand dunes 40 km south of Tel-Aviv, Israel, between the cities of Ashdod and Ashkelon (Fig. 1). The climate is Mediterranean, with an annual average rainfall of 450–500 mm, all in wintertime, with maximum rainfall in December (Bitan and Rubin, 1991). The average daily maximum and minimum temperatures in summer are 29°C and 21°C, respectively.

Proximity to the sea boosts the average relative humidity year round and may reach 70% and higher during the summer.

The origin of the sand along the Israeli coast is mainly from the Nile delta via the longshore currents near the coast and the anti-clockwise Mediterranean current in the deep water (Emery and Neev, 1960). Eolian sand transport from the beach inland occurs under the influence of high winds from the south-west to the north-east, mainly in wintertime (Goldsmith et al., 1990). The southern-half of the study area is part of Nizanim Nature Reserve, while the northern section is protected under Israel's National Master Plan No. 22 for forestry. The vegetation associations typical of the southern coastal dunes of Israel that match our study area were defined by Danin and Nukrian (1991) near Netiv HaAsara, 10 km south of Ashkelon (see Table 1). They note that with increasing sand stability, the germination and establishment of more species is enabled and the monospecific community of *Ammophilia arenaria* thickens and changes into associations where *Artemisia monosperma* is the dominant plant.

### 2.2. Data base and digital processing

To monitor the stabilization process of the sand dunes, a temporal sequence of gray-scale aerial photographs was obtained from the Survey of Israel, mostly for summer and autumn months, when vegetation cover by annuals is minimal. Aerial photographs for 12 years (1944, 1956, 1963, 1965, 1968, 1974, 1977, 1982, 1987, 1990, 1995, 1999) were acquired for the northern dunes of Ashdod, and for 11 years

Table 1
Vegetation associations of the southern coastal dunes of Israel, as defined by Danin and Nukrian (1991), Nukrian (1988)

| Association | Habitat | Silt + clay content at soil surface (%) | Absolute cover of perennial species (%) |
|---|---|---|---|
| *Asthenatherum forsskalii–Polycarpon succulentum* | Windward slope of the dune | 0–3 | 3.8 |
| *Ammophilia arenaria–Senecio joppensis* | Summit of dunes, top of leeward slopes and blowouts | 0.5–4 | 44.3 |
| *Ononis natrix–Artemisia monosperma* | Stable and small sand dunes | 2–5 | 51.9 |
| *Artemisia monosperma–Retama raetam* | Fossil soils in interdune valleys | 6–15 | 130.5 |
| *Artemisia monosperma–Launaea tenuiloba* | Fossil soil covered with 50–100 cm sand | 1.5–5 | 110.0 |
| *Asthenatherum forsskalii–Lotus halophilus* | Slightly mobile sand, up to 100 cm deep, in the interdune valleys | 3–4 | 55.7 |

(1945, 1949, 1956, 1963, 1968, 1972, 1974, 1977, 1982, 1988, 1997) for the southern dunes of Nizanim. All the photographs were scanned at a resolution of 400 dpi, and then georectified using a digital orthophoto as the basis image from which ground control points (GCPs) were collected. For each photograph, more than 100 GCPs (the average was 235; mostly bushes and trees) were identified. A local affine transformation (a linear combination of translation, rotation and scaling adapted locally using the triangulation technique available in ENVI 3.5 package 2001; Research Systems, Inc., 2001) was applied to account for the non-systematic geometric effects caused by the dunes' topography (5–20 m high) and the low flight altitude (about 2300 m above surface) from which the aerial photos were taken (Buiten and Putten, 1997).

### 2.3. Calculation of the dunes' movement

The advance rate of sand dunes (barchan, transverse, or parabolic) can be measured by locating the front of the dune (slip face) at successive times. The slip face can be manually identified either by the shaded areas or by the area at the foot of the dune where vegetation begins. The method (Gay, 1999) traditionally employed to then determine the advance rate (and used by Tsoar and Blumberg (2002) for the Ashdod srea) is based on measuring the distance between two successive lines, each representing a different year. Several arrows/lines are then drawn between those successive lines, their average length representing the average distance moved by the dune between those years (see the arrows in Fig. 2). The main problems of the method are, therefore, related to the way those arrows are drawn (Goudie, 1994, pp. 347–348): how densely should the arrows be drawn? In what direction do they point, and how can the starting and end points of each arrow be objectively determined? In addition, as the method does not take into account those parts of dunes that did not advance, an overestimation of the calculated advance rate is expected.

Alternatively, we suggest the following technique and steps for determining dune movement rate (Fig. 2): (a) the lines representing the dune's front in successive years are joined, forming a polygon, which represents the area covered by sand during those years; (b) for each polygon, the length of the dune's moving front is automatically extracted as the skeleton line, using a vectorizing technique (Peuquet, 1981); (c) the advance rate of a dune is then calculated as follows:

$$v = S/t/L, \tag{1}$$

where $v$ is the movement rate, $S$ the area covered by sand between successive years, $t$ the time between successive aerial photographs and $L$ the dunes' front length.

The "modified method" represents the dune's movement rate more accurately than its traditional counterpart, for the following theoretical reasons (a comparison of the two methods is presented in the results below): (1) completeness: as the calculation is based on a skeleton line integrating the movement all along the dune's front, and not on a limited number of points; (2) objectivity: as the skeleton lines are created by established vectorizing techniques; (3) compatibility with the geomorphological process: In order to insure that the calculations include not only the area

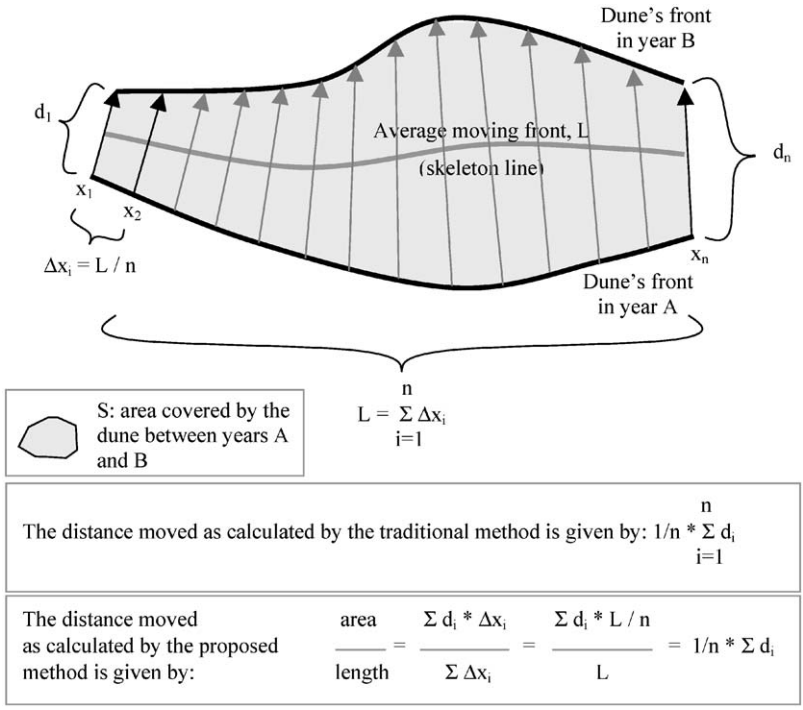


Fig. 2. Schematic chart presenting methods for measuring dunes' movement advance from aerial photographs, and the mathematical relationships between the traditional and the proposed methods for the measurement of dunes' movement. The lettering in the figure is the following: $L$ = dunes' front length; $x_i$ = distance between arrows along the dune's front; $d_i$ = distance moved by the dune along a selected arrow/line $i$; $n$ = number of arrows used by the traditional method to measure the average distance moved by the dune.

where the sand was moved over but also that part of the dune's front that did not move (for example, in the case of vegetation establishment or morphological changes of a dune; e.g. dune A in Fig. 3, where the flanks have stabilized in the mid-1980s while the center of the dune was still advancing), we suggest that for each dune, a constant front length should be defined. This front length will be the longest skeleton line extracted for each of the dunes (from the time when they were fully mobile) and will enable calculation of the exact rate of movement, thus considering also the areas where no movement occurred.

Based on this technique, the dune's movement rate was calculated separately for each area (27 dunes in the northern part, 28 dunes in the southern part, shown in Fig. 3). The dune's movement rate was first calculated using the front dune's length found for each of the respective years (the "traditional method") and then applying the fixed front length (our "modified method") for each of the dunes separately (total of 55 dunes as compared to 15 measured by Tsoar and Blumberg, 2002).

The new method can be extended to calculate the volume (or weight) of sand moved across a width of 1 m, by multiplying the yearly movement rate of a dune by

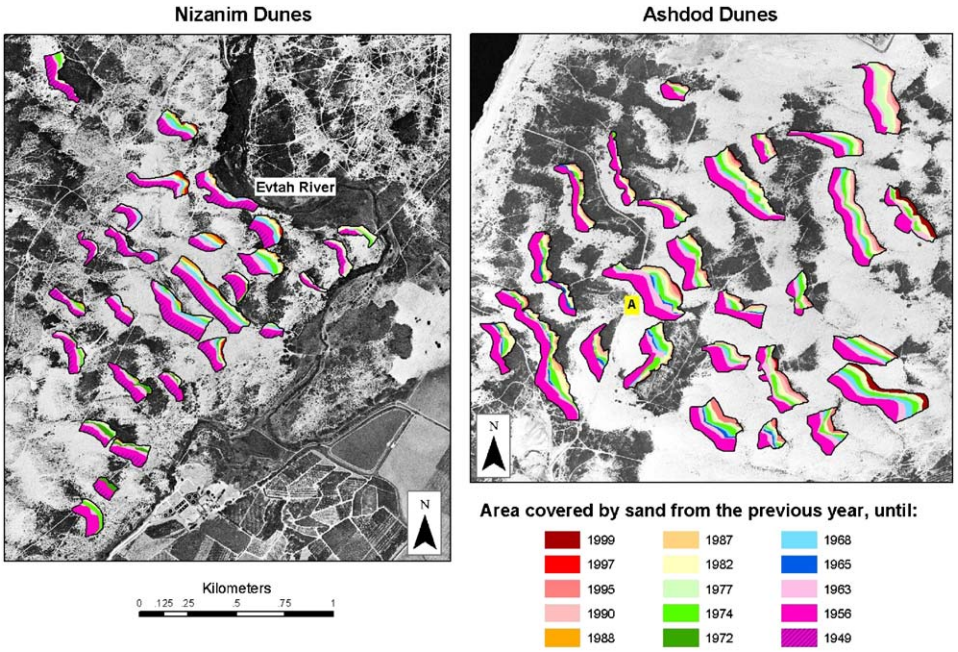


Fig. 3. Areas covered by sand as a consequence of dunes' movement in the Nizanim dunes and Ashdod dunes, as extracted from a temporal series of aerial photographs.

its height. This is based on the assumption that the dune maintained a constant height for the calculation period.

In addition to the new technique to monitor the dune's movement, we have calculated the temporal changes in the vegetation coverage using the gray-scale aerial photographs (similar to the method described by Kadmon and Harari-Kremer, 1999), after applying radiometric corrections, in the following way: (1) in each image, several regions of interest (ROIs) representing bare sand (0%) and dense vegetation (100% cover) in the interdune areas were identified; (2) the average gray-scale value of these ROIs was calculated; (3) the gray-scale values were then calibrated according to the percentage of vegetation cover. Validation of vegetation cover accuracies was preformed against vegetation cover as measured in the field in 16 quadrants of 100 $m^2$ by Ron M. (these measurements were preformed in the months of August and October 2000 for Israel's Nature and Parks Authority), obtaining $R^2$ values of 60%, significant at more than 99%.

### 2.4. *Physical factors time-series analysis*

The following physical factors of dune mobility were examined for the study area: annual average rainfall as measured in Nizanim, average ground-water level along the dunes of Ashdod (data received from Melloul A., Israeli Water Commission),

frequency of Saharan dust storms (Ganor, 1994) as an indicator for the amount of dust deposited, DP and RDP/DP values (indices developed by Fryberger, 1979; see below) in Gaza and Tel-Aviv (data obtained from the Israel Meteorological Service).

### 2.5. Documentation of human activities in the study area

Human activities in the study area relevant to dune mobility include military training, recreational activities, fixation of dunes by plants, and nomadic population pressure of grazing, trampling and cutting. These were reconstructed using archival records (of the Israel Nature and Parks Authority (INPA), Kibbutz Nizanim and the Society for the Protection of Nature in Israel), personal interviews with locals and officials who know the area, and a visual analysis and interpretation of historical aerial photographs.

## 3. Results and discussion

### 3.1. Temporal changes in the stabilization process

Figs. 3 and 4 indicate that the dunes' movement rate is not constant neither in space nor in time. The results of the dune's movement rate, along with those of the vegetation cover, are given in Fig. 4. Several points should be made here: First, the traditional method (variable front length) to estimate the dunes' movement rates results in higher rate values than the modified method. This overestimation might hinder some of the temporal trends within the dune dynamics. The effect explains the higher rates of movement found by Tsoar and Blumberg (2002) who used the traditional method (1.9 m/year between 1980 and 1990) whereas for the same area the modified method depicted values of $<1$ m/year.

Second, the range of the modified method's movement rates of the southern coastal dunes reached values of $>4$ m/year for selected dunes in the late 1940s, while in the late 1990s this value decreased significantly to $<1$ m/year. These values are quite low compared to other dune fields in the world (e.g. the coastal barchan dunes of Peru) that move at rates of up to 80 m/year; Gay, 1999) and are explained by the low wind magnitude in Israel (Tsoar and Blumberg, 2002). Third, a general trend of dune stabilization is clearly seen: in the late 1940s the dunes' movement rate was about 3 m/year, while 50 years later it stood at 0.5 m/year or less. With increased vegetation cover, the effective wind decreases, slowing down the entire dunes' movement accordingly. However, Fig. 4 indicates that in both areas the dunes were reactivated in the late 1960s, with the lowest vegetation cover values and movement rates 50% higher (than in the mid-1960s) achieved in the mid-1970s. From the late 1970s onwards the stabilization process resumed.

Fourth, the southern dunes (Nizanim) became stabilized much faster than the northern dunes (Ashdod). Several human and environmental factors may explain this difference: (1) the coastal cliffs along the southern dunes reach heights of more than 15 m along 2500 m, while along the northern dunes cliffs higher than 15 m

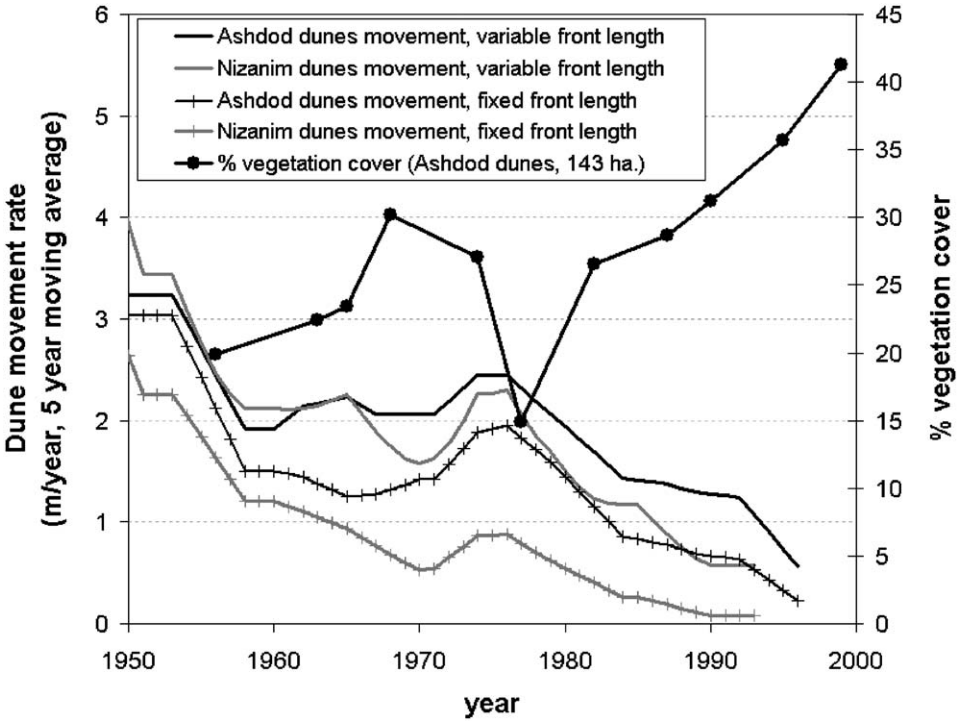


Fig. 4. Temporal changes in the stabilization process of Ashdod–Nizanim dunes, as monitored by dunes' movement rate and vegetation cover.

stretch along less than half that distance (1000 m; see Fig. 1), therefore diverting the wind and narrowing the areas where sand encroaches inland (Tsoar, 1990); (2) the Evtah stream that crosses the southern dunes forms an obstacle for the movement of sand to its northeastern side; (3) the proportion of the area used for agriculture until 1948 (as analysed from historical 1:20,000 British maps) was much larger in the southern dunes, and thus was more suitable for stabilization by vegetation.

For the northern dunes of Ashdod the late 1940s average annual amount of sand that moved across 1 m of a dune was about 26 ton. This figure gradually decreased, reaching a minimum of 11 ton/year in 1965. Reactivation of the dunes since the late 1960s resulted in an increase in sand movement to a peak of about 17 ton/year around 1975. From the late 1970s, the dunes stabilized again with values of about 2 ton/year in the late 1990s.

The direction in which the dunes advance, which is perpendicular to the orientation of the dunes' fronts, can be calculated based on the orientation of the extracted skeleton lines. It was thus found that the dunes' orientation, 130–140°, did not change in the past 50 years, indicating a consistency in the wind regime's direction and that the dunes move from the south-west to the north-east.

### 3.2. Physical factors influencing dune stabilization

Amongst the various physical factors that influence dunes some may encourage stabilization, while others may encourage mobility. Indices of sand mobility are traditionally based on precipitation, evaporation and wind magnitude (Lancaster, 1997). Among the above, wind regime was found to be the most important physical factor in determining the mobility of dunes (Tsoar and Werner, 1998; Tsoar, 2002). The wind parameters to be considered are both wind velocity (above the threshold wind velocity required to keep sand in saltation) and wind directionality. The drift potential (DP) of the sand by the wind can be calculated by applying the method developed by Fryberger (1979), deriving the following indices:

(1) DP, a measure of the wind's energy and potential sand drift, and
(2) RDP/DP, a measure of the wind's directionality, where unidirectional winds result in RDP/DP close to unity, while multi-directional equally spread winds result in RDP/DP values close to zero.

Based on Tsoar and Werner (1998), in areas with an annual average of rainfall $>90$ mm and no human influences, the wind magnitude DP and wind directionality factor RDP/DP can determine the dunes' mobility potential very accurately. Two other factors that may be considered in this respect are ground-water level (Carter, 1991) and eolian dust deposition rate (Tsoar and Moller, 1986; Zaady et al., 2001).

The temporal sequence of the various physical factors analysed is given in Fig. 5, and the correlation coefficients between them and the dunes' movement rate is given in Table 2. It can be seen from the above figure and table that no significant correlation exists between the physical factors' annual values and the dunes' movement rate. However, after the application of a consecutive 5-year running average on the physical factors' values, some relationships emerge: slower movement rates are weakly correlated with higher amounts of rainfall and increased frequency of dust storms. However, a careful examination of the temporal changes given in Fig. 5 reveals that the correlation found with rainfall data is an outcome of the rainy year of 1991/1992 that came when the dunes were already quite inert, while during the 1960–1970s no correlation between these factors exists. As for dust storm frequency, the correlation found is merely an expression of a long-term agreement between an increase in dust episodes and dune stabilization; however, no correlation exists between the two during the 1970s (when the dunes were reactivated).

Ranwell (1972) notes that plant growth on sand dunes may be related to the water table only in those places where the water table is less than 2 m below the surface. In our area, the average dune height (relative to their surroundings) is 10 m, and the ground-water level has dropped by more than 10 m since the 1950s due to intensive pumping (Yair Farjun, pers. comm.), and is now only a few meters above sea level (see Fig. 5). It is hence understood why ground-water level had no effect on dune mobility in the study area.

We therefore conclude that the determining factor is most favorably related to human influence, which can change and impact coastal systems faster than physical disturbances (Gabriel and Kreutzwiser, 2000).

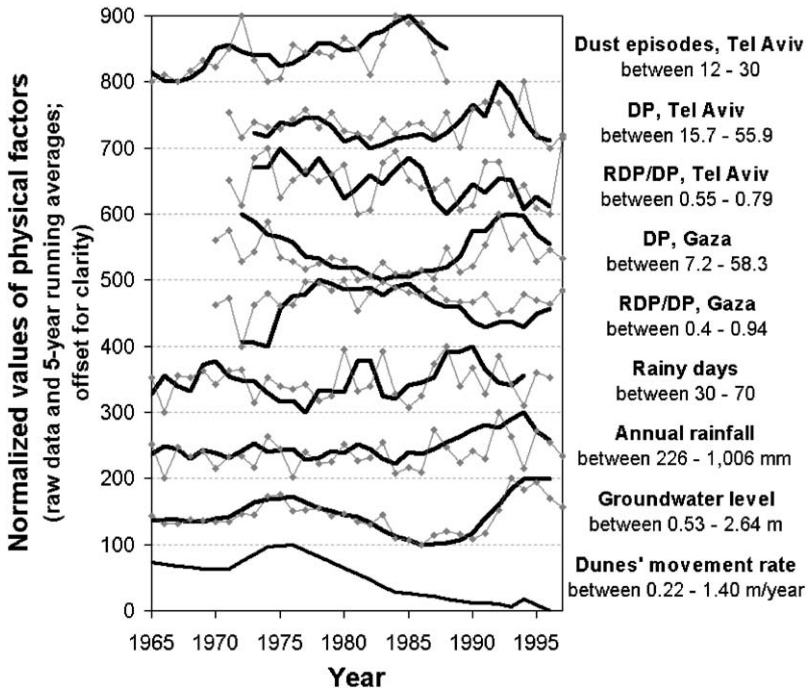


Fig. 5. Temporal series of dunes' movement rate and physical factors examined. Raw data of the physical factors are presented by the thin gray lines, while the running averages are shown by thick black lines. The values given to the right relate to the raw data values' range during the period shown in the chart.

Table 2
Correlation coefficients between selected environmental factors and the dunes' movement rate

| Factor examined | Period of measurement | Linear correlation coefficient ($R$) with dunes' average movement rate in both areas | |
|---|---|---|---|
| | | Raw data | 5 years running average |
| Annual average rainfall,[a] Nizanim | 1960–1996 | −0.36 | −0.68 |
| Rainy days,[a] Nizanim | 1960–1996 | −0.11 | −0.01 |
| Groundwater level,[b] Ashdod dunes | 1960–1998 | 0.21 | 0.17 |
| Frequency of Saharan dust storms,[c] Tel Aviv | 1956–1990 | −0.36 | −0.63 |
| DP,[a] Gaza | 1970–1998 | 0.01 | −0.02 |
| DP,[a] Tel Aviv | 1971–1998 | −0.01 | −0.18 |
| RDP/DP,[a] Gaza | 1970–1998 | 0.01 | 0.04 |
| RDP/DP,[a] Tel Aviv | 1971–1998 | 0.29 | 0.63 |

[a] Calculated from Israel Meteorological Service data.
[b] Calculated from Israel Water Commission data, received from Melloul A.
[c] Ganor (1994).

### 3.3. Human factors and dune stabilization

Among the human impacts affecting sand dunes activity are livestock grazing and cutting of vegetation by nomadic populations (Meir and Tsoar, 1996; Barth, 1998), planting of vegetation to stabilize dunes (Liphschitz and Biger, 1997), and disruption caused by military maneuvers (Al-Dabi et al., 1997) and recreational activities, such as off-road vehicles (ORVs) and hikers (Curr et al., 2000).

Fig. 6 presents maps of the tracks identified from aerial photographs over an area of 166 ha located in the Ashdod dunes. From these maps (a similar analysis applied to an area of military training in Nizanim dunes gave similar results, and is therefore not shown) it is clear that there is an increase in the density of tracks since the 1960s, a process that still continues, and known from Mediterranean dunes outside Israel too (Curr et al., 2000). The higher density of tracks, whether a result of recreational or military activities, removes vegetation from the track. Itself, but did not lead to the reactivation of the dunes, for several reasons: (1) vehicle traffic is mostly confined to linear routes; (2) invasive species (e.g. *Acacia saligna*) were found to spread faster in disturbed areas and a linear pattern was found in their advance along tracks (Cohen et al., 2001); (3) soil compaction along tracks was found to be beneficial for vegetation in the sand dune habitat (Liddle and Greig-Smith, 1975a, b); (4) stabilized

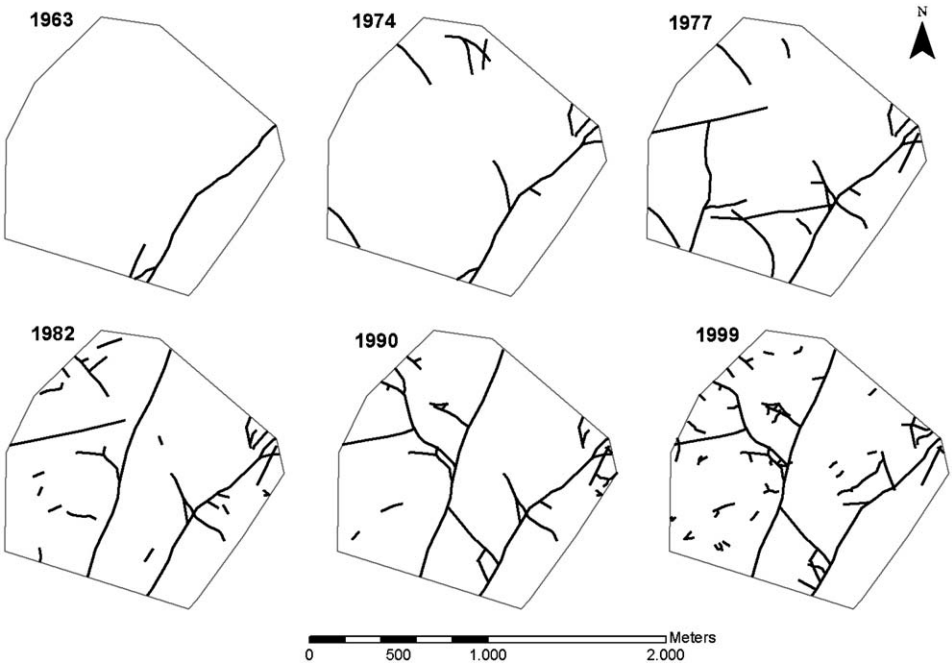


Fig. 6. Changes in the tracks' network as identified from aerial photographs over an area of 166 ha, Ashdod dunes.

Mediterranean coastal dunes are highly resistant and recover quickly from the effects of pedestrian and even vehicle traffic (Kutiel et al., 2001).

Actions taken to stabilize the Ashdod dunes during the British mandate (1920–1940s) and later by the Jewish National Fund (JNF; during the early 1960s), were mostly targeted to the eastern part of the dunes, and to the creation of a foredune. However, it was found that *Acacia saligna* (planted during the 1960s by the JNF) does not spread spontaneously to bare sand dunes (Cohen et al., 2001). Furthermore, stabilization actions cannot explain the reactivation of the dunes, that took place during the late 1960–late 1970s.

Prior to 1948, there was no control on grazing or the cutting of vegetation by the local population, and as almost every plant is useful for the Bedouins and Arabs that lived in the area (either as livestock pasture, or as medicine, building material, firewood, etc. See Table 3 and Bailey and Danin, 1981), the pressure exerted did not allow vegetation establishment on the dunes. Israel's establishment in 1948 brought with it a drastic decrease in the Bedouin population along the coastal dunes and in the Negev, from about 70,000 to 11,000 (Abu-Rabia, 1994), and those left were concentrated under military rule in the northern Negev, in the surroundings of Beer Sheva (see Fig. 1). Due to the poor state of the natural forests and maquis in Israel after decades of uncontrolled cutting, fire and grazing, a special law for the *protection of vegetation* (*goat damages*) was passed in 1950 that determined the allowed density of grazing by goats and forbade it in forest areas and all other places to be declared by the Ministry of Agriculture. As a result, vegetation cover was able to recover along the coastal dunes.

The nullification of military rule in 1966 and Israel's occupation of Sinai and the West Bank areas in 1967 opened the doors for the Bedouin to pasture their flocks all over the Negev and the central area of Israel. Formally, free grazing was not allowed; however, no government ministry was put in charge to replace the military rule and supervise grazing (State of Israel, 1979). In the mid-1970s a severe drought in the northern Negev encouraged many of the Bedouin to move northwards. Fig. 7 demonstrates the temporal correspondence between the Bedouin's livestock size, the years of drought in the Negev desert and the maximum reactivation of the coastal dunes.

The damage to vegetation along the coastal dunes (and elsewhere) caused by the cutting and grazing practices was noted by several of Israel's Nature and Parks Authority rangers:

- "Nizanim dune area is one of the only places along the coasts of Israel, where sand dunes, kurkar hills and hidden swamps that comprise the unique ecosystems of the coast have survived, without being disturbed heavily by man for many years. Now, grazing has returned and in some areas even overgrazing, because of the invasion of livestock herds from the south that endanger the dunes' vegetation and their stabilization" (Rabinovitch, 1975).
- "Nizanim dunes reserve—area of 700 ha … uncontrolled grazing by Bedouin's cattle and flock, along with their illegal settlement damages the reserve" (Ortal, 1975).

Table 3
Sand dunes' vegetation uses by Bedouin and their livestock

| Plant species | Uses | | | | |
|---|---|---|---|---|---|
| | Grazing by livestock | Medicine | Veterinary medicine | Plants as food | Other uses |
| *Polygonum* | | | | Condiment for tea[a] | Windbreak of shrubs around the tent[a] |
| *Tamarix aphylla* | | | | | Tent poles,[b] bowl for milking camels,[a] camel saddle[a] |
| *Teucrium capitatum* | | The leaves for head colds, purulent sores and digestive problems[a] | | | |
| *Artemisia monosperma* | During the months of May–July[a] | | | | Huts from the branches,[c] Windbreak of shrubs around the tent,[a] Insulation for handle of coffee pot[a] |
| *Capparis spinosa* | | The leaves for head colds, aches in joints, limbs and back, women's disorders[a] | | | |
| *Populus euphratica* | | | | | Poles supporting the center of the tent[a] |
| *Phragmites australis* | | | | | Flute,[a] Mats[a] |

| | | | | | |
|---|---|---|---|---|---|
| *Retama raetam* | Grazing of young branches that renew after being cut down[d] | Branches and green leaves for aches in joints, limbs and back[a] | Branches and green leaves for swelling in camel's leg | | Charcoal,[a,e] pins that fasten the roof to the outer curtain,[a] partridge traps,[a] tent poles,[b] insulation for hand of coffee pot[a] |
| *Ziziphus spina-christi* | | | | Fruit of the Ziziphus[a] | Boat's skeleton[f] |
| *Acacia albida* | In autumn—the camels graze the tree tops, while the goats graze the lower branches and offsprings[g] | | | | Charcoal[g] |
| *Ficus sycomorus* | | | | Fruit of the Ficus[a] | |
| *Phoenix dactylifera* | | | | Dates[a] | Construction of booth dwelling in summer,[a] baskets,[a] tent poles,[b] tent ropes[a] |

[a] Bailey and Danin (1981).
[b] Khwaldi (1992).
[c] Danin (1983).
[d] Berliner (1979).
[e] Levi (1983).
[f] Dar (1973).
[g] Ortal (1976).

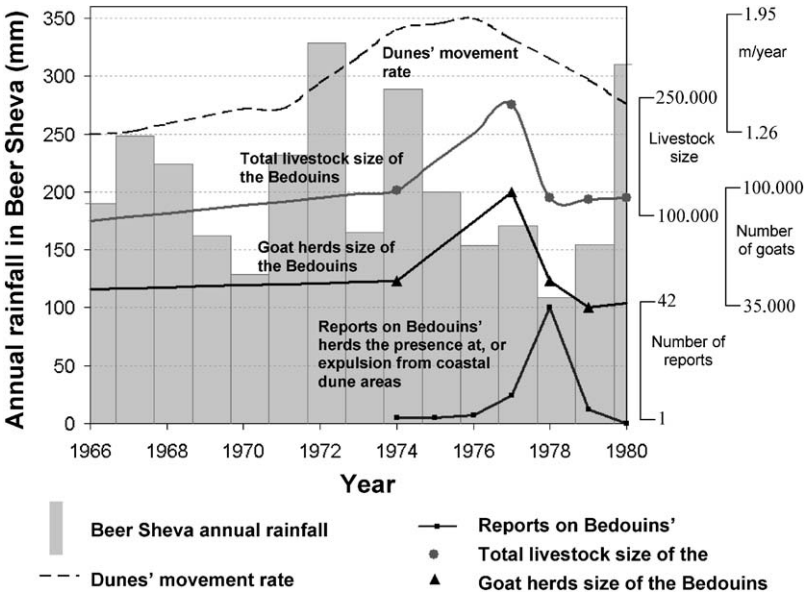


Fig. 7. Livestock and goat herds sizes of the Bedouin (based on Abu-Rabia, 1994, and other sources), reports regarding the presence of Bedouins and their herds in the coastal dunes, and annual rainfall in the northern Negev (Beer Sheva), between the years 1966 and 1980.

- "But in the last year spring 1976… along the dunes of Ashdod, Nizanim and Shikma river, considerable grazing by Bedouin's livestock of goats, sheep and camels was observed in autumn time, when migrating from the south to the north. In this season pasture is scarce and the flocks prefer the *Acacia* trees that carry abundant leaves. The camels graze the treetops while the goats graze the lower branches…" (Ortal, 1976).

In response, a new agency was established under Israel's Nature Reserves Authority in 1976 to protect state lands: the "Green Patrol", formally named as the "Unit for Overseeing Open Spaces". Yoel Dov (2001, pers. comm.) who worked in the Green Patrol estimates that during the 1970s there were about 30 Bedouin families in the area of Ashdod–Ashkelon. Alon Galili (2001, pers. comm.), the Green Patrol's first manager, estimates that the coastal dunes between Tel-Aviv and Gaza were under grazing pressures from about 10,000 goats, 5000 sheep and 200 camels.

Amendments made in 1977 to the 1950 law determined that grazing in nature reserves and national parks is forbidden and that rangers who catch illegally grazing goats will have the power to confiscate and sell them. The Green Patrol has taken various actions aimed at returning the Bedouin's flocks to the Negev. For example, between 1978 and 1992 about 104 operations of goat confiscation were conducted by the Green Patrol, with more than 10,100 goats captured and sold, most of them concentrated in the center of Israel during the first year of goat operations—1978

(Galili, 1978). Between 1977 and 1984, some 544,000 sheep, goats and cows were temporarily caught by the Green Patrol and removed from the areas they invaded (State of Israel, 1985). The reported operations against illegal grazing in the dunes, and the following reduction in the Bedouin's livestock size and in the dunes' mobility are clearly evident in Fig. 7.

These and other actions led to a dramatic decrease in the number of flocks held by the Bedouin (shown in Fig. 7), a drop in the goats population numbers (from 40% to 10% of the total livestock), and to the exit of the Bedouin from the central area of Israel. Vegetation recovery along the coastal dunes north of Shikma river (south of Ashkelon) was noted by Nature Reserves Authority ranger Berliner (1979) already in summer 1979:

- "… while the tall *Retama reatam* bushes were cut down until a year ago by invading Bedouin and their herds, and only now they start to recover after the pressures of cutting and grazing have been removed" (there, p. 6).
- "Cutting and grazing have stopped during the last year, after the invading herds were expelled, and already now the local vegetation can be seen to recover. *Retama reatama* bushes, that were in the past sought after as firewood and charcoal while the flocks were grazing the soft offshoots from their bases, have renewed their growth, although their relative cover in the area is still quite sparse. *Artemisia* bushes are also increasing all the time from seeds and covering the front of the moving sand. These contribute a lot to the dunes' stabilization and to soils' enrichment with organic matter, therefore facilitating the establishment of other species. It's possible that in a short while it will be possible to observe here a rise in the relative cover by more developed and species' rich vegetation associations, as the *Retama–Helianthemum* association, and the stabilization of sand in many places from which vegetation cover was previously removed" (there, p. 8).

Indeed, the observed peak in the dunes' movement between 1974 and 1977 corresponds to the time when the size of the Bedouin's livestock was at its peak and to the time of the drought in the Negev (see Figs. 4 and 7), just before the operations of the Green Patrol began, in 1978.

This historical exploration together with temporal aerial photographs observations suggests a human reason for the anomaly found in the sand dune movement and demonstrates that man's impact on the dune ecosystem is both rapid and obvious.

## 4. Summary and conclusions

The use of more accurate methods for georectification of gray-scale aerial photographs and for measuring dunes' movement rates allowed us to record subtle changes in the dunes' stabilization process. Increasing the spatial and temporal resolutions enabled for the first time the identification of when and where these changes occurred. In general, it was found that dune movement decreased over the

years with an anomaly observed around the late 1960s–late 1970s. None of the meteorological and environmental factors examined was able to explain this anomaly or the other declining sand movement trend. Rather, human activities have a more dramatic and immediate effect on natural ecosystems and provide a more convincing explanation for the observations made. Among these activities, recreational pedestrian and ORV traffic seems to cause fragmentation but not to destabilize the dunes, as they tend to follow fixed lines, and even encourage the establishment of invading species along them. Based on historical evidences, we conclude that the combined cutting and grazing practices of the Bedouin led to the reactivation of Israel's southern coastal dunes during the 1970s, once military rule over their area ended and borders between Israel, Sinai, the Gaza Strip and the West Bank were removed. The establishment of the Green Patrol in 1976 and the changing grazing laws resulted in a decrease in the size of livestock populations and moved the Bedouin back from central Israel to the Negev, thereby allowing the vegetation to recover.

While livestock grazing was perceived in the past as harmful to nature conservation (the common property problem; see Livingstone, 1977, 1986), Perevolotsky (1999) claims that the long history of grazing in the Negev (and in other areas of Israel) converted it into a "grazing-incorporated system", and that the grazed state is, in fact, the most "natural" state. It may be stated that the preservation of sand-living flora and fauna and a landscape of mobile sand dunes, will be greatly facilitated if grazing by Bedouin herds (or other equivalent ecological processes) will be reintroduced to that area. For certain purposes, such as infiltration of rain into aquifers underlying the dunes, the dunes' vegetation cover and state of mobility are not important, while for other issues (e.g. species richness) stabilization of the dunes is favorable (as mobile dunes present a habitat poor in nutrients, supporting fewer species than adjacent habitats receiving the same amount of rainfall). However, the desired landscape of Israel in general and of the Israeli coastal dunes in particular ("grazed and mobile" or "ungrazed, vegetated and more stable") is out of the scope of this article (for further discussion, see Kutiel, 2000; Schorsch, 2002; Kutiel et al., 2003).

In conclusion, it is has been found that historical exploration aided by a series of aerial photographs may shed light on dune activity, and it was demonstrated that human impact on the dune ecosystem is remarkably rapid and much more significant than short-term natural environmental factors.

## Acknowledgements

We wish to thank all the people and institutions that helped us in this work: Israel Nature and Parks Authority (Zeev Kuler, Shay Cohen and Zvi Horesh), the Green Patrol (Alon Galili, Naomi Altshuler, Gile'ad Altman, Yoel Dov and Noam Eldan), Kibbutz Nizanim (Nava Zelinger and Arye Adelheit), the Society for the Protection of Nature in Israel (Mimi Ron, Yair Farjun, Iris Han and the GIS unit), Israel Water Commission (Avi Melloul), the Survey of Israel, the Israel Meteorological Service,

the Jewish National Fund GIS unit, Amiad Bresner and Amiram Oren. In addition we thank the anonymous reviewers for their helpful comments and contribution to the manuscript.

## References

Abu-Rabia, A., 1994. The Negev Bedouin and Livestock Rearing, Mediterranea Series. Berg, Oxford, 139pp.

Al-Dabi, H., Koch, M., Al-Sarawi, M., El-Baz, 1997. Evolution of sand dune patterns in space and time in north-western Kuwait using Landsat images. Journal of Arid Environments 36, 15–24.

Bailey, C., Danin, A., 1981. Bedouin plant utilization in Sinai and the Negev. Economic Botany 35 (2), 145–162.

Barth, H.J., 1998. Status of vegetation and an assessment of the impact of overgrazing in an area north of Jubail, Saudi Arabia. In: Omar, S.A.S., Misak, R., Al-Ajmi, D., Al-Awadhi, N. (Eds.), Sustainable Development in Arid Zones, Management and Improvement of Desert Resources, Vol. 2. A.A. Balkema, Rotterdam, Beookfield, pp. 435–450.

Berliner, R., 1979. Proposal for a nature reserve in the southern Shfela sand dunes near Zikim, 12.7.1979. Israel Nature Reserves Authority archives, Tel Aviv (in Hebrew).

Bitan, A., Rubin, S., 1991. Climatic Atlas for Physical and Environmental Planning in Israel. Geography Department, Tel Aviv University, Meteorological Service, Ministry of Transportation, Research and Development Section, Ministry of Energy and Infrastructure, Ramot Publishing, Tel Aviv University.

Buiten, H.J., van Putten, B., 1997. Quality assessment of remote sensing image registration—analysis and testing of control point residuals. ISPRS Journal of Photogrammetry and Remote Sensing 52, 57–73.

Carter, R.W.G., 1991. Near-future sea level impacts on coastal dune landscapes. Landscape Ecology 6 (1/2), 29–39.

Cohen, O., Shub, M., Kutiel, P., Shoshany, M., 2001. Distribution characteristics of the *Acacia saligna* in the Nizanim dunes, between 1962–1995—Rates, patterns and trends of expansion. In: Abstracts of the 2000 Israeli Geographic Association Conference, Jerusalem, pp. 46–47 (in Hebrew).

Curr, R.H.F., Edwards, Koh.A., Williams, A.T., Davies, P., 2000. Assessing anthropogenic impact on Mediterranean sand dunes from aerial digital photography. Journal of Coastal Conservation 6, 15–22.

Danin, A., 1983. Weed vegetation that accompanied the Israeli settlements in Sinai. Teva va Aretz 25 (4), 36–38 (in Hebrew).

Danin, A., Nukrian, R., 1991. Dynamics of dune vegetation in the southern coastal area of Israel since 1945. Documents Phytosociologiques XIII, 281–296.

Dar, S., 1973. Crafts in Gaza, summer 1973. Teva va Aretz 16 (3), 124–126 (in Hebrew).

Emery, K.O., Neev, D., 1960. Mediterranean beaches of Israel. Israel Geological Survey Bulletin 26, 1–24.

Fryberger, S.G., 1979. Dune forms and wind regime. In: McKee Edwin, D. (Ed.), A Study of Global Sand Seas, Geological Survey Professional Paper, Vol. 1052. United States Geological Survey, Washington, DC, pp. 137–169.

Gabriel, A.D., Kreutzwiser, R.D., 2000. Conceptualizing environmental stress: a stress-response model of coastal sandy barriers. Environmental Management 25 (1), 53–69.

Galili, A., 1978. Goat Operation Reports, Nos. 2-104, Green Patrol archives, Israel Nature Reserve Authority (in Hebrew).

Ganor, E., 1994. The frequency of Saharan dust episodes over Tel Aviv, Israel. Atmospheric Environment 28 (17), 2867–2871.

Gay Jr., S.P., 1999. Observations regarding the movement of barchan sand dunes in the Nazca to Tanaca area of southern Peru. Geomorphology 27, 279–293.

Goldsmith, V., Rosen, P., Gertner, Y., 1990. Eolian transport measurements, winds, and comparison with theoretical transport in Israeli coastal dunes. In: Nordstrom, K.F., Psuty, N.P., Carter, R.W.G. (Eds.), Coastal Dunes: Form and Process. Wiley, New York, pp. 79–101 (Chapter 5).

Goudie, A., 1994. Geomorphological Techniques, 2nd Edition (edited for the British Geomorphological Research Group). Routledge, London, New York.

Kadmon, R., Harari-Kremer, R., 1999. Studying long-term vegetation dynamics using digital processing of historical aerial photographs. Remote Sensing of Environment 68, 164–176.

Khwaldi, O., 1992. The impact of changes in Bedouin land uses on the natural environment along the Israeli–Egyptian border since the 1940s. M.A. Thesis, Ben-Gurion University of the Negev, Israel (in Hebrew), unpublished.

Kutiel, P., 2000. Preservation and management of open landscape areas along the dunes of Israel's coastal strip. Ecology and Environment 6 (2), 91–96 (in Hebrew).

Kutiel, P., Eden, Z., Zhevelev, J., 2001. The impact of motorcycle traffic on soil and vegetation of stabilized coastal dunes, Israel. Journal of Coastal Conservation 7, 81–90.

Kutiel, P., Cohen, O., Shoshany, M., Shub, M. 2003. Vegetation establishment on the southern Israeli coastal sand dunes between the years 1965 and 1999, Landscape and Urban Planning, in press.

Lancaster, M., 1997. Response of eolian geomorphic systems to minor climate change: examples from the southern Californian deserts. Geomorphology 19, 333–347.

Levi, S., 1983. Preservation of acacia trees in Sinai. Teva va Aretz 25 (4), 42–43 (in Hebrew).

Liddle, M.J., Greig-Smith, P., 1975a. A survey of tracks and paths in a sand dune ecosystem: I. Soils. Journal of Applied Ecology 12, 893–908.

Liddle, M.J., Greig-Smith, P., 1975b. A survey of tracks and paths in a sand dune ecosystem: II. Vegetation. Journal of Applied Ecology 12, 909–930.

Liphschitz, N., Biger, G., 1997. Sand dunes reclamation by vegetation in palestine during the British mandate period. Horizons in Geography 46–47, 21–38 (in Hebrew).

Livingstone, I., 1977. Economic irrationality among pastoral peoples: myth or reality? Development and Change 8, 209–230.

Livingstone, I., 1986. The common property problem and pastoralist economic behaviour. The Journal of Development Issues 23 (1), 5–19.

Meir, A., Tsoar, H., 1996. International borders and range ecology: the case of bedouin transborder grazing. Human Ecology 24 (1), 39–64.

Nukrian, R., 1988. Vegetation and its habitats in the sand dunes to the south of Shikma river. M.Sc Thesis, Department of Botany, Hebrew University of Jerusalem, Israel (in Hebrew).

Ortal, R., 1975 (printed in 1983). A Survey of Nature Reserves along the Judean Coastal Plain, Israeli Nature Reserves Authority archives (in Hebrew).

Ortal, R., 1976. Survey of Acacia Albida, Israeli Nature Reserves Authority archives (in Hebrew).

Perevolotsky, A., 1999. Interrelationships between conservation, landscape development and grazing in the Northern Negev. Ecology and Environment 5 (2–3), 190–199 (in Hebrew).

Peuquet, D.J., 1981. An examination of techniques for reformatting cartographic data part 1: The raster-to-vector process. Cartographica 18 (1), 34–48.

Rabinovitch, A., 1975. Let the Nizanim dunes be a nature reserve. Teva va Aretz 17 (2), 76 (in Hebrew).

Ranwell, D.S., 1972. Ecology of Salt Marshes and Sand Dunes. Chapman & Hall, London, 258pp.

Research Systems, Inc., 2001. The Environment for Visualizing Images. ENVI Version 3.5, 4990 Pearl East Circle, Boulder, CO 80301, USA.

Schorsch, J., 2002. Israel, a land of asphalt and concrete? A conversation with Israeli Environmentalist Yoav Sagi. Tikkun 17 (1). Accessed in June 9, 2003: http://www.tikkun.org/magazine/index.cfm/action/tikkun/issue/tik0201/article/020112b.html.

State of Israel, 1979. Illegal Overtaking of State Lands—Final Report, directed to Dr. Burg J., chairman of the minister's committee for internal affairs, services and environment, September 1979, Jerusalem (in Hebrew).

State of Israel, 1985. State Comptroller's Report for 1984, Jerusalem (in Hebrew).

Tsoar, H., 1990. Trends in the development of sand dunes along the southeastern Mediterranean coast. In: Bakker, Th.W., Jungerius, P.D., Klijn, J.A. (Eds.), Dunes of the European Coasts, Catena Suppl. 18, Elsevier, Amsterdam, pp. 51–60.

Tsoar, H., 2002. Climatic factors affecting mobility and stability of sand dunes. In: Proceedings of ICAR5/GCTE-SEN Joint Conference. International Center for Arid and Semiarid Land Studies, Texas, Publication 02-2, pp. 423–426.

Tsoar, H.A., Blumberg, D.G., 2002. Formation of parabolic dunes from barchan and transverse dunes along Israel's Mediterranean coast. Earth Surface Processes and Landforms 27, 1147–1161.

Tsoar, H., Moller, J.T., 1986. The role of vegetation in the formation of linear sand dunes. In: Nickling, W.G. (Ed.), Aeolian Geomorphology. Allen and Unwin, Boston, pp. 75–95.

Tsoar, H., Werner, I., 1998. Reevaluation of sand dunes' mobility indices. Journal of Arid Land Studies 7S, 265–268.

Tsoar, H., Zohar, Y., 1985. Desert dune sand and its potential for modern agricultural development. In: Gradus, Y. (Ed.), Desert Development. D. Reidel Pub. Co., Dordrecht, Holland, pp. 184–200.

Zaady, E., Offer, Z.Y., Shachak, M., 2001. The content and contributions of deposited aeolian organic matter in a dry land ecosystem of the Negev Desert, Israel. Atmospheric Environment 35, 769–776.

*In the fifth article* the aim was to quantify the spatial variability in the wind speed, or to be more specific, in the aerodynamic surface roughness ($Z_0$) across a coastal dune field, focusing on two areas: the Ashdod dunes and those of Bet Yanay.
Understanding the spatial variability of the wind field and how it is influenced by vegetation and topography are a key for better models of dune stabilization. In this chapter the importance of analyzing the influence of the area upwind of a selected location to understand its wind speed characteristics was demonstrated. The same principle was expected to be true also for the movement of sand, as measured in the field.

# Prediction of surface roughness ($Z_0$) over a stabilizing coastal dune field based on vegetation and topography

**Levin Noam, Eyal Ben-Dor, Giora J. Kidron and Yaron Yaakov**
The Department of Geography and Human Environment, Tel-Aviv University, Israel

## Abstract

The aerodynamic surface roughness ($Z_0$) is related to the density, height and shape of the surface and of the various land-cover types and obstacles covering the surface and creating the friction. Surface roughness has a direct influence over the winds' speed and therefore also on the potential sand drift, and is thus an important factor in understanding the stabilization process of sand dunes. In this study we have aimed at quantifying the influence of vegetation cover and topography on $Z_0$ values over a stabilizing coastal dune field. We have performed 39 wind measurements (at a height of 2.5m) at two coastal dunes fields in Israel (Ashdod and Bet Yanay) at various distances from the coastline, ranging from 10m to 2,800m, including the beach, the fore dune and the inland dune areas. We have then applied the method suggested by Wieringa (1973, 1986) to calculate $Z_0$ values from wind measurements that were done on a single height, based on the ratio between the wind gust and the average wind speed. These ranged from 0.00005m at the coastline to 0.36m inland. We estimated vegetation cover from aerial photographs and using the Normalized Difference Vegetation Index (NDVI) and Soil Adjusted Vegetation Index (SAVI) from Landsat satellite images taken in winter, spring and summer. This was done for each location where the wind was measured as well as for the upwind sector at various lengths, ranging from 15m to 400m. We calculated the topographic variables of the relative heights of the stations in a similar way, based on digital elevation models and differential GPS field measurements. It was found that the $Z_0$ values are positively correlated with SAVI values (R=0.86 for the winter SAVI at an upwind length of 200m, when all stations are included) and negatively correlated with the relative height (R=-0.68 for the relative height at an upwind length of 200m-400m, for the inland dune stations). Using these variables we were then able to model and create a map of predicted $Z_0$ values

with accuracy higher than 64%. Such maps enable us to have a better understanding of the spatial variability in both the wind speed and the sand movement over coastal dune areas, and to predict future changes in vegetation cover and dune movement.

## Keywords

Sand dunes, roughness, wind, vegetation, topography, digital elevation models, Landsat, NDVI, SAVI

## 1. Introduction

### 1.1 Wind profiles and estimations of $Z_0$

The wind field in the atmospheric boundary layer is largely controlled by the frictional drag imposed on the flow by the underlying surface (Oke, 1987). As a result of the drag, the horizontal wind speed decreases towards the ground. Accurate knowledge of the surface roughness and the resultant wind speed are important for many applications, such as climatic models, wind power meteorology, agriculture and erosion hazards, especially in arid and semi-arid environments, where vegetation cover is scarce (Peterson et al., 1997; Pike, 2000).

The actual form of the wind variation with height under neutral stability has been found to be accurately described by a logarithmic decay curve, as follows:

$$U_z = ( U_* / k ) \ln([z-d] / Z_0) \qquad (1)$$

Where $U_z$ – mean wind speed (m $s^{-1}$) at the height z, $U_*$ - frictional velocity (m $s^{-1}$), k – von Karman's constant (≈0.40), $Z_0$ – roughness length (m), and d - the zero plane displacement height that represents the apparent level of the bulk drag exerted by the vegetation (or any other roughness elements) on the air (depending on the surface characteristics, the displacement height may be negligible, as in Lancaster and Baas, 1998, and see in Wieringa, 1993) . The length $Z_0$ is a measure of the aerodynamic roughness of the surface, and is related to the height of the roughness elements, their

shape and distribution. Common values of $Z_0$ range from $0.1*10^{-5}$ to $10*10^{-5}$ m for water, 0.0003 m for sand, 0.01-6 m for vegetation (Oke, 1987).

The various methods existing for the estimation of $Z_0$ values may be divided among field methods and remote sensing methods, as well as between direct methods (that measure the roughness elements themselves) and indirect methods (that infer $Z_0$ values from other variables, e.g. wind). The traditional wind profile approach for estimating $Z_0$ values is based on measuring the wind speed simultaneously at several heights vertically above the ground, while applying a stability function that accounts for buoyancy effects on the wind profile (for a review, see Högström, 1988, 1996, and Bauer et al., 1992). However the assumption of log-linearity of wind velocity with height (below 1.5 m in height) over sand dunes is inappropriate, due to the changes in both topography and vegetation cover (Jackson and Hunt, 1975; Wiggs, 2001).

As vegetation cover increases, soil erosion decreases, partly because of the reduction in the force of the wind near the ground (Wolfe and Nickling, 1993; Wiggs et al., 1995). Consequently, various field methods were devised for estimating $Z_0$ values based on parameters of the vegetation (e.g. Dong et al., 2001). A classic relation was given by Lettau (1969):

$$Z_0 = 0.5\ h\ (A^* / A') \qquad (2)$$

Where h is the canopy height, A* - the silhouette area (the upwind face of the average roughness element), and A' – the per unit ground area occupied by each element. Further adjustments of Lettau's equation are given by De Vries et al. (2004).

An alternative method for deriving $Z_0$ values from wind data, measured at a single height that we used in this study was suggested by Wieringa (1973, 1986). This non-spectral model suggested by Wieringa is based on the assumption of a normal wind fluctuation distribution and on the fact that the turbulence level $\sigma_u/U$ increases with increasing roughness. Therefore, $Z_0$ can be derived from single-level stations wind measurements by way of a gustiness analysis. If at a station anemometer height $Z_s$, for some upwind azimuth sector the median value of the observed gust factor $G = U_{max}/U$ is known (where

U is the average wind speed, and $U_{max}$ is the maximum wind gust speed), then a gustiness-derived sector roughness length $Z_0g$ can be estimated from:

$$Z_{og(sector)} = Z_s \exp ( - [A f_T \{1.42 + 0.3013 \ln (-4 + 990 / U_t) \}] / [G_{sector} - 1 + A - f_T A ]) \quad (3)$$

Where A (≈ 0.9) is the attenuation of $U_{max}$ by the anemometry, and $f_T$ is a factor which is unity for 10-minute averaging periods and increases to 1.1 for hourly averages. $U_t$ is the average wavelength (wind run) of maximum gusts observed by the given station combination of anemometer and recorder, and varies usually between 50 and 100 m. The roughness value obtained by a gustiness analysis is an area-integrated parameter, taking into account both nearby and far-off obstacles, vegetation etc. in the upwind direction within a distance of ~3 km (for wind measurements at 10 m) over a sector of 20º to 30º width. The gustiness method for deriving $Z_0$ values has been evaluated by Barthelmie et al. (1993) in comparison with the profile, terrain and standard deviation methods and was found to be acceptable (see discussion in Wieringa, 1996). In the case of turbulent observations such as these, the measurement does not furnish a value for d (vegetation displacement) at all, however for modeling of wind-flow at meso- or macro-scale it is of little importance (Wieringa, 1993).

As it is impossible to conduct field measurements of either wind or vegetation parameters in many places over large areas, approximations of $Z_0$ values are often used for different land-use categories to derive numerical weather prediction models (Petersen et al., 1997), wind damage maps (Blennow and Sallnäs, 2004), etc. Representative roughness parameters for homogeneous and heterogeneous terrains are given by Wieringa (1992, 1993).

Active remote sensing methods provide an alternative method for mapping $Z_0$ values over large areas. Blumberg and Greeley (1993) demonstrated for various geological terrains (Sand-mantled pahoehoe, Pahoehoe, Alluvium, Playa and Playa/gravel) in the south-western deserts of the United States (Death Valley, Central Nevada and the Mojave

Desert) that airborne radar backscatter can be used as an indication of variations in $Z_0$ on a regional scale. In addition, laser altimeters, whether airborne or space-borne are used to derive roughness estimations (See Garvin et al., 1998). In this regard, a new method to derive effective aerodynamic roughness of a complex dune area using high resolution laser altimeter measurements of land surface roughness was recently presented by de Vries et al. (2003). However, the technology of laser altimeters is very expensive and out of reach for most of the scientific community.
Passive remote sensing tools may also serve for the estimation of vegetation of aerodynamic roughness as offered by Jasinski and Crago (1999). They have used Landsat TM images over a coniferous forest in France, based on a characterization of the bulk canopy geometry.

## 1.2 Wind flow over coastal dunes

Sand dunes present an aeolian landscape, a landscape shaped by wind, that in itself transforms the wind field. Desert and coastal dunes cover about 10% of the land area between latitudes 30˚N and 30˚S (Sarnthein, 1978). Sand dune areas are dynamic in nature, with the dunes changing their location, length, or height, depending on the dune type (Tsoar, 2001; Andrews et al., 2002). An understanding of the aerodynamic roughness of dune areas is therefore highly important for understanding the spatial variability in dune movement and in dune stabilization processes.
Coastal dune areas are commonly characterized by wind flowing in from the sea inland, passing from the smooth surface of the water, to a rougher surface at the beach, and then passing over the dune field itself, where vegetation may or may not exist.
As the wind passes from one surface-type to another one, it must adjust to a new set of boundary conditions. The adjustment is not immediate throughout the depth of the air layer, rather it is generated at the surface and diffuses upward (Oke, 1987). As the wind passes from a smooth to a rough surface the wind speed will decrease and its direction will deflect towards the lower pressure, that is to the left in the northern hemisphere (Plate, 1982; Warren, 1976).
When considering the wind flow over topographic features, they are commonly classified according to whether or not flow separation occurs (Jackson and Hunt, 1975; Oke, 1987):

- Slopes up to about 30% (17°) are considered as moderate topography, allowing the boundary layer flow to adjust without separation. In such cases a hill will cause the wind to speed-up over its vicinity with a maximum near summit. This behavior corresponds to the wind flow in the upwind part of most dunes. In such cases a maximum amplification factor can be estimated using simple mathematical formulas that incorporate the height H of the topographic feature and the distance X from the crest of the hill to the upstream point where the height equals H/2.
- If the upwind or downwind slope of the ground exceeds about 17°, flow separation occurs. In sand dunes this happens in the dunes' slip face, where the slope reaches an angle of 33°. In such complex systems where secondary flows occur, a simple mathematical analysis is not possible.

Many studies that deal with the effects of topography on wind flow have considered only isolated hills (e.g. Ishihara et al., 1999), or have used wind tunnels and simulations (e.g. Kim et al., 1997; Neff and Meroney, 1998), and only few of them have conducted field measurements of actual wind flow (e.g. Kim et al., 2000).

The same is true also for sand dunes, where many studies have been restricted to computer simulations and wind tunnel measurements of the wind flow (e.g. Walker and Nickling, 2003, and Parsons et al., 2004), or to the measurements and modeling of wind flow over a single dune (e.g. Sauermann et al., 2003; McKenna Neuman et al., 2000; Sweet and Kocurek, 1990) or to field measurements only between the beach and the fore dune (e.g. Arens, 1996; Hesp et al., 2004).

Studies of wind flow over sand dunes apply many principles that were studied over hills. In this regard, the following points may be highlighted: (1) Wind speed is generally expected to gradually decrease with the distance from the coastline (modified locally by topography and vegetation), and along with the wind so is the sand transport rate decreasing (Troen and Peterson, 1989; Illenberger and Rust, 1988; Ranwell, 1958); (2) However, analyzing a succession of symmetrical sinusoidal ridges, maximum speed-up of the wind was found in the first hill crest, whereas in the second and third hills the speed-up is much reduced relative to the first one, remaining unchanged downstream of the third hill (Miller and Davenport, 1998; Carpenter and Locke, 1999). Thus, the most

significant decrease in wind speed is expected to be at the interaction between the beach and the fore dune area; (3) As reviewed by Wiggs (2001), shear velocity ($U_*$) cannot be successfully measured for windflow over dunes or related to sand flux on dune surfaces. Wiggs therefore recommends to concentrate on wind velocity in field studies and not on shear velocity; (4) the wind flow characteristics over dunes include flow compression over their stoss slope (Frank and Kocurek, 1996a), and flow separation on their lee slope (Frank and Kocurek, 1996b),

### 1.3 Objectives

Not only that there are few studies that have estimated $Z_0$ values for landscapes comprised of sparse vegetation typical of arid and semi-arid regions, there are also logistical and theoretical limitations inherent to wind profile techniques in such areas (Sherman, 1995; Wiggs, 2001; Prueger et al., 2004). The objectives of our study were therefore two fold:

- To study the combined influence of vegetation cover and topographic variables on the aerodynamic roughness length ($Z_0$) across a coastal dune field.
- To evaluate the feasibility of creating a map of $Z_0$ values using simple field measurements and using GIS and remote sensing techniques.

## 2. Methods

### 2.1 Study area

The Israeli coastline is characterized by an alternating mosaic of coastal dunes and coastal cliffs of aeolianites up to 50m high (Tsoar, 1990). These coastal dunes are about 1,000-1,500 years old and have the Nile River as their main source of sand.
The area covered by coastal dunes in Israel has diminished from 462 $km^2$ (Tsoar, 1990), to only 185 $km^2$ at the end of the 1990's (Frumkin-Ahiron et al., 2003), due to the quarrying of sand, and the construction of cities, military bases and water reservoirs over dune areas. In addition, the remaining dunes are undergoing processes of stabilization by vegetation, due to changes in human land uses along the coast, mainly the ending of the

practice of the "mawasi" agricultural system (in which the high level of coastal underground water was used for growing grapes, palm trees and other crops; see Tsoar and Zohar, 1985) and grazing by Arab and Bedouin local populations since the establishment of the state of Israel (Tsoar and Blumberg, 2002; Levin and Ben-Dor, 2004).

Two sites were chosen for the wind measurements: the dunes of Ashdod/Nizzanim in the south, and the dunes of Bet-Yanay in the north (see Figure 1). We chose to work on two dune areas so that in our analysis each one in its turn will be used for the calibration of the model and the other for its validation. The average movement rate of the Ashdod/Nizzanim dunes is now estimated to be less than one meter/year (Levin and Ben-Dor, 2004), their average vegetation cover being about 31% (based on Frumkin-Ahiron et al., 2003; Kutiel et al., 2004, estimated it at 29%), and the average yearly rainfall about 485mm.The dunes of Ashdod/Nizzanim represent the largest remaining tract of relatively undisturbed coastal dunes in Israel, covering 31 $km^2$ (out of 49 $km^2$ originally) between the cities of Ashdod and Ashkelon (Frumkin-Ahiron et al., 2003).

The dunes of Bet-Yanay were formed at the mouth of the Alexander stream and cover a much smaller area (with only 0.36 $km^2$ of active dunes remaining out of 1.82 $km^2$ 60 years ago), intersected in the middle by the Tel-Aviv Haifa highway. Their average vegetation cover is about 22% (based on Frumkin-Ahiron et al., 2003), the average yearly rainfall there being about 550mm.

The average height of Israel's coastal dunes is about 10m (Levin et al., 2004). The vegetation associations common to Israel's southern coastal dunes are described by Danin and Nukrian (1991); They note that with increasing sand stability the germination and establishment of more species is enabled and the monospecific community of *Ammophilia arenaria* thickens and changes into associations where *Artemisia monosperma* is the dominant plant (see also Levin et al., in preparation). The vegetation associations common to Israel's northern coastal dunes are described by Kutiel et al. (1979/80).

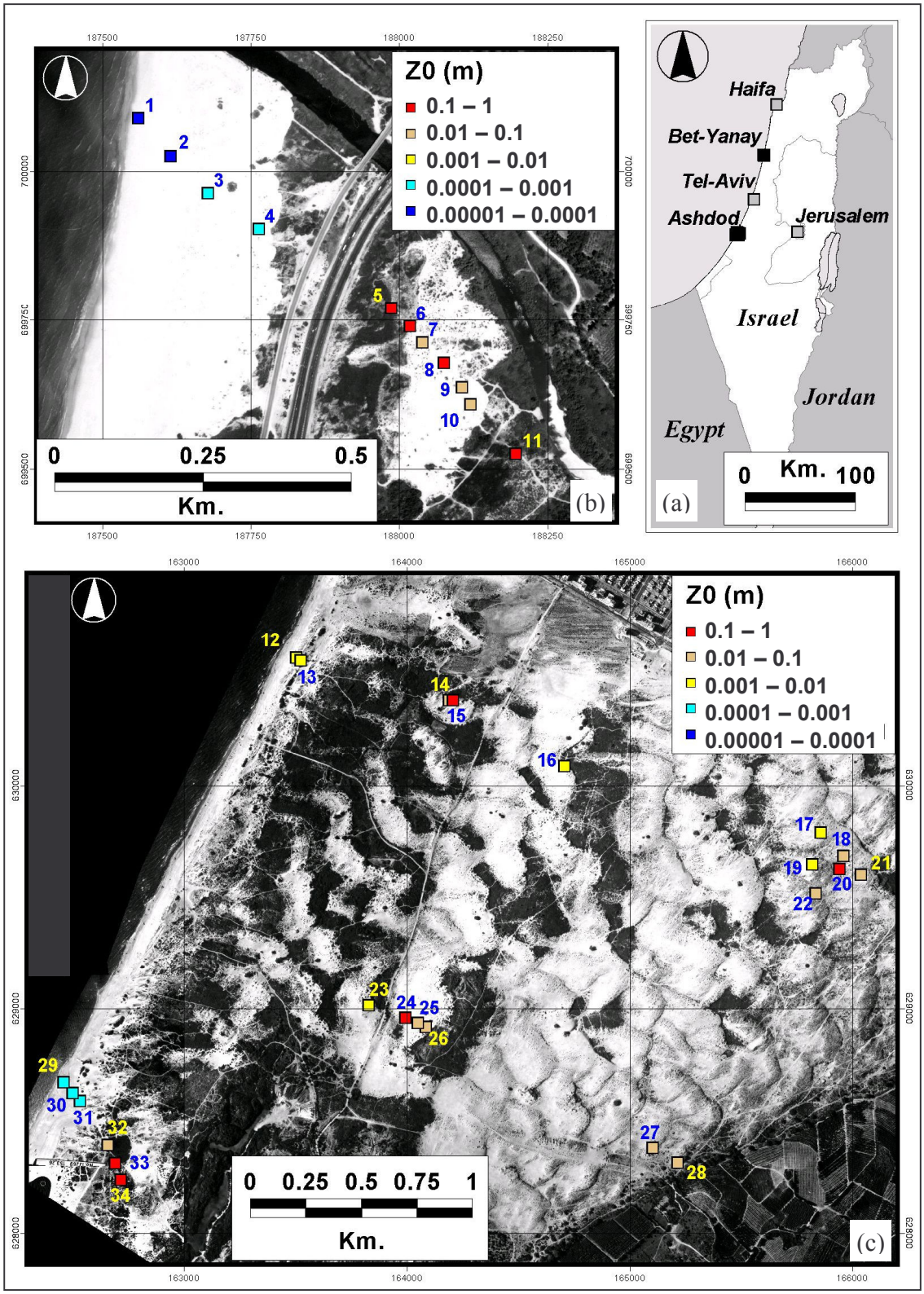


**Figure 1**: Map of study area, wind stations sites and measured values of $Z_0$ (a. location map; b. Bet Yanay; c. Ashdod)

| Id on map | Location | X | Y | Date | Time | μ (σ) of the winds' | | | $Z_0$ (m) | | Upwind variables | | |
|---|---|---|---|---|---|---|---|---|---|---|---|---|---|
| | | | | | | speed (m/s) | gust speed (m/s) | direction | Median | CV | SAVI, 200m | CV of SAVI | Height difference, 400m |
| 1 | C, beach | 187560 | 700090 | 1/4/04 | 9:35-16:25 | 9.7 (2.8) | 11.5 (3.4) | 337.7 (26.1) | 0.00005 | 2.68 | 0.000 | | 0.0 |
| 2 | C, beach | 187615 | 700026 | 1/4/04 | 9:15-12:55 | 7.1 (1.8) | 8.5 (2.1) | 306.7 (16.6) | 0.00006 | 1.76 | 0.020 | 146% | 0.7 |
| 3 | C, beach | 187677 | 699963 | 1/4/04 | 13:00-16:25 | 11.7 (0.8) | 14.5 (1.3) | 333.8 (6.3) | 0.00050 | 1.97 | 0.059 | 40% | 1.0 |
| 4 | C, fore dune | 187763 | 699903 | 1/4/04 | 9:00-16:40 | 9.9 (2.8) | 12.5 (3.8) | 324.6 (27.1) | 0.00042 | 2.87 | 0.083 | 13% | 3.1 |
| 5 | D, vegetated slack | 187987 | 699770 | 1/4/04 | 15:25-16:15 | 7.3 (0.7) | 12.9 (1.4) | 340.6 (5.1) | 0.21628 | 0.53 | 0.149 | 25% | -1.2 |
| 6 | D, vegetated slack | 188017 | 699739 | 1/4/04 | 12:20-15:15 | 7.0 (0.6) | 11.7 (1.0) | 294.5 (24.0) | 0.14602 | 0.47 | 0.141 | 22% | 0.0 |
| 7 | D, top of nebka | 188038 | 699712 | 1/4/04 | 10:05-12:10 | 6.5 (0.7) | 9.0 (1.1) | 291.8 (11.6) | 0.01798 | 0.74 | 0.141 | 21% | 2.7 |
| 8 | D, behind nebka | 188075 | 699678 | 1/4/04 | 15:15-16:30 | 6.1 (0.5) | 12.0 (1.1) | 350.5 (8.2) | 0.36352 | 0.34 | 0.146 | 16% | -0.9 |
| 9 | D, dune top | 188106 | 699637 | 1/4/04 | 12:15-15:10 | 9.9 (0.8) | 14.1 (1.0) | 354.9 (22.1) | 0.02690 | 1.11 | 0.127 | 16% | 4.1 |
| 10 | D, dune top | 188120 | 699608 | 1/4/04 | 9:50-16:35 | 9.0 (1.2) | 12.7 (2.3) | 340.1 (20.4) | 0.01982 | 1.24 | 0.118 | 12% | 5.1 |
| 11 | D, vegetated slack | 188196 | 699525 | 1/4/04 | 9:35-12:10 | 4.3 (0.7) | 7.8 (1.1) | 311.6 (15.3) | 0.22676 | 0.46 | 0.139 | 26% | -3.4 |
| 12 | C, *Ammophila* nebka | 163503 | 630575 | 18/2/03 | 10:35-16:20 | 14.4 (2.0) | 18.4 (3.0) | 220.9 (4.1) | 0.00195 | 1.24 | 0.037 | 99% | 4.0 |
| 13 | C, fore dune | 163523 | 630560 | 18/2/03 | 10:35-13:30 | 15.3 (3.4) | 20.1 (3.6) | 235.5 (6.9) | 0.00367 | 1.54 | 0.065 | 49% | 3.5 |
| 13 | C, fore dune | 163523 | 630560 | 18/2/03 | 13:35-16:20 | 16.8 (2.4) | 21.8 (2.9) | 265.3 (6.9) | 0.00447 | 1.09 | 0.012 | 242% | 6.4 |
| 14 | D, dune top | 164189 | 630383 | 18/2/03 | 10:35-13:30 | 14.9 (1.8) | 21.0 (2.4) | 243.1 (5.7) | 0.02567 | 0.76 | 0.140 | 15% | 12.0 |
| 14 | D, dune top | 164189 | 630383 | 18/2/03 | 13:35-16:20 | 13.7 (2.3) | 20.3 (3.4) | 268.6 (6.3) | 0.05183 | 0.58 | 0.155 | 16% | 8.8 |
| 15 | D, dune top | 164206 | 630383 | 18/2/03 | 10:35-13:30 | 14.0 (1.2) | 19.8 (1.7) | 230.8 (6.4) | 0.02745 | 0.59 | 0.134 | 13% | 11.0 |
| 15 | D, dune top | 164206 | 630383 | 18/2/03 | 13:35-16:20 | 11.2 (2.2) | 17.8 (3.3) | 261.9 (7.8) | 0.11857 | 0.52 | 0.153 | 18% | 7.7 |
| 16 | D, dune top | 164707 | 630088 | 18/2/03 | 10:35-13:30 | 15.2 (1.0) | 20.4 (1.0) | 252.3 (5.4) | 0.00786 | 0.87 | 0.122 | 15% | 3.5 |
| 16 | D, dune top | 164707 | 630088 | 18/2/03 | 13:35-16:20 | 16.9 (2.6) | 22.6 (3.4) | 276.6 (5.1) | 0.00893 | 1.47 | 0.113 | 10% | 8.1 |
| 17 | D, dune top | 165858 | 629791 | 26/10/04 | 10:20-14:15 | 8.8 (1.1) | 11.5 (1.2) | 256.1 (10.3) | 0.00428 | 1.08 | 0.123 | 9% | 8.5 |
| 18 | D, dune top | 165958 | 629687 | 26/10/04 | 10:40-14:25 | 7.1 (0.7) | 10.5 (1.2) | 265.4 (12.3) | 0.04189 | 0.79 | 0.122 | 5% | 2.9 |
| 19 | D, dune top | 165819 | 629648 | 26/10/04 | 9:55-11:05 | 8.7 (1.4) | 12.4 (1.1) | 220.6 (20.5) | 0.02707 | 1.17 | 0.120 | 4% | 5.2 |
| 19 | D, dune top | 165819 | 629648 | 26/10/04 | 11:10-14:05 | 8.8 (0.8) | 11.7 (1.1) | 250.1 (7.0) | 0.00799 | 1.03 | 0.133 | 9% | 7.9 |
| 20 | D, vegetated slack | 165942 | 629629 | 26/10/04 | 11:20-14:55 | 4.4 (0.5) | 7.7 (0.9) | 268.4 (10.7) | 0.19008 | 0.43 | 0.123 | 5% | -1.9 |
| 21 | D, dune top | 166039 | 629602 | 26/10/04 | 11:05-14:45 | 7.1 (0.9) | 10.3 (1.2) | 265.5 (9.6) | 0.04208 | 0.77 | 0.130 | 5% | 4.6 |
| 22 | D, dune top | 165836 | 629520 | 26/10/04 | 10:50-14:35 | 6.9 (0.9) | 10.1 (1.1) | 263.4 (27.8) | 0.03999 | 0.71 | 0.128 | 13% | 7.7 |
| 23 | D, dune top | 163827 | 629017 | 11/8/04 | 11:45-15:10 | 13.4 (0.8) | 17.9 (1.3) | 266.1 (4.8) | 0.00962 | 1.74 | 0.131 | 15% | 9.1 |
| 24 | D, windward slope | 163993 | 628960 | 11/8/04 | 11:45-15:10 | 8.9 (0.6) | 14.3 (1.0) | 249.5 (7.2) | 0.11366 | 0.47 | 0.117 | 14% | 2.8 |
| 25 | D, windward slope | 164048 | 628937 | 11/8/04 | 11:45-15:10 | 11.1 (0.5) | 15.7 (1.1) | 261.3 (6.4) | 0.02544 | 0.67 | 0.119 | 15% | 8.2 |
| 26 | D, dune top | 164084 | 628919 | 11/8/04 | 11:45-15:10 | 10.6 (0.8) | 16.7 (1.0) | 265.5 (6.6) | 0.08454 | 0.53 | 0.117 | 15% | 13.6 |
| 27 | D, dune top | 165103 | 628380 | 11/8/04 | 11:45-15:10 | 12.0 (0.8) | 17.4 (1.2) | 257.7 (5.8) | 0.03898 | 0.59 | 0.124 | 8% | 6.5 |
| 28 | D, dune top | 165216 | 628314 | 11/8/04 | 11:45-15:10 | 10.8 (0.9) | 16.8 (1.1) | 271.8 (7.3) | 0.08668 | 0.77 | 0.130 | 7% | 8.7 |
| 29 | C, beach | 162458 | 628673 | 25/5/03 | 11:50-17:25 | 11.4 (2.2) | 13.7 (2.6) | 331.3 (5.2) | 0.00014 | 1.52 | 0.000 | | 1.3 |
| 30 | C, beach | 162497 | 628624 | 25/5/03 | 12:20-14:30 | 9.8 (1.1) | 12.1 (1.2) | - | 0.00057 | 1.03 | 0.011 | 235% | 1.8 |
| 31 | C, beach | 162532 | 628588 | 25/5/03 | 11:50-17:15 | 10.9 (2.0) | 13.3 (2.5) | 330.9 (5.0) | 0.00032 | 1.41 | 0.031 | 117% | 1.8 |
| 32 | D, vegetated slack | 162655 | 628393 | 25/5/03 | 14:40-16:40 | 8.1 (0.6) | 12.9 (0.7) | - | 0.09879 | 0.39 | 0.102 | 24% | -1.1 |
| 33 | D, vegetated slack | 162689 | 628313 | 25/5/03 | 11:55-16:55 | 6.7 (0.9) | 11.3 (1.5) | 332.9 (6.0) | 0.15203 | 0.40 | 0.133 | 22% | -1.2 |
| 34 | D, vegetated slack | 162714 | 628238 | 25/5/03 | 12:05-16:55 | 6.0 (0.6) | 10.5 (1.2) | 339.8 (6.6) | 0.17549 | 0.38 | 0.158 | 12% | -1.0 |

**Table 1**: Wind measurement stations (per wind direction): x, y, date, time, wind direction and speed, $Z_0$, topography and vegetation. The stations in the table are numbered as on the map in Figure 1, from north to south. Stations tagged as C under the heading of location are the coastal stations, located between the coastline and the fore dune. Stations tagged as D under the same heading are the inland dune stations, located beyond the fore dune. CV stands for Coefficient of Variation.

## 2.2 Wind measurements

A total of 5 days of measurements were conducted, four at Ashdod/Nizzanim (February 18th, 2003, May 25th, 2003, August 11th, 2004 and October 26th, 2004) and one at Bet-Yanay (April 1st, 2004), at 34 different points spread from the coastline up to 2,800m inland (see Table 1 and Figure 1 for the date, time and exact location of the stations). The position of all the wind stations was measured using a differential GPS (± 1m). Out of the 34 points, 9 were located between the coastline to the fore dune, and the remaining 25 points further inland behind the fore dune. Most of the stations were located at dune tops, or at the windward side of dunes as well as on the beach. Few stations were located at inter-dune areas, and no stations were located in the lee-slope of dunes (see Table 1 for details). This setting was aimed to avoid further complexity in the analysis of the data that might have been encountered due to the separation of the winds' flow lines and the creation of a separation cell in the lee side of a dune (Parsons et al., 2004).

The wind measurements were performed at a height of 2.5m. According to the guide lines given by Wieringa (1993, p. 333) we performed such measurements only in areas where the canopy height was less than 1 m. We used a RM Young 05103 Wind Monitor cabled to a Campbell Scientific 21X data logger. The 05103 Wind Monitor can measure wind speed at the range of 0-60 m $s^{-1}$, with an accuracy of 0.3 m $s^{-1}$. Wind Data were sampled every second and recorded in the data logger for intervals of five minutes. The recorded variables included for each interval the average wind speed, the maximum wind gust speed, and the most common wind direction.

## 2.3 Calculation of $Z_0$ from the wind data

Estimation of $Z_0g$ was carried out based on Equation 3, for 10 minutes averaging periods. As we recorded the data every five minutes, and considering that the average wavelength (wind run) of maximum gusts ($U_t$) lasts less than half a minute, we were not to calculate it from our data and assumed it to be 75 m (as this was the average of the values suggested by Wieringa, 1986). As the variable of $Z_0g$ is a sector derived variable depending on the upwind surface characteristics, we defined for each station the direction from which the wind blew, as either coming from the south-west, from the west or from the north-west. In the measurements conducted at the dunes of Ashdod/Nizzanim on

February 18th, 2003, and on October 26th, 2004, the wind changed its direction from south-westerly in the morning to westerly in the afternoon. We have therefore separated these two time periods, and calculated $Z_0$g values for each of them. Thus we arrived at a total of 39 measurements of $Z_0$, 10 of them related to locations between the coastline and the fore dune, and the remaining 29 further inland behind the fore dune (11 in the dunes of Bet Yanay, and 28 in the dunes of Ashdod). We have concentrated this study on the estimation of $Z_0$ values and not on evaluating the speed-up of the wind, so as to be able to compare between measurements performed on different days and places, with different wind velocities and directions.

## 2.4 Remote sensing of vegetation

Remote sensing analyses of vegetation included the calculation of vegetation cover from grey-scale aerial photographs taken by the Survey of Israel (as in Levin and Ben-Dor, 2004), and the calculation of the Normalized Difference Vegetation Index (NDVI) from Landsat 7 ETM+ satellite images. NDVI was calculated as follows (Clark Labs, 2002):

$$NDVI = (NIR - R) / (NIR + R) \quad (4)$$

where NIR = Value in the Near Infra Red band of an image pixel
R = Value in the Red band of an image pixel

As the values of NDVI are affected by the background soil, especially in arid and semi-arid areas where vegetation cover is low, we have also applied the Soil Adjusted Vegetation Index (SAVI), following Huete (1988):

$$SAVI = (NIR - R) / (NIR + R + L) * (1 + L) \quad (5)$$

Where L = A constant soil adjustment factor ranging between 0-100. We have tried several values and found in a preliminary study that L=0.25 gave the best results in our area for estimating vegetation cover (see also Levin and Ben-Dor, in review).

For the dunes of Bet-Yanay we used an aerial photograph taken by the Survey of Israel at 11:42 on May 3rd, 2003 (strip AR/2, photograph 712). For the dunes of Ashdod/Nizzanim we used two aerial photographs, one taken at 13:36 on February 11th, 2000 (photograph 7092), the other taken at 17:11 on June 8th, 2002 (strip BA-163, photograph B135). All the aerial photographs were rectified to the Israel New Grid (Israel Transverse Mercator; Mugnier, 2000), using Ground Control Points (GCPs) identified on a color orthophoto (1m. resolution).

We have calculated NDVI and SAVI values for both study areas based on Landsat 7 ETM+ satellite images (path 174 row 38) from August 7th, 1999, January 14th, 2000 and May 21st, 2000. This was done after performing atmospheric corrections using the MODTRAN (Berk et al., 1999) and ACORN (AIG, 2001) atmospheric models and fusing the spectral bands with high resolution (15m) pan chromatic band 8 of the Landsat, using Envi 3.4 (RSI, 2001).

We have calculated the vegetation cover and the NDVI and SAVI values for the locations of the wind stations, as well as for the upwind sectors of these stations at the following distances, using directional filters at a width of about 60º: 15 m, 25 m, 50 m, 100 m, 200 m and 400 m. Directional filters (see Lillesand and Kiefer, 1994) are a tool that enables the detection of directional objects in images, or in our case, to analyze the values of a certain variable for a certain sector, whose width and length are defined by the filter, with respect to the wind direction.

Since vegetation cover in the dunes area increases at an annual rate of about 1% between 1990-1999 (Levin and Ben-Dor, 2004, and Kutiel et al., 2004), we assume ed that our estimations regarding the effects of vegetation cover on the aerodynamic roughness, will not be hampered by using satellite images and aerial photographs that were acquired up to four years prior to the field measurements.

Although biological soil crusts have considerable influence on surface roughness and wind erosion (see Belnap and Gillette, 1998), their presence over the coastal dunes of Ashdod and Bet-Yanay is quite low, and was therefore not included in our analysis. In addition we did not include in our analysis possible effects due to soil moisture. All wind measurements that we conducted and the images that we used were on dry surface after at

least four days with no rainfall, so we estimated that except at the beach itself, our results will not be influenced by soil moisture.

## 2.5 Topographic analyses

Topographic data for our analyses was based on several sources that included digital contours files, orienteering maps and field measurements using differential GPS.

For the northern part of the Ashdod Dunes, detailed contours (at a vertical spacing of 0.5 meter) were obtained from a photogrammetric survey by Fishman (1994). For the southern part of the Ashdod Dunes, contour lines (at a vertical spacing of 2.5 meters) were digitized from the Nizzanim orienteering map (published in 1995 by the Israel Sport Orienteering Association, at a scale of 1:10,000), The data from the contours were converted into a digital elevation model (DEM) using the triangulation method described by Zhu et al. (2001), and implemented in the Idrisi software (Eastman, 2001).

For the dunes of Bet-Yanay no digital elevation data or detailed topographic maps were found, and we have therefore measured the topographic profile between the stations along the direction from which the wind blew using the differential GPS elevation information (with an estimated vertical accuracy of 1-2 m).

We have then used the following parameters to estimate the influence of topography on the measured surface roughness: (1) the distance of the station from the nearest dune upwind; (2) the height difference between the place where the station was located and crest of the nearest dune upwind; (3) the slope angle between the place where the station was located and the crest of the nearest dune upwind; (4) difference between the height of place where the station was located and the average height of the upwind sectors of the station at the following distances, using directional filters at a width of about 60º: 15 m, 25 m, 50 m, 100 m, 200 m and 400 m.

**Table 2**: Correlation values between $Z_0$ and the topographic and vegetation variables examined for the inland dune stations (n = 29).

| | **The location** | **The length of the upwind sector (m)** | | | | | |
|---|---|---|---|---|---|---|---|
| **The vegetation and topographic variables analyzed** | **of the station** | **15** | **25** | **50** | **100** | **200** | **400** |
| Average vegetation cover based on aerial photographs | 0.29 | 0.41 | 0.44 | **0.49** | 0.43 | -0.06 | -0.20 |
| Average NDVI value as of August 1999 | | 0.49 | 0.53 | **0.54** | 0.52 | 0.03 | -0.12 |
| Average NDVI value as of January 2000 | | 0.55 | 0.56 | **0.57** | 0.53 | 0.44 | 0.22 |
| Average NDVI value as of May 2000 | | 0.40 | 0.46 | **0.49** | 0.47 | 0.06 | -0.13 |
| Average SAVI (L=0.25) value as of January 2000 | | 0.52 | 0.54 | **0.57** | 0.56 | 0.41 | 0.29 |
| The difference in the height of the station from the average height of area upwind of the station | | -0.12 | -0.21 | -0.43 | -0.64 | -0.68 | **-0.68** |
| Height above sea level | -0.56 | | | | | | |
| Distance perpendicular to the coastline | -0.34 | | | | | | |
| Distance from the coastline along the winds' direction | -0.42 | | | | | | |
| Distance upwind to the nearest dune | -0.44 | | | | | | |
| Distance downwind to the nearest dune | 0.42 | | | | | | |
| Difference between the upwind & downwind distances | -0.56 | | | | | | |
| Height difference relative to the nearest dune upwind | -0.68 | | | | | | |
| The slope angle between the wind station and the dune upwind | -0.76 | | | | | | |

## 3. Results

### 3.1 Wind measurements and calculation of $Z_0$

The average and standard deviation of the wind speed, wind gust and wind direction are given in Table 1, as well as the calculated values of the surface roughness $Z_0$ and its coefficient of variation (CV; the values of the $Z_0$ standard deviation divided by its average). The calculated values of $Z_0$ range from a minimum of 0.00005 m (at station 1, located at the coastline itself; this value corresponds to those given by Oke, 1987, p. 57, for water) to a maximum of 0.36 m (at station 8 located at an inter-dune area behind a large nebka dune; this value corresponds to rough terrains, as described by Wieringa, 1992, p. 363). The CV of the $Z_0$ ranged between 0.36 and 2.87, and was found to be negatively correlated with $Z_0$ on a log-log plot ($R^2 = 76\%$, $p < 0.01$) This might mean that this method is more stable for estimating $Z_0$ over rougher areas, as in smooth areas there is much less difference between average wind speed and wind gusts. In Figure 2 it can be seen that there is a gradual increase in the values of $Z_0$ with the distance from the coastline, especially in the first 300 m. The variance explained in the values of $Z_0$ by the distance from the coastline is 50% and significant ($p < 0.01$), when all the stations are pooled together. When considering only the inland dune stations (those beyond a distance of about 300m from the coastline) a more or less random fluctuation in the values of $Z_0$ can be seen.

### 3.2 Correlation between vegetation and topography to $Z_0$

The correlation values between $Z_0$ and the various vegetation and topographic variables we have examined are given in Table 2, for the inland dunes. The table focuses on the area beyond the fore dune because some of the topographic variables relating to the distance to the first dune upwind, could not be calculated for the coastal stations (as for them, there is no dune upwind, only the beach and the sea).

As for the topographic variables, the following relationship emerges, in which the higher and farther is the wind station located with respect to the crest of the nearest dune upwind, the lower will the value of $Z_0$ found there. The variable that gave the highest correlation was that of the slope angle upwind ($R = -0.76$; see Table 2).

The topographic variables relating to the distance upwind from the nearest dune were not examined any further due to the following reasons: (1) they cannot be calculated for the coastal stations; (2) in a stabilizing coastal dune system, where the shape of the dune is under transformation, many nebkha dunes are forming and the clear discrimination of dune ridges disappears, it is not straight forward to determine where the nearest dune upwind is located, and some subjective decisions are needed. We have therefore chosen to focus on the topographic variable of relative height that can be easily calculated automatically using a digital elevation model as follows: the difference in the height of the station from the average height of area upwind of the station (examining variable length sizes, from 15 m to 400 m).

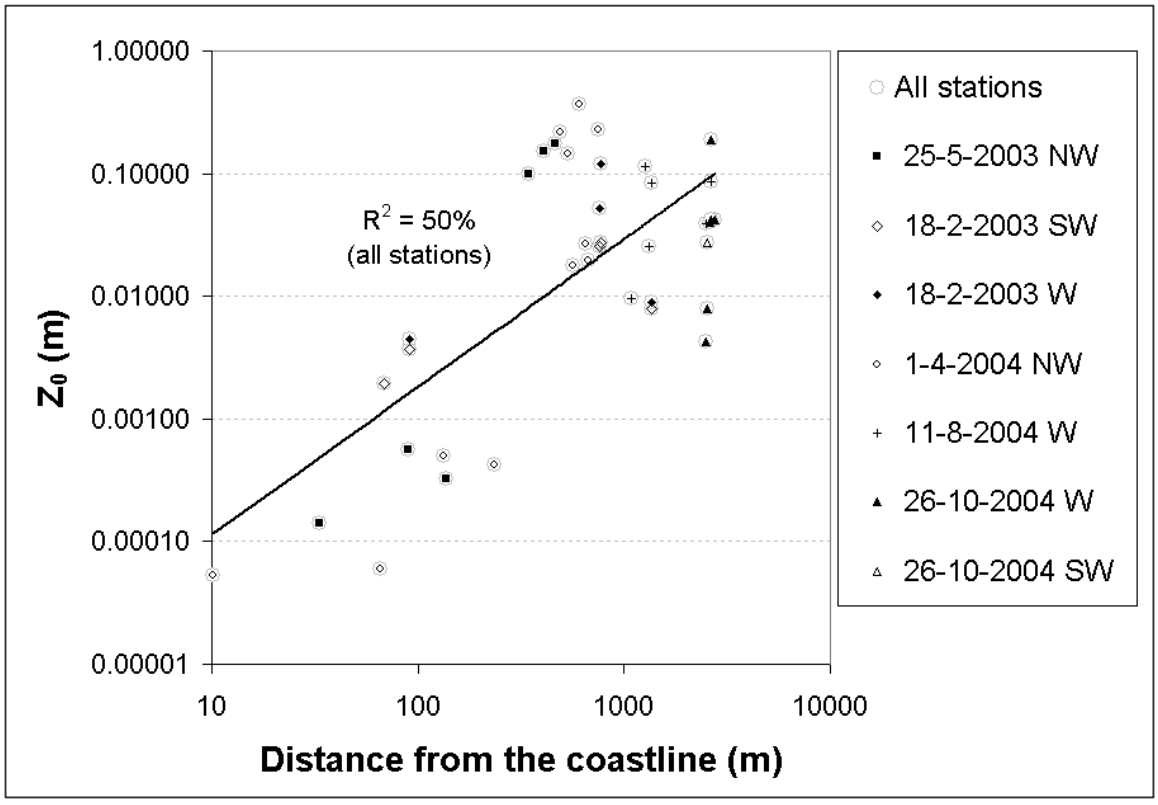


**Figure 2**: The variability in $Z_0$ values as a function of the distance from the coastline (n = 39). The stations are symbolized according to the date of measurement and the dominant wind direction at the time of the measurement. Notice that both axes are plotted on a logarithmic scale.

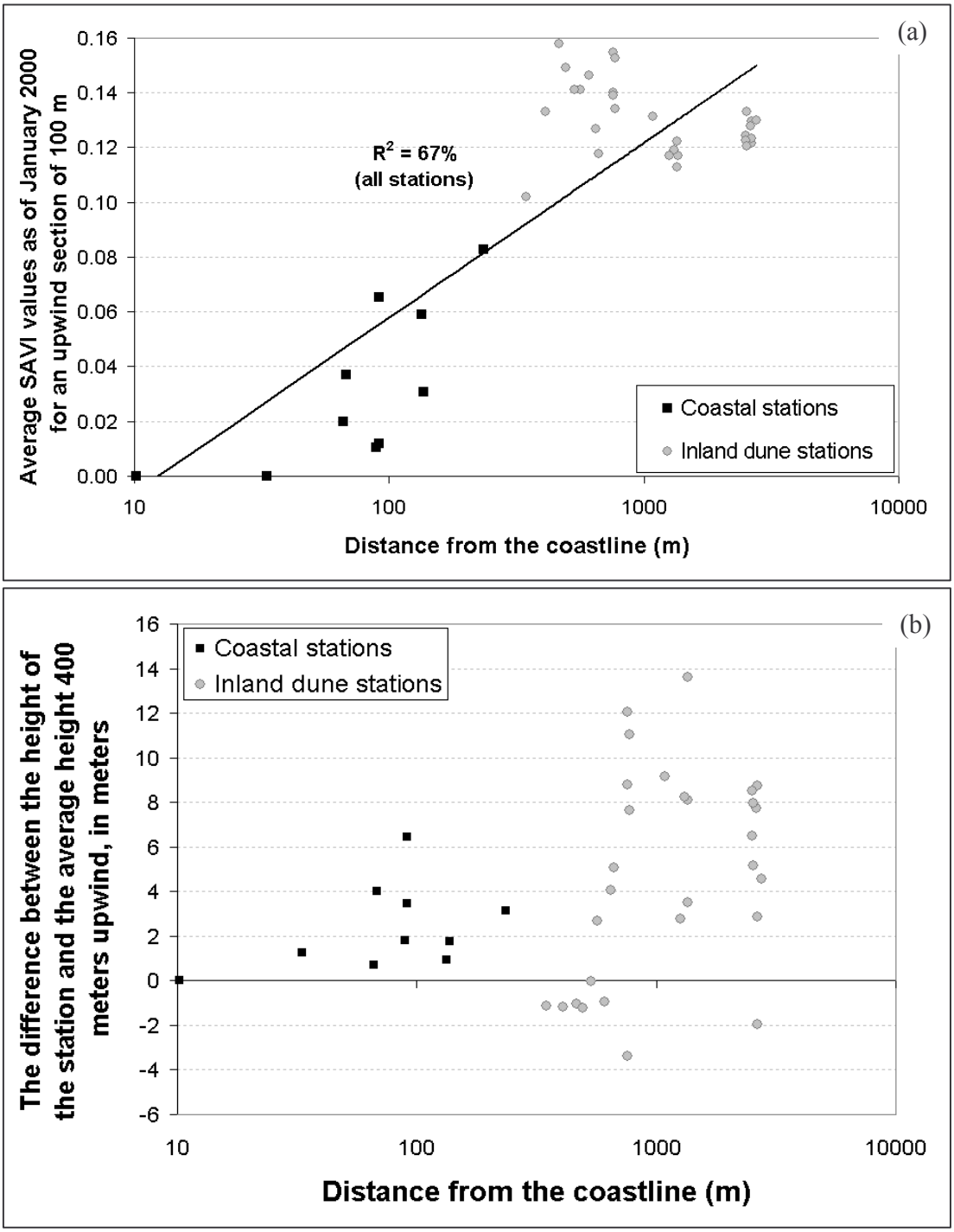


**Figure 3**: The variability in the variables of (a) SAVI (as of January 2000 for an upwind section of 200 m) and (b) topography (the difference between the height of the station and the average height at an upwind section of 400 m) as a function of the distance from the coastline, as measured in the locations of the wind stations. Notice that the x-axis is plotted on a logarithmic scale.

As for the vegetation variables, the highest correlation values were found at the same upwind length for all four variables: at 50 m (when only the inland dune stations were considered). In addition, it was found that Landsat images (whether they are of the winter, spring or summer seasons) give higher correlation values then black and white aerial photographs that have a higher resolution (see Table 2). In the results presented in Table 2 (for the inland dune stations), the variability explained by SAVI and by NDVI is equal. However, when considering all the stations, SAVI performs a little better than NDVI, and we will therefore focus most of our discussion on it below.

To examine the variability of the topography and the vegetation in the locations where wind was measured, and to understand the correlation found between the distance from the coastline and $Z_0$, we have selected two variables (one for each group) and drawn them with respect to the distance from the coastline (see Figure 3). The two variables are (1) SAVI as of January 2000 for an upwind section of 200 m, and (2) the difference between the height of the station and the average height at an upwind section of 400 m. As can be seen in Figure 3, these two variables behave differently for the coastal stations (0-300 m from the coastline) and for the inland dune stations (>300 m from the coastline), similar to the values of $Z_0$ shown in Figure 2. When all stations are pooled together, 67% ($p < 0.001$) of the variability in the values of the vegetation can be explained by the distance from the coastline (no such correlation was found for the relative height variable). In the coastal stations (defined as those stations located between the coastline and the crest of the fore dune), both the vegetation cover (as estimated by NDVI or SAVI) and to a lesser degree also the height difference increase gradually with the distance from the coastline. As for the inland dune stations, no clear pattern could be observed with respect to the distance from the coastline.

When comparing the correlograms (charts presenting the correlation between two variables as a function of another variable; in our case as a function of the length of the upwind sector) of the vegetation and the topographic variables (Figure 4), it can be seen that the highest correlations are reached at an upwind sector 100-200 m long (depending on the variable), and that vegetation as a whole explains more of the variability in the values of $Z_0$ than topography.

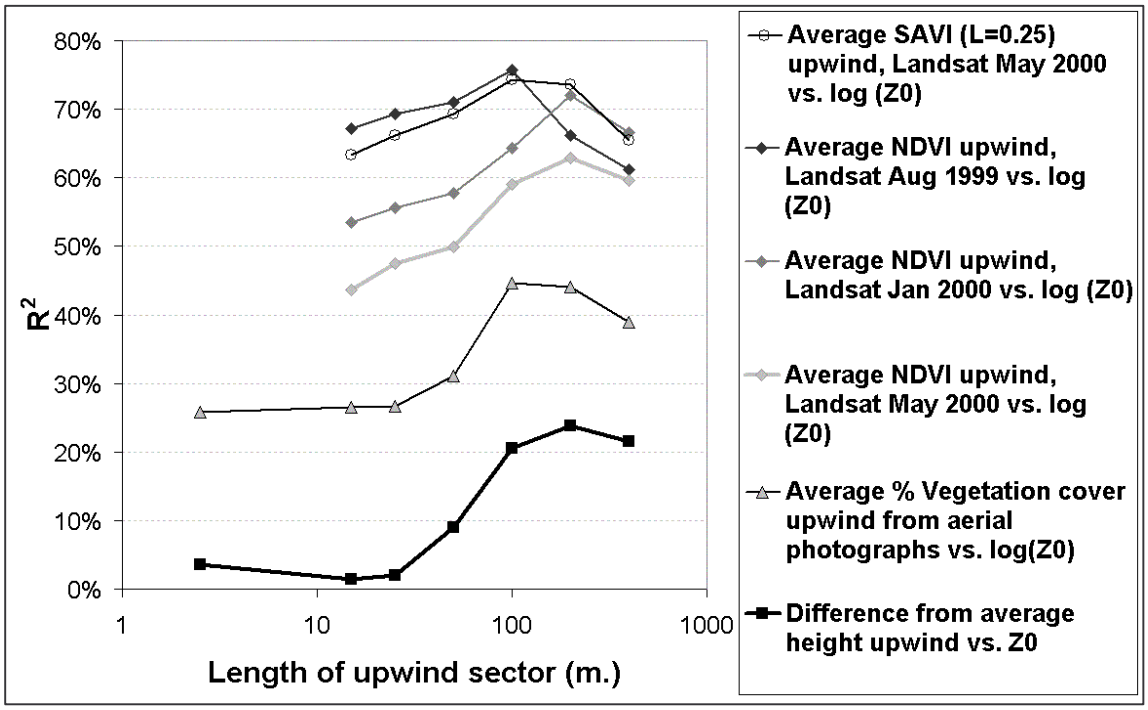


**Figure 4**: A correlogram presenting the correlation values between $Z_0$ and various vegetation and topographic variables as a function of the length of the upwind sector (all stations included). The leftmost point of each of the lines represents the correlation found between $Z_0$ and the analyzed variable at the position of the station. Notice that the x-axis is plotted on a logarithmic scale.

However, in Figure 4 all the stations were included – the coastal stations and the inland dune stations. When only vegetation is considered, mixing together the two areas is reasonable, as can be seen in Figure 5 – both for the coastal stations and for the inland dune stations, the higher is the vegetation cover, the roughness increases and the higher will be the values of $Z_0$. The higher correlation values obtained when combining all stations then for each of the areas separately may be explained that ranging from the coastline to the inland dunes, the values of $Z_0$ change on a scale of five orders, whereas in each area separately they change on a scale of only three orders. This is clarified in Figure 6, presenting scatter plots between the SAVI values of January 2000 (at upwind lengths of 50, 100 and 200 m, respectively).

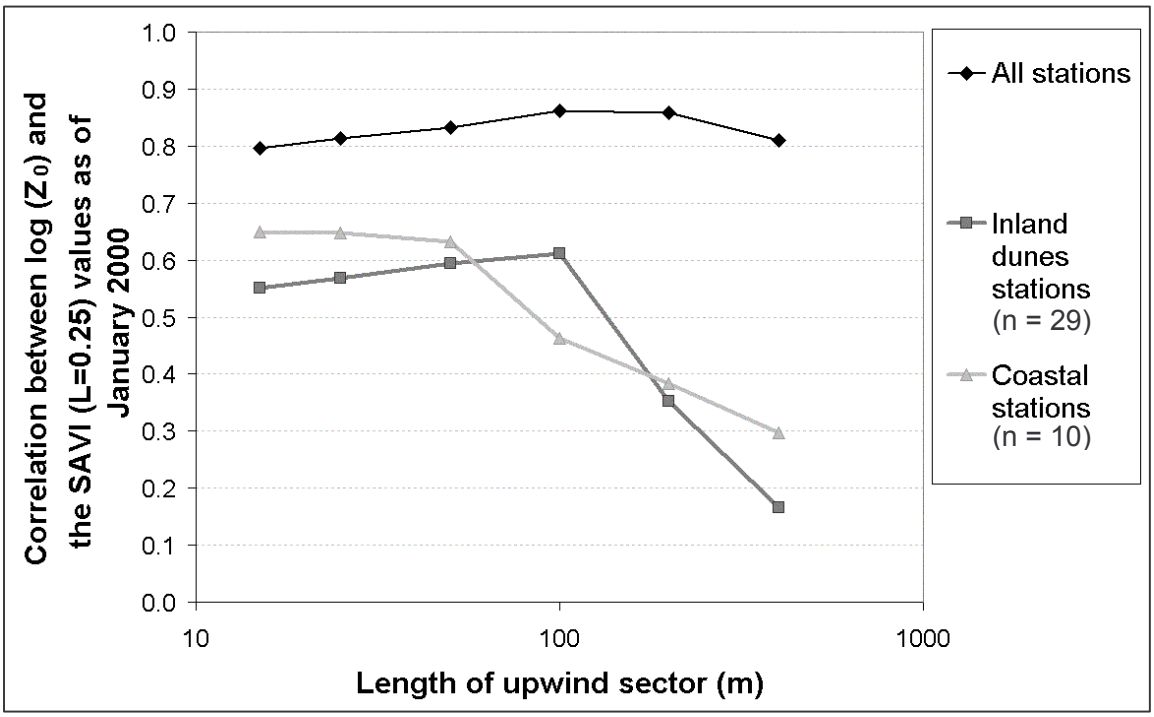


**Figure 5**: A correlogram presenting the correlation values between log ($Z_0$) and the SAVI (L=0.25) values as of January 2000, as a function of the length of the upwind section. The leftmost point of each of the lines represents the correlation found between log ($Z_0$) and the analyzed variable at the position of the station. Notice that the x-axis is plotted on a logarithmic scale.

The topographic variable of the difference in the height of the station from the average height of area upwind of the station behaves differently among the two areas however. In Figure 7 we present the correlation values between $Z_0$ and the topographic variable of the difference between the height of the station and the average height upwind, as a function of the length of the upwind sector, whereas Figure 8 presents the variability in $Z_0$ values as a function of the difference between the height of the station and the average height 400 meters upwind of the station, for the coastal and inland stations separately. Examining Figure 7 and Figure 8 we can see that whereas for the inland dune stations the values of $Z_0$ decrease with the relative height of the station (as expected), for the coastal stations a positive relationship exists, with higher $Z_0$ values the higher is the station located.

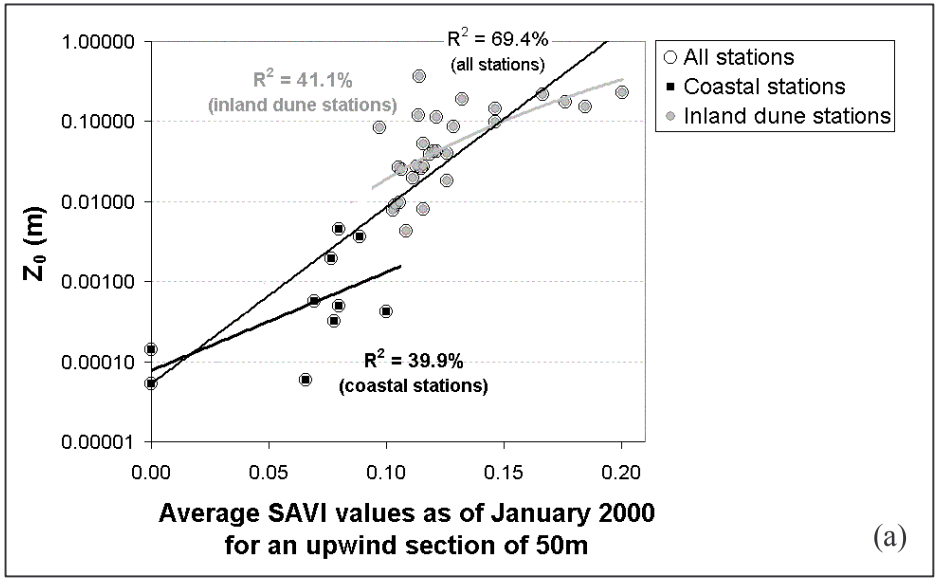


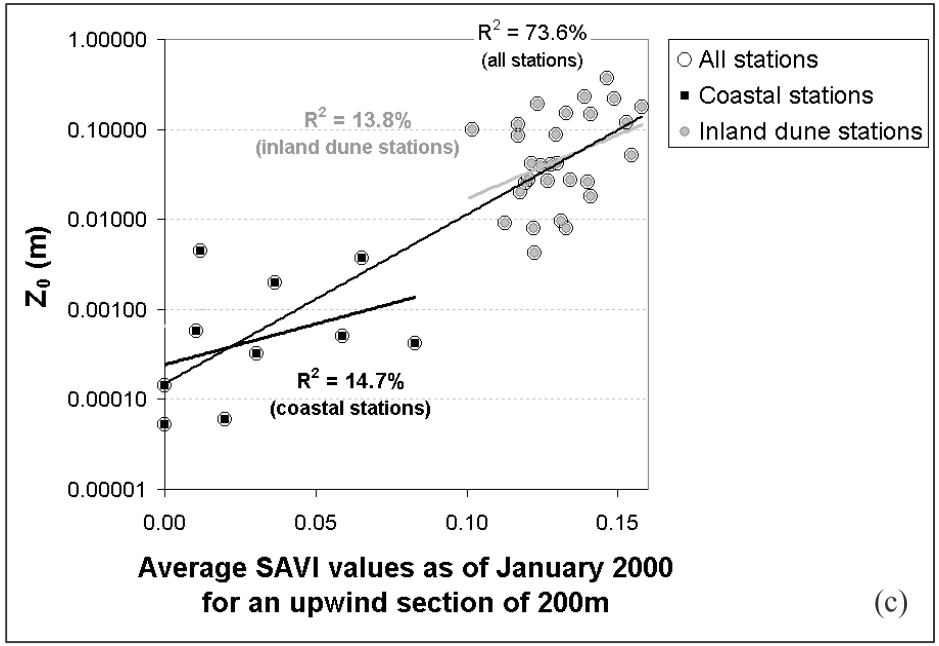


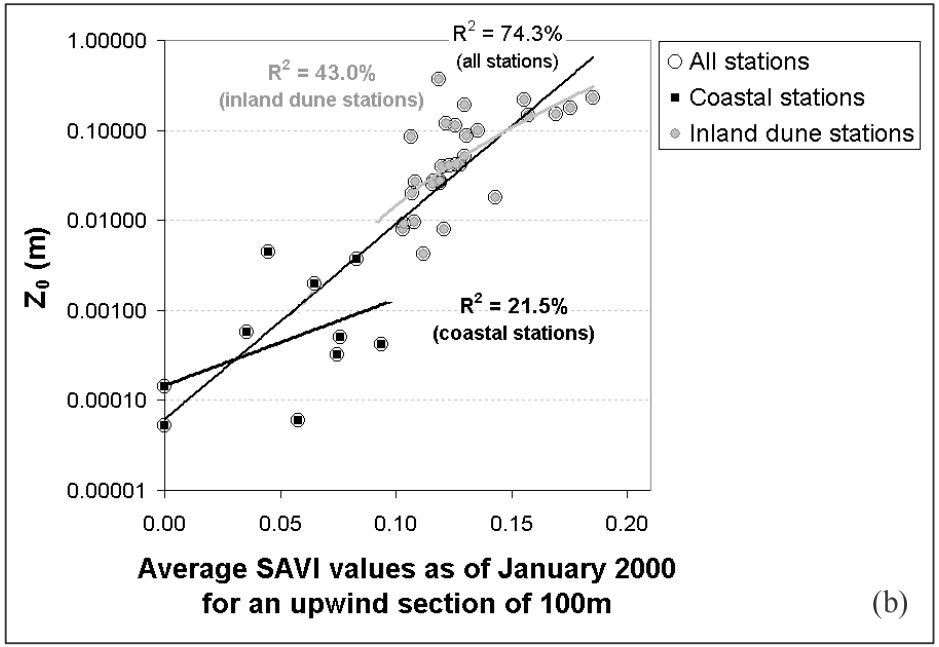


**Figure 6**: The variability in $Z_0$ values as a function of the SAVI values as of January 2000 for an upwind section of (a) 50 m, (b) 100 m, (c) 200 m. The stations are symbolized according to their location, either as coastal stations (n=10; on the beach or on the fore dune) or inland dune stations (n=29). Notice that the y-axis is plotted on a logarithmic scale.

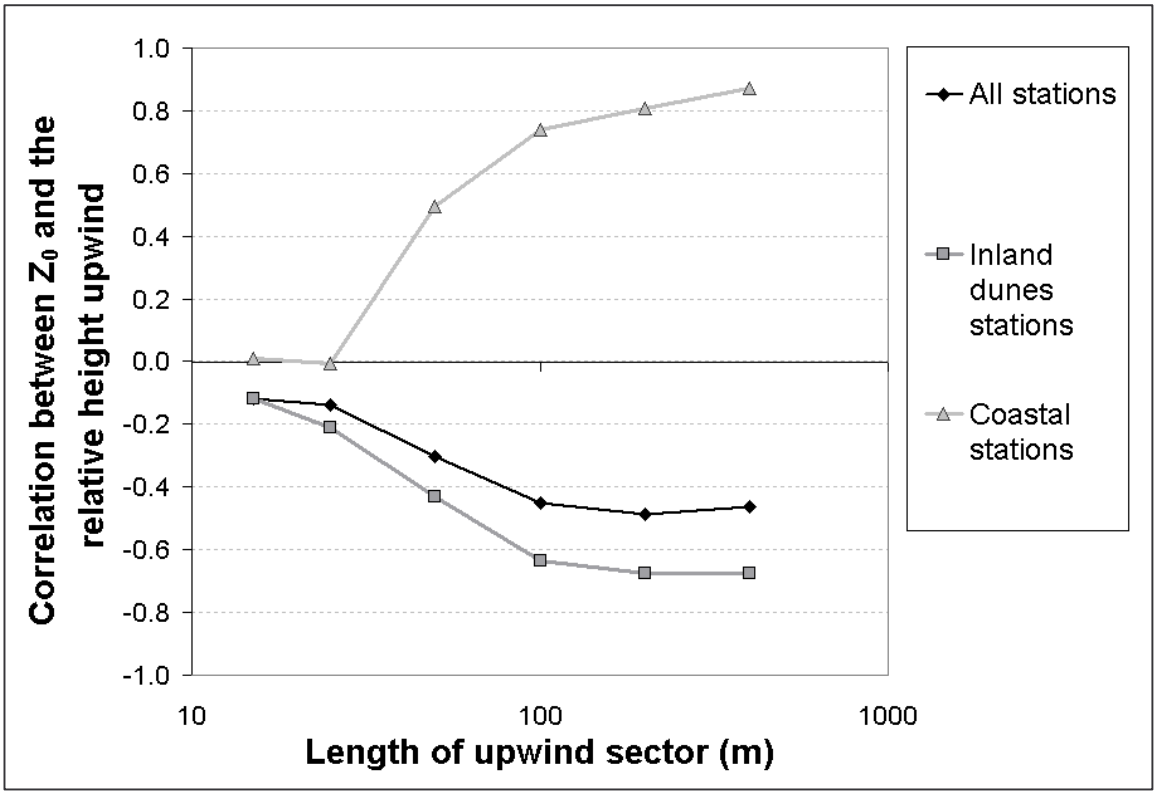


**Figure 7**: A correlogram presenting the correlation values between $Z_0$ and the topographic variable of the difference between the height of the station and the average height upwind, as a function of the length of the upwind sector. Notice that the x-axis is plotted on a logarithmic scale.

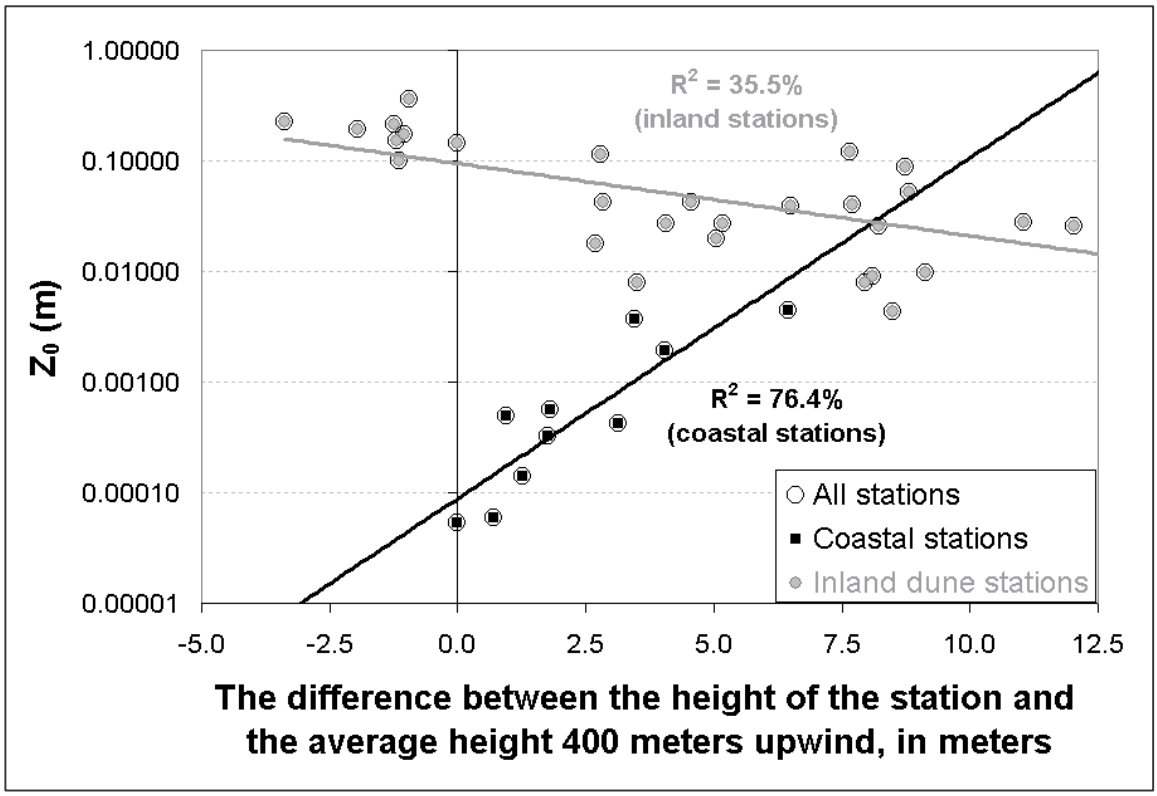


**Figure 8**: The variability in $Z_0$ values as a function of the difference between the height of the station and the average height 400 meters upwind of the station. The stations are symbolized according to their location, either as coastal stations (n =10; on the beach or on the fore dune) or inland dune stations (n = 29). Notice that the y-axis is plotted on a logarithmic scale, and that vegetation cover (not shown here) is not the same for all stations.

## 3.3 Validation of the predicted $Z_0$ values

To validate the accuracy of predicted $Z_0$ values based on the upwind variables of relative height and vegetation (either NDVI or SAVI, both of January 2000) we separated the stations according to their area, Bet Yanay (n = 11) and Ashdod (n = 28).

In tables 3 and 4 we present the variability in the values of log $Z_0$ in one dune area, explained by a regression model based on the other dune area, using two variables: the relative height 400m upwind and SAVI (or NDVI) values at 50, 100 and 200m upwind. From these tables it can be seen that the predictions done based on SAVI are better than those done based on NDVI. However the differences between the two are not large, and in almost all the combinations examined the $R^2$ value are higher than 64%.

**Table 3**: The variability in the values of log $Z_0$ in one dune area, explained by a regression model based on the other dune area, using two variables: the relative height 400m upwind, and SAVI values at 50, 100 and 200m upwind.

| Dune area on which the model is based | Bet Yanay (n = 11) | | | Ashdod (n = 28) | | | | |
|---|---|---|---|---|---|---|---|---|
| Topographic variable used | Relative height 400m upwind | | | | | | | |
| Vegetation variable used | SAVI 50m upwind | SAVI 100m upwind | SAVI 200m upwind | SAVI 50m upwind | SAVI 100m upwind | SAVI 200m upwind | | |
| $R^2$ between observed and predicted values of log $Z_0$ | 70.7% | 76.8% | **95.4%** | 70.4% | 76.4% | **94.6%** | Bet Yanay (n = 11) | Dune area on which the model is tested |
| | 72.2% | **75.3%** | 68.6% | 74.6% | **77.3%** | 71.2% | Ashdod (n = 28) | |

**Table 4**: The variability in the values of log $Z_0$ in one dune area, explained by a regression model based on the other dune area, using two variables: the relative height 400m upwind, and NDVI values at 50, 100 and 200m upwind.

| Dune area on which the model is based | Bet Yanay (n = 11) | | | Ashdod (n = 28) | | | | |
|---|---|---|---|---|---|---|---|---|
| Topographic variable used | Relative height 400m upwind | | | | | | | |
| Vegetation variable used | NDVI 50m upwind | NDVI 100m upwind | NDVI 200m upwind | NDVI 50m upwind | NDVI 100m upwind | NDVI 200m upwind | | |
| $R^2$ between observed and predicted values of log $Z_0$ | 64.8% | 68.9% | **93.2%** | 64.4% | 68.9% | **92.8%** | Bet Yanay (n = 11) | Dune area on which the model is tested |
| | 66.2% | **75.9%** | 67.9% | 72.0% | **76.3%** | 69.8% | Ashdod (n = 28) | |

The best results were obtained at upwind distances of 100m or 200m for the Landsat derived vegetation indices. Figure 9 presents in the form of a scatter plot the predicted $Z_0$ values of each dune area as derived from a regression model that was based on the other dune area. Notice that the predicted values are closer to the 1:1 line of perfect fit when the $Z_0$ values are higher. This may be due to the higher coefficient of variation (CV) of $Z_0$ data when $Z_0$ values are low.

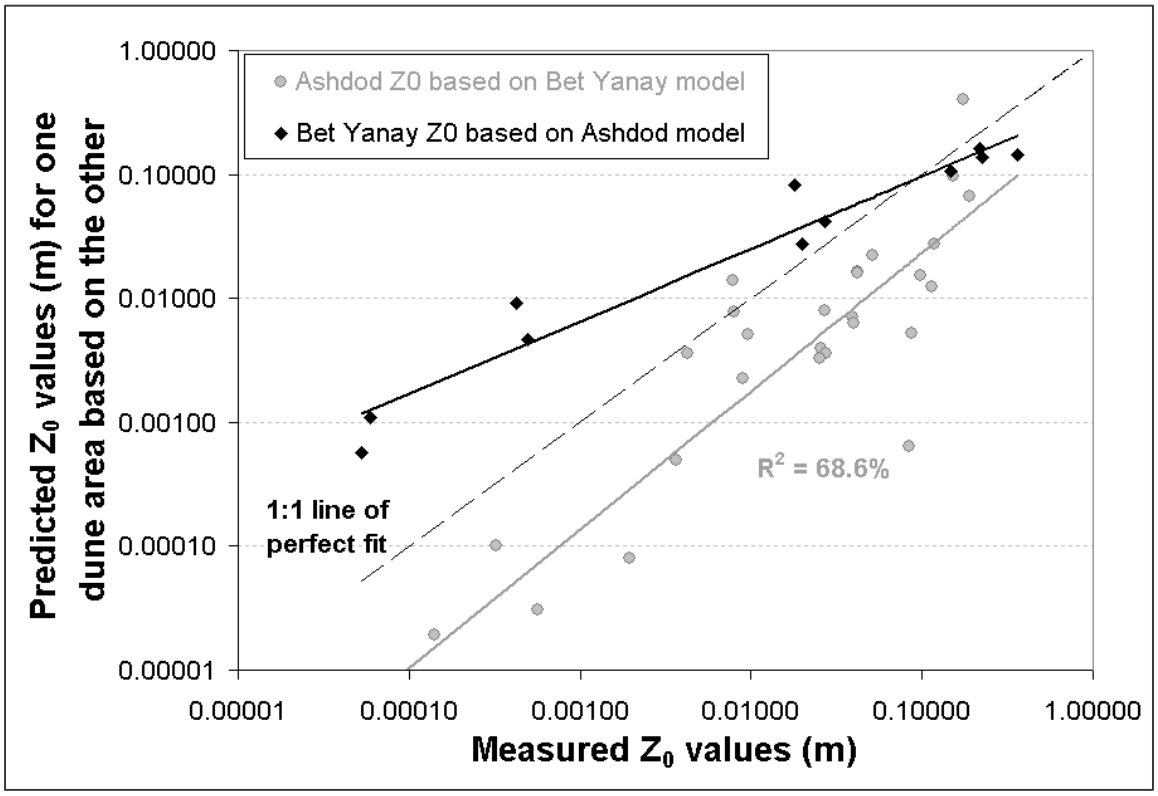


**Figure 9**: The predicted $Z_0$ values of each dune area derived from a regression model based on the other dune area, using the variables of relative height at an upwind distance of 400m and SAVI at an upwind distance of 200m. Notice that both axes are plotted on a logarithmic scale.

## 3.4 Mapping the predicted values of $Z_0$

To create a map of predicted $Z_0$ values, we have used a multiple regression model, using two variables, that served as topography and vegetation derived indices: the height difference at an upwind length of 400 m, and the SAVI values as of January 2000 at an upwind distance of 200 m. We chose these two variables as we found that these gave the

best results after examining various possible combinations of the SAVI and the relative height variables at various upwind distances. In addition, only when we used an upwind distance of 200m for SAVI we obtained a negative coefficient in the regression model for the relative height variable (see Equations 6 and 8 below). We chose to use the winter SAVI values as the sand moving winds in Israel blow in this time of the year (Goldsmith et al., 1990). We calculated the $Z_0$ model for winds blowing from the SW, as this corresponds to sand movement along the coast of Israel as well as to the dunes orientation (Tsoar, 1990).

The topographic variable was found to be positively correlated with the surface roughness for the coastal stations because there the wind is moving from the relatively smooth surface of the water to the rougher land surface, which is also gradually rising towards the foredune over a short distance of 50-300 m. For the inland dune stations however, the topographic variable was found to be negatively correlated with the surface roughness, as over land surfaces at higher locations, the wind flow is compressed, and wind speed increases, thus meaning lower $Z_0$ values. We therefore decided to compare two predictive models. In the so called "unified model" all stations are included. In the so called "separated model", we build a multiple regression separately for the coastal stations and for the inland dune stations. In order to avoid the possibility of obtaining negative values of $Z_0$, we have used a log-normal model, in which the topographic and vegetation variables are used to model the predicted values of log ($Z_0$).

Thus we received the following three regression models:

For the unified regression model, including both the coastal and the inland dune stations:

$$\text{Log}(Z_0) = -3.744 - 0.0373 * \Delta H + 19.514 * \text{SAVI} \quad (6)$$

($n = 39$, $p < 0.001$, adjusted $R^2 = 74\%$)

For the separated model, for the coastal stations:

$$\text{Log}(Z_0) = -4.170 + 0.292 * \Delta H + 4.87 * \text{SAVI} \quad (7)$$

($n = 10$, $p < 0.005$, adjusted $R^2 = 75\%$)

For the separated model, for the inland dune stations:

$$\text{Log}(Z_0) = -2.405 - 0.0606 * \Delta H + 10.290 * SAVI \quad (8)$$

$(n = 29, p < 0.001$ , adjusted $R^2 = 38\%)$

where $\Delta H$ = Height difference 400m upwind

SAVI = SAVI values as of January 2000, 200m upwind

Figure 10 presents a scatter plot in which the predicted values of the unified model and of the separated model (combining the coastal and the inland stations) are plotted against the measured values of $Z_0$. The separated model presents a higher correlation than the unified model ($R^2 = 87.6\%$, $R^2 = 75.8\%$, respectively).

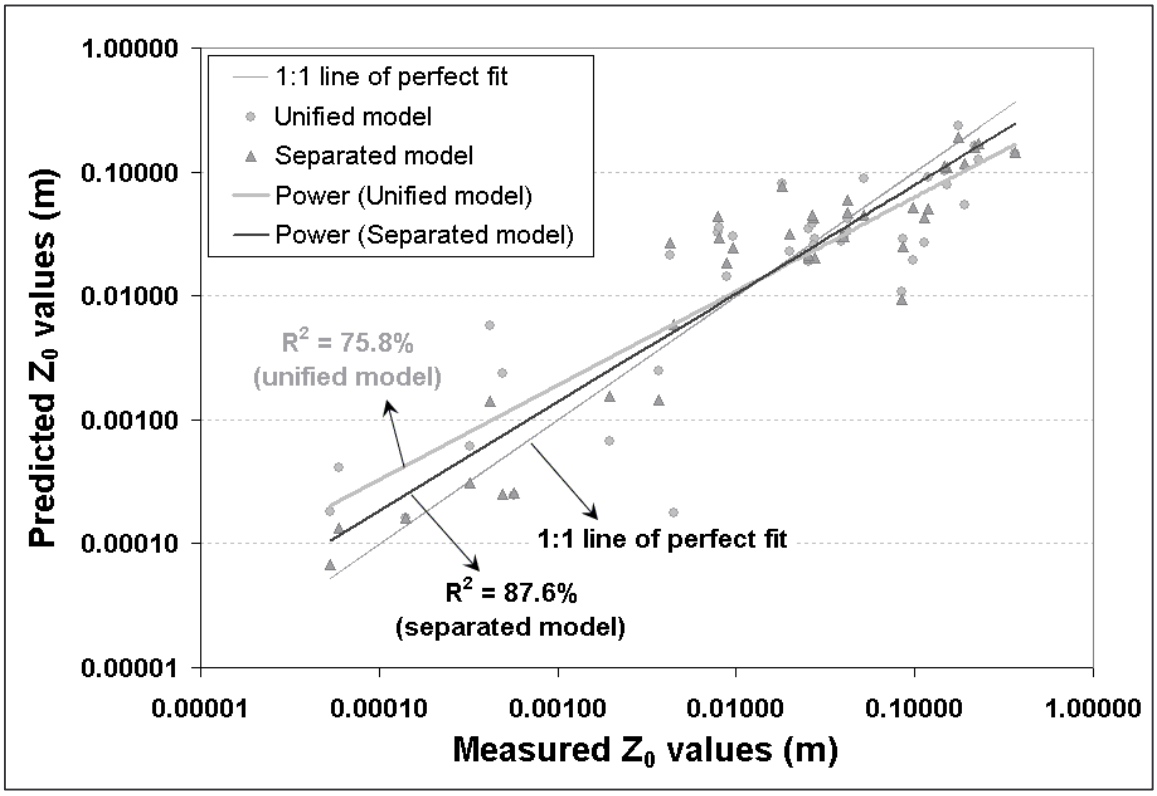


**Figure 10**: A scatter plot comparing the predicted values of $Z_0$ vs. the measured values of $Z_0$, between the two regression models: the unified and the separated (in which the coastal stations and the inland dune stations are not modeled together). Both models used two independent variables: the height difference at an upwind distance of 400 m, and the SAVI values as of January 2000 at an upwind distance of 200 m. Notice that both axes are plotted on a logarithmic scale.

To map $Z_0$ values according to the separated model one needs to first identify the foredune so as to be able to apply different equations for the coastal and inland areas. We therefore chose to use the unified model for the final map of the predicted $Z_0$ values (for winds coming from the south-west, the dominant winds carrying sand along the Israeli coastal dunes), as presented in Figure 11.

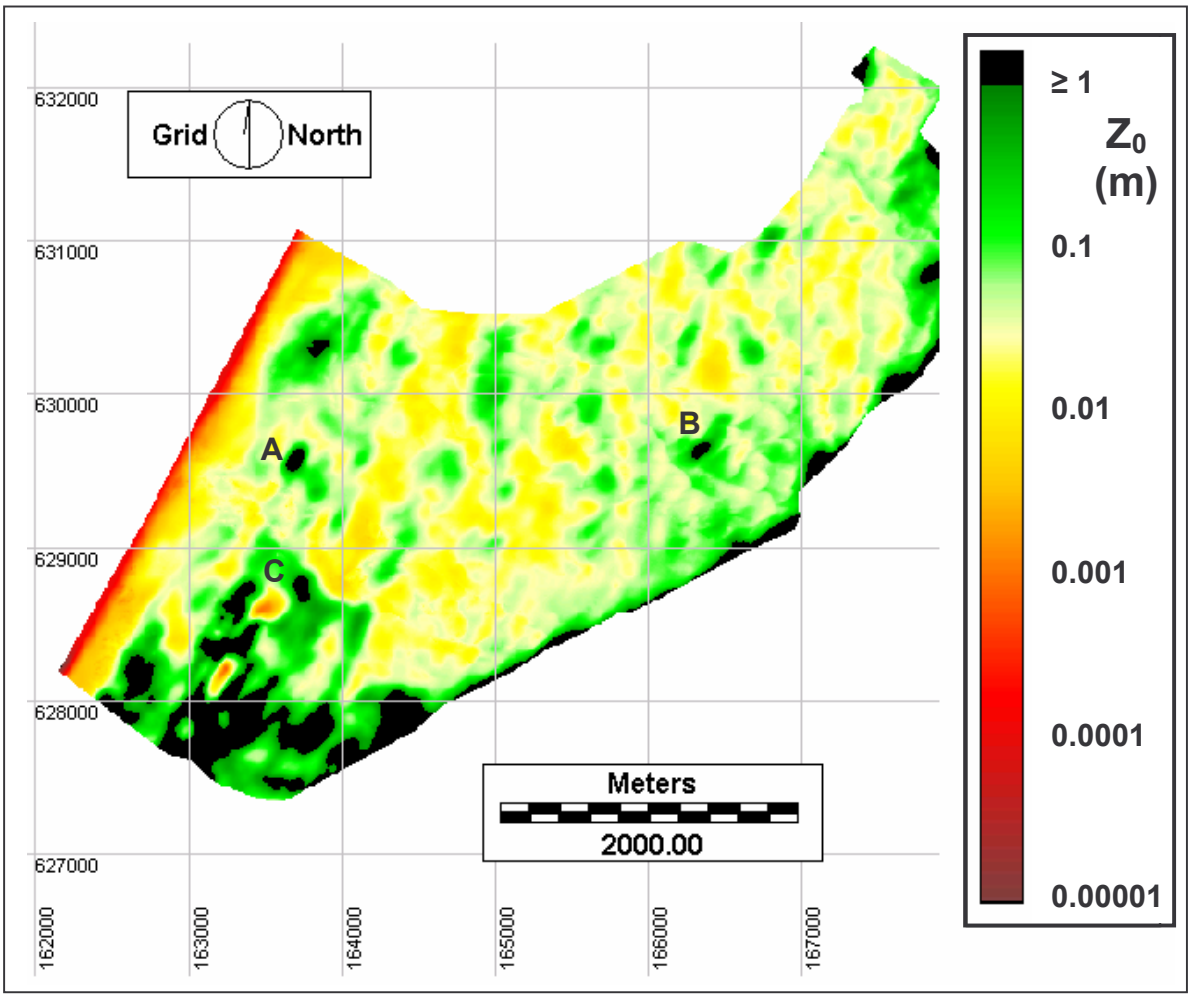


**Figure 11**: Map of the predicted values of $Z_0$ (m) over the coastal dunes of Ashdod according to the unified model, for south-westerly winds. Locations A, B and C are described in the text. Notice that the map legend is given in a logarithmic scale.

This map is based on two layers: (1) A digital elevation model from which we calculated the relative height of each pixel with respect to those upwind of it at a distance of 400m to the south west; (2) A Landsat derived winter (January 2000) SAVI image, from which

we calculated for each pixel the average value of SAVI at a distance of 200m to the south west. As our measured values of $Z_0$ range between 0.00005 m and 0.36 m, those areas in the map presented in Figure 11 in which the predicted values exceeded 1 m are shown in black, as they are extrapolations of our set of data. This map seems to present correctly several places were the expected $Z_0$ values are either very high or very low. For example: (1) in location A (shown on the map in Figure 11) the predicted $Z_0$ value is high due to a large concentration of the invasive tree species *Acacia Saligna* (see also Kutiel et al., 2004); (2) in location B the predicted $Z_0$ value is high as in this inter dune slack there are many palm trees and two tall eucalyptus trees; (3) in location C the predicted $Z_0$ value is low is it an area of bare soil on top of a cliff that was created by a quarry of sand and aeolionites.

The sensitivity of the predicted values of $Z_0$ to the variables of SAVI and relative height in each of the three regression models is presented in Figure 12. In all three models the $Z_0$ values are positively correlated with those of the SAVI values. As for the topography (relative height), in the unified as well as in the inland dunes model it is negatively correlated with the $Z_0$ values, and only in the coastal model is it positively correlated with the $Z_0$ values. From these figures it can also be seen that in both the unified model and the inland separated model, the $Z_0$ values are mostly influenced by the vegetation cover (using SAVI as a surrogate variable), whereas in the coastal separated model the topographic variable has more influence on the $Z_0$ values.

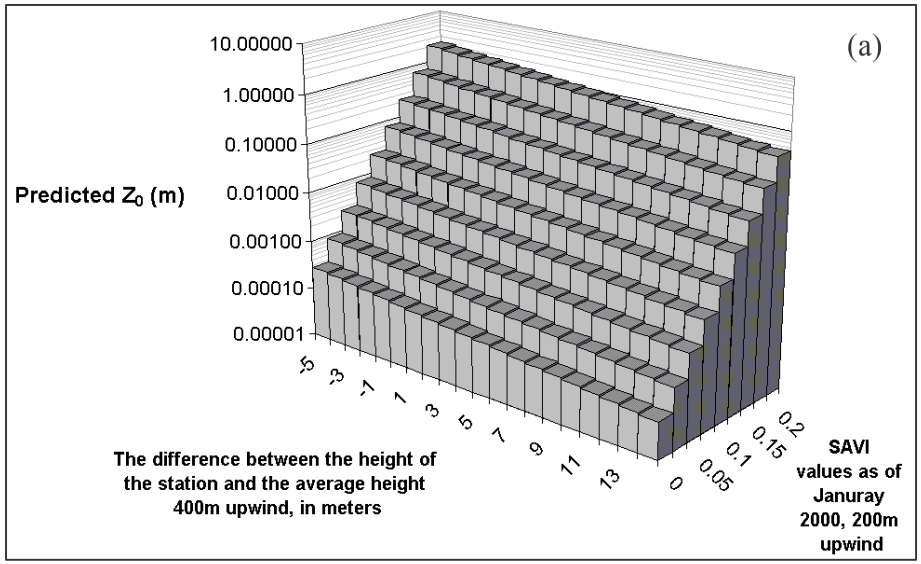


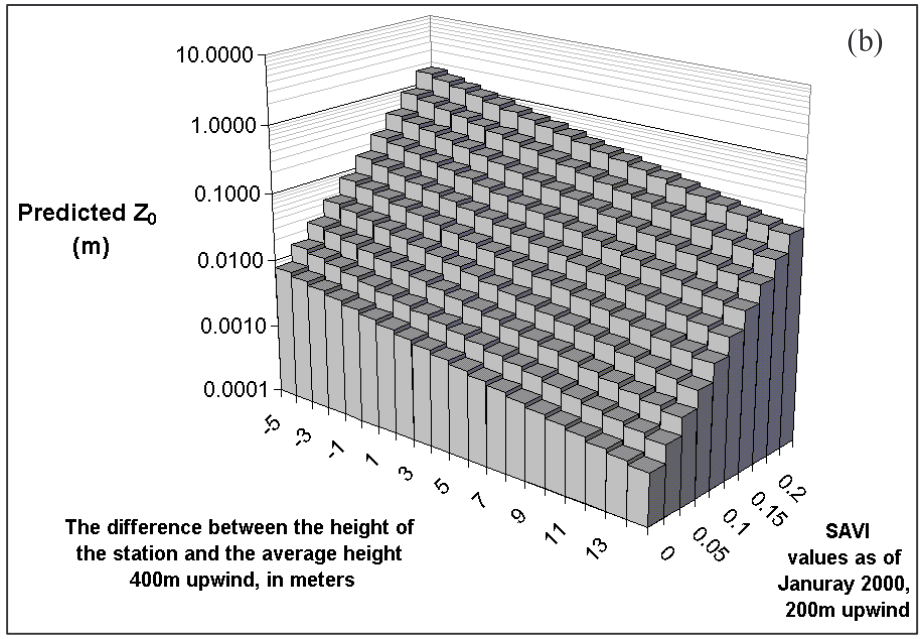


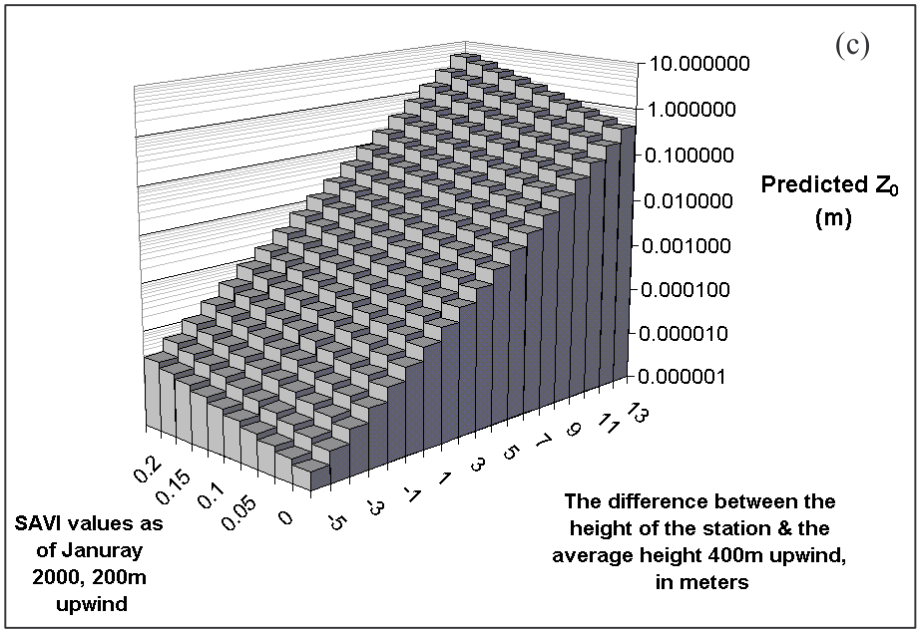


**Figure 12**: The sensitivity of the predicted $Z_0$ values to the variables of SAVI and relative height in the three regression models: (a) unified model, (b) the inland dunes model, (c) the coastal model. Notice that the z-axis is plotted on a logarithmic scale.

## 4. Discussion

### 4.1 Influence of vegetation vs. topography on the predicted values of $Z_0$

Overall our results have shown that to model $Z_0$ values at a certain place located in a stabilizing coastal dune field, two major factors should be considered: the relative height of that place and the vegetation cover. As the surface roughness of a certain location is influenced not only by the local surface characteristics but also by the area upwind of that place, spatially designed directional filters should be applied to calculate the relative height and vegetation cover upwind of a location. These filters should be constructed with respect to the direction from which the sand bearing wind is coming (as for the width of the directional sector), and with respect to the height of measurement that is modeled (as for the length of the directional filter).

The factor of vegetation cover is relatively straight forward in its influence over the surface roughness: the higher is the vegetation cover, the higher will be the surface roughness. However different plants may have different structures, and therefore even with the same vegetation cover, the wind flow characteristics may be different when the plant composition is different. As for the influence of topography, we have received different results for the coastal stations and for the inland dune stations (see Figure 12). For the inland dunes as well for the unified model, the higher is a certain location with respect to the upwind area, the lower will be its surface roughness, and thus a higher wind speed is expected there. Our explanation for the opposite phenomena in the coastal model in which the higher is a certain location, the higher will be its surface roughness, is related to the special interaction between the sea, the beach and the vegetation that is forming the fore dune. At the coastline, the wind is moving from a relatively smooth surface to a rougher surface – that of the sand. In addition to the sand, on the beach one may find various types of litter brought on the shore by the waves as well as pioneer plants, further increasing the surface roughness with the distance from the sea. The fore dune itself is a topographic obstacle that is formed by the accumulation of sand due to vegetation (Arens, 1996). Thus in beaches there is a steady increase in both vegetation cover and height away from the coastline, increasing the surface roughness all the way from the smooth sea surface to the fore dune.

Dune systems are highly dynamic both in space and in time, and modeling of these dynamics, even without including vegetation is a complex task. One of the main variables that need to be modeled in order to improve our predictions of sand movement in coastal system is that of the surface roughness. We have shown here that it can be indeed predicted (with $R^2$ values of 75% and higher) using geographic information systems (see Andrews et al., 2002) and two simple databases: a topographic layer and a satellite derived vegetation index. Both layers can be created using remote sensing techniques, and thus maps of surface roughness can be constructed for large coastal areas, improving our understanding of both dune dynamics and wind flow.

## 4.2 Regarding the combination of data sets from different spatial scales

In his manuscripts presenting his method for estimating $Z_0$ values from wind measurements taken at a single height, Wieringa (1973, 1986) was referring to wind measurements taken at a standard height of 10 m. He therefore expected that the surface roughness values will take into account both nearby and far-off obstacles, vegetation etc. in the upwind direction within a distance of ~3 km over a sector of 20° to 30° width. Our measurements were performed at a height of 2.5 m, and are indeed influenced by obstacles (whether related to topography or vegetation) that lie within a shorter distance upwind (up to 400 m). As our roughness measurements are influenced by a relatively large area upwind, it can be understood why we have succeeded in explaining the variability in the $Z_0$ values, using GIS and remote sensing layers of a coarse nature – Landsat images at a resolution of 15-30 m and digital elevation models that were ten years old.

Satellite images are superior over aerial photographs for monitoring vegetation also due to other reasons: (1) Their measurements of radiance values can be easily transformed into quantitative values of reflectance and other bio- and geo-physical variables, whereas the grey values of aerial photographs are relative to that specific setting of camera, time and day and atmospheric conditions, and their transformation into reflectance values is more difficult; (2) On black and white aerial photographs taken over sand dunes, darker areas may represent vegetation but may also be the result of shading effects, either due to vegetation or to the topographic shape of the dunes. Vegetation indices that are based on

a ratio between an infra-red band and a red band (such as the NDVI and SAVI) are less prone to errors due to shading effects (Lillesand and Kiefer, 1994).
Wieringa (1973, 1986) also cautions that the assumptions behind his method for calculating $Z_0$ based on the gust speed become doubtful when the heights at which the measurements are being done become too close to the actual surface elements ($Z/Z_0 < 25$). As our wind measurements were conducted at a height of 2.5 m, they are supposed to be reliable only up to $Z_0$ values of 0.1 m.

## 4.3 Sources of errors

We believe that our results of estimating $Z_0$ values for a coastal dune area based on satellite images and digital elevation models are quite promising. However, the following factors might have contributed errors into our final model and results:

- That areas with a very low vegetation cover may not be adequately monitored using satellite images in arid and semi-arid areas (Tueller, 1987). More specifically, using a Landsat satellite image (its highest resolution being 15 m) isolated bushes cannot be detected.
- That data regarding the vegetation height, from which the zero plane displacement height was not incorporated in our model, although it is considered important for estimating surface roughness (and see Jasinski and Crago, 1999, in this regard).
- Vegetation indices are known to be influenced by variability in the soil background properties (mineralogy, moisture content and particle size [roughness]) even when no vegetation cover is present (Huete, 1988; Rondeaux et al., 1996; Schmidt and Karnieli, 2000). This might have even created some artifacts that improved our results; thus, the NDVI (and to a certain degree also the SAVI) values at the interaction between the sea and the beach decrease from the fore dune towards the coastline and on to the sea, due to the increased moisture of the sand near the water line, when the vegetation cover is zero. The values of NDVI and SAVI may have also been influenced by the changing content of free iron oxides, affecting the color of the sand to change from almost white on the beach to a darker and

more yellow-brown hue inland. This change is especially strong in the first 500m from the beach (Ben-Dor et al., 2005). Using the same data set of 42 sand samples used by Levin et al. (2005), we have found a positive correlation between the content of free iron oxides and NDVI (R = 0.61), whereas a weaker correlation was found with SAVI (R = 0.49).

- That the digital elevation model we used, although being quite detailed for a coastal dune area, was not detailed enough to show small nebkha dunes. In addition, this DEM was measured in the mid 1990's whereas our wind measurements were done in 2003/4. Although the Ashdod dunes are now stabilizing and their movement rate is lower than 1 m/year (Levin and Ben-Dor, 2004), their topography is expected to change at the least due to their transformation from transverse to parabolic (Tsoar and Blumberg, 2002).
- That the presence of biogenic soil crusts in the study area, although having less effect on the wind flow when compared with higher vegetation, was not incorporated.

## 5. Summary and Conclusions

In this paper we have shown that wind flow over sand dunes, as characterized by the surface aerodynamic roughness can be predicted with accuracies higher than 64%. To this end only two base layers are needed: a digital elevation model, and a satellite image from which vegetation indices can be calculated. As we conducted our wind measurements at a height of 2.5 m above the ground, they were influenced from a relatively large area upwind of them, up to 400 m. This may explain why medium resolution data layers were sufficient for our needs. To extend this study for prediction of sand movement rates it may be beneficial to apply this method of estimating surface roughness using anemometers that will be placed at a lower height. To explain wind flow at heights of about 0.5 m above ground however, higher resolution data of topography and vegetation cover, as obtained by airborne LIDAR sensors may be needed.

## Acknowledgments

We thank Daniela Heller, Michael Winograd, Rami Almog, Matt Freedman, Yair Farjun from the Shikmim Field School of the Society for the Protection of Nature in Israel and Ofri Cohen (from the Israel's Nature and Parks Authority) for their help in the wind measurements at the dunes of Ashdod. We wish to thank the students from the Israel Maritime College for their help in the wind measurements at the dunes of Bet Yanay. We also thank Prof. Arye Bitan and Dr. Oded Potchter of the climatology laboratory of Tel-Aviv Geography and Human Environment department for their support for this research. We would also like to thank Ravid Pik and Yoav Eshel from the Israeli Green Patrol (Ha Sayeret ha Yeruka) for the use of the differential GPS.

## References

Analytical Imaging and Geophysics LLC (AIG), 2001, ACORN User's Guide, Stand Alone Version, Analytical Imaging and Geophysics LLC, 64 p.

Andrews B.D., P.A. Gares and J.D. Colby, 2002, Techniques for GIS modeling of coastal dunes, Geomorphology, 48: 289-308

Arens S.M., 1996, Patterns of sand transport on vegetated foredunes, Geomorphology, 17: 339-350

Barthelmie R.J., Palutikof J.P. and Davies D., 1993, Estimation of sector roughness lengths and the effect on prediction of the vertical wind speed profile, Boundary Layer Meteorlogy, 66: 19-47.

Bauer B.O., Sherman D.J. and Wolcott J.F., 1992, Sources of uncertainty in shear stress and roughness length estimates derived from velocity profiles, Professional Geographer, 44 (4): 453-464

Belnap J. and D.A. Gillette, 1998, Vulnerability of desert biological soil crusts to wind erosion: the influences of crust development, soil texture, and disturbance, Journal of Arid Environments, 39: 133-142

Ben-Dor E., Levin N., Singer A., Karnieli A., Braun O. and Kidron G., 2005, Quantitative Mapping of the Soil Rubification Process on Sand Dunes Using an Airborne CASI Hyperspectral Sensor, *Geoderma*, accepted for publication

Berk , A. G. P. Anderson, L. S.Bernstein, P. K. Acharya, H. Dothe, M. W. Matthew, S. M.Adler-Golden, J. H. Chetwynd, Jr., S. C. Richtsmeier, B. Pukall, C. L. Allred, L. S. Jeong, and M. L. Hoke, 1999, MODTRAN4 Radiative Transfer Modeling for Atmospheric Correction, SPIE Proceeding, Optical Spectroscopic Techniques and Instrumentation for Atmospheric and Space Research III, Volume 3756.

Blennow K. and O. Sallnäs, 2004, WINDA – a system of models for assessing the probability of wind damage to forest stands within a landscape, Ecological Modelling, 175: 87-99

Blumberg D.G. and Greeley R. (1993), Field studies of aerodynamic roughness length, Journal of Arid Environments, 25: 39-48

Carpenter P. and Locke N., 1999, Investigation of wind speeds over multiple two-dimensional hills, Journal of Wind Engineering and Industrial Aerodynamics, 83: 109-120

Clark Labs. 2002. Idrisi 32. The Idrisi Project, 950 Main Street, Worcester MA 01610-1477, USA

Danin A. and Nukrian R., 1991, Dynamics of dune vegetation in the southern coastal area of Israel since 1945, *Documents Phytosociologiques*, XIII: 281-296

De Vries A.C., W.P. Kustas, J.C. Ritchie, W. Klassen, M. Menenti and J.H. Prueger, 2003, Effective aerodynamic roughness estimated from airborne laser altimeter measurements of surface features, International Journal of Remote Sensing, 24 (7): 1545-1558

Dong Z., Gao S. and Fryrear D.W. (2001), Drag coefficients, roughness length and zero-plane displacement height as disturbed by artificial standing vegetation, Journal of Arid Environments, 49: 485-505

Eastman J.R. (2001), Idrisi 32 Release 2—Guide to GIS and Image Processing, Vol. 2, Clark University, U.S.A., 144pp.

Fishman A. (1994), Photogrammetric survey of Ashdod dunes, AutoCAD layers received from the GIS unit of the Society for the Protection of Nature in Israel.

Frank A.J. and Kocurek G., 1996a, Airflow up the stoss slope of sand dunes: limitations of current understanding, Geomorphology, 17: 47-54

Frank A. and Kocurek G., 1996b, Toward a model for airflow on the lee side of aeolian dunes, Sedimentology, 43: 451-458

Frumkin-Ahiron, T., Frumkin, R., Roudich, R., Melloul, A., Levin, N. and Papay, N. (2003), Conservation of the Coastal Sand Dunes – a Policy Report, The Surveys Unit – Open Landscape Institute – The Society for the Protection of Nature in Israel, The Ministry of Environment, The Nature and Parks Authority, The Jewish National Fund, The Water Commission and the Jerusalem Institute for Israel Studies, 126 p. (in Hebrew)

Garvin J., Bufton J., Blair J., Harding D., Luthcke S., Frawley J., and Rowlands D., 1998, Observations of the Earth's topography from the Shuttle Laser Altimeter (SLA): Laser-pulse echo-recovery measurements of terrestrial surfaces, Physics and Chemistry of The Earth, 23 (9-10): 1053-1068

Goldsmith V., Rosen P. and Gertner Y., (1990), Eolian transport measurements, winds, and comparison with theoretical transport in Israeli coastal dunes, Chapter Five in Nordstrom K.F., Psuty N.P. and Carter R.W.G. (eds.), *Coastal Dunes: Form and Process*, John Wiley & Sons, 79-101

Hesp P.A., Davidson-Arnott R., Walker I.J. and Ollerhead J., 2004, Flow dynamics over a foredune at Prince Edward Island, Canada, Geomorphology, in press (14 p.)

Högström U., 1988, Non-dimensional wind and temperature profiles in the atmospheric surface layer: a re-evaluation, Boundary-Layer Meteorology, 42: 55-78

Högström U., 1996, Review of some basic characteristics of the atmospheric surface layer, Boundary-Layer Meteorology, 78: 215-246

Huete A.R., 1988, A soil-adjusted vegetation index (SAVI), Remote Sensing of Environment, 25: 295-309

Illenberger W.K. and I.C. Rust, 1988, A sand budget for the Alexandria coastal dunefield, South Africa, Sedimentology, 35: 513-521

Ishihara T., Hibi K. and Oikawa S., 1999, A wind tunnel study of turbulent flow over a three-dimensional steep hill, Journal of Wind Engineering and Industrial Aerodynamics, 83: 95-107

Jackson, P.S., Hunt, J.C.R. 1975. Turbulent windflow over a low hill. Quarterly Journal of the Royal Meteorological Society, 101, 929–955

Jasinski M.F. and R.D. Crago, 1999, Estimation of vegetation aerodynamic roughness of natural regions using frontal area density determined from satellite imagery, Agricultural and Forest Meteorology, 94: 65-77

Kim H.G., Lee C.M., Lim H.C. and Kyong N.H., 1997, An experimental and numerical study on the flow over two-dimensional hills, Journal of Wind Engineering and Industrial Aerodynamics, 66: 17-33

Kim H.G., Patel V.C. and Lee C.M., 2000, Numerical simulation of wind flow over hilly terrain, Journal of Wind Engineering and Industrial Aerodynamics, 87: 45-60

Kutiel P., Cohen O., Shoshany M. and Shub M., 2004, Vegetation establishment on the southern Israeli coastal sand dunes between the years 1965 and 1999, Landscape and Urban Planning, 67: 141-156

Kutiel P., Danin A., and Orshan G., 1979/80, Vegetation of the sandy soils near Caesarea, Iarael. I. Plant communities, environment and succession, Israel Journal of Botany, 28: 20-35

Kutiel P., O. Cohen, M. Shoshany and M. Shub, 2004, Vegetation establishment on the southern Israeli coastal sand dunes between the years 1965 and 1999, Landscape and Urban Planning, 67: 141-156

Lancaster N. and A. Baas, 1998, Influence of vegetation cover on sand transport by wind: field studies at Owens Lake, California, Earth Surface Processes and Landforms, 23: 69-82

Lettau H. (1969), Note on aerodynamic roughness-parameter estimation on the basis of roughness-element description, Journal of Applied Meteorology, 8: 828-832

Levin N. and E. Ben-Dor, 2004, Monitoring sand dune stabilization along the coastal dunes of Ashdod-Nizanim, Israel, 1945-1999, Journal of Arid Environments, 58: 335-355

Levin N., Ben-Dor E. and Karnieli A. (2004), Topographic information of sand dunes as extracted from shading effects using Landsat images, Remote Sensing of Environment, 90: 190-209

Levin N., Ben-Dor E. and Singer A. (2005), A digital camera as a tool to measure colour indices and related properties of sandy soils in semi-arid environments, Submitted to *International Journal of Remote Sensing*, December 2003, received from

reviewers on October 2004, corrected version submitted to *IJRS* on December 2004, accepted on December 15th, 2004

Levin N. and E. Ben-Dor, in review, Remote sensing as a tool for monitoring coastal sand dunes – a review, an invited chapter to a book edited by Prof. Pua Bar (Kutiel) titled: Conservation and Management of Mediterranean Coastal Sand Dunes in Israel: Dilemmas and Challenges at Nitzanim Sand Park; Submitted in September 2004

Levin N., Kidron G.J. and Ben-Dor E., in preparation, A field quantification of the adaptations of costal dune plants to erosion and deposition of sand

Lillesand T.M. and R.W. Kiefer, 1994, Remote Sensing and Image Interpretation, John Wiley & Sons, Inc., 3rd edition, New York

McKenna Neuman C., N. Lancaster and W.G. Nickling, The effect of unsteady winds on sediment transport on the stoss slope of a transverse dune, Silver Peak, NV, USA, Sedimentology, 47: 211-226

Miller C.A. and Davenport A.G., 1998, Guidelines for the calculation of wind speed-ups in complex terrain, Journal of Wind Engineering and Industrial Aerodynamics, 74-76: 189-197

Mugnier C.J. 2000. Grids and Datums: the State of Israel. Photogrammetric Engineering and Remote Sensing, 66 (8): 915-917

Neff D.E. and Meroney R.N., 1998, Wind-tunnel modeling of hill and vegetation influence on wind power availability, Journal of Wind Engineering and Industrial Aerodynamics, 74-76: 335-343

Oke T.R. (1987), Boundary Layer Climate, Routledge, London and New York

Parsons D.R., Walker I.J. and Wiggs G.F.S., 2004, Numerical modeling of flow structures over idealized transverse aeolian dunes of varying geometry, Geomorphology, 59: 149-164

Peterson E.L., N.G. Mortensen, L. Landberg, J. Højstrup and H.P. Frank, 1997, Wind Power Meteorology, Riso-I-1206(EN), Risø National Laboratory, Roskilde, Denmark, 46p.

Pike R.J., 2000, Nano-metrology and terrain modeling – convergent practice in surface characterization, Tribology International, 33: 593-600

Plate E.J. (1982), Engineering Meteorology, Elsevier, Amsterdam – Oxford – New York

Prueger J.H., Kustas W.P., Hipps L.E. and Hatfield J.L., 2004, Aerodynamic parameters and sensible heat flux estimates for a semi-arid ecosystem, Journal of Arid Environments, 57: 87-100

Ranwell D., 1958, Movement of vegetated sand dunes at Newborough Warren, Anglesey, Journal of Ecology, 46 (1): 83-100

Research Systems, Inc. (RSI), 2001, ENVI Version 3.4, 4990 Pearl East Circle, Boulder, CO 80301, USA: The Environment for Visualizing Images

Rondeaux G., Steven M. and Baret F., 1996, Optimization of soil-adjusted vegetation indices, Remote Sensing of Environment, 55: 95-107

Sarnthein M., 1978, Sand deserts during glacial maximum and climatic optimum, Nature, 272: 43–46

Sauermann G., Andrade Jr. J.S., Maia L.P., Costa U.M.S., Araujo A.D. and Herrmann H.J., 2003, Wind velocity and sand transport on a barchan dune, Geomorphology, 54: 245-255

Schmidt H. and Karnieli A., 2000, Sensitivity of vegetation indices to substrate brightness in hyper-arid environment: the Makhtesh Ramon Crater (Israel) case study, International Journal of Remote Sensing, 22 (17): 3503-3520

Sherman D.J., 1995, Problems of scale in the modeling and interpretation of coastal dunes, Marine Geology, 124: 339-349

Sweet M.L. and Kocurek G., 1990, An empirical model of aeolian dune lee-face airflow, Sedimentology, 37: 1023-1038

Troen I. and Peterson E.L. (1989), European Wind Atlas, Commission of the European Community, Risø National Laboratory, Roskilde, Denmark, 656 p.

Tsoar, H. (1990). 'Trends in the development of sand dunes along the southeastern Mediterranean coast', in Dunes of the European Coasts, Catena Supplement, 18, ed. by Bakker, Th.W., Jungerius, P.D., and Klijn, J.A., 51-60

Tsoar H., 2001, Types of Aeolian Sand Dunes and Their Formation, in: Balmforth N.J., & A. Provenzale (Eds.): Lecture Notes in Physics 582, pp. 403-429, Berlin Heidelberg: Springer-Verlag

Tsoar, H. and Blumberg, D.G. (2002). 'Formation of parabolic dunes from barchan and transverse dunes along Israel's Mediterranean coast', Earth Surface Processes and Landforms, 27, 1147-1161.

Tsoar, H. and Zohar, Y., (1986). 'Desert dune sand and its potential for modern agricultural development'. In Desert Development, ed. by Gradus Y., pp. 184-200, D. Reidel Pub. Co.

Tueller P.T., 1987, Remote sensing science applications in arid environments, Remote Sensing of Environment, 23: 143-154

Walker I.J. and Nickling W.G., 2003, Simulation and measurement of surface shear stress over isolated and closely spaced transverse dunes in a wind tunnel, Earth Surface Processes and Landforms, 28: 1111-1124

Warren A. (1976), Dune trend and the Ekman Spiral, Nature, 259, pp. 653-654

Wieringa J. (1973), Gust factors over open water and built-up country, Boundary-Layer Meteorology, 3: 424-441

Wieringa J. (1986), Roughness-dependent geographical interpolation of surface wind speed averages, Quarterly Journal of the Royal Meteorological Society, 112: 867-889

Wieringa J. (1992), Updating the Davenport roughness classification, Journal of Wind Engineering and Industrial Aerodynamics, 41-44: 357-368.

Wieringa J. (1993), Representative roughness parameters for homogeneous terrain, Boundary-Layer Meteorology, 63: 323-363.

Wieringa J. (1996), Does representative wind information exist? Journal of Wind Engineering and Industrial Aerodynamics, 65: 1-12.

Wiggs G.F.S., 2001, Desert dune processes and dynamics, Progress in Physical Geography, 25 (1): 53-79

Wiggs G.F.S., Thomas D.S.G., Bullard J.E. and Livingstone, I. (1995), Dune mobility and vegetation cover in the southwest Kalahari Desert, Earth Surface Processes and Landforms 20: 515–529.

Wolfe, S. A., and Nickling W.G. (1993), The protective role of sparse vegetation in wind erosion, Progress in Physical Geography, 17(1): 50-68.

Zhu H., Eastman, J.R., and Toledano J. (2001), "Triangulated irregular network optimization from contour data using bridge and tunnel edge removal," International Journal of Geographical Information Science 15 (3), pp. 271–286

*In the sixth article* the rates of erosion and deposition of sand that were measured using erosion pins across the dunes of Ashdod and Nizzanim at 315 locations for 25 periods along two years (2002-2004) are presented. Using this dataset the effect of wind and of rainfall on sand movement along Israel's coastal dunes is explored. In addition, the spatial variability in sand movement was quantified, as governed by vegetation cover and topography upwind of the erosion pins.

# The spatial and temporal variability of sand erosion across a stabilizing coastal dune field

**Levin Noam*†, Giora J. Kidron‡ and Eyal Ben-Dor†**

† The Department of Geography and the Human Environment, Tel-Aviv University, Israel

‡ Institute of Earth Sciences, The Hebrew University of Jerusalem, Givat Ram Campus, Jerusalem 91904, Israel

* Corresponding author. E-mail: levinnoa@post.tau.ac.il

E-mail of Giora Kidron: kidron@vms.huji.ac.il

E-mail of Eyal Ben-Dor: bendor@post.tau.ac.il

## Abstract

This study aimed at quantifying the temporal and spatial variability in sand erosion and deposition over a coastal dune field in Israel. These were measured monthly over two years using 315 erosion pins over four transects that were placed perpendicular to the coastline. Vegetation cover was estimated based on aerial photographs and Landsat satellite images, whereas the relative height was based on a digital elevation model. These variables were calculated for the area upwind (south west) of the erosion pins, at various lengths, ranging from 15 to 400 m. Nine geomorphologic units found in coastal dunes were defined, five related to active units, and four to stabilized units. In active units at least 65% of the temporal variance in the annual absolute changes in sand level was explained by the index of Resultant Drift Potential, with most of the sand movement occurring during winter storms. Local rainfall had no apparent impact on sand mobility, due to the low coincidence of sand moving winds and rainfall in Israel during the passage of frontal cyclones. As for the spatial variables, only a weak correlation was found between sand mobility with the distance from the coastline ($R^2$ = 18%). Rather, sand erosion and deposition at the pins were influenced by vegetation cover and the relative height of an area of 100-200 m upwind of them. The values of Soil Adjusted Vegetation Index (SAVI) were significantly negatively correlated with annual absolute changes ($R^2$ = 40%), whereas the relative height was significantly positively correlated ($R^2$ = 36%).

Applying a multiple regression model, 68% of the spatial variability in sand mobility was explained. The resulting map of sand activity clearly shows that at this stage of the stabilization process, most of the dunes are now disconnected, and movement of sand grains to them from the beach or between them, is very limited. These methods can be applied into spatial and temporal models of sand mobility, to assess the impact of different management practices on coastal dunes.

## Keywords

Coastal dunes, dune mobility, wind, rainfall, vegetation, topography, remote sensing.

## 1. Introduction

### 1.1 Stabilization of coastal dunes

The stabilization or re-activation of sand dunes may be a result of either climate changes (e.g. Anthonsen et al., 1996; Lancaster, 1997; Hugenholtz and Wolfe, 2005) or of human activities (e.g. Tsoar and Møller, 1986; Al-Dabi et al., 1997; Chapter 4 of this thesis). Dune stabilization processes are commonly described by many works as a feedback mecahnism (Danin and Yaalon, 1982; Tsoar and Møller, 1986; Danin et al., 1989; Danin, 1991; Hesp, 1991). In addition to the increase in vegetation cover, and the decrease in the movement of sand grains, stabilizing dunes also experience morphological and topographic changes (Anthonsen et al., 1996; Tsoar and Blumberg, 2002).

The coastal dunes of Israel are undergoing processes of stabilization by vegetation since the establishment of the state of Israel, in 1948. This is attributed to a combination of the low energy wind regime in the eastern Mediterranean climate and changes in human land uses along the coast, mainly the ending of the practice of the "mawasi" agricultural system (Tsoar and Zohar, 1985) and the use of dune vegetation by Arab and Bedouin local populations and their stocks since the establishment of the state of Israel (Danin and Nukrian, 1991; Tsoar and Blumberg, 2002; Chapter 4 of this thesis). Efforts for reactivating dunes are done in recent years both in the Netherlands (Arens et al., 2004; Turnhout et al., 2004) and in Israel. To assess the success of such efforts a quantitative understanding of the spatial factors affecting sand mobility, as well as identification of spatial indicators are needed.

## 1.2 Spatial and temporal variability of sand erosion

Indices of sand mobility are traditionally related to precipitation, evaporation and wind magnitude (Lancaster, 1997). In a study considering a remobilized parabolic dune in the Netherlands, activity of the dune was strongly influenced by precipitation (Arens et al., 2004); However, this may change between different climate regions. Indeed, other studies identify wind regime as the most important physical factor in determining the mobility of dunes (Fryberger, 1979; Tsoar and Werner, 1998; Tsoar, 2002). The wind parameters to be considered are both wind velocity (above the threshold required to keep sand in saltation) and directionality, both of which may be affected by: topography (e.g. the relative height, the slope and aspect, wind fetch; see Yeaton, 1988; White and Tsoar, 1998; Iversen and Rasmussen, 1999; Wiggs, 2001; Bauer and Davidson-Arnott, 2002; Sauermann et al., 2003; Hesp et al., 2005), vegetation (cover, height, arrangement; e.g. Lettau, 1969; Wasson and Nanninga, 1986; Buckley, 1987; Yeaton, 1988; Raupach et al., 1993; Musick et al., 1996; Lancaster and Baas, 1998; Dong et al., 2001), biogenic crust (cover and type; see Belnap and Gillette, 1998; McKenna Neuman et al., 2005), surface moisture content (Belly, 1964; Hotta et al., 1984; Sherman et al., 1998; Arens et al., 2004; Cornelis et al., 2004; Wiggs et al., 2004), underground water table (Munoz-Reinoso and de Castro, 2005), and the aeolian deposition of fine particles (Fearnehough et al., 1998).

Although some studies used remote sensing techniques for assessing the effect of some of these variables on dune mobility (Illenberger and Rust, 1986; Chapter 4 of this thesis), a comprehensive study that aims to combine field measurement and remote sensing techniques on a whole dune field was not yet, to our knowledge, performed. As stated by Walsh et al. (1998, p. 201) the combination of remote sensing with geographic information systems (GIS) allows "geomorphologists to examine spatial relationships at a variety of scales that would not be feasible using only fieldwork or traditional aerial photography". A multiple scale approach can be applied by using spatial filters at various sizes. However, these were not utilized so far to examine quantitative relationships in space between sand mobility, vegetation and topography. In the current study we conducted a field research using erosion pins (as in Ranwell, 1958; Moreno-Casasola, 1986; Gertner, 1989; Harel, 1990; Kadmon and Leschner, 1995; Wiggs et al., 1995; White and Tsoar, 1998; Arens et al., 2004) to assess the spatial and temporal variability

in sand erosion and deposition. We then analyzed these data with respect to time series of meteorological data, and using selected remote sensing and geographic information system (GIS) layers to quantitatively study the effect of upwind topography and vegetation on sand mobility.

### 1.3 Objectives

The objectives of this study are therefore the following:

- To study the relative importance of wind power and rainfall in influencing sand movement across a stabilizing dune field in an eastern Mediterranean climate.
- To study the combined influence of vegetation cover and topographic variables on the erosion and deposition of sand through a multi-scale analysis combining remote sensing and GIS.
- To identify which of the geomorphologic units of a sand dune is the best indicator of aeolian processes.
- To derive a predictive spatial model of sand movement as a function of topography and vegetation.

## 2. Methods

### 2.1 Study area

The area selected for this study consists of coastal sand dunes 40 km south of Tel-Aviv, Israel, between the cities of Ashdod and Ashkelon (Fig. 1). This area represents the largest remaining tract of coastal dunes that was spared from urban sprawl. The climate is Mediterranean, with an annual average rainfall of 450-500mm, all in wintertime, with maximum rainfall in December (Bitan and Rubin, 1991). The average daily maximum and minimum temperatures in summer are 29˚C and 21˚C, and in winter are 18˚C and 10˚C, respectively. Proximity to the sea boosts the average relative humidity year round and may reach 70% and higher during the summer.The wind regime in the study area is uni-directional (Tsoar and Blumberg, 2002: RDP/DP = 0.71).

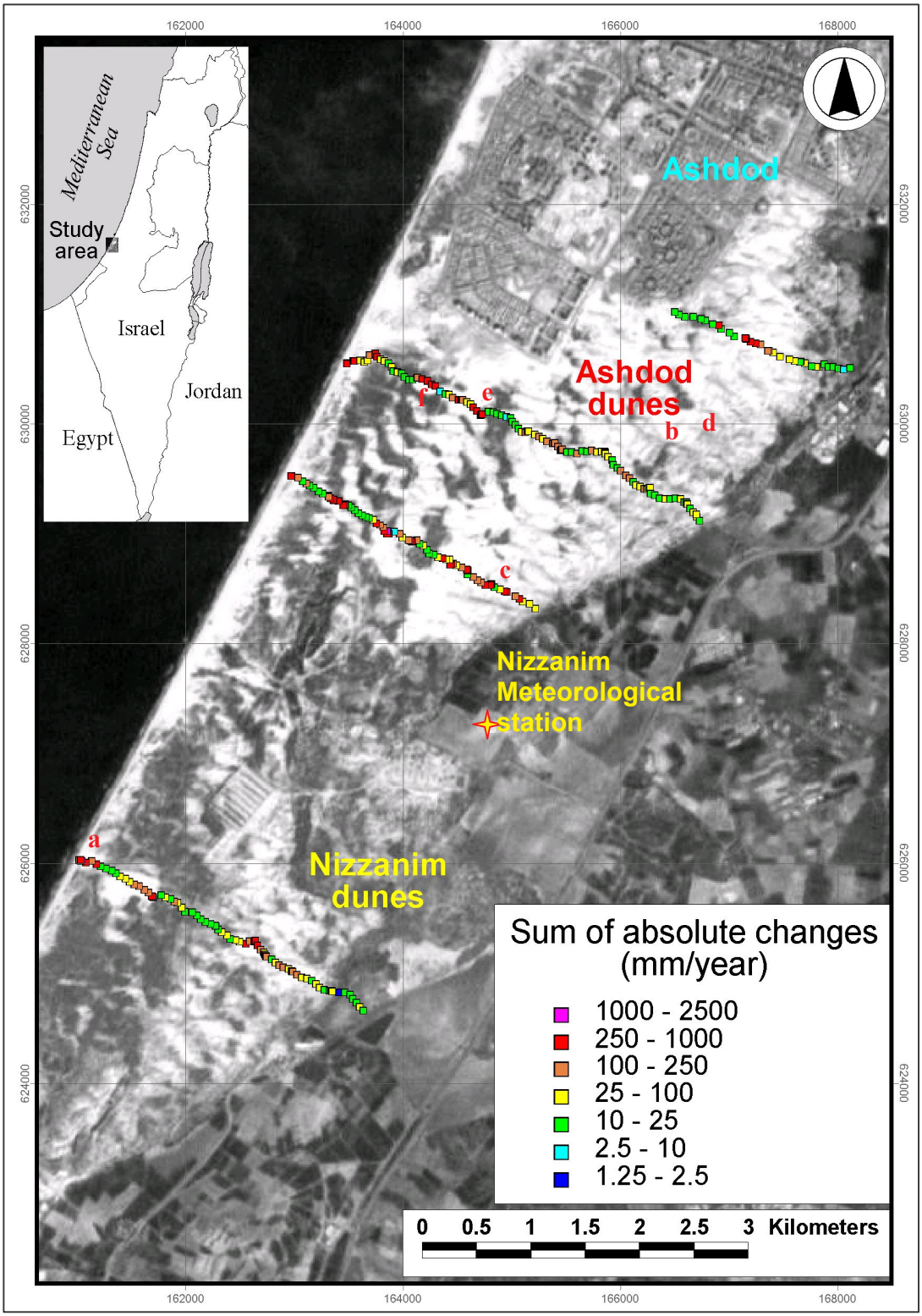


**Figure 1**: A Landsat satellite image (January 2000) covering the study area of the Ashdod and Nizzanim Dunes. The locations of the erosion pins as well as the yearly sum of absolute changes are shown on the map for the four transects. Locations of the photographs shown in Fig. X are given by bold letters a-f.

The origin of the sand along the Israeli coast is mainly from the Nile delta via the longshore current near the coast and the anti-clockwise Mediterranean current in the deep water (Emery and Neev, 1960). Aeolian sand transport from the beach inland occurs under the influence of high winds from the southwest towards the northeast, mainly in wintertime (Goldsmith et al., 1990). The vegetation associations typical of the southern coastal dunes of Israel that match the study area were defined by Danin and Nukrian (1991) near Netiv HaAsara, 10 km south of Ashkelon. They note that with increasing sand stability the germination and establishment of more species is enabled and the monospecific community of *Ammophila arenaria* thickens and changes into associations where *Artemisia monosperma* is the dominant plant.

## 2.2 Field measurements of sand erosion/deposition

To study the spatial and temporal variability in the current rates of erosion and deposition of sand, four transects were chosen, lying perpendicularly to the coastline (see fig .1). Erosion pins were inserted perpendicular to the shoreline (~ NW-SE) and not in the direction of storm wind and dune advance (SW-NE) to avoid spatial autocorrelation (Legendre, 1993). Three of the four transects begin at the foredune, and all the transects end at the dunes' easternmost edge. Along these transects, 315 erosion pins were placed at intervals of about 50 meters in December 2002. As maximum changes of sand deposition were expected to occur in the dunes' slip faces, three erosion pins were placed across each slip face to represent them more accurately. Most of the erosion pins were 50 cm long, except those located at the dunes slip faces (where sand movement was expected to be higher), that were 100 cm long. All pins were buried to a depth of 50% of their total length (mentioned above), and reset once the level at the pin has either increased or decreased by 66% of the full length of the erosion pin. On the average some 8.7% of the erosion pins had to be reset every time as they were disturbed by human or faunal activities (Table 1).

| Serial number | Start date | End date | Length of the measured period (days) | Number of erosion pins visited & measured | % of erosion pins with no-data for that period, attributed to: faunal activities: e.g. footprints of dears or an ant nest changing the micro topography | % of erosion pins with no-data for that period, attributed to: human activities: e.g. off road vehicles, erosion pins found outside of their location | Nizzanim meteorological station data completeness |
|---|---|---|---|---|---|---|---|
| 1 | 5/12/2002 | 28/12/2002 | 23 | 308 | 0.3% | 3.9% | 99.8% |
| 2 | 28/12/2002 | 11/1/2003 | 14 | 308 | 0.3% | 3.2% | 61.3% |
| 3 | 11/1/2003 | 1/2/2003 | 21 | 308 | 0.3% | 6.2% | 14.5% |
| 4 | 1/2/2003 | 23/2/2003 | 22 | 72 | 0.0% | 1.4% | 96.4% |
| 5 | 23/2/2003 | 1/3/2003 | 6 | 314 | 0.0% | 5.4% | 34.7% |
| 6 | 1/3/2003 | 16/3/2003 | 15 | 151 | 0.0% | 7.3% | 83.3% |
| 7 | 16/3/2003 | 29/3/2003 | 13 | 315 | 0.0% | 4.1% | 99.7% |
| 8 | 29/3/2003 | 1/5/2003 | 33 | 315 | 0.0% | 7.9% | 99.5% |
| 9 | 1/5/2003 | 31/5/2003 | 30 | 315 | 0.3% | 5.7% | 99.9% |
| 10 | 31/5/2003 | 28/6/2003 | 28 | 315 | 1.6% | 7.0% | 99.9% |
| 11 | 28/6/2003 | 31/7/2003 | 33 | 315 | 1.6% | 6.3% | 99.9% |
| 12 | 31/7/2003 | 30/8/2003 | 30 | 315 | 1.3% | 7.3% | 99.6% |
| 13 | 30/8/2003 | 3/10/2003 | 34 | 315 | 2.5% | 10.2% | 99.9% |
| 14 | 3/10/2003 | 31/10/2003 | 28 | 315 | 2.9% | 6.7% | 99.7% |
| 15 | 31/10/2003 | 15/11/2003 | 15 | 315 | 1.0% | 2.5% | 99.7% |
| 16 | 15/11/2003 | 11/12/2003 | 26 | 315 | 1.0% | 6.0% | 99.8% |
| 17 | 11/12/2003 | 31/12/2003 | 20 | 315 | 0.3% | 5.7% | 99.6% |
| 18 | 31/12/2003 | 17/1/2004 | 17 | 315 | 0.6% | 7.6% | 99.8% |
| 19 | 17/1/2004 | 28/1/2004 | 11 | 315 | 0.0% | 4.8% | 99.6% |
| 20 | 28/1/2004 | 17/2/2004 | 20 | 315 | 0.3% | 6.7% | 99.8% |
| 21 | 17/2/2004 | 20/3/2004 | 32 | 315 | 1.6% | 11.4% | 99.9% |
| 22 | 20/3/2004 | 1/5/2004 | 42 | 314 | 2.2% | 12.1% | 99.7% |
| 23 | 1/5/2004 | 19/6/2004 | 49 | 315 | 5.7% | 8.9% | 99.5% |
| 24 | 19/6/2004 | 11/8/2004 | 53 | 200 | 12.0% | 11.5% | 70.6% |
| 25 | 11/8/2004 | 4/10/2004 | 54 | 307 | 8.8% | 13.0% | 87.4% |

**Table 1**: All the sampling events – date, number of iron rods samples, number of missing data, remarks

Sand erosion and deposition were measured with an accuracy of about 1-2 mm every 2-6 weeks since December 2002 until October 2004, thus covering two winter seasons (Table 1). From these we calculated both the net and absolute values of sand erosion and deposition. Assuming that surface changes of up to 2 mm may be due to measurement errors and not due to real changes, and as the measurements were done on a monthly basis, cumulative absolute yearly changes of up to 24 mm may be considered as measurement noise. The exact location and height above sea level of the erosion pins were determined using a differential GPS, whereas the surface slope and aspect angles were determined in situ using a clinometer and a hand compass, as well as from a digital elevation model (see below). The presence or absence of biogenic crust was estimated visually for each erosion pin on January 31st-February 3rd 2003 (i.e. during winter time). As part of the analysis the erosion pins were classified into nine geomorphologic units in which they were located: foredune (FD), slip face (SF), dune top or on a nebka (DT), lee facing slope of the dune, moderate slope (MF), wind facing slope of the dune (WS), urkar (aeolionite) hill (K), inter dune area, usually lower than its surroundings and vegetated (L), stabilized sand hill, located to the east of an existing or a past river (SH), alluvial plain of the Evtah River crossing the Nizzanim Dunes (AL) (Table 2 and Fig. 2). The topographic profiles of the four transects are presented in Fig 3. The overall statistics regarding the completeness of the field data and of the meteorological data for the 25 measurement periods are presented in Table 1.

| Geomorphologic unit code | Description | Unit type | No. of erosion pins | Sum of absolute change (mm/year) | | Net absolute change (mm/year) | |
|---|---|---|---|---|---|---|---|
| | | | | Average | Standard deviation | Average | Standard deviation |
| FD | Foredune | Active | 13 | 749.0 | 767.0 | -22.8 | 404.0 |
| SF | Slip face | Active | 33 | 345.2 | 366.6 | 228.8 | 385.0 |
| DT | Dune top or on a nebka | Active | 88 | 218.7 | 203.3 | 54.8 | 163.1 |
| MF | Lee facing slope of the dune, moderate slope | Active | 44 | 181.5 | 198.7 | 114.2 | 144.4 |
| WS | Wind facing slope of the dune | Active | 47 | 133.9 | 101.2 | -61.2 | 84.5 |
| K | Kurkar (aeolionite) hill | Stabilized | 12 | 19.9 | 6.1 | -1.5 | 2.7 |
| L | Inter dune area, usually lower than its surroundings and vegetated | Stabilized | 62 | 19.2 | 10.5 | 1.5 | 9.5 |
| SH | Stabilized sand hill, located to the east of an existing or a past river | Stabilized | 14 | 18.9 | 5.9 | 1.2 | 6.3 |
| AL | Alluvial plain of the Evtah River crossing the Nizzanim Dunes | Stabilized | 2 | 6.2 | 6.9 | 0.0 | 0.0 |
| Grand Total | | | 315 | 178.9 | 281.1 | 45.5 | 198.3 |

**Table 2**: Definition of the geomorphologic units used in the study.

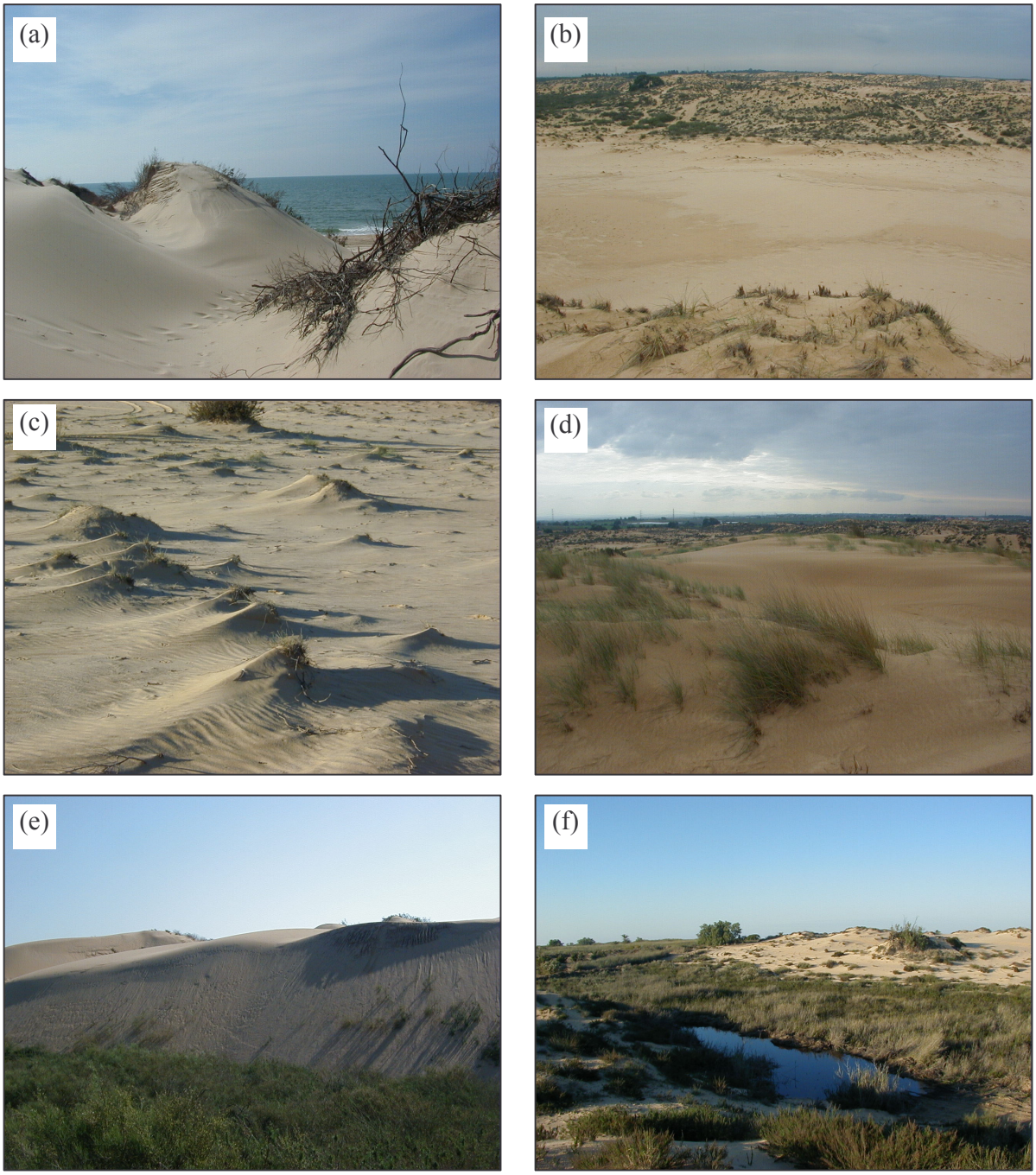


**Figure 2**: Photographs representing some of the geomorphologic units and their vegetation. The location of the photographs is shown in Fig. 1 by bold letters a-f. (a) A disturbed foredune (unit FD) with a wind tunnel between the large nabkas. The dead branches on the right are of a Tamarix tree. Image taken in March 29th, 2003; (b) An area without vegetation on the wind facing slope of a dune (unit WS). In the background: semi-stabilized dunes covered by *Artmeisia monosperma*. Image taken in January 28th, 2004; (c) Nebkas of *Cyperus macrorrhizus* on a wind facing slope (unit WS); (d) Nebkas of Ammophila arenaria on the top a dune (unit DT). Image taken in January 28th, 2004; (e) An active slip face (unit SF). Image taken in March 30th, 2003; (f) In the lower-left part of the photo: a non-active moderate slip face (unit MF) mainly covered by *Artmeisia monosperma*. In the center of the image: a fully vegetated interdune area (unit L) covered by *Artmeisia monosperma*, *Retama raetam* and . Image taken in January 27th, 2001.

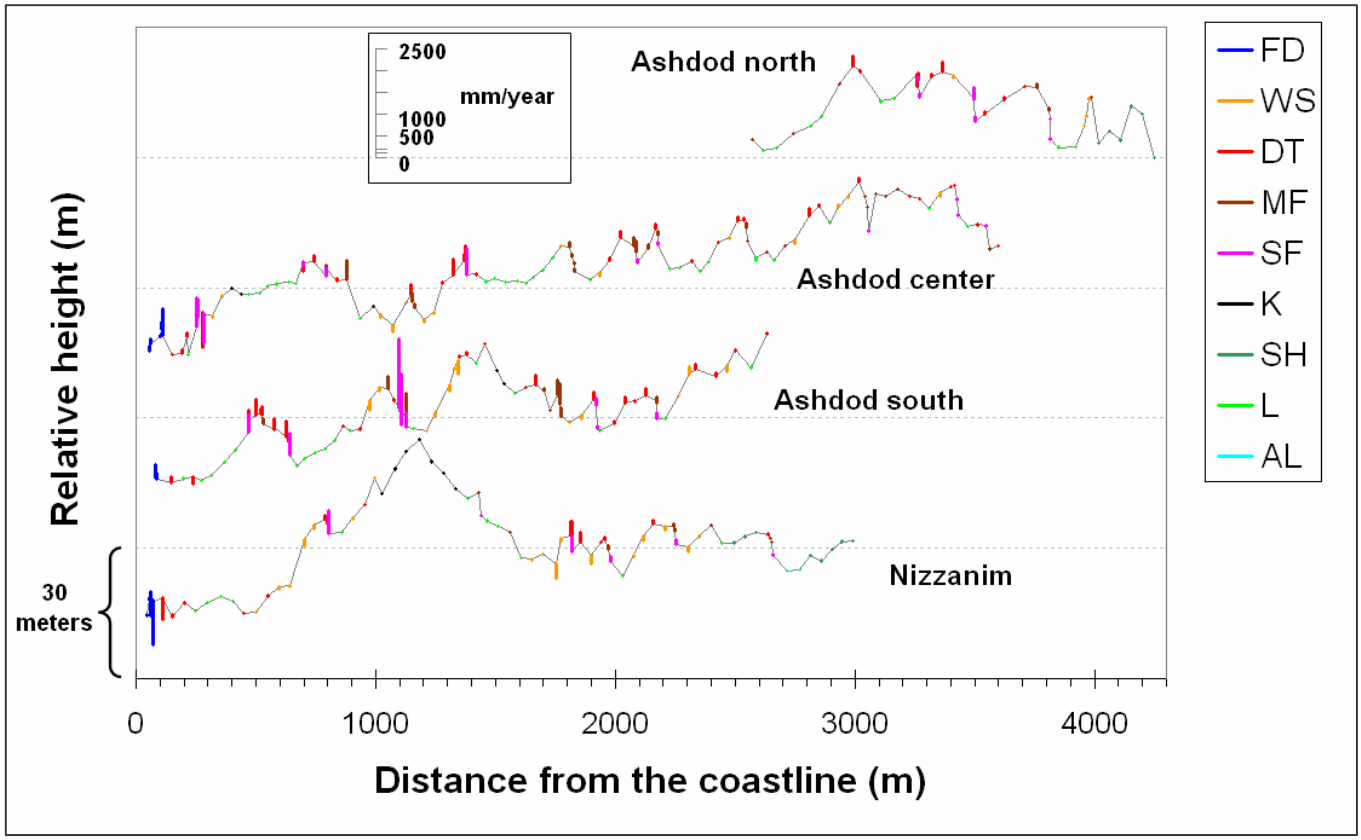


**Figure 3**: The positions of the erosion pins laid upon the topographic profiles of the four transects, and the sum of net changes in the sand level (mm/year) as measured in each of the erosion pins. The following initials were used for the geomorphologic units: FD (foredune), WS (wind facing slope), DT (dune top), MF (moderate lee facing slope), SF (slip face), K ('kurkar' aeolionite hill), SH (stabilized sand hill), L (inter dune area), AL (alluvial plain).

## 2.3 Temporal analyses of meteorological data

Meteorological data of rainfall, wind speed and direction, temperature and relative humidity were measured by the Nizzanim meteorological station located on the roof of the building of the Shikmim Field School (see map in Fig. 1) and operated by the Ashkelon Metropolitan Union for the Environment. This building is located on a hill and surrounded by trees about 500m south-east of the Ashdod Dunes, and about 2.8km from the coastline. The data are recorded in periods of every 5 minutes, and were here analyzed at a temporal resolution of one hour. As the wind regime is one of the most important physical factors in determining the mobility of dunes (Bagnold, 1941; Tsoar and Werner, 1998; Tsoar, 2002), the drift potential of the sand by the wind was estimated by applying the method developed by Fryberger (1979), using the indices of the Drift

Potential (DP), the Resultant Drift Potential (RDP) index, and the Resultant Drift Direction (RDD). These indices were calculated for each of the 25 time periods for which the sand erosion/deposition was measured in the field ($\mu$ = 26.8 days, $\sigma$ = 12.8 days; Table 1). The variable of DP is calculated as follows (Fryberger, 1979):

$$DP = \sum q_s \text{ , where } q_s = \sum U^2 (U - U_t) * t \qquad (1)$$

Where $q_s$ = the rate of sand drift for a certain wind sector (vector units)

$U$ = wind velocity (m/s)

$U_t$ = the threshold wind velocity for sand movement (m/s)

$t$ = percent of the time the wind blew above the threshold

We did not include the time factor (t) presented in equation 1 in our calculations because the measurement periods of sand movement that we compared were not equal in their length (see Table 1; a similar approach was adapted by Arens et al., 2004). We therefore refer to these variables as DP-t, RDP-t and RDD-t as they are calculated without the time factor. Determining a single threshold wind speed for the calculation of these indices is somewhat arbitrary, as in reality it varies with the surface roughness from place to place over the sand dunes, as a function of the vegetation cover and the relative height. The wind speed of 4 m/s (as recorded in the Nizzanim meteorological station) was chosen as the threshold wind speed for the calculation of those indices (compare with Arens, 2004, equation 12); the corresponding wind speed as measured on the beach at a height of 2.5 m was about 10 m/s, and in such events sand movement was observed. In addition, the corresponding rainfall amounts were calculated, as well as the percent of the time in which the wind speed was above the threshold and there was rainfall. For those periods in which there was no data available from the Nizzanim station, the corresponding wind and rainfall data from the Ashkelon station were used, located about 15 km to the south-west near the coastline (The correlation coefficient between the hourly wind speed and daily rainfall amounts of the two stations are 0.74 and 0.63, respectively).

## 2.4 Remote sensing of vegetation

Remote sensing analyses of vegetation included the calculation of vegetation cover from grey-scale aerial photographs taken by the Survey of Israel (as in Chapter 4 of this thesis), and the calculation of the Normalized Difference Vegetation Index (NDVI; Tucker, 1979) from Landsat 7 ETM+ satellite images. As the values of NDVI are affected by the background soil, especially in arid and semi-arid areas where vegetation cover is low, the Soil Adjusted Vegetation Index (SAVI) was also applied, following Huete (1988):

$$SAVI = (NIR - R) / (NIR + R + L) * (1 + L) \qquad (2)$$

where NIR = Value in the Near Infra Red band of an image pixel

R = Value in the Red band of an image pixel

L = A constant soil adjustment factor ranging between 0-100. Several values were tested in a preliminary study and it was found that L=0.25 gave the best results in the study area for estimating vegetation cover.

The aerial photograph covering the Ashdod dunes was taken at 17:11 on June 8th, 2002 (strip BA-163, photograph B135). The two aerial photographs covering the Nizzanim Dunes were taken at 12:15 on June 27th, 2003 (strip AR-7, photographs 2783 and 2792). All the aerial photographs were rectified to the Israel New Grid (Israel Transverse Mercator; Mugnier, 2000), using Ground Control Points (GCPs) identified on a color orthophoto (1m. resolution).

NDVI and SAVI values were calculated for both study areas based on Landsat 7 ETM+ satellite images (path 174 row 38) from August 7th, 1999, January 14th, 2000 and May 21st, 2000. This was done after performing atmospheric corrections using the MODTRAN (Berk et al., 1999) and ACORN (AIG, 2001) atmospheric models and merging the spectral bands with high resolution pan chromatic band 8 of the Landsat, thus obtaining a spatial resolution of 15 m. The NDVI and SAVI values served us as surrogate variables for vegetation cover. These two are known to be correlated with the aboveground net primary productivity and the absorbed photosynthetically active radiation (Kerr and Ostrovsky, 2003). Such estimates (derived from a CASI airborne

sensor; see Ben-Dor et al., 2006) were validated using field estimates done in the field by Mimi Ron (personal communication; these measurements were preformed in the months of August and October 2000 for Israel's Nature and Parks Authority) in 16 quadrats of 100m$^2$ located on dunes whose location was measured by a highly accurate differential global positioning system (GPS). As vegetation cover estimates often have a poisson distribution, a square-root transformation (Sokal and Rohlf, 1995) was applied to them prior to the correlation analyses. From this we found that NDVI and SAVI were able to explain 78.6% and 83.5% (respectively) of vegetation cover as sampled in the field (ranging between 0% to 45% in the sampled quadrats).

Vegetation cover, NDVI and SAVI values were calculated for the locations of the erosion pins, as well as for the upwind (towards the SW) sectors of these stations at the following distances, using directional filters at a width of about 60º: 15 m, 27.5 m, 50 m, 100 m, 200 m and 400 m. This was done to analyze the influence of upwind plant cover on the sand erosion, a factor mentioned by Hupy (2004).

Although biological soil crusts have considerable effect on both surface roughness and wind erosion (see Belnap and Gillette, 1998), their presence over the coastal dunes of Ashdod and Nizzanim is quite low (see below) and patchy, and was therefore not included in the analysis.

## 2.5 Topographic analyses

Topographic data for this study was based on several sources that included digital contours files, orienteering maps and field measurements using differential GPS.

For the northern part of the Ashdod Dunes, detailed contours (at a vertical spacing of 0.5 meter) were obtained from a photogrammetric survey by Fishman (1994). For the southern part of the Ashdod Dunes, contour lines (at a vertical spacing of 2.5 meters) were digitized from the Nizzanim orienteering map (published in 1995 by the Israel Sport Orienteering Association, at a scale of 1:10,000). The data from the contours were converted into a digital elevation model (DEM) with a spatial resolution of 2.5 meters using the triangulation method described by Zhu et al. (2001), and implemented in the Idrisi software (Eastman, 2001). For the dunes of Nizzanim the most detailed topographic data existing consists of contours with a vertical spacing of 5 m. As this is not enough for

the dunes under study (whose average height is about 10 m), no topographic analyses were conducted for the dunes of Nizzanim.

The following parameters were applied to estimate the influence of topography on the measured sand erosion and deposition: (1) the elevation, slope and aspect at the location of the erosion pin, as well as the first derivative of the slope; (2) the difference between the height of a place where the station was located and the average height (i.e. 'the relative height') of the upwind (towards the SW) sectors of the station at the following distances, using directional filters at a width of about 60º: 15 m, 27.5 m, 50 m, 100 m, 200 m and 400 m.

We expected that the higher is an erosion pin located relatively to the area upwind of it, the greater will be sand erosion or deposition there, as wind speed increases. Erosion pins that are located beyond the dune crest (especially those at the slip face) were however hypothesized to deserve a special treatment. Considering the case of a slip face for example, when sand grains start sliding over it, they can slide the whole way down. Thus, the exact position of an erosion pin on a slip face (whether it is 5 m higher or lower) will not change the values of sand movement that were measured. In fact, when calculating the relative height of an erosion pin located in either the slip face or another position behind (and usually lower than) the dune top, a negative value may result. A negative relative height is associated with weaker winds that are not able to carry sand (see Frank and Kocurek, 1996). This happens on a slip face, where the wind speed decreases suddenly: sand grains are deposited, and the winds' flow lines form a separation bubble (Parsons et al., 2004). The height difference variable was therefore calculated for those erosion pins located in the lee slopes of the dunes (units MF and SF) both in their correct location and also as if they were located on their respective dune top (that is, as if they are moved by a few meters or dozens of meters upwind towards the coastline).

## 2.6 Aerodynamic surface roughness ($Z_0$)

In Chapter 5 of this thesis we have modeled the aerodynamic surface roughness ($Z_0$) over two coastal dune areas in Israel (Ashdod and Bet Yanay) based on wind measurements at a single height of 2.5m (following Wieringa, 1973, 1986), and the same vegetation and topographic variables presented above. Here we examined whether the observed patterns of sand erosion and deposition can be explained by the modeled map of $Z_0$ values.

## 3. Results

### 3.1 Temporal analysis of sand erosion and its influencing factors: wind and rain

Measured figures of sand erosion/deposition are presented in Figures 3 and 4 and in Table 2. Since some of the geomorphologic units (AL, K, L, SH) are relatively stable (with a net absolute change of <2 mm/year), presentation of only the active units is given here. The sand erosion/deposition changes are shown separately for five active geomorphologic units (DT, MF, SF, WS and FD) as it varies greatly between them (see also Table 2). Foredunes were included here in spite of their small samples size (n=13). The greatest values of net or absolute sand deposition were found in the fore dunes as these are expected to experience the strongest wind. However the fore dune experiences periods in which it is being built and eroded, and therefore the highest levels of consistent net accumulation of sand were found as expected on the lee slope of the dunes, as this part of the dune occupies a small part of the dune yet is suspected to deposition of sand grains from the stoss slope of the dune.

Most of sand erosion/deposition (both the absolute and the net values) over the dunes is during the winter months (November to March; Figure 4). During this period, the coastal areas of Israel experience both high wind speeds (as expressed by the RDP-t values) and rainfall. While during the winter months, sand moving winds are moving the sand towards the north-east (~ 45º, as estimated by RDD-t; fig 4d), during the summer months, the sand moving winds are moving the sand towards the south-east (~ 135º, as estimated by RDD-t; fig 4d). Although the strongest winds and almost all the rainfall are experienced in the same months, no correlation was found between the sand erosion/deposition to the rainfall. This lack of correlation is explained by the low coincidence of strong winds and rainfall. Figure 5 presents a histogram showing the co-occurrence of wind speed and rainfall events on an hourly basis, for the period between January 2000 – October 2004, as measured in the Nizzanim meteorological station. Most of the sand moving winds occur when there is no rain at all, and the rainy events usually coincide with wind speed of below 8 m/s.

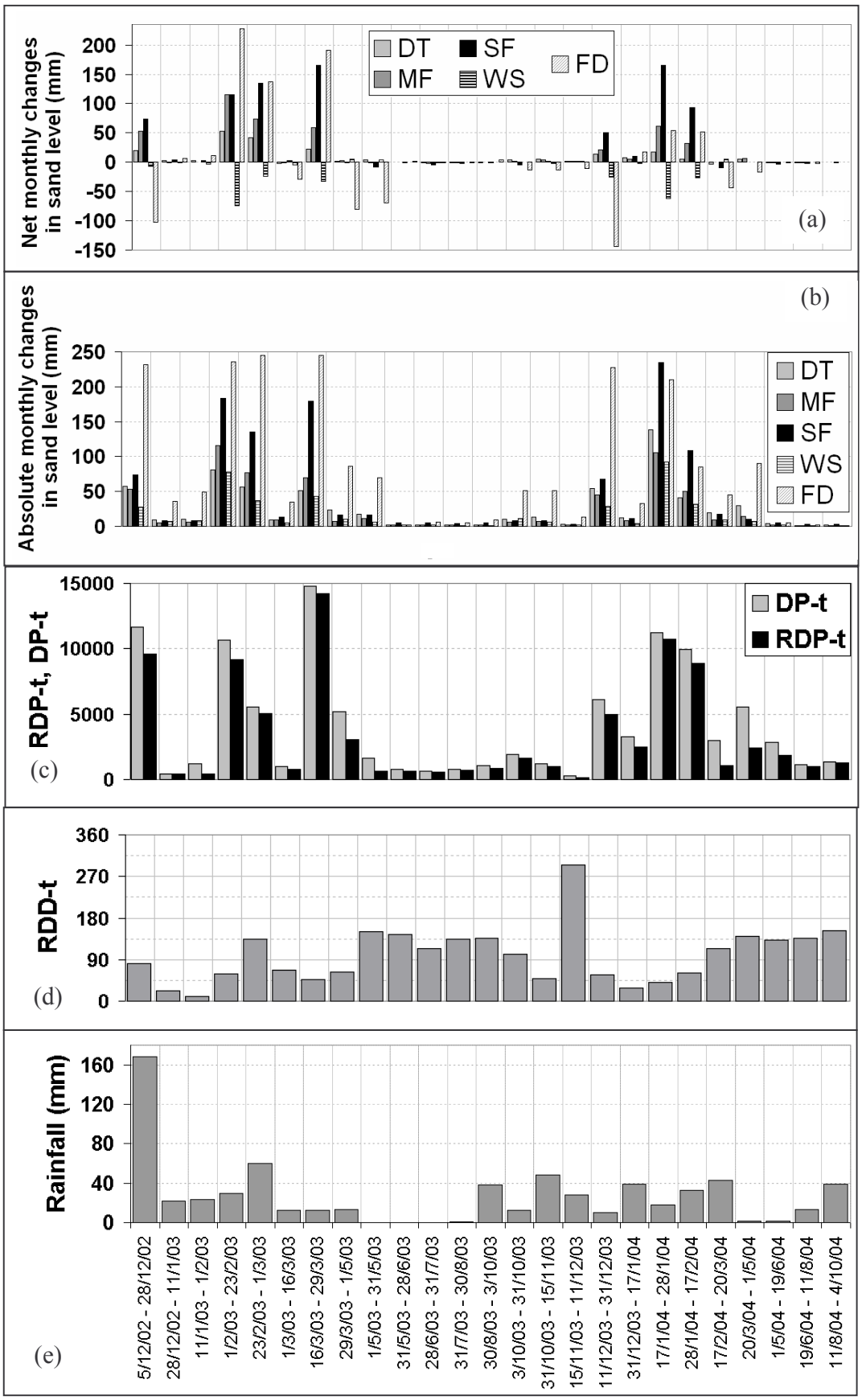


**Figure 4**: Temporal series of rainfall, wind, and sand movement data: (a) The average net monthly change in the sand level for four active geomorphologic units, (b) The average absolute monthly change in the sand level for four active geomorphologic units, (c) Resultant Drift Potential (RDP-t) and Drift Potential (DP-t), (d) Resultant Drift Direction (RDD-t): in the grey bars, (e) Rainfall. The following initials were used for the geomorphologic units: DT (dune top), MF (moderate lee facing slope), SF (slip face) WS (wind facing slope), and FD (fore dunes).

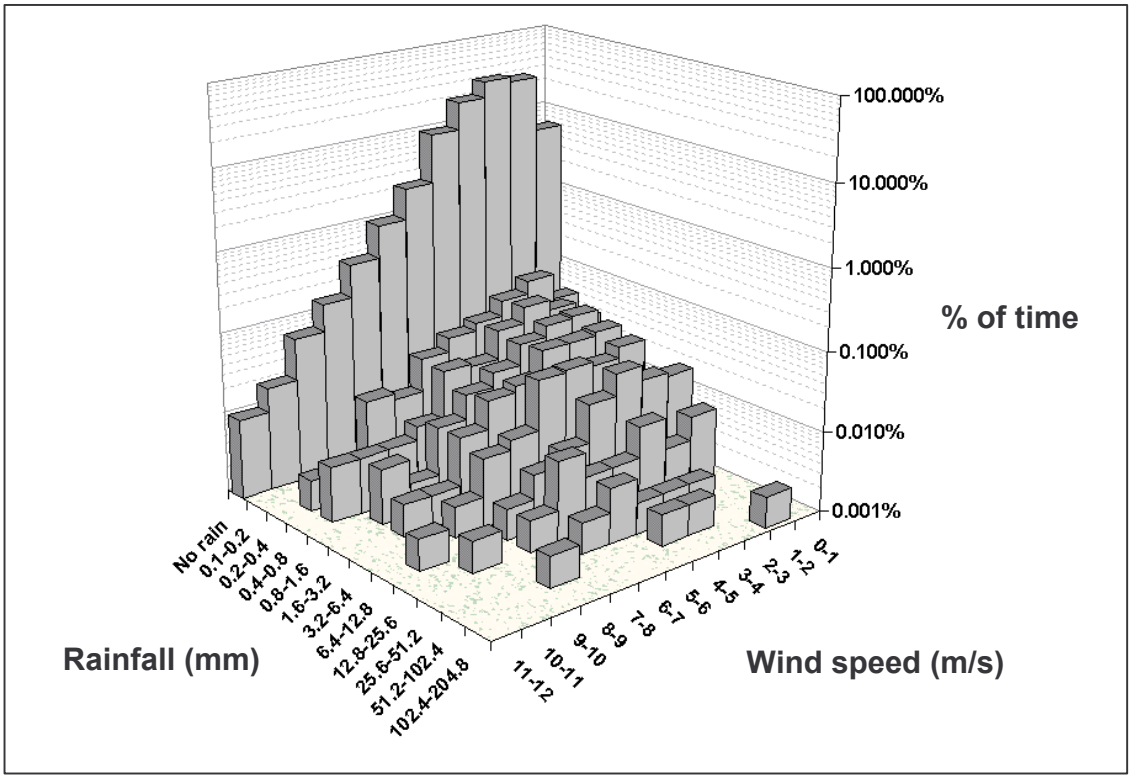


**Figure 5**: A 3-d histogram presenting the co-occurrence of wind speed and rainfall events on an hourly basis, for the period between January 2000 – October 2004, as measured in the Nizzanim meteorological station. Note that the z-axis is drawn on a logarithmic scale.

Rather, it is the variable of RDP-t (and to a lesser degree also DP-t) that is highly correlated with the sand movement. High correlation was found between RDP-t (or DP-t) and sand movement over the five active geomorphologic units (Table 3, Fig. 4). The variance in the absolute values of sand erosion explained by RDP-t is higher than 65% for all five units, and higher than 44% when net sand erosion is considered (except for the fore dunes, were it was only 19%-25%). The geomorphologic unit that was the most indicative of the wind power was the slip face (SF), with $R^2$ values of 81% and 85% for the absolute and net values of sand erosion/deposition, respectively (Table 3).

| | | Absolute monthly changes in the sand level | | | | | Net monthly changes in the sand level | | | | |
|---|---|---|---|---|---|---|---|---|---|---|---|
| | | DT | MF | SF | WS | FD | DT | MF | SF | WS | FD |
| Correlation coefficient | DP-t | 0.81 | 0.85 | 0.86 | 0.81 | 0.85 | 0.67 | 0.81 | 0.87 | -0.74 | 0.43 |
| | RDP-t | 0.81 | 0.86 | 0.90 | 0.83 | 0.84 | 0.67 | 0.82 | 0.92 | -0.78 | 0.50 |
| % of variance | DP-t | 66% | 72% | 74% | 65% | 72% | 44% | 65% | 76% | 55% | 19% |
| | RDP-t | 66% | 75% | 81% | 68% | 70% | 46% | 68% | 85% | 61% | 25% |

**Table 3**: The correlation between the Drift Potential (DP-t) and Resultant Drift Potential (RDP-t) of sand by the wind as measured in the Nizzanim station, with respect to the absolute and monthly changes in the sand level as measured in four active geomorphologic units in the Ashdod and Nizzanim dunes, between December 2002 and October 2004 (n = 25). The following initials were used for the geomorphologic units: SF (slip face), MF (moderate lee facing slope), DT (dune top), WS (wind facing slope) and FD (fore dunes).

## 3.2 Influence of spatial variables on sand erosion and deposition

Out of the 315 erosion pins, 190 experienced net deposition, 111 experienced net erosion and only 14 of them resulted with a net balance between erosion and deposition. The yearly absolute and net sand level changes were found to be highly correlated: $R^2$ = 82.9% for net increase (deposition) in the sand level, and $R^2$ = 68.2% for net decrease (erosion) in the sand level (Fig 6). Thus, as the spatial analysis is focused on absolute annual sand level changes, in places where high absolute changes in sand level occurred, an apparent deposition or erosion, rather than a net balance, was taking place. All erosion pins (but one) for which no change was documented in the sand level were located in stabilized units.

The annual changes in sand erosion and deposition over stabilizing coastal dunes present a highly variable spatial pattern. The spatial patterns of the annual absolute changes in sand level are mapped in Fig. 1 (where the location of the erosion pins with respect to varying vegetation cover can be appreciated) and in Fig. 3 (where annual net changes in the sand level are presented over topographic profiles of the four transects).

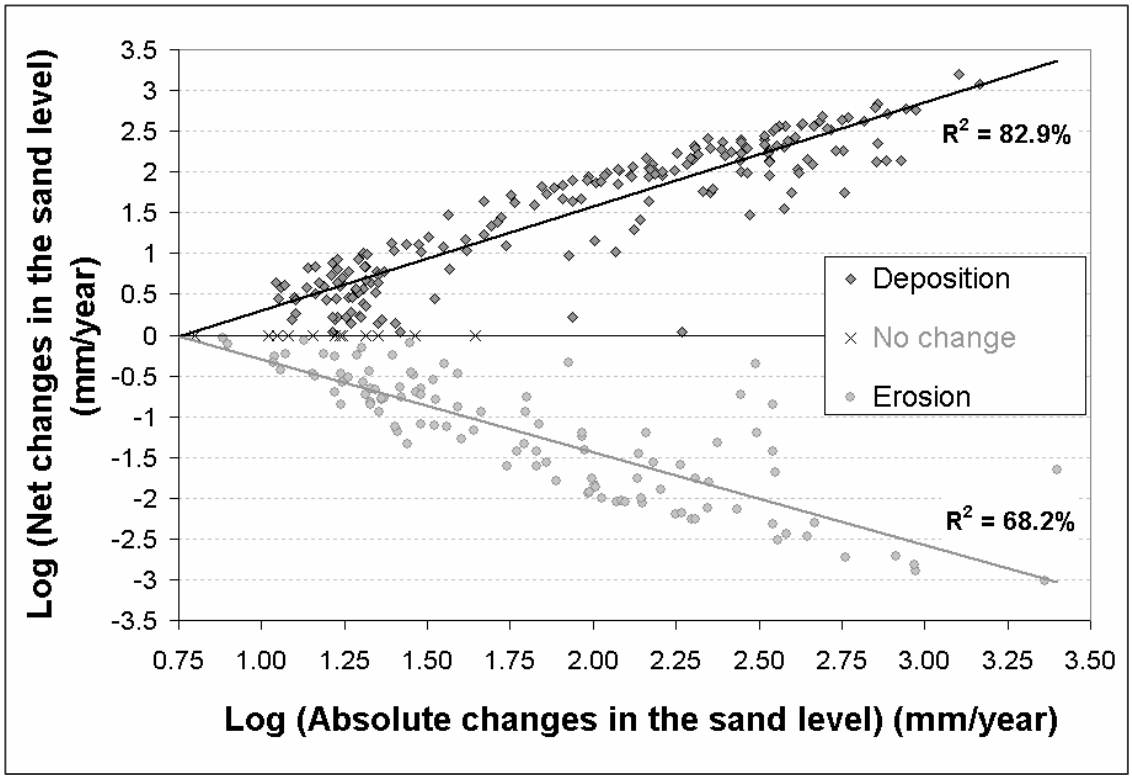


**Figure 6**: The correlation between the absolute and net yearly changes in the sand level.

Not all geomorphologic units experience sand movement (Table 2). Results for the fore dunes are not shown as none of the spatial variables we examined was able to explain more than 15% of the differences between the erosion pins located on them. This may be related to their disturbance by human presence, which causes local variability in vegetation and topography, in addition to tunneling effects, that are beyond the resolution of our digital elevation model and of the Landsat satellite images. A significant but weak pattern of a general decrease in sand movement with distance from the coastline was found when all erosion pins were included in the analysis ($R^2$ = 18%, $p < 0.001$, n = 315; Table 4. Compare with Illenberger and Rust, 1988). Only when using a subset of the data, this expected trend is indeed found, being especially evident in the lee slope units (MF, $R^2$ = 38%, $p < 0.001$, n = 44; SF, $R^2$ = 56%, $p < 0.001$, n = 33).

As expected sand movement was positively correlated with the relative height of the erosion pins (with respect to the preceding upwind topography), and negatively correlated with vegetation cover (Tables 4 and 5). The correlation values reached their peak at an upwind distance of about 100 m (depending on the variable).

| | Upwind distance | All erosion pins | WS | DT | MF | SF |
|---|---|---|---|---|---|---|
| Distance from the coastline (m) | | 18% | 5% | 19% | 38% | 56% |
| SAVI January 2000 for an upwind distance of | 100 m | 40% | 12% | 35% | 48% | 61% |
| The difference between the height of the erosion pin (corrected location, see text) and the average height of the erosion pin for an upwind distance of | 100 m | 36% | 4% | 21% | 46% | 44% |
| | 200 m | 31% | 8% | 20% | 23% | 42% |
| Predicted values of sum of absolute change (mm/year), according to the regression model | | 69% | 48% | 63% | 67% | 71% |

**Table 4**: The % of the variance explained in the sum of absolute yearly changes in the sand level as a function of: (a) the distance from the coastline; (b) average SAVI values (as of January 2000) for an upwind (SW) distance of 100 m.; (c, d) the difference between the height of the erosion pin and the average height 100 and 200 meters upwind (SW) of the erosion pin. The positions of all the erosion pins located behind the dunes' crest lines (mainly the MF and SF units) were moved as if they were on the dune tops; (e) the predicted values of sum of absolute yearly change in the sand level, based on the multiple regression model presented in equation 7. Included are all the erosion pins from the transects of the dunes of Ashdod (n = 230) for which DEM data exist. The following initials were used for the geomorphologic units: DT (dune top), FD (foredune), MF (moderate lee facing slope), SF (slip face) and WS (wind facing slope).

| | | Distance upwind (SW) in meters | | | | | |
|---|---|---|---|---|---|---|---|
| Factor examined | Subset of erosion pins | 15 | 27.5 | 50 | 100 | 200 | 400 |
| % Vegetation cover on aerial photographs | All (n=315) | -0.50 | -0.64 | -0.68 | **-0.66** | -0.45 | -0.35 |
| NDVI, August 1999 | | -0.49 | -0.57 | -0.60 | **-0.62** | -0.49 | -0.43 |
| NDVI, January 2000 | | -0.57 | -0.63 | **-0.66** | **-0.66** | -0.54 | -0.48 |
| NDVI, May 2000 | | -0.29 | -0.41 | -0.48 | **-0.52** | -0.40 | -0.38 |
| Average height difference (erosion pins with DEM data) | All (n=230) | -0.30 | -0.22 | -0.07 | 0.19 | 0.36 | **0.40** |
| Average height difference, positions corrected (erosion pins with DEM data) | All (n=230) | 0.24 | 0.38 | 0.50 | **0.60** | 0.56 | 0.52 |
| | DT (n=72) | -0.01 | 0.08 | 0.19 | **0.46** | 0.45 | 0.38 |
| | MF (n=37) | 0.55 | 0.61 | **0.73** | 0.68 | 0.48 | 0.32 |
| | SF (n=27) | 0.54 | 0.60 | 0.64 | **0.66** | 0.65 | 0.46 |
| | WS (n=30) | -0.10 | -0.07 | 0.09 | 0.21 | 0.28 | **0.44** |
| SAVI (L=0.25), January 2000 | All (n=315) | -0.57 | -0.60 | -0.62 | **-0.63** | -0.54 | -0.48 |
| | DT (n=88) | -0.54 | -0.57 | -0.58 | **-0.59** | -0.34 | -0.36 |
| | MF (n=44) | -0.48 | -0.59 | -0.65 | **-0.69** | -0.60 | -0.40 |
| | SF (n=33) | -0.55 | -0.67 | -0.75 | **-0.78** | -0.61 | -0.47 |
| | WS (n=47) | -0.39 | **-0.42** | -0.39 | -0.35 | -0.12 | -0.10 |

**Table 5**: The correlation coefficients between the sum of absolute yearly change in the sand level, and several topographic and vegetation factors, as a function of the distance upwind (SW), for all the erosion pins (n = 315). For the topographic variables, only erosion pins for which DEM data was available (i.e., over the Ashdon Dunes) were included. In the second topographic variable the positions of all the erosion pins located behind the dunes' crest lines (mainly the MF and SF units) were moved as if they were on the dune tops (see text for details). The following initials were used for the geomorphologic units: DT (dune top), MF (moderate lee facing slope), SF (slip face) and WS (wind facing slope).

The correlation values obtained from vegetation cover as calculated from aerial photographs, were not superior to those obtained from NDVI or SAVI values of a much lower resolution (1m and 15m, respectively).In contrast with the variable of distance from the coastline (Table 4), vegetation (as estimated by the SAVI values of January 2000 at an upwind distance of 100m) directly affects sand movement and here the general trend also for all the erosion pins pooled together is clearly evident ($R^2$ = 40%; $p < 0.001$, n = 315). A higher explanatory power was obtained for the slip face (SF; $R^2$ = 61%) and for the moderate lee slope (MF; $R^2$ = 48%).

As for the relative height difference of an erosion pin with respect to the average topographic height preceding it in the 400m upwind towards the SW, there is hardly any positive trend with respect to the annual absolute changes ($R^2$ = 16% for all erosion pins for which DEM data was available; $p < 0.001$, n =230).

Correcting the positions of the erosion pins located behind the dunes' crest lines (see section 2.5) revealed the expected positive trend of greater sand movement for erosion pins located higher with respect to the area upwind of them ($R^2$ = 36%, $p < 0.001$, n = 230; Table 4). As before, highest explanatory power was obtained for the slip face (SF; $R^2$ = 44%, $p < 0.001$, n = 27) and the moderate lee slope (MF; $R^2$ = 46%, $p < 0.001$, n = 37).

One of the main factors affecting whether a certain place is undergoing erosion or deposition, is the aspect of the surface with respect to the main direction of the sand moving winds. Thus, a higher magnitude of net accumulation of sand was expected when the surface aspect was closer to the NE, and a higher magnitude of net erosion of sand when the surface aspect was closer to the SW. As in dunes that are undergoing stabilization the development of nebkha dunes modifies the initial classic shape of the dune, only the slip face (SF) and the wind facing slope (WS) units were included in the analysis. Indeed, when all erosion pins are included, only 25% of the variance was explained. However, when SF and WS were examined, surface aspect had a significant effect on the yearly net changes in the sand level, with 53.2% of the variance explained when both units were pooled together (Figure 7). Notice also that the overall net values are higher for the slip face (even surpassing 1000 mm/year in two places; see also the results in Table 2). In contrast to the winter months, during the summer months the slip face unit was experiencing net erosion under the influence of sand moving winds blowing

from the NW (Fig. 4a). This phenomena was marginal however, and the average annual erosion from the slip face amounted to only 20.7 mm/year in contrast with an average annual deposition of 448.7 mm/year on the slip face (Figure 4a).

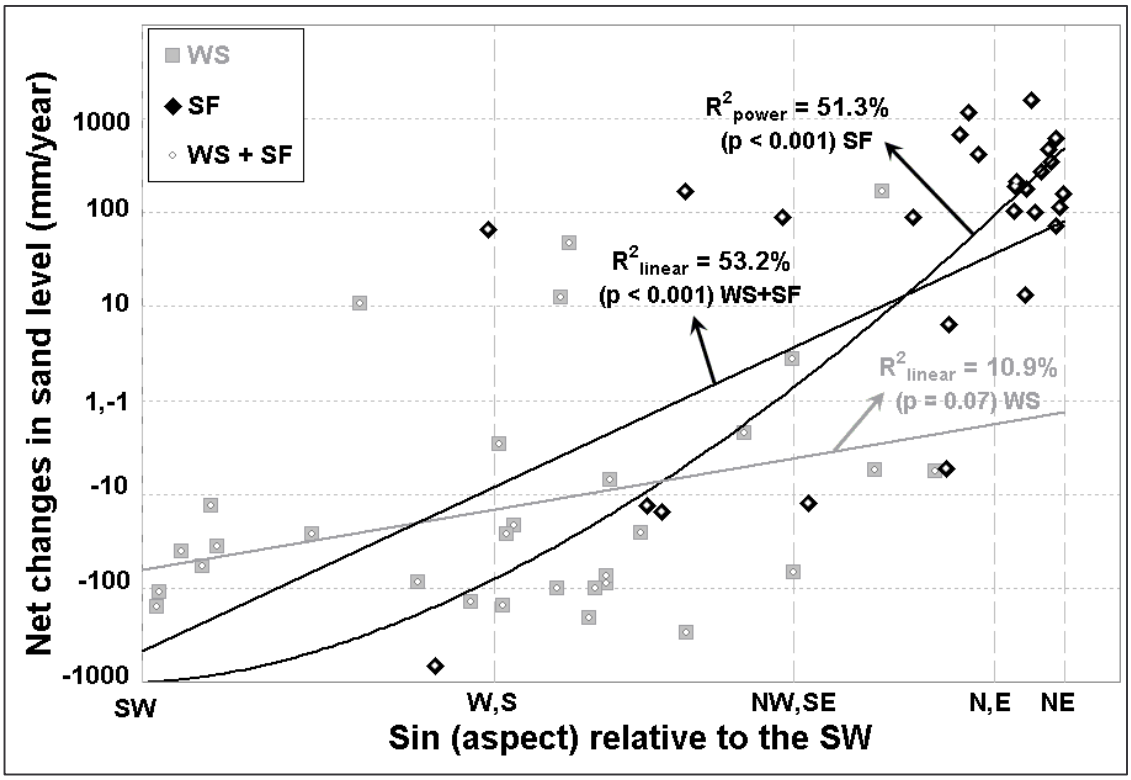


**Figure 7**: Sum of net yearly changes in the sand level as a function of the aspect (relative to the SW) of the surface, as calculated from a digital elevation model. Only the two opposing geomorphologic units are presented, WS (wind facing slope) and SF (slip face), separately and combined.

## 3.3 Predictive models of sand erosion and deposition

The best vegetation variable was that of SAVI for an upwind distance of 100 m (Table 5). The best topographic variable was that of the relative height for an upwind distance of 100 m (Table 5). However as the spacing between the dunes is about 200-300 m, we preferred to use for the regression models the variable of the relative height for an upwind distance of 200 m. These variables were inserted into a multiple regression analysis from which we then derived various empirical models to estimate the yearly absolute changes

in sand level. The first of these models included the following basic vegetation and topographic variable to estimate the yearly absolute changes in sand level:

$$\text{Log (year-abs)} = 4.128 + 0.0415 * (\Delta H200sw) - 17.96 * (SAVI100sw)$$
($\mathbf{R^2 = 52\%}$, n = 230; $p < 0.001$ for all coefficients) (3)

Where:

| | |
|---|---|
| year-abs: | Annual absolute changes in the sand level (mm) |
| SAVI100sw: | SAVI values as of January 2000, at an upwind distance of 100 m to the SW |
| ΔH200sw: | The difference between the height of the erosion pin and the average height 200 meters upwind (SW) of the erosion pin. |

The variable 'distance to sea' was not incorporated for two reasons: (1) As we have shown above and claim here, the distance itself is not an explanatory variable, rather it is the topography and vegetation cover which affect wind flow and therefore also sand movement; (2) adding the 'distance' variable to the model presented in equation 3 did not change the value of $R^2$ and the coefficient of the 'distance' variable within the regression model was not significant. However, adding variables relating to the surface slope and aspect into the regression model enabled us to increase the variability explained by the model:

$$\text{Log (year-abs)} = 3.388 + 0.056 * (\Delta H200sw) - 15.54 * (SAVI100sw) + 0.021 * (slope) + 0.305 * (aspect) + 0.0012 * (\Delta slope) \quad (4)$$
($\mathbf{R^2 = 62\%}$, n = 230; $p < 0.001$ for all coefficients, except for last one where $p = 0.03$)

Where:

| | |
|---|---|
| Slope | The surface slope |
| Aspect | Sqrt (sin (surface aspect relative to the dunes movement direction)); maximum values obtained at surface aspect of 45º (NE). |

Δslope The 1st derivative of the surface slope in the direction of the dunes movement (45º, NE)

Correcting for the location of the erosion pins located on the lee slope of the dunes, as explained in section 2.5, greatly improved the model presented in Equation 3, with the same two variables:

$$\text{Log (year-abs)} = 3.842 + 0.0669 * (\Delta\text{H200sw-moved}) - 16.46 * (\text{SAVI100sw})$$
$$(\mathbf{R^2 = 63\%,}\ n = 230;\ p < 0.001 \text{ for all coefficients}) \quad (5)$$

Where:

ΔH200sw-moved: The difference between the height of the erosion pin and the average height 200 meters upwind (SW) of the erosion pin. The positions of all the erosion pins located behind the dunes' crest lines (mainly the MF and SF units) were moved as if they were on the dune tops.

Including the variable of upwind vegetation cover as estimated from aerial photographs to the model improved it but not by much:

$$\text{Log (year-abs)} = 3.336 + 0.0568 * (\Delta\text{H200sw-moved}) - 10.48 * (\text{SAVI100sw}) - 0.0056 * (\text{vegcover-50sw})$$
$$(\mathbf{R^2 = 68\%},\ n = 230;\ p < 0.001 \text{ for all coefficients}) \quad (6)$$

Where:

vegcover-50sw: Vegetation cover at an upwind distance of 50 m to the SW, based on aerial photographs.

The % of variability in the predicted values of sum of absolute yearly change in the sand level explained by the measured values, based on the multiple regression model presented in Equation 6, is given in Table 4.

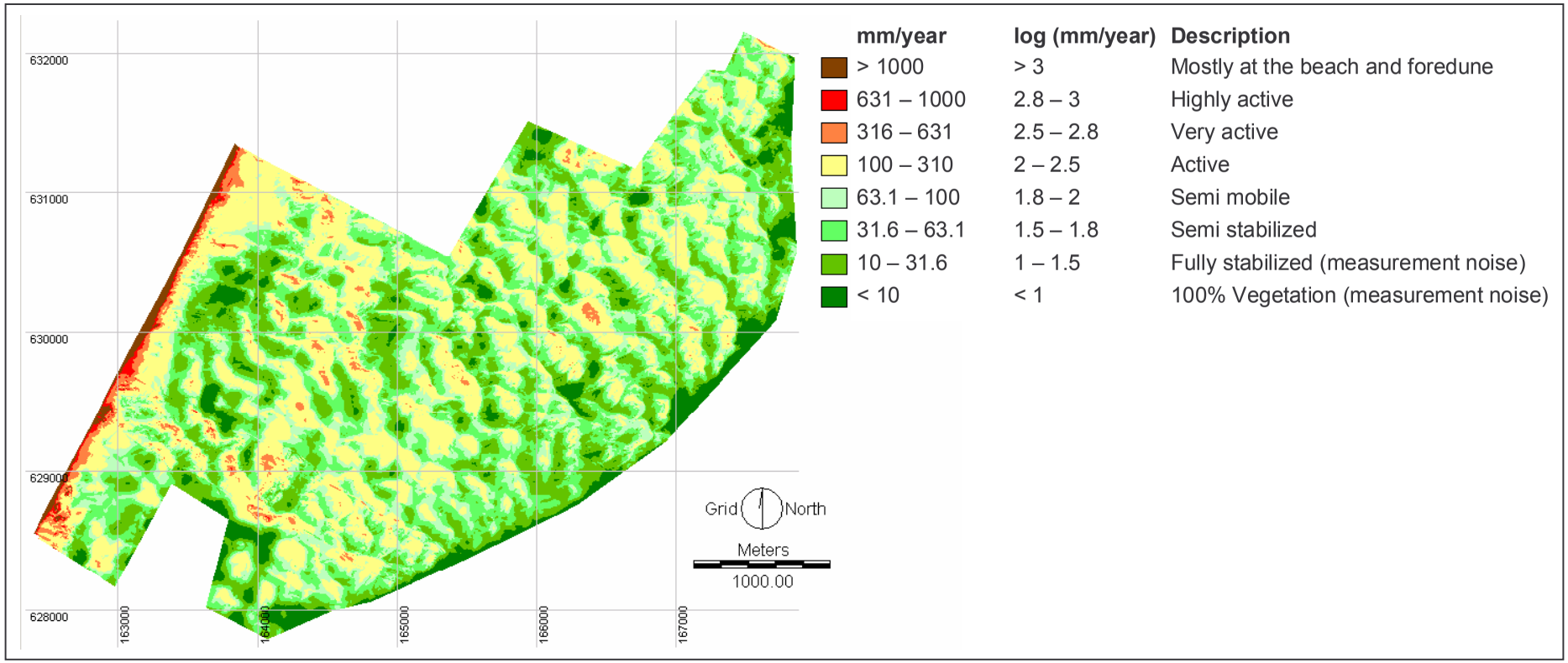


**Figure 8**: Predicted values of absolute change in sand level (mm/year), according to equation 4.

As Equations 5 and 6 were based on corrected positions of the erosion pins, they were not used to create a map of estimated values of surface stability. Rather, Equation 4 of the multiple regression model was applied (see fig 8) to derive this map.

## 3.4 Sand erosion and deposition as predicted by $Z_0$ map

The map of $Z_0$ (Chapter 5 in this thesis, Figure 11) was able to significantly explain 40% ($p < 0.001$, $n = 230$) of the variability in the absolute changes in sand movement when all erosion pins for which DEM data was available were included, and 60% of the variability for the erosion pins located on dunes slip faces ($p < 0.001$, $n = 27$; see fig 9).
When comparing the correlation between the $Z_0$ map (serving as the independent variable: $Z_0$ MAP) and the map of absolute changes in sand level (serving as the dependent variable: SAND_MAP), a highly significant relationship emerges (fig 10):

$$SAND\_MAP = 0.8437 - 0.7315 * Z_0\_MAP \qquad (7)$$

($\mathbf{R^2 = 66\%}$, $p < 0.001$)

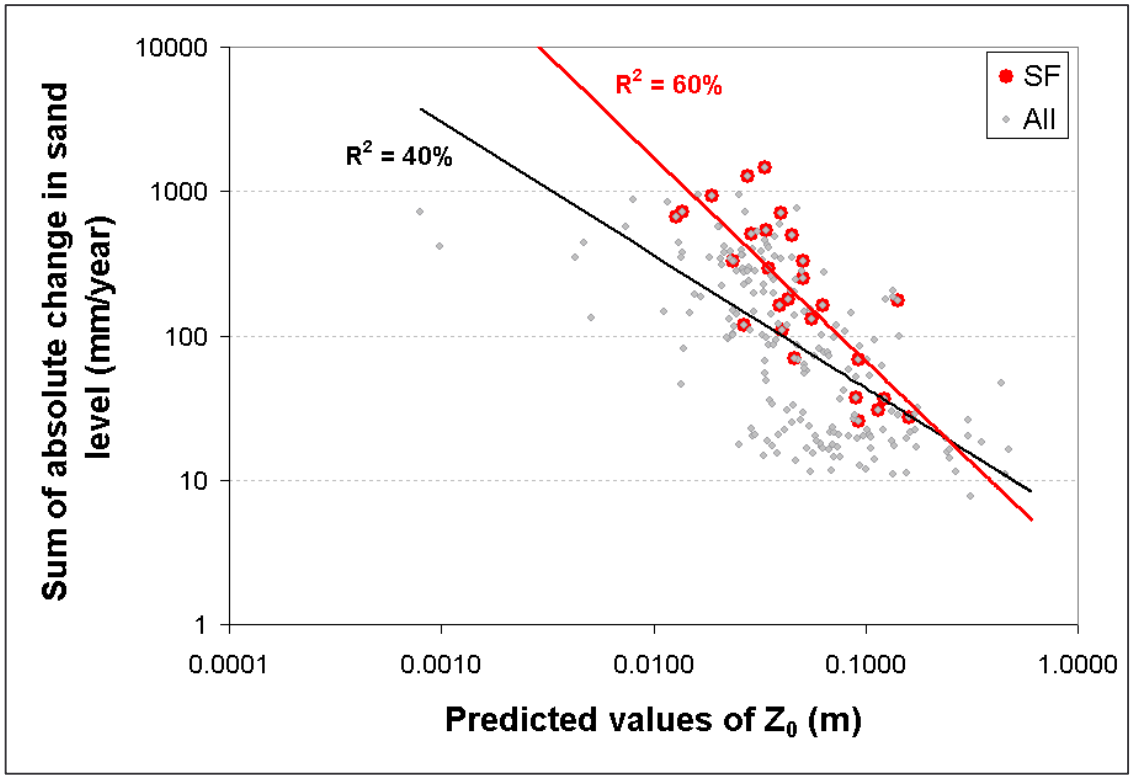


**Figure 9**: The correlation between the predicted values of $Z_0$ (based on the map presented in chapter 5) and the sum of absolute yearly changes in the sand level. The red color highlights the erosion pins located on dune slip faces (SF).

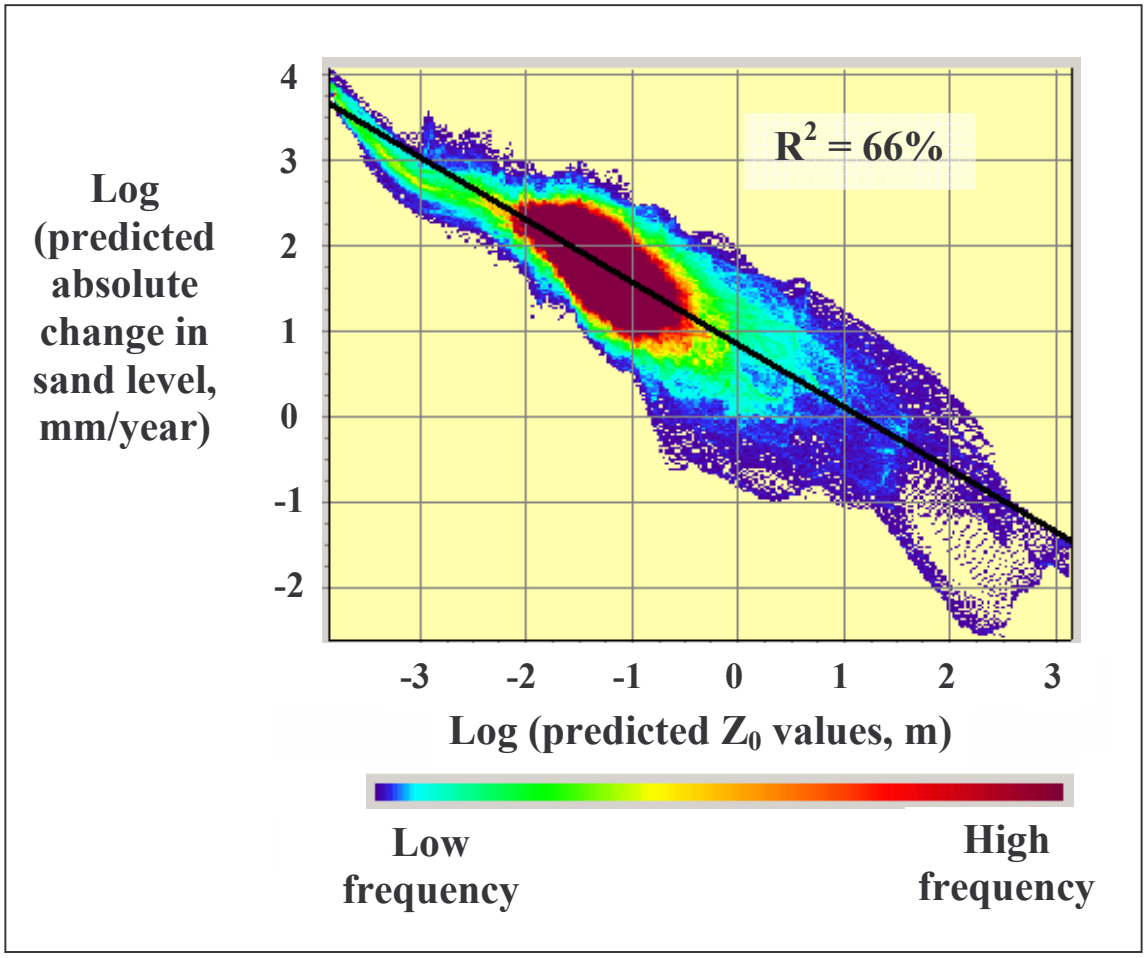


**Figure 10**: The correlation between the predictive map of Z0 values (Levin et al., submitted, fig. 11) and the predictive map of absolute yearly changes in sand level (fig. 16), on a log-log plot.

## 4. Discussion

### 4.1 Sources of errors and scaling issues

Measurements using erosion pins are commonly expected to be representative of only a small area surrounding the pin (Arens et al., 2004). Therefore, when conducting a research that uses erosion pins, care should be taken in choosing their exact locations as well as in their interpretation. Nevertheless, 68% in the variability of the annual absolute changes in the level of the sand was explained by three variables: the relative height, SAVI (or NDVI) value and vegetation cover from aerial photographs (the latter added only 5% to the variability explained). As the sand erosion/deposition at a certain place is

influenced by the upwind surface roughness, these variables were best correlated with sand movement when they were calculated for an upwind length of up to 100-200 m. This distance may well vary between dune systems e.g. depending on the spacing of the dunes. Thus, although erosion pins may seem meager and unrepresentative, when placed carefully they offer an insight into aeolian processes.

A result that may seem at first surprising was the better performance of NDVI and SAVI values derived from Landsat satellite images (with a spatial resolution of 30 m) in explaining sand movement, when compared with grey scale aerial photographs with a much higher spatial resolution (~1 m). This is due to: (1) As the sand movement across an erosion pin is influenced by the wind speed and the upwind surface roughness (at about 100 m), there is no need to use high resolution aerial photographs or topographic GIS layers; (2) The measurements of radiance values recorded on satellite images can be transformed into quantitative values of reflectance and other bio- and geo-physical variables, whereas the grey values of aerial photographs are relative to that specific setting of camera, time and day and atmospheric conditions, and cannot be transformed into reflectances; (3) On black and white aerial photographs taken over sand dunes, darker areas may represent vegetation but may also be the result of shading effects, either due to vegetation or to the topographic shape of the dunes (Chapter 2 of this thesis). Vegetation indices (calculated from satellite images) that are based on a ratio between an infra-red band and a red band (such as the NDVI) are less prone to errors due to shading effects (Lillesand and Kiefer, 1994).

Of the three seasons from which SAVI (or NDVI) values were calculated (January representing winter, May representing spring and August representing the summer), the best results in explaining sand movement were obtained by those of January, and the worst for May. The differences in the vegetation indices values between the different seasons are most probably related to the phenology of the plants (as in Schmidt and Karnieli, 2000). During the summer season rainfall events are rare in Israel, and the dunes are mainly influenced by sea breeze winds. The lowest values of vegetation indices were obtained in August, when the biogenic crust is not active and no annual plants are present. These appear and influence the values of vegetation indices following rainfall (first the crust and then germinating annuals plants). As biogenic crust was found at only 31% of the erosion pins located in the five active geomorphologic units (compared with

only 2% of the erosion pins where no perennial plants were found), and as it is usually covered by a thin layer of sand grains in this area, we estimate that its effect on vegetation indices is not very high. As most of the sand movement occurs during winter, it is therefore probable that also the spatial patterns of winter vegetation are the most effective in explaining the spatial variability in the movement of sand. The lowest correlations were obtained at spring time, probably due to the presence of annual plants at that time of the year, when almost no sand movement occurs.

Whereas $Z_0$ values were best modeled when using upwind distances of up to 200-400m for the variables of vegetation and topography (Chapter 5 in this thesis), shorter distances of up to 100-200m were found to perform better to model erosion and deposition rates of sand. Some of the difference between the $Z_0$ and the erosion pins is related to the scale of the measurements. Erosion pins measuring actual sand erosion/deposition are affected by the near surface wind flow, whereas our $Z_0$ values were based on wind measurements conducted at a height of 2.5m above ground. Over homogeneous surface conditions, estimations of $Z_0$ based on wind measurements will be unrelated to the heights at which the wind was measured. However, on dune areas, due to changing topography as well as variability in vegetation cover (on stabilizing dunes), the law of the wall does not operate (Wiggs, 2001). Thus, in heterogeneous areas, the higher is the measurement of the wind, the less it will reflect the local surface conditions and more will it be reflecting upwind surface conditions. Wieringa (1973, 1986) applied the equation that we also used for calculating $Z_0$, only he applied it to wind measurements taken at a standard height of 10 m. He therefore expected that the surface roughness values will take into account both nearby and far-off obstacles, vegetation etc. in the upwind direction within a distance of ~3 km over a sector of 20° to 30° width. Our measurements were performed at a height of 2.5 m, and are indeed influenced by obstacles (whether related to topography or vegetation) that lie within a shorter distance upwind (up to 400 m). In Chapter 5 of this thesis the aim was to see if the factor of $Z_0$ (that is related to the more researched variable of shear stress, U*), that is supposed to be an indicator of the potential for wind erosion, can be modeled by vegetation and topography, as was indeed demonstrated. In this respect Wiggs (2001) states that "Empirical field approaches of the types described above have now encountered a problem because it has become clear that shear velocity (U*) cannot be successfully measured for wind flow over dunes and it is futile to attempt to

relate sand flux on dune surfaces to meaningless values of U*. Future field research may therefore be obliged to consider the redundancy of U* in favour of $U_z$ (wind velocity)…". Seen under this light, our ability to explain 40% of the variability in all erosion pins measurements by $Z_0$ are all the more promising – that although it is problematic to measure U* (or $Z_0$ in our case) in the field, we were able to relate it to sand flux.
Other sources of errors that might have lowered the success in explaining sand movement include the following:

- Areas with a very low vegetation cover may not be adequately monitored using satellite images in arid and semi-arid areas (Tueller, 1987).
- The digital elevation model used, although being quite detailed for a coastal dune area, was not detailed enough to show small nebkha dunes These do not appear also on the satellite images. We expect that this fact affected our ability to adequately estimate erosion and deposition of sand in the fore dunes and on the dune top and to model net (instead of absolute) changes in the sand surface for the whole dune.

## 4.2 The temporal influence of wind and rainfall on sand movement

It is well known that when sand dunes are wetted by rainfall, the high moisture content of the sand inhibits sand movement to some degree ( Wiggs et al., 2004). It was therefore expected that as sand movement in Israel occurs mainly during the winter months, the amount and the regime of rainfall may have a secondary impact on the sand movement, in addition to the wind (as found by Arens et al., 2004). However, no such effect of rainfall was found regarding sand mobility in the examined dunes in Israel.
Along the Israeli coastline the strongest winds and most sand transport occur during the winter months (as found by us and by Goldsmith et al., 1990). Although the strongest winds and almost all the rainfall are experienced in the same months, strong winds and rainfall do not coincide (see Fig 5) in the mid-latitude cyclones passing over Israel (see also Alpert and Ziv, 1989; Lutgens and Tarbuck, 2001; Schultz and Trapp, 2003; Szeto and Stewart, 1997; Yumao et al., 1997). It is explained by the fact that even when the sand is wet, the wind is drying the upper layer of sand grains, enabling them to move, and exposing the moist layer of sand underneath them (Jackson and Nordstrom, 1997, 1998;

Cornelis et al., 2004), and thus sand erosion/deposition and rainfall were only poorly correlated.

## 4.3 Vegetation and topography effect on sand dune movement

Distance from the coastline explained only 18% of the variability in sand erosion/deposition – in contrast with the common concept that wind velocity decreases gradually inland and therefore dune movement is lower (Illenberger and Rust, 1988). As the dominant wind direction controlling sand and dune movement across the Israeli coastline is from the south-west (Goldsmith et al., 1990), the effect of vegetation and topography was calculated for each one of the erosion pins at various upwind distances towards the south west. As expected, a negative relationship was found between either NDVI or SAVI values (that are related to vegetation cover) and the yearly absolute sand movement. In addition, a positive relationship was found between the relative height and the absolute sand movement. Best correlation coefficients with sand movement were obtained for the two units at the lee slope of the dunes (SF and MF), for almost all the variables analyzed, temporal and spatial (RDP, distance from the coastline, vegetation and topography; see Tables 3, 4 and 5). This is explained by the fact that in barchan, transverse and parabolic dunes the area of the lee slope of a dune is much smaller than that of the windward side; the sand eroded by the wind from the windward side is later deposited in the lee side of the dune (this pattern is only partly applicable to parabolic dunes, as over them nebkha dunes develop of the dune top, capturing sand; see Tsoar and Blumberg, 2002). Thus, the overall net accumulation of sand per erosion pin (or per unit area) is highest there (see Table 2).

The variables of both vegetation and topography were able to explain most of the variability when the upwind length considered was up to 100-200 m. By using directional filters we were thus able to incorporate the large scale effect of air flow over topography and vegetation, and by comparing correlation values obtained from various upwind distances, we accordingly identified the optimal predicting distance. The consideration of the upwind characteristics of vegetation and topography on sand erosion and deposition has therefore proven to be of value, as hypothesized by Hupy (2004). Combining three variables in a multiple regression model (see Equation 6) resulted with a $R^2$ value of 68%, for the annual absolute changes of the sand level. From the map of predicted values

of surface stability (Figure 8) it is clear that most of the active dune areas are disconnected now from each other, being separated by areas with high vegetation cover, which inhibit most of the transport of sand grains. There are also are very few places where beach sand is still able to feed the dunes beyond the foredune. Such a map may be useful in currently proposed efforts for reactivating this coastal dune field

Net annual changes, especially near the dune crest are very irregular and may mask the actual fluctuation that occurs (Ranwell, 1958). This is because on dune tops, especially those of stabilizing dunes (that are in the transformation from transverse to parabolic), but also anywhere where nebkha dunes exist, there may be areas of both sand accumulation and of sand erosion, depending on the exact location of the erosion pin with respect to the nebkas and the wind direction. On the whole, the height of the dune tops over the Ashdod-Nizzanim dunes is increasing, most probably due to sand capture by plants (Table 2). For this reason the analysis was focused on absolute changes in the sand level (as in other studies, e.g. Yeaton, 1988, and Arens, 2004).

## 5. Summary and conclusions

- Monthly changes in sand mobility along the coastal dunes of Israel were shown to be mainly affected by winds during winter storms. As most of the winds occur prior to the onset of rainfall and they hardly coincide, rainfall (i.e. moisture content) was not found to significantly affect yearly sand erosion and deposition in this Mediterranean setting. The results indicate that in the active geomorphologic units at least 66% of the temporal variance in the annual absolute changes in sand level can be explained by the RDP-t (81% for the slip face unit).
- To understand the spatial variation in sand mobility over a dune field, consideration of the distance from the coastline may give only a partial understanding of the system. It is the upwind vegetation and topography variables that directly affect surface roughness and wind speed that should be treated rather than the mere distance from the coastline which is commonly used.
- Vegetation and topographic variables enabled us to explain more than 65% of the variability found in the spatial and temporal patterns of sand

mobility as measured by the erosion pins ($p < 0.001$, $n = 230$). This model can be applied into spatial and temporal models (such as markov chains or other spatial models and simulations) of sand mobility, or to direct management practices on coastal dunes activity in Israel.

- Considering the question of field monitoring of sand dunes, it is suggested that the sampling of dunes' slip faces may represent sand mobility over the whole dune. Such a sampling approach is economic as the slip face unit is usually smaller, easier to define and more homogeneous than the other units of a dune. In addition this unit is easily recognized on aerial photographs.
- As a dune field stabilizes, the sand dunes become disconnected from each other. Sand grains from the beach are not able to pass easily over the foredune and feed the inner dune areas, while sand grains from one dune are not able to easily cross areas with vegetation separating it from the next dune. Thus when the current dunes transform from transverse to parabolic, their interaction becomes very limited. Efforts to reactivate stabilizing dunes should take this factor in consideration. Reconnection of dunes by removing vegetation from corridors between dunes, along the direction of the sand moving winds, may serve as a useful mean to reactivate stabilized dunes.

## Acknowledgments

We wish to express our thanks to Rachel Lugassi from the Remote Sensing and GIS Lab at the Department of Geography in Tel Aviv University for performing the atmospheric and geometric corrections of the Landsat images. We would also like to thank Ravid Pik and Yoav Eshel from the Israeli Green Patrol (Ha Sayeret ha Yeruka) for the use of the differential GPS, and Uri Goldstein from the Ashkelon Metropolitan Union for the Environment for his help in obtaining the meteorological data. We appreciate the remarks made by the anonymous referees, and thank for their contribution to the improvement of this manuscript.

## References

**Al-Dabi, H., Koch, M., Al-Sarawi, M. and El-Baz,** F. (1997) Evolution of sand dune patterns in space and time in north-western Kuwait using Landsat images. *Journal of Arid Environments*, **36**, 15-24.

**Alpert, P. and Ziv, B.** (1989) The Sharav cyclone: observations and some theoretical considerations. *Journal of Geophysical Research*, **94 (D15)**, 18,495-18,514.

**Analytical Imaging and Geophysics LLC (AIG)** (2001) ACORN User's Guide. Stand Alone Version, Analytical Imaging and Geophysics LLC, 64 p.

**Anthonsen, K.L., Clemmensen, L.B. and Jensen, J.H.** (1996) Evolution of a dune from crescentic to parabolic form in response to short-term climatic changes: Rabjerg Mile, Skagen Olde, Denmark. *Geomorphology*, **17**, 63-77.

**Arens, S.M., Slings, Q. and de Vries, C.N.** (2004) Mobility of a remobilized parabolic dune in Kennemerland, The Netherlands. *Geomorphology,* **59**, 175-188.

**Bagnold, R.A**. (1941) *The Physics of Blown Sand and Desert Dunes*, Methuen, London, 265 p.

**Bauer, B.O. and Davidson-Arnott, R.G.D.** (2002) A general framework for modeling sediment supply to coastal dunes including wind angle, beach geometry, and fetch effects. *Geomorphology*, **49**, 89-108.

**Belly, P.-Y.** (1964) Sand Movement by Wind. U.S. Army Corps Eng. CERC. Tech. Mem. 1, Washington D.C., 38 pp.

**Belnap, J. and Gillette, D.A.** (1998) Vulnerability of desert biological soil crusts to wind erosion: the influences of crust development, soil texture, and disturbance. *Journal of Arid Environments*, **39**, 133-142.

**Ben-Dor E., Levin, N., Singer, A., Karnieli, A., Braun, O. and Kidron, G.J.** (2006) Quantitative Mapping of the Soil Rubification Process on Sand Dunes Using an Airborne CASI Hyperspectral Sensor. *Geoderma*, in press

**Berk, A.G.P., Anderson, L.S., Bernstein, P.K., Acharya, H., Dothe, M.W., Matthew, S.M., Adler-Golden, J.H., Chetwynd, Jr., S.C., Richtsmeier, B., Pukall, C.L. Allred, L., Jeong, S., Hoke, M.L.** (1999) MODTRAN4 Radiative Transfer Modeling for Atmospheric Correction. SPIE Proceeding, *Optical Spectroscopic*

*Techniques and Instrumentation for Atmospheric and Space Research III*, Volume **3756**

**Bitan, A. and Rubin, S.** (1991) *Climatic Atlas for Physical and Environmental Planning in Israel*, Geography Department – Tel Aviv University, Meteorological Service – Ministry of Transportation, Research and Development Section – Ministry of Energy and Infrastructure, Ramot Publishing, Tel Aviv University.

**Buckley, R.** (1987) The effect of sparse vegetation on the transport of dune sand by wind. *Nature*, **325**, 426-428.

**Cornelis, W.M., Gabriels, D. and Hartmann, R.** (2004) A parameterization for the threshold shear velocity to initiate deflation of dry and wet sediment. *Geomorphology*, **59**, 43-51.

**Danin, A.** (1991) Plant adaptations in desert dunes. *Journal of Arid Environments*, **21**, 193-212.

**Danin, A. and Nukrian, R.** (1991) Dynamics of dune vegetation in the Southern Coastal area of Israel since 1945. *Documents Phytosociologiques*, **XIII**, 281-296.

**Danin, A. and Yaalon, D.H.** (1982) Silt plus clay sedimentation and decalcification during plant succession in sands on the Mediterranean coastal plain of Israel. *Israel Journal of Earth Sciences*, **31**, 101-109.

**Danin, A., Bar-Or, Y., Dor, I. and Yisraeli, T.** (1989) The role of cyanobacteria in stabilization of sand dunes in southern Israel. *Ecologia Mediterranea*, **15**, 55-64.

**Dong, Z., Gao, S. and Fryrear, D.W.** (2001) Drag coefficients, roughness length and zero-plane displacement height as disturbed by artificial standing vegetation. *Journal of Arid Environments*, **49**, 485-505.

**Eastman, J.R.** (2001) *Idrisi 32 Release 2—Guide to GIS and Image Processing*. Vol. **2**, Clark University, U.S.A., 144pp.

**Emery, K.O. and Neev, D.** (1960) Mediterranean beaches of Israel. *Israel Geological Survey Bulletin*, **26**, 1-24.

**Fearnehough, W., Fullen, M.A., Mitchell, D.J., Trueman, I.C. and Zhang, J.** (1998) Aeolian deposition and its effect on soil and vegetation changes on stabilized desert dunes in northern China. *Geomorphology*, **23**, 171-182.

**Fishman, A.** (1994) *Photogrammetric survey of Ashdod dunes - AutoCAD layers*. gis1@spni.org.il, The GIS unit of the Society for the Protection of Nature in Israel, Tel Aviv, Israel.

**Frank, A. and Kocurek, G.** (1996) Toward a model for airflow on the lee side of aeolian dunes. *Sedimentology*, **43**, 451-458.

**Fryberger, S.G.** (1979) Dune forms and wind regime. In: *A Study of Global Sand Seas* (Ed. E.D. McKee), pp. 137-169, Geological survey professional paper **1052**, Geological Survey, Washington, D.C., United States.

**Gertner, Y.** (1989) *The Influence of Vegetation on the Rates of Erosion and Deposition of Wind Blown Sand in the Coastal Dunes of Neve Yam*. Unpublished M.A. thesis under the supervision of M. Inbar, P. Kutiel and V. Goldsmith, Department of Geography, University of Haifa (in Hebrew)

**Goldsmith, V., Rosen, P. and Gertner, Y.** (1990) Eolian transport measurements, winds, and comparison with theoretical transport in Israeli coastal dunes. In *Coastal Dunes: Form and Process* (Eds. K.F. Nordstrom, N.P. Psuty and R.W.G. Carter), pp. 79-101, John Wiley & Sons, New-York.

**Harel, R.** (1990) *The Change in Space and Time in the Balance of Wind Blown Sand in the Dunes of Atlit Bay*. Unpublished M.A. thesis under the supervision of H. Kutiel and V. Goldsmith, Department of Geography, University of Haifa (in Hebrew).

**Hesp, P.A.** (1991) Ecological processes and plant adaptations on coastal dunes. *Journal of Arid Environments*, **21**, 165-191.

**Hesp, P.A., Davidson-Arnott, R., Walker, I.J. and Ollerhead, J.** (2005) Flow dynamics over a foredune at Prince Edward Island, Canada. *Geomorphology*, **65**, 71-84.

**Hotta, S., Kubota, S., Katori, S., Horikawa, K.** (1984) Sand transport on a wet sand surface. Proc. 19th Coastal Eng. Conf. New York, American Society of Civil Engineers, pp. 1265-1281.

**Huete, A.R.** (1988) A soil-adjusted vegetation index (SAVI). *Remote Sensing of Environment*, **25**, 295-309.

**Hugenholtz, C.H. and Wolfe, S.A.** (2005) Biogeomorphic model of dunefield activation and stabilization on the northern Great Plains. Geomorphology, **70**, 53-70.

**Hupy, J.P.** (2004) Influence of vegetation cover and crust type on wind-blown sediment in a semi-arid climate. *Journal of Arid Environments*, **58**, 166-178.

**Illenberger, W.K. and Rust, I.C.** (1988) A sand budget for the Alexandria coastal dunefield, South Africa. *Sedimentology*, **35**, 513-521.

**Iversen, J.D. and Rasmussen, K.R.** (1999) The effect of wind speed and bed slope on sand transport. *Sedimentology*, **46**, 723-731.

**Jackson, N.L. and Nordstrom, K.F.** (1997) Effects of time-dependent moisture content of surface sediments on aeolian transport rates across a beach, Wildwood, New Jersey, U.S.A. *Earth Surface Processes and Landforms*, **22**, 611-621.

**Jackson, N.L. and Nordstrom, K.F.** (1998) Aeolian transport of sediment on a beach during and after rainfall, Wildwood, NJ, USA. *Geomorphology*, **22**, 151-157.

**Kadmon, R. and Leschner, H.** (1995) Ecology of linear dunes: effect of surface stability on the distribution and abundance of annual plants. *Advances in GeoEcology*, **28**, 125–143.

**Kerr, J. T. And Ostrovsky, M.** (2003) From space to species: ecological applications for remote sensing. *Trends in Ecology and Evolution*, **18**, 299-305

**Lancaster, M.** (1997) Response of eolian geomorphic systems to minor climate change: examples from the southern Californian deserts. *Geomorphology*, **19,** 333-347.

**Lancaster, N. and Baas, A.** (1998) Influence of vegetation cover on sand transport by wind: field studies at Owens Lake, California. *Earth Surface Processes and Landforms*, **23**, 69-82.

**Legendre, P.** (1993) Spatial autocorrelation: trouble or new paradigm? *Ecology*, **74 (6)**, 1659-1673

**Lettau, H.** (1969) Note on aerodynamic roughness-parameter estimation on the basis of roughness-element description. *Journal of Applied Meteorology*, **8**, 828-832.

**Lillesand, T.M. and Kiefer, R.W.** (1994), *Remote Sensing and Image Interpretation*. 3rd edition, John Wiley & Sons, Inc., New York.

**Lutgens, F.K. and Tarbuck, E.J.** (2001) *The Atmosphere, an Introduction to Meteorology*. Prentice Hall, New Jersey.

**McKenna Neuman .C., Maxwell, C. and Rutledge, C.** (2005) Spatial and temporal analysis of crust deterioration under particle impact. *Journal of Arid Environments*, **60**, 321-342.

**Moreno-Casasola, P.** (1986) Sand movement as a factor in the distribution of plant communities in a coastal dune system. *Vegetatio*, **65**, 67-76.

**Mugnier, C.J.** (2000) Grids and Datums: the State of Israel. *Photogrammetric Engineering and Remote Sensing*, **66 (8)**, 915-917.

**Munoz-Reinoso, J.C. and de Castro, F.J.** (2005) Application of a statistical water-table model reveals connections between dunes and vegetation at Donana. *Journal of Arid Environments*, **60 (4)**, 663-679.

**Musick, H.B., Trujillo, S.M. and Truman, C.R.** (1996), Wind-tunnel modeling of the influence of vegetation structure on saltation threshold. *Earth Surface Processes and Landforms*, **21**, 589-605.

**Parsons, D.R., Walker, I.J. and Wiggs, G.F.S.** (2004), Numerical modeling of flow structures over idealized transverse aeolian dunes of varying geometry. *Geomorphology*, **59**, 149-164.

**Ranwell, D.** (1958) Movement of vegetated sand-dunes at Newborough Warren, Anglesey. *Journal of Ecology*, **46 (1)**, 83-100.

**Raupach, M.R., Gillette, D.A. and Leys, J.F.** (1993) The effect of roughness elements on wind erosion threshold. *Journal of Geophysical Research*, **98 (D2)**, 3023-3029

**Sauermann, G., Andrade Jr., J.S., Maia, L.P., Costa, U.M.S., Araujo, A.D. and Herrmann, H.J.** (2003) Wind velocity and sand transport on a barchan dune. *Geomorphology*, **54**, 245-255.

**Schmidt, H. and Karnieli, A.** (2000) Remote sensing of the seasonal variability of vegetation in a semi-arid environment. *Journal of Arid Environments*, **45**, 43-59.

**Schultz, D.M. and Trapp, R.J.** (2003) Nonclassical cold-frontal structure caused by dry subcold air in Northern Utah during the Intermountain Precipitation Experiment (IPEX). *Monthly Weather Review*, **131**, 2,222-2,246.

**Sherman, D.J., Jackson, D.W.T., Namikas, S.L. and Wang, J.** (1998) Wind-blown sand on beaches: an evaluation of models. *Geomorphology*, **22**, 113-133.

**Sokal, R.R. and Rohlf, F.J.** (1995) *Biometry – the principles and practice of statistics in biological research*, W.H. Freeman and Company, New York.

**Szeto, K.K. and Stewart, R.E.** (1997) Cloud model simulations of surface weather elements associated with warm frontal regions of winter storms. *Atmospheric Research*, **44**, 243-269.

**Tsoar, H.** (1983) Dynamic processes acting on a longitudinal (seif) sand dune, *Sedimentology*, **30**, 567-578.

**Tsoar, H.** (1990), Trends in the development of sand dunes along the southeastern Mediterranean coast. In: *Dunes of the European Coasts* (Eds. Th.W. Bakker, P.D. Jungerius and J.A. Klijn), Catena supplement **18**, pp. 51-60, Catena-Verlag, Cremlingen-Destedt, Germany.

**Tsoar, H.** (2002) Climatic factors affecting mobility and stability of sand dunes. In: *Proceedings of ICAR5/GCTE-SEN Joint Conference*, International Center for Arid and Semiarid Land Studies, Texas, Publication **02-2**, 423-426

**Tsoar, H. and Blumberg, D.G.** (2002) Formation of parabolic dunes from barchan and transverse dunes along Israel's Mediterranean coast. *Earth Surface Processes and Landforms*, **27**, 1147-1161.

**Tsoar, H. and Møller, J.T.** (1986) The role of vegetation in the formation of linear sand dunes. *Eolian Geomorphology Proceedings from the 17th annual Binghamton Geomorph. Symp.*, 75-95.

**Tsoar, H. and Werner, I.** (1998) Reevaluation of sand dunes' mobility indices. *Journal of Arid Land Studies*, **7S**, 265-268.

**Tsoar, H. and Zohar, Y.** (1985) Desert dune sand and its potential for modern agricultural development. In: *Desert Development* (Ed. Y. Gradus), pp. 184-200, D. Reidel Pub. Co.

**Tucker, C.J.** (1979) Red and photographic infrared linear combinations for monitoring vegetation. *Remote Sensing of Environment*, **8**, 127-150.

**Tueller, P.T.** (1987) Remote sensing science applications in arid environments. *Remote Sensing of Environment*, **23**, 143-154.

**Turnhout, E., Hisschemöller, M. and Eusackers, H.** (2004) The role of views of nature in Dutch nature conservation: the case of the creation of a drift sand area in the Hoge Veluwe National Park. *Environmental Values*, **13**, 187-198.

**Walsh, S.J., Butler, D.R. and Malanson, G.P.** (1998) An overview of scale, pattern, process relationships in geomorphology: a remote sensing and GIS perspective. *Geomorphology*, **21**, 183-205.

**Wasson, R.J. and Nanninga, P.M.** (1986) Estimating wind transport pf sand on vegetated surfaces. *Earth Surface Processes and Landforms*, **11**, 505-514.

**White, B.R. and Tsoar, H.** (1998) Slope effect on saltation over a climbing sand dune. *Geomorphology*, **22**, 159-180.

**Wiggs, G.F.S.** (2001) Desert dune processes and dynamics. *Progress in Physical Geography*, **25 (1)**, 53-79.

**Wiggs, G.F.S., Thomas, D.S.G. and Bullard, J.E.** (1995) Dune mobility and vegetation cover in the southwest Kalahari Desert. *Earth Surface Processes and Landforms*, **20**, 515-529.

**Wiggs, G.F.S., Baird, A.J. and Atherton, R.J.** (2004) The dynamic effects of moisture on the entrainment and transport of sand by wind. *Geomorphology*, **59**, 13-30.

**Yeaton, R.I.** (1988) Structure and function of the Namib dune grasslands: characteristics of the environmental gradients and species distributions. *Journal of Ecology*, **76**, 744-758.

**Yumao, X., Yinong, P. and Aidong, S.** (1997) Spectral characteristics and multi-scale structure of the boundary-layer wind field during cold front passages over East China. *Boundary-Layer Meteorology*, **85**, 423-446.

**Zhu, H., Eastman, J.R. and Toledano, J.** (2001) Triangulated irregular network optimization from contour data using bridge and tunnel edge removal. *International Journal of Geographical Information Science*, **15 (3)**, 271–286.

*In the seventh article* it was shown that even when no measurements of sand erosion and deposition are conducted, the composition and cover of the perennial plants at a certain location may indicate whether it is stable or active, and whether it is undergoing erosion or deposition. To this end nine perennial plant species that are abundant across these coastal dunes, were analyzed using a specially devised visual exploratory data analysis method (the gradient visualization) in combination with established statistical methods.

# A field quantification of coastal dune perennial plants as indicators of surface stability, erosion or deposition

**Levin Noam, Giora J. Kidron and Eyal Ben-Dor**
The Department of Geography and Human Environment, Tel-Aviv University, Israel

## Abstract

Dune plants both modify the wind field around them and are impacted by various stress factors, among them sand erosion and sand deposition. As coastal dunes are being either stabilized or remobilized, in addition to the changes in the rates of sand and dune movement, the vegetation cover and composition are expected to differ, reflecting the changes in the environmental conditions. In this field study we have analyzed 315 quadrats of 10*10 m for which the perennial plant species were sampled, with respect to annual rates of sand erosion and deposition that were measured using erosion pins. We developed a visual exploratory data analysis which we termed as gradient visualization, that combined with traditional statistical tools, enabled us to uncover the inclination and indicative power of nine perennial dune plants to either a stabilized or a mobile environment, and whether they are more present in places undergoing sand erosion or sand burial. Two species were found to be clear indicators of a stabilized environment, *Stipagrostis lanata*, and *Retama raetam*. Of the species indicating a mobile environment, only one may be stated as a clear indicator of sand erosion: *Silene succulenta*, with *Cyperus macrorrhizus* coming close to indicate a less mobile erosive environment. The best indicator species for sand burial was found to be as expected *Ammophila arenaria*, with *Artemisia monosperma* also indicating high rates of sand mobility especially when its relative cover is higher than 80%. The rest of the species analyzed (*Polygonum palestinum*, *Scrophularia hypericifolia*, and *Sporobolus pungens*) may also serve as indicators of lower rates of sand mobility and sand burial, as a function of their relative cover and of the relative cover by *Artemisia monosperma,* but their indicative power is weaker, as evident from their low significance values in a regression model. Such information is necessary to monitor processes of dune stabilization or reactivation, whether occurring naturally, or to assess the success of a management plan that aims at stabilizing a dune, or remobilizing it by removing vegetation.

## Keywords

Coastal dunes, sand erosion, sand deposition, vegetation, plant indicators

## 1. Introduction

Coastal sand dunes are an unstable habitat in which plants suffer several stresses imposing unique adaptations. Among the severe a-biotic stresses are the burial and exposure by sand moved by the wind, salt spray, dryness and nutrient deficiency (Danin, 1991; Hesp, 1991; Danin, 1996a;). Working on coastal foredunes Van der Valk (1974) has found that sand erosion and deposition is the main factor controlling the distribution of plant species, with salt spray playing only a secondary role, whereas soil moisture, soil nutrients and soil temperatures appear to have little influence. The level of these stresses is highest in the beach-fore dune environment and generally decreases with distance from the coast in fully vegetated coastal dune systems (Hesp, 1991). However, in a stabilizing dune field and even within a single dune many microenvironments and local habitats may be found (e.g. active mobile dunes, stabilized dune slacks, deflation basins, etc), according to the rate of environmental stress there, and the stage of the plant succession.

One of the most used indicators for the stabilization rate of sand dunes is that of vegetation cover (e.g. in Chapter 4 in this thesis). However, perennial plant cover, easily quantified using remote sensing methods, does not inform us on the succession stage of the vegetation, or on the species composition. In fact, vegetation cover may be similar among different local habitats where different magnitudes of the same stress are exerted on the vegetation (Jauffret and Visser, 2003). Identifying plant species that may serve as indicators of geomorphologic processes may be a useful tool for assessing current dune activity, or for evaluating the progress of any restoration and rehabilitation project.

Much information has been gathered on stress factors and their corresponding plant adaptations in desert and coastal dune plants. Adaptations to sand burial include the development of adventitious roots and of new shoots from the plants rhizome system (Danin, 1991). Yeaton (1988) noted that plants reproducing from seed in areas of rapidly moving sand can only do so when rainfall events are frequent. Adaptation to

sand exposure includes the enabling of transportation activity through the roots even when they are exposed (Danin, 1991).

Dune grasses are the most studied dune plants with respect to sand burial (Kent et al., 2001), and especially *Ammophila arenaria*, a pioneer plant adapted to sand burial, common on fore dunes, dune tops that begin to stabilize, and a plant used to stabilize dunes around the world, also outside its native range (Tsuriell, 1959; Wiedemann and Pickart, 1996). Other plants common to coastal dunes that their adaptations and role in stabilization were studied include *Artemisia monosperma* (Huang and Gutterman, 1998; Li et al., 2002), and the *Stipagrostis* species (Danin, 1996b).

Many studies concerning the adaptations of plants to dunes have focused on one or more species using a certain experimental design altering the stress factor studied (e.g. Sykes and Wilson, 1990). Few studies have quantitatively compared the influence of stress factors comparing various dune plant species in their natural environment. Thus the distribution and abundance of annual plants on linear desert dunes with respect to surface stability was studied by Kadmon and Leschner (1995), whereas their responses to the shrub-opening gradient were analyzed by Tielbörger and Kadmon (1997) as well as by El-Bana et al. (2002). Moreno-Casasola (1986) has studied the presence of coastal dune plants with respect to sand movement, whereas Willis et al. (1959) have created histograms presenting the distribution of the chief species in relation to water level, and Ranwell (1958) has mentioned annual accretion limits for *Ammophila* and *Salix repens*. Over the Namib dunes Yeaton (1988) concluded that the amount of rainfall is the ultimate factor controlling their stabilization as well as the dynamics of four species of perennial grasses. As for the major perennial plant species common to the coastal dunes of Israel, most of the knowledge regarding their adaptations to burial by sand or to the exposure of their roots is qualitative and descriptive (Danin, 1996a; Waisel et al., 1975; Kutiel et al., 1979/80, Danin and Nukrian, 1991), and a quantitative study was therefore called for.

Following the call of Kent et al. (2001) for further research into plant response to burial in desert environments, and given the paucity of studies related to plant adaptations to erosion, our objective were therefore: To quantitatively characterize indicator coastal dune perennial plant species corresponding to stable environments or to mobile environments of sand burial (deposition) or sand exposure (erosion), as measured in the field.

## 2. Methods

### 2.1 Study area

The area selected for this study consists of coastal sand dunes 40 km south of Tel-Aviv, Israel, between the cities of Ashdod and Ashkelon (Figure 1). The climate is Mediterranean, with an annual average rainfall of 450-500mm, all in wintertime, with maximum rainfall in December (Bitan and Rubin, 1991). The average daily maximum and minimum temperatures in summer are 29˚C and 21˚C, respectively. Proximity to the sea boosts the average relative humidity year round and may reach 70% and higher during the summer.

The origin of the sand along the Israeli coast is mainly from the Nile delta via the longshore currents near the coast and the anti-clockwise Mediterranean current in the deep water (Emery and Neev, 1960). Aeolian sand transport from the beach inland occurs under the influence of high winds from the southwest to the northeast, mainly in wintertime (Goldsmith et al., 1990). The southern half of the study area (here referred to as the Nizzanim Dunes) is part of Nizzanim Nature Reserve, while the northern section (here referred to as the Ashdod Dunes) is protected under Israel's National Master Plan No. 22 for forestry.

The vegetation associations typical of the southern coastal dunes of Israel that match our study area were defined by Danin and Nukrian (1991) near Netiv HaAsara, 10 km south of Ashkelon (see Table 1). They note that with increasing sand stability the germination and establishment of more species is enabled and the monospecific community of *Ammophilia arenaria* thickens and changes into associations where *Artemisia monosperma* is the dominant plant. Photos of three of the perennial plants that will be discussed below are given in Figure 2. Information about the content of fine particles and regarding the presence of biogenic crust in these associations is detailed in Danin and Nukrian (1991) and partly in Table 1 here.

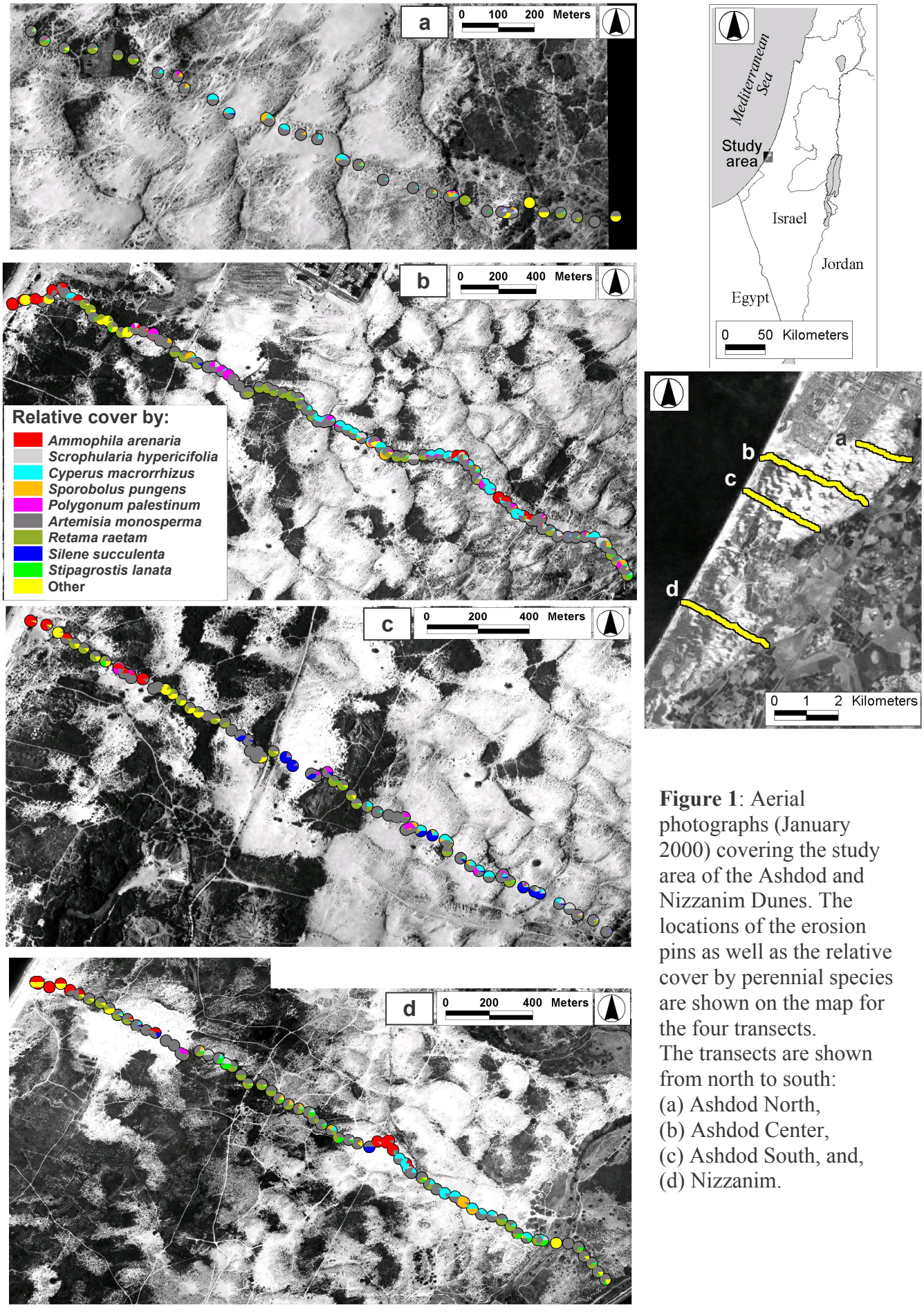


**Figure 1**: Aerial photographs (January 2000) covering the study area of the Ashdod and Nizzanim Dunes. The locations of the erosion pins as well as the relative cover by perennial species are shown on the map for the four transects.
The transects are shown from north to south:
(a) Ashdod North,
(b) Ashdod Center,
(c) Ashdod South, and,
(d) Nizzanim.

**Table 1**: Vegetation associations of the southern coastal dunes of Israel, as defined by Danin and Nukrian (1991), Nukrian (1988)

| Association | Habitat | Silt + clay content at soil surface | Absolute cover of perennial species |
|---|---|---|---|
| *Asthenatherum forsskalii – Polycarpon succulentum* | Windward slope of the dune | 0-3% | 3.8% |
| *Ammophilia arenaria – Senecio joppensis* | Summit of dunes, top of leeward slopes and blowouts | 0.5-4% | 44.3% |
| *Ononis natrix – Artemisia monosperma* | Stable and small sand dunes | 2-5% | 51.9% |
| *Artemisia monosperma – Retama raetam* | Fossil soils in interdune valleys | 6-15% | 130.5% |
| *Artemisia monosperma – Launaea tenuiloba* | Fossil soil covered with 50-100 cm sand | 1.5-5% | 110.0% |
| *Asthenatherum forsskalii – Lotus halophilus* | Slightly mobile sand, up to 100 cm deep, in the interdune valleys | 3-4% | 55.7% |




**Figure 2**: Photographs of selected plant species: (a) *Silene succulenta* exposed by erosion (January 28th, 2004); (b) *Cyperus macrorrhizus* nebkhas in an area undergoing erosion (January 12th, 2003); (c) *Ammophila arenaria* being partly buried on a dune top (January 27th, 2001).

## 2.2 Field measurements of sand erosion/deposition

To study the spatial and temporal variability in the current rates of erosion and deposition of sand, we chose four transects, lying perpendicularly to the coastline (see fig .1). Three of the four transects begin at the fore dune, and all the transects end at the dunes' easternmost edge. Along these transects, we placed 315 erosion pins at intervals of about 50 meters in December 2002 (further details given in Chapter 6 in this thesis). As we expected maximum changes of sand deposition to occur in the dunes' slip faces, we have placed three erosion pins at each slip face to represent them more accurately. Most of the erosion pins were 50 cm long, except those located at the dunes slip faces (where sand movement was expected to be higher), that were 100 cm long. They were buried to a depth of 50% of their length, and replaced when after sand movement the level at the pin has changed to either 33% or 166% of their original length. We measured the sand erosion and deposition at an accuracy of 1 mm subsequently every 2-6 weeks since December 2002 until October 2004, thus covering two winter seasons. We determined the exact location and height above sea level of the erosion pins using a differential GPS. A detailed description and analysis of the yearly rates of sand erosion and deposition with respect to climatic and spatial variables, is given in Chapter 6 in this thesis. 225 of the 315 erosion pins were placed in active geomorphologic units (see Chapter 6 in this thesis details): the fore dune, the wind facing slope of the dunes, the dune tops, the slip face, and at some dunes a moderate lee slope behind the dune top..

## 2.3 Vegetation cover measurements

Vegetation cover was estimated in the field for each one of the erosion pins. Total perennial vegetation cover and the relative cover of each perennial species were estimated visually for a quadrat area of 10*10 meters, on March 29-30$^{th}$ 2003 (spring time). Annual vegetation cover over a radius of 13 centimeters around each erosion pin was quantitatively estimated twice during spring time, on March 29-30$^{th}$ 2003 and on March 20-21$^{st}$ 2004. In the analyses presented here we averaged these two estimates. All data were expressed as a percent ($p$) of cover. We transformed the

proportional data with arcsin($\sqrt{p}$) to stabilize variances (Sokal and Rohlf, 1981). The botanic nomenclature follows Feinbrun-Dothan and Danin (1998) and Danin (2000).

**2.4 Gradient visualization of indicator plants**

In contrast with controlled experiments, that isolate each plant species and subject it to different stresses (e.g. Sykes and Wilson, 1990), when working in the field, the situation is more complicated (Kent et al., 2001): (1) multiple habitat factors are influencing plants at the same time; (2) the magnitude of stress factors is not controlled by us; (3) plants of different species are found together and have various interactions, such as competition, facilitation, or other indirect relationships; and (4) the presence of a species may also reflect past conditions that no longer exist.

In our case study over a stabilizing dune field, the stress factor we measured in the field and analyzed was the erosion or deposition of sand.

To partly overcome the above mentioned problems and in an attempt to isolate plant species to some extent, at least in the analysis, we suggest the following graphic exploratory data analysis and visualization approach: for each plant species, we have calculated the average annual absolute and net rates of erosion and deposition, on several gradients, ranging from 0% to 100%, at intervals of 5%: (1) The minimum relative % cover of each species in a vegetation sample; (2) The maximum relative % cover by *Artemisia monosperma* in a vegetation sample; (3) The minimum % vegetation cover in a vegetation sample.

We devised the first and the second gradients to identify indicator plant species based on their relative cover with respect to measured value of sand erosion and deposition. In the first gradient, we aimed to see the average net rates of erosion/deposition for each species with respect to its relative cover in a vegetation sample, expecting to identify indicator species as the relative cover of each species gets higher. In the second gradient we aimed to reduce the influence of the most common plant species, *Artemisia monosperma*, on our results, expecting to identify indicator species as the relative cover of *Artemisia monosperma* gets lower. With the third gradient, we aimed to study the influence of perennial vegetation cover (estimated in the field) on the rates of sand movement for the plants species analyzed.

### 2.5 Statistical analyses

To assess the reliability of the results from the gradient visualization we have applied established statistical graphic tools (box plots) as well statistical analyses, such as stepwise regression and cluster analysis, using the statistical software JMP IN 5.1 (SAS, 2003).

To quantitatively assess the indicative power of the nine perennial species analyzed with respect to the annual absolute change in sand level, we have conducted a multiple regression analysis, applying three models:

1. Linear model, using the nine species as the independent variables.
2. Log-normal model, using the nine species as the independent variables.
3. Log-normal model, using the nine species as well as the perennial vegetation cover as the independent variables.

These models were applied twice: (1) Including all the independent variables, and (2) Using a forward stepwise regression.

As for the cluster analysis, we applied a hierarchical cluster analysis using the Ward method (Milligan, 1980) for standardized data, with the following variables: absolute and net rates of sand erosion/deposition (after a log transformation), perennial and annual cover, as well as the relative cover of all nine perennial species (all the variables relating to % cover were included only after an arcsin√%p transformation).

## 3. Results

### 3.1 General

As demonstrated in Chapter 6 in this thesis and in Figure 3a vegetation cover (perennial or annual) is negatively correlated with sand movement. However, at the same vegetation cover, different aeolian processes may occur: erosion, deposition or surface stability (fig 3b). We focused here on perennial plants, not only because they can be identified throughout the year, but also because they can withstand higher rates of either sand erosion or sand deposition, when compared with annual plants (fig 3).

To better understand the relationships between vegetation and sand movement, we have chosen to focus on the nine most common perennial plant species that we found in the field survey. The relative cover of the nine most common perennial species is presented in Figure 1 using pie charts on the background of aerial photographs, and in Figure 4 using bar charts laid upon the topographic profiles of the transects.

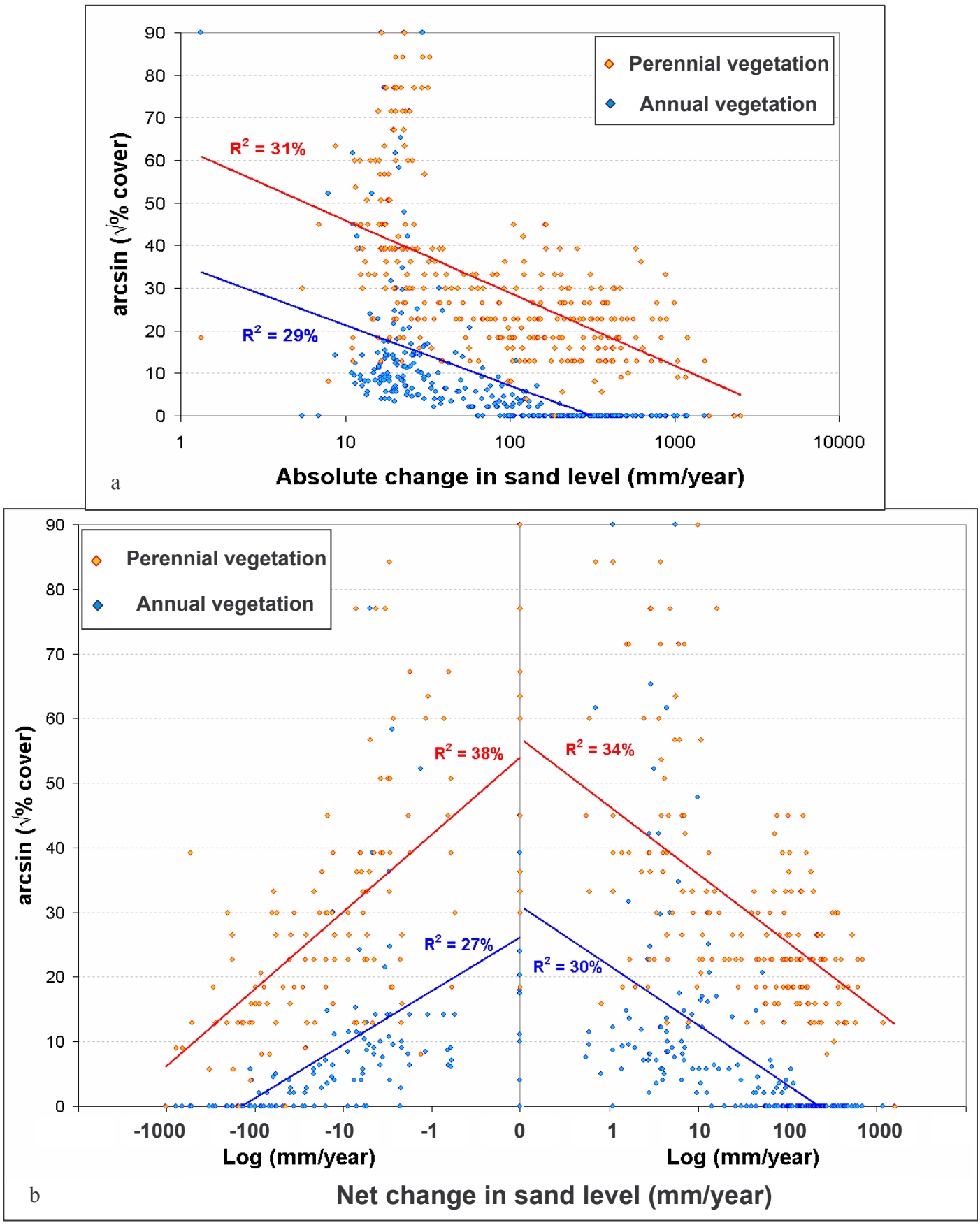


**Figure 3**: The relationship between vegetation cover (perennial and annual) and yearly rates of erosion/deposition: (a) absolute changes, (b) net changes.

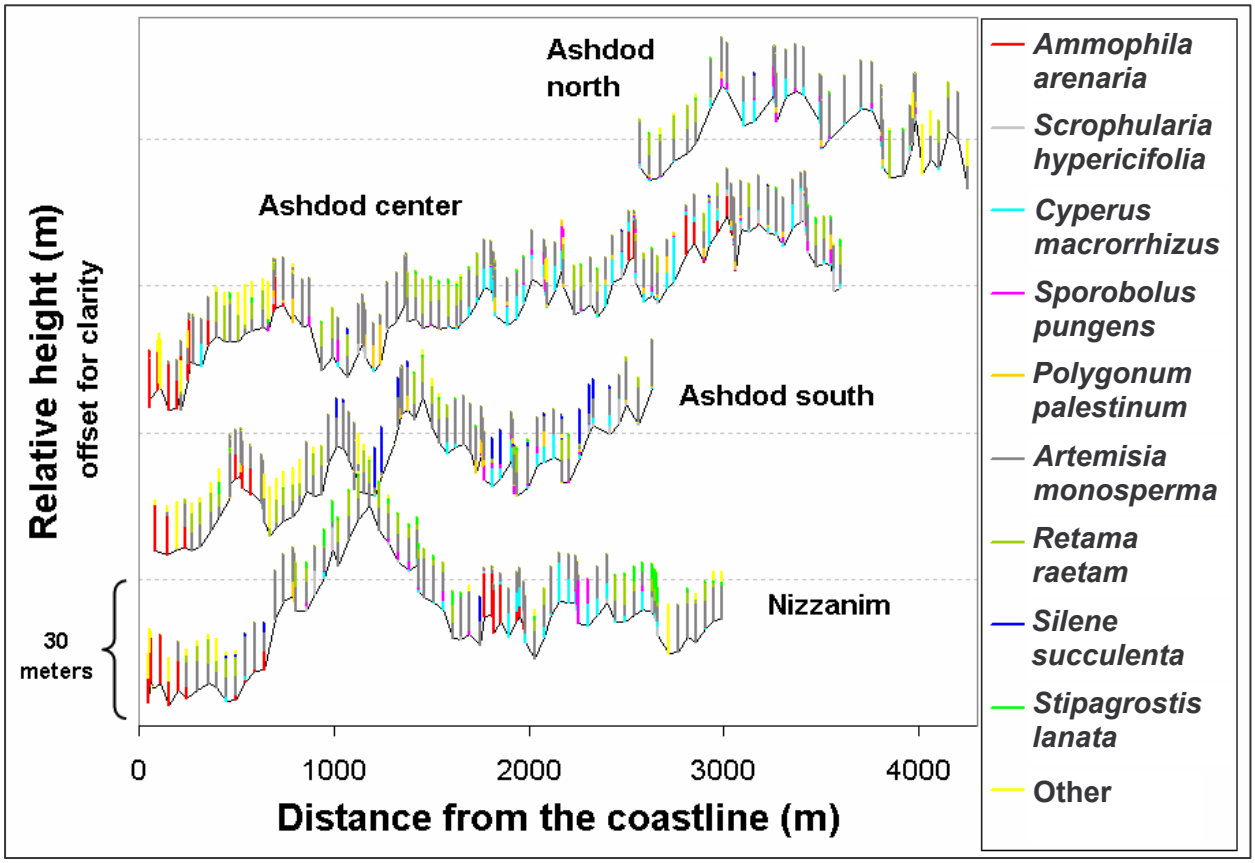


**Figure 4**: The relative cover of the perennial plant species sampled in quadrats of 10*10 m around the erosion pins. The height of each bar represents 100%, and the coloring of each bar represents the % of relative cover by each of the plant species. The bars are laid upon the topographic profiles of the four transects.

The presence of these species in active geomorphologic units as a function of the distance from the coastline is presented in Figure 5. It can be clearly seen that *Artemisia monosperma* was present in more than 90% of the quadrats (except near the coastline). The only species whose presence decreased with the distance from the coastline was *Ammophila arenaria*, whereas for *Scrophularia hypericifolia*, *Cyperus macrorrhizus*, *Sporobolus pungens* and *Polygonum palestinum* their presence increases with the distance from the coastline:

In Figure 6 we show histograms presenting the presence of perennial species as a function of the net yearly change in sand level, for all the sand samples. In this figure (as well as in Figures 8 and 11 that follow below) in addition to the box plots presenting the net yearly change in sand level per species, we assigned warm-dark colors (yellow-orange-red-black) to bars representing sand accumulation, whereas cold colors (green-blue) were assigned to bars representing sand erosion.

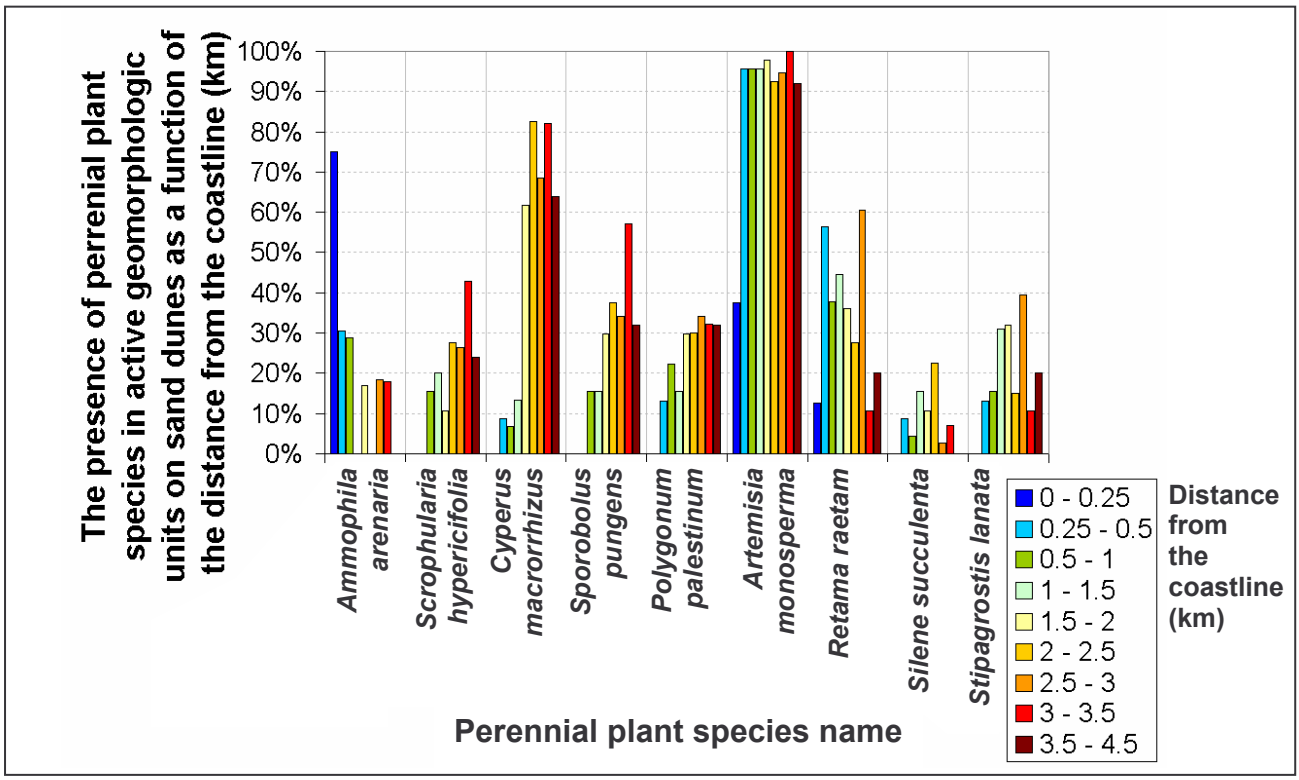


**Figure 5**: The presence of perennial plant species in active geomorphologic units on sand dunes as a function of the distance from the coastline (km).

Notice the clear inclination of *Ammophila arenaria* towards places with sand accumulation and that two species (*Retama raetam* and *Stipagrostis lanata*) are mostly present in stabilized places where the annual rates of sand erosion or of sand accumulation are low (usually less than ±8 mm).

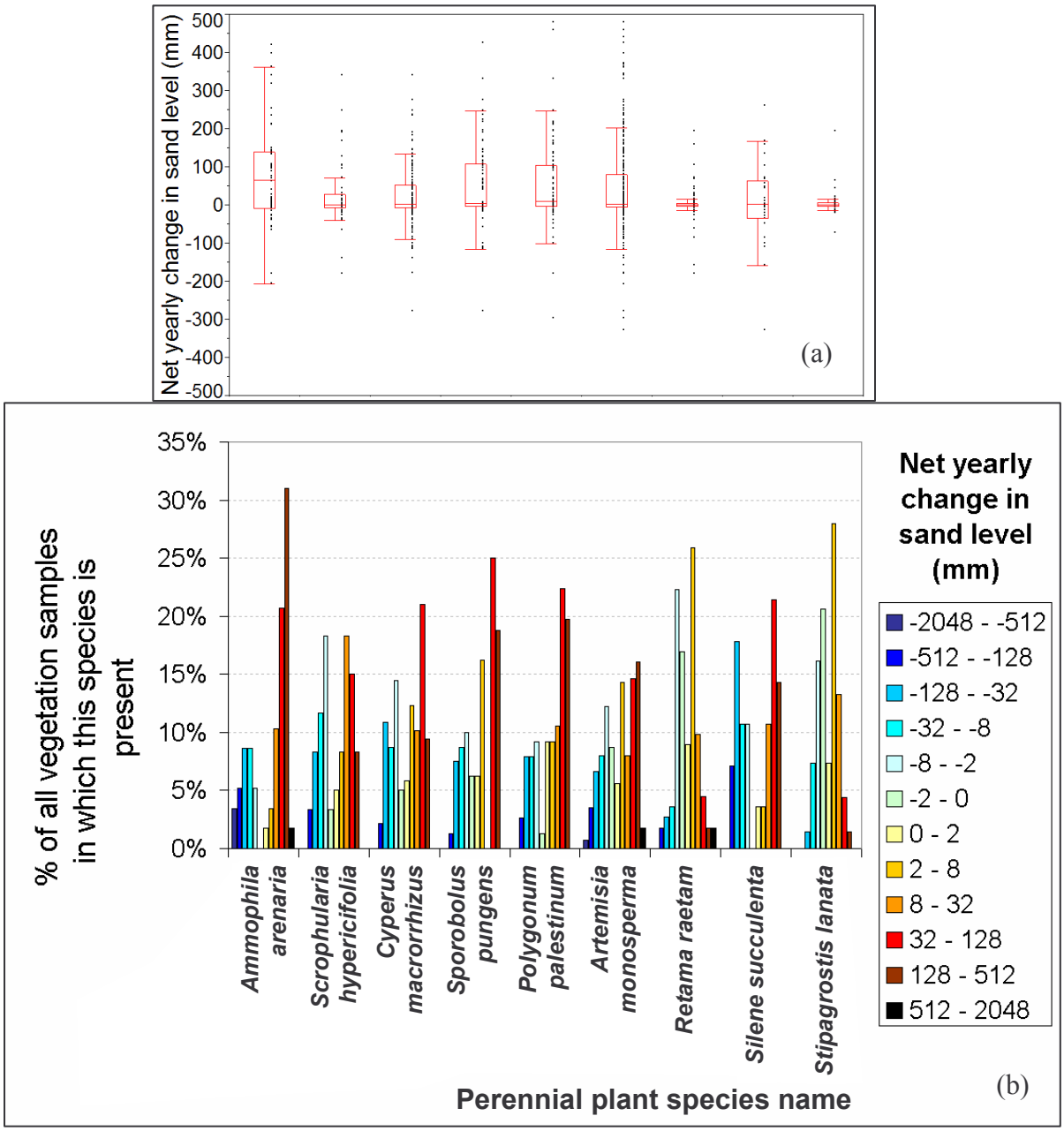


**Figure 6**: Including all vegetation samples in this figure: (a) Box plots presenting the net yearly change in sand level, (b) Histograms presenting the presence of perennial species as a function of the net yearly change in sand level (focusing on the range of ±500 mm); We assigned warm-dark colors (yellow-orange-red-black) to bars representing sand accumulation, whereas cold colors (green-blue) were assigned to bars representing sand erosion.

### 3.2 The first gradient: the minimum relative % cover of each species in a vegetation sample

Analyzing the first gradient, that of the minimum relative % cover of each species in a vegetation sample, recall that we expect to see identify indicator species when their respective relative cover is higher. Before entering the analysis itself, and to make the reader familiar with the method used here for visualizing the data (applied in Figures 7, 9, 10, 12 and 13) an example is given, referring to Figure 7. The x-axis on these figures acts as a filter, determining the condition whether a vegetation quadrat will be included in the analysis or not. Turning our attention for example to *Cyperus macrorrhizus* (shown in cyan), when all vegetation quadrats in which it is present are included (i.e., 5% on the x-axis), the average net change in those quadrats was 25mm/year. As one moves along the x-axis to the right, less qudrats are included in the analysis. For *Cyperus macrorrhizus* the net change turns to negative (meaning erosion) only when reaching qudrats where it was more than 80% of the vegetation cover. Indeed, it is common to see that areas undergoing erosion are dominated by small nebkhas of *Cyperus macrorrhizus* (Figure 2b).

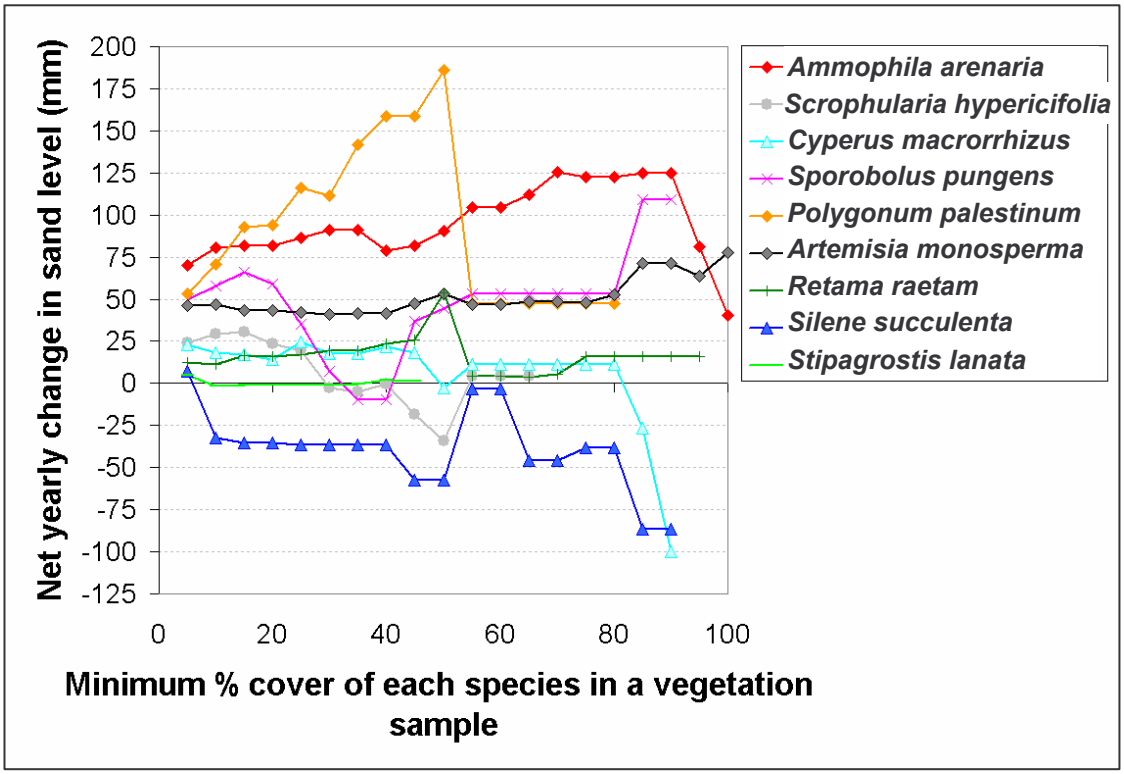


**Figure 7**: The average net yearly change in sand level as a function of the relative cover of plant species in vegetation samples.

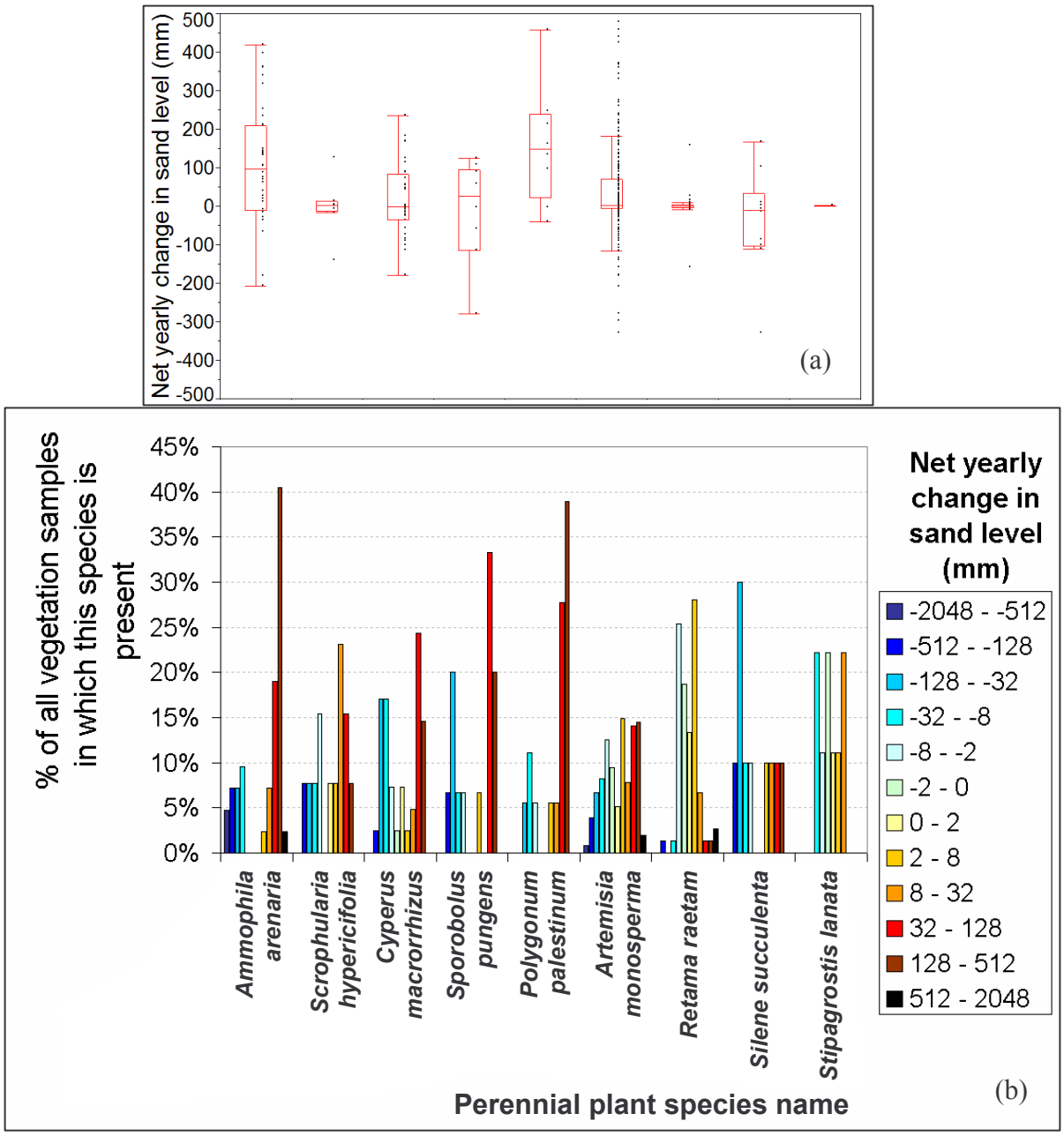


**Figure 8**: Including for each species only those vegetation samples in which its relative cover is higher than 30%: (a) Box plots presenting the net yearly change in sand level, (b) Histograms presenting the presence of perennial species as a function of the net yearly change in sand level (focusing on the range of ±500 mm); We assigned warm-dark colors (yellow-orange-red-black) to bars representing sand accumulation, whereas cold colors (green-blue) were assigned to bars representing sand erosion.

Following this explanation, several patterns can be seen from Figure 7:
In Figure 7 we show the average net yearly change in sand level as a function of the relative cover of plant species in vegetation samples. Based on Figure 7, the following plants may be said to be indicators of sand accumulation, in a decreasing order: *Ammophila arenaria*, *Polygonum palestinum*, *Sporobolus pungens*, and *Artemisia monosperma*. As indicators for sand erosion, the following species may be stated in a decreasing order: *Silene succulenta*, *Cyperus macrorrhizus* (the latter may indicate erosion processes only in places where it comprises more than 80% of the plant species). Three species may serve as indicators of stabilized dunes, in decreasing order: *Stipagrostis lanata*, *Retama raetam* and to a certain degree, also *Scrophularia hypericifolia*.
In Figure 8, which is built in the same principle as Figure 6, we show box-plots and histograms presenting the presence of perennial species as a function of the net yearly change in sand level; this time however, for each species only those vegetation samples in which its relative cover is higher than 30% are included in the figure. The inclination of several species to places with sand accumulation is clearly evident (in a decreasing order): *Ammophila arenaria*, *Polygonum palestinum* and *Sporobolus pungens*. In the majority of the places where *Retama raetam* and *Stipagrostis lanata* are present, the net yearly changes in sand level are between –8 mm to 8 mm. In addition, the tendency of *Silene succulenta* to be present in places with sand erosion is apparent here.
Figure 9 is modeled after Figure 7, only this time we show the average absolute yearly change in sand level as a function of the relative cover of plant species in vegetation samples. Based on this figure, we may conclude that two species, when comprising a high percentage of the plant species, may serve as indicators of high rates of sand movement (in decreasing order): *Ammophila arenaria*, and *Artemisia monosperma*. As in the previous Figures (6, 7 and 8), *Stipagrostis lanata*, *Retama raetam* and *Scrophularia hypericifolia* are again clear indicators of a stabilized environment.

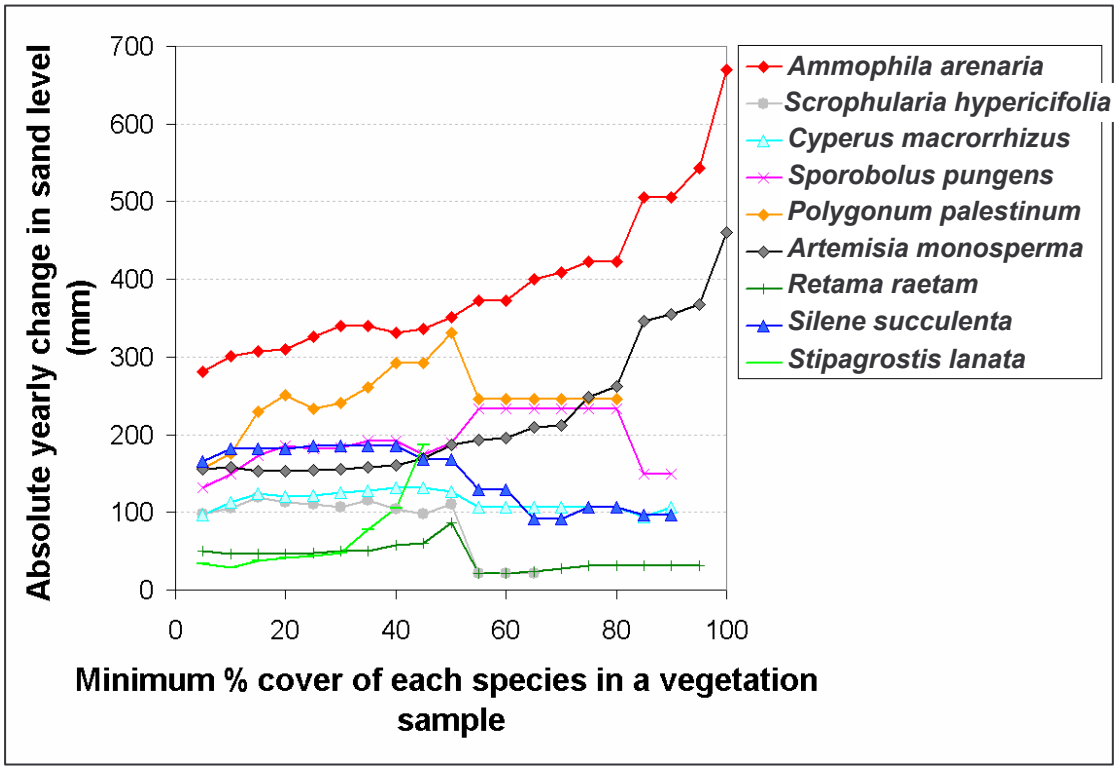


**Figure 9**: The average absolute yearly change in sand level as a function of the relative cover of plant species in vegetation samples.

### 3.3 The second gradient: the maximum relative % cover by *Artemisia monosperma* in a vegetation sample

Analyzing the second gradient, that of the maximum relative % cover of *Artemisia monosperma* in a vegetation sample, recall that we expect to identify indicator species when the relative cover of *Artemisia monosperma* (the most common species in the study area) is lower. We can therefore see the following patterns:

In Figure 10 we show the net yearly change in sand level as a function of the maximum relative cover by *Artemisia monosperma* in vegetation samples. From this figure two species emerge as indicators of sand accumulation when the % cover by *Artemisia monosperma* is low (in a decreasing order): *Ammophila arenaria* and *Sporobolus pungens.* According to this figure, *Scrophularia hypericifolia* and *Cyperus macrorrhizus* may serve as indicators for sand accumulation when the relative cover by *Artemisia monosperma* is lower than 40%. The identification of *Siliene succulenta* as an indicator for sand erosion is again apparent here, in places where the relative cover by *Artemisia monosperma* is lower than 20%.

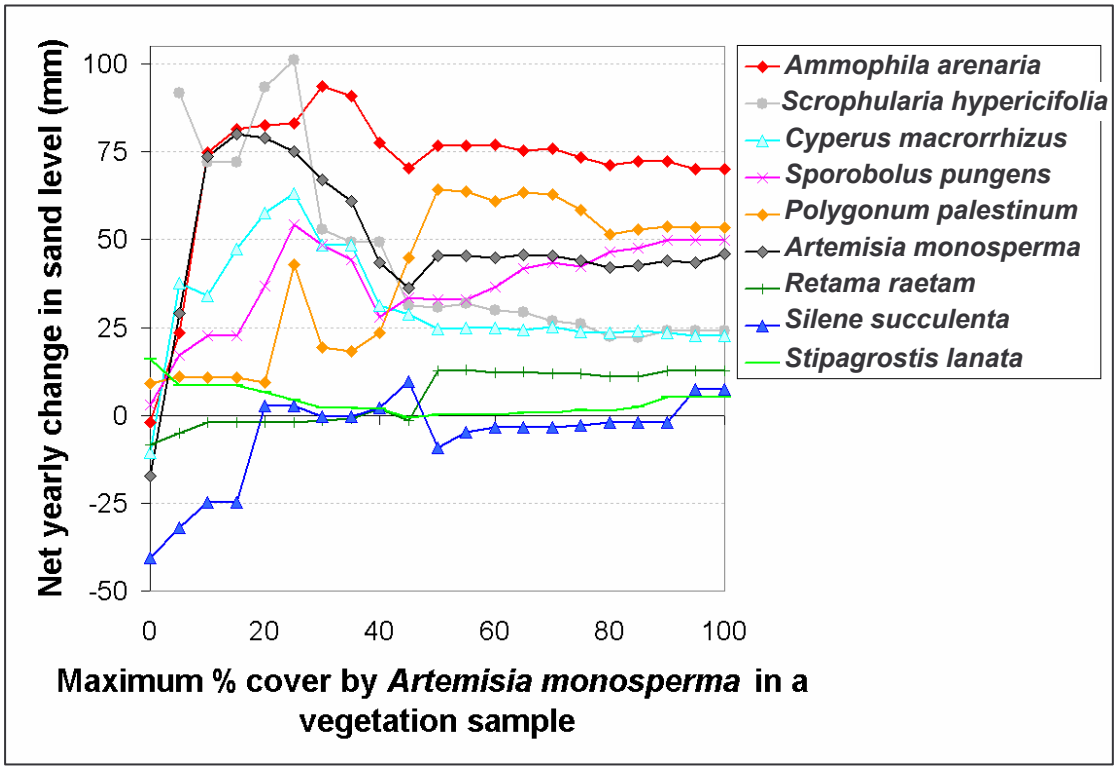


**Figure 10**: The average net yearly change in sand level as a function of the maximum relative cover by *Artemisia monosperma* in vegetation samples.

In Figure 11, that is modeled after Figures 6 and 8, we show box-plots and histograms presenting the presence of perennial species as a function of the net yearly change in sand level; this time however, for each species only those vegetation samples in which the relative cover by *Artemisia monosperma* is lower than 25% are included in the figure. From this figure the inclination of several species to places with sand accumulation is clearly evident, especially (in a decreasing order): *Ammophila arenaria*, *Scrophularia hypericifolia* and *Artemisia monosperma.* Again, the tendency of *Silene succulenta* to be present in places with sand erosion is apparent here.

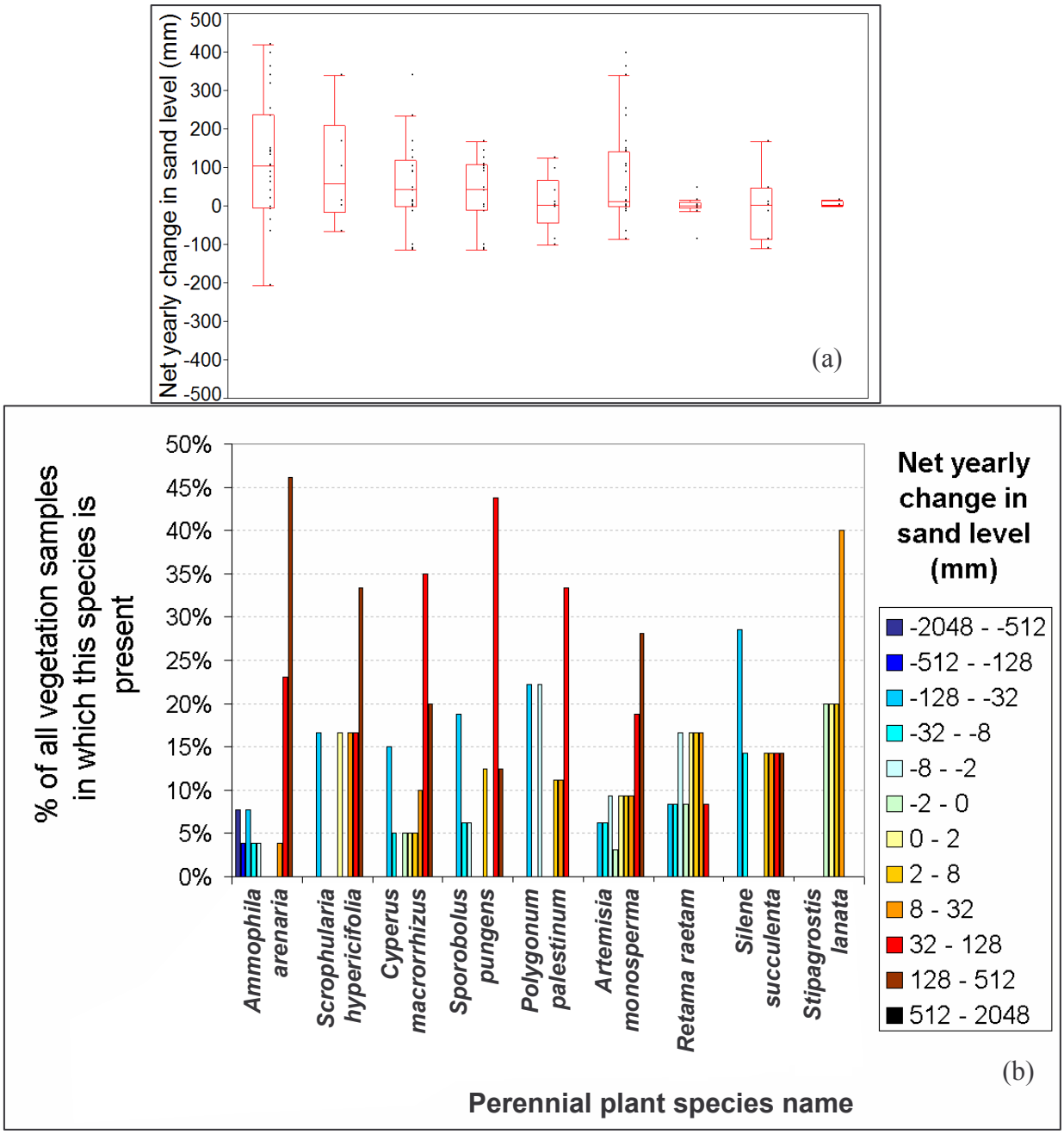


**Figure 11**: Including for each species only those vegetation samples in which the relative cover of *Artemisia monosperma* is lower than 25%: (a) Box plots presenting the net yearly change in sand level, (b) Histograms presenting the presence of perennial species as a function of the net yearly change in sand level (focusing on the range of ±500 mm); We assigned warm-dark colors (yellow-orange-red-black) to bars representing sand accumulation, whereas cold colors (green-blue) were assigned to bars representing sand erosion.

### 3.4 The third gradient: the minimum % vegetation cover in a vegetation sample

Analyzing the third gradient, of the minimum % cover of vegetation cover in a vegetation sample, recall that here we expect to identify indicator plant species with respect to the stabilization stage of a place. We can therefore see the following patterns:

In Figure 12 we show the absolute yearly change in sand level as a function of the minimum % of perennial vegetation cover in the vegetation samples. Clearly, as vegetation cover increases, sand movement decreases, with vegetation cover higher than 50% being the threshold above which there is hardly anymore sand movement. *Ammophila arenaria* stands out as the plant indicating highest mobility rates. The sudden rise in the mobility rates in places with *Silene succulenta* at higher vegetation cover, is probably an artifact due to the low sample size for that plant above vegetation cover of 30% ($n \leq 2$). Again, *Stipagrostis lanata*, and *Retama raetam* present the lowest rates of sand movement and are therefore clear indicators of a stabilized environment.

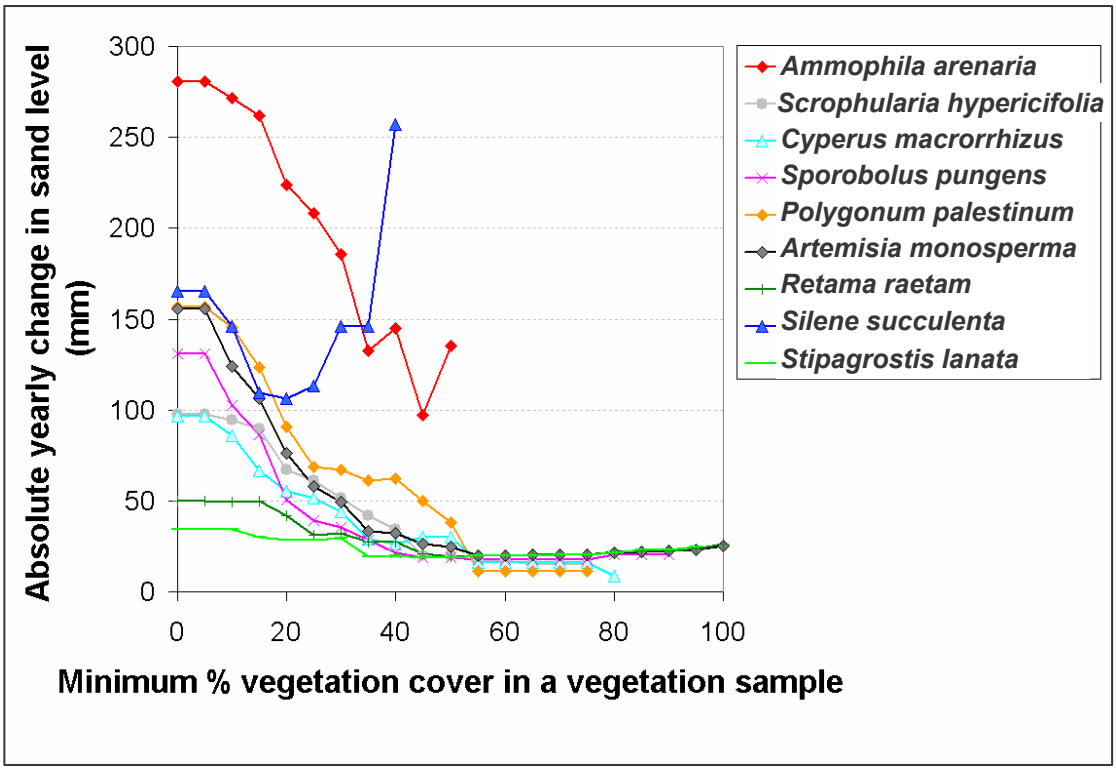


**Figure 12**: The average absolute yearly change in sand level as a function of the minimum % of perennial vegetation cover in vegetation samples.

In Figure 13 we show the relative presence of perennial plant species in vegetation samples as a function of the minimum % of perennial vegetation cover. This figure

emphasizes, in addition to the abundance of *Artemisia monosperma* in most of the dune areas, also the relationship between vegetation cover and the presence of other perennials. Three species may be found in the most stabilized places: *Artemisia monosperma, Retama raetam*, and *Stipagrostis lanata.* As for places that have a more mobile nature (i.e. lower vegetation cover), species may be ordered as follows in their dependence on a low vegetation cover (in a descending order): *Silene succulenta, Ammophila arenaria*, *Scrophularia hypericifolia, Polygonum palestinum, Sporobolus pungens*, and *Cyperus macrorrhizus*.

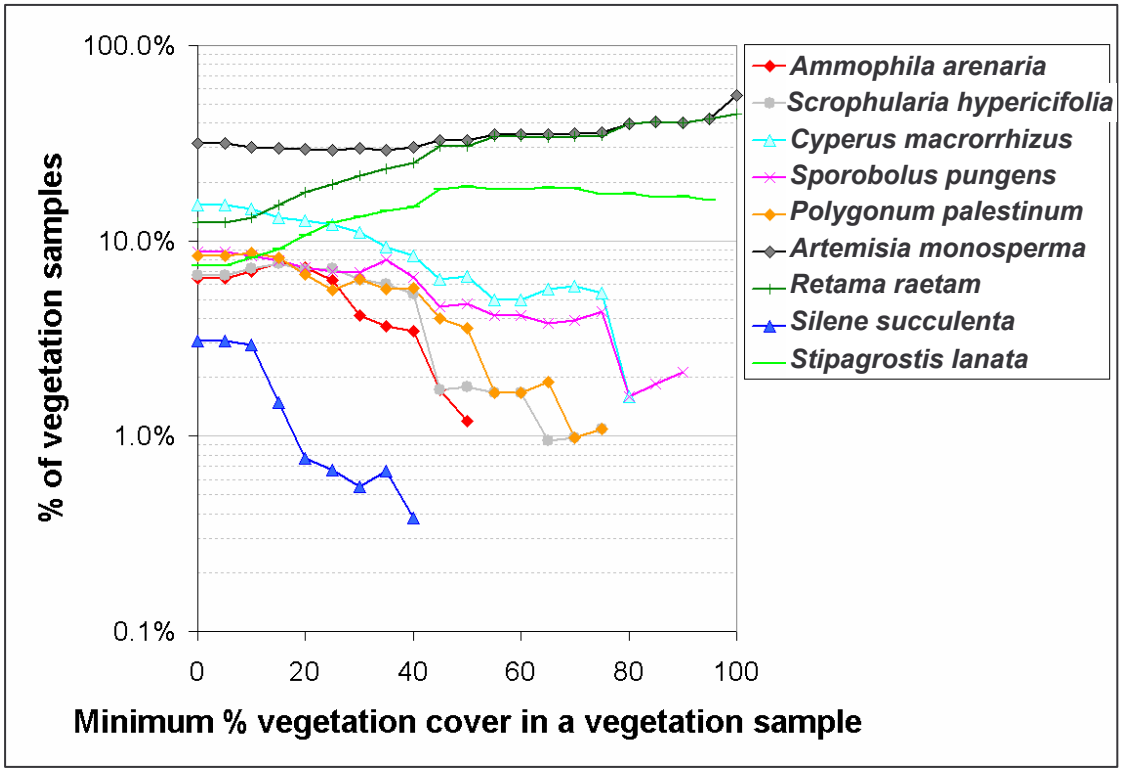


**Figure 13**: The average relative presence of perennial plant species in vegetation samples as a function of the minimum % of perennial vegetation cover.

### 3.5 Statistical analyses

By calculating a correlation matrix between the vegetation variables (after an arcsin(√p) transformation of the relative cover values) and the sand movement variable (Table 2) we have found that the majority of the perennial species are not strongly correlated one to the other (although of low values, many of the correlations were statistically significant). The only relatively strong negative correlation found was between *Ammophila arenaria* and *Artemisia monosperma* ($R = -0.42$, $p < 0.001$, $n = 315$), whereas a positive correlation was found between *Retama raetam* and

perennial cover ($R = 0.63$, $p < 0.001$, $n = 315$) and between *Retama raetam* and *Stipagrostis lanata* ($R = 0.33$, $p < 0.001$, $n = 315$). As for the annual absolute rate of erosion/deposition, this was found to be negatively correlated with perennial vegetation cover ($R = -0.56$, $p < 0.001$, $n = 315$), *Retama raetam* ($R = -0.55$, $p < 0.001$, $n = 315$) and *Stipagrostis lanata* ($R = -0.38$, $p < 0.001$, $n = 315$), and positively correlated with *Ammophila arenaria* ($R = 0.35$, $p < 0.001$, $n = 315$).

The results of the regression models are presented in Table 3. It is interesting to note that not only are we able to explain 39% of the variability in the annual absolute change by the species composition alone (or 49% when incorporating the perennial vegetation cover into the model), when sorting the plant species by their model coefficients on a decreasing order, they give similar patterns to those noted by us above.

**Table 2**: Correlation matrix of vegetation variables (after an arcsin(√p) transformation) and sand movement variable (after a log transformation). Values marked with *** are significant at $p < 0.001$, those marked with ** are significant at $0.01 < p < 0.001$and those marked with * are significant at $0.05 < p < 0.01$.

| | Perennial cover | *Ammophila arenaria* | *Scrophularia hypericifolia* | *Cyperus macrorrhizus* | *Sporobolus pungens* | *Polygonum palestinum* | *Artemisia monosperma* | *Retama raetam* | *Silene succulenta* | *Stipagrostis lanata* |
|---|---|---|---|---|---|---|---|---|---|---|
| Annual absolute rate of sand movement | **-0.56*** ** | **0.35*** ** | -0.06 | -0.05 | 0.04 | 0.10 | -0.02 | **-0.55*** ** | 0.09 | **-0.38*** ** |
| Perennial cover | | -0.08 | -0.03 | -0.28*** | -0.14* | -0.15** | -0.17** | **0.63*** ** | -0.17** | 0.26*** |
| *Ammophila arenaria* | | | -0.07 | -0.18** | -0.16** | -0.12* | **-0.42*** ** | -0.24*** | -0.08 | -0.19*** |
| *Scrophularia hypericifolia* | | | | 0.03 | 0.00 | -0.04 | -0.01 | -0.11* | -0.02 | 0.14* |
| *Cyperus macrorrhizus* | | | | | 0.23*** | 0.01 | -0.10 | -0.22*** | 0.04 | -0.05 |
| *Sporobolus pungens* | | | | | | 0.10 | -0.12* | -0.18** | -0.01 | -0.04 |
| *Polygonum palestinum* | | | | | | | -0.01 | -0.19** | 0.02 | -0.15** |
| *Artemisia monosperma* | | | | | | | | -0.12* | -0.14* | -0.03 |
| *Retama raetam* | | | | | | | | | -0.08 | **0.33*** ** |
| *Silene succulenta* | | | | | | | | | | -0.10 |

**Table 3**: Regression model coefficients for predicting the annual absolute rate of sand movement based on the composition of perennial dune plants (after an arcsin(√p) transformation). The table is ordered according to column d. See text for details.

| a | b | c | d | e | f | g | h | i | j | k | l | m |
|---|---|---|---|---|---|---|---|---|---|---|---|---|
| | Multiple regression | | | | | | Forward stepwise multiple regression | | | | | |
| | 1st model (Adj. $R^2$ = 25.6%, p < 0.001) | | 2nd model (Adj. $R^2$ = 39.0%, p < 0.001) | | 3rd model (Adj. $R^2$ = 48.8%, p < 0.001) | | 4th model (Adj. $R^2$ = 25.6%, p < 0.001) | | 5th model (Adj. $R^2$ = 39.5%, p < 0.001) | | 6th model (Adj. $R^2$ = 49.2%, p < 0.001) | |
| Dependent variable | Annual absolute change | | Log (Annual absolute change) P-value | | Log (Annual absolute change) | | Annual absolute change | | Log (Annual absolute change) P-value | | Log (Annual absolute change) | |
| | Coef. | P-value | Coef. | P-value | Coef. | P-value | Coef. | P-value | Coef. | P-value | Coef. | P-value |
| Intercept | 654.38 | p < 0.001 | 2.2206 | p < 0.001 | 2.699 | p < 0.001 | 654.38 | p < 0.001 | 2.157 | p < 0.001 | 2.650 | p < 0.001 |
| *Ammophila arenaria* | -2.70 | P < 0.01 | 0.0041 | P < 0.05 | 0.003 | P < 0.05 | -2.70 | P < 0.01 | 0.005 | p < 0.001 | 0.004 | P < 0.05 |
| *Silene succulenta* | -3.63 | P < 0.05 | 0.0031 | 0.29 | -0.001 | 0.74 | -3.63 | P < 0.05 | 0.004 | 0.20 | | |
| *Polygonum palestinum* | -3.76 | P < 0.01 | -0.0002 | 0.95 | -0.001 | 0.57 | -3.76 | P < 0.01 | | | | |
| *Sporobolus pungens* | -3.81 | P < 0.01 | -0.0002 | 0.93 | -0.001 | 0.68 | -3.81 | P < 0.01 | | | | |
| *Artemisia monosperma* | -4.07 | p < 0.001 | -0.0010 | 0.51 | -0.003 | P < 0.05 | -4.07 | p < 0.001 | | | -0.003 | P < 0.05 |
| *Scrophularia hypericifolia* | -5.45 | p < 0.001 | -0.0049 | 0.08 | -0.004 | 0.09 | -5.45 | p < 0.001 | -0.005 | 0.09 | -0.004 | 0.10 |
| *Cyperus macrorrhizus* | -6.87 | p < 0.001 | -0.0060 | P < 0.01 | -0.009 | p < 0.001 | -6.87 | p < 0.001 | -0.006 | P < 0.01 | -0.009 | p < 0.001 |
| *Stipagrostis lanata* | -5.59 | P < 0.01 | -0.0138 | p < 0.001 | -0.013 | p < 0.001 | -5.59 | P < 0.01 | -0.014 | p < 0.001 | -0.012 | p < 0.001 |
| *Retama raetam* | -8.62 | p < 0.001 | -0.0167 | p < 0.001 | -0.010 | p < 0.001 | -8.62 | p < 0.001 | -0.016 | p < 0.001 | -0.009 | p < 0.001 |
| Perennial cover | | | | | -0.014 | p < 0.001 | | | | | -0.014 | p < 0.001 |
| Correlation with the values shown in column d (for the 9 species) | 0.89 | | 1.00 | | 0.92 | | 0.89 | | 1.00 | | 0.89 | |

Notice also that the coefficients in the three models are highly correlated between themselves. *Ammophila arenaria* stands out as the species indicating highest sand mobility, followed by the following four species (not necessarily in this order): *Silene succulenta, Polygonum palestinum, Artemisia monosperma,* and *Sporobolus pungens*. These are followed by *Scrophularia hypericifolia* and *Cyperus macrorrhizus*. The two species closing the list are *Stipagrostis lanata* and *Retama raetam*, clear indicators of a stabilized dune environment.

The forward stepwise regression analysis is helpful in highlighting those species that have a stronger indicative power – those species that are significant enough to enter the regression model. The best indicative species (as seen in columns j-m of Table 3) for a mobile environment is *Ammophila arenaria*, whereas for a more stabilized environment the indicative species are (in a decreasing order) *Retama raetam*, *Stipagrostis lanata*, *Cyperus macrorrhizus*, and *Scrophularia hypericifolia*.
To accommodate the existing correlations between the relative cover of different species, we have used a cluster analysis as another method to identify indicator species. From the dendogram tree (fig 14) we extracted four clusters, and then used

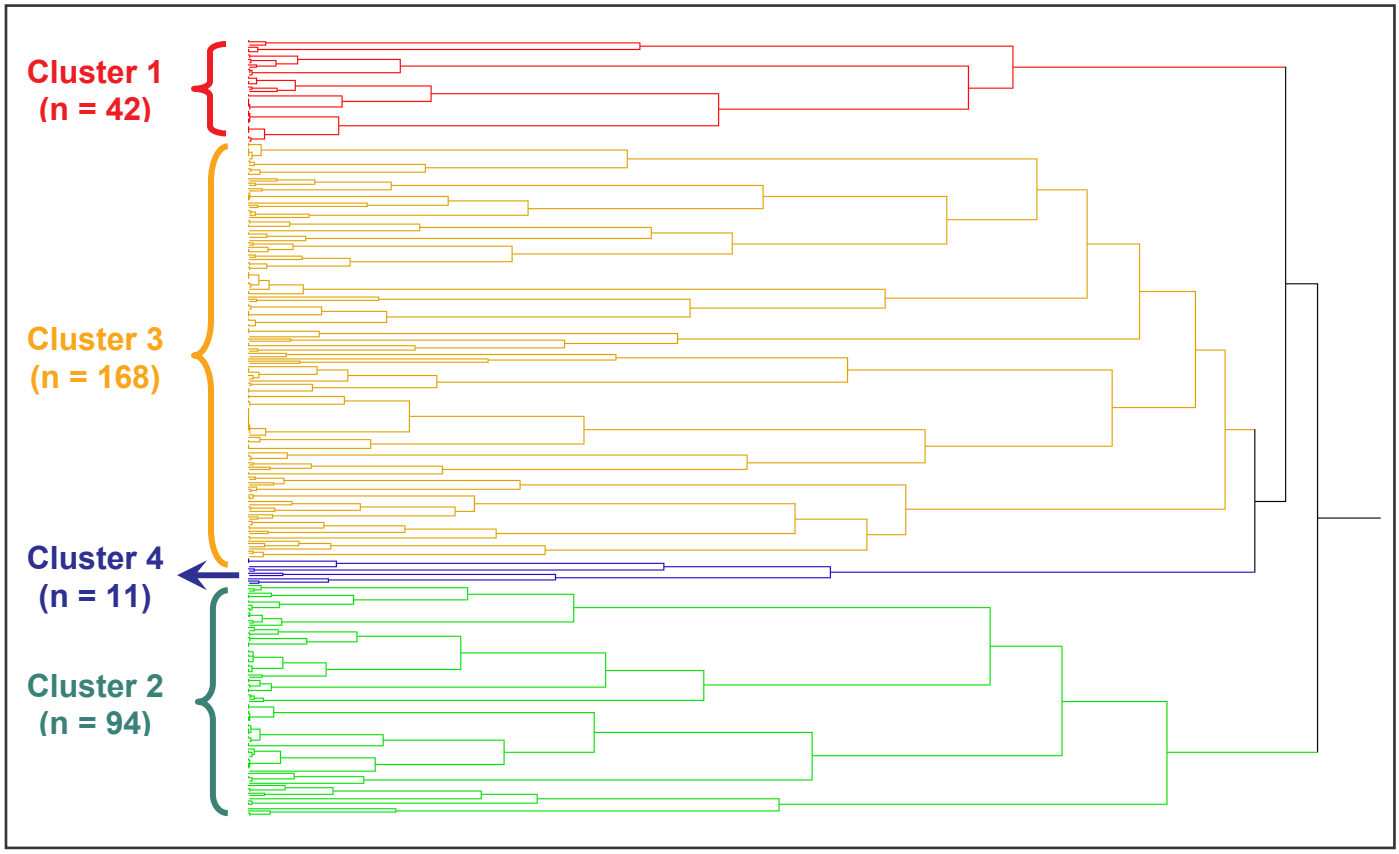


**Figure 14**: The dendogram tree of the cluster analysis (Ward method, standardized data). See text for details.

them as the grouping variable for box plots charts (fig 15). The four clusters correspond therefore to the following habitats:

1. Cluster 1 comprises 13% of all quadrats (n = 42). This cluster is characterized by high absolute rates of sand erosion/deposition (fig 15b), mostly sand deposition (fig 15c). Almost no annual plants exist here (fig 15d) and the relative cover of *Ammophila arenaria* is highest in this cluster (fig 15e).
2. Cluster 2 comprises 30% of all quadrats (n = 94). This cluster is characterized as the most stable habitat, exhibiting lowest absolute changes in sand level (fig 15b), with similar rates of erosion and deposition (fig 15c). In this habitat vegetation cover by both perennial plants (fig 15a) and annual plants (fig 15d) is the highest. Correspondingly, the relative cover of two species, *Retama raetam* (fig 15g) and *Stipagrostis lanata* (fig 15h), is highest in this cluster.
3. Cluster 3 is the largest of the four comprising 53% of al quadrats (n = 168). This cluster may is characteristic of active geomorphologic units in which neither erosion nor deposition are extreme, with a moderate cover by either perennial and annual vegetation. The relative cover of *Artemisia monosperma* (fig 15i) is highest in this cluster.
4. Cluster 4 is the smallest of the above, comprising only 3% of all quadrats (n = 11). In these locations, vegetation cover is relatively low (fig 5a) although some annual plants may be present (fig 15d) unlike cluster 1, and there is an overall erosion of the surface (fig 15c). The relative cover of *Silene succulenta* is highest in this cluster (fig 15f).

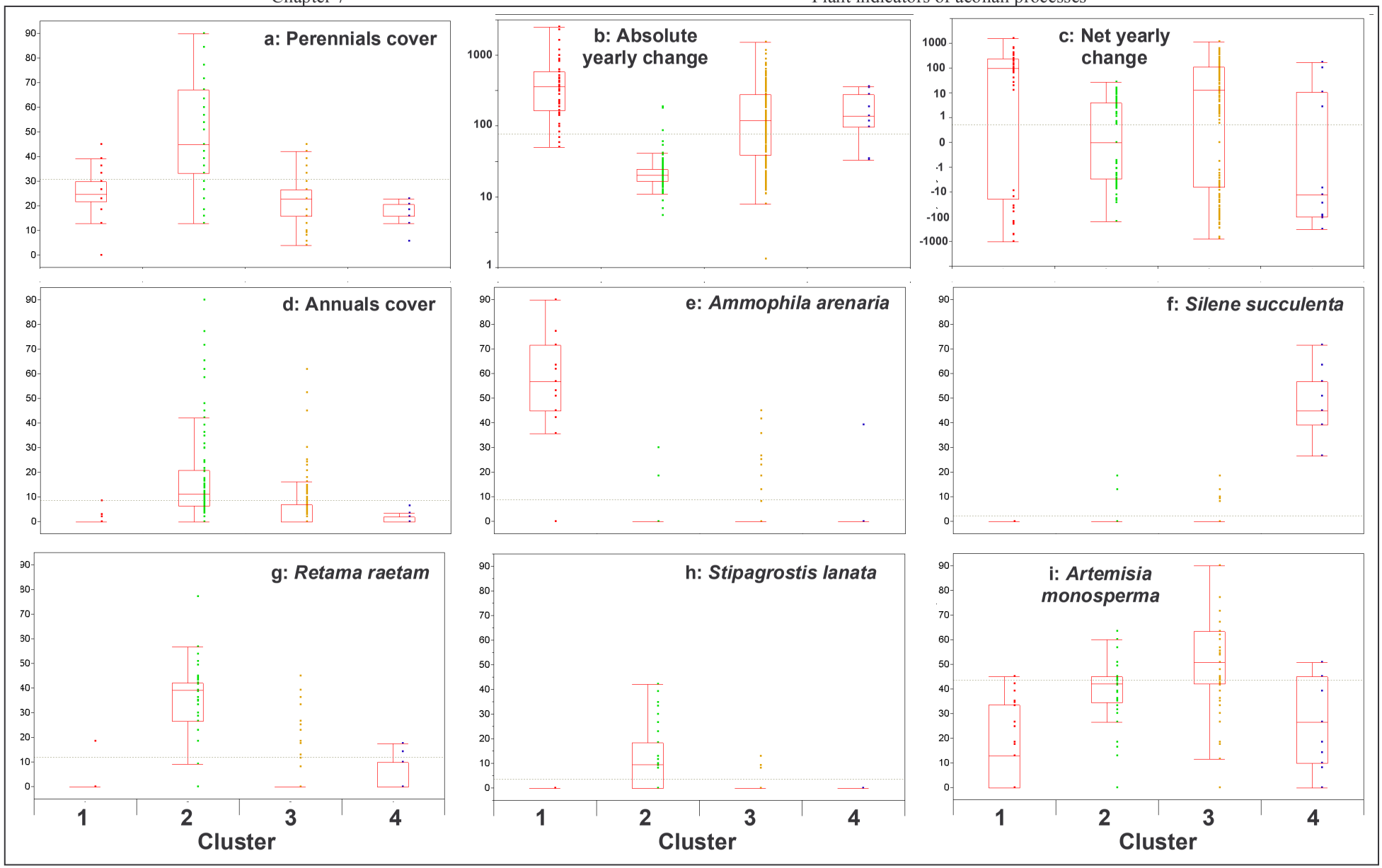


**Figure 15**: Box plots of nine selected variables grouped by the four clusters: (a) Perennials cover, (b) Absolute yearly change, (c) Net yearly change, (d) Annuals cover, (e) *Ammophila arenaria*, (f) *Silene succulenta*, (g) *Retama raetam*, (h) *Stipagrostis lanata*, (i) *Artemisia monosperma*. Sand changes variables were calculated following a log transformation, whereas the vegetation cover variables were calculated following an arcsin √% transformation.

## 4. Discussion

Vegetation cover, although being commonly used as an indicator of the stabilization stage of a dune field (Chapter 4 in this thesis) as it generally increases with lower rates of sand movement (as shown in fig 3a) is not informative regarding other aspects of aeolian processes. Thus, certain places may experience erosion or deposition, but have the same amount of vegetation cover (fig 3b; see also in Tsoar and Blumberg, 2002). However, both the magnitude of sand movement and the net outcome (erosion or accumulation of sand) at a certain place may be inferred from the composition of the perennial species found there.

Computer models that simulate the formation of sand dunes are now starting to incorporate also vegetation, as influenced by various factors, such as the groundwater table or by the erosion/deposition balance (de Castro, 1995; Baas, 2002). Obtaining field information on indicator dune plants can help calibrate the growth functions that are used in such models to relate the erosion/deposition balance at each grid cell with the increase or decrease of vegetation effectiveness.

Presently, identification of plant species/communities over coastal dunes is done in the field, although there are some promising developments lately in the application of the remote sensing technology using hyper spectral sensors for mapping plant communities (compare the negative success of Lucas et al., 2002, with the reported success of de Lange et al., 2004, and of Kempeneers et al., 2004).

We have therefore used traditional field methods to sample the absolute and relative cover of perennial plant species, along with the rates of sand erosion and accumulation, along four transects ranging from the coastline inland. However, in order to identify indicator plant species, we needed to devise an analysis method that will be able overcome the fact that the presence of plant species in a certain locality in the field may reflect also past conditions, and other stress factors, that were not measured by us (e.g. competition between different plant communities, as in Tielbörger and Kadmon, 1997, or the effects of microbiotic crusts on the emergence of vascular plants, as in Prasse and Bornkamm, 2000).

The gradient visualization method we have devised aims at overcoming these difficulties, by calculating the average annual absolute and net rates of erosion and deposition, on three gradients, ranging from 0% to 100%, at intervals of 5%:

(1) The minimum relative % cover of each species in a vegetation sample;

(2) The maximum relative % cover by *Artemisia monosperma* (the most common perennial species in the coastal dunes of Israel) in a vegetation sample;
(3) The minimum % vegetation cover in a vegetation sample.
Using this method we were then able to identify indicator species that may inform us on the geomorphologic process and the magnitude of the stress exerted on plants in a specific place.
As for species indicating (or found in) a stabilized environment, two species stand out clearly: *Stipagrostis lanata*, and *Retama raetam*. Both species are mostly found in units where the annual rate of sand erosion/deposition is between -8mm to 8mm. *Retama raetam* however is much more dominant, and may dominate the vegetation in the low inter dune areas, whereas *Stipagrostis lanata* did not reach more than 45% of the relative cover in neither one of the vegetation samples. *Artemisia monosperma* is also very common in stabilized places, however is not an indicator of such an environment. Another species that is mostly found in less mobile areas is *Scrophularia hypericifolia*.
As for species indicating a highly mobile sand environment, these may be classified as to whether they indicate a habitat of sand erosion or sand deposition.
Only one species may be stated as a clear indicator of sand erosion: *Silene succulenta*. This species is found only when vegetation cover is lower than 50%, and is almost always associated with sand erosion, especially when the relative cover by *Artemisia monosperma* is lower than 20% (see photo in fig 2a). In this regard, we may also note that places that are dominated by more than 80% of their relative cover by *Cyperus macrorrhizus* are also experiencing sand erosion (see photo in fig 2b). However, *Cyperus macrorrhizus* is also common in forming small nebkhas on dune tops.
As for species indicating sand accumulation, *Ammophila arenaria* as expected is almost always the leader, whether in the annual rates of sand accumulation (75mm/year and higher) or of the absolute change in sand level (see photo in fig 2c). And, *Ammophila arenaria* was not found in places where the vegetation cover was higher than 50%. The presence of *Artemisia monosperma* on the other hand may be an indicator of a very high rate of absolute sand change when its relative cover is higher than 80% (> 300 mm/year), and is generally associated with sand burial. Other species that were found to indicate sand burial, although on lower rates, include *Polygonum palestinum* (especially when its relative cover is between 20%-50%), *Sporobolus pungens, Cyperus macrorrhizus* (especially when the relative cover by *Artemisia*

*monosperma* is lower than 40%) and to a certain degree also *Scrophularia hypericifolia* (when the relative cover of *Artemisia monosperma* is lower than 25%). However, the p-values attached to *Polygonum palestinum*, *Sporobolus pungens* and *Cyperus macrorrhizus* in the regression models (columns d-g, j-m in Table 2) are quite low and therefore may not serve as strong indicators. Also *Artemisia monosperma*, being such an abundant plant in these dunes, is not a strong indicator, although it does enter most of the regression models and is negatively correlated with *Ammophila arenaria*. These results were derived by the gradient visualization depicted in the figures and further reinforced by the statistical regression models presented in Table 2, as well as by the cluster analysis presented in Figures 14 and 15. This confirms not only the gradient visualization method as an adequate exploratory graphic data analysis method, but also our identifications of indicator species. However, for most of those species (excluding the much studied Ammophila arenaria; see Kent et al., 2001), the physiological mechanisms enabling them to adapt to different habitats were not studied.

## 5. Conclusions

The results presented here have several important implications. First, they demonstrate an analysis method that is able to unveil important relationships between plants and the physical stresses influencing them, when studied in the field. Secondly, by identifying the inclination of specific perennial plant species to stabilized vs. mobile parts of the dunes, or to those parts experiencing erosion or deposition, we can proceed in two ways: (1) have an immediate insight whether a certain place undergoes erosion or deposition, based on the composition of the perennial plants found there; (2) predict which plant species will be found at different parts of the dunes, based on our knowledge about the physical factors influencing sand mobility (see Chapter 6 in this thesis): vegetation cover and the relative height upwind of a certain place, and the angle of the surface aspect with respect to the direction from which the sand moving winds are coming. Such knowledge is important to monitor processes of dune stabilization or reactivation, whether occurring naturally, or to assess the success of a management plan that aims at stabilizing a dune, or remobilizing it by removing vegetation.

## Acknowledgments

We wish to express our thanks to Rachel Lugassi from the Remote Sensing and GIS Lab at the Department of Geography in Tel Aviv University for performing the atmospheric and geometric corrections of the Landsat images. We would also like to thank Ravid Pik and Yoav Eshel from the Israeli Green Patrol (Ha Sayeret ha Yeruka) for the use of the differential GPS. For their comments on the manuscript we thank Anna Trakhtenbrot from the department of Ecology, Systematics and Evolution of the Hebrew University of Jerusalem (Israel).

## References

Baas A.C.W., 2002, Chaos, fractals and self-organization in coastal geomorphology: simulating dune landscapes in vegetated environments, Geomorphology, 48: 309-328

Bitan A. and Rubin S., (1991), *Climatic Atlas for Physical and Environmental Planning in Israel*, Geography Department – Tel Aviv University, Meteorological Service – Ministry of Transportation, Research and Development Section – Ministry of Energy and Infrastructure, Ramot Publishing, Tel Aviv University

Clark Labs. 2002. Idrisi 32. The Idrisi Project, 950 Main Street, Worcester MA 01610-1477, USA

Danin A., 1996a, Plants of Desert Dunes, Springer-Verlag, Berlin, 177 p.

Danin A., 1996b, Adaptations of *Stipagrostis* species to desert dunes, Journal of Arid Environments, 34: 297-311

Danin A., 2000, The Nomenclature News of Flora Palaestina, Flora Mediterranea, 10: 109-172.

Danin A. and Nukrian R., 1991, Dynamics of dune vegetation in the southern coastal area of Israel since 1945, *Documents Phytosociologiques*, XIII: 281-296

De Castro F., 1995, Computer simulations of the dynamics of a dune system, Ecological Modelling, 78: 205-217

El-Bana M.I., Nijs I. and Kockelbergh F., 2002, Micorenvironmental and vegetational heterogeneity induced by phytogenic nebkhas in an arid coastal ecosystem, Plant and Soil, 247: 283-293

Emery K.O. and Neev D., (1960), Mediterranean beaches of Israel, *Israel Geological Survey Bulletin*, 26: 1-24

Feinbrun-Dothan N., and Danin A., (1998), Analytical Flora of Eretz-Israel, second edition, CANA, Jerusalem (in Hebrew)

Goldsmith V., Rosen P. and Gertner Y., (1990), Eolian transport measurements, winds, and comparison with theoretical transport in Israeli coastal dunes, Chapter Five in Nordstrom K.F., Psuty N.P. and Carter R.W.G. (eds.), *Coastal Dunes: Form and Process*, John Wiley & Sons, 79-101

Hesp P.A., 1991, Ecological processes and plant adaptations on coastal dunes, Journal of Arid Environments, 21: 165-191

Huang Z. and Gutterman Y., 1998, *Artemisia monosperma* achene germination in sand: effects of sand depth, sand/water content, cyanobacterial sand crust and temperature, Journal of Arid Environments, 38: 27-43

Jauffret S. and Visser M., 2003, Assigning life-history traits to plant species to better qualify arid land degradation in Presaharian Tunisia, Journal of Arid Environments, 55: 1-28

Kadmon, R. & Leschner, H. (1995). Ecology of linear dunes: effect of surface stability on the distribution and abundance of annual plants. Advances in GeoEcology, 28: 125–143

Kempeneers P., S. de Backer, S. Delalieux, B. Nechad, W. Debruyn, P. Coppin, K. Ruddick, and P. Scheunders, 2004, HYPERWAVE Generic classification technique for Hyperspectral Data, a Powerpoint presentation presented at: Stereo & Vegetation, May 6 2004

Kent M., Owen N.W., Dale P., Newnham, R.M., and Giles, T.M., 2001, Studies of vegetation burial: a focus for biogeography and biogeomorphology?, Progress in Physical Geography, 25 (4): 455-482

Kutiel P., Danin A., and Orshan G., 1979/80, Vegetation of the sandy soils near Caesarea, Iarael. I. Plant communities, environment and succession, Israel Journal of Botany, 28: 20-35

de Lange R., M. van Til and S. Dury, 2004, The use of hyperspectral date in coastal zone vegetation monitoring, EARSeL eProceedings 3,2/2004, pp. 143-153

Li S.G., Harazono Y., Zhao H.L., He Z.Y., Chang X.L., Zhao X.Y., Zhang T.H., and Oikawa T., 2002, Micrometeorlogical changes following establishment of artificially established artemisia vegetation on desertified sandy land in the

Horqin island land, China and their implication on regional environmental change, Journal of Arid Environments, 52: 101-119

Lucas N.S., Shanmugam S. and Barnsley M., 2002, Sub-pixel habitat mapping of a coastal dune ecosystem, Applied Geography, 22: 253-270

Milligan, G.W., 1980, An Examination of the effect of six types of error perturbation on fifteen clustering algorithms, *Psychometrika*, 45: 325–342

Mugnier C.J. 2000. Grids and Datums: the State of Israel. Photogrammetric Engineering and Remote Sensing, 66 (8): 915-917

Nukrian R., (1988), *Vegetation and its Habitats in the Sand Dunes to the South of Shikma River*, M.Sc thesis, Department of Botany, Hebrew University of Jerusalem, Israel (in Hebrew)

Prasse, R., and Bornkamm, R., 2000, Effect of microbiotic soil surface crusts on emergence of vascular plants, Plant Ecology, 150: 67-75

SAS, 2003, JMP IN release 5.1, SAS Institute Inc.

Sokal, R. R., and F. J. Rohlf, 1981, Biometry, Second edition, W. H. Freeman and Company, New York, New York, USA

Sykes M.T. and Wilson J.B., 1990, An experimental investigation into the response of New Zealand sand dune species to different depths of burial by sand, Acta Botanica Neerlandica, 39 (2): 171-181

Tielbörger, K., and Kadmon, R., 1997, Relationships between shrubs and annual communities in a sandy desert ecosystem: a three-year study, Plant Ecology, 130: 191-201

Tsoar, H. and D.G. Blumberg, 2002, Formation of parabolic dunes from barchan and transverse dunes along Israel's Mediterranean coast, Earth Surface Processes and Landforms, 27: 1147-1161

Tsuriell E.D., 1959, Physiological – Ecological Studies on Ammophila arenaria as a Pioneer Plant for Israel's Sand Dunes, unpublished PhD thesis, The Hebrew University of Jerusalem, Israel

Van der Valk A.G.,1974, Environmental factors controlling the distribution of forbs on coastal foredunes in Cape Hatteras National Seashore, Canadian Journal of Botany, 52: 1057-1073

Waisel Y., Litav M. and Agami M., 1975, Coastal Plants of Israel, Tel Aviv University, Tel Aviv, 96 p.

Wiedermann A.M. and Picakart A., 1996, The *Ammophila* problem on the Northwest

Coast of North America, Landscape and Urban Planning, 34: 287-299

Willis B.F.F., Hope-Simpson J.F. and Yemm E.W., 1959, Braunton Burrows: the dune system and its vegetation, part II, Journal of Ecology, 47 (2): 249-288

Yeaton, R.I., 1988, Structure and function of the Namib dune grasslands: characteristics of the environmental gradients and species distributions, Journal of Ecology, 76: 744-758

*In the eighth article* a new method is presented to measure the reflectance of biogenic crust in the field along a vertical micro-profile. This was achieved by using a specially constructed Subsurface Biogenic Crust Sampler, that enabled to remove 2mm layers of sand one after the other, and thus to measure the reflectance at several layers. Furthermore, a study on the effect of moisture on spectral indices related to the chlorophyll content has been conducted, and a relationship was established between the content of fine particles in a sand sample and its spectral properties in the short wave infra-red region of the electromagnetic spectrum. Using these techniques it was possible to quantify the content of biogenic soil crust and of fine particles, in addition to iron oxides, in the field, and relate them to the variables of surface aspect and surface stability (mobile or stabilized, erosion or deposition) that occur in different places on the dune. Studying in detail the spatial variability in these variables, in a basin that has begun stabilizing only 30 years ago, was intended to reveal the differences in the temporal responses of these indicators to dune stabilization.

# The relationship between coastal dunes' stabilization and the content of biogenic soil crusts, free iron-oxides and fine particles – a field spectral analysis

Noam Levin, Giora J. Kidron and Eyal Ben-Dor
Department of Geography and Human Environment, Tel Aviv University, Israel

## Abstract

The coastal dunes of Israel are undergoing a process of stabilization since 1948. One of the major features of this process is a change in surface properties of the dunes – the development of a biogenic soil crust, and a change in the properties of the sand grains themselves. Over a small area covering three dunes we have analyzed in detail the factors influencing the spatial distribution of biogenic crust, fine particles and free iron-oxides, using field and lab spectroscopy methods. Biogenic crust was measured in the field after rainfall along a vertical micro-profile at several layers, and in the lab when dry, from both the surface and the sub-surface samples. Sand erosion and deposition was measured using erosion pins to determine its effect on the presence of biogenic crust. It was found that the biogenic crust over these dunes is comprised of green algae that differs in its reflectance spectra from cyanobacterial crust, especially in the blue band. The crust is usually covered by a thin layer of sand grains, and is more abundant in the stable areas. It was found that the surface aspect plays only a secondary role in its spatial distribution, with a preference for north-facing slopes over south-facing slopes. The content of fine particles was correlated with the presence of biogenic crust, being higher in the stable areas. In addition, the color of sand grains in the stable areas was found to be of a lower albedo and a slightly more developed reddish color, indicating a higher rate of rubification in those places. This study clearly demonstrated that the intensity of sand erosion/deposition rates affects soil properties, with the biogenic crust being the fastest to react to the stabilization process, followed by the content of fine particles and to a lesser degree also the rubification process.

# 1. Introduction

## 1.1 Coastal dune stabilization processes

The coastal dunes of Israel are undergoing processes of stabilization by vegetation since the establishment of the state of Israel, in 1948 (Danin and Nukrian, 1991; Tsoar and Blumberg, 2002; Chapter 4 in this thesis). Dune stabilization processes are commonly described as follows (Danin and Yaalon, 1982; Tsoar and Møller, 1986; Danin et al., 1989; Danin, 1991; Hesp, 1991): (1) With sufficient rainfall (above 50 mm/year) pioneer plants of perennial grasses germinate; (2) The presence of vegetation leads to a decrease in the wind speed, causing a local deposition of sand forming biogenic hillocks (nebkhas) and at a lower rate also the trapping of fine-grained particles transported via aerosols that are washed by the rainfall; (3) This amelioration in the water regime enables the development of filamentous cyanobacteria and the formation of a biogenic crust; (4) This in turn increases surface roughness, leading to less sand movement, enabling plant succession, an increase in nutrient levels and a decrease in stress levels for the plants. In addition, the percentage of free iron oxides in sand dunes and in sandy soils may represent their stage in the rubification process (Norris, 1969; Walker, 1979). However some studies report that iron oxides stimulate soil aggregation whereas others observed no effect (Duiker et al., 2003); their role possible role in the dune stabilization process is therefore not clear. In this study we focus on three soil properties that develop on stabilized dunes, and their spectral characteristics: the formation of biogenic crusts, the reddening of the sand, and the increase in the content of fine particles.

## 1.2 Changing properties of sand over stabilizing dunes

### 1.2.1 Biogenic soil crusts in desert and coastal dunes

Many areas of sand dunes in arid and semiarid regions are covered by biogenic soil crusts, where they have important ecological and environmental roles, e.g. in aggregating soil particles (Clough and Sutton, 1978), controlling wind erosion especially on sandy soils (Belnap and Gillette, 1998), inhibiting the germination of vascular plants (Huang and Gutterman, 1998; Prasse and Bornkamm, 2000), initiating runoff following rainfall events (Kidron and Yair, 1997), and are sensitive to destruction by human activities of grazing and trampling (Karnieli and Tsoar, 1995).

Ancker et al. (1985) have found algae and cyanobacteria are the first plants to colonize dune blowouts in The Netherlands: four filamentous species were distinguished by them, three cyanobacteria and the fourth, which seemed to be the most numerous, was a green alga, *Ulothrix sp*. The total number and weight of aggregates (formed by algae, cyanobacteria, bacteria, fungi and actinomycetes) was found to increase in a dune succession ranging from unstable foredunes to early fixed dunes (Forster and Nicolson, 1981). Working in the stabilized dunes of Park ha Sharon located at the center of Israel's coastal plain, where the annual amount of rainfall is 600 mm., Kutiel et al. (1996) have found that more than 50% of the surface was covered by biogenic soil crusts. These were found to increase both the content of organic matter and that of the water in the soil.
At the southern coastal dunes of Israel, where the present study is located (precipitation above 480mm/year), the presence of biogenic soil crusts is lower than that of the more rainy area of Park HaSharon (P = 600 mm/year), and much lower than that of Nizzana in the Negev Desert (P = 95 mm/year). The higher presence of biogenic soil crusts in the desert dunes of Nizzana is probably related to higher deposition rates of fine particles, due to shorter distance to dust sources (Tsoar and Møller, 1986, p. 84). The only study to date that has analyzed the presence of biogenic crusts in this area is that of Danin and Nukrian (1991), based on the M.A. thesis of Nukrian (1988). They have found that the first species of blue-green algae on the sand found among stems and leaves of *Ammophilia arenaria* was the filamentous *Microcoleus vaginatus*, that was also the most common species in all the cyanobacterial crusts throughout the area studied. At later stages of vegetation succession and older sites a species of *Nostoc* was found as well. They noted that in young and unstable sites viable crust may be found up to 1-10 mm below the soil surface, whereas in older sites the cyanobacteria were found at soil surface. However, as mentioned by West (1990), the role of microphytes in plant succession and ecosystem development is not yet clear, and whether the development of a microphytic crust is a prerequisite to the development of higher plant cover or vice versa, or whether both processes proceed simultaneously, is yet to be understood.
The decisive role of solar insolation and direction of exposure (surface aspect) on the vegetation cover and composition in semi-arid and arid regions is a well known phenomena (Boyko, 1947; Kutiel, 1992; Nevo et al., 1999; Pavlicek et al., 2003).

As for microclimatic and other environmental factors influencing the presence of biogenic crusts, the following may be stated:

(1) Active sand movement effectively limits any establishment of crusts (Tsoar, 1990);

(2) Algae are apparently more sensitive than mosses and lichens to annual variations in precipitation and temperature (West, 1990);

(3) Cyanobacterial crusts begin photosynthetic activity soon after being wetted (Lange et al., 1992);

(4) Areas of higher dust deposition do not coincide with the distribution of the biological crust within the dune field; however, the net input balance of dust may account for the different amounts of fines in the crust areas of opposing slopes (Littmann, 1997). In addition, biogenic crust was found to regenerate within two years, with differences in the microhydrological budget relative to aspect and slope probably playing a much more important role than fine material input;

(5) On the dunes of Nizzana all the properties of biomass checked (thickness, organic matter, chlorophyll, protein and carbohydrate) showed significant differences between the south-facing and the north-facing foot-slopes of the dunes, the north-facing foot-slopes being richer. In addition, much higher diversity of species characterized the moss-dominated crust (including green algae and lichens) which are abundant in the dune-interdune interface of the northern exposure, whereas the south-facing slopes are inhabited by cyanobacterial crust (Kidron et al., 2000). Rain, temperatures or aeolian input were not found to explain the distribution of cyanobacterial- and moss-dominated crusts at the south- and north-facing dune footslopes, respectively. Longer daytime moistness (a 2.5 fold increase) characterized the north-facing foot slopes following rain, in comparison to the south-facing foot slopes, as a result from a difference in evaporation due to aspect and slope angle. In addition, runoff and apparently subsurface flow contribute substantially to the differential water distribution.

(6) Dew and fog contribution to the cyanobacterial crust is negligible, however it might be contributing for the reproduction of mosses (Kidron et al., 2002);

(7) The intensity of particle emission and the spatial extent of crust breakdown caused by wind carried sand grains, were found to be dependent on the thickness and strength of the crust examined. While fungal crusts were two to three times stronger than the photoautotrophic crusts, they were also two to three time thicker, further explaining their

relative high resistance to breakdown (McKenna Neuman et al., 1999). The duration of the wind gust was found to be of prime importance in this regard, more than the impact intensity associated with the external sediment supply.
(8) Crust deflation features were found to be aligned with the air stream on average and regardless of size (McKenna Neuman et al., 2005).

### 1.2.2 The rubification process on sand dunes

The rubification is defined as a pedogenesis stage in which iron is released from primary minerals to form free iron oxides that coat quartz particles in soils with a thin reddish film (Buol et al. 1973). There is abundant evidence that many dune sands become reddened with the passage of time that is promoted by warm temperatures, oxidizing conditions and periodic presence of moisture (Norris, 1969). Williams and Yaalon (1977) have demonstrated reddening in sand dune under laboratory weathering conditions and concluded that organic matter is not necessary to initiate the process. Differences in the pedoclimatic conditions (soil moisture tension and soil temperature) were found by Singer et al. (1998) to cause the differences in color and iron-oxide mineralogy between two Mediterranean soils, the red Terre Rosse (Rhodoxeralfs according to the USDA classification) being dominated by hematite and the yellower Rendzina by goethite. Given the estimated young age of the coastal dunes of Israel (c. 1000 years; Tsoar, 1990), the free iron-oxide content found on active dune areas in the Ashdod dunes is quite low, ranging from 0.02% at the beach to 0.05% in the innermost dunes (Ben-Dor et al., 2005). Exposed *Hamra* soil (Haploxeralf according to the USDA classification) found in the same area, has a higher content of free iron oxides, ranging between 0.1% to 0.4%, representing the other end of the pedogenetic sequence, starting with sand dunes.

### 1.2.3 The content of fine particles in stabilizing sand dunes

The amount of fine particles increases during sand succession and dune stabilization processes (Danin and Yaalon 1982) and in sandy soils is important for estimating the water holding capacity of these soils as it determines the availability of water to plants (Tsoar and Zohar 1985). In addition, Danin (1983) observed that the sandy deserts of Israel and Sinai need to have at least 4-5% clay and silt to support measurable microphytic cover.

## 1.3 Spectral properties of sand characteristics over stabilizing dunes

### 1.3.1 Spectral studies of biogenic crust

Remote sensing approaches on a micro-scale have been suggested as a non-destructive in situ means for quantifying crust properties (West, 1990). So far, much attention has been given for the spectral study of cyanobacteria soil crust over sand dunes, with the following conclusions (for desert dunes in Israel – Karnieli and Tsoar, 1995; Karnieli and Sarafis, 1996; Karnieli, 1997; Karnieli et al., 1999; for semi-arid regions in Australia – O'Neill, 1994): (1) biogenic soil crusts exhibit absorption features of chlorophyll at 670-685nm, that are more conspicuous when the crust is wetted (see also O'Neill, 1994); (2) the closer the red edge inflection point is to the longer wavelengths, the higher the relative abundance and distribution of the microphytic community; (3) the phycobilin pigments, that are unique to cyanobacteria, contribute to higher reflectance in the blue relative to the sand substrate, and therefore enable to differentiate them from higher plants, in which phycobilins are generally not detectable; (4) as more intense biogenic crust forms, the iron oxide and the clay minerals absorption features are masked and the organic matter features of the crust become dominant.

### 1.3.2 Spectral studies of free iron-oxide content in sand dunes

Fe in the free iron oxides is spectrally active across the VIS-NIR region via the electron transition (of 6A1→T1g between 750-950nm and 6A1-→T2g between 550-650nm) and is responsible for the Fe absorption of radiation that gives the soil its red color. Based on the free iron oxides that redden the sand, and using spectral color indices or linear mixing models, Madeira et al. (1997) and White et al. (1997, 2001) showed that it is possible to account for iron oxides status using the Landsat Thematic Mapper data (only six bands in the VIS-NIR-SWIR region) over lateritic soils in Brazil, and sand dunes at the Namib, and at the Northern Rub' Al Khali (United Arab Emirates), respectively. Field spectroscopy was used by Bullard and White (2002) to quantify iron oxide coatings on dune sand in the Simpson-Strzelecki Desert, Australia

Although the content of free iron-oxides in the dunes of Ashdod is low, remote sensing methods based on the visible spectrum were found to be very accurate in monitoring it, either using a simple digital camera (Chapter 2 in this thesis), or by using a CASI

hyperspectral airborne sensor (Ben-Dor et al., 2005). In these two studies, several spectral indices using the red, green and blue bands were evaluated (see below in the methods), of which the redness index (see below) was found as the best predictor of iron oxide content.

### 1.3.3 Spectral studies of the content of fine particles in sand dunes

Differences in the particle size of soils affect their reflectance. If multiple scattering dominates, as is usually the case in the visible and near- infrared, the over all reflectance is expected to decrease as the grain size increases (Clark 1999). This was indeed observed by Okin and Painter (2004) who studied sand plumes from abandoned agricultural fields, in which effective particle size decreased towards the toe of the plume. Analyzing a hyperspectral AVIRIS image, they demonstrated the expected negative correlation between effective grain size of sand in the plume, and its reflectance, with the most significant correlations in the short-wave infrared. Nevertheless, in chapter 2 of this thesis I have shown that the iron oxides spectral redness index based on three visible bands, was able to explain 81% of the variability in fine particles content in sand samples; this was explained by them to be due to the high correlation between the content of free iron oxides and fine particles (see also Dematte et al., 2004, as well as by Sanchez-Maranon et al., 2004).

## 2. Aims

Based on the proven capability of spectral indices to quantify the above mentioned soil properties over sand dunes, our aims are to study the effect of the stability of the surface (i.e. erosion or deposition of sand) and of the surface aspect over the presence of biogenic crusts, the content of fine particles and of free iron oxides on recently stabilizing coastal dunes.

## 3. Methods

### 3.1 Study area

The specific area chosen for this study is located at the heart of the Ashdod Dunes, at a distance of c. 2.5km. from the coastline, and c. 1km. from the nearest buildings in the city of Ashdod (see Figure 1).


**Figure 1**: Location map of the Ashdod Dunes area

This area was chosen as it represents a semi-stabilized dune area, where in some places biogenic crust is to be found, and because in it various surface aspect and slope angles are found. In addition we estimated that this area is less disturbed by off road vehicles, relative to other places in this coastal dune system. Two additional databases were also available for us for the area under study: a Landsat satellite image taken in January 2000 (see Chapter 5 in this thesis), and a detailed Digital Elevation Model prepared in 1992 (see Chapter 1 in this thesis). From the Landsat image NDVI and SAVI values were calculated at several upwind (SW) distances from the erosion pins, as in
chapters 5 and 6 in this thesis.

Samples of cyanobacterial biogenic crust common to Israel's desert dunes were collected from the Sede Hallamish (Nizzana) dune field along the Israel/Egypt border, about 50 km south of the Mediterranean coastline. Five microphytic communities were defined in the Sede Hallamish dune field (Kidron, 1995). These are denoted in this article as communities A, B, C, D, and E, as in Mazor et al. (1996). These communities represent a gradient in which the amount of chlorophyll content, organic matter, protein content and crust thickness increase steadily from community A to community E (Mazor et al., 1996; Karnieli et al., 1999).

## 3.2 Field measurement of the erosion and deposition of sand

To study current rates of erosion and deposition of sand, seven transects were chosen, representing various aspect and slope angles (see Figures 2 and 3). Along these transects, 64 erosion pins (following Arens et al., 2004) were placed in December 2003, and measured at an accuracy of 1-2 mm subsequently every 2-4 weeks since the winter of 2003/4 until October 2004. The exact location and height above sea level of the erosion pins were determined using a differential GPS, whereas the surface slope and aspect angles were determined in situ using a clinometer and a hand compass.

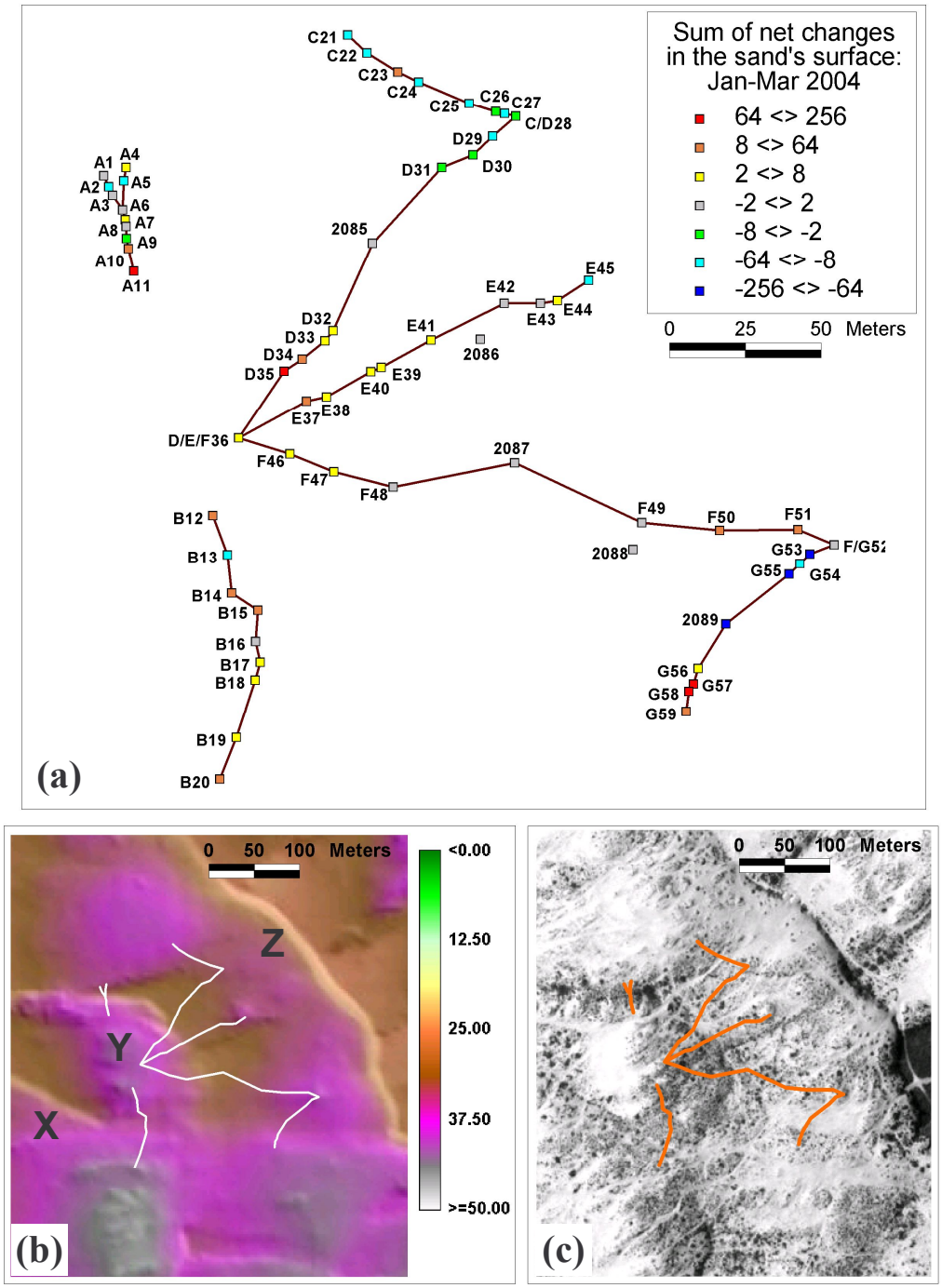


**Figure 2**: Detailed maps of the transects: (a) The specific locations of the erosion pins, their serial numbers, and the sum of net changes in the sand's surface height between Jan-Mar 2004; (b) An analytically shaded digital elevation model, the letters X, Y and Z marking the locations of the dunes whose movement is analyzed in Fig 7; (c) An aerial photograph taken in June 2002

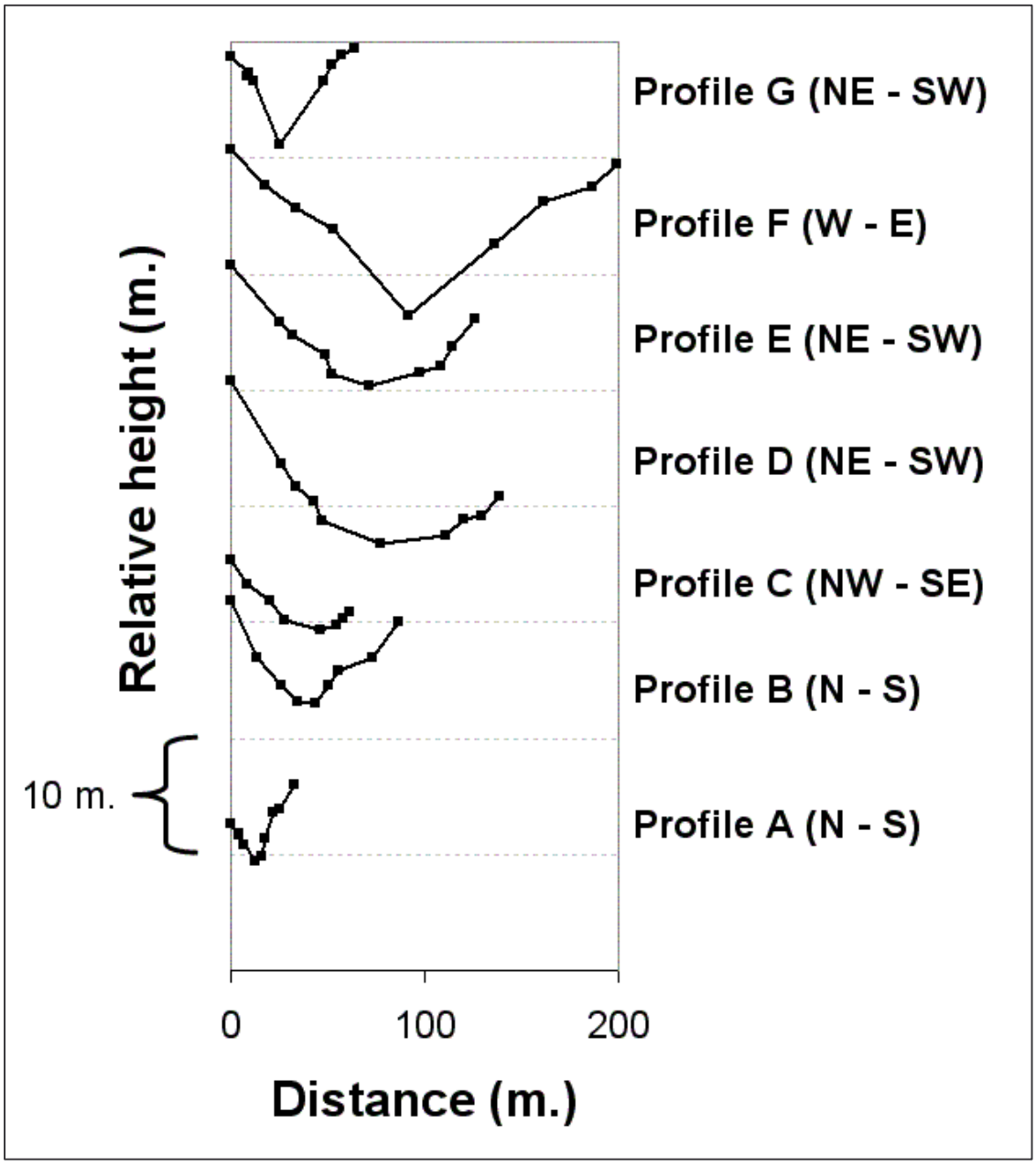


**Figure 3**: Topographic profiles of the transects

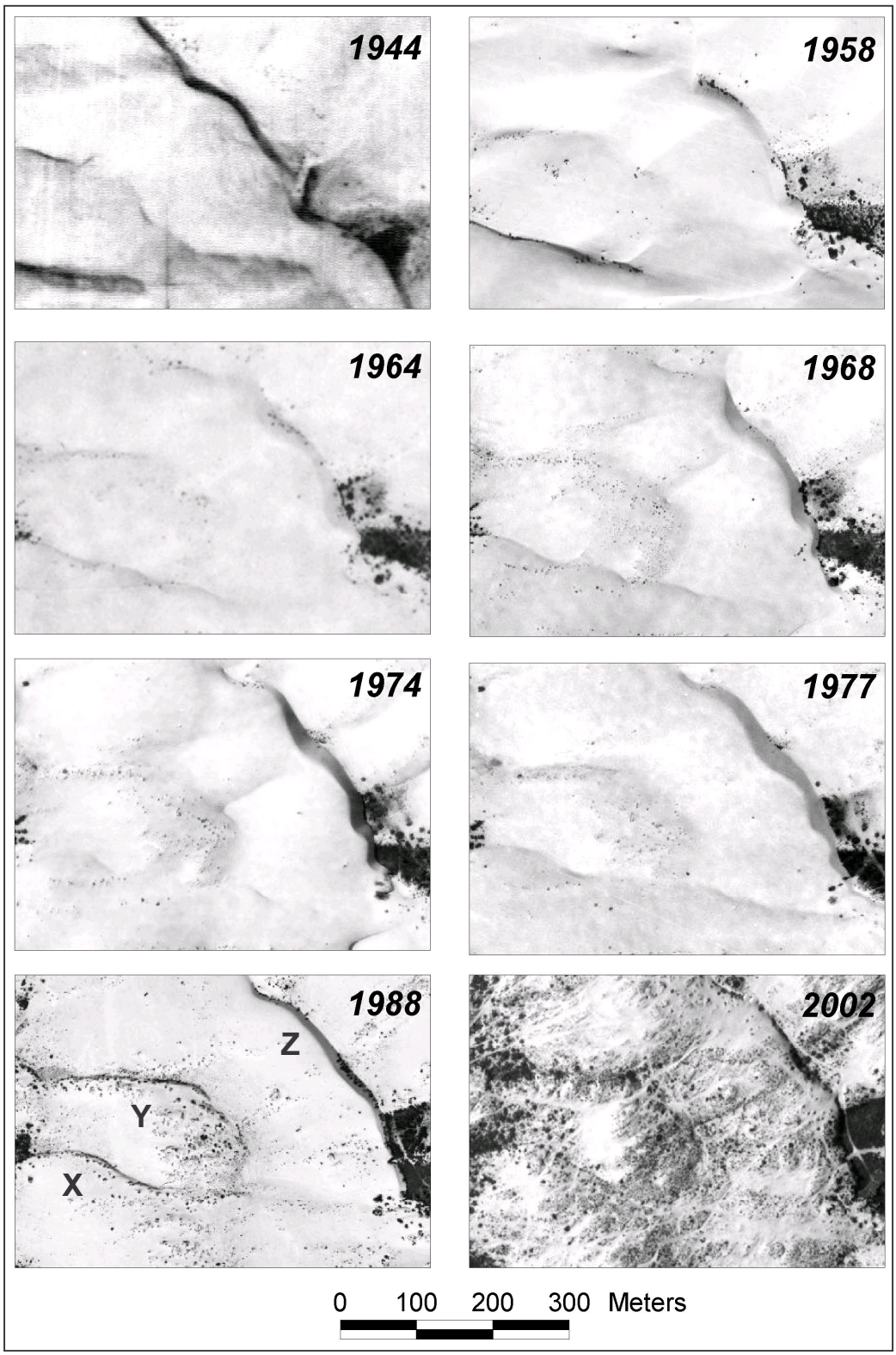


**Figure 4**: A time series of selected historical aerial photographs presenting the stabilization process of the dunes in the study area.

## 3.3 Dune movement analysis and vegetation cover from aerial photos

To determine the time when the dunes in the study area have started to stabilize, we have analyzed dune movement rates and vegetation cover from historical aerial photographs, as in chapter 4 in this thesis. This was done using historical aerial photographs from 1944 to 2002 over three dunes, shown in Figures 2 and 4. Vegetation cover was analyzed from the same photographs for the locations of the erosion pins.

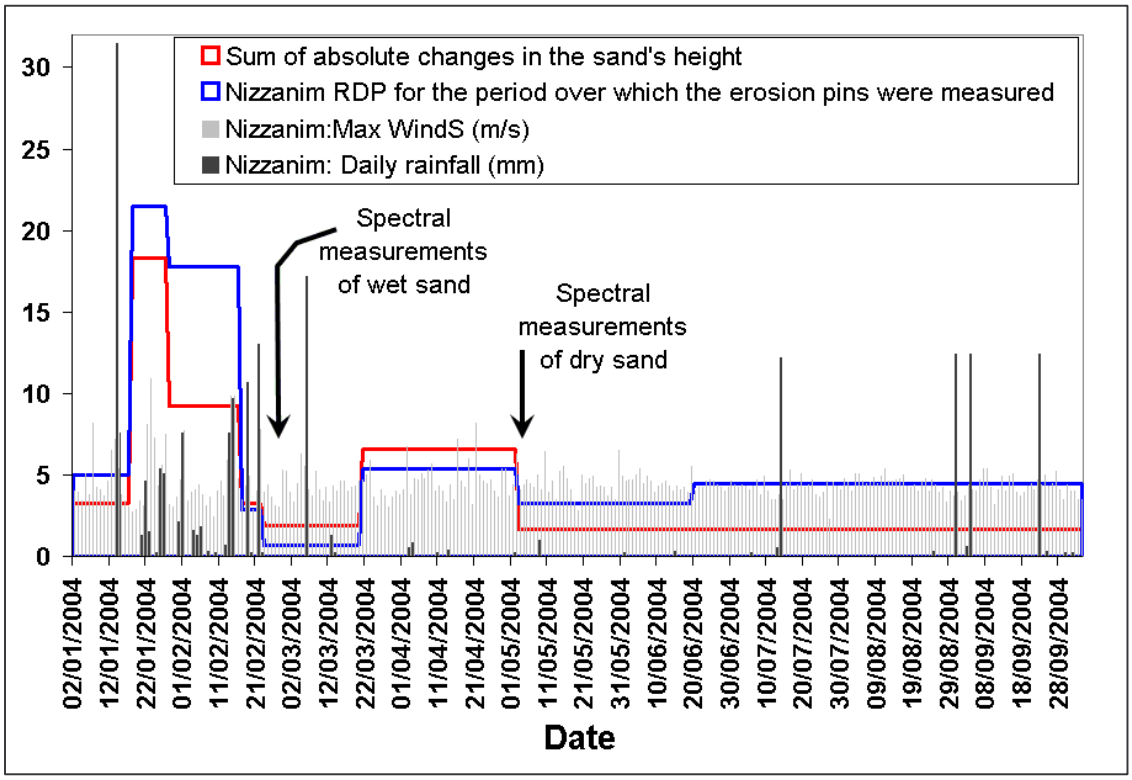


**Figure 5**: Temporal series of daily rainfall and daily maximum wind speed as measured in the Nizzanim meteorological station. Also shown are the average of the sum of the absolute changes in the height of sand as measure by the erosion pins (in mm.), and the corresponding Resultant Drift Potential (RDP) values (divided by 500 to match the scale of the chart) calculated from the wind data.

## 3.4 ASD measurements and calculation of indices

### 3.4.1 ASD measurements

Spectral measurements of the sand's surface and subsurface were performed both in situ and in the laboratory. This was done using an ASD field spectrometer (ASD, 2001) that covers the VIS-NIR-SWIR spectral region (0.4-2.5um) using a contact probe with

constant and self Tungsten illumination. For each sample, twenty spectral measurements were taken and averaged to present the spectral characteristics of the sample.
Following rainfall events (see Figure 5), we have measured the spectral properties of the surface and subsurface of the dunes in-situ using a Subsurface Biogenic Crust Sampler that was developed especially for this mission (SBCS, described below). This was completed in three days in the month of February 2004 ($16^{th}$, $20^{th}$ and $23^{rd}$), when the sand was still wet from the rain. On the $23^{rd}$ the surface was dried by the winds following the rain, so we have carefully wetted the surface ourselves. The wetness of the surface was a prerequisite for us, not only because it enhances spectral features of the biogenic crust, rather because it is necessary for using the SBCS.
In addition, sand samples were collected from the surface (0-1 cm.) and subsurface (below 2cm., where no biogenic crust exists) in the $2^{nd}$ week of the month of May 2004, during an event of a sharav (the flow of hot and dry air from deserts to the south of Israel – Alpert and Ziv, 1989). The last significant rainfall event before the sand was collected was about a month earlier, and the sand was already dry (see also Figure 5 for the climatic details). The crust samples from Sede Hallamish were measured with the ASD in the laboratory, once dry, and again one hour after wetting them.

### 3.4.2 Iron-oxide spectral indices

To estimate the free iron-oxide content of the sand we have used the following color indices, following Mathieu et al., 1998:

$$\text{Brightness Index, BI} = \text{sqrt}\ \{ (B^2 + G^2 + R^2) / 3 \} \quad (1)$$

$$\text{Colouration Index, CI} = (R - G) / (R + G) \quad (2)$$

$$\text{Hue Index, HI} = (2 * R - G - B) / (G - B) \quad (3)$$

$$\text{Redness Index; RI} = R^2 / (B * G^3) \quad (4)$$

$$\text{Saturation Index, SI} = (R - B) / (R + B) \quad (5)$$

Where R, G, and B represent the reflectance at the wavelengths of Red (693nm), Green (556nm) and Blue (477nm).

### 3.4.3 Chlorophyll and moisture spectral indices

Based on the chlorophyll absorption feature located between 670-685nm (Karnieli, 1997; Karnieli et al., 1999) and based on the same logic of the above color indices of Mathieu et al. (1998), we identified for our samples the location of the chlorophyll absorption peak at 680nm, with the following two wavelengths representing the "shoulders" of the absorption peak: 635nm and 710nm. Using these wavelengths for Equations 1-5 we then checked their ability to model biogenic crust content. Of these, the best spectral index was the following one (similar to Equation 2):

$$\text{Crust Red Slope, CRS} = (710\text{nm}-680\text{nm})/(710\text{nm}+680\text{nm}) \qquad (6)$$

Another index calculated was the Crust Red Absorption Depth, CRAD. This was calculated using the continuum removal method (Clark and Roush, 1984), that calculates the ratio between the observed reflectance at a certain wavelength (680nm in our case), and that predicted according to a linear line drawn between the two wavelengths representing the "shoulders" of the absorption peak.

To estimate which of these two indices is better in predicting chlorophyll concentrations, and to be able to correct for possible effects of variable moisture content on the spectral indices of the crust, we have taken 39 sand samples from the study area representing the gradient of chlorophyll values found there (including places with sand ripples to stabilized, places in the interdune area, and in different dune aspects). These were measured using the ASD in the laboratory in a dry state, and then at three different moisture contents. The moisture was determined by weighing the moist sample and then reweighing it following oven drying at 105$^{o}$C until reaching a constant weight. The chlorophyll *a* content was measured on 1 cm$^2$ samples, 1 cm thick, according to Vollenweider (1969)

As soil water content increases the reflectance diminishes (until a critical point; Liu et al., 2002), affecting the spectral features of other soil constituents (Whiting et al., 2004; Lobell and Asner, 2002; Karnieli et al., 1999). One of the strongest spectral absorption features of water is located at 1.9nm (Whiting et al., 2004; Ben-Dor et al., 1998). Based on the same logic of the above color indices of Mathieu et al. (1998), we identified for our samples the location of the water absorption peak at 1925nm, with the following two wavelengths representing the "shoulders" of the

absorption peak: 1860nm and 2140nm. Using these wavelengths for Equations 1-5 we then checked their ability to model moisture content. Of these, the best spectral index was the following one (similar to Equation 1):

$$\text{Sand Moisture Index; SMI} = \text{sqrt} \{ (A^2 + B^2 + C^2) / 3 \} \qquad (7)$$

Where A, B, and C represent the reflectance at the wavelengths of left shoulder of the water absorption feature (1860nm), its center (1925nm) and its right shoulder (2140nm), respectively.

### 3.4.4 Fine particles spectral indices

Clay minerals are characterized by absorption features near 2200-2300nm (Ben-Dor et al., 1998; Chabrillat et al., 2002). Based on the same logic of the above color indices of Mathieu et al. (1998), we identified for our samples the location of the clay absorption peak at 2209nm, with the following two wavelengths representing the "shoulders" of the absorption peak: 2133nm and 2225nm. Using these wavelengths for Equations 1-5 we then checked their ability to model the content of fine particles. Of these, the best spectral index was the following one (similar to Equation 4):

$$\text{SWIR Fine particles Index; FI} = D^2 / (F * E^3) \qquad (8)$$

Where D, E, and F represent the reflectance at the wavelengths of left shoulder of the clay absorption feature (2133nm), its center (2209nm) and its right shoulder (2225nm), respectively. To evaluate the performance of this SWIR spectral index for estimating the content of fine particles, we have used the same 42 sand samples used in chapter 2 of this thesis. From this set of 42 sand samples, an amount of 40 g. was taken to analyze the content of fine particles (silt and clay) in the soil, as described in Kidron (2001).

## 3.5 Subsurface Biogenic Crust Sampler (SBCS)

To measure the spectral reflectance of the sand and of the biogenic crust along a vertical micro-profile of about 2cm, we have constructed a Subsurface Biogenic Crust Sampler (SBCS), shown in Figure 6.

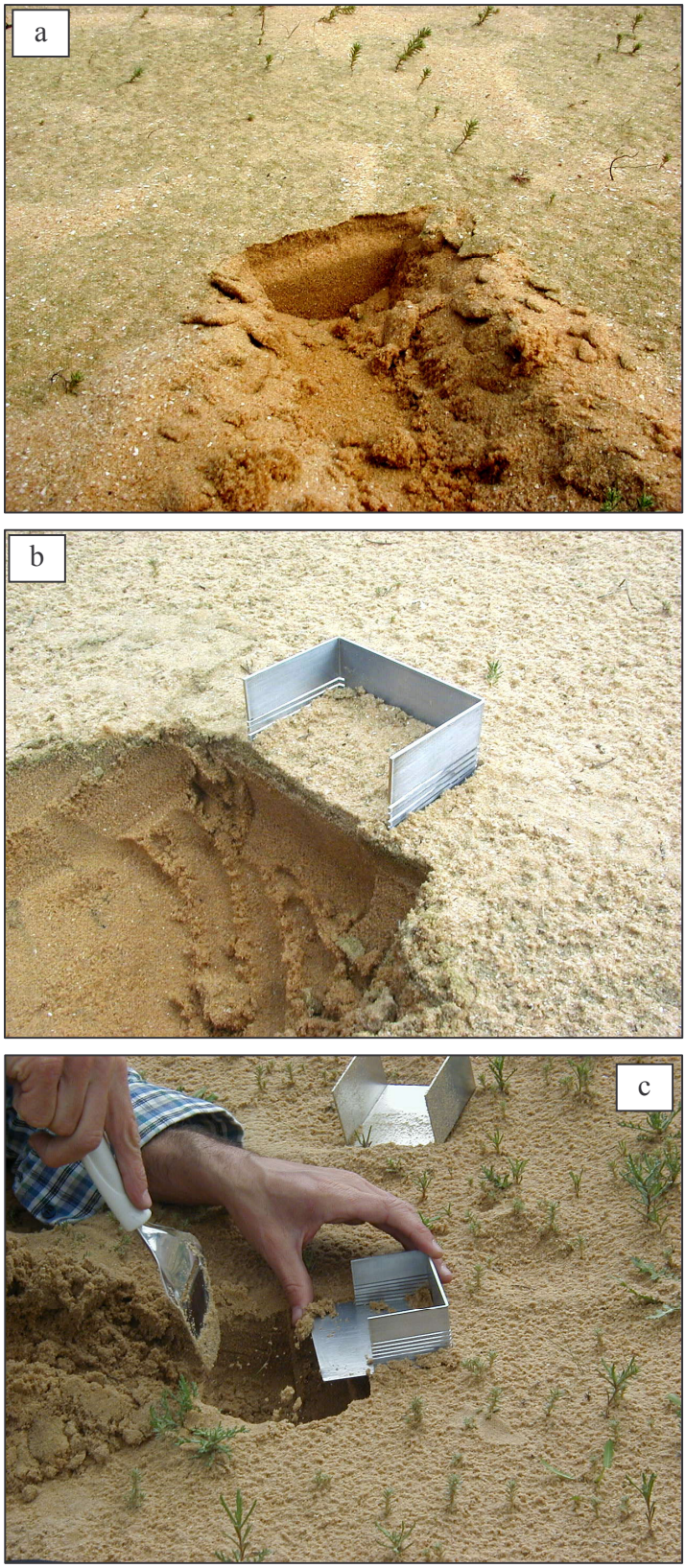


**Figure 6**: (a) Exposed biogenic crust by the wind; (b) Biogenic crust below a thin layer of sand grains. Also shown is the Subsurface Biogenic Crust Sampler (SBCS); (c) One of the steps in applying the SBCS for removing top layers and unveiling those lying beneath them. Notice the wetness of the sand, as seen from the surface shaped by rain drops. All photographs were taken during the second half of February 2004 when the in situ spectral measurements were performed.

The sampler has 1mm slots every 2mm through which a metal plate of a width less than 1mm can be inserted. The procedure for using the SBCS was the following: (1) Insert a sampler unit (without slots) into the wet sand, and then take it out; (2) Insert the sampler that has the slots on it into the opening that was created; (3) Dig away the wet sand in front of the sampler, so that the profile will be seen; (4) Measure the upper surface of the sand/crust using the ASD; (5) Insert a thin metal plate into the first slot located under the surface, and remove the sand/crust above the plate; (6) Remove the plate and measure the spectral reflectance of the surface revealed; (7) Repeat steps 5 and 6 again. This procedure was repeated until at least 5 spectral measurements were conducted for each of the sampled locations. If there were signs for the presence of biogenic crust at deeper layers, the above procedure was continued. These measurements were conducted at all of the 64 erosion pins.

### 3.6 Meteorological data

Meteorological data of rainfall, wind speed and direction, temperature and relative humidity were measured by the Nizzanim Field School meteorological station. This station is located at the edge of the Ashdod Dunes, about 2.8km from the coastline and is operated by the Ashkelon Metropolitan Union for the Environment. These data are recorded in periods of every 5 minutes, and were here analyzed at a temporal resolution of one hour. As the wind regime is one of the most important physical factors in determining the mobility of dunes (Tsoar and Werner, 1998; Tsoar, 2002), we have estimated the drift potential of the sand by the wind by applying the method developed by Fryberger (1979), using the Resultant Drift Potential (RDP) index.

## 4. Results

### 4.1 Surface stability

The dunes in the study area are stabilizing, as are the rest of the coastal dunes in Israel. This can be clearly seen in Figure 4 that presents historical time series of aerial photographs covering the study area. In an overall view, it can be seen that the dunes were quite active until 1977, and started stabilizing faster since then (in accordance with chapter 4 of this thesis). A quantitative analysis of the dune movement of the main three

dunes in this area, termed here as dunes X, Y and Z, is presented in Figure 7. Whereas during the 1950's the movement rate of these dunes was above 2.5 m/year, it decreased to less than 0.5 m/year by the late 1990s. The central dune in the study area (dune Y) was the first to stabilize - already during the 1960's, followed by dune X in the late 1970's, and dune Z in the late 1980's.

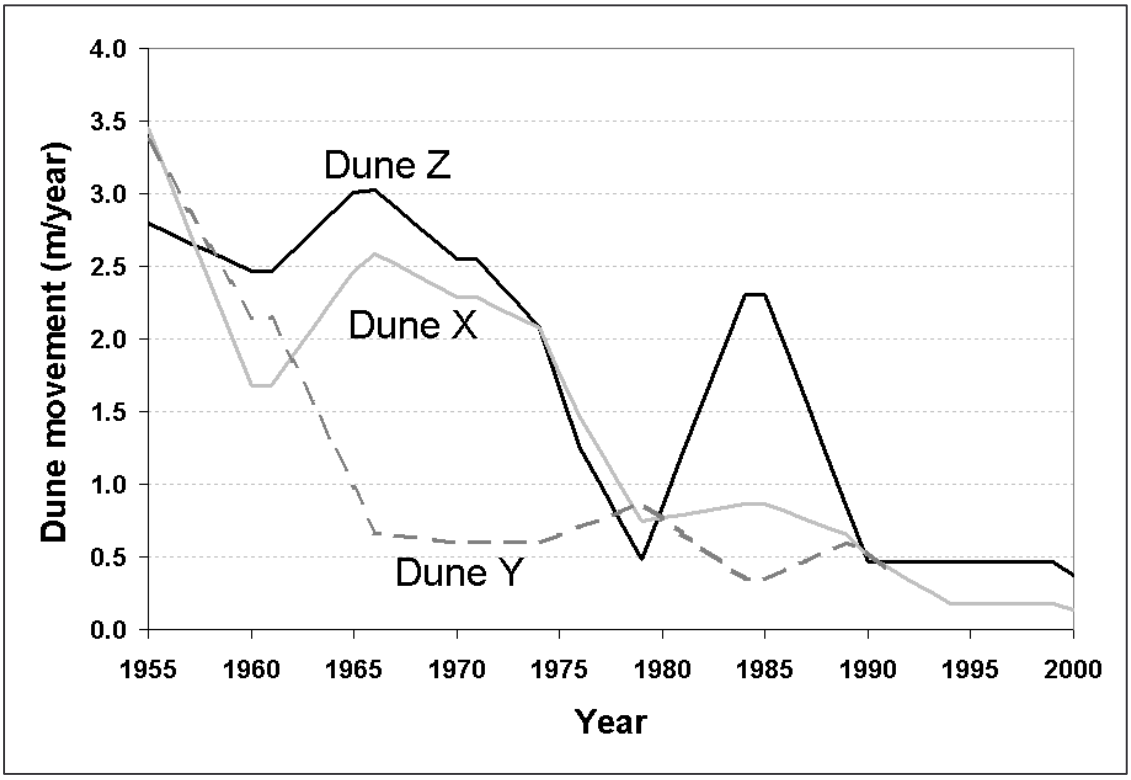


**Figure 7**: Rate of dune movement in the area analyzed between the years 1955-2000 as determined from time series of historical aerial photographs. The locations of the three dunes analyzed is shown in Figs. 2 and 4. No movement was detected for dune Y beyond 1990.

To analyze local processes of erosion and deposition of sand by the wind, we have analyzed the erosion pins data. In Figure 5 it can be seen that most of the movement of the sand occurred during the winter and spring months and is negligible during the summer. This is in accordance with Goldsmith et al. (1990) and with chapter 6 in this thesis. Locally it can be seen in Figures 2, 8 and 9 that there are three topographic factors influencing sand movement: elevation, vegetation cover and aspect.

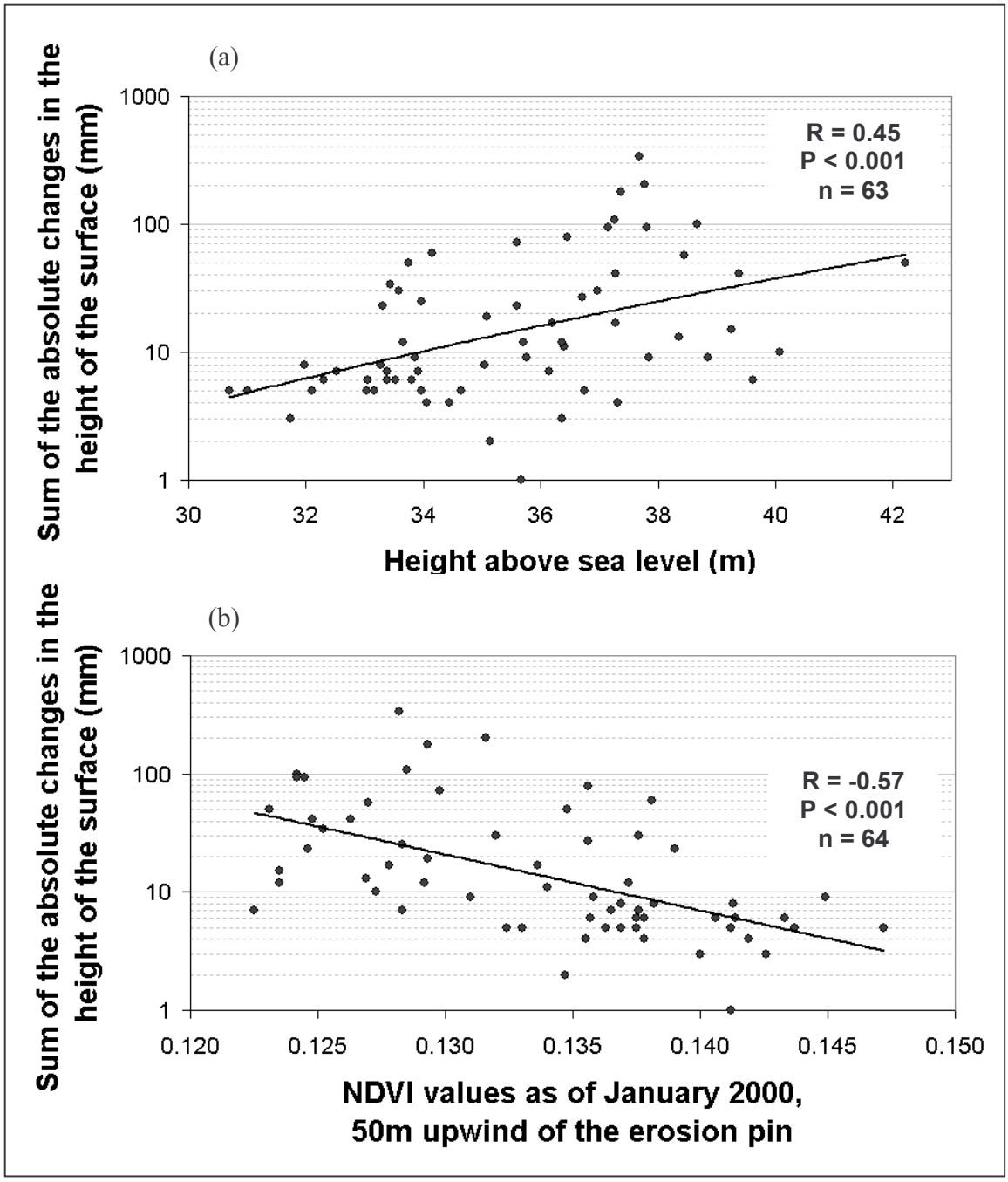


**Figure 8**: The influence of (a) the height above sea level at which the erosion pin was located, and (b) the NDVI values upwind (SW of the erosion pin), on the sum of absolute changes in the height of the surface, as measured between the months of January and March 2004, prior to the field spectral measurements of the crust.

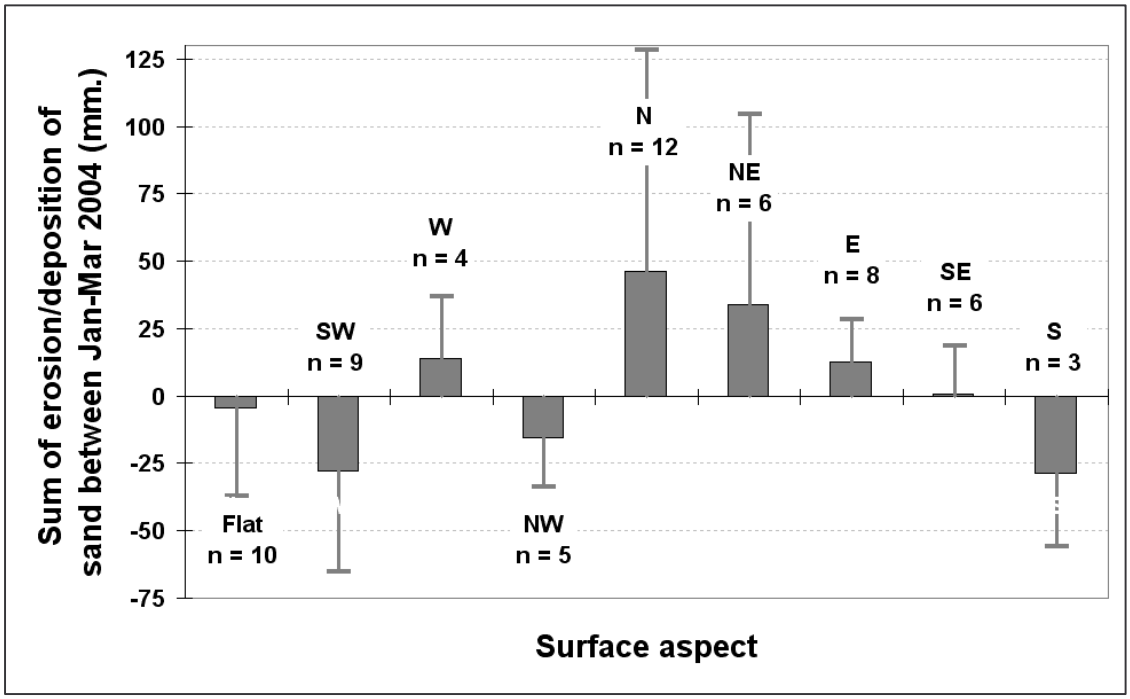


**Figure 9**: The influence of the surface aspect at which the erosion pin was located, on the sum of net changes in the height of the surface, as measured between the months of January and March 2004, prior to the field spectral measurements of the crust

Erosion pins that are located at higher places (e.g. dune tops) are under the influence of stronger winds, and therefore experience more erosion/deposition of sand (Figure 8a; $R = 0.45$, $p < 0.001$, $n = 63$). Erosion pins that are located downwind of higher vegetation cover (as estimated by NDVI or by SAVI) are under the influence of weaker winds (due to increased surface roughness), and therefore experience less erosion/deposition (Figure 8b; $R = -0.57$, $p < 0.001$, $n = 64$). The surface aspect angle with respect to the direction from which the strong wind blows, determines whether erosion or deposition will take place. In Figure 9 it can be seen that the wind facing slopes (SW and S) are indeed being eroded, whereas the sand is being deposited mainly on the slopes facing the N and NE. This is in accordance with the resultant drift direction of sand by the wind in the area as calculated in Chapter 6 of this thesis (see Figure 4 there) for the same period. The unexpected erosion in the NW facing slopes may be partly explained by wind tunnel effects.

We have then proceeded in analyzing the affect of changes in surface stability on the presence of crust, fine particles and free iron oxides.

**Figure 10**: The southern part of transect G: development of biogenic crust at the interface between a north-facing dune slope and the inter-dune area. Indication for subsurface flow or merely exposure of crust by wind? The photograph was taken on January 28th, 2004, from the ESE to the WNW.

## 4.2 The biogenic crust

### 4.2.1 Spectral characteristics of the biogenic crust

Indeed, the spectral reflectance obtained from crust covered areas exhibits a chlorophyll absorption at 680nm. In Figure 11 the spectral curves obtained at one of the erosion pin are presented, both when wet (in March 2004) in the five measured layers of the vertical micro-profile, and when dry (in May 2004) – at the surface and the subsurface. Notice that in both states of the sand (wet and dry), the chlorophyll absorption feature at 680nm is present at the surface and just below the surface (L-1), and disappears at the subsurface – indicating no subsurface crust presence below 1cm (and see also Figure 18 below).

The biogenic crust in the Ashdod dunes has a distinctive green color when wetted, as can be clearly seen in Figures 6 and 10. As the two spectral indices used to quantify the presence of crust, CRS and CRAD, were highly correlated ($R^2$ = 99.3%), and as the concentration of chlorophyll was better explained by CRAD then by CRS ($R^2$ = 73% and 71%, respectively), we have used the CRAD index. Figure 12 presents a scatter-plot of the CRAD values obtained in March 2004 (wet) with respect to those of May 2004 (dry). It can be clearly seen that there is high correlation ($R^2$ = 60%) between the CRAD values obtained from the wet micro-profile and the dry surface – two months later.

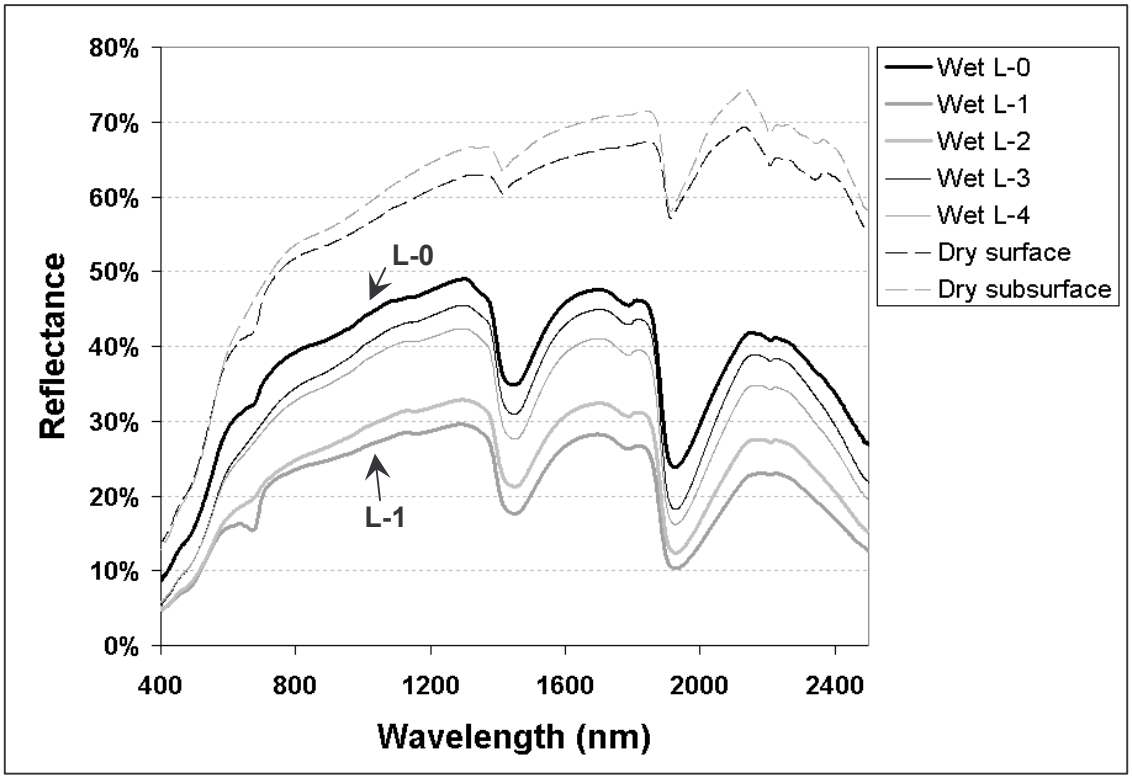


**Figure 11**: Spectral reflectance of the dunes' surface and subsurface at erosion pin A9 (ID 5009). Shown in the chart are both the spectral measurements taken in situ when the sand was wet at five different layers (from the surface L-0 downwards), and those taken from the dry samples of the surface and subsurface of the sand.

However, as no crust is present two centimeters below the surface, no correlation was obtained with CRAD measured from the sub-surface (CRAD values of 1 indicating no crust).

The values of CRAD were found to be negatively correlated with moisture content as can be seen in Figure 13, with higher moisture levels expressed in deeper absorption features by the chlorophyll (notice the slope factors of the three regression lines in Figure 13, representing different moisture level: 0.16%, 12% and 23%). The Sand Moisture Index (SMI) was found to explain more than 97% in the variability of moisture content in the sand samples (Figure 14).

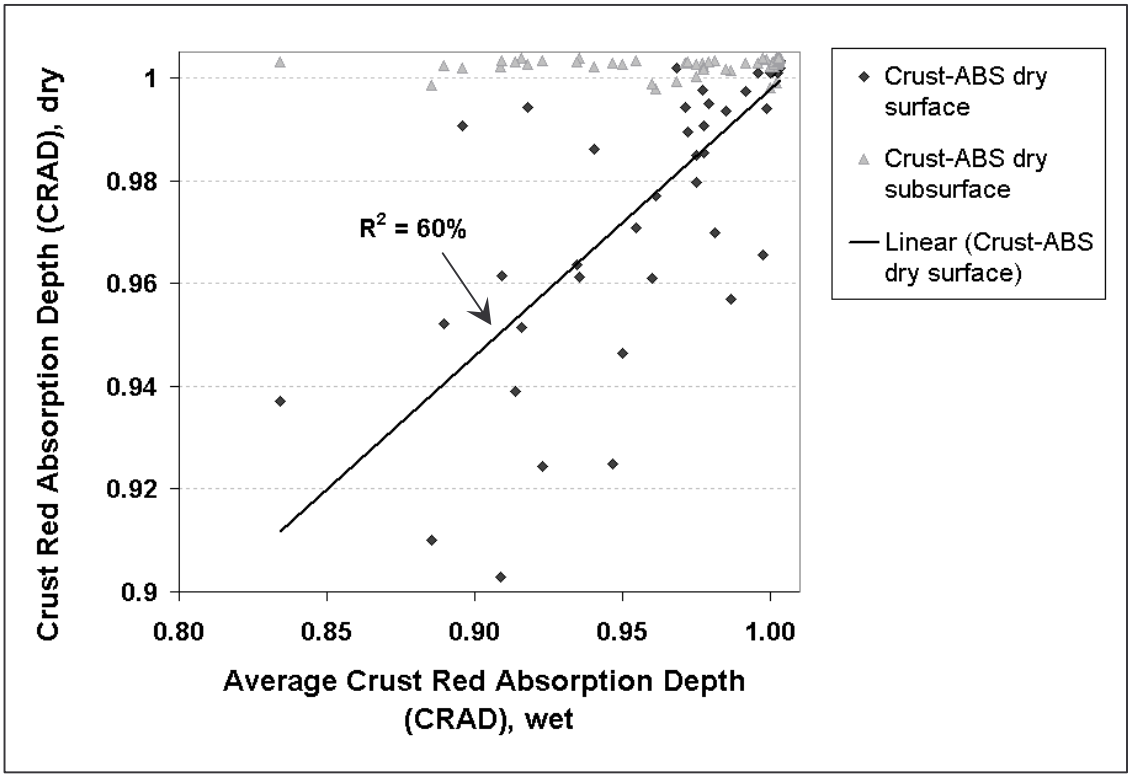


**Figure 12**: Scatter-plot showing the correspondence between the Crust Red Absorption Depth (CRAD) spectral index of crust presence, as averages from in situ measurements at five layers when the sand was wet in March 2004, compared with measurements performed in the lab for dry samples of sand collected in May 2004 both from the surface and the sub-surface.

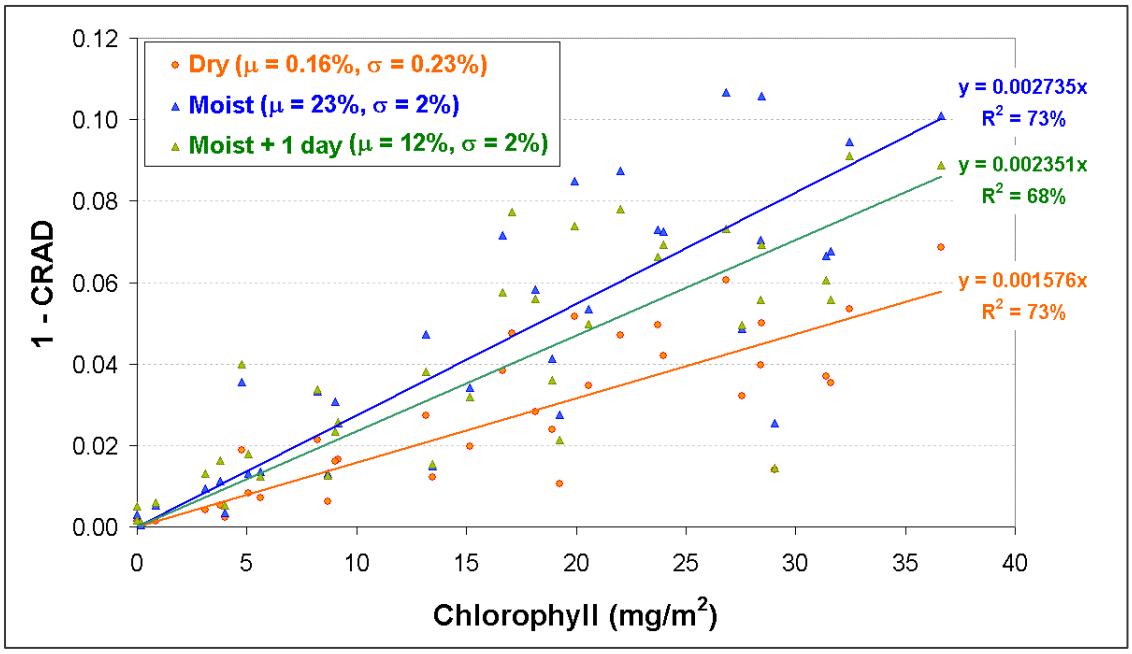


**Figure 13**: The correlation between the Crust Red Absorption Depth (CRAD) and the chlorophyll content at three moisture levels. In the legend are given the average (μ) and standard deviation (σ) values of the moisture content of the sand samples. Notice that the y-axis shows the values of (1 – CRAD), and not CRAD (thus values of 0 mean no crust).

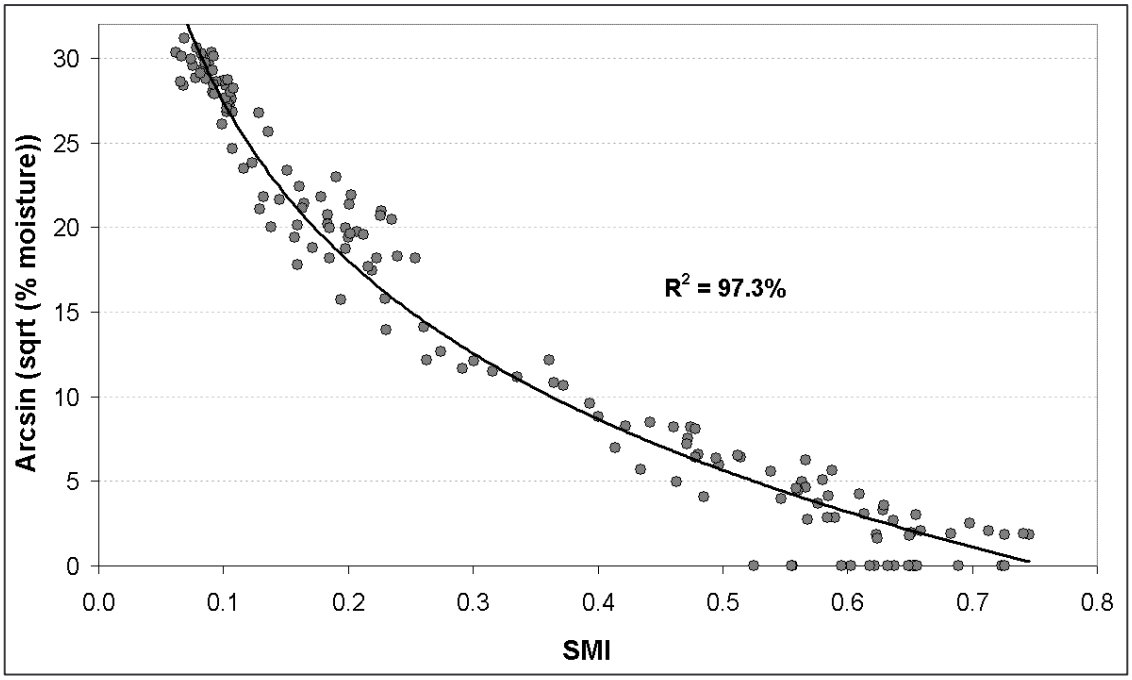


**Figure 14**: The correlation between the Sand Moisture Index (SMI) and the moisture content of the sand samples. Notice that the values moisture content values are transformed using arcsin ( sqrt (moisture) ).

To incorporate the MSI values with CRAD for determining the concentration of chlorophyll in a sand sample, the following steps were taken:

a) We first found the following empirical relationship between MSI values and the slope factor shown on the three regression lines in Figure 13:

$$\text{Slope factor} = 0.001406 * \text{MSI}^{-0.288397} \qquad (R^2 = 98\%, n = 3) \qquad (9)$$

b) We then found the following relationship between the chlorophyll content and the values of 1-CRAD for the dry samples:

$$\text{Chlorophyll (mg/m}^2) = 563.582 * (1 - \text{CRAD}) \qquad (R^2 = 69\%, n = 39) \qquad (10)$$

c) Incorporating Equations 9 and 10 with the regression line of the dry samples shown in Figure 13, we obtained the following relationship:

$$\text{Chlorophyll} = (1 - \text{CRAD}) / ((0.001406 * \text{MSI}^{-0.288397}) / 0.001576) * 563.582 \qquad (11)$$

d) Equation 11 may be them rewritten as follows:

$$\text{Chlorophyll (mg/m}^2) = (1 - \text{CRAD}) / (0.001583 * \text{MSI}^{-0.288397}) \qquad (12)$$

To compare the spectral characteristics of the biogenic crust found in different dune areas in Israel, we have chosen to compare it with that of the much researched cyanobacterial crust found in the Nizzana dunes, which exhibits distinctive reflectance features in the blue region of the visible spectra (Karnieli and Sarafis, 1996). The biogenic crust found over the Ashdod dunes (comprised mostly of green algae) differs in its spectral features from the cyanobacterial crust of Nizzana, as can be seen in Figure 15. In Figure 15a the reflectance curves of biogenic crust and reference bare sand from both the Nizzana and the Ashdod dunes are presented. To facilitate the comparison between the two, we have calculated ratio spectra of the biogenic crust, with respect to the bare sand reference.

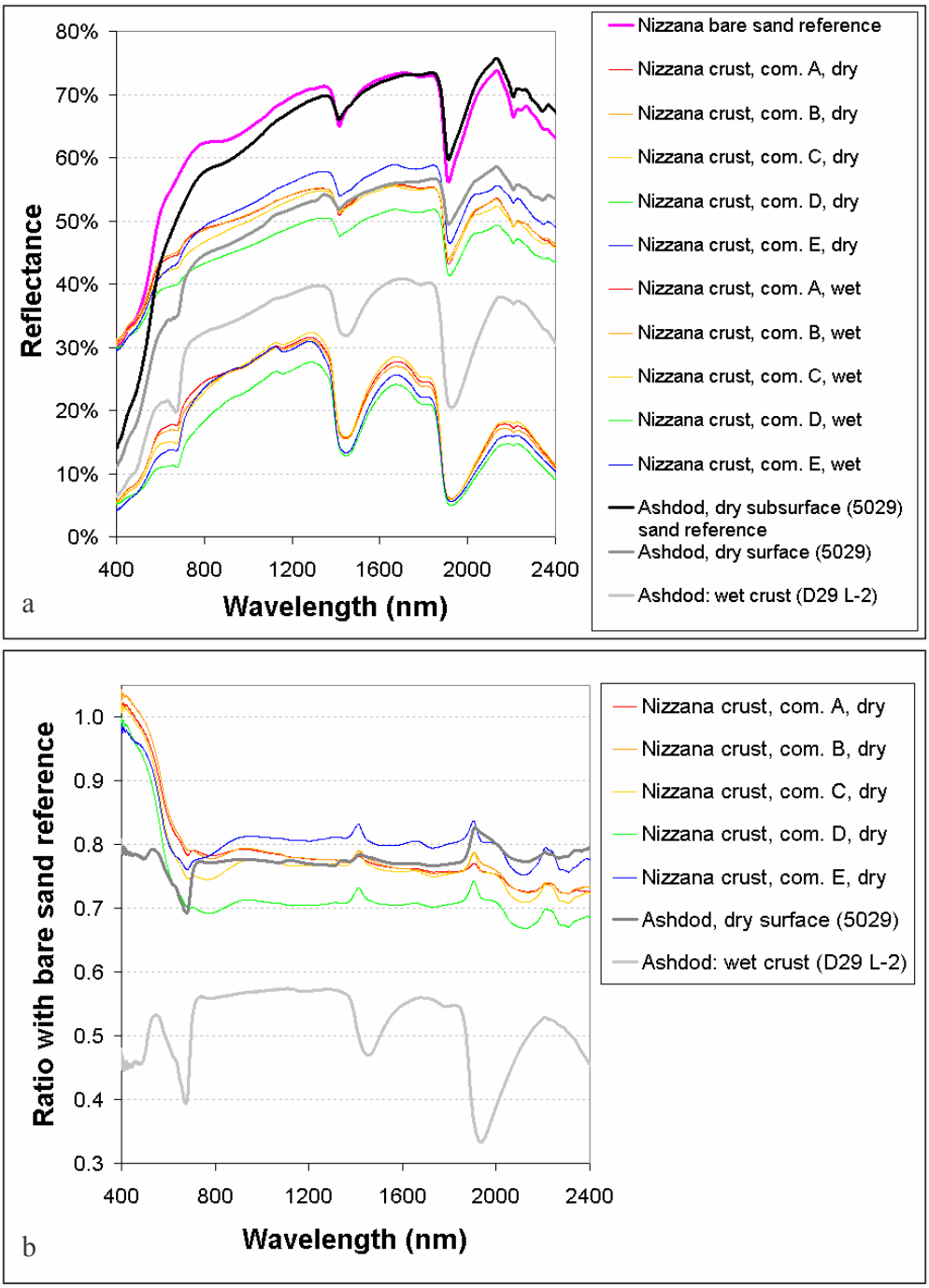


**Figure 15**: A comparison between the spectral properties of biogenic crust in Nizzana and Ashdod Dunes: (a) Reflectance spectra; (b) Ratio spectra with respect of dry bare sand reference from each location, respectively (The ashdod spectra were divided by the dry subsurface spectra).

In Figure 15b the ratio spectra are shown, and it can be clearly seen that the Nizzana samples exhibit a rise in the reflectance towards the shorter wavelengths (towards the blue), whereas in the Ashdod sample the second chlorophyll absorption feature at 490nm is present, and there is no rise towards the blue. This enables us to differentiate between cyanobacterial crust and the green algae biogenic crust.

Therefore, to quantify the presence of biogenic crust, we have used both the CRAD and the MSI indices, and not a spectral index similar to the one suggested by Karnieli (1997), which relates to the blue region.

### 4.2.2 Spatial distribution of the biogenic crust

The spatial distribution of the crust was therefore analyzed using Equation 12 that calculates the concentration of chlorophyll taking into account both the CRAD and the MSI indices. This concentration of chlorophyll was studied with respect to the surface aspect and to the surface stability (erosion/deposition of sand).

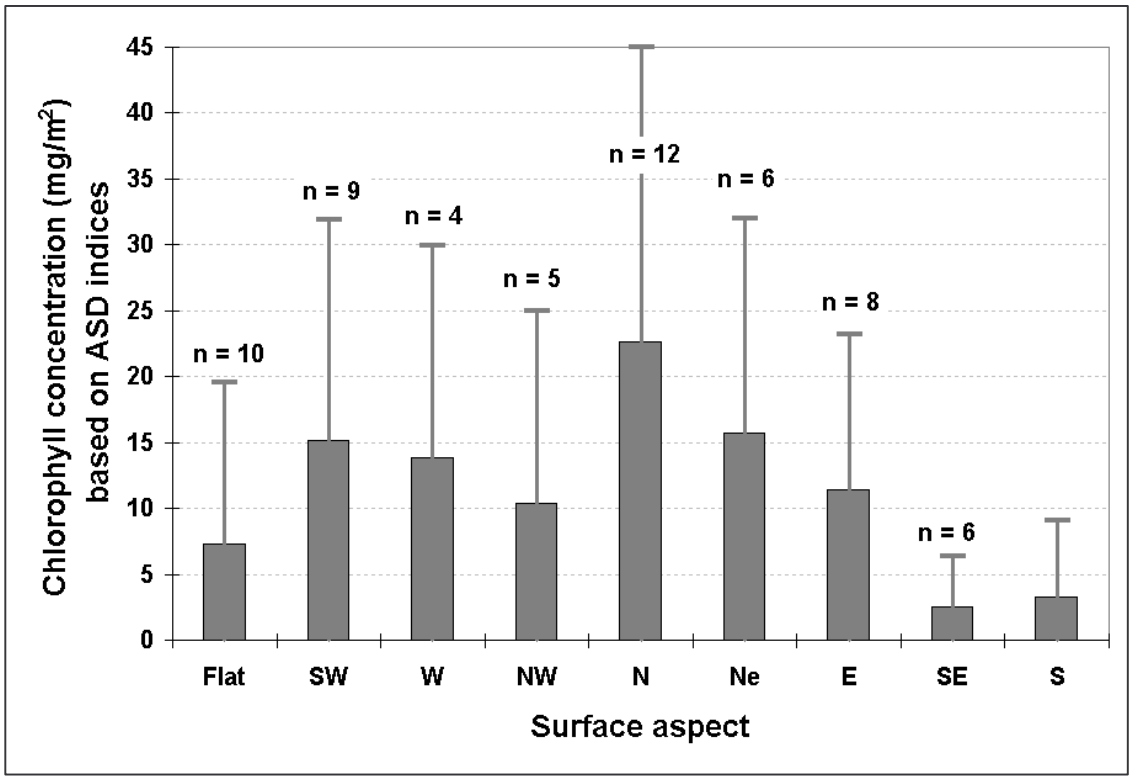


**Figure 16**: Average presence of biogenic crust (along the vertical micro-profile), as calculated using equation 12 based on the spectral indices of CRAD and MSI, with respect to the surface aspect

Figure 16 presents the chlorophyll values with respect to the aspect, and it can be seen that there is a clear preference of crust development in the north-facing slopes, with much less crust presence in the south- and southeast-facing slopes. This is in accordance with Kidron (2001). However, the factor that has most of the affect in determining the development of the crust is the amount of erosion/deposition of sand by the wind, presented in Figures 17 and 18 (Figure 18 'breaks' Figure 17a for each of the surface and subsurface layers separately). From these figures it can be concluded that in places with high deposition rates (over 8 mm for a period of three months) or high erosion rates (over 8 mm for the same period), almost no crust was present. From Figure 18 the vertical distribution of the biogenic crust is also apparent, wherein the maximum concentration of the algal crust is usually at the first layer beneath the surface (L-1), where it is covered by some grains of sand (see also in Figure 11 above). However, the response of the system to erosion or to deposition is not symmetric, as the peak in the presence of crust was not found in the most stable places (between -2mm erosion and 2mm deposition) when all data was included, rather in the places that underwent slight deposition (2-8mm; see Figure 17a); however this difference was not statistically significant. If erosion and/or deposition events of up to 2mm are considered as possible noise due to measurement errors, then the expected pattern of maximum presence of crust in the most stable areas is obtained (Figure 17b). Nonetheless, biogenic crust can withstand low rates of sand deposition, apparently due to its ability to move vertically (see Chapman, 1976). In Figure 6b a photograph of crust covered by sand grains is given. That this situation is very common, can be seen in Figure 18, which emphasizes the evidence that crust presence is always greater at the immediate subsurface, and not on the surface itself. The lower presence of crust in eroded places may indicate that the development of crust is less adapted to places undergoing erosion than to places experiencing deposition of sand. However, to a certain degree, the biogenic crust is able to stabilize the surface. This can be seen in the photographs given in Figures 6a and 10, where the biogenic crust is seen to be exposed on the surface with no sand grains. Furthermore, whereas ripple marks characterized the non-crusted surfaces during high velocity winds, they were not observed on most encrusted surfaces. above it. The sand above the biogenic crust was carried by the wind, however it was apparently not strong enough to break the crust directly, or through the impact of the hitting sand grains.

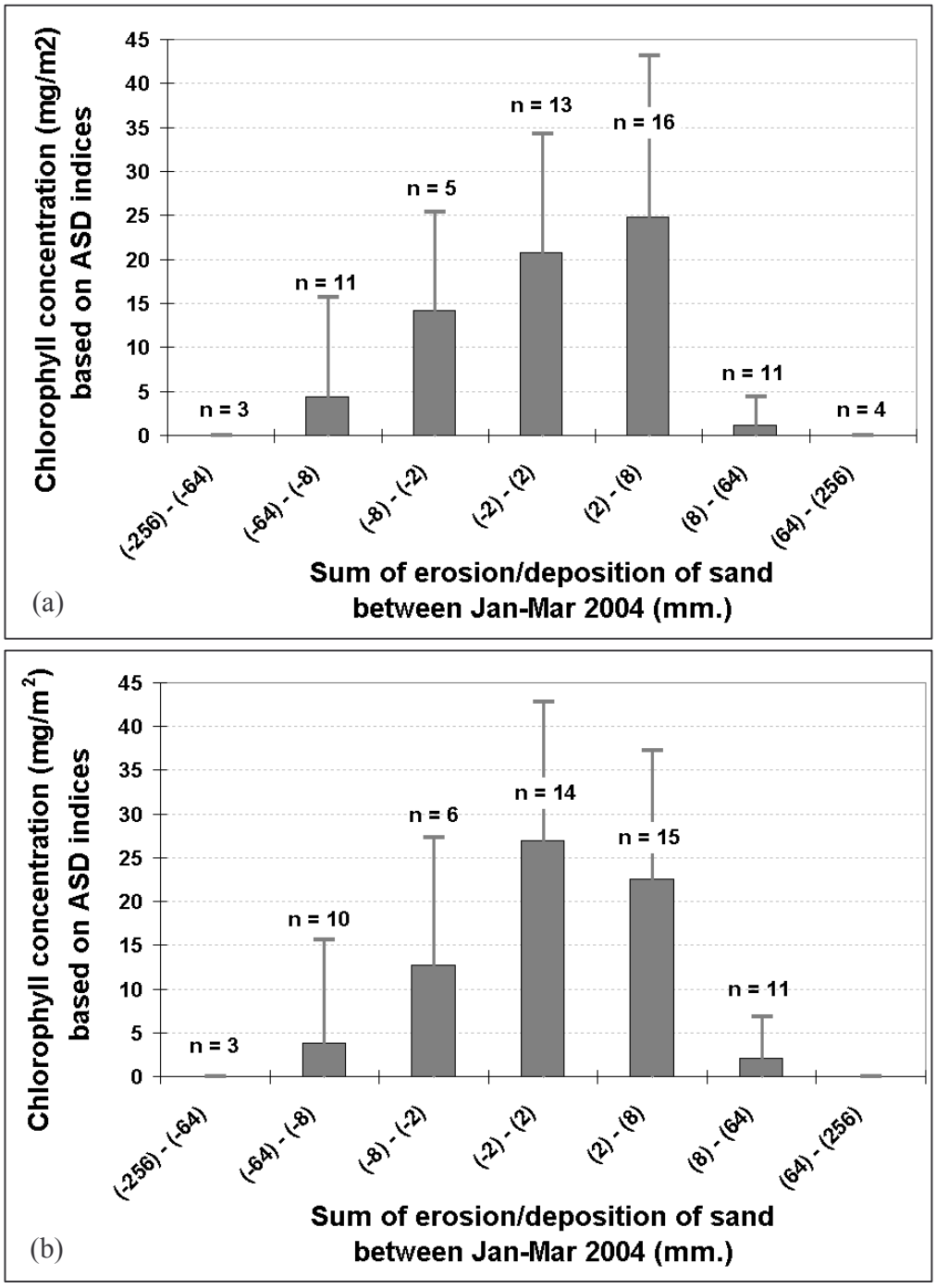


**Figure 17**: Average presence of biogenic crust (along the vertical micro-profile), as calculated using equation 12 based on the spectral indices of CRAD and MSI, with respect to the erosion/deposition of sand in January-March 2004: (a) net values of erosion/deposition of sand; (b) net values of erosion/deposition of sand considering only events greater than 2mm.

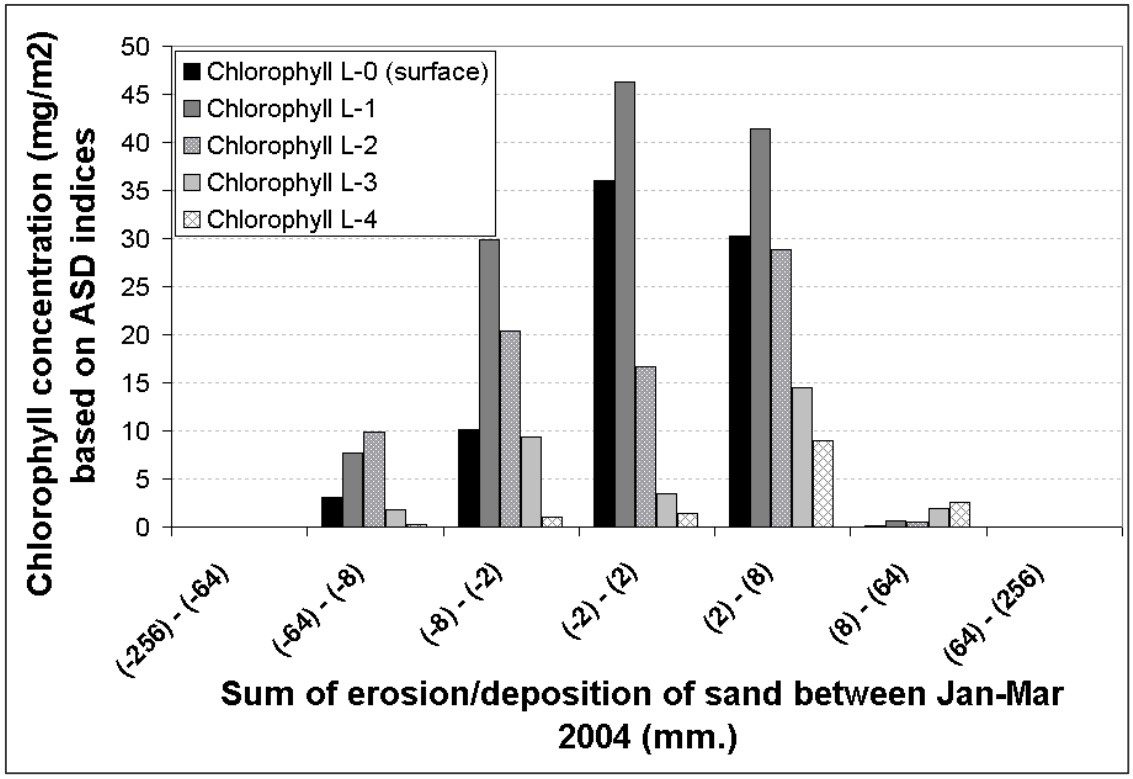


**Figure 18**: Average presence of biogenic crust (along the vertical micro-profile), as calculated using equation 12 based on the spectral indices of CRAD and MSI for each of the surface and subsurface layers separately, with respect to the erosion/deposition of sand in January-March 2004.

The two factors of sand erosion/deposition and surface aspect act jointly in influencing the crusts' presence. An example to this can be seen in the photograph shown in Figure 10, where the crust is exposed in the interface between an active north-facing slope and the inter-dune area. This may be because of wind removing the sand grains that covered the crust there, or may indicate the role of subsurface flow moistening sand in this area (Rutin, 1983; Kidron et al., 2000).

## 4.3 Spatial differences in the rubification process

To estimate the degree of the rubification process in the area, we have calculated several spectral color indices (Equations 1-5). However, we first wanted to evaluate if the values of these indices are influenced by the presence of crust. To this end, we have calculated the correlation between the CRAD index and all the five color indices, for both the dry

surface measurements, and for the average of the five layers from the wet micro vertical profile. The results are shown in Figure 19.

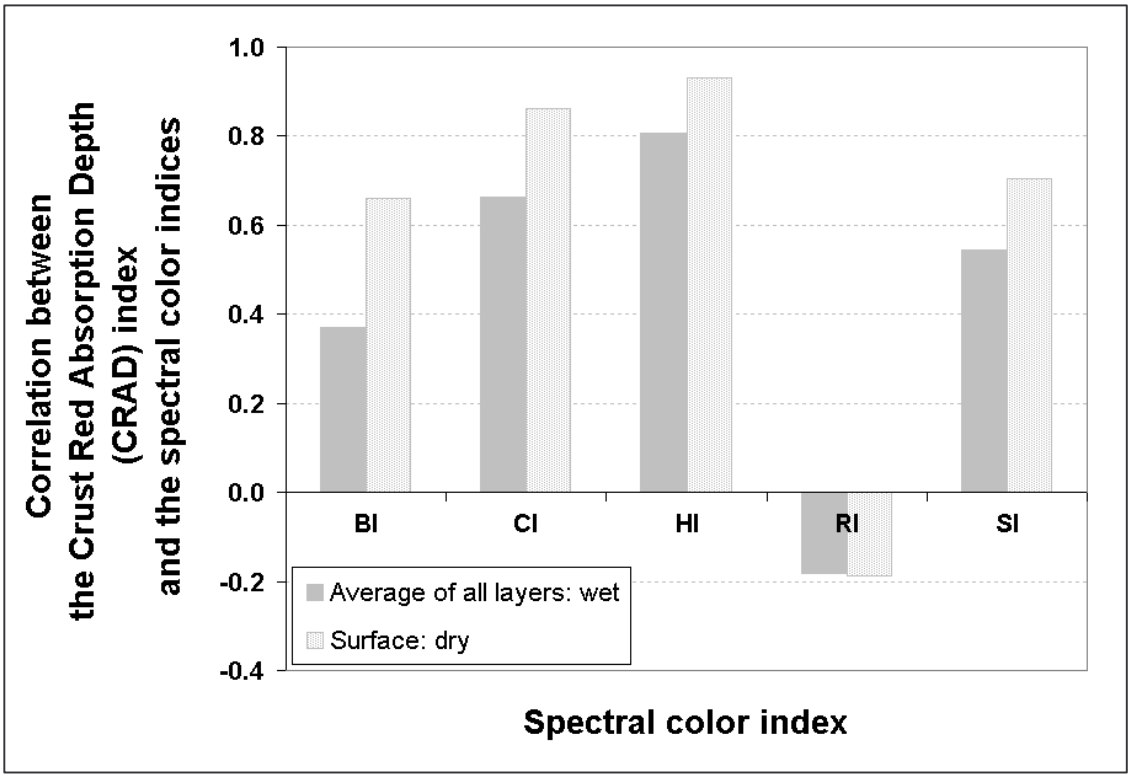


**Figure 19**: Correlation coefficient values between the spectral index of the crust (CRAD) and the spectral color indices, for the wet and dry sand measurements.

It can be seen that in both cases, the Redness Index (RI) showed very low negative correlation with CRAD. All other indices (and especially CI and HI) exhibited more significant and positive correlation with CRAD. In previous studies (Chapter 2 in this thesis; Ben-Dor et al., 2005) it was shown that the RI was also superior to the other indices both when compared to the content of free iron-oxides extracted in the laboratory, when correlated with the distance from the coastline, and the most stable when compared between sensors (ASD, CASI and a digital camera).

The values of RI found over on the surface over the transects presented in Figure 2 range between 28 and 41, indicating fine iron oxides content of up to 0.04% using models derived in Chapter 2 of this thesis (Figure 4a there) and Ben-Dor et al. (2005; Figure 8).

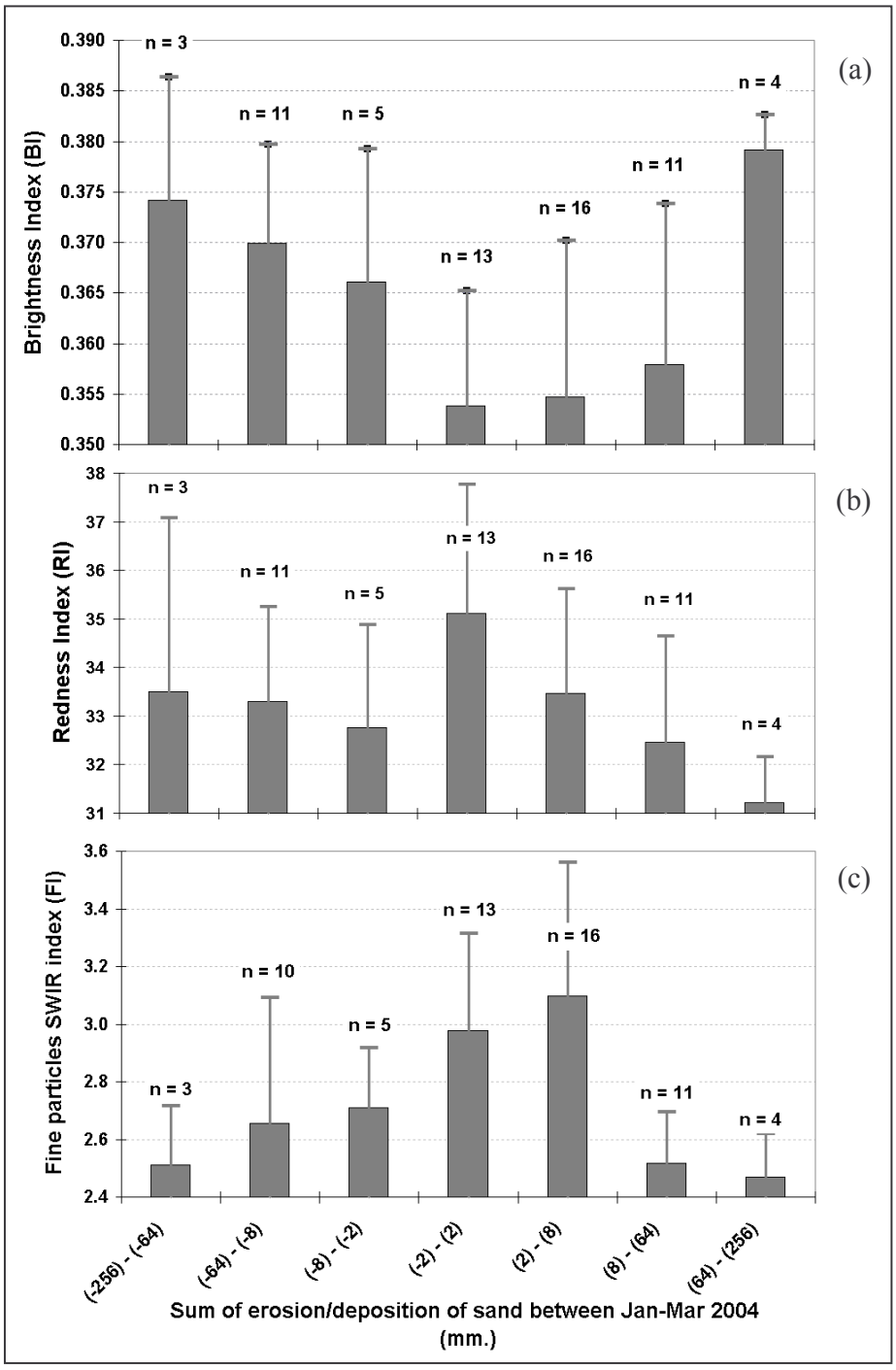


**Figure 20**: Average properties of the dunes' surface with respect to the erosion/deposition of sand in January-March 2004: (a) albedo, (b) content of free iron-oxides, as indicated by the Redness Index (RI), (c) content of fine particles, as indicated by the SWIR fine particles index (FI).

Relying on this, Figures 20a and 20b present the degree of rubification of the dry subsurface at 2cm (where no biogenic crust exists, as measured in May 2004) with respect to the surface erosion/deposition. For both the RI and the BI, it can be seen that maximum rubification (highest RI values and lowest BI values) occurs in the stable places, those without erosion/deposition of sand. No such correlation was found between either color index and the surface aspect.

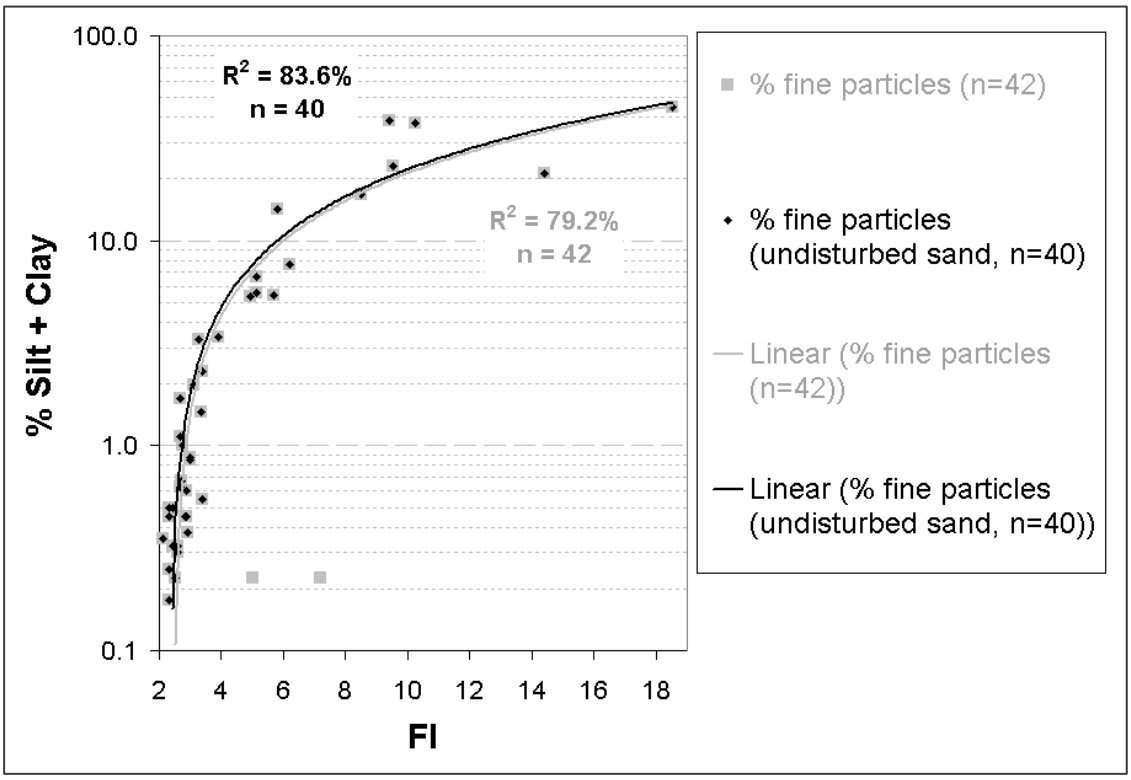


**Figure 21**: The correlation between the SWIR fine particles spectral index and the content of fine particles.

## 4.4 Spatial differences in the content of fine particles

Figure 21 presents high correlation between the SWIR fine particles index (FI) and the content of fine particles, reaching a value of $R^2$>83% when only the 40 undisturbed sand samples are included in the analysis. The surface values of FI found for the transects presented in Figure 2 range between 2 and 4, indicating fine particles content of up to 4% (according to the model in Figure 21). The spatial pattern of the fine particles at the surface (as measured in May 2004) is well correlated with that of the biogenic crust (R=0.58 between FI and the chlorophyll content). As can be seen in Figure 20c, the

highest content of fine particles is found not as might be expected on the most stable places, rather in those places where there is moderate sand accumulation; however this difference was not statistically significant, and therefore we cannot conclude that the highest content of fine particles is not in the most stable places. This pattern is the same as we found for the presence of biogenic crust, presented in Figure 17a, and did not change when omitting possible measurement errors from events when up to 2mm of erosion/deposition was recorded.

## 5. Discussion

Several sub-processes may be identified in the process of sand dunes stabilization: the development of vegetation cover, an increase in the amount of fine particles, the development of biogenic soil crusts, and the rubification of the sand. Each one of these sub-processes operates on a different spatial and temporal scale. We have used field spectral and geomorphologic methods to analyze the development of biogenic soil crust, content of fine particles and the rubification of the sand over a semi-stabilized dune in the coastal dunes of Ashdod.

The stabilization process of Israel's coastal dunes has started after the establishment of the state of Israel, in 1948. The dunes in our study area however have started stabilizing only in the late 1960's – late 1980's. Locally, we have shown that the rates of erosion and deposition of sand are influenced by the same factors that affect wind flow: the topography (relative height and aspect) as well as the vegetation cover. These findings, calculated here for a small "basin" of three dunes, resemble our findings regarding the factors influencing the spatial variability in the aerodynamic roughness length ($Z_0$) and annual rates of erosion and deposition of sand for the whole area of these coastal dunes (Chapters 5 and 6 in this thesis).

In this short time period of three decades, biogenic soil crusts have successfully established themselves in the more stable parts of the dunes, and even differences in the presence of the crusts are now evident when comparing north- and south-facing slopes. Biogenic crusts are known from the literature to be able to develop very fast (in two years) on stabilized dunes (Littmann, 1997). We have demonstrated here that both biogenic crust and a higher content of fine particles formed in a short time period, most

probably much less than the 30 years over which the dunes in this study area have started stabilizing.

The presence of biogenic crusts, and in this case of green algae, was easily quantified by us in the field, using a field spectrometer, both when the crust was wet (following rainfall) and even when it was dry (during the spring season). For green algae this was done utilizing the chlorophyll absorption feature at 680nm. In contrast with cyanobacterial crust, green algae do not possess phycobilin pigments that have characteristic features in the blue band, so it is more difficult to distinguish between vegetation and green algae from airborne sensors, than is the case with cyanobacterial crust. These may be differentiated however using images taken at different times, utilizing the phonological differences between them and especially the quick response of biogenic crusts to wetting by rainfall (see Schmidt and Karnieli, 2000; Karnieli, 2003).

In contrast with our understanding of the formation of biogenic crusts, less is known regarding the development rate of the rubification process in natural conditions. We have therefore compared several spectral indices to quantify the free iron oxides content, and found that the redness index (RI) performed better than all other spectral color indices (see also chapter 2 in this thesis; Ben-Dor et al., 2005). In addition the RI values were found to be almost independent of the values of the spectral crust index used (CRAD), therefore increasing its indicative power, as it is not affected by the presence of biogenic crust.

The results of this study indicate that the development rate of free iron-oxides coating on the sand particles (as evident from their color) is much slower than that of the biogenic crust cover and of fine particles content for the following reasons:

1. The variability explained by the surfaces' stability in the chlorophyll content is much higher than that explained for the iron-oxides content (as indicated by the RI), 64% ($p<0.001$, $n=63$) and 17% ($p<0.001$, $n=63$), respectively (see Figure 22). The explained variability in the content of fine particles (as indicated by the FI) is intermediate between the above, reaching 26% ($p<0.001$, $n=63$).
2. The presence of crust is higher in north-facing slopes than in the south-facing slopes, whereas such a pattern was not found for the sand's color or for the content of fine particles.

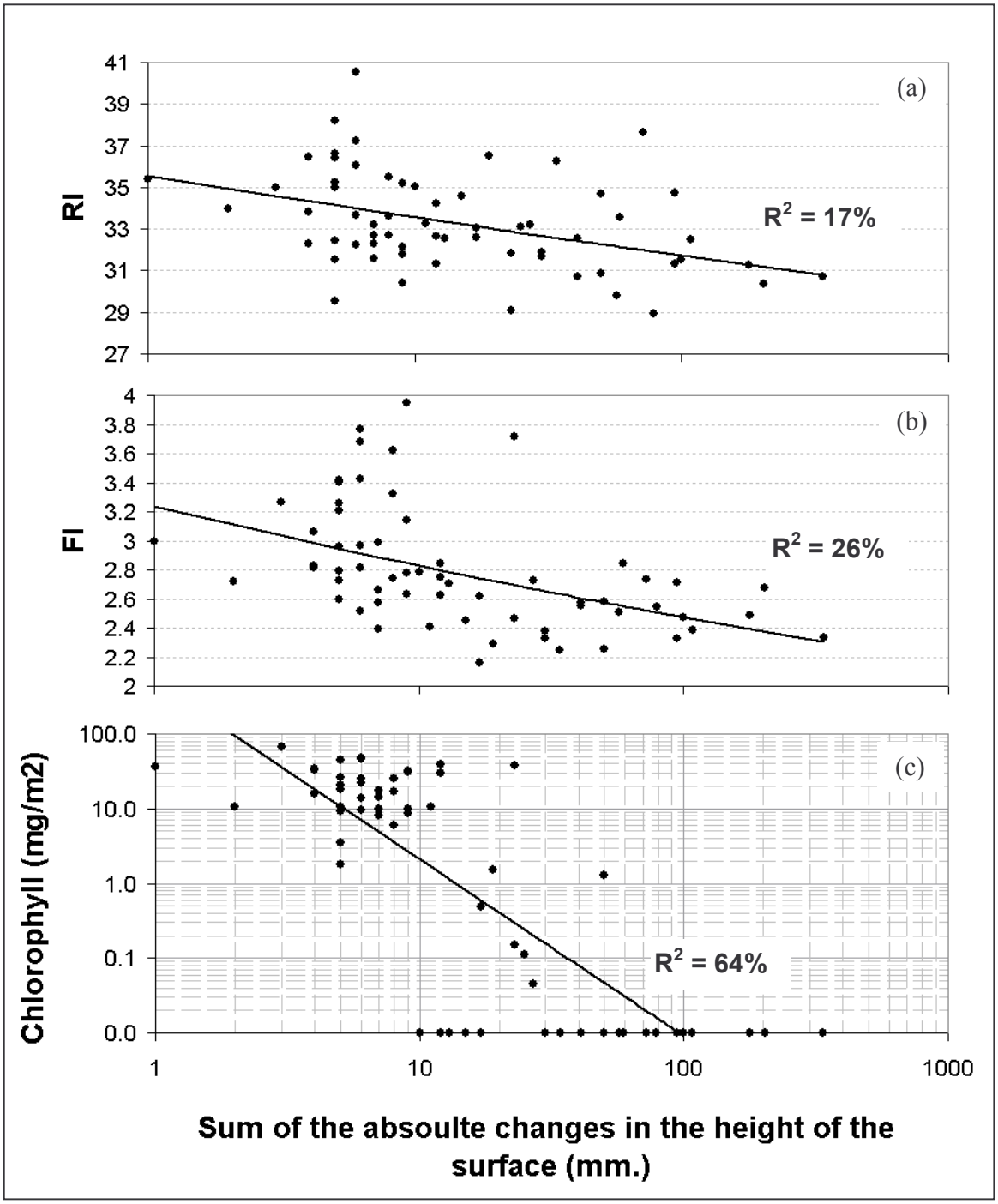


**Figure 22**: The correlation between the dunes' surface stability and the following spectral indices: (a) free iron-oxides content (RI), (b) fine particles content (FI) and (c) the chlorophyll content. Notice that the more stabilized is the dune, the higher will be its content of free iron oxides, fine particles and the presence of biogenic crust.

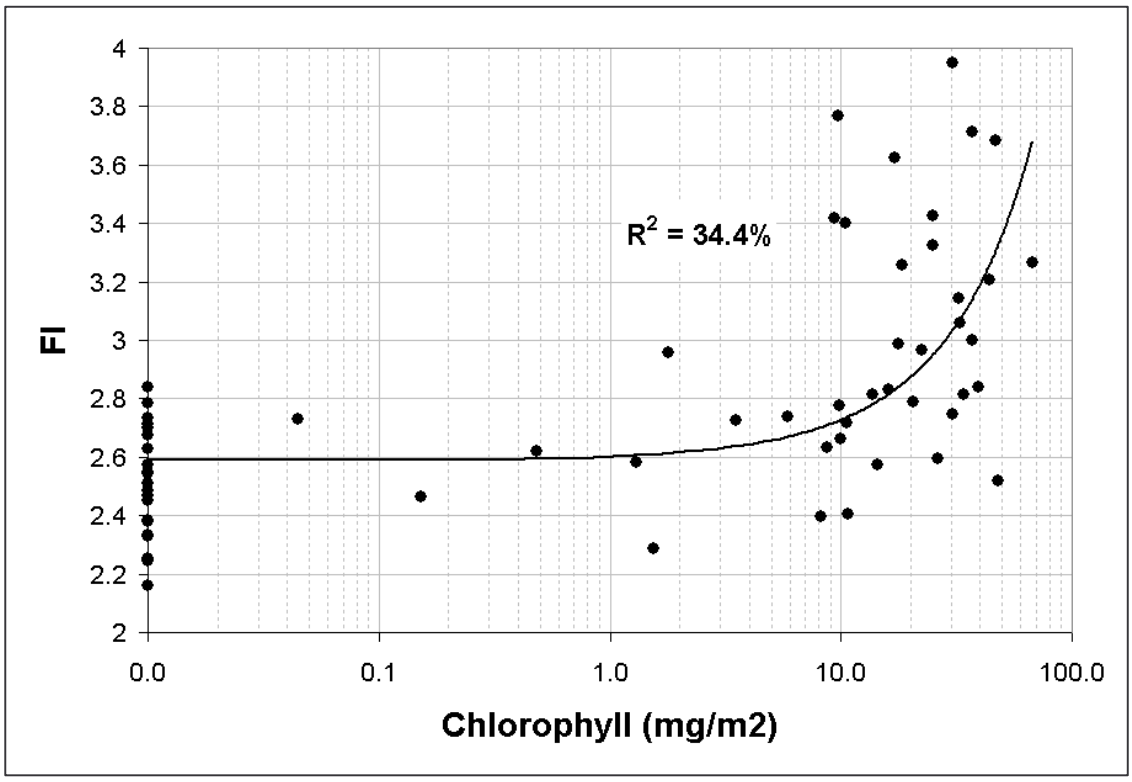


**Figure 23**: The correlation between the chlorophyll content and spectral index of fine particles content.

Biogenic crust was found to develop in placed where the sum of absolute changes in the height of the surface were less than 25mm over a period of about two months during the wintertime, when most sand movement takes place (Figure 22c). The chlorophyll content found there was mostly above 8mg/m$^2$. No correlation was found between the rubification level and the chlorophyll content, probably due to the much longer time scales over which the color of sand changes (decades) with respect to the quick formation of biogenic crust and fine particles (months – several years). Although the spectral features of the crust may react over an even very shorter time-scale (minutes-hours) to wetting, this effect was accounted here by modeling the effect of moisture content on the chlorophyll absorption feature. The content of fine particles was found to be related with chlorophyll content ($R^2$ = 34%; Figure 23), and in places where the chlorophyll content was above 8mg/m$^2$, the content of fine particles increased dramatically (Figure 23). This may be stated also in the other direction: in places where FI was higher than 3 (which is equal to a content of fine particles above 2%; note that this is below the threshold of 4-

5% given by Danin, 1983, for sandy desert in Sinai and Israel), the chlorophyll content was above 8mg/$m^2$.

We may therefore conclude that the rubification of sand dunes does not require pedogenetic processes that occur in stabilized places, and that as an indicator for the stabilization stage of coastal dunes, the presence of biogenic crust is more informative than the content of fine particles or of free iron oxides.

## Acknowledgments

We would like to thank Rachel Lugassi, Daniela Heller and Oded Levanoni for their help with the field measurements of the biogenic crusts. We also thank Ravid Pik and Yoav Eshel from the Israeli Green Patrol (Ha Sayeret ha Yeruka) for the use of the differential GPS, and Uri Goldstein from the Ashkelon Metropolitan Union for the Environment for his help in obtaining the meteorological data.

## References

Van den Ancker J.A.M., P.D. Jungerius and L.R. Mur, The role of algae in the stabilization of coastal dune blowouts, Earth Surface Processes and Landforms, 10: 189-192

Alpert, P., and Ziv, B., 1989, The Sharav cyclone: observations and some theoretical considerations, *Journal of Geophysical Research*, 94 (D15): 18,495-18,514

Arens S.M., Q. Slings and C.N. de Vries. 2004. Mobility of a remobilized parabolic dune in Kennemerland, The Netherlands, Geomorphology, 59: 175-188

ASD. 2001. Analytical Spectral Devices website: http://www.asdi.com/. Accessed on November 13, 2003

Belnap J. and D.A. Gillette, 1998, Vulnerability of desert biological soil crusts to wind erosion: the influences of crust development, soil texture, and disturbance, Journal of Arid Environments, 39: 133-142

Ben-Dor, E., J.R. Irons, and G. Epema, 1998, Soil reflectance, In Remote Sensing for the Earth Sciences, edited by Rencz, A.N., in Manual of Remote Sensing Volume 3, edited by Ryerson R.A. (New York: John Wiley & Sons, Inc.), pp. 111-188

Ben-Dor E., N. Levin, A. Singer, A. Karnieli, O. Braun and G.J. Kidron., 2005, Quantitative Mapping of the Soil Rubification Process on Sand Dunes Using an Airborne CASI Hyperspectral Sensor, Geoderma, in press

Boyko H., 1947, On the role of plants as quantitative climate indicators and the geo-ecological law of distribution, Journal of Ecology, 35: 138-157

Bullard J.E. and K. White, 2002, Quantifying iron oxide coatings on dune sands using spectrometric measurements: An example from the Simpson-Strzelecki Desert, Australia, *Journal of Geophysical Research*, 107 (B6): 2125-2138

Buol S.W., F.D. Hole, and R.J. McCracken, 1973, Soil Genesis and Classification, The Iowa State University Press, Ames pp. 360

Chabrillat S., A.F.H Goetz, L. Krosley, and H.W. Olsen, 2002, Use of hyperspectral images in the identification and mapping of expansive clay soils and the role of spatial resolution, Remote Sensing of Environment, 82: 431-445

Chapman V.J., 1976, Coastal Vegetation, 2nd edition, Pergamon Press, Oxford

Clark R.N and T.L. Roush, 1984, Reflectance spectroscopy: Quantitative analysis techniques for remote sensing applications, Journal of Geophysical Research, 89:B7:6

Clough K.S. and J.C. Sutton, 1978, Direct observation of fungal aggregates in sand dune soil, Canadian Journal of Microbiology, 24: 333-335

Danin A., 1983, Desert Vegetation of Israel and Sinai, Cana, Jerusalem, 148pp.

Danin A., 1991, Plant adaptations in desert dunes, Journal of Arid Environments, 21: 193-212

Danin A., Bar-Or Y., Dor I. and Yisraeli T., 1989, The role of cyanobacteria in stabilization of sand dunes in southern Israel, Ecologia Mediterranea, 15: 55-64

Danin A. and R. Nukrian, 1991, Dynamics of dune vegetation in the Southern Coastal area of Israel since 1945, Documents Phytosociologiques, XIII: 281-296

Danin A. and Yaalon D.H., 1982, Silt plus clay sedimentation and decalcification during plant succession in sands on the Mediterranean coastal plain of Israel, Israel Journal of Earth Sciences, 31: 101-109

Dematte, J.A.M., Campos, R.C., Alves, M.C., Fiorio, P.R. and Nanni, M.R., 2004, Visible-NIR reflectance: a new approach on soil evaluation, *Geoderma*, **121**, pp. 95-112

Duiker S.W., Rhoton F.E., Torrent J., Smeck N.E. and Lal R., 2003, Iron (hydr)oxide crystallinity effects on soil aggregation, Soil Science Society of America Journal, 67: 606-611

Forster S.M. and T.H. Nicolson, 1981, Microbial aggregation of sand in a maritime dune succession, Soil Biology and Microbiology, 13: 205-208

Fryberger S. G., 1979, Dune forms and wind regime, In: McKee Edwin D. (ed.), A Study of Global Sand Seas, Geological survey professional paper 1052, Washington, D.C. : United States Geological Survey, 137-169

Goldsmith V., Rosen P. and Gertner Y., (1990), Eolian transport measurements, winds, and comparison with theoretical transport in Israeli coastal dunes, Chapter Five in Nordstrom K.F., Psuty N.P. and Carter R.W.G. (eds.), *Coastal Dunes: Form and Process*, John Wiley & Sons, 79-101

Hesp P.A., 1991, Ecological processes and plant adaptations on coastal dunes, Journal of Arid Environments, 21: 165-191

Huang Z. and Y. Gutterman, 1998, *Artemisia monosperma* achene germination in sand: effects of sand depth, sand/water content, cyanobacterial sand crust and temperature, Journal of Arid Environments, 38: 27-43

Karnieli A., 1997, Development and implementation of spectral crust index over dune sand, International Journal of Remote Sensing, 18 (6): 1207-1220

Karnieli, A., 2003, Natural vegetation phenology assessment by ground spectral measurements in two semi-arid environments, International Journal of Biometeorology, 47: 179-187

Karnieli A. and V. Sarafis, 1996, Reflectance spectroscopy of cyanobacteria within soil crusts – a diagnostic tool, International Journal of Remote Sensing, 17 (8): 1609-1615

Karnieli A. and H. Tsoar, 1995, Spectral reflectance of biogenic crust developed on desert dune sand along the Israel-Egypt border, International Journal of Remote Sensing, 16 (2): 369-374

Karnieli A., G.J. Kidron, C. Glaesser and E. Ben-Dor, 1999, Spectral characteristics of cyanobacteria soil crust in semiarid environments, Remote Sensing of Environment, 69: 67-75

Kidron G.J., 1995, The impact of microbial crust upon rainfall-runoff-sediment yield relationships on longitudinal dune slopes, Nizzana, western Negev Desert, Israel, Ph.D. thesis, The Hebrew University of Jerusalem (Hebrew with English summary), 113 pp. (unpublished)

Kidron, G.J., 2001, Runoff-induced sediment yield over dune slopes in the Negev Desert. 2: Texture, carbonate and organic matter, *Earth Surface Processes and Landforms*, **26**, pp. 583-599

Kidron G.J. and A. Yair, 1997, Rainfall-runoff relationships over encrusted dune surfaces, Nizzana, Western Negev, Israel, Earth Surface Processes and Landforms, 22: 1169-1184

Kidron G.J., E. Barzilay and E. Sachs, 2000, Microclimate control upon sand microbiotic crusts, Western Negev Desert, Israel, Geomorphology, 36: 1-18

Kidron G.J., I. Herrnstadt and E. Barzilay, 2002, The role of dew as a moisture source for sand microbiotic crusts in the Negev Desert, Israel, Journal of Arid Environments, 52: 517-533

Kutiel P., 1992, Slope aspect effect on soil and vegetation in a Mediterranean ecosystem. Israel Journal of Botany. 41: 243-250

Kutiel P., H. Dangur, H. Moses and S. Levi, 1996, The role and function of biogenic soil crusts in the succession process of the Sharon dunes, Ecology and Environment, 4(3): 177-183 (in Hebrew)

Lange O.L., G.J. Kidron, B. Budel, A. Meyer, E. Kilian, and A. Abeliovich, 1992, Taxonomic composition and photosynthetic characteristics of the biological soil crusts covering sand dunes in the Western Negev District, Functional Ecology, 6: 519-527

Littmann T., 1997, Atmospheric input of dust and nitrogen into the Nizzana sand dune ecosystem, north-western Negev, Israel, Journal of Arid Environments, 36: 433-457

Liu W., F. Baret, G. Xingfa, T. Qingxi, Z. Lanfen and Z. Bing, 2002, Relating soil surface moisture to reflectance, Remote Sensing of Environment, 81: 238-246

Lobell D.B. and G.P. Asner, 2002, Moisture effects on soil reflectance, Soil Science Society of America Journal, 66: 722-727

Madeira, J., A. Bedidi, B. Cervelle, M. Pouget, and N. Flay, 1997, Visible spectrometric indices of hematite (Hm) and goethite (Gt) content in lateritic soils: the application of a Thematic Mapper (TM) image for soil-mapping in Brasilia, Brazil, International Journal of Remote Sensing, 18 (13): 2835-2852

Mathieu, R., M. Pouget, B. Cervelle, and R. Escadafal, 1998, Relationships between satellite-based radiometric indices simulated using laboratory reflectance data and typic soil colour of an arid environment, Remote Sensing of Environment, 66: 17-28

Mazor, G., G.J. Kidron, A. Vonshak, and A. Abeliovich, 1996, The role of cyanobacterial exopolysaccharides in structuring desert microbial crusts, FEMS Microbiology Ecology, 21: 121-130

McKenna Neuman C. and C. Maxwell, 1999, A wind tunnel study of the resilience of three fungal crusts to particle abrasion during aeolian sediment transport, Catena, 38: 151-173

McKenna Neuman .C., C. Maxwell and C. Rutledge, 2005, Spatial and temporal analysis of crust deterioration under particle impact, Journal of Arid Environments, 60: 321-342

Nevo E., O. Fragman, A. Dafni and A. Beiles, 1999, Biodiversity and interslope divergence of vascular plants caused by microclimatic differences at "Evolution Canyon", lower Nahal Oren, Mount Carmel, Israel, Israel Journal of Plant Sciences, 47: 49-59

Norris R. M., 1969, Dune reddening and time, Journal of Sedimentary Petrology, 39 (1): 7-11

Nukrian R., 1988, Vegetation and its Habitats in the Sand Dunes south of Nahal Shikma, unpublished M.A. thesis, Department of Botany, Hebrew University of Jerusalem, Israel (in Hebrew)

O'Neill A.L., 1994, Reflectance spectra of microphytic soil crusts in semi-arid Australia, International Journal of Remote Sensing, 15 (3): 675-681

Pavlicek T., D. Sharon, V. Kravchenko, H. Saaroni and E. Nevo, 2003, Microclimatic interslope differences underlying biodiversity contrasts in "Evolution Canyon", Mt. Carmel, Israel, Israel Journal of Earth Sciences, 52: 1-9

Prasse R. and Bornkamm R., 2000, Effect of microbiotic soil surface crusts on emergence of vascular plants, Plant Ecology, 150: 67-75

Rutin J., 1983, Erosional Processes on a Coastal Sand Dune, De Blink, Noordwijkerhout, The Netherlands, Ph.D. Thesis, Kaal B.V. Amsterdam

Sanchez-Maranon, M., Soriano, M., Melgosa, M., Delgado, G. and Delgado, R., 2004, Quantifying the effects of aggregation, particle size and components on the colour of Mediterranean soils, *European Journal of Soil Science*, **55**, pp. 551-565

Schmidt H. and A. Karnieli, 2000, Remote sensing of the seasonal variability of vegetation in a semi-arid environment, Journal of Arid Environments, 45: 43-59

Singer A., U. Schwertmann and J. Friedl, 1998, Iron oxide mineralogy of Terre Rosse and Rendzinas in relation to their moisture and temperature regimes, European Journal of Soil Sciences, 49: 385-395

Tsoar H., 1990, The ecological background, deterioration and reclamation of desert dune sand, Agriculture, Ecosystems and Environment, 33: 147-170

Tsoar H., 2002, Climatic factors affecting mobility and stability of sand dunes, in Proceedings of ICAR5/GCTE-SEN Joint Conference, International Center for Arid and Semiarid Land Studies, Texas, Publication 02-2: 423-426

Tsoar, H. and Y. Zohar, 1985, Desert dune sand and its potential for modern agricultural development. In Desert Development, ed. by Gradus Y., pp. 184-200, D. Reidel Pub. Co.

Tsoar, H. and D.G. Blumberg, 2002, Formation of parabolic dunes from barchan and transverse dunes along Israel's Mediterranean coast, Earth Surface Processes and Landforms, 27: 1147-1161

Tsoar H. and Møller T. (1986), "The role of vegetation in the formation of linear sand dunes", in Aeolian Geomorphology, Nickling William G. (ed.), Boston, pp. 75-95

Tsoar H. and I. Werner, 1998, Reevaluation of sand dunes' mobility indices, Journal of Arid Land Studies, 7S: 265-268

Vollenweider, R.A. 1969. A manual on methods for measuring primary production in aquatic environments. Blackwell Scientific Pub. Oxford Edinburgh

West N.E., 1990, Structure and function of microphytic soil crusts in wildland ecosystems of arid to semi-arid regions, Advances in Ecological Research, 20: 179-223

White K., J. Walden, N. Drake, F. Eckardt, and J. Settle, 1997, Mapping the iron oxide content of dune sands, Namib Sand Sea, Namibia, using Landsat Thematic Mapper data. *Remote Sensing of Environment,* 62:30-39

White K., A. Goudie, A. Parker and A. Al-Farraj, 2001, Mapping the geochemistry of the Northern Rub' Al Khali using multispectral remote sensing techniques, Earth Surface Processes and Landforms, 26: 735-748

Whiting M.L., Li L., and Ustin S.L., 2004, Predicting water content using Gaussian model on soil spectra, Remote Sensing of Environment, 89: 535-552

Williams C. and D.H. Yaalon, 1977, An experimental investigation of reddening in dune sand, Geoderma, 17:181-191

# Integration of papers and general discussion

## 1. Preface

As sand dunes are being stabilized, both their biotic and a-biotic characteristics change. As a result, at different stages of a dune stabilization (or re-activation) process, different remote sensing methods, field indicators, and physical factors are becoming more or less relevant. Throughout the different chapters of this thesis various variables and indicators of dune stabilization have been developed and analyzed (see Table 1 for a selected list of the most important variables). Two variables however that were collected during the field survey for each of the erosion pins were only partly incorporated in the above chapters, and will be referred more in the discussion. These include the presence/absence of biogenic crust and the cover by annual plants.

**Table 1**: Selected list of the major variables and indicators of dune stabilization that were used in the study

| Variable | Type | Based on | *n* | Reference for detailed description of methods |
|---|---|---|---|---|
| Dune movement (m/year) | Direct indicator of dune activity | Aerial photographs | 90 | Chapter 4 (Levin and Ben-Dor, 2004) |
| Annual rates of erosion and deposition of sand | Direct indicator of dune activity | Erosion pins in the field | 315 | Chapter 6 |
| Aerodynamic surface roughness | Indicator of potential sand drift by the wind | Wind measurements | 39 | Chapter 5 |
| Soil Adjusted Vegetation Index | Indicator of vegetation cover | Landsat image, January 2000 | | Chapters 5,6 |
| Perennial vegetation cover | Common indicator of stabilized dunes | Field measurements at quadrats of 10*10 m | 315 | Chapter 7 |
| Relative cover of selected perennial plants | Common indicators for the succession stage of dunes' vegetation | Field measurements at quadrats of 10*10 m | 315 | Chapter 7 |
| Annual vegetation cover and presence | | Field measurements | 315 | Chapter 7, here |
| Presence of biogenic crust | Common on indicator of stabilized dunes | Field observations as of winter 2003<br>ASD measurements<br>Chlorophyll content | 315<br>64<br>39 | Here<br>Chapter 8<br>Chapter 8 |
| Rubification | Common indicator for dunes' age / source materials | ASD measurements<br>Lab measurement of % Fe<br>CASI image | 315<br>42 | Ben-Dor et al., 2006; Chapter 2 (Levin et al., 2005) |
| Content of fine particles | Common on indicator of stabilized dunes | ASD measurements<br>Lab measurement of % fines | 315<br>42 | Chapter 2 (Levin et al., 2005);<br>Chapter 8 |
| Distance from the coastline | Rough indicator of dunes activity | DGPS measurements in the field combined with a GIS analysis | 315 | |

## 2. Remote sensing methods for monitoring of coastal dunes at different stages

### 2.1 Extraction of topography over mobile and bare sand dunes

When dunes are highly active, often no vegetation cover may be found on the dunes themselves. In such cases, monitoring of the dunes' mobility can be based on either the dunes movement rate (in the case of barchan and transverse dunes), or on volumetric changes (relevant for all dunes). To analyze the 3D structure of coastal dunes, their topography should be accurately known (Andrews, 2002). Traditionally, this has been done using photogrammetry based on aerial photographs, a method that has been extended to satellite based sensors, such as Spot, Aster and Ikonos, and even Landsat (see comparison and references in Toutin, 2002; Toutin, 2004). Active sensors such as RADAR and LIDAR are recently being applied to map the topography of the Earth. Although Landsat images are being taken since the early 1970s, enabling to monitor changes in sand dunes around the globe for a long period, they were not used for extracting topographic data. In Chapter 1 we presented a method to extract slope, aspect and elevation data of bare sand dunes from multi-date Landsat images of the same path and row. The accuracies achieved for heights and slopes along selected profile lines were to the order of 1 m and 3°, respectively (at a spatial resolution of 15 m). Such photometric stereo methods for the extraction of topographic information have several important advantages, for example: (1) Creating digital elevation models with a spatial resolution similar to that of the sensor; (2) The extraction of topographic information from satellite images acquired by early Landsat MSS and TM missions, thus enabling global monitoring of topographic changes in sand dunes for over 30 years. So far, optical satellite images were used to gain information regarding the spatial extent of sand dunes, their vegetation cover and mineralogical composition. The method developed here offers new opportunities for studies of aeolian geomorphology, adding the ability to analyze dynamic aspects of sand dunes topography in time and space. Knowledge of the volume of sand in a dune is also crucial when comparing the movement rate of sand dunes that have different sizes (Jimenez et al., 1999).

### 2.2 Studying dunes movement rate of mobile and semi-mobile dunes

The method traditionally employed to determine the advance rate of dunes (Gay, 1999) is based on measuring the distance between two successive lines (usually slip faces or brink

lines, or cuspate vegetation marks where they exist, as presented by Jimenez et al., 1999), each representing a different year. Several arrows/lines are drawn between those successive lines, their average length representing the average distance moved by the dune between those years. This method is widely utilized in the world, as seen in Table 2:

| Region | Period analyzed | Dune movement rate (m/year) | Dunes height (m) | Reference |
|---|---|---|---|---|
| Coastal dunes of Oregon | 1939-1975 | 3.8 | 25 | Hunter et al., 1983 |
| Coastal dunes of Alexandria, South Africa | 1939/42-1980 | 1.8 | 22 | Illenberger and Rust, 1988 |
| Desert dunes of Peru | 1943-1952/1957 | 10-70 | 7-20 | Gay, 1999 |
| Coastal dunes of Ceara, Brazil | 1958-1988 | 15-20 | 20-50 | Jimenez et al., 1999 |
| Coastal dunes of Ashdod | 1944-1956 | 3.36 | 10 | Tsoar and Blumberg, 2002a |
| Coastal dunes of Ashdod | 1980-1990 | 1.9 | 10 | Tsoar and Blumberg, 2002a |

**Table 2**: Dune movement rates as reported in various studies

Although the reported movement rate for the coastal dunes of Ashdod is quite low with respect to other dune fields in the world (as demonstrated in the table), we have found (see Chapter 4) that currently they are even lower, as the traditional method tends to exaggerate. The main problems of the traditional method are related to the way those arrows are drawn (Goudie, 1994, pp. 347-348): how densely should the arrows be drawn, in what direction do they point, and how can the starting and ending points of each arrow be objectively determined? In addition, the method assumes that all the different parts of the dune advance at the same rate, which may not be the case in stabilizing dunes, that also change their form from transverse to parabolic. In Chapter 4 we have therefore presented a new method that accommodates these problems: (1) we calculate the area covered by the moving dune between two successive years, and mot measure only the distance moved by a certain part of the dune; (2) to find the distance the dune has moved as a whole, we divide this area by the full width of the dune, even if only part of the dune is advancing; thus we compensate for the fact that not all the dune is necessarily moving together.

However, at advanced stages of dune stabilization, dunes may change their shape, transform from transverse or barchan dunes to parabolic dunes (Tsoar and Blumberg,

2002a), and become disconnected from each other in terms of sand movement (see Figure 8 in Chapter 6). Even if sand is still being transported by the wind, the dune may not be moving anymore, as sand is eroded from the wind facing slope will be deposited on nebkhas on the dunes crest. In such a stage an analysis of dunes movement rate from aerial photographs is futile, and other methods are needed to assess spatial variability in the activity of the dune field. These may still include 3D volumetric change analysis using LIDAR, or spectral methods analyzing the characteristics of the sand itself.

## 2.3 Assessing spectral properties of dune sand to determine their stabilization stage

Over semi-stabilized dunes, local differences in the dune stabilization state may be inferred by the color of the sand in the visible range, that is related to the content of organic matter, water molecules, iron oxides, carbonates and chemical composition of transition metals in clay minerals (Ben-Dor et al., 1998). Whereas this is usually accomplished using sophisticated field spectrometers or airborne hyperspectral sensors (e.g. Levin, 2002; Ben-Dor et al., 2006), we demonstrated in Chapter 2 the ability to measure such attributes using a simple digital camera. Using 370 samples of sandy soils, we have developed a method used the red, green and blue (RGB) values from digital images and their derived soil indices correlate highly with similar measurements preformed by a field spectrometer. When checked against free iron-oxide content and against the percentage of fine particles in a sub-sample set of 42 soils, the redness index as measured by the digital camera gave similar or better correlations than those obtained from a field spectrometer, against both free iron oxides and fine particle contents ($R^2$ of 89% for the iron oxides, and of 81% for the fine particles). We therefore propose the use of a digital camera as a field analytical tool to determine precisely soil color, iron oxide and fine particle content in sandy soils of arid and semi-arid environments.

The chlorophyll absorption of biogenic crust is enhanced when wetted (Karnieli et al., 1999). We have established an empirical relationship between biogenic crust spectral features of water and chlorophyll absorptions (around 1925nm and 680nm, respectively) that estimates the content of chlorophyll of a sand sample regardless of its moisture content (see Figures 13, 14 and Equation 12 in Chapter 8). Thus we measured the chlorophyll content of biogenic crust in the field at several depths along a vertical micro-profile in 64 sites (see Chapter 8), and found that the maximum presence of biogenic crust

was not on the surface, rather immediately below the surface (see also Danin and Nukrian, 1991, and Nukrian, 1988). We have also found that there is a high correlation between the absorption of chlorophyll on the surface when the sand is wet and dry ($R^2$ = 60%; at least during in spring time; see Figure 12 in Chapter 8). Thus, the presence of biogenic crusts can be mapped in the field quickly even when the surface is dry using a field spectrometer, after there has been some rain that activated it.

All these soil characteristics may also be mapped from an airborne- or space-borne platform (as indeed was performed with respect to iron oxides over the Ashdod Dunes by Levin, 2002; Ben-Dor et al., 2006); however this option is somewhat limited in stabilizing dunes due to vegetation cover that might mask the spectral characteristics of the sand.

## 3. Indicators of dune stabilization at various spatial and temporal scales

### 3.1 Indicators of dunes' activity for mobile dunes

When dunes are mobile and without vegetation – their volume changes and annual movement rates are direct indicators of their mobility. Dune movement rates may be further transformed into assessments of the amount transport of sand transported annually, when knowledge on their shape and height and/or width is known (as in Illenberger and Rust, 1988).

Dune sand becomes redder with time, however its initial degree of redness is also dependent upon its parent material (Norris, 1969). Changes in the colour of the sand from white to yellow and then to red, i.e. changes in the amount of free iron oxides thus cannot be interpreted immediately as changes in the stability of the dune field. Although areas where sand is more stable may become a little redder as demonstrated in Figure 20 and 22 in Chapter 8, and areas with increased sand mobility may lead to abrasion of the red coatings of Fe-oxides (Nanson et al., 1992; Bullard et al., 2004), areas of active red sand dunes are known in Namibia (White et al., 1997) as well as in Australia (Bullard et al., 2004).

## 3.2 Indicators of dune activity in stabilizing dunes

As dunes are starting to stabilize vegetation starts to play a leading role, and can serve as an indicator for the activity of a dune. Vegetation is a complicated variable to deal with as it is composed of several types acting on different time scales (Schmidt and Karnieli, 2000): (1) perennial plants that reflect changes on a time scale of years, decades or even centuries, (2) annual plants that may germinate as a function of the seasonal conditions, and are present only for a short period of several weeks or months, and (3) biogenic soil crusts, that are the quickest to respond to environmental changes becoming active upon wetting. In addition, in arid and semi-arid environments there is a high extent of senescent plant canopies (standing litter; Asner and Lobell, 2000; Asner and Heidebrecht, 2002). Regardless of the type of vegetation under consideration, it may be quantified in several ways, e.g.: (1) absolute cover as measured in the field, (2) relative cover of different plant species, (3) remotely sensed based vegetation indices, that are related to the health of the plant, and to the absorption of incoming solar radiation by chlorophyll. One of the advantages of using vegetation indices calculated from satellite images is in our ability to examine the influence of vegetation on wind erosion in several spatial scales (as in chapters 5 and 6).

On a temporal scale of five decades, vegetation cover as estimated from aerial photographs was indeed an indicator of increased dune stabilization, being negatively correlated with dune movement (see Figure 4, Chapter 4). Among the various remotely sensed based vegetation variables, we have shown that often vegetation cover estimates that are based on aerial photographs are poor predictors of wind erosion when compared with satellite based indices such as NDVI or SAVI (see Figure 4, Chapter 5). This is mainly due to the better identification of vegetation when including information from the infra-red spectral region.

Nonetheless, places with similar values of absolute cover of perennial vegetation may be undergoing different aeolian processes: erosion or deposition (see Figure 3b in Chapter 7). The relative cover of selected perennial plant species may thus be an indicator not only of the stability of an area, but also of erosion or deposition as we demonstrated in Chapter 7. Two species were found to be clear indicators of a stabilized environment, *Stipagrostis lanata*, and *Retama raetam*. Of the species indicating a mobile environment, only one may be stated as a clear indicator of sand erosion: *Silene succulenta*, with *Cyperus macrorrhizus* coming close to indicate a less mobile erosive environment.

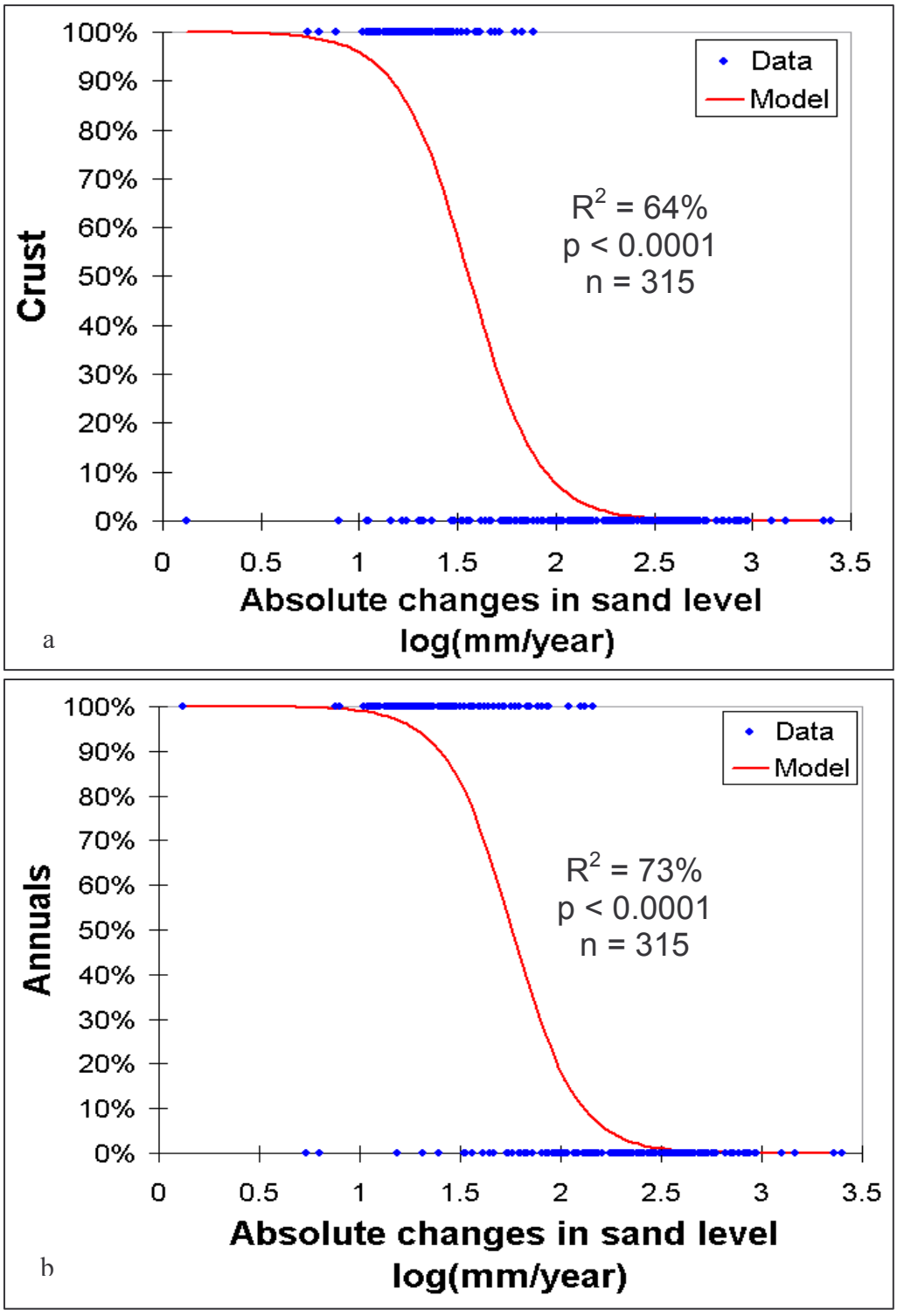


**Figure 1**: (a) Logit model of crust presence as a function of absolute changes in sand level; (b) Logit model of annual plants presence as a function of absolute changes in sand level.

The most adapted species to sand burial was found to be as expected *Ammophila arenaria*, with *Artemisia monosperma* also indicating high rates of sand mobility especially when its relative cover is higher than 80%.

However, when looking for indicators of mobility on a shorter time scale, it would be more beneficial to use the cover/presence of annual plants or of biogenic soil crust[1]. Their correlation with the absolute annual change in sand/erosion deposition as measured in the field was the highest (73% for the annuals, and 64% for the biogenic crust; see Figure 1 here), as they cannot survive in areas where sand movement is very high.

Annual vegetation cover over a radius of 13 centimeters around each iron rod was quantitatively estimated twice during spring time, on March 29-30$^{th}$ 2003 and on March 20-21$^{st}$ 2004. In addition, the presence or absence of annual vegetation was recorded in two additional visits, on January 31$^{st}$-February 3$^{rd}$ 2003 and on February 28$^{th}$-March 2$^{nd}$ 2003. Thus from all four visits the probability of the occurrence of annual vegetation was calculated for each iron rod (being either 0%, 25%, 50%, 75% or 100%). For further analysis of the presence/absence of annual plants, we used an occurrence threshold of 50%. The presence or absence of biogenic crust was estimated visually for each erosion pin on January 31$^{st}$-February 3$^{rd}$ 2003.

In addition to its role in increasing the aerodynamic surface roughness and lowering wind speed (except in special cases, i.e. in local tunneling of the wind between bushes), vegetation also changes the topography of the dunes. In the first stage small nebkhas form, changing the wind field. Later on, the whole shape of the dune might change, e.g. from transverse to parabolic (Tsoar and Blumberg, 2002a). As a result of the formation of nebkhas, when a dune is in a stage where it is semi-mobile, the spatial variability in sand movement increases and the dune can no longer be regarded as being in a steady state in which it is maintaining its shape. Autocorrelation is a measure for spatial variability, and it tends to decrease with the distance from a certain point.

[1] Annual vegetation cover over a radius of 13 centimeters around each iron rod was quantitatively estimated twice during spring time, on March 29-30$^{th}$ 2003 and on March 20-21$^{st}$ 2004. In addition, the presence or absence of annual vegetation was recorded in two additional visits, on January 31$^{st}$-February 3$^{rd}$ 2003 and on February 28$^{th}$-March 2$^{nd}$ 2003. Thus from all four visits the probability of the occurrence of annual vegetation was calculated for each iron rod (being either 0%, 25%, 50%, 75% or 100%). For further analysis of the presence/absence of annual plants, we used an occurrence threshold of 50%. The presence or absence of biogenic crust was estimated visually for each erosion pin on January 31$^{st}$-February 3$^{rd}$ 2003.

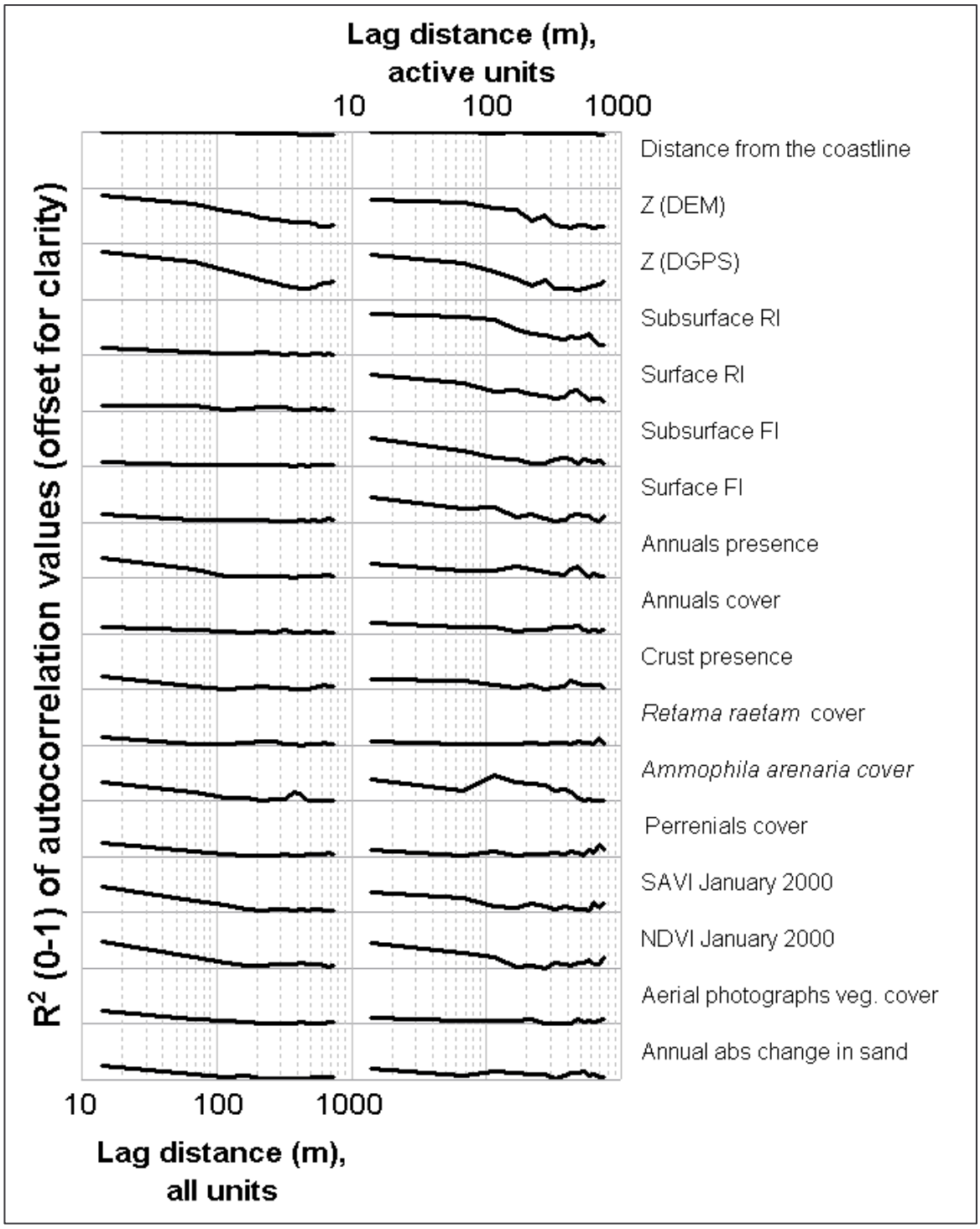


**Figure 2**: $R^2$ values of autocorrelation of the various variables measured at the erosion pins, as a function of 15 lag distances of 50m (up to 750m). On the left hand side of the chart we present the autocorrelation values for all erosion pins (n = 315), and on the right hand side of the chart, those for the active units (n = 225). RI stands for the Redness spectral Index indicating the content of free iron oxides, whereas FI stands for the Fine particles spectral Index, indicating the content of clay and silt.

High autocorrelation means a low spatial variability. In Figure 2 we can see that the autocorrelation of different variables is not the same. Generally, the autocorrelation is lower when all units are included. Notice however that autocorrelation of the elevation values is very high (with $R^2 > 50\%$, $p < 0.001$, in some cases) regardless of the data set used, and is much higher than that of the NDVI or SAVI. Notice also the very low autocorrelation in the annual rate of sand erosion/deposition.

The spatial autocorrelation of many variables (e.g. wind speed, sand mobility and vegetation) increases in the stage when nebkhas form on the dune changing its topography. Variables whose spatial autocorrelation remains relatively high even at this stage are those related to the topography and to the red coating of sand grains by iron oxides. To quantify sand movement in such an environment, requires high resolution data for both topography and vegetation, such as is available from LIDAR sensors (see Rango et al., 2000; Woolard and Colby, 2002), or a combination of a very detailed photogrammteric survey for the DEM creation accompanied with a hyperspectral sensor for vegetation monitoring.

This may partly explain why topographic variables were weaker predictors of aerodynamic surface roughness and of the annual rates of sand erosion/deposition, when compared with vegetation (compare Figures 6 and 8 in Chapter 5, and see also Table 5 in Chapter 6). It should be noticed that the autocorrelation of the topography as measured by DGPS was lower than when based on the DEM. We may therefore presume that if we had a better DEM (e.g. LIDAR based) our predictions of sand movement will be improved.

When only the active units are included, we can see that the soil (sand) characteristics (especially Redness Index, RI, but also the Fine particles Index, FI) change much slowly (are more autocorrelated) than vegetation. The influence of spatial resolution on autocorrelation can also be seen when comparing the higher autocorrelation of the satellite based indices (SAVI and NDVI) with ground resolution of 30m, with that calculated from aerial photographs (ground resolution of about 1m), or with the field estimation of perennial vegetation cover.

The spatial autocorrelation of the annual absolute changes in the sand level at the first lag distance is relatively low ($R^2 = 21\%$). Variables with a high spatial autocorrelation are therefore not expected to be highly correlated with it, as is indeed demonstrated in Figure 3. Notice that the two variables with the highest correlation with sand movement, annuals and crust presence, have a low value of spatial autocorrelation.

When sand dunes are further stabilized, the dunes may be not moving anymore, and sand that is eroded from the wind facing (stoss) slopes of the dune will not reach the dunes' slip face anymore but be deposited on nebkhas on the dunes' crest. Indeed, in the dunes of Ashdod and Nizzanim only nine out of 90 dunes that were analyzed (the 55 dunes that were discussed in Chapter 4, and 35 additional dunes in the eastern part of the Ashdod Dunes park) were still detected as mobile when analyzed using aerial photographs (see Figure 4). Therefore, in this stage dune movement rate can no longer serve as an indicator of spatial variability in sand activity.

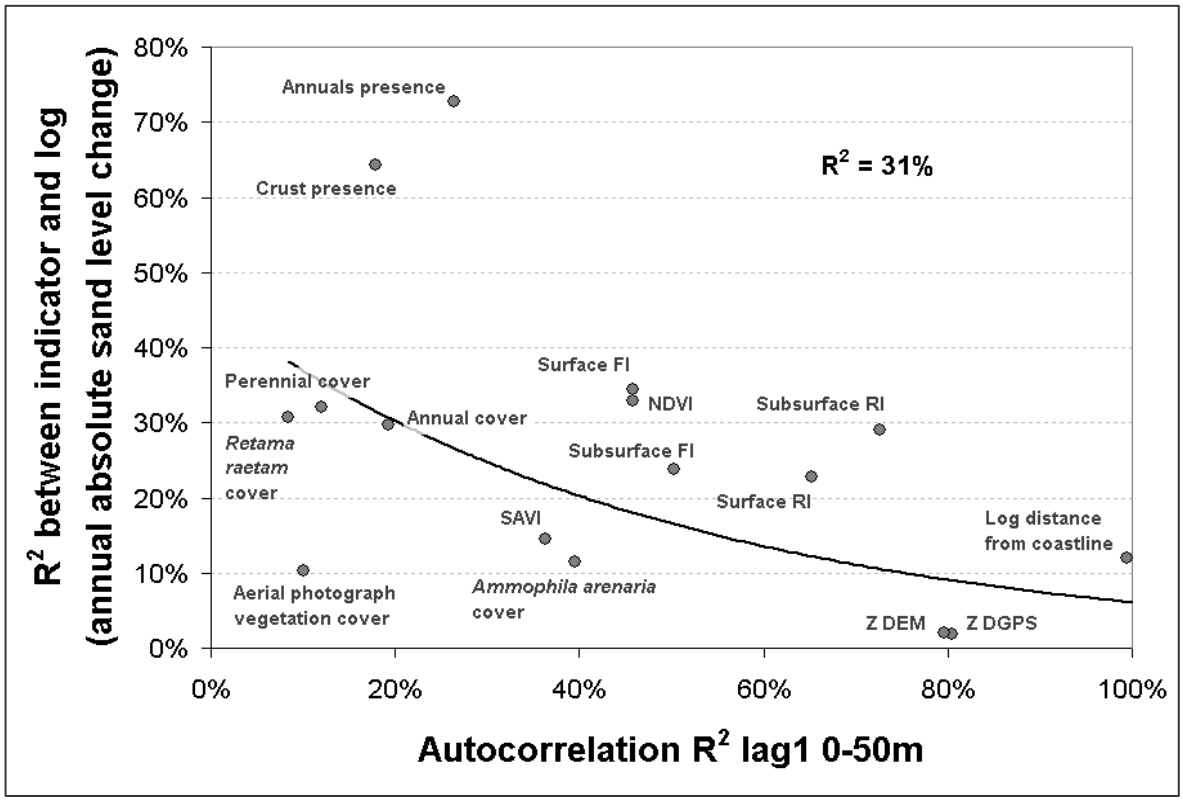


**Figure 3**: The relationship between the spatial autocorrelation of stabilization indicators (based on the active units, n=225), and their ability to explain the annual absolute changes in the sand level (based on all units, n=315).

Of the three soil properties that we analyzed using spectral indices (content of iron oxides, fine particles and presence of biogenic soil crust), the latter two may serve as indicators of a dunes' activity. The content of fine particles, deposited as dust, is a recognized indicator for desertification (McTainsh, 1985). This is expected to increase gradually with time, as a dune area undergoes weathering processes and more deposition of fine particles during following dust storms occurs (being kept in place by vegetation after it has been washed

down by rainfall). The relatively high spatial autocorrelation in the content of fine particles (see Figure 2 and 3) and its correlation with the content of free iron oxides (reported in Chapter 2) indicate that it is indeed slowly increasing with the dunes' age. However, the relatively high correlation of fine particles with annual sand movement ($R^2$ = 35%, $p < 0.001$; Figure 3) as well as its higher content in relatively stabilized areas (see Figures 20 and 22 in Chapter 8) indicate that it also influenced by local changes in

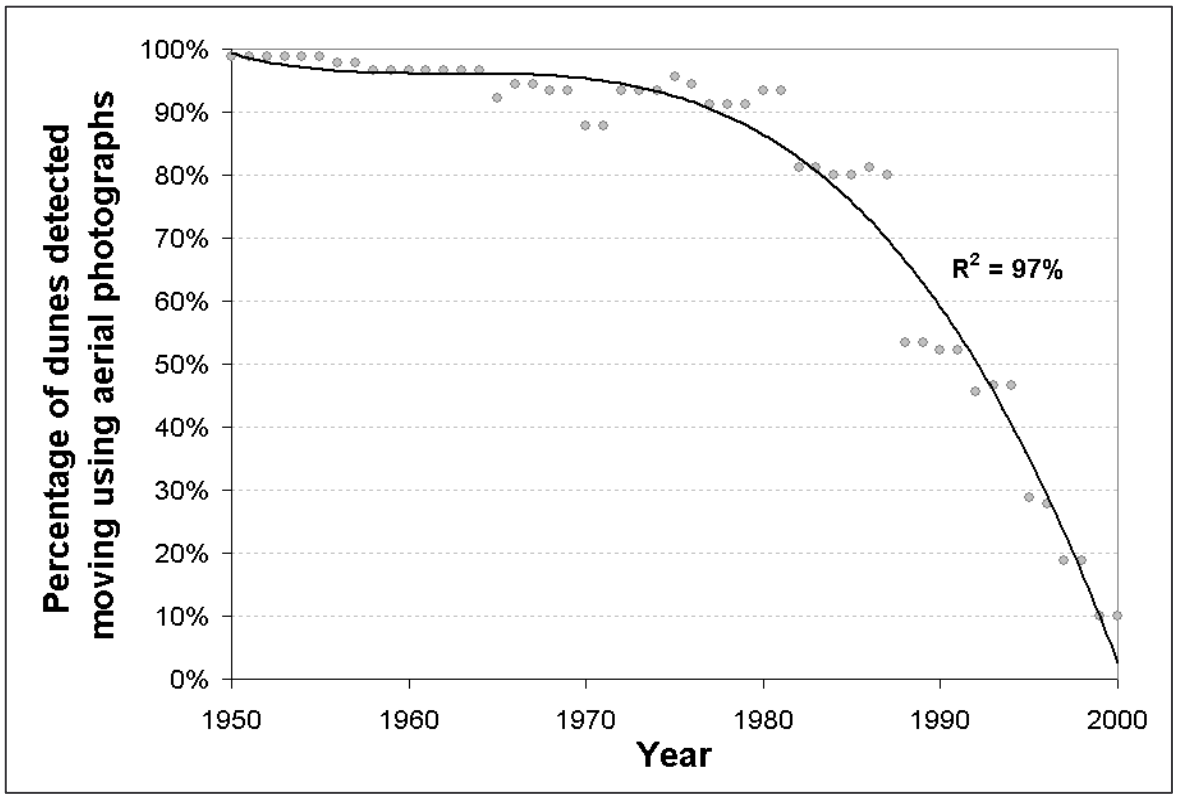


**Figure 4**: The percentage of dunes detected as moving using aerial photographs. In this figure were included 90 dunes between the cities of Ashdod and Nizzanim.

vegetation cover.

This is seen again in Figure 5, from which we can conclude that RI is principally an indicator of the dunes' age, as it is the only variable whose correlation with the distance from the coastline is higher than with the surface stability and with $Z_0$. FI is influenced by both distance from the coastline (~age) and by surface stability (local conditions). Annual cover and crust presence are clear indicators of a dunes' stability, least affected by the distance from the coastline.

To be able to predict sand erosion rates without field measurements however, one may rely on a map of predicted $Z_0$ values, as presented in Chapter 5. This map was based on two variables relating to the area upwind of a certain location: the relative height and the

Soil Adjusted Vegetation Index (SAVI). As the $Z_0$ map was based on wind measurements performed at a height of 2.5 m, it was influenced by a larger area upwind of the wind stations than experienced by the erosion pins (200-400m vs. 100m, respectively; compare Figure 11 in Chapter 5 with Figure 8 in Chapter 6). As reviewed by Wiggs (2001) it is very difficult to measure shear velocity (u*) for wind flow over dunes, and it is even more challenging to relate it to sand flux on dune surfaces. Our map of $Z_0$ was able to significantly explain 40% ($p < 0.001$, $n = 230$) of the variability in the absolute changes in sand movement when all erosion pins for which DEM data was available were included, and 60% of the variability for the erosion pins located on dunes slip faces ($p < 0.001$, $n = 27$; see Chapter 6, Figure 9). Moreover, 66% of the variability in the predictive map of absolute yearly changes in sand level (Chapter 6 Figure 8) is explained by the predictive map of $Z_0$ (Chapter 5 Figure 11), on a log-log plot (Chapter 6 Figure 10).
In addition, as both variables of SAVI and relative height are of a relatively medium resolution, the expected correlation between the $Z_0$ map and stabilization indicators was expected to be lower than those obtained with respect to field measured values of sand movement. However, this map was still able to explain more than 50% in the variability of the absolute annual rate of sand erosion/deposition and content of free iron oxides (subsurface RI) and of fine particles (Surface FI), and annual plant cover, as measured in the dunes slip faces along the field transects (Figure 5). We thus believe that maps of surface roughness that will be based on higher resolution datasets (e.g. LIDAR derived DEMs) will be able to predict even better sand mobility as measured in the field using a similar approach. In addition, future measurements of $Z_0$ should be based on wind measurements taken at lower heights (of about 0.5 m), that will better reflect the near surface wind flow that is affecting sand movement.

## 3.3 The slip face as an indicator of dune stabilization processes

As dune stabilization or re-activation efforts and monitoring programs are budget limited, it would be of great value to know not only which indicators of dune stabilization are worth measuring, but also where to do the field sampling. We claim that the most indicative geomorphologic unit for assessing the stabilization stage of a sand dune is its slip face.

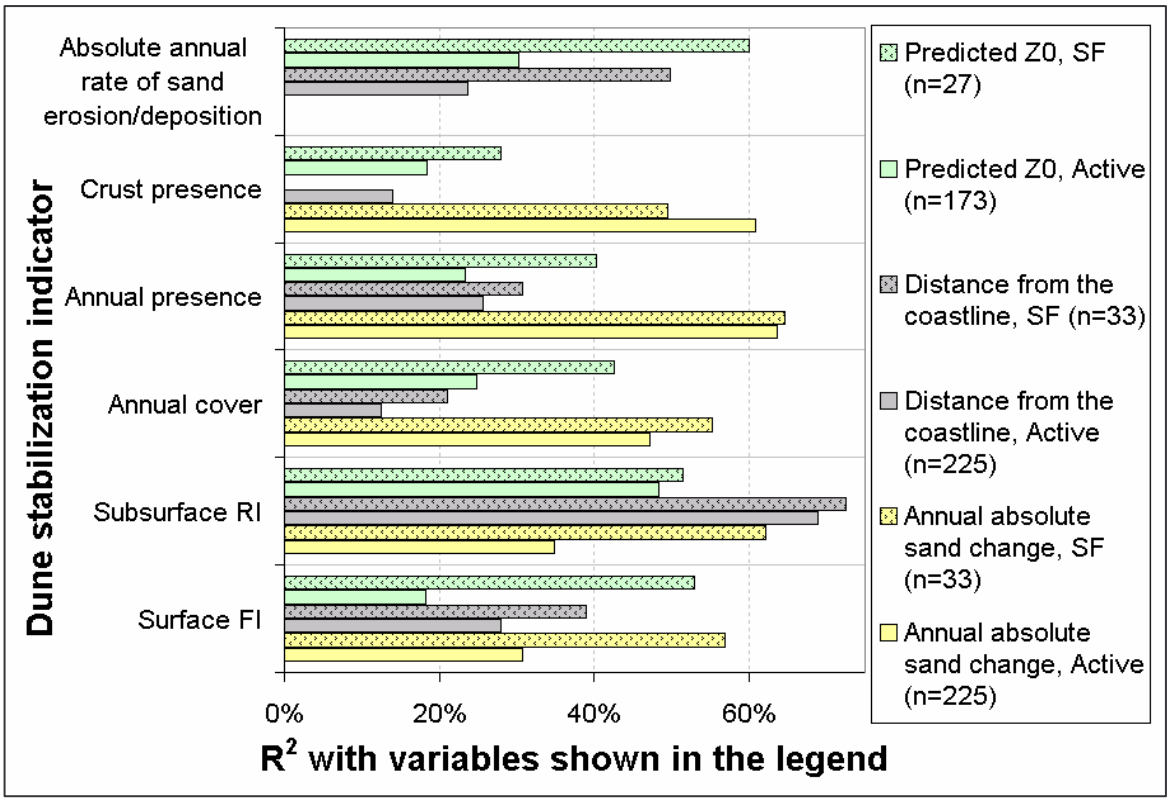


**Figure 5**: The variability in the values of five dune stabilization indicators, as a function of the surface stability (log of annual absolute change in the sand level), the log of the distance from the coastline, and the predicted $Z_0$ values as of the year 2000. In this analysis we included two subsets of the data: all active units (n=225), and all the dune slip faces (n=33).

Over active sand dunes, the slip face is oriented perpendicularly to the direction of sand moving winds, having an angle of 33º when dry – the angle of repose (Bagnold, 1941). In all sand dunes, and especially in barchan, transverse and parabolic dunes, the area of the slip face is quite small relative to the area of the whole dune. In active dunes, the sand that is eroded from the wind facing slopes, is expected to be deposited on the slip face. This small area therefore is supposed to receive all the sand that is transported by the wind. In addition, the vertical changes in the volume of sand will be more pronounced over this unit (see Figures 3 and 4 in Chapter 6), as here we find the maximum slope on a sand dune. It is due to these reasons that we found the best correlations between various indicators of dune stabilization when using only the data subset relating to the slip face. Indeed, the highest correlations between absolute and net weekly changes in the sand level and the resultant drift potential (RDP-t) were found at the slip face ($R^2$ = 81%, 85%, respectively; Table 3 in Chapter 6). We also found over the slip face the highest

correlations between sand movement and the distance from the coastline (Table 4 in Chapter 6), satellite images derived vegetation indices (Tables 4 and 5 in Chapter 6), topography (Tables 4 and 5 in Chapter 6), surface aspect (Figure 7, Chapter 6), predicated values of $Z_0$, annuals plants cover, content of iron oxides and of fine particles (Figure 5 here). In addition, the slip face is used to define the dunes' front when analyzing the movement rate of sand dunes, as it is the most easily identified unit of a sand dune from remote sensing imagery, because of its uniform slope of 33º. As a dune further stabilizes its slip face will gradually lose the steep angle of repose, due to the establishment of plants, and due to the passage of animals and man.
Thus by carefully monitoring various indicators at the slip faces of sand dunes in a dune field, spatial patterns of dune activity can be obtained.

## 4. Physical factors affecting coastal dune activity in space and time

### 4.1 Temporal variability

Of all the various physical factors that affect the transport of sand and movement of dunes, wind regime, composed of the winds' direction and velocity, is clearly the most direct and important factor (Bagnold, 1941; Tsoar, 2002). These are commonly estimated using the indices of Drift Potential (DP) devised by Fryberger (1979), as done by Tsoar and Werner (1998) as well as by Arens et al. (2004). The wind regime may change in space and in time, due to climate changes (on a temporal scale of decades-centuries), due to different synoptic systems (on a temporal scale of days-weeks-months), and due to spatial heterogeneity whether it is natural or caused by human obstructions.
Analyzing dune movement and various climatic factors on a years-decades scale (chapters 3 and 4) we found that the average dune movement rate between the 1874-1930 was similar to that found in 1950 (about 5.1 m/year; see also Tsoar and Blumberg, 2002a). Based on this it can be presumed that the wind regime did not change dramatically during the first half of the 20$^{th}$ century. In addition, we did not find any significant changes in the past 30 years in the sand drift indices that may have caused any changes in the dunes' movement rate (Figure 5 and Table 2 in Chapter 4). In this regard it should be noted that the mesoclimatic change found by Alpert and Mandel (1986) is not in the wind speed, but in the wind variability. Also for other factors that are known from the literature to affect dune activity, such as rainfall and evapotranspiration (Lancaster, 1988), aeolian deposition of fine particles (Tsoar and Møller, 1986) and the underground

water table height (Ranwell, 1972), we did not find any significant changes that may be related to the observed changes in the dunes' movement rates (Figure 5 and Table 2 in Chapter 4). Thus, none of the meteorological and environmental factors that we examined was able to explain the anomaly in the dune movement rates during the late 1960s-late 1970s or the general declining dune movement trend. Rather, human activities appeared to responsible to these changes, as will be discussed below.

On a shorter time-scale however, we found a strong relationship between changes in sand movement and the wind power, as detailed in Chapter 6. Based on the measurements of sand erosion and deposition that we conducted along four transects between December 2002 – October 2004, we found as expected (Goldsmith et al., 1990; Tsoar, 1990), most of the sand is moved during the winter storms (Figure 4 Chapter 6) from the south-west towards the north-east. More than 80% in the variability of sand movement over the dunes' slip faces could be explained by the resultant drift potential (Table 3 Chapter 6). More interesting, and in contrast to Arens et al. (2004) we did not find any indication that rainfall had any significant influence on the overall transport of sand. We explain this by the fact that the rainfall over the Israeli coast hardly coincides with sand moving winds, due to the characteristics of mid-latitude cyclones over Israel (Figure 5 in Chapter 6). These have a dominant cold front (Alpert and Ziv, 1989), in which the strong winds (that are able to move sand) are preceding the rainfall. In addition, rainfall in Israel is usually fragmented, so that winds may dry the sand between rainfall periods and mobilize it. And, as reported by Jackson and Nordstrom (1998), light rain, resulting in bulk surface moisture values below 7% are not sufficient to eliminate sand transport.

The rainfall activity, wind speed and the consequent sand movement associated with a passing cyclone are influenced by the wider synoptic and climatic conditions. Analyzing monthly time series of rainfall and wind speed along Israel's southern coastal plain I did not find any significant trends over the years that may influence changes in the dunes' movement (Chapter 4 in this thesis). Lionello et al. (2002) have applied a model that investigated the variations in the cyclonic activity in the Mediterranean Region that would be produced by the doubling of the $CO_2$ atmospheric content; the climate variations identified by them were not large and the only clear effect of the $CO_2$ doubling expected by their model is the diminished overall cyclonic activity.

We may therefore expect that given no changes in human land-uses (Chapter 4 in this thesis) the coastal dunes along the coast of Israel will continue their gradual stabilization process, and remain active only in limited periods during the winter.

## 4.2 Spatial variability

As the major factor influencing sand and dune movement is wind power, to understand spatial variability in the mobility of sand, one should be able to understand the factors controlling the wind field. We focused our study on two variables that seemed to us as the major ones: topography and vascular vegetation. Although biological soil crusts have considerable effect on surface roughness and wind erosion (see Belnap and Gillette, 1998), their presence over the coastal dunes of Ashdod and Nizzanim is generally quite low (being present in 36% of the 315 erosion pins, but on only 17% of the 225 erosion pins that were located on active units, and on 12% of the erosion pins located on dune slip faces) and was therefore not included in our analysis.

As it is quite difficult, if not impossible, to measure the wind speed simultaneously at many locations across a dune field, we have instead studied the spatial variability in the aerodynamic surface roughness, $Z_0$. This was calculated from single height wind measurements following Wieringa (1973, 1986). In addition we have measured actual sand erosion and deposition using 315 erosion pins along four transects ranging from the coastline to the dunes' edge.

We have quantified the influence of vegetation using Landsat derived vegetation indices (SAVI and NDVI) whereas the influence of topography was estimated using relative heights. Both variables were calculated at each position with respect to the area upwind of it, at various spatial scales ranging from 15-400m.

We have found (Figures 4-8, Chapter 5) the $Z_0$ values to be significantly positively related to SAVI values ($R=0.86$, $p<0.001$, for the winter SAVI at an upwind length of 200m, when all stations are included) and negatively related to the relative height ($R=-0.68$, $p<0.001$, for the relative height at an upwind length of 200m-400m, for the inland dune stations). Using these variables with the same stations we were then able for the first time to model and create a map of predicted $Z_0$ values (Figure 11 in Chapter 5) with an accuracy higher than 64% (tables 3-4 and Figure 9 in Chapter 5).

Sand erosion and deposition rates were also found to be influenced by the same variables of vegetation and topography (Tables 4 and 5 in Chapter 6). Whereas in many coastal dunes studies spatial variability in sand movement is attributed as being related to a general decrease in wind speed with the distance from the coastline (as in Illenberger and Rust, 1988), as far as we know this is the first study that has aimed at quantifying the

effects of topography and vegetation on sand and dune movement across a whole dune field. In addition we show that although the distance from the coastline is correlated with $Z_0$ (Figure 2 Chapter 5), sand movement (Table 4 in Chapter 6) and other indicators of dune stabilization (Figure 5 here), the correlation of these variables with vegetation or topography is higher.

Generally we found that spatial vegetation indices were better than relative height in explaining the variability in $Z_0$ and in sand erosion/deposition rates. This is due to the fact that these are dunes that are stabilizing. As mentioned before, as sand dunes are becoming less mobile, vegetation cover increases, and nebkha dunes form on them, capturing sand, increasing surface roughness and reducing sand movement. Whereas on bare sand dunes no vegetation exists, and the major control on wind velocity and on sand movement is the dunes' topography, as vegetation cover increases, it is expected to have more and more effect on aeolian processes, and to eventually stop sand erosion when vegetation cover reaches a certain limit (above 45%, according to Wasson and Nanninga, 1986 or above 25% according to Lancaster and Baas, 1998; see also Figure 12 in Chapter 7). As vegetation cover increases, the continuous bare sand dune areas become increasingly fragmented, further reducing potential sand drift (see map in Figure 8, Chapter 6). This is important, as sand erosion at a certain location, as well as other indicators of dune stability (such as annual cover and biogenic soil crust) are influenced by the characteristics of the area upwind (see Table 5 in Chapter 6; see also Hupy, 2004, and Lancaster and Baas, 1998).

To improve our estimates of wind erosion and sand mobility based on vegetation indices and topography improved data sets are needed. As our vegetation indices were based on medium resolution Landsat images (15-30m) single bushes could not be identified. Also our digital elevation model was not detailed enough to present nebkha dunes. Indeed, the spatial autocorrelation of both the DEM and vegetation indices that we used was much higher than that of sand erosion/deposition rates (or of annual plants cover and biogenic soil crust; see Figure 2 here) further reducing our ability to quantify spatial variability in sand movement. In addition, vegetation parameters that influence wind erosion of sand include not only vegetation cover, but also its height, spacing and frontal area (Lettau, 1969; Dong et al., 2001). These variables can be estimated in the future using LIDAR sensors mounted on airborne platforms (Rango et al., 2000; de Vries et al., 2003). Nonetheless, although our map of predicted $Z_0$ values was based on medium resolution maps of vegetation and topography, over the dunes' slip faces it was able to significantly

explain more than 50% in the variability of fine particles content and 60% in the variability of the absolute annual rate of sand erosion/deposition (Figure 5 here, and Figure 9 in Chapter 6). Such maps can be thus used to predict future changes in vegetation cover over sand dunes, using available satellite data.

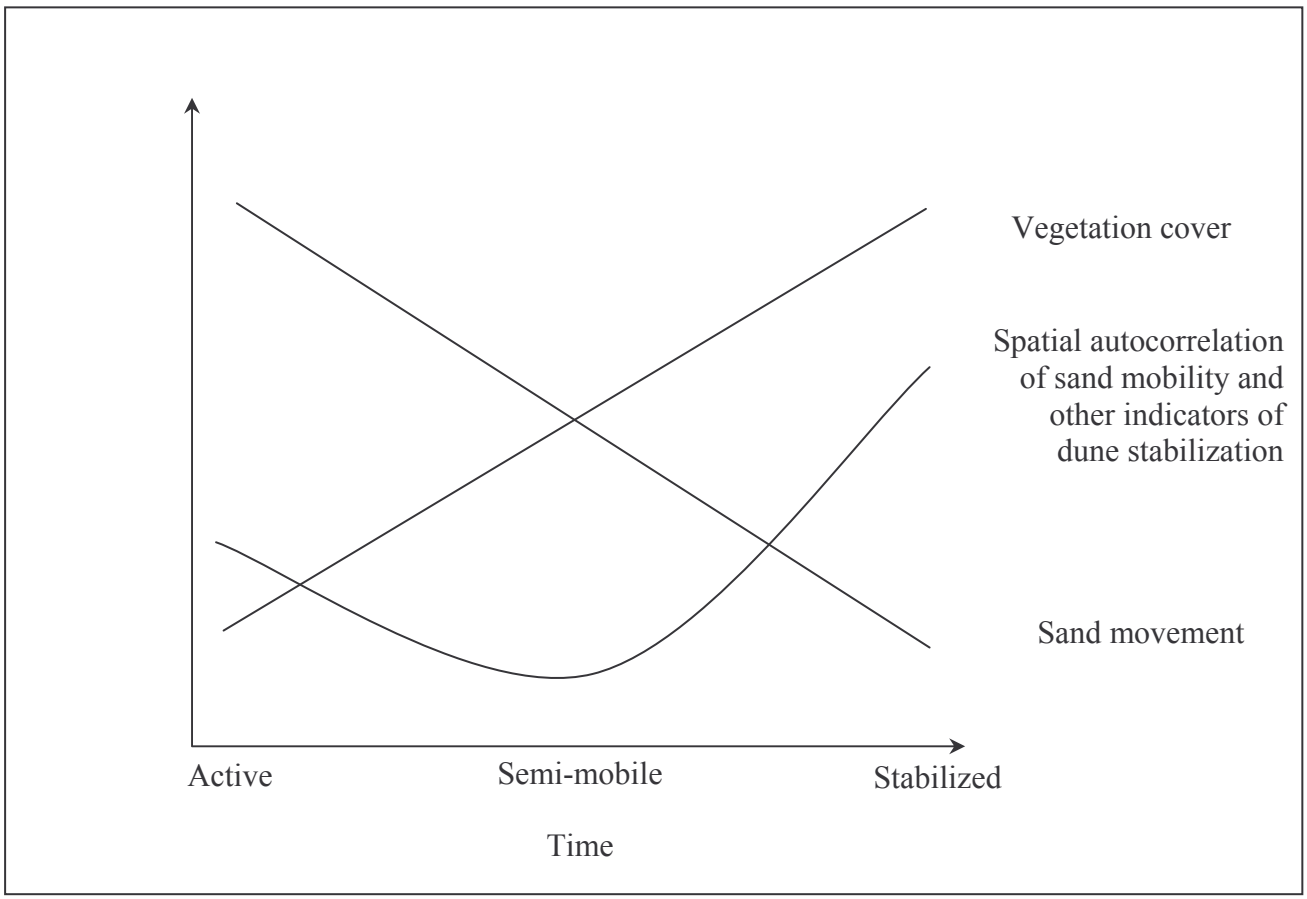


**Figure 6**: Schematic representation of temporal changes in dunes vegetation cover, sand movement and spatial autocorrelation as they stabilize.

As the dunes go on stabilizing eventually the autocorrelation of the various stabilization indicators is expected to increase again in the future once vegetation cover will reach higher values. This idea is presented schematically in Figure 6. When dunes are active, their vegetation cover is low, sand mobility high, and spatial autocorrelation is moderate-low, mainly influenced by the dunes topography and age dependent variables (such as free iron oxides content). As dune stabilize and vegetation establishes on them, the spatial autocorrelation becomes very low (for most variables) as the dunes area becomes spotted with nebkha dunes and plants of varying sizes and phenology, and the dunes themselves become disconnected one from the other. This off course affects sand mobility that decreases. Towards the ultimate stages of dune stabilization, vegetation cover may

surpass values of 40% (and eventually 100% when soil formation processes are more advanced), thereby limiting all sand mobility, and bringing spatial autocorrelation to its highest values, as even the dunes topography becomes slowly flattened by erosion processes induced by rainfall, surface runoff, animal and human activities.

## 5. The possibility of directing coastal dune processes by changing human activities

The current phase of coastal dunes started to encroach on the coastal plain of Israel between the 7$^{th}$ and 9$^{th}$ centuries A.D, based on archaeological remains that are covered by them (Tsoar, 1990). Our estimation of the dunes movement rate between the 1874-1930 of about 5.1 m/year is further evidence for this, based on the maximum extent of the coastal dunes, reaching about six kilometers south of Jaffa (see details in Chapter 3). Although coastal dunes may seem to be a natural ecosystem, some authors attribute this recent encroachment of sand to processes of soil erosion in Palestine, caused by changes in human land uses, following the occupation of the area by the Arabs from the hands of the Byzantine Empire (Reifenberg, 1947, 1950; Rubin, 1989). The harbor of Caesarea, built by Herod 2,000 years ago, is also given as an example for an impediment of sand movement, and in consequent, the formation of sand dunes of Caesarea to the south of it (Reifenberg, 1951).

Whether or not human activities or climate changes were behind the formation of these coastal dunes, it is clear that coastal dunes may be influenced by anthropogenic land-uses. Although sand dunes may seem as a non fertile area, a special kind of agricultural system has developed among the dunes, called "Mawasi". In this system the high level of coastal underground water was used for growing grapes, palm trees and other crops (Tsoar and Zohar, 1985), shown on various historical maps (e.g. on Jacotin maps of Palestine from Napoleon's military campaign in 1799, on the Palestine Exploration Fund Survey of Western Palestine from 1871-1877, and on British Mandate maps from ca. 1930) as well as mentioned by various travelers and botanists (Guerin, 1868; Warren 1871; Zohary and Feinbrun, 1941; Ashkenazi, 1947). In addition, local Arab and Bedouin populations living in nearby villages or in temporary huts were using local vegetation for burning, building materials, medicinal purposes as well as for grazing (Bailey and Danin, 1981). The influence of such practices on reducing vegetation cover over the dunes north of the

Alexander River (Israel) was noticed by Kosovsky et al. (1996) that compared aerial photographs from 1918 and 1944.

Activities of nomadic populations leading to a decrease in dune vegetation cover and the re-activation of sand dunes are well known, whether from grazing and trampling by their livestock and by the direct use of dune plants (in the Negev desert of Israel: Meir and Tsoar, 1986; in the Rajasthan Desert of India: Kumar and Bhandari, 1993; in Eastern Saudi Arabia: Barth, 1998), or due to the traditional use of fire as a way of promoting young grass for cattle (in Australia: Wasson and Nanninga, 1986).

In Chapter 4 we discuss the land use changes that followed the drastic decrease in the Bedouin population along Israel's coastal dunes after its establishment in 1948. Thus the removal nomadic pressure from this area enabled vegetation cover to recover along the coastal dunes. However, the Bedouins and their livestock were able to return to Israel's coastal dunes between the late 1960's – late 1970's due to the coincidence of three events: the nullification of military rule over the Arab population in Israel in 1966, Israel's occupation of Sinai and the West Bank areas in 1967, and a severe drought in the northern Negev Desert In the mid-1970s that encouraged many of the Bedouin to move northwards. Based on historical archives and government reports from this time we demonstrated that Bedouins agricultural practices led to a reactivation of the dunes, as measured by the dunes movement rate and vegetation cover. The establishment of the Green Patrol in 1976 and the changing grazing laws resulted in a decrease in the size of livestock populations and moved the Bedouin back from central Israel to the Negev, thereby allowing the vegetation to recover and the dunes to stabilize again.

However, there are other human activities along Israel's coastal dunes that may lead to their stabilization or re-activation. Actions taken to stabilize the Ashdod dunes during the British mandate (1920's-1940's; Liphschitz and Biger, 1997) and later by the Jewish National Fund (JNF; during the early 1960's), were mostly targeted to the eastern part of the dunes, and to the creation of a foredune. However, it was found that the invasive tree *Acacia saligna* (planted during the 1960's by the JNF) does not spread spontaneously to bare sand dunes (Cohen, 2002). Furthermore, stabilization actions can not explain the reactivation of the dunes, that took place during the late 1960's – late 1970's. We therefore conclude that directed stabilization efforts apparently did not influence the geomorphologic processes in this area. In areas where sand dunes were blocked behind man-made obstructions (e.g. buildings), as between the cities of Holon and Rishon le Zion (Peery and

Dmiel, 1995), this may also be a cause to further dune stabilization. However, in our study area of the Ashdod Dunes, other than some beach bungalows, the south-westerly storm winds are unobstructed.

Removal of the protective vegetation cover and consequent sand erosion may be result from disruption caused by military maneuvers (Al-Dabi et al., 1997) or recreational activities, such as off-road vehicles (ORVs) and hikers (Curr et al., 2000). However in our study area (see Chapter 4 as well as results presented in Levin et al., 2003 in the appendix) it seems that military maneuvers, recreational pedestrian and ORV traffic caused fragmentation but their intensity was not sufficient to destabilize the dunes, as they tend to follow fixed lines, and may have even encouraged the establishment of invading *Acacia saligna* species in disturbed areas (see Cohen, 2002, for the spatial pattern of the invading Acacia, and compare with Liddle and Greig-Smith, 1975, and Kutiel et al., 1999, for the effects of visitors on trails and adjacent vegetation).

According to the morphodynamic classification of Rust and Illenberger (1996), as dunes become stabilized by vegetation they also become more sensitive and fragile. Thus, active dunes are more able to retain their character in response to anthropogenic impacts such as those done by hikers or off road vehicles, as sand moved by the wind will tend to erase them with sufficient time (depending on the type of impact and annual rates of sand movement; see also Lemauviel and Roze, 2003). We have shown that over the coastal dunes of Israel, human activities have had more impact on the stabilization processes than did climate change in the past 100 years.

In areas where dunes are being stabilized as a result of human actions (whether in purpose or indirectly), the ecological consequences are now being questioned. In such areas, not only does the landscape change, populations of sand-living organisms decrease as a result of the loss of their habitat – shifting sand, and are replaced by other organisms, more adapted to stabilized dunes (Kutiel et al., 2000). In Israel, this may result with the loss of species that are endemic to the Israeli coastal dunes. Consequently experiments are being conducted that aim at reactivating stabilized dunes to restore their ecological values (Kutiel et al., 2000; Arens et al., 2004). Similar efforts are now starting also in the Ashdod and Nizzanim Dunes (Tsoar and Blumberg, 2002b). However, as the drift potential of sand by the wind in Israel is low (Tsoar, 2002) the reactivation of the dunes will most probably require repeated actions of vegetation removal. These may take the form removing vegetation by hand, by mechanical means, fire or by grazing. While livestock grazing was perceived in the past as harmful to nature conservation (the common property

problem; see Livingstone 1977, 1986), Perevolotsky (1999) claims that the long history of grazing in the Negev (and in other areas of Israel) converted it into a 'grazing-incorporated-system', and that the grazed state is, in fact, the most 'natural' state. It may be stated that the preservation of sand-living flora and fauna and a landscape of mobile sand dunes, will be greatly facilitated if grazing by Bedouin herds (or other equivalent ecological processes) will be reintroduced to that area. How practical is this solution in Israel's urbanizing society, in which the Bedouins are moving away from their traditional agricultural practices, remains to be seen.

Quantifying the relative contribution of human and physical factors to dune activity is hard to achieve, as human activities are not monitored on a daily basis (as done in meteorological stations). Some variables regarding human activity over sand dunes may be quantified using aerial photographs (e.g. density of trails and tracks, see Chapter 4), whereas others may be retrieved from statistical records (e.g. the size of nomadic populations and their herds; albeit the uncertainties in such figures) however the type and intensity of actual activity is hard to assess, unless done in controlled experiments (as in Lemauviel and Roze, 2003; Kutiel et al., 1999). An alternative which we did not explore here is the use of logistic regression, to examine the effect of the presence or absence of human activity on dune parameters. Rather, we followed an approach in which we examined the changes in both physical and human factors over time with the best data available, and analyzed these with respect to changes in dune activity. By excluding the possibility of physical effects on the temporal changes (on a semi-decadal scale) in dune activity, we were left with the hypothesis of human effects. We then proceeded by examining them one by one, each time discarding another type of human activity, until arriving to the conclusion that changes in the presence of Bedouins and their livestock over the coastal dunes, is the cause to the apparent changes in their activity.

## 6. Summary of the scientific contributions of the thesis

Throughout the different chapters of this thesis various new methods and approaches for studying dune dynamics and characteristics that may be applied in other systems were developed. These include:

- Extraction of topographic variables of active dunes based on shading effects from passive satellite images (Chapter 1).

- Establishment of quantitative relationships between spectral properties of dune sand and their content of fine particles, free iron oxides, and biogenic crust (chapters 2 and 8).
- The use of a digital camera to derive the content of fine particles and fre iron oxides in sand samples (Chapter 2).
- A method to calculate dune movement rates from either historical maps or aerial photographs, using an objective method that takes into account also those parts of the dunes that did not move (chapters 3 and 4).
- The application of directional filters on satellite images and digital elevation models to model the effects of vegetation and topography on the surface aerodynamic roughness ($Z_0$) and sand erosion/deposition rates (chapters 5 and 6).
- The use of a graphic exploratory data analysis method to unveil the adaptations of perennial dune plants to sand activity, erosion and deposition (Chapter 7).
- The impact of the scale of the analysis on the explanatory power of different variables was demonstrated using an autocorrelation analysis (in the discussion).

In addition to new methods, in this thesis an assessment and comparison of various indicators of dune activity/stability was done. The relevance of such indicators depends on the stage on the dune stabilization/re-activation process:

- When dunes are active, variables relating to their topography and movement rates are the best to quantify dune dynamics.
- As dunes start to stabilize, the role of vegetation increases and variables that are related to it in addition to vegetation cover, such as the percent cover of specific plant species and the presence of biogenic soil crusts may indicate the level of stabilization.
- As later stages when most of the dune is stabilized, soil properties such as the content of fine particles may indicated differences in stabilization levels. The content of free iron oxides was shown to be more dependent on the age of the dunes, then on their stability.

Last but not least, the role of man in this ecosystem was found to be most significant, with past activities of nomadic populations held responsible to the dunes previous state of

activity, and to their current stabilization, due to changes in land use along the coast. Current human uses of the dunes in this area, for recreation or for military training are apparently not as intensive and do not hamper further stabilization.

## References for Discussion

Al-Dabi H., Koch M., Al-Sarawi M. and El-Baz (1997), Evolution of sand dune patterns in space and time in north-western Kuwait using Landsat images, *Journal of Arid Environments*, 36: 15-24

Alpert P. and Mandel M., 1986, Wind variability – an indicator for a mesoclimatic change in Israel, Journal of Climate and Applied Meteorology, 25: 1568-1576

Alpert, P., and Ziv, B., 1989, The Sharav cyclone: observations and some theoretical considerations, *Journal of Geophysical Research*, 94 (D15): 18,495-18,514

Andrews B.D., P.A. Gares and J.D. Colby, 2002, Techniques for GIS modeling of coastal dunes, Geomorphology, 48: 289-308

Arens S.M., Q. Slings and C.N. de Vries. 2004. Mobility of a remobilized parabolic dune in Kennemerland, The Netherlands, Geomorphology, 59: 175-188

Ashkenazi T., 1947, The Bedouin tribes in the Shfela, Teva v eha Aretz, 7 (3-4): 157-160 (in Hebrew)

Asner G.P. and Heidebrecht K.B., 2002, Spectral unmixing of vegetation, soil and dry carbon cover in arid regions: comparing multispectral and hyperspectral observations, International Journal of Remote Sensing, 23 (19): 3939-3958

Asner G.P. and Lobell D.B., 2000, A biogeophysical approach for automated SWIR unmixing of soils and vegetation, Remote Sensing of Environment, 74: 99-112

Bagnold, R.A., 1941, The Physics of Blown Sand and Desert Dunes, Methuen, London, 265 p.

Bailey C. and Danin A., (1981), Bedouin plant utilization in Sinai and the Negev, *Economic Botany*, 35 (2): 145-162

Barth Hans-Jorg (1998), "Status of vegetation and an assessment of the impact of overgrazing in an area north of Jubail, Saudi Arabia", in Omar Samira A.S., Misak Raafat, Al-Ajmi Dhari and Al-Awadhi Nader (Eds.): Sustainable Development in Arid Zones, Volume 2: Management and Improvement of Desert Resources, pp. 435-450, A.A. Balkema, Rotterdam, Beookfield

Belnap J. and D.A. Gillette, 1998, Vulnerability of desert biological soil crusts to wind erosion: the influences of crust development, soil texture, and disturbance, Journal of Arid Environments, 39: 133-142

Ben-Dor, E., J.R. Irons, and G. Epema, 1998, Soil reflectance, In Remote Sensing for the Earth Sciences, edited by Rencz, A.N., in Manual of Remote Sensing Volume 3, edited by Ryerson R.A. (New York: John Wiley & Sons, Inc.), pp. 111-188

Ben-Dor E., N. Levin, A. Singer, A. Karnieli, O. Braun and G.J. Kidron, 2006, Quantitative Mapping of the Soil Rubification Process on Sand Dunes Using an Airborne CASI Hyperspectral Sensor, Geoderma, 131: 1-21.

Bullard J.E., McTainsh G.H. and Pudmenzky C., 2004, Aeolian abrasion and modes of fine particle production from natural red dune sands: an experimental study, Sedimentology, 51: 1103-1125

Cohen O., 2002, Landscape Changes in the Vegetation Coverage in the Southern Coastal Plain of Israel in the Years 1965 to 1999: Nitsanim Sand Dune Park, unpublished M.A. thesis, Department of Geography, Bar Ilan University (in Hebrew)

Curr R.H.F., Edwards Koh. A., Williams A.T. and Davies P., (2000), Assessing anthropogenic impact on Mediterranean sand dunes from aerial digital photography, *Journal of Coastal Conservation*, 6: 15-22

Danin A. and R. Nukrian, 1991, Dynamics of dune vegetation in the Southern Coastal area of Israel since 1945, Documents Phytosociologiques, XIII: 281-296

Dong Z., Gao S. and Fryrear D.W. (2001), Drag coefficients, roughness length and zero-plane displacement height as disturbed by artificial standing vegetation, Journal of Arid Environments, 49: 485-505

Fryberger S. G., (1979), Dune forms and wind regime, In: McKee Edwin D. (ed.), *A Study of Global Sand Seas*, Geological survey professional paper 1052, Washington, D.C. : United States Geological Survey, 137-169

Gay S.P., 1999, Observations regarding the movement of barchan sand dunes in the Nazca to Tanaca area of southern Peru, Geomorphology, 27: 279-293

Goldsmith V., Rosen P. and Gertner Y., 1990, Eolian transport measurements, winds, and comparison with theoretical transport in Israeli coastal dunes, in Coastal dunes: form and process, Nordstrom K.F., Psuty N.P. and Carter R.W.G. (eds.), John Wiley & Sons LTD., pp. 79-101

Goudie A., 1994, Geomorphological Techniques, 2nd edition, edited for the British Geomorphological Research Group, London and New York: Routledge

Guerin V., 1868, Description Geographique, Historique et Archeologique De La Palestine Accompagnee De Cartes Detaillees, Paris : Imprimerie imperiale

Hunter R.E., Richmond B.M. and Alpha T.R., 1983, Storm-controlled oblique dunes of the Oregon coast, Geological Society of America Bulletin, 94: 1450-1465

Hupy J.P., 2004, Influence of vegetation cover and crust type on wind-blown sediment in a semi-arid climate, Journal of Arid Environments, 58: 166-178

Illenberger W.K. and I.C. Rust, 1988, A sand budget for the Alexandria coastal dunefield, South Africa, Sedimentology, 35: 513-521

Jackson N.L. and Nordstrom K.F., 1997, Effects of time-dependent moisture content of surface sediments on aeolian transport rates across a beach, Wildwood, New Jersey, U.S.A., Earth Surface Processes and Landforms, 22: 611-621

Jimenez J.A., L.P. Maia, J. Serra and J. Morias, 1999, Aeolian dune migration along the Ceara coast, north-eastern Brazil, Sedimentology, 46: 689-701

Karnieli A., G.J. Kidron, C. Glaesser and E. Ben-Dor, 1999, Spectral characteristics of cyanobacteria soil crust in semiarid environments, Remote Sensing of Environment, 69: 67-75

Kumar M. and Bhandari M.M. (1993), Impact of human activities on the pattern and process of sand dune vegetation in the Rajasthan desert, Desertification Bulletin, 22: 45-54

Kutiel P., Zhevelev H. and Harrison R., 1999, The effect of recreational impacts on soil and vegetation of stabilized coastal dunes in the Sharon Park, Israel, Ocean and Coastal Management, 42: 1041-1060

Kutiel P., Peled Y. and Geffen E., 2000, The effect of removing shrub cover on annual plants and small mammals in a coastal sand dune ecosystem, Biological Conservation, 94: 235-242

Lancaster N., 1988, Development of linear dunes in the southwestern Kalahari, Southern Africa, Journal of Arid Environments, 14: 233-244

Lancaster N. and A. Baas, 1998, Influence of vegetation cover on sand transport by wind: field studies at Owens Lake, California, Earth Surface Processes and Landforms, 23: 69-82

Lettau H. (1969), Note on aerodynamic roughness-parameter estimation on the basis of roughness-element description, Journal of Applied Meteorology, 8: 828-832

Lemauviel S. and Roze F., 2003, Response of three plant communities to trampling in a sand dune system in Brittany (France), Environmental Management, 31(2): 227-235

Levin N., 2002, Quantitative Mapping of the Soil Rubification Process on the Coastal Sand Dunes of Israel Using an Airborne CASI Hyperspectral Sensor: The Sand Dunes of Ashdod as a

Case Study, unpublished M.A. thesis, Department of Geography and Human Environment, Tel-Aviv University, Israel

Levin N. and Ben-Dor E. (2004), ”Monitoring sand dune stabilization along the coastal dunes of Ashdod-Nizanim, Israel, 1945-1999”, Journal of Arid Environments, 58: 335-355.

Levin N., Ben-Dor E. and Kidron G.J. (2003), ”The influence of human factors on the temporal changes in the stabilization rate of the Ashdod-Nizzanim dunes”, Horizons in Geography, 57-58: 224-241 (in Hebrew; abstract in English in p. viii)

Levin N., Ben-Dor E. and Singer A. (2005), "A digital camera as a tool to measure colour indices and related properties of sandy soils in semi arid environments", International Journal of Remote Sensing, 26 (24): 5475 – 5492.

Liddle M.J. and Greig-Smith P., 1975, A survey of tracks and paths in a sand dune ecosystem, I. Soils, Journal of Applied Ecology, 12: 893-908

Lionello P., Dalan F. and Elvini E., 2002, Cyclones in the Mediterranean Region: the present and the doubled $CO_2$ climate scenarios, Climate Research, 22: 147-159

Livingstone Ian (1977), Economic irrationality among pastoral peoples: myth or reality?, Development and Change, 8: 209-230

Livingstone Ian (1986), The common property problem and pastoralist economic behaviour, *The Journal of Development Issues*, 23 (1): 5-19

McTainsh G., 1985, Desertification and dust moinitoring in West Africa, Desertification Control Bulletin, 12: 26-33

Meir A. and Tsoar H. (1996), “International borders and range ecology: the case of bedouin transborder grazing”, Human Ecology, 24 (1): 39-64

Nanson G.C., Chen X.Y., and Price D.M., 1992, Lateral migration, thermoluminescence chronology and colour variation of longitudinal dunes near Birdsville in the Simpson Desert, Central Australia, Earth Surface Processes and Landforms, 17: 807-819

Norris, R. M., 1969, Dune reddening and time, *Journal of Sedimentary Petrology*, 39 (1): 7-11

Nukrian R., 1988, Vegetation and its Habitats in the Sand Dunes south of Nahal Shikma, unpublished M.A. thesis, Department of Botany, Hebrew University of Jerusalem, Israel (in Hebrew)

Peery G. and Dmiel R., 1995, Urbanization and sand dunes in Israel: direct and indirect effects, Israel Journal of Zoology, 41: 33-41

Perevolotsky A., (1999), Interrelationships between conservation, landscape development and grazing in the Northern Negev, Ecology and Environment, 5 (2-3): 190-199 (in Hebrew)

Rango A., M. Chopping, J. Ritchie, K. Havstad, W. Kustas and T. Schmugge, 2000, Morphological characteristics of shrub coppice dunes in desert grasslands of Southern New Mexico derived from scanning LIDAR, Remote Sensing of the Environment, 74: 26–44

Ranwell D.S., 1972, Ecology of Salt Marshes and Sand Dunes, London: Chapman and Hall, 258pp.

Reifenberg A. (1947), The Soils of Palestine, Studies in Soil Formation and Land Utilization in the Mediterranean, London, Thomas Murby & Co.

Reifenberg A. (1950), The War between the Sown Land and the Wilderness, Jerusalem, The Bialik Institute, 132 p. (in Hebrew)

Reifenberg A. (1951), Caesarea, a study in the decline of a town, Israel Exploration Journal, 1, pp. 20-32

Rubin R. (1989), The debate over climatic changes in the Negev, fourth-seventh centuries C.E., Palestine Exploration Quarterly, 121, pp. 71-78

Rust I.C. and Illenberger W.K., 1996, Coastal dunes: sensitive or not?, Landscape and Urban Planning, 34: 165-169

Schmidt H. and A. Karnieli, 2000, Remote sensing of the seasonal variability of vegetation in a semi-arid environment, Journal of Arid Environments, 45: 43-59

Toutin, T., 2002, Three-dimensional topographic mapping with ASTER stereo data in rugged topography, IEEE Transactions on Geoscience and Remote Sensing, 40 (10): 2241-2247

Toutin, T., 2004, Comparison of stereo-extracted DTM from different high-resolution sensors: SPOT-5, EROS-a, IKONOS-II, and QuickBird, IEEE Transactions on Geoscience and Remote Sensing, 42 (10): 2121-2129

Tsoar, H., 1990, Trends in the development of sand dunes along the southeastern Mediterranean coast, in Dunes of the European Coasts, Catena Supplement, 18, ed. by Bakker, Th.W., Jungerius, P.D., and Klijn, J.A., 51-60.

Tsoar H., 2002, Climatic factors affecting mobility and stability of sand dunes, in Proceedings of ICAR5/GCTE-SEN Joint Conference, International Center for Arid and Semiarid Land Studies, Texas, Publication 02-2: 423-426

Tsoar, H. and D.G. Blumberg, 2002a, Formation of parabolic dunes from barchan and transverse dunes along Israel's Mediterranean coast, Earth Surface Processes and

Landforms, 27: 1147-1161

Tsoar H. and D.G. Blumberg, 2002b, The Effect of Vegetation Removal on the Rate of Aeolian Sand Transportation and the Morphologic and Dynamic Changes in the Dunes of Ashdod,

Annual report presented to the Jewish National Fund, Research no. 90-2-537-01 (in Hebrew), available at: http://www.geocities.com/parkholot1/tsohar2002.pdf

Tsoar H. and Møller J.T., 1986, The role of vegetation in the formation of linear sand dunes, Eolian Geomorphology Proceedings from the 17th annual Binghamton Geomorph. Symp., 75-95

Tsoar H. and Werner I., (1998), Reevaluation of sand dunes' mobility indices, Journal of Arid Land Studies, 7S: 265-268

Tsoar H. and Zohar Y., (1986), Desert dune sand and its potential for modern agricultural development, in Gradus Y. (ed.), Desert Development, 184-200, D. Reidel Pub. Co

de Vries A.C., W.P. Kustas, J.C. Ritchie, W. Klassen, M. Menenti and J.H. Prueger, 2003, Effective aerodynamic roughness estimated from airborne laser altimeter measurements of surface features, International Journal of Remote Sensing, 24 (7): 1545-1558

Warren, C.W., 1871, The recovery of Jerusalem :A narrative of exploration and discovery in the city and the Holy Land, London : R. Bentley

Wasson R.J. and Nanninga P.M., 1986, Estimating wind transport of sand on vegetated surfaces, Earth Surface Processes and Landforms, 11: 505-514

Wieringa J. (1973), Gust factors over open water and built-up country, Boundary-Layer Meteorology, 3: 424-441

Wieringa J. (1986), Roughness-dependent geographical interpolation of surface wind speed averages, Quarterly Journal of the Royal Meteorological Society, 112: 867-889

Wiggs G.F.S., 2001, Desert dune processes and dynamics, Progress of Physical Geography, 25 (1): 53-79

Woolard J.W. and J.D. Colby, 2002, Spatial characterization, resolution, and volumetric change of coastal dunes using airborne LIDAR: Cape Hatteras, North Carolina, Geomorphology, 48: 269-287

Zohary M. and Feinbrun N., 1941, A Geo-botanic Agricultural Survey of the Southern Shfela, Department of Botany, Hebrew University of Jerusalem, Jerusalem

Tsoar, H. 1990: "Trends in the development of sand dunes along the southeastern Mediterranean coast", in **Dunes of the European Coasts**, Catena Supplement 18, Bakker Th.W., Jungerius, P.D. and Klijn, J.A. (ed.), pp .51-60

Tsoar, H. 2002: "Climatic factors affecting mobility and stability of sand dunes", in **Proceedings of ICAR5/GCTE-SEN Joint Conference**, International Center for Arid and Semiarid Land Studies, Texas, Publication 02-2, pp. 423-426

Tsoar, H. and Blumberg, D.G. 2002: "Formation of parabolic dunes from barchan and transverse dunes along Israelís Mediterranean coast", **Earth Surface Processes and Landforms**, **27**, pp. 1147-1161

Tsoar, H. and Moller T. 1986: "The role of vegetation in the formation of linear sand dunes", in **Aeolian Geomorphology**, Nickling, W. G. (ed.), Boston, pp. 75-95

Wartena, L., van Boxel, J.H. and Veenhuysen, D. 1991: "Macroclimate, microclimate and dune formation along the West European coast", **Landscape Ecology**, **6** (1/2), pp. 15-27

Wasson, R.J. and Hyde, R. 1983: "Factors determining desert dune type", **Nature**, **304**, pp.337-339

Zaady, E., Offer, Z.Y. and Shachak, M. 2001: "The content and contributions of deposited aeolian organic matter in a dry land ecosystem of the Negev Desert, Israel", **Atmospheric Environment**, **35**, pp. 769-776

Blumberg, D.G. and Greeley, R. 1993: "Field studies of aerodynamic roughness length", **Journal of Arid Environments**, **25**, pp. 39-48

Carter, R.W.G. 1991: "Near-future sea level impacts on coastal dune landscapes", **Landscape Ecology**, **6** (1/2), pp. 29-39

Chen, X.Y., Spooner, N.A., Olley, J.M. and Questiaux, D.G. 2002: "Addition of aeolian dusts to soils in southeastern Australia: red silty clay trapped in dunes bordering Murrumbidgee River in the Wagga Wagga region", **Catena**, **47**, pp. 1-27

Cohen, S., Ianetz, A. and Stanhill, G. 2002: "Evaporative climate changes at Bet Dagan, Israel, 1964-1998", **Agricultural and Forest Meteorology**, **111**, pp. 83-91

Curr, R.H.F., Koh, A., Edwards, E., Williams, A.T. and Davies, P. 2000: "Assessing anthropogenic impact on Mediterranean sand dunes from aerial digital photography", **Journal of Coastal Conservation**, **6**, pp. 15-22

Danin, A. 1996: **Plants of desert dunes**, Springer, 177p.

Fryberger, S.G. 1979: "Dune forms and wind regime", in **A Study of Global Sand Seas**, McKee E.D. (ed.), Geological survey professional paper 1052, United States Geological Survey, Washington, pp. 137-169

Gabriel, A.D. and Kreutzwiser, R.D. 2000: "Conceptualizing environmental stress: a stress-response model of coastal sandy barriers", **Environmental Management**, **25** (1), p. 53-69

Ganor, E. 1994: "The frequency of Saharan dust episodes over Tel Aviv, Israel", **Atmospheric Environment**, **28** (17), pp. 2867-2871

Gay, Jr. S.P., 1999: Observations regarding the movement of barchan sand dunes in the Nazca to Tanaca area of southern Peru, **Geomorphology**, **27**: 279-293

Goudie, A., 1994: **Geomorphological Techniques**, 2nd edition, edited for the British Geomorphological Research Group, London and New York : Routledge

Khalidi, W. 1992: **All That Remains: The Palestinian Villages Occupied and Depopulated by Israel in 1948**, Institute for Palestine Studies, Washington D.C.

Kutiel, P., Eden, Z. and Zhevelev, H. 2001: "The impact of motorcycle traffic on soil and vegetation of stabilized coastal dunes, Israel", **Journal of Coastal Conservation**, **7**, pp. 81-90

Lancaster, M. 1997: "Response of eolian geomorphic systems to minor climate change: examples from the southern Californian deserts", **Geomorphology**, **19**, pp. 333-347

Molina, C., Rubinoff, P. and Carranza, J. 2001: **Guidelines for Low-Impact Tourism along the Coast of Quintana Roo, Mexico**, Amigos de Sian Kaían, A.C., Coastal Resources Center, Cancun, Quintana Roo, Mexico, (accessed January 10th, 2003)

Meir, A. and Tsoar, H. 1996: "International borders and range ecology: the case of bedouin transborder grazing", **Human Ecology**, **24** (1), pp. 39-64

Noy-Meir, I. 1975: **Primary and Secondary Production in Sedentary and Nomadic Grazing Systems in the Semi-arid Region: Analysis and Modelling**, Final Research Report submitted to the Ford Foundation (Project 7/E-3), Department of Botany, Hebrew University, Jerusalem, Israel

Ranwell, D.S. 1972: **Ecology of salt marshes and sand dunes**, Chapman and Hall, London, 258p.

זיוון, ז. 1990: **יחסי הישוב היהודי והבדווים בנגב - חזית המגע והשפעתה על עיצוב ספר ההתיישבות בשנות הארבעים והחמישים**, חיבוד לשם קבלת התואר "מוסמך למדעי הרוח והחברה", אוניברסיטת בן-גוריון, הפקולטה למדעי הרוח והחברה, המחלקה לגאוגרפיה

חואלדי, ע. 1992: **השפעת שינויים בשימושי קרקע בדווים על הסביבה הטבעית בגבול ישראל-מצרים מאז שנות הארבעים**, עבודת גמר לתואר "מוסמך", הפקולטה למדעי הרוח והחברה, אוניברסיטת בן גוריון בנגב

כהן, ע., קותיאל, פ., שושני, מ. ושו"ב, מ. 2002: "התפשטות שיטה כחלחלה (Acacia saligna) בחולות ניצנים: דוגמא לחדירה ביולוגית במערכת חופית", **אופקים בגאוגרפיה**, **55**, ע"ע 79-96

ליפשיץ, נ. וביגר, ג. 2000: **נלבישך שלמת ירק: הייעור בארץ ישראל: מאה שנים ראשונות, 1850-1950**, קרן קיימת לישראל, ירושלים, 265 ע'

מדינת ישראל 1979: **השתלטות בלתי חוקית על קרקע המדינה - דו"ח מסכם**, מוגש לד"ר יוסף בורג, יו"ר ועדת השרים לענייני פנים, שרותים ואיכות הסביבה, ספטמבר 1979, ירושלים

מלול, א. 2000: "חשיבות התווך החולי למשק המים", **שמירת טבע בחולות מישור החוף - מטרות וממשק**, הרשות לשמירת הטבע והגנים הלאומיים - מחוז מרכז - חטיבת המדע: אוסף תקצירים, ניצנים 6-7 דצמבר 2000

מרקס, ע. 1974: **החברה הבדוית בנגב**, הוצאת רשפים

פרבולוצקי, א. 1991: "רהביליטציה של העז השחורה או האם מעז ייצא מתוק?", **השדה**, ע"א (**ד'**), ע"ע 619-622

צוער, ח. ובלומברג, ד. 1990: "השפעת המצוק החופי על חדירת חול איאולי למישור החוף הדרומי של ישראל", **אופקים בגאוגרפיה**, **31**, ע"ע 155-168

קותיאל, פ. 2000: "שימור וממשק של שטחים פתוחים ברצועת החולות של מישור החוף בישראל", **אקולוגיה וסביבה**, כרך **6 (2)**, ע"ע 91-96

קרסל, ג. מ. 1976: **פרטיות לעומת שבטיות - דינמיקה של קהילת בדוים בתהליך התעיירות**, הוצאת הקיבוץ המאוחד

רטנר, ד. 1959: "נדידת הבדוים בשנות בצורת", **טבע וארץ**, א' (ה'), ע"ע 175-178

רשות שמורות הטבע 1989: **סיכום סיור הנהלת רשות במישור החוף מתאריך ה 9/3/89**, רשות שמורות הטבע מחוז מרכז, נכתב ב-15/3/1989, תיק ביולוגי שמורת ניצנים

Al-Dabi, H., Koch, M., Al-Sarawi, M. and El-Baz 1997: "Evolution of sand dune patterns in space and time in north-western Kuwait using Landsat images", **Journal of Arid Environments**, **36**, pp.15-24

Almagor, G., Gill, D. and Perath, I. 2000: "Marine sand resources offshore Israel", **Marine Georesources and Geotechnology**, **18**, pp. 1-42

Barret, E.C. and Curtis, L.F. 1992: **Introduction to environmental remote sensing**, Chapman and Hall, London, 426p.

Barth, H.J. 1998: "Status of vegetation and an assessment of the impact of overgrazing in an area north of Jubail, Saudi Arabia", in Omar, S.A.S., Misak, R., Al-Ajmi, D. and Al-Awadhi, N. (Eds.): **Sustainable Development in Arid Zones, Volume 2: Management and Improvement of Desert Resources**, pp. 435-450, A.A. Balkema, Rotterdam, Beookfield

Belnap, J. and Gillette, D.A. 1998: "Vulnerability of desert biological soil crusts to wind erosion: the influences of crust development, soil texture, and disturbance", **Journal of Arid Environments**, **39**, pp. 133-142

(שינויים של יותר מ-10% לשנה במהירות הדיונות או כיסוי הצומח).

פינוי הבדווים בסוף שנות השבעים היה סופי, כפי שניתן ללמוד מאיור 10 והוא מצביע על כך שלא היה צורך במבצעי עזים נוספים בחולות מישור החוף הדרומי לאחר שנת 1978.

**סיכום ומסקנות**

עד אמצע המאה העשרים היו חולות מישור החוף חשופים מכיסוי צומח. ניתוח סדרות זמן של צילומי אוויר והדמאות לוויין בחולות אשדוד-ניצנים העלה שמאז קום המדינה חלו שינויים עתיים בתהליך ההתייצבות של החולות. עד לסוף שנות הששים חלו תהליכי התייצבות, בין סוף שנות הששים לסוף שנות השבעים הייתה פעילות מחודשת של הדיונות ומאז סוף שנות השבעים התחדשו תהליכי ההתייצבות של הדיונות. המחקר הנוכחי מצביע על הגורם האנושי - לחץ הרעייה, הרמיסה והכריתה של הצמחייה ע״י הבדווים - כגורם המרכזי בהסברת השינויים העתיים בקצב תנועת הדיונות. עוצמת הרעייה יכולה איפוא לשמש ככלי מרכזי בויסות תנועת הדיונות. שימוש בעדרים יכול לסייע לשמירת הנופים של דיונות נודדות במישור החוף וכך לסייע לשמירתם של צמחים, בעלי חיים וצורות נוף הייחודיים לחולות נודדים. השימוש ברעייה לצורכי ממשק בחולות יכול איפוא להצטרף למגוון פעולות ממשק אחרות העושות שימוש בעדרים, כגון פתיחת אזורים של חורש סבוך ומניעת שריפות (פרבולוצקי 1991).

**תודות**

אנו מבקשים להודות לכל האנשים והמוסדות אשר סייעו לנו בעבודה זו: רשות הטבע והגנים (זאב קולר, שי כהן, צבי חורש), הסיירת הירוקה (אלון גלילי, נעמי אלטשולר, גלעד אלטמן, יואל דב ו נעם אלדן), קיבוץ ניצנים (נאוה זלינגר, אריה אדלהייט), החברה להגנת הטבע (יאיר פרג׳ון, איריס האן ויחידת ה GIS), נציבות המים (אבי מלול), רשות הניקוז שקמה-בשור (אלחנן ויינברגר), המרכז למיפוי ישראל, השירות המטאורולוגי, הקרן הקיימת לישראל, עמיעד ברזנר ועמירם אורן. כמו כן אנו מביעים תודתנו למבקרים אשר קראו את המאמר ותרמו לו ע״י הערותיהם.

**מקורות**

אורטל, ר. 1975: הודפס יולי 1983, **סקר שמורות טבע במישור חוף יהודה**, רשות שמורות הטבע

אשכנזי, ט. 1947: ״שבטי הבדוים בשפלה״, **טבע והארץ**, **ז׳** (ג-ד), ע״ע 157-160

ביילי, י. ודנין, א. 1975: ״צמחי מדבר בחיי הבדווים״, **רשימות בנושא הבדווים, ב׳**, קובץ 5, ע״ע 67-107

ביתן, א. ורובין, ש. 1994: **אטלס אקלימי לתכנון פיסי וסביבתי בישראל**, אוניברסיטת תל-אביב, משרד התחבורה ומשרד האנרגיה והתשתיות

ברזילי, ע. 2001: **השינויים הגיאומורפולוגיים שחלו בחוליות החופיות של אזור אשדוד מאמצע שנות ה-40 ועד אמצע שנות ה-90**, עבודת גמר לתואר ״מוסמך למדעי הרוח והחברה״, המחלקה לגאוגרפיה ופיתוח סביבתי, אוניברסיטת בן גוריון בנגב

ברלינר, ר. 1979: **הצעה לשמורת הטבע בחולות השפלה הדרומית באזור זיקים**, 12.7.1979, רשות שמורות הטבע, תל-אביב

גרן, ו. 1982: **תיאור גאוגרפי, היסטורי וארכיאולוגי של ארץ-ישראל כרך שני: יהודה (ב)**, יד יצחק בן-צבי, ירושלים

**דו״ח מבקר המדינה מספר 30 לשנת 1979**

**דו״ח מבקר המדינה מספר 35 לשנת 1984, חלק א׳**

זהרי, מ. ופינברון, נ. 1941: **סקירה גיאובוטנית - חקלאית של השפלה הדרומית**, המחלקה לבוטניקה של האוניברסיטה העברית, ירושלים

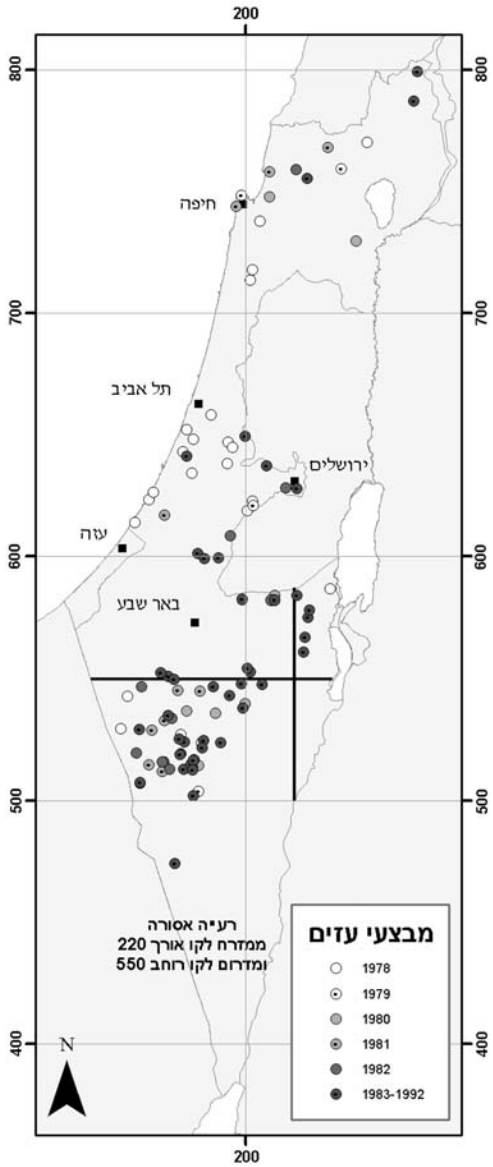


**איור 10**: מפת מבצעי עזים שנערכו בכל שטח המדינה, בשנים 1978-1992 (לפי נתוני הסיירת הירוקה)

"קרקעות חול - חמרה... שטחים המעובדים כיום נמצאים תחת משטר רעייה חזק של עדרי הבדואים, המכרסמים את הצמחים עד פני הקרקע... לעתים מתכסות הקרקעות ע"י חולות נודדים..." "שמורת כרמיה - שטחה כ-400 דונם באזור החוליות המיוצבות... השמורה נמצאת תחת לחץ רעייה חזק של עדרי כבשים ועזים, השייכים לבדואים ואלה אינם נותנים לצמחיה להתפתח..." "שמורת חולות ניצנים - שטחה כ-7,000 דונם... רעייה בלתי מבוקרת של עדרי צאן ובקר של הבדואים וכן התיישבותם הבלתי חוקית פוגעת בשמורה" "שמורת חולות נחל שקמה - בשל היותו בעבר הקרוב סמוך לגבול המדיני, הרעייה בו מצומצמת ביותר..." "שמורת אשדוד - שטח השמורה כ-700 דונם, מגודרת ושמורה מפני רעית צאן ובקר... העזים אשר רעו כאן בעבר העדיפו באופן ברור את השיטה המלבינה...".

הנדידה וההתיישבות הבלתי מבוקרת של הבדווים הובילו להקמת ה"סיירת הירוקה" באוקטובר 1976. פעולות הסיירת הירוקה כללו תפישת עדרים ופינוי הבדווים ממרכז הארץ בחזרה לבקעת באר-שבע (דו"חות מבקר המדינה לשנים 1979 ו-1984). פעילותה של הסיירת הירוקה הייתה מהירה וכבר ב-1979 מדווחת ברלינר על השתקמות צמחיית החולות שמצפון לנחל שקמה (דרומית לאשקלון):

"...ואילו שיחי הרותם הגבוהים נכרתו עד לפני כשנה ע"י בדואים פולשים על עדריהם ורק עתה הם מתעודדים לאחר שלחץ הכריתה והרעיה הוסר" (שם, ע' 6).

"לחצי הכריתה והרעיה פסקו בשנה האחרונה, לאחר גרוש העדרים הפולשים וכבר עתה ניתן לראות התאוששות בצמחיה המקומית. שיחי הרותם, שהיו מבוקשים בעבר כחומר בעירה והצאן ליחך את הענפים הרכים שנתחדשו מבסיסם, שבו לצמח ולפתח נוף חדש, אם כי כיסויים היחסי בשטח עדיין דל למדי. גם שיחי הלענה מתרבים כל העת מזרעים ומכסים את חזית החול הנודד. אלה תורמים הרבה לייצוב החולות ולהעשרת הקרקע בחומר אורגני ומסייעים ע"י כך להתיישבות מינים נוספים. יתכן כי תוך זמן קצר ניתן יהיה לצפות כאן בעליית הכיסוי היחסי בשטח ע"י חברות הצמחים המפותחות יותר ועשירות המינים, כחברת רותם-שמשון והתייצבות החול במקומות רבים בהם הוסר קודם הכיסוי הצמחי" (שם, ע' 8).

כפי שניתן לראות באיור 9 קיימת התאמה טובה בין תחילת הנדידה של הבדווים (סוף שנות ה-60) לעלייה בקצב התנועה של הדיונות ובין פינויים מחולות מישור החוף (סוף שנות ה-70) לתחילת התייצבותם של הדיונות. מגמה זו עולה בקנה אחד עם הירידה בתנועת הדיונות מיד לאחר פינוי הבדווים ממישור החוף עם סיומה של מלחמת העצמאות. מתוך המגמות המוצגות באיור 9 ניתן ללמוד גם על התגובה המהירה של המערכת האקולוגית להסרת הלחץ האנושי. זו התבטאה בקצב הירידה המהיר של תנועת הדיונות

הפיזיים. בפרמטר היחיד בו נמצאה התאמה גבוהה יחסית (התאדות; $R_2$= 23%), ההתאמה נמצאת בניגוד להיגיון העומד מאחורי המשתנה, שהרי עלייה בהתאדות אמורה לפי Lancaster (1997) להגביר את פעילות הדיונות ואילו לפי הנתונים הנוכחיים התקבלה דווקא מגמה הפוכה המעידה על קשר מקרי שאיננו נסיבתי.

ההתאמה הנמוכה שנמצאה בין כמות המשקעים לתנועת הדיונות מתאימה למודל של Tsoar (2002). לפי מודל זה משום שבמישור החוף כמות המשקעים היא מעל 50 מ״מ לשנה משטר הרוחות הוא הקובע אם דיונה תהיה מיוצבת או פעילה ולא פרמטרים אקלימיים של משקעים והתאדות. עוצמות הרוח שאיפיינו את האזור בשנות המחקר היו נמוכות ולא נמצאה התאמה מובהקת בין משטר הרוחות לקצב תנועת הדיונות. לא נמצא גם קשר בין מפלס מי התהום לבין פעילות הדיונות וזאת בהתאמה למסקנות Ranwell (1972) אשר מציין כי רק מי תהום גבוהים המגיעים לשני מטר לפחות מתחת לפני הקרקע ישפיעו על הצומח וכך על מידת יציבותן של הדיונות. מאחר ומפלס מי התהום באזור המחקר נמוך בממוצע משלושה מטרים מעל לפני הים, השפעתם על התייצבות הדיונות (שגובהן הממוצע כעשרה מטר והן מגיעות עד לגבהים של 50 מטר מעל לפני הים) מזערית.

היעדר קשר בין הגורמים הפיזיים מחד וההתאמה העתית שנמצאה בין פעילות הבדווים לשינויי המגמה בתנועת החולות מצביעים על קשר לכאורה בין מידת יציבותן של הדיונות ללחצי הרעייה של הבדווים. כאן מן הראוי לציין שלמרות שהפעילות האנושית לא הייתה מוגבלת לבדווים, הרי שהן העלייה בתיירות ונופש (החל משנות ה-80) והן העלייה בשימוש ברכבי שטח (החל משנות ה-90, Kutiel et al. 2001) לא התבטאה בעלייה בתנועת הדיונות ודווקא בשנות השמונים והתשעים נרשמה ירידה בקצב התנועה של הדיונות. ההסבר נעוץ בכך שרוב הפעילות הנ״ל מוגבלת לאורך דרכי עפר, כך שהשפעתה על הדיונות עצמן מוגבלת ביותר. שימוש נרחב בדרכים והפרעה בעלת אינטנסיביות נמוכה יכולה גם להסביר את העובדה שלא נמצא קשר בין הפעילות הצבאית לנדידת הדיונות.

הגורם המשמעותי להערכתנו שהביא לשינויים העתיים בתהליך ההתייצבות, כפי שהם באים לידי ביטוי באיורים 3 ו-6, הוא השינויים שחלו בפעילות הערבים והבדווים, אשר הושפעו ממדיניות ממשלות ישראל לגביהם. עד ל-1948 גרו בכפרים הערביים שבסמוך לחולות אשדוד-ניצנים, קרוב ל-15,000 איש (לפי נתוני המפקד הבריטי מ-1945; Khalidi 1992) כשבנוסף להם ישבו בסמוך לחוף הים מעל ל3,000 בדווים (אשכנזי, 1947). חקלאות המוואסי שהייתה נפוצה בשקעים הבין-דיונריים באזור זה (כפי שניתן לראות בצילומי אוויר משנת 1944/5), מעידה על נוכחות פעילה של האדם בחולות, הן של הערבים תושבי הכפרים הסמוכים לחוף (זהרי ופינברון 1941; גרן 1982) והן של הבדווים אשר ישבו שם (אשכנזי 1947). לאחר מלחמת השחרור לא נותרו עוד ישובים ערביים במישור החוף הדרומי. אותם בדווים שלא עזבו את שטח המדינה (כ-13,000 במספר) רוכזו בבקעת באר-שבע (אזור ה׳סייג׳; זיוון 1990) והיו נתונים תחת ממשל צבאי אשר לא אפשר להם לנדוד כרצונם עם עדריהם. ההתייצבות המהירה של חולות מישור החוף בשנים הראשונות להקמת המדינה (ברזילי 2001; Tsoar and Blumberg 2002; וראה גם איור מספר 3), מיוחסת לכן להסרת לחץ הרעייה, הרמיסה וכריתת הצמחייה ע״י הבדווים ותושבי הכפרים הערביים (ראה ביילי ודנין 1975, לגבי השימושים השונים שעושים הבדווים בצמחיית המדבר).

ביטול הממשל הצבאי בדצמבר 1966 הביא בעקבותיו לנדידה של הבדווים צפונה. מאחר ולא היה בנמצא גוף שיתבע מבעלי העדרים לשוב דרומה, ״החלו הבדואים להשתקע ולהכות שורשים בכל רחבי הארץ - בתוך שטחי ישובים חקלאיים, שטחי אש ועל אדמות מדינה - איש איש בהישג ידו״ (דו״ח הועדה הבין משרדית להשתלטות בלתי חוקית על קרקע המדינה, 1979, ע׳ 2). הסרת הגבול בין ישראל לסיני ב-1967 הביאה בעקבותיה גם לחדירת עדרי הבדווים של צפון-מזרח סיני (חואלדי 1992) ובמקביל החלה גם חדירה של עדרי עזים מרצועת עזה לתחומי הקו הירוק.

נדידתם של הבדווים התעצמה בשנת 1970 ואמצע שנות השבעים שהיו שנות בצורת בצפון הנגב (ראה איור מספר 10). נדידה זו תועדה ע״י Noy-Meir (1975) ומוזכרת גם ע״י אורטל (1975) המציין גם את הנזקים שנגרמו:

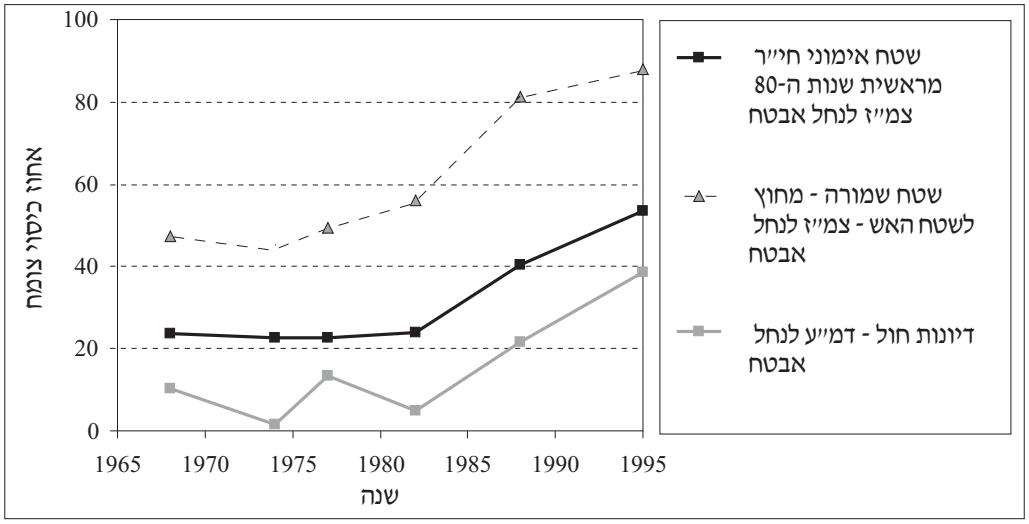


**איור 8**: השינויים בכיסוי הצומח בחולות ניצנים באזור של נחל אבטח, השוואה בין האזורים המוצגים באיור 7, בהם הייתה אינטנסיביות שונה של פעילות צבאית.

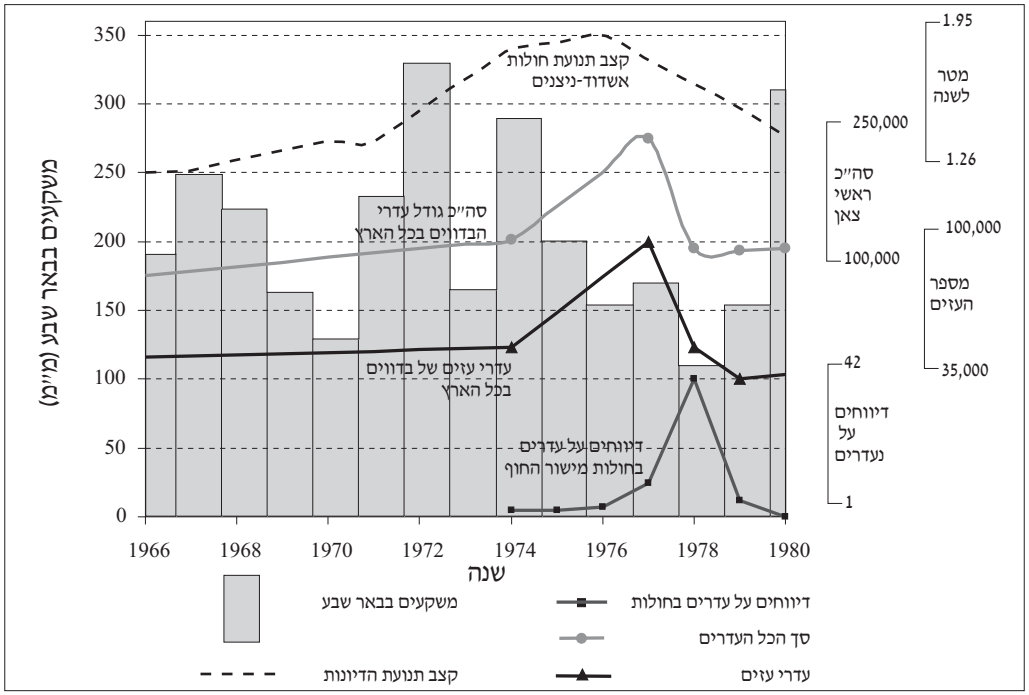


**איור 9**: הדינמיקה של משטר הרעייה של הבדווים בחולות מישור החוף בשנים 1966-1980: כמות המשקעים בבאר שבע בעונת החורף (לפי נתוני השירות המטאורולוגי) ניתנת במ״מ ומתייחסת לעונת החורף; דיווחים על נוכחות עדרים בחולות מישור החוף הדרומי, השינויים במספר ראשי הצאן ובמספר העזים שבידי הבדווים (לפי מקורות שונים; קווי המגמה של גודל העדרים מבוססים על ממוצע רץ של שלוש שנים), קצב תנועת הדיונות בחולות אשדוד-ניצנים (הנתונים המתייחסים לבדווים ולתנועת הדיונות מוסטים לשם בהירות).

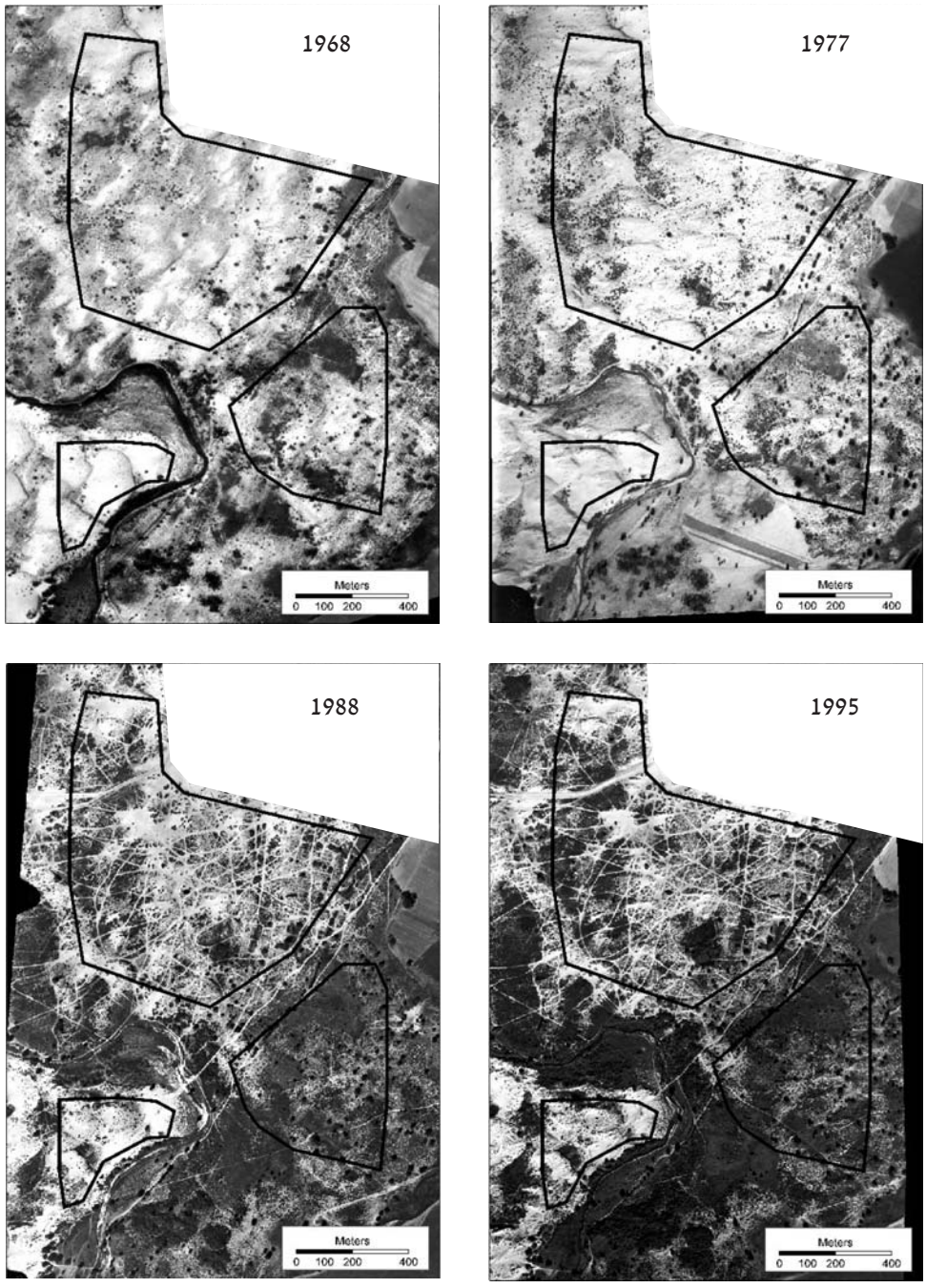


**איור 7**: סדרת זמן של צילומי אוויר (מהשנים 1968, 1977, 1988 ו-1995) המציגים את אזור נחל אבטח, חולות ניצנים. השטח התחום מצפון לנחל מתייחס לאזור בו מרוכזים עיקר האימונים בשטח האש, השטח במזרח מתייחס לחלק משמורת הטבע שמחוץ לשטח האש והשטח ממערב לנחל כלול בשטח האש אך כמעט ואין בו פעילות צבאית.


**איור 6**: השינויים בכיסוי הצומח בחולות אשדוד, בשטח בו נותרו כיום גרוטאות צבאיות רבות (האזור שצבעו אפור באיור 5) ובשאר השטח (אזורי האפור הבהיר והכהה באיור 5)

1989; שי כהן, ראיון אישי 2002). ניתוח סדרת זמן של צילומי אוויר המתמקדת בשטח שבין בסיס ניצנים לקריית המטווחים שבו מרוכזים רוב האימונים מראה כי בטרם הקמת הבסיס, כיסוי הצומח היה נמוך וכמעט שלא היו שם דרכי עפר (איור 7). לאחר הקמת הבסיס בראשית שנות השמונים, ניתן להבחין בעלייה מהירה בצפיפות דרכי העפר, אך גם בכיסוי הצומח. העלייה בכיסוי הצומח בשטח האש מקבילה לעלייה בכיסוי הצומח באזורים אחרים בחולות ניצנים בהם לא היו אימונים צבאיים (איור 8). ניתן להסיק לפיכך כי לא נראה שלאימונים הצבאיים בחולות אשדוד-ניצנים הייתה השפעה על תהליכי ההתייצבות של החולות שם.

נוכחותם של בדווים בחולות מישור החוף הדרומי בכלל וחולות אשדוד-ניצנים בפרט, בשנים שלאחר קום המדינה, זוכה לאזכורים רבים בשנים 1974-1979. באיור 9 ניתן לראות שמספר הדיווחים לשנה מגיע לשיאו בסוף שנות השבעים, לאחר הקמת הסיירת הירוקה, אותן השנים בהן התחדש תהליך ההתייצבות של הדיונות. כך למשל פקח אזור השפלה של רשות שמורות הטבע (בזמנו) מעריך את מספר התנחלויות הבדווים באזור השפלה באותה התקופה ב-49 (צבי חורש 2001, ראיון אישי). לפי יואל דב מהסיירת הירוקה (2001, ראיון אישי) היו באותה תקופה כ-30 משפחות של בדווים באזור אשדוד-אשקלון ואילו לפי אלון גלילי (2001, ראיון אישי) - מנהלה הראשון של הסיירת הירוקה - רעו בשנות השבעים בחולות שבין תל-אביב לרצועת עזה כ-15,000 ראשי צאן.

שיעור עדרי הבדווים בכלל ועדרי העזים בפרט ירד באופן חד בסוף שנות השבעים בכל הארץ, כפי שניתן לראות באיור 9. לפי הערכת הסיירת, בעקבות מבצעי העזים (בהם הוחרמו ונמכרו עזים שרעו בניגוד לחוק) ופעולות ההסברה, קטן מספר העזים השחורות שבידי הבדווים בנגב מ-100,000 ראש בקירוב בסוף 1977, לכ-43,000 בקירוב באמצע 1978 (דו"ח מבקר המדינה לשנת 1979). באיור 10 מוצגת הפרישה הארצית של מבצעי העזים בין השנים 1978-1992, לפי נתוני הסיירת הירוקה. מתוך המפה ניתן ללמוד על הפרישה הארצית של עדרי הבדווים בשנות השבעים וכן לראות כי בשנה הראשונה בה נערכו מבצעי העזים (1978), הם רוכזו במרכז הארץ וחלקם אף נערכו בחולות מישור החוף הדרומי, בין תל-אביב לרצועת עזה.

## דיון

השוואה בין השינויים בקצב התקדמות הדיונות לגורמים פיזיים לימדה על התאמה נמוכה המעידה על היעדר קשר בין מידת התייצבות הדיונות לגורמים

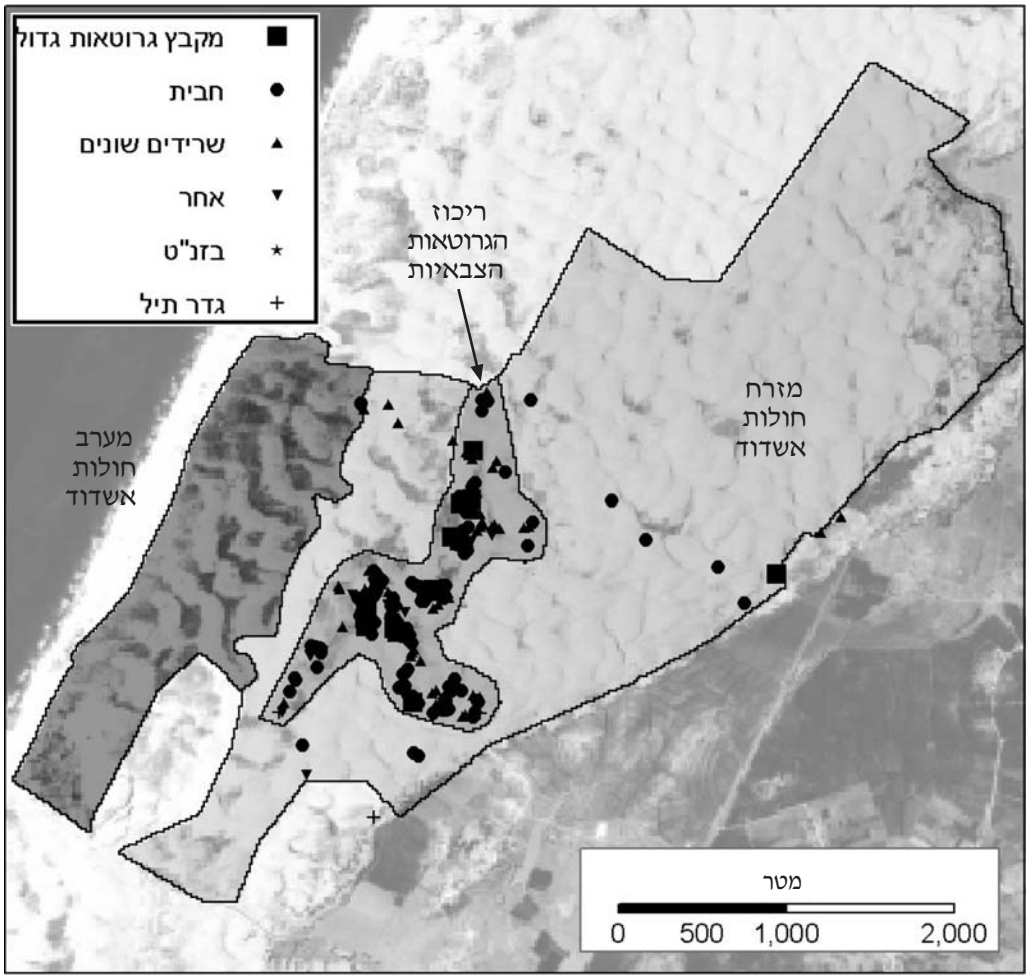


**איור 5**: מיפוי של שרידי גרוטאות צבאיות בחולות אשדוד באמצעות מכשיר GPS, על רקע צילום לוויין Corona מ-1963

הפעילות הצבאית בחולות אשדוד כללה אימוני טנקים (מבסיס גיוליס) בין אמצע שנות החמישים ועד מלחמת ששת הימים (עמירם אורן, ראיון אישי 2002) ואימוני רגלים של טירוני חיל השריון שהסתיימו עם מלחמת יום הכיפורים (עמיעד ברזנר, ראיון אישי 2002). מיפוי של שרידי גרוטאות צבאיות שנותרו עד היום בשטח (איור 5) גילה שקיים אזור בו הריכוז של השרידים הללו גבוה מאד. בהנחה שלפעילות הצבאית הייתה השפעה על תהליכי ההתייצבות ושבאזור זה הפעילות הצבאית הייתה אינטנסיבית יותר, הרי שנצפה לראות שהשינויים בכיסוי הצומח שם גבוהים מאשר בשאר השטח. אך כפי שניתן לראות באיור 6, המגמות העתיות בשינויים בכיסוי הצומח בשטח בו מרוכזים השרידים הצבאיים נמצאו זהות לאלה של שאר השטח. הנתונים לא הצביעו איפה על כך שהפעילות הצבאית גרמה לשונות מרחבית בתהליכי ההתייצבות.

משנות השמונים ואילך החלו חולות ניצנים לשמש כשטח אימונים של בסיס הטירונים שהוקם שם עם הפינוי מסיני. עיקר הפעילות רוכזה בשטח שבין כביש הגישה לחוף ניצנים מצפון, נחל אבטח מדרום וקריית המטווחים ממערב (ראה איור 1). הפעילות כוללת בעיקר אימונים רגליים, כאשר אימוני הנסיעה בחולות הופסקו באמצע שנות התשעים (רשות שמורות הטבע,

**טבלה 2**: מידת ההתאמה בין קצב תנועת הדיונות השנתי הממוצע בחולות אשדוד-ניצנים, למספר פרמטרים אקלימיים וסביבתיים

| שם המשתנה האקלימי/סביבתי | R | המקום אליו מתייחסים הנתונים | השנים בהן הוא נבחן 1970-1996 | מקור הנתונים |
|---|---|---|---|---|
| כיווניות סחיפת החול: RDP/DP | 0.01 | עזה | 1970-1996 | השירות המטאורולוגי |
| פוטנציאל סחיפת החול: DP | 0.01 | עזה | 1971-1996 | השירות המטאורולוגי |
| כיווניות סחיפת החול: RDP/DP | 0.29 | תל-אביב | 1971-1996 | השירות המטאורולוגי |
| פוטנציאל סחיפת החול DP | -0.01 | תל-אביב | 1950-1996 | השירות המטאורולוגי |
| כמות המשקעים השנתית | -0.12 | ניצנים | 1950-1996 | השירות המטאורולוגי |
| מספר ימי הגשם | -0.31 | ניצנים | 1965-1996 | השירות המטאורולוגי |
| התאדות מגיגית | -0.48 | בית דגן | 1960-1996 | Cohen et al. (2002) |
| מפלס מי התהום בסתיו | 0.21 | קידוחים בחולות אשדוד | 1958-1960 | נציבות המים |
| מספר ספות האבק | -0.36 | תל-אביב | | Ganor (1994) |

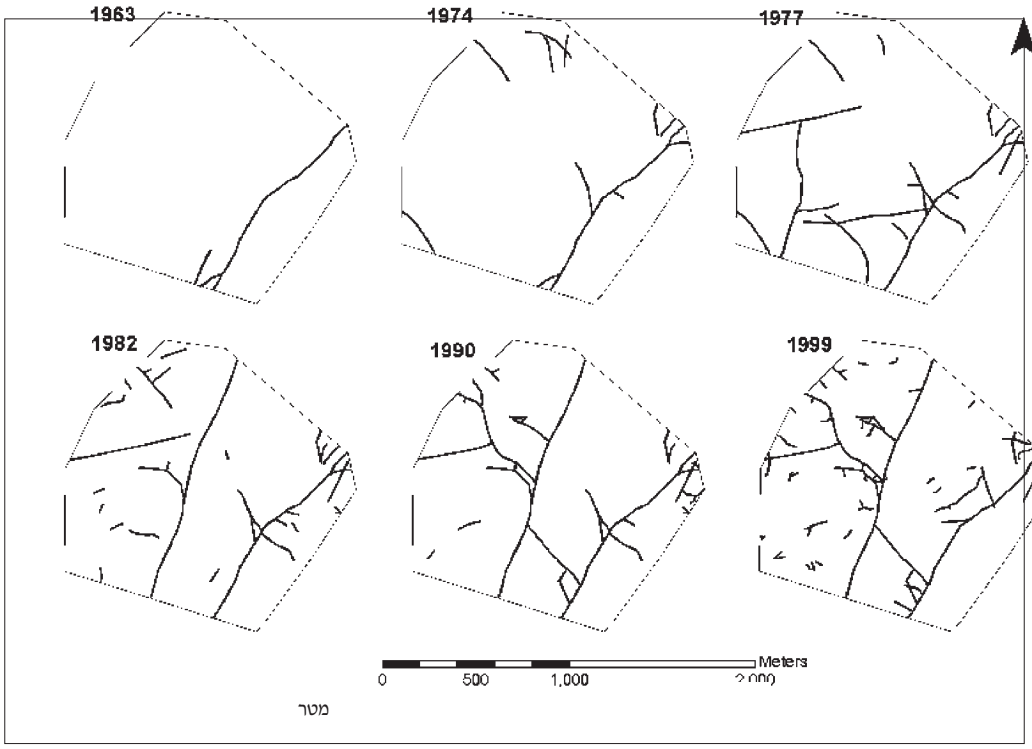


**איור 4**: מיפוי השינויים בצפיפות דרכי העפר במערב חולות אשדוד, לפי צילומי אוויר

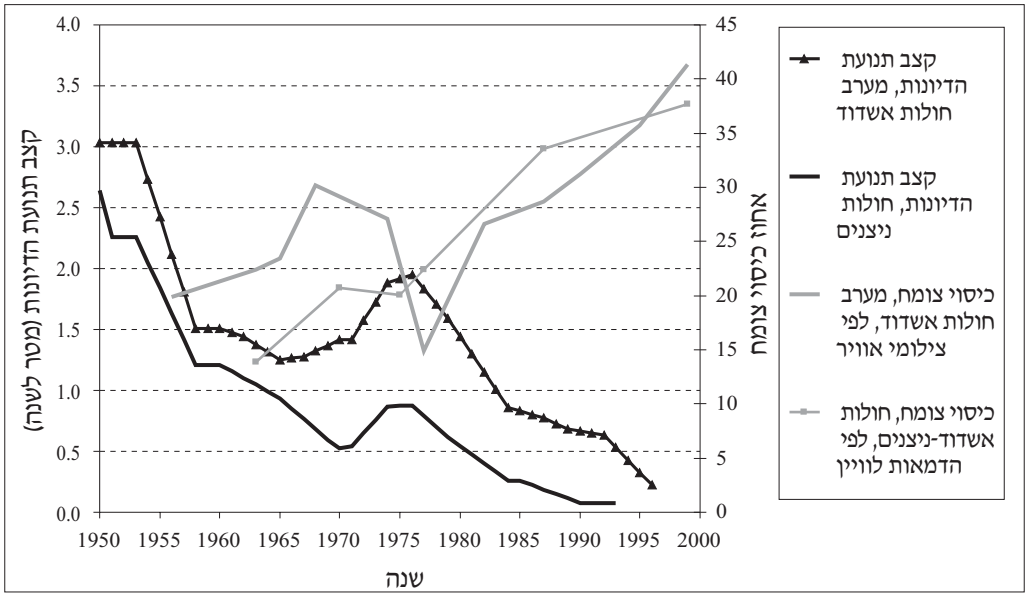


**איור 3**: שינויים עתיים בתהליך ההתייצבות של חולות אשדוד-ניצנים, לפי ניתוח צילומי אוויר והדמאות לוויין

בית ספר שדה שקמים בניצנים של החברה להגנת הטבע ומקורות נוספים. כן נערכו שיחות עם אנשים המכירים את האזור. מיפוי ההתפתחות של דרכי העפר נעשה מתוך צילומי אוויר היסטוריים ואילו מיפוי השרידים שנותרו בשטח נערך בסתיו 2002 באמצעות מכשיר GPS.

**תוצאות**

המגמות העתיות בכיסוי הצומח ובקצב התנועה של הדיונות מוצגות באיור 3 ונמצאות בהתאמה האחת לשנייה ($R_2$=72% עבור חולות אשדוד). מקום המדינה ועד סוף שנות הששים הדיונות היו נתונות בתהליך של התייצבות (איור 3), דהיינו, עלייה בכיסוי הצומח וירידה בקצב התנועה של הדיונות, כשקצב התנועה ירד מ-3 ל-1.25 מטר לשנה. בין סוף שנות הששים לסוף שנות השבעים הייתה פעילות מחודשת של הדיונות, המתבטאת בירידה בכיסוי הצומח ובעלייה בקצב התנועה של הדיונות מ-1.25 ל-2 מטר לשנה. תהליך ההתייצבות של הדיונות התחדש בסוף שנות השבעים והוא נמשך עד היום, כאשר קצב התנועה של הדיונות עמד בסוף שנות התשעים על כ-0.25 מטר לשנה. הגורמים להבדלים המרחביים בקצב ההתייצבות לא ייסקרו במסגרת המאמר הנוכחי.

טבלה מספר 2 מציגה את התוצאות של מבחנים סטטיסטיים שבחנו האם קיימת התאמה בין הקצב הממוצע של תנועת הדיונות בחולות אשדוד-ניצנים לבין מספר משתנים אקלימיים: שכיחות סופות אבק, משטר הרוחות (DP ו-RDP/DP), כמות המשקעים השנתית ומספר ימי הגשם, ההתאדות השנתית וממוצע מפלס מי התהום בחולות אשדוד. כפי שניתן לראות, לא נמצאה התאמה גבוהה בין אף אחד מהמשתנים הפיזיים שנבחנו לבין השינויים העתיים בקצב התנועה של הדיונות, כאשר השונות המוסברת ($R_2$) נמוכה מ-25% בכל המשתנים שנבחנו.

באיור 4 ניתן לראות שעם השנים חלה עלייה מתמדת בצפיפות דרכי העפר. עלייה זו נובעת מהעלייה ברמת החיים שהביאה לגידול במספר רכבי השטח בשנות התשעים (Kutiel et al. 2001) וכן מגידול האוכלוסייה בארץ בכלל ובישובים הסמוכים. הפגיעה של רכבי שטח קשה מאד והורסת לחלוטין את הצומח. ברם, פגיעה זו מוגבלת לדרכים ספורות שרוחבן אינו עולה על 2-3 מטר ולכן סה"כ השטח המופרע ביחס לכלל השטח הוא קטן ביותר.

ניצנים מדרום לנחל אבטח. קצבי תנועת הדיונות המוצגים באיורים המלווים את המאמר מתייחסים לממוצע רץ 5-שנתי של קצב תנועת הדיונות.

ניתוח השפעת הגורמים האקלימיים נעשה על סמך סדרות זמן של:

- **נתוני רוח**: נתונים יומיים של מהירות וכיוון הרוח בתחנות של עזה ותל-אביב בשנים 1970-2000 בשעות היום (09:00, 12:00, 15:00 GMT). מתוך נתוני הרוח חושבו ערכי DP ו-RDP/DP שנתיים עבור השנים 1970-2000, תוך הנחת מהירות סף של 7 מ'/ש' (צוער ובלומברג 1990). ניתן לחשב את ערכי DP לפי טבלאות המציגות את שכיחות הרוחות שנשבו לפי כיוונן ועוצמתן, תוך שימוש בנוסחה הבאה (כאשר החישוב נעשה בנפרד לכל כיוון רוח):

$$DP = \Sigma q = U_2 (U-U_t) * t/100$$

כאשר U מבטא את מהירות הרוח (בגובה עשרה מטר), $U_t$ את מהירות הסף של הרוח ו-t את משך הזמן בו נשבה הרוח (באחוזים) מכיוון מסוים בעוצמה נתונה.

ההתחממות הדיפרנציאלית של היבשה והים גורמת לכך שמהירות הרוח גבוהה יותר בד"כ בשעות היום מאשר בשעות הלילה (Wartena et al. 1991) ולכן נעשה שימוש רק בנתוני יום. החלטתנו זו נתמכה בבדיקות פרילימנריות שערכנו. מתוך טבלאות המצויות באטלס האקלימי של ביתן ורובין (1994) המתייחסות לתחנות של עזה ושדה-דוב, חשבנו את ערכי DP, RDP/DP ו-RDD פעם אחת לפי כל שעות היממה ובפעם השניה רק לפי נתוני השעות 09:00, 12:00, 15:00. התוצאות מוצגות בטבלה מספר 1. מתוך הנתונים שבטבלה ניתן לראות כי פוטנציאל הסחיפה של הרוח (DP) גבוה יותר בשעות 09:00, 12:00, 15:00 לעומת זה של כל שעות היום, אך לא נמצאו הבדלים מובהקים (לפי מבחן t-test) בין הפרמטרים של פוטנציאל סחיפת החול (ערכי DP, RDP/DP או RDD) בין הנתונים של כל שעות היממה לאלה של השעות 09:00, 12:00, 15:00 בלבד.

- **משקעים**: נתונים חודשיים של כמות משקעים ומספר ימי גשם בתחנת ניצנים, עבור השנים 1949/50-1999/2000, שהתקבלו מהשירות המטאורולוגי.
- **התאדות**: נתוני התאדות שנתיים לבית-דגן לשנים 1964-1998 כפי שפורסמו במחקרם של Cohen et al. (2002).
- **מפלס מי התהום**: על סמך נתוני מפלס מעונת הסתיו כפי שנמדדו ב-46 קידוחים בחולות אשדוד שנעשו בשנים 1960-2000 ואשר התקבלו מנציבות המים.
- **סופות אבק**: שכיחות סופות האבק השנתיות בתל-אביב עבור השנים 1958/9-1990/1 (מתוך Ganor 1994) כאינדיקטור לכמות החומר הדק המושקע. הקריטריונים ששימשו להגדרת אירוע של סופת אבק ע"י Ganor (1994) הם ראות אופקית מתחת לעשרה ק"מ, ריכוזי אבק מרחף מעל 120 $\mu g\ m^{-3}$ וכמות אבק שוקע מעל 0.1 $g\ m^{-2}$.

ניתוח השינויים בפעילות האנושית באזורי החולות מבוסס על חומר שנאסף בארכיונים שונים (ארכיון רשות הטבע והגנים, ארכיון קיבוץ ניצנים). אלו כוללים דו"חות של הסיירת הירוקה (דו"חות מבצעי עזים ודו"חות במסגרת הועדה לשמירה ופיתוח של שטחים שאינן מעובדים), דו"ח הועדה להשתלטות בלתי חוקית על קרקע המדינה (נספח ו') משנת 1979, תיקים של

**טבלה 1**: פוטנציאל סחיפת החול בתחנות שדה-דוב ועזה, בכל שעות היממה לעומת שעות היום בלבד (15,12,9), כפי שחושב מתוך הטבלאות המופיעות באטלס האקלימי של ביתן ורובין (1994).

| עזה | DP | RDP/DP | RDD | | שדה דוב | DP | RDP/DP | RDD |
|---|---|---|---|---|---|---|---|---|
| כל השעות | 13.6 | 0.82 | 74.0 | | כל השעות | 10.2 | 0.88 | 63.1 |
| 9, 12, 15 | 18.5 | 0.73 | 69.4 | | 9, 12, 15 | 11.1 | 0.83 | 56.8 |

שנבחרה הייתה "אפינית לוקאלית" (local affine triangulation) הזמינה בתוכנת ENVI 3.4 (Research Systems, Inc. 2001), וזאת, על מנת להתגבר על העיוותים הגיאומטריים הלא סיסטמטיים הנגרמים עקב הטופוגרפיה של הדיונות וגובה הטיסה הנמוך.

כמו כן נעשה שימוש בצילומי לוויין הריגול האמריקאי Corona מהשנים 1963 ו-1970 ובהדמאות לוויין ה-Landsat מהשנים 1975, 1977, 1987 ו-1999. הדמאות הלוויין עוגנו לרשת ישראל החדשה באותה השיטה בה עוגנו צילומי האוויר.

**כיסוי הצומח** חושב מצילומי האוויר ומהדמאות הלוויין ע"י זיהוי אזורי עניין של חול חשוף (0% כיסוי צומח) ושל צמחיית חולות בשקעים (100% כיסוי צומח). בצילומי האוויר ובצילומי לוויין ה-Corona כוילו ערכי האפור של הצילום לאחוזי כיסוי צומח לפי אזורי העניין הללו (אזור בהיר: חול חשוף, אזור כהה: צמחייה), בעוד שבהדמאות לוויין ה-Landsat אינדקס ה-NDVI (Normalized Difference Vegetation Index) שימש כייחוס לחישוב אחוזי כיסוי הצומח. אינדקס ה-NDVI מבוסס על ההבדלים בהחזרה של קרינת השמש בין אורכי הגל של האינפרה-אדום הקרוב (NIR) והאדום (R), אשר נובעים ממאפייני הבליעה של הצמחייה וערכיו נמצאים בהתאמה לפעילות הכלורופיל בצמח, לכיסוי הצומח ולביומסה (Barret and Curtis 1992). חישוב האינדקס נעשה כך:

$$NDVI = (NIR - R) / (NIR + R)$$

קצב התנועה של הדיונות ניתן למדידה ע"י השוואת המיקום של חזית הדיונה (מישור ההחלקה) בזמנים שונים. חזית הדיונה ניתנת לזיהוי ויזואלי בצילומי אוויר אם ע"י מאפייני ההצללה האופייניים לה, או ע"י כיסוי הצומח הרב המתפתח למרגלות הדיונה כאשר זו נמצאת בשלבים מתקדמים של התייצבות. השיטה המסורתית לחישוב קצב התנועה של דיונות מבוססת על מציאת המרחק בין קווי חזית הדיונה במספר נקודות נבחרות, כמתואר ע"י Gay (1999). בשיטה זו, בה עשה שימוש ברזילי (2001) בניתוחו את חולות אשדוד, ישנן בעיות הקשורות לאופן הדגימה של הנקודות הנבחרות (Goudie 1994: 347-348) ולכך שהשיטה מתייחסת רק לאותם חלקים של חזית הדיונה אשר נעו קדימה. גישה זו אפשרית רק בדיונות פעילות ללא כיסוי צומח, שאינן משנות את צורתן. בתהליך התייצבות של דיונות, חלים שינויים בצורת הדיונה (למשל, מדיונה רוחבית לדיונה פרבולית: Tsoar and Blumberg 2002) וישנם חלקים מחזית הדיונה שמתייצבים ולא נעים יותר. חישוב קצב התנועה של הדיונה, תוך התייחסות רק לאותם חלקים שנעו קדימה, בלא להתייחס לאלה שנותרו במקומם, יביא לכן להערכת יתר של קצב התנועה של הדיונות.

במסגרת המחקר פיתחנו שיטה חדשה, אשר מחשבת את קצב התנועה של חזית הדיונה תוך התחשבות בתנועת חזית הדיונה לכל רוחבה ותוך כדי שקלול אותם חלקים של חזית הדיונה שלא נעו קדימה. דרך החישוב (המתוארת באיור 2) נעשית כך: קווי חזית הדיונה מצילומים עוקבים, מחוברים תוך יצירת פוליגון. לכל פוליגון מחושב קו השלד (המייצג את האורך הממוצע של חזית הדיונה בין שני התאריכים של צילומי האוויר). המרחק השנתי הממוצע שעברה חזית הדיונה בין התאריכים של שני הצילומים מחושב ע"י חלוקת שטח הפוליגון, באורך קו השלד, במספר השנים שבין הצילומים. על מנת להתחשב באותם חלקים של הדיונה שלא נעו (למשל קצוות הדיונה באיור 2 בין השנים 1960-1970), קו השלד בו עושים שימוש הוא זה הארוך ביותר לכל דיונה, המייצג את התקופה בה הדיונה התקדמה לרוחב כל החזית שלה, לפני שהחלו תהליכי ההתייצבות. בסך הכל נמדד קצב התנועה של 27 דיונות (שרוחב חזיתותיהן מגיע יחדיו ל-9,570 מטר) במערב חולות אשדוד ו-28 דיונות (שרוחב חזיתותיהן מגיע יחדיו ל-6,750 מטר) בחולות

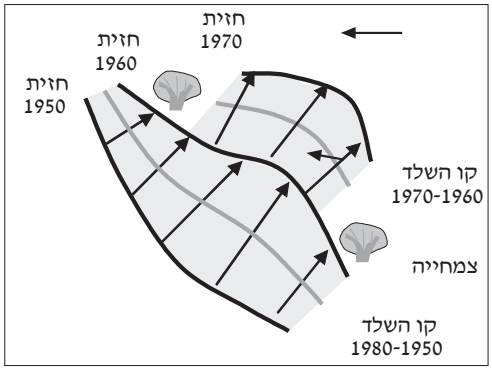


**איור 2**: תיאור סכימטי של התקדמות חזית הדיונה והקווים המשמשים למדידת קצב התנועה

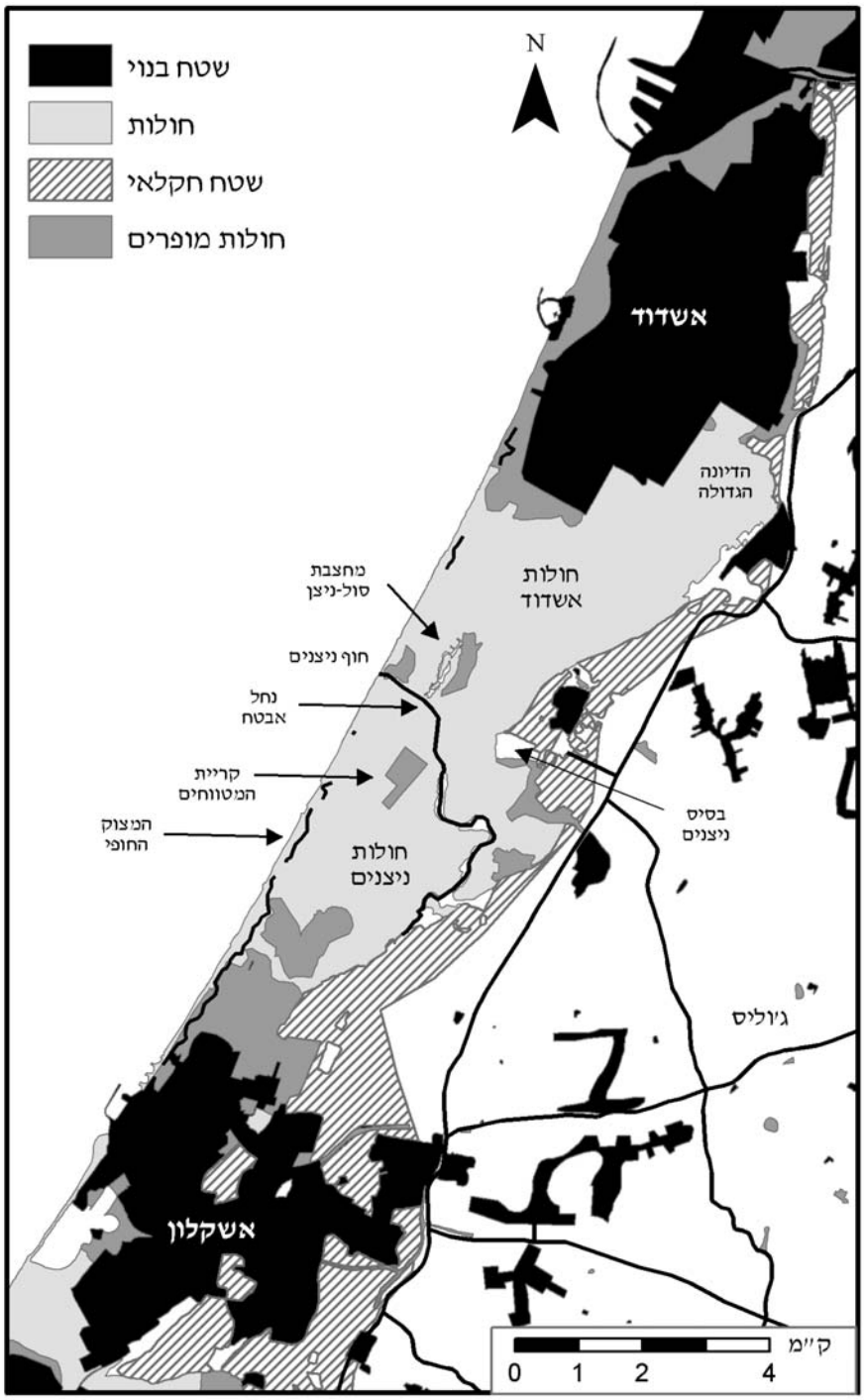


**איור 1**: מפת אזור המחקר (מבוססת ברובה על נתונים מיחידת ה-GIS של החברה להגנת הטבע)

הסעודית: Barth 1998). רמיסת הקרומים הביוגניים ע"י תנועת אנשים ועדרים בחולות וכריתת הצמחים הגדלים בחולות (ביילי ודנין 1975), מביאים להקטנת החיכוך של פני השטח ולהורדת מהירות הסף של סחיפת החול ע"י הרוח.

- **תנועת אנשים ורכבים:** אלו עשויים להוריד את כיסוי הצומח ולשבור קרומים ביוגניים וכך לחשוף את הדיונות לסחיפה ע"י הרוח (Curr et al. 2000).
- **אימונים צבאיים**: אלו עלולים להגביר את הפעילות האיאולית עקב פגיעה בפני השטח, כמוסבר בסעיף הקודם (Al-Dabi et al.1997).
- **נטיעת צמחים:** זו עשויה לסייע לייצוב החולות (ליפשיץ וביגר 2000).
- **בנייה לאורך החוף:** זו עשויה לנתק את הדיונות ממקור אספקת החול ולהוריד את מהירות הרוח (Molina et al. 2001).

נראה שאין בשני הגורמים האחרונים (נטיעת צמחים לייצוב חולות ובנייה לאורך החוף), כמו גם בכמות החומר הזמין להשפיע על תהליך ההתייצבות בחולות אשדוד-ניצנים.

לפי ההערכות המקובלות (Almagor et al. 2000) לא יחולו שינויים באספקת החול לחופי ישראל בעתיד הנראה לעין, מאחר ובדלתא של הנילוס (כולל חלקיה התת-מימיים) ולאורך חופי סיני עדיין מצויות כמויות גדולות של חול.

פעולות הנטיעה לייצוב חולות, אשר נעשו ע"י הבריטים בתקופת המנדט (ליפשיץ וביגר 2000) היו בגבול המזרחי של החולות על מנת להוות מחסום בפני תנועתם מזרחה. בעקבות הנטיעה של שיטה כחלחלה ע"י הקרן הקיימת לישראל בראשית שנות הששים (כהן וחובריו 2002) חלה אמנם פלישה ביולוגית של צמח זה לבתי גידול חוליים, אך נמצא כי השיטה אינה מתפשטת לדיונות חול חשופות (כהן וחובריו 2002) ולפיכך אינה יכולה להוות גורם בייצובן; בנוסף, פעולות לייצוב חולות לא יכולות להוות גורם המסביר פעילות מחודשת של הדיונות בשנים מסוימות.

אשר לשינויים בשטח הבנוי, מלבד מספר מבנים קטן ביותר בחוף ניצנים, לא נגרמה הפרעה משמעותית לזרימת הרוח ולהסעת החול מהחוף פנימה.

לפיכך הצבנו את המטרות הבאות:

- ראשית, להעריך במדויק את השינויים העתיים בתהליך ההתייצבות של חולות אשדוד-ניצנים בשיטות של חישה מרחוק.
- לאתר את הגורמים הפיזיים (משקעים, התאדות, עוצמה וכיוון הרוח, מפלס מי תהום והשקעה של חומר דק) והאנושיים (פעילויות הקשורות בנוכחותם של בדווים, מטיילים או חיילים בשטח החולות), אשר מסבירים את השינויים העתיים בתהליך ההתייצבות.

**אזור המחקר**

עיקר השטח של הדיונות החופיות בישראל נמצא במישור החוף הדרומי (בין תל-אביב לרצועת עזה) עקב הקרבה למקור החול (הדלתא של הנילוס) והיעדרו של מצוק חופי המהווה מחסום בפני תנועת החול פנימה (Tsoar 1990). האזור בו מתמקד המחקר הוא שטח החולות שבין הערים אשדוד ואשקלון אשר מוגדר במחקר זה כחולות אשדוד-ניצנים (בשם חולות אשדוד מכנים את השטח שבין אשדוד לכביש הרוחב המוביל מכביש מספר 4 לחוף ניצנים ובשם חולות ניצנים מכנים את החולות שמדרום לכביש הרוחב הנ"ל ועד לאשקלון; ראה מפה באיור 1).

**מתודולוגיה**

על מנת לנטר את תהליך ההתייצבות של הדיונות, נרכשה מהמרכז למיפוי ישראל סדרת זמן של צילומי אוויר (רובם מחודשי הקיץ והסתיו, כאשר כיסוי הצומח החד-שנתי מינימלי). בחולות אשדוד נעשה שימוש בצילומי אוויר מ-12 שנים (1944, 1956, 1963, 1965, 1968, 1974, 1977, 1982, 1987, 1990, 1995, 1999) ובחולות ניצנים נעשה שימוש בצילומי אוויר מ-11 שנים (1945, 1949, 1956, 1963, 1968, 1972, 1974, 1977, 1982, 1988, 1997). כל הצילומים עוגנו לאורתופוטו תוך שימוש ביותר מ-100 נקודות בקרה לכל צילום אוויר (רוב נקודות הבקרה בהן נעשה שימוש היו שיחים ועצים). שיטת הטרנספורמציה

והתשעים, כפי שמתבטא בכיסוי הצומח.

המחקרים שנערכו בחולות דרום מישור החוף כיסו תחומי זמן שונים; בהקשר זה רק ברזילי (2001) מתייחס לשינויים שחלו מאז קום המדינה. המחקרים הללו גילו שקיימת שונות בזמן בקצב ההתייצבות של הדיונות אך לפי ברזילי (2001) תהליך ההתייצבות של הדיונות התחדש בשנות השבעים, בעוד שלפי כהן וחובריו (2002) שנות השמונים מהוות את נקודת המפנה. יתרה מזו, לא ניתן הסבר לשינויים העתיים בקצב התנועה של הדיונות.

מספר גורמים פיזיים מוזכרים בספרות כמשפיעים על התייצבות הדיונות (וכך גם על כיסוי הצומח):

- **משטר הרוחות:** רוחות חזקות מגבירות את הסעת החול וגורמות להורדת כיסוי הצומח ע"י חשיפת שורשי הצמחים, קבירתם ושחיקת רקמותיהם (ע"י פגיעת גרגרי החול בצמח). Fryberger (1979) פיתח שיטה לחשב את פוטנציאל סחיפת החול ע"י הרוח DP ( Drift Potential), כיווניות הרוח RDP/DP ( RDP: Resultant Drift Potential) וכיוון פוטנציאל סחיפת החול RDD (Resultant Drift Direction) במחקר שהשווה בין אזורי חולות מרחבי העולם. פרמטרים אלו נמצאו כמתאימים להבחין בין תנאים אקלימיים בהם דיונות תהיינה מיוצבות לאלה בהם דיונות תהיינה פעילות (Tsoar 2002).
- **כמות המשקעים וההתאדות:** כמות משקעים גבוהה והתאדות נמוכה מעלים את כיסוי הצומח (Lancaster 1997); כשפני השטח רטובים, מהירות הסף של הרוח הנדרשת להתחלת ההסעה של גרגרי החול (דהיינו, כוח הגזירה של הרוח) עולה ולפיכך יורדת תנועת הדיונות.
- **כיסוי הצומח**: הצומח משפיע על הסביבה החולית, דרך שינויים בכיוון ובמהירות הרוח המביאים לשינוי הטופוגרפיה והמורפולוגיה של הדיונה (Danin 1996; Tsoar and Blumberg 2002).
- **קרומים ביוגניים**: קרומים ביוגניים מייצבים את הקרקע ומקטינים את סחיפת החול ע"י הרוח (Belnap and Gillette 1998).
- **חספוס פני השטח**: חספוס פני השטח $Z_0$ הוא אותו גובה מעל פני השטח בו מהירות הרוח היא אפס (Blumberg and Greeley 1993). ערכו של $Z_0$ מושפע ממאפייני הצמחייה והקרקע ומשפיע על פרופיל הרוח. ככל שחספוס פני השטח גדול יותר, כך סחיפת החול ע"י הרוח תהיה קטנה יותר.
- **השקעת חומר דק:** החומר הדק עשוי לסייע ליציבות הדיונות ולכיסוי גבוה יותר של צמחים וקרומים, בעיקר בדיונות בהן כבר החלו תהליכי התייצבות (Tsoar and Moller 1986). אבק שוקע יכול לחדור לתוך הקרקע ע"י הגשם ( Chen et al. 2002; Zaady et al. 2001) שבא לעתים לאחר שבירת השרב.
- **מפלס מי תהום:** מפלס מי תהום גבוה (התלוי בכמות המשקעים ובפעילות האדם - שאיבה או החדרה) מעלה את האזור הרטוב ומגדיל את כוח הגזירה של הרוח. מפלס מי תהום גבוה מאפשר גם לחברות צומח עשירות יותר להתפתח בשקעים שבין הדיונות ובתנאים מסוימים (כאשר שורשי הצמחים מגיעם למפלס מי התהום) אף לייצב דיונות נמוכות (עד שני מטר; Ranwell 1972) מאידך, ירידה במפלס מי התהום עלולה להביא לדפלציה ולהגברת הפעילות של הדיונות (Carter 1991).
- **כמות החומר הזמין:** זו מכתיבה את אופי הסביבה החופית. כך, היווצרות דיונות חופיות תלויה באספקת חול מהחוף (Wasson and Hyde 1983).

אחד ההבדלים בין לחצים אנושיים ללחצים אקלימיים/פיזיים, הוא שלחצים אנושיים לרוב מצטברים ולא מחזוריים ואינם מותירים זמן למערכת הטבעית להתאושש (Gabriel and Kreutzwiser 2000). מאפיין נוסף של הפרעות אנושיות הוא באינטנסיביות ההפרעה ובמהירות ההשפעה שלה על הסביבה. בין הגורמים האנושיים המוזכרים בספרות כמשפיעים על פעילות הדיונות:

- **לחץ הרעייה ו/או הכריתה של הצמחייה:** שינויים בלחץ הרעייה והכריתה של הצמחייה מביא לפעילות מחודשת (או לייצוב) של הדיונות (למשל בנגב: Meir and Tsoar 1996 ; במזרח ערב

# השפעתם של גורמים אנושיים על השינויים העיתיים בקצב ההתייצבות של חולות אשדוד-ניצנים

**נעם לוין, איל בן-דור, גיורא קדרון**
החוג לגיאוגרפיה ולסביבת האדם, אוניברסיטת תל-אביב

מחקרים קודמים שנערכו בחולות אשדוד-ניצנים הצביעו על כך שקצב תהליך ההתייצבות של הדיונות, אשר החל עם קום המדינה, איננו קבוע בזמן או במרחב. עם זאת, קיימות אי-התאמות בין תוצאות המחקרים הללו ולא ניתנו הסברים לגורמים הפיזיים והאנושיים אשר עומדים מאחורי השינויים שנצפו. במסגרת מאמר זה אנו מצביעים על הפעילות האנושית בחולות כגורם המרכזי בהסברת השינויים העיתיים בתהליך ההתייצבות. באמצעות שיטות ייחודיות לניתוח צילומי אוויר והדמאות נמצאו שלושה שלבים עתיים בתהליך : 1948-1966 התייצבות, 1966-1977 פעילות מחודשת של הדיונות ומ-1977 ואילך - התייצבות מחודשת.

על מנת להסביר את השונות העתית בקצב ההתייצבות נבחנו השינויים בקצב תנועת החול ובכיסוי הצומח וזאת ביחס לגורמים פיזיים (משקעים, התאדות, עוצמת הרוח וכיווניות הרוח, מפלס מי התהום ושכיחות סופות האבק) וגורמים אנושיים (נוכחות בדווים באזורי חולות, אימוני הצבא, תיירות ונופש). לא נמצאה התאמה בין הגורמים הפיזיים שנבחנו לבין השינויים שחלו בפעילות הדיונות. מאידך, הנתונים מצביעים על קשר בין פעילות הדיונות לנוכחות אנתרופוגנית של הערבים ובעיקר של הבדווים באזור, כאשר תחילת התייצבות הדיונות עם הקמת המדינה מוסברת בהפסקת פעילותם של הערבים והבדווים שם. ריכוז הבדווים בצפון הנגב לאחר קום המדינה הביא להורדת הלחץ האנושי על החולות ואיפשר לצמחייה להתבסס. פעילות הבדווים באזור התחדשה בשנים 1966-1977 על רקע ביטול הממשל הצבאי, תוצאות מלחמת ששת הימים והבצורות שאירעו בנגב בשנות השבעים, והתבטאה בתנועה מחודשת של הדיונות. פעילות הסיירת הירוקה בסוף שנות השבעים הביאה לפינוי הבדווים ממישור החוף ולהסדרת הרעייה ובעקבות כך להתייצבות הדיונות. תהליכים אלו נמשכים עד היום.

**מלות מפתח** : דיונות חופיות, בדואים, תהליך התייצבות, צילומי אוויר, שימושי קרקע

**מבוא**

תהליך ההתייצבות של חולות מישור החוף הנו תהליך דינמי המאפשר ללמוד על הקשרים שבין האקלים, הקרקע, הצומח ופעילות האדם. ככלל, תהליך ההתייצבות של דיונות הנו התהליך בו חלה עלייה בכיסוי הצומח, עלייה בשיעור החומר הדק (סילט וחרסית) ועלייה בכיסוי הקרומים הביוגניים אשר בעקבותיהם חלה ירידה בקצב תנועת החול. תהליך זה מלווה גם בשינוי מורפולוגי של הדיונות ( Tsoar and Moller 1986; Tsoar and Blumberg 2002). תהליך ההתייצבות מושפע מגורמים אקלימיים (Tsoar 2002) ומפעילות אנושית (ליפשיץ וביגר 2000 ; חואלדי 1992) אשר עשויה להביא לייצוב החולות או להסרת כיסוי הצומח.

לחולות מישור החוף יש חשיבות רבה עבור משק המים (מלול 2000), לקיומם של צמחים ובעלי חיים המותאמים לאזורי חולות (קותיאל 2000) וכאזור לפעילות פנאי ונופש. תהליך ההתייצבות של הדיונות מביא לאובדן בית הגידול של החול הנודד הנחוץ לקיומם של בעלי חיים וצמחים אשר הותאמו אליו ולאובדן של אחת מיחידות הנוף האופייניות למישור החוף. הבנה של היקף וקצב התהליכים והגורמים להם נחוצה על מנת לנהל את אזורי החולות כיאות.

מחקרים שנעשו בחולות אשדוד אשר ניתחו את קצב תנועת הדיונות בחולות אשדוד בין השנים 1945-1995 ואת השינויים בכיסוי הצומח בשטח של 560 אקר, מצאו כי קיימת שונות עתית בקצב ההתייצבות (ברזילי 2001; Tsoar and Blumberg 2002). מחקרים אלו הצביעו על עצירה של תהליך ההתייצבות בין השנים 1966-1974 (תהליך אשר החל עם קום המדינה). לפי כהן וחובריו (2002) התייצבות הדיונות התחדשה בשנות השמונים

(עד למרחק של כ 100 מטר), כך שהרזולוציה הבינונית של הדמאות לוויין היא מספיקה. עם זאת, שימוש בהדמאות לוויין ברזולוציה גבוהה (של 1-2 מטר) עשוי לשפר את המודל, כיוון שאז יהיה ניתן לעמוד על המבנה המרחבי של הצומח ברמת הנבח׳ות. דבר זה נכון גם לגבי הגורם הטופוגרפי – אשר ניתן יהיה לעמוד על ההשפעה שלו באשר לסחיפת החול ע״י הרוח תוך שימוש בהדמאות LIDAR של לייזר מוטס, אשר מאפשרות למפות בצורה מפורטת מאד את הטופוגרפיה, כולל את הנבח׳ות.

מאחר וכיסוי הצומח החד-שנתי ונוכחותם של קרומי קרקע ביוגניים נבדקו בכל אחד מהיתדות, וכיוון שהם רגישים מאד לתנאים של יציבות פני השטח, זו אפשרה להסביר 64% מהשונות בנוכחותם של הקרומים ו 73% מהשונות בנוכחותו של צומח חד-שנתי.

מפת החספוס האירודינאמי ($Z_0$) נמצאה כמסבירה רק 40% מהשונות ביציבות פני השטח כפי שזו נמדדה ביתדות. עם זאת, עבור מישור ההחלקה של הדיונות יכולת החיזוי הייתה גבוהה בהרבה והגיעה ל 60%. הסיבה העיקרית לכך היא שמהירות הרוח ממנה חושבו ערכי החספוס נמדדה בגובה של 2.5 מטר, בעוד שתנועת החול מושפעת ממהירות הרוח בגובה נמוך הרבה יותר. מאחר ומהירות הרוח ככל שעולים בגובה מושפעת מאוחר יותר משינויים בחספוס פני השטח, על מנת לאפשר חיזוי טוב יותר של הסעת חול ע״י הרוח מתוך מדידות של מהירות רוח וחספוס, יש לערוך את מדידות הרוח בגובה של כחצי מטר.

עבודה זו מציגה חידושים באשר ל: (1) כלים של מערכות מידע גיאוגרפיות וחישה מרחוק לניטור אזורי דיונות - חילוץ טופוגרפיה, השימוש במצלמה דיגיטאלית, שיטה לחישוב קצב תנועת הדיונות מצילומי אוויר, מיפוי נוכחותם של קרומים ביוגניים, שימוש בפילטרים כיווניים על מנת לאמוד את השפעת הצומח והטופוגרפיה על סחיפת החול; (2) כימותם של מדדים שונים של התייצבות תוך השוואה ביניהם והצבעה על כך שמדדים שונים הינם יותר או פחות רלוונטיים לניטור תהליכי התייצבות בהתאם לשלב בו נמצא תהליך ההתייצבות; (3) בחינה של גורמים פיסיים ואנושיים שונים והשפעתם על תהליך התייצבות הדיונות; (4) הצבעה על מישור ההחלקה של הדיונות כיחידה הגיאומורפולוגית המתאימה ביותר לניטור תהליכי התייצבות, כיוון שבה הם באים לידי הביטוי הרב ביותר.

בעוד שבעבר נטו לראות בדיונות נודדות איום על אזורים חקלאיים ועל תשתיות שונות, באזורים בהם דיונות מתייצבות בהשפעת פעילויות אנושיות בעבר או בהווה (במכוון או שלא במכוון) מתחילים לבחון גם את ההשלכות האקולוגיות והנופיות של ההתייצבות. זו מובילה לכך שבעלי חיים וצמחים שהותאמו לבית גידול של חול נודד נמצאים בסכנת הכחדה מקומית, ולעתים אף עולמית, אם המדובר במינים אנדמיים. על רקע זה נערכים כיום ניסיונות, בארץ ובעולם לגרום לדיונות מיוצבות להיות פעילות מחדש ע״י הסרה של הצומח, אם באמצעים מכניים או ידניים. מאחר ובארץ פוטנציאל הסחיפה של החול ע״י הרוח חלש, תידרש הסרה חוזרת ונשנית של הצומח. בעוד שרעייה נתפשה בעבר כאיום על הצומח הטבעי בארץ, מזה כעשרים שנה שהיא משמשת ככלי לממשק של שטחים פתוחים. עם זאת, השבתם של עדרי עזים לחולות וחזרתם של הבדואים להשתשמש בצמחי החולות לצרכים ביתיים לא נראים ריאליים עוד, עם תהליכי העיור של הבדואים.

## סיכום ומסקנות

הדיונות החופיות בארץ היו פעילות עד לאמצע המאה העשרים ומאז הן עוברות תהליכי התייצבות עקב השינויים שחלו בשימושי הקרקע לאורך החוף אשר הביאו להפסקה פתאומית בלחץ האנושי על הצומח בחולות. לחץ זה שהופעל בעבר ע״י בדואים ועדריהם ואשר כלל כריתה של צמחים לצורכי בעירה ובנייה, רעייה של הצמחים ורמיסה של פני השטח היה הגורם לכך שהדיונות היו בעבר פעילות. לחץ זה הוחלף כיום ברכבי שטח ומטיילים, אך אלה ככל הנראה אינם מספיקים להפחתת כיסוי הצומח ולהפעלת הדיונות, למעט לאורך צירים או באתרים המושכים אליהם קהל רב (כמו הדיונה הגדולה באשדוד). כל זאת, על רקע פוטנציאל הסחיפה הנמוך של החול ע״י הרוח בארץ, כאשר אירועים של רוחות סערה המסוגלות להסיע את החול הינם קצרים.

עם תהליך ההתייצבות של דיונות המאפיינים הביוטיים והא-ביוטיים שלהן משתנים. בהתאם, בתנאי יציבות שונים, שיטות שונות של חישה מרחוק, מדדים שונים של יציבות דיונות, וגורמים פיסיים שונים נעשים יותר או פחות מתאימים ומשפיעים.

כאשר דיונות הינן פעילות, די לנטר את מידת הפעילות שלהן באמצעות מאפייני הטופוגרפיה לבדם או באמצעות קצב התנועה שלהן. עם העלייה בכיסוי הצומח, קצב התנועה של הדיונות פוחת עד לשלב בו הן עשויות לא לנוע יותר, גם אם יש בחלקים מסוימים שלהן תנועת חול. בשלב מתקדם שכזה תכונות הקרקע (המתבטאות בצבע) ובייחוד נוכחותם של קרומים ביוגניים, צומח חד-שנתי אך גם תכולת החומר הדק, עשויים להעיד על מידת היציבות של פני השטח.

מבין היחידות הגיאומורפולוגיות השונות המרכיבות דיונה חופית, נמצא שמישור ההחלקה של הדיונה יכול לשמש כיחידה המלמדת בצורה הטובה ביותר על מידת היציבות של הדיונה כולה, כמעט בכל משתנה שנבדק. זאת כיוון שליחידה זו, המהווה אחוזים בודדים בלבד משטח הדיונה כולה, אמורים להגיע כמעט כל גרגרי החול מהצד הפונה לרוח. עם התייצבות הדיונה והעלייה בכיסוי הצומח על ראש הדיונה ובחלקים אחרים שלה, חלק מגרגרי החול יושקעו בנבח׳ות ולא יגיעו למישור ההחלקה. כך שעם הזמן גם היחידה הזו תיעשה פחות דינאמית, עד שלבסוף גם בה יתפתחו קרומים ביוגניים, צמחים עילאיים והשיפוע שלה יתמתן.

יכולת החיזוי של משתנה מרחבי כלשהו ע״י משתנה מרחבי אחר תלויה אם כך גם ברמת הרזולוציה בה כל אחד מהם נמדד. בחינה של האוטוקורלציה המרחבית לאורך ארבעת חתכי הדיגום העלתה כי האוטוקורלציה של קצבי הסחיפה/השקעה של חול ביתדות נמוכה בהרבה לעומת זו של מדדי הצומח מהדמאות הלוויין או של הגובה היחסי אשר חושב ממודל הגבהים הספרתי. מאחר והסעת החול נעשית ע״י הרוח, וזו מושפעת מחספוס פני השטח, על מנת לחזות בצורה טובה את סחיפת החול ע״י הרוח יש להתייחס למאפייני הטופוגרפיה והצומח שבמעלה הרוח. את הגורמים הללו ניתן לכמת באמצעות מודל גבהים ספרתי והדמאות לוויין תוך שימוש בפילטרים כיווניים. למרות שהרזולוציה המרחבית של הדמאות Landsat היא בינונית (30 מטר) יחסית לצילומי אוויר, נמצא שהן מבטאות טוב יותר את השפעת הצומח על הסעת החול ע״י הרוח. זאת עקב מספר גורמים: (1) השימוש במידע ספקטרלי בתחום האינפרה-אדום בנוסף לתחום הנראה, אשר מאפשר לכמת בצורה טובה יותר את הצומח; (2) העובדה שהסעת החול המתרחשת בנקודה כלשהיא מושפעת משטח די גדול במעלה הרוח

מספר שנים והשתנו מאז) פותחה **בפרק השביעי** שיטה חקר נתונים גראפית המבוססת על שלושה גרדיינטים בין 0% ל 100% : (1) אחוז הכיסוי היחסי המינימאלי של כל מין בתרשים צומח, (2) אחוז הכיסוי היחסי המכסימאלי של לענה חד-זרעית (המין הנפוץ ביותר) בתרשים צומח, ו (3) אחוז הכיסוי המוחלט המינימאלי של הצומח בתרשים צומח. שיטה זו בשילוב עם כלים סטטיסטיים מקובלים אפשרה לי לחשוף את מידת ההתאמה של המינים הללו לסביבות חוליות שונות. שני מינים נמצאו כמעידים על סביבה מיוצבת : רותם המדבר ומלענן החוף. מבין המינים המצביעים על סביבות של תנועת חול, רק מין אחד היה באופן מובהק מייצג של סביבות בהן יש חשיפה של חול : ציפורנית בשרנית. עם זאת, ישנם אזורים של חשיפת חול בצד הפונה לרוח של הדיונה בהם הגומא המגובב תופש מעל ל 80% מכלל מיני הצמחים. המין שנמצא כמותאם ביותר לקבירת חול היה כצפוי ידיד החולות, אך גם אזורים בהם יותר מ 80% ממיני הצמחים הם לענה חד-זרעית, הם אזורים של השקעת חול. שאר המינים לא נמצאו כמעידים בצורה מובהקת על סביבה חולית כלשהי, אם כי בהתאם לכיסוי היחסי שלהם ושל הלענה החד-זרעית הם עשויים להעיד על אזורים פעילים בהם ישנה קבירה ע״י חול. בסה״כ מתוך נתונים של תרשימי הצומח (כיסוי מוחלט ויחסי של המינים השונים) ניתן היה להסביר 49% מהשונות בערכים המוחלטים של השינוי במפלס פני השטח. המידע האקולוגי הזה עשוי להיות שימושי ביותר לצורך ניטור ההצלחה של פעולות ממשק באזורי דיונות, בין אם הן מכוונות לייצב את הדיונות או להפעיל אותן מחדש.

במקביל לשינויים החלים במיני הצמחים הרב-שנתיים עם התייצבותה של דיונה, חלים גם שינויים בתכונות הקרקע החולית של הדיונה. על מנת לבחון את מהירות התגובה של שלוש תכונות קרקע ליציבות פני השטח, הוצבו 64 פיני ארוזיה לאורך שבעה חתכים באגן קטן הנמצא בין שלוש דיונות אשר החלו להתייצב מאז שנות הששים של המאה העשרים, ואשר מצויות במרחק של כ 2.5 ק״מ מהחוף. שלוש התכונות שנבחנו **בפרק השמיני** הן כמות הכלורופיל של הקרומים הביוגניים, תכולת החומר הדק (סילט וחרסית) ותחמוצות הברזל החופשי. אלה נמדדו באמצעים ספקטראליים, ובחנתי ביחס לקצבי החשיפה וההשקעה של החול כפי שנמדדו בפיני הארוזיה, וכן ביחס למפנה של פני השטח. מצאתי שהקרום הביוגני נמצא לרוב מתחת לשכבה דקה של גרגרי חול, ורק לעתים הוא נחשף ע״י הרוח. ריכוזי הקרום הגבוהים ביותר נמצאים במקומות היציבים יותר (ריכוז ממוצע של 27 מ״ג כלורופיל למ״ר), ונמצא יותר באזורים בהם ישנה קבירה קלה ע״י חול (ריכוז ממוצע של 22.5 מ״ג למ״ר במקומות של עד 1 מ״מ לשבוע של קבירה ע״י חול) מאשר באזורים בהם ישנה סחיפה קלה. זאת ככל הנראה עקב יכולת התנועה האנכית של הקרום. כמו כן נמצא שריכוז הכלורופיל הממוצע גבוה יותר במפנה הצפוני (22.5 מ״ג למ״ר) מאשר במפנה הדרומי (3 מ״ג למ״ר), עובדה נוספת המעידה על מהירות התגובה של משתנה זה ליציבות פני השטח. באשר לשני המשתנים האחרים לא נמצאה כל השפעה למפנה של פני השטח על תכולת החומר הדק או על ריכוז תחמוצות הברזל. עם זאת כן נמצא שהם מושפעים מיציבות פני השטח, אם כי במידה פחותה לעומת הקרום הביוגני. בעוד ש 64% מהשונות בריכוז הכלורופיל מוסברת ע״י השינויים המוחלטים במפלס פני השטח, יציבות פני השטח מסבירה רק 26% מהשונות בתכולת החומר הדק ורק 17% מהשונות בריכוז תחמוצות הברזל. מכאן ניתן להסיק שתהליך הרוביפיקציה מושפע רק במידה קלה ע״י תהליכים פדוגניים של מצב נייח, ומעיד יותר על גיל הדיונה או על חומר המוצא, מאשר על מידת היציבות שלה.

התחנות החופיות (מקו החוף ועד לדיונה החזיתית), ובין 0.36-0.008 מטר ל- 22 התחנות הפנימיות (מעבר לדיונה החזיתית). ערכי אינדקס הצומח המתוקן לקרקע (Soil Adjusted Vegetation Index, SAVI) בעונת החורף (בטווח של 100-200 מטר במעלה הרוח) נמצאו כמסבירים יותר מ 70% מהשונות של ערכי $Z_0$ עבור כל התחנות. המודל הסופי כלל גם את גורם הטופוגרפיה - הגובה של התחנה יחסית לגובה הממוצע של פני השטח בטווח של 400 מטר במעלה הרוח. המודל הליניארי המשולב שהתקבל מאפשר למפות את ערכי $Z_0$ וכך להבין טוב יותר את השונות המרחבית במהירות הרוח ובתנועת החול באזורים של דיונות חופיות.

על מנת לאפיין בצורה ישירה את קצבי הסחיפה וההשקעה של החול הוצבו 315 פיני ארוזיה לאורך ארבעה חתכים בחולות אשדוד-ניצנים. חתכים אלה השתרעו מקו החוף ועד לגבול אזור החולות עם השדות החקלאיים. גובהם של הפינים דלעיל מעל פני החול נמדד 25 פעמים בין דצמבר 2002 לאוקטובר 2004. בדומה למשתנה של חספוס פני השטח, **בפרק השישי** של העבודה נבחנה ההשפעה של משתני הצומח והטופוגרפיה במעלה הרוח על קצבי הסחיפה וההשקעה של החול. כאן נמצא שמרחק ההשפעה במעלה הרוח היה קצר יותר (100 מטר), ובעזרת משתני צומח וטופוגרפיה היה ניתן להסביר כ- 70% מהשונות בערכים המוחלטים של השינוי במפלס פני השטח. בחלוקה ליחידות גיאומורפולוגיות נמצא שהיחידה הדינאמית ביותר הייתה כצפוי מישור ההחלקה של הדיונות (שינוי ממוצע של 345 מ״מ לשנה בערכים מוחלטים, או 229 מ״מ קבירה נטו), בעוד שבצד הפונה לרוח של הדיונה השינויים היו קטנים יותר (134 מ״מ לשנה בערכים מוחלטים בממוצע, עם חשיפה ממוצעת של 61 מ״מ לשנה). בראשי הדיונות נמצא שתהליך ההשקעה גובר על תהליך החשיפה, ככל הנראה עקב התפתחותן של נבח׳ות. מיפוי הערכים החזויים של השינוי במפלס החול על סמך המודל הראה שהדיונות החופיות מנותקות כיום לא רק מהחוף, אלא גם זו מזו, כך שהן כבר כמעט אינן מזינות זו את זו. זאת, עקב כיסוי הצומח הצפוף שהתפתח באזורים הנמוכים שביניהן.

למרות שכיסוי צומח מהווה מדד מקובל למידת יציבותה של דיונה, זה אינו מדד מספק, מאחר וברמות זהות של כיסוי צומח יכולים להתרחש תהליכים איאוליים שונים: יציבות או מוביליות, חשיפה או השקעה. הרכב המינים של הצמחייה לעומת זאת יכול להוות מדד לאופי ועוצמת התהליכים האיאוליים המתרחשים במקום מסוים, מאחר ולמיני צמחים שונים התאמות שונות לתנועת חול, לחשיפה או לקבירה. לשם כך נרשם כיסוי הצומח המוחלט והיחסי של המינים הרב-שנתיים בכל אחד מפיני הארוזיה, בקואדראט של 10*10 מטר. לצורך הניתוח נבחנו תשעת המינים הרב-שנתיים שנמצאו כנפוצים ביותר בחולות אשדוד-ניצנים: ידיד החולות (*Ammophila arenaria*), לוענית החולות (*Scrophularia hypericifolia*), גומא מגובב (*Cyperus conglomerates*), מד-חול דוקרני (*Sporobolus pungens*), ארכובית ארצישראלית (*Polygonum palestinum*), לענה חד-זרעית (*Artemisia monosperma*), רותם המדבר (*Retama raetam*), צפורנית בשרנית (*Silene succulenta*) ומלענן החוף (*Stipagrostis lanata*). על מנת להתגבר על הבעייתיות שבאפיון מידת ההתאמה של מיני צמחים לתנועת חול בשדה כאשר זו אינה נשלטת על ידי החוקר, וגורמים נוספים משפיעים על נוכחות מיני צמחים (כמו למשל תחרות בין מינים, או התנאים ששררו במקום לפני

תוצאות מלחמת ששת הימים והבצורות שאירעו בנגב בשנות השבעים, והתבטאה בתנועה מחודשת של הדיונות. פעילות הסיירת הירוקה בסוף שנות השבעים הביאה לפינוי הבדווים ממישור החוף ולהסדרת הרעייה ובעקבות כך להתחדשות תהליכי ההתייצבות של הדיונות. תהליכים אלו נמשכים עד היום. הגורם האנושי הרבה פעמים אינו זוכה להתייחסות הראויה לו עקב הקושי במציאת תיעוד היסטורי הולם. במסגרת העבודה הזו הראיתי את התרומה של מחקר גיאוגרפי-היסטורי בארכיונים שונים, תוך שילוב של ראיונות עם אנשים על מנת לחשוף את השפעת האדם על הסביבה.

תנועה של חול ע״י הרוח עדיין מתקיימת בחלקים הלא מיוצבים של הדיונות, בעיקר בעונת החורף, כאשר עוברים מעל אזור החוף שקעים ברומטריים המלווים ברוחות סערה דרום-מערביות. **בפרק השישי** של העבודה נבחנו סדרות זמן של קצבי הסרת והיערמות החול כפי שנמדדו ב 315 פיני ארוזיה שהוצבו בשטח של חולות אשדוד-ניצנים, ביחס לסדרות זמן של נתוני רוח ומשקעים כפי שנמדדו בתחנה המטאורולוגית בבית ספר שדה שקמים בניצנים. בניגוד לאזורי דיונות אחרים בעולם, נמצא כי באזור המחקר, תנועת החול כמעט ואינה מושפעת מכמות המשקעים, וזאת למרות שידוע כי לרוח קשה יותר להסיע חול רטוב לעומת חול יבש. ניתן להסביר זאת באופיים של מערכות מזג האוויר האחראיות לרוחות הסערה ולגשמים בחורף בארץ. בשל אופיו המקוטע של הגשם בארץ ומאחר והרוחות החזקות מגיעות לפני החזית הקרה, אין כמעט חפיפה בזמן בין רוחות הסערה לגשם היורד. אינדקס פוטנציאל הסחיפה של החול ע״י הרוח (Resultant Drift Potential, RDP) אפשר להסביר יותר מ 66% מהשונות בקצבי סחיפת/השקעת החול (81% עבור פיני הארוזיה שנקבעו במישור ההחלקה של הדיונות).

## ציר המרחב

מאחר והרוח נמצאה כגורם העיקרי המשפיע על תנועת החול, על מנת להסביר את הפסיפס המרחבי של אזורים מיוצבים ולא מיוצבים בחנו את הגורמים המשפיעים על זרימת הרוח באזורי דיונות, ובעיקר את כיסוי הצומח והטופוגרפיה.

גובה החספוס $Z_0$ המבטא את החספוס האירו-דינאמי של פני השטח, נמצא בהתאמה לצפיפות, גובה וצורת האלמנטים בפני השטח אשר יוצרים את החספוס. החספוס של פני השטח משפיע ישירות על מהירות הרוח ולפיכך גם על סחיפת החול הפוטנציאלית, ומהווה גורם חשוב בהבנת תהליך ההתייצבות של דיונות. **בפרק החמישי** נערך כימות של ההשפעה של כיסוי הצומח והטופוגרפיה על ערכי $Z_0$ כפי שהם באים לידי ביטוי בחולות מישור החוף. לשם כך נערכו מדידות רוח ב 32 מקומות שונים (בגובה של 2.5 מטר) בחולות אשדוד ובחולות של חוף בית-ינאי, מקו החוף ועד למרחק של כ 2.5 ק״מ מהחוף. ערכי ה $Z_0$ חושבו (בנפרד לכל סקטור של כיוון רוח) מתוך מדידות של מהירות הרוח בגובה אחד בלבד, על סמך היחס שבין מהירות הרוח הממוצעת למשבי הרוח הקיצוניים. אחוזי כיסוי הצומח חושבו מתוך צילומי אוויר והדמאות לוויין Landsat לתחנות בהן נמדדה מהירות הרוח, וכן לדרך שעברה הרוח עד לתחנה (במספר מרחקים, בין 15 ל 400 מטר) תוך שימוש בפילטרים כיווניים. מאפייני הטופוגרפיה חושבו על סמך מודלים ספרתיים של גבהים (Digital Elevation Models) וכן על סמך מדידות של GPS דיפרנציאלי בשדה. ערכי $Z_0$ בתחנות נעו בין 0.00005-0.005 מטר ל- 10

## ציר הזמן

מחקר היסטורי של אזורי דיונות מוגבל לרוב ע״י הזמן בו נעשו לראשונה הדמאות לוויין או צילומי אוויר. **בפרק השלישי** מוצגת האפשרות לחקור את קצב החדירה פנימה של דיונות חופיות תוך שימוש במפות היסטוריות. לשם כך הועלתה לראשונה למערכת מידע גיאוגרפית מפת הקרן לחקירת ארץ ישראל (Palestine Exploration Fund, PEF) המבוססת על סקר שנערך בארץ בשנים 1871-1877. מפה זו, המהווה את המיפוי המדעי המקיף ביותר של הארץ לפני המנדט הבריטי, מציגה במפורט את הנוף האנושי והטבעי של הארץ לפני העלייה הראשונה. לשם כך נסרקו 26 הגיליונות של מפת ה PEF, אשר עוגנו לרשת ישראל החדשה. על מנת לבחון את הדיוק של מפת ה PEF כולה, ושל האלמנטים השונים (מעיינות, ישובים וכיו״ב) המופיעים עליה, נאספו 1,104 זוגות של נקודות בקרה (ground control points) ממפה זו וממפות טופוגרפיות מודרניות (1:50,000). מצאתי שהשגיאה האופקית הממוצעת במפה עומדת על 74.4 מטר, והשגיאה האנכית החציונית היא 11.6 מטר, על סמך 123 נקודות טריאנגולציה, אשר היוו את הבסיס למיפוי. נבחרו ששה אזורים של דיונות חופיות על מנת לבחון את השינויים בשטח הדיונות, תוך השוואת השטחים המופיעים במפת ה PEF עם מפות טופו-קדסטריות (1:20,000) מתקופת המנדט הבריטי. בכל האזורים שנבדקו, מצאתי גידול בשטח המכוסה ע״י הדיונות, אשר שקול לקצב התקדמות של 5.1 מטר לשנה (בין 3.9-6.3 מטר לשנה, בהתאם לשיטת עיגון המפה). קצב התקדמות זה היה גדול מהערכת השגיאה האפשרית של 2.96 מטר לשנה, הנובעת מהצטברות הטעויות של תהליך המיפוי בשדה, שרטוט המפות, סריקתן למחשב, עיגונן לרשת ישראל והדיגיטציה של אזורי הדיונות. קצב ההתקדמות שחושב נמצא בהתאמה למחקרים ארכיאולוגיים וגיאומורפולוגיים המעריכים שגיל חולות מישור החוף נע בין 1,000-1,500 שנה. עם זאת, יש לציין שיש להיזהר כאשר מנתחים מפות היסטוריות על מנת לבחון שינויי נוף, מאחר ולא ניתן להניח שכל חלקי המפה או שכל האלמנטים המופיעים על המפה נמדדו באותה מידה של דיוק. בעוד שבמחצית הראשונה של המאה העשרים הדיונות החופיות היו פעילות, מאז הקמת המדינה הן הולכות ומתייצבות. מחקרים קודמים שעסקו בנושא לא עמדו על הגורמים הפיזיים והאנושיים אשר עומדים מאחורי תהליך ההתייצבות. **הפרק הרביעי** מצביע על הפעילות האנושית בחולות כגורם המרכזי בהסברת השינויים העתיים בתהליך ההתייצבות. באמצעות שיטות ייחודיות לניתוח צילומי אוויר (ר׳ לעיל), נמצאו שלושה שלבים עתיים בתהליך: 1948-1966 התייצבות, 1966-1977 פעילות מחודשת של הדיונות ומ- 1977 ואילך – התייצבות מחודשת. על מנת להסביר את השונות העתית בקצב ההתייצבות נבחנו השינויים בזמן בקצב תנועת החול ובכיסוי הצומח וזאת ביחס לגורמים פיזיים (משקעים, התאדות, עוצמת הרוח וכיווניות הרוח, מפלס מי התהום ושכיחות סופות האבק) וגורמים אנושיים (נוכחות בדווים באזורי חולות, אימוני הצבא, תיירות ונופש). לא נמצא מתאם בין הגורמים הפיזיים שנבחנו לבין השינויים שחלו בפעילות הדיונות. מאידך, הנתונים מצביעים על קשר בין פעילות הדיונות לנוכחות אנתרופוגנית של הערבים ובעיקר הבדווים באזור, כאשר תחילת התייצבות הדיונות עם הקמת המדינה מוסברת בהפסקת פעילותם של הערבים והבדווים שם. ריכוזם של הבדווים בצפון הנגב לאחר קום המדינה הביא להורדת הלחץ האנושי על החולות ואפשר לצמחייה להתבסס. פעילות הבדווים באזור התחדשה בשנים 1966-1977 על רקע ביטול הממשל הצבאי,

אפשרויות חדשות בפני מחקרים בתחום של גיאומורפולוגיה איאולית, תוך הוספת היכולת לנתח מאפיינים דינאמיים של הטופוגרפיה של דיונות, במרחב ובזמן.
עם זאת, כאשר בוחנים דיונות על פני שטחים נרחבים, מגלים שהתכונות המינרלוגיות שלהן גם הן משתנות. צבע החול מאפשר לנו ללמוד על התכונות הכימיות והפיסיקליות שלו, אשר מושפעות מתהליכי הבלייה של החול בהשפעת תנאי האקלים, הזמן ובנוכחות צומח. השיטות המקובלות לקביעת הצבע של דוגמאות חול (או קרקע) המבוססות על טבלאות מונסל אינן מספקות בשל אופיין הסובייקטיבי ומספר הקטגוריות המוגבל שהן מכילות. חסרונם של כלים מתוחכמים יותר כמו ספקטרומטר שדה ו/או מעבדה הוא בכך שהם יקרים מאד ולא נוחים לשימוש בשדה. **בפרק השני** של העבודה מוצגת שיטה חדשה המאפשרת לאפיין את הצבע של דוגמאות חול וכן תכונות כימיות ופיסיקליות של הקרקע, תוך שימוש במצלמה דיגיטאלית ובלוחות פלסטיק צבעוני המשמשים לכיול. תוך שימוש ב 370 דוגמאות של חול וקרקעות חוליות, הראיתי שערכי האדום, הירוק והכחול בתמונות דיגיטאליות ואינדקסים ספקטראליים של קרקע אשר חשבתי מתוכם, נמצאים בהתאמה גבוהה מאד למדידות דומות שנעשו עם ספקטרומטר שדה ($R > 0.9$).על סמך 42 דוגמאות שנלקחו לבדיקת מעבדה של ריכוז תחמוצות הברזל ותכולת החומר הדק (סילט וחרסית), נמצא כי האינדקסים שחושבו מתוך התמונות של המצלמה הדיגיטאלית (ובייחוד ה Redness Index), היו זהים ביכולתם לאלו שחושבו על סמך מדידות הספקטרומטר, או אף עלו עליהן ביכולתם לחזות את ריכוזי תחמוצות הברזל והחומר הדק ($R^2$ של 89% ו 81%, בהתאמה). מצלמה דיגיטאלית המצויה בידי כל חוקר יכולה לפיכך לשמש ככלי מדעי לאפיין במדויק את צבע הקרקע החולית, את ריכוז תחמוצות הברזל והחומר הדק – תכונות העשויות להעיד על גיל הדיונות, תנאי האקלים שבהן הן התפתחו, ובאופן חלקי אף על דרגת הייצוב של הדיונות.
אחד המדדים המקובלים לפעילות דיונות הוא קצב התנועה שלהן כפי שהוא מחושב לרוב מצילומי אוויר. עם זאת, בדיונות העוברות תהליכי התייצבות ההנחה שהדיונות שומרות על צורתן וגודלן אינה תקפה. על מנת למדוד את קצב התנועה של דיונות במקרים כאלה בהם חלקים שונים של הדיונה נעים בקצב שונה, פותחה שיטה חדשה המוצגת **בפרק הרביעי**. שיטה זו מחלקת את כלל השטח שכוסה בחול ע״י דיונה מתקדמת בין שתי נקודות זמן ברוחבה של הדיונה כולה על מנת לחשב את מרחק ההתקדמות הממוצע של הדיונה.
בדיונות מתייצבות מתפתחים גם קרומי קרקע ביוגניים. על מנת לאפשר מיפוי כמותי של קרומים אלה בשדה נעשה שימוש בכלי אשר אפשר להסיר בהדרגה שכבות חול (כאשר זה היה רטוב) וכך למדוד את ההחזרה הספקטרלית של הקרום במספר עומקים. על יסוד מדידות אלה פותחה משוואה אמפירית שמתוכה ניתן היה לחשב את ריכוז הכלורופיל בקרום תוך התחשבות בתכולת הלחות של דוגמת החול. מדדים אלה אפשרו (כפי שהדגמתי **בפרק השמיני**) לקבוע את מידת ההשפעה של המפנה והיציבות של פני השטח על התפתחות הקרום של אצות ירוקיות בחולות אשדוד.

# תקציר


## מבוא

דיונות חופיות מהוות דוגמא למערכת מורכבת הנוצרת בהשפעתם המשולבת של גורמים פיזיים, ביולוגיים ואנושיים. הדינאמיות הרבה של דיונות חופיות, קרבתן לריכוזי אוכלוסיה ועקב כך ללחצי פיתוח, והמערכת האקולוגית המיוחדת של צמחים ובעלי חיים אשר נוצרה בהן עושים אותן לא רק לנושא מחקר מעניין, אלא גם לכזה שיש לו השלכות חשובות של שמירת טבע וסביבה. במהלך המאה העשרים, וביתר שאת מאז קום המדינה, הולך ומצטמצם שטחן של הדיונות בעיקר עקב פעולות של בנייה, כרייה וחקלאות הנערכות עליהן. בנוסף הולכות הדיונות ומתייצבות עם השנים, כך שכיסוי הצומח גדל ותנועת החול קטנה.

בעבודה זו בקשנו לבחון ולהבין את הגורמים הפיזיים והאנושיים המסבירים את השונות במרחב ובזמן של תהליך ההתייצבות של דיונות חופיות, תוך התמקדות בשדה הדיונות הגדול ביותר שנותר במצב טבעי יחסית לאורך מישור החוף: חולות אשדוד-ניצנים, בין הערים אשדוד לאשקלון. לשם כך נקטתי בגישה בין-תחומית שאפשרה לי לבחון את הנושא במספר רבדים תוך שילוב כלים של חישה מרחוק, מערכות מידע גיאוגרפיות (ממ"ג או GIS) ועבודת שדה גיאומורפולוגית. המאמרים המדעיים המרכיבים עבודה זו נעים לאורכם של שלושה צירים מחקריים: ציר השיטות, ציר הזמן וציר המרחב. בציר השיטות פותחו כלים חדשים של חישה מרחוק על מנת לחקור אזורים של דיונות, בציר הזמן נבחנו השינויים שחלו בקצב תנועת הדיונות ואת הגורמים הפיזיים והאנושיים האחראיים להם, בעוד שבציר המרחב כומתו הגורמים המשפיעים על השונות המרחבית בהסעת החול ע"י הרוח. להלן עיקרי החידושים והממצאים של העבודה בהתאם לשלושת הצירים שפורטו:

## ציר השיטות

אחד הגורמים החשובים ביותר להבנת הדינאמיקה של שדה דיונות הוא המבנה הטופוגרפי של הדיונות והשינויים החלים עם הזמן. עם זאת בשל אופיין המשתנה וקשיי הנגישות שלהן, אזורי דיונות לרוב אינם ממופים במפורט. **בפרק הראשון** של העבודה מוצגת שיטה חדשה המאפשרת לחלץ מידע טופוגרפי של השיפוע, המפנה והגובה של דיונות מתוך הדמאות לוויין של חיישנים אופטיים (דוגמת ה Landsat), על בסיס ההצללה (shading) של פני השטח כאשר אלה אחידים בהרכבם המינרלוגי ונטולי כיסוי צומח. נמצא כי שילוב של שתי הדמאות לוויין, האחת מעונת החורף והשנייה מעונת הקיץ, יוצר את השילוב הטוב ביותר להפקת מפות שיפועים ומפנים לדיונות בחולות אשדוד וכן באזור ניצנה. הדיוק בחישוב הגובה והשיפוע לאורך חתכים שנבחרו לצורך האימות הגיע למטר אחד ושלוש מעלות, בהתאמה (בהדמאה עם רזולוציה מרחבית של 15 מטר). שיטה זו מאפשרת לחלץ מידע טופוגרפי מהדמאות לוויין עוד משנות השבעים וכך לעקוב אחרי שינויים שחלו בטופוגרפיה של דיונות ברחבי העולם ללא מדידה בשטח. עד היום, הדמאות לוויין אופטיות שימשו בעיקר על מנת ללמוד על היקף השתרעותן של דיונות, כיסוי הצומח שלהן וההרכב המינרלוגי. השיטה המוצעת כאן פותחת

# תוכן העניינים

**עבודה זו נעשתה בהדרכתם של**

**פרופ׳ איל בן-דור**

**וד״ר גיורא קדרון**

# ניטור, הבנת הגורמים וחיזוי תהליך ההתייצבות של חולות מישור החוף באמצעים של חישה מרחוק ומערכות מידע גיאוגרפיות (ממ"ג): חולות מישור החוף הדרומי כמקרה מבחן

**חיבור לשם קבלת התואר "דוקטור לפילוסופיה"**

**במסגרת ביה"ס להיסטוריה, הפקולטה למדעי הרוח**

**מאת**

**נעם לוין**

**מוגש לסנאט של אוניברסיטת תל-אביב**

**פברואר 2006**